

Current Cancer Research

Ian Y. Wong  
Michelle R. Dawson *Editors*

# Engineering and Physical Approaches to Cancer

 Springer

# **Current Cancer Research**

## **Series Editor**

Wafik El-Deiry, Legoretta Cancer Center, Brown University, Providence, RI, USA

Current Cancer Research is a highly regarded series covering new and emerging topics in cancer research and oncology. Volumes are current and timely, edited by experts in the related field, and chapters are authored by renowned scientists and physicians in their fields of interest. All volumes undergo single blind peer review and review by the series editor prior to acceptance and publication in the series. Current Cancer Research is indexed in SCOPUS.

Ian Y. Wong • Michelle R. Dawson  
Editors

# Engineering and Physical Approaches to Cancer

 Springer



*Editors*

Ian Y. Wong  
School of Engineering Department of  
Pathology & Laboratory Medicine  
Legoretta Cancer Center  
Brown University  
Providence, RI, USA

Michelle R. Dawson  
Department of Molecular Biology, Cell  
Biology, & Biochemistry, School of  
Engineering, and Legoretta Cancer Center  
Brown University  
Providence, RI, USA

ISSN 2199-2584

ISSN 2199-2592 (electronic)

Current Cancer Research

ISBN 978-3-031-22801-8

ISBN 978-3-031-22802-5 (eBook)

<https://doi.org/10.1007/978-3-031-22802-5>

© The Editor(s) (if applicable) and The Author(s), under exclusive license to Springer Nature Switzerland AG 2023

This work is subject to copyright. All rights are solely and exclusively licensed by the Publisher, whether the whole or part of the material is concerned, specifically the rights of translation, reprinting, reuse of illustrations, recitation, broadcasting, reproduction on microfilms or in any other physical way, and transmission or information storage and retrieval, electronic adaptation, computer software, or by similar or dissimilar methodology now known or hereafter developed.

The use of general descriptive names, registered names, trademarks, service marks, etc. in this publication does not imply, even in the absence of a specific statement, that such names are exempt from the relevant protective laws and regulations and therefore free for general use.

The publisher, the authors, and the editors are safe to assume that the advice and information in this book are believed to be true and accurate at the date of publication. Neither the publisher nor the authors or the editors give a warranty, expressed or implied, with respect to the material contained herein or for any errors or omissions that may have been made. The publisher remains neutral with regard to jurisdictional claims in published maps and institutional affiliations.

This Springer imprint is published by the registered company Springer Nature Switzerland AG  
The registered company address is: Gewerbestrasse 11, 6330 Cham, Switzerland

# Preface

Outcomes for cancer patients are ultimately governed by tumor cell invasion and metastasis, as well as therapeutic resistance. The functional phenotypes that drive these aberrant behaviors have been conceptually understood via the classic “Hallmarks of Cancer” and associated signaling pathways. Furthermore, the complex interactions between cancer cells and their surrounding microenvironment are now recognized to suppress or promote cancer progression. It should be noted that these dysregulated genetic and biochemical traits are intimately linked with disruption of the physical and mechanical conditions within a tissue. For example, uncontrolled cell growth can result in profound increases in solid stress, vessel compression, interstitial fluid pressure, extracellular matrix stiffness, as well as dramatic alterations in the tissue architecture. Emerging technologies enable precise measurements of cell and tissue dynamics with exquisite resolution, reverse engineering of the complex tumor microenvironment, and ultrasensitive diagnostics for early cancer detection. Physical and mathematical concepts enable fundamental insights into how cells within a tumor are influenced by external forces and flows, and can dynamically reciprocate to maintain tensional homeostasis by reprogramming the surrounding microenvironment.

*Engineering and Physical Approaches to Cancer* addresses the newest research at this interface between cancer biology and the physical sciences. Several chapters address the mechanobiology of collective and individual cell migration, including experimental, theoretical, and computational perspectives. Other chapters consider the crosstalk of biological, chemical, and physical cues in the tumor microenvironment, including the role of senescence, polyploid giant cells, TGF-beta, metabolism, and immune cells. Further chapters focus on circulating tumor cells and metastatic colonization, highlighting both bioengineered models as well as diagnostic technologies. Finally, one chapter is a meta-analysis of recent successes from the National Cancer Institute’s Physical Sciences in Oncology Network. We are proud to feature the work of emerging and diverse investigators in this field, who have already made impressive cross-disciplinary scientific contributions.

This book is designed for a general audience, particularly researchers conversant in cancer biology but less familiar with engineering (and vice versa). Thus, we

envision that this book will be suitable for faculty, postdoctoral fellows, and advanced graduate students across medicine, biological sciences, and engineering. We also anticipate this book will be of interest to medical professionals and trainees, as well as researchers in the pharmaceutical and biomedical device industry. We hope that this work will inspire new directions for the diagnosis, prevention, and treatment of cancer in order to improve the lives of patients worldwide.

Providence, RI, USA  
Providence, RI, USA  
September 2022

Ian Y. Wong  
Michelle R. Dawson

# Contents

<b>Mechanobiology of Collective Cell Migration in 3D Microenvironments..</b>	1
Alex M. Hruska, Haiqian Yang, Susan E. Leggett, Ming Guo, and Ian Y. Wong	
<b>Collective Cellular Phase Transitions in Cancer.....</b>	33
Adrian F. Pegoraro, Thien-Khoi N. Phung, and Jennifer A. Mitchel	
<b>Biophysical and Biochemical Mechanisms Underlying Collective Cell Migration in Cancer Metastasis.....</b>	77
Ushasi Roy, Tyler Collins, Mohit K. Jolly, and Parag Katira	
<b>Hallmarks of an Aging and Malignant Tumor Microenvironment and the Rise of Resilient Cell Subpopulations .....</b>	113
Carolina Mejia Peña, Amy H. Lee, Mateo F. Frare, Deepraj Ghosh, and Michelle R. Dawson	
<b>Physical Regulations of Cell Interactions and Metabolism in Tumor Microenvironments.....</b>	139
Hydari Masuma Begum, Jeong Min Oh, Diane S. Kang, Min Yu, and Keyue Shen	
<b>Biophysical Regulation of TGF<math>\beta</math> Signaling in the Tumor Microenvironment .....</b>	159
Chinmay S. Sankhe, Jessica L. Sacco, and Esther W. Gomez	
<b>Bioengineering and Bioinformatic Approaches to Study Extracellular Matrix Remodeling and Cancer-Macrophage Crosstalk in the Breast Tumor Microenvironment .....</b>	201
Youngbin Cho, Ruxuan Li, and Ioannis K. Zervantonakis	
<b>Engineering Approaches in Ovarian Cancer Cell Culture .....</b>	231
Marcin Iwanicki, Tonja Pavlovic, and Panteha Behboodi	

<b>Biophysical Properties and Isolation of Circulating Tumor Cells</b> .....	255
Diane S. Kang, Aidan Moriarty, Jeong Min Oh, Hydari Masuma Begum, Keyue Shen, and Min Yu	
<b>In Vitro and In Vivo Host Models of Metastasis</b> .....	285
Sam H. Au	
<b>Physical Sciences in Cancer: Recent Advances and Insights at the Interface</b> .....	301
Olalekan H. Usman and Jerome Irianto	
<b>Index</b> .....	329

# Mechanobiology of Collective Cell Migration in 3D Microenvironments



Alex M. Hruska, Haiqian Yang, Susan E. Leggett, Ming Guo,  
and Ian Y. Wong

**Abstract** Tumor cells invade individually or in groups, mediated by mechanical interactions between cells and their surrounding matrix. These multicellular dynamics are reminiscent of leader-follower coordination and epithelial-mesenchymal transitions (EMT) in tissue development, which may occur via dysregulation of associated molecular or physical mechanisms. However, it remains challenging to elucidate such phenotypic heterogeneity and plasticity without precision measurements of single-cell behavior. The convergence of technological developments in live cell imaging, biophysical measurements, and 3D biomaterials is highly promising to reveal how tumor cells cooperate in aberrant microenvironments. Here, we highlight new results in collective migration from the perspective of cancer biology and bioengineering. First, we review the biology of collective cell migration. Next, we consider physics-inspired analyses based on order parameters and phase transitions. Further, we examine the interplay of metabolism and phenotypic heterogeneity in collective migration. We then review the extracellular matrix and new modalities for mechanical characterization of 3D biomaterials. We also explore epithelial-mesenchymal plasticity and implications for tumor progression. Finally, we speculate on future directions for integrating mechanobiology and cancer cell biology to elucidate collective migration.

**Keywords** Biomaterials · Epithelial-mesenchymal transition · Extracellular matrix · Metabolic heterogeneity · Order parameter · Traction force microscopy

---

A. M. Hruska · I. Y. Wong (✉)

School of Engineering, Center for Biomedical Engineering, and Legorreta Cancer Center,  
Brown University, Providence, RI, USA  
e-mail: [ian\\_wong@brown.edu](mailto:ian_wong@brown.edu)

H. Yang · M. Guo

Department of Mechanical Engineering, Massachusetts Institute of Technology, Cambridge, MA,  
USA

S. E. Leggett

Department of Bioengineering, University of Illinois at Urbana-Champaign, Urbana, IL, USA

© The Author(s), under exclusive license to Springer Nature Switzerland AG 2023

I. Y. Wong, M. R. Dawson (eds.), *Engineering and Physical Approaches to Cancer*,  
Current Cancer Research, [https://doi.org/10.1007/978-3-031-22802-5\\_1](https://doi.org/10.1007/978-3-031-22802-5_1)

## 1 Introduction

Collective migration occurs when a group of individual cells exhibit coordinated movements with similar speed and directionality [1]. This phenomenon is intriguing in cancer biology as a demonstration of how heterogeneous phenotypes cooperate to enhance solid tumor progression within a dysregulated microenvironment [2]. Indeed, patient histopathology sections often include packs of tightly connected cancer cells organized as rounded clusters or linearly extended strands within an aberrant tissue architecture [3]. Such behaviors are reminiscent of leader-follower interactions in development and wound healing [4]. Moreover, the epithelial-mesenchymal transition (EMT) is associated with developmental transcription factors that weaken cell-cell adhesions and promote tumor invasion [5]. Collective migration is also intriguing from a physical science perspective as an emergent phenomenon driven by interactions between many individuals [6]. These behaviors are further influenced by abnormal solid and fluid stresses from their surroundings, which impact metastatic dissemination and drug delivery [7]. Thus, a cross-disciplinary approach is required to understand how heterogeneous groups of invasive cells interact with the surrounding matrix via biological and physical mechanisms.

Recent advances in assay development have enabled new mechanistic insights into collective migration via exquisitely sensitive measurements as well as biomimetic culture conditions. For example, single-cell molecular profiling technologies have revealed the interplay of myriad signaling pathways, which previously involved dissociation of tissues into single cells [8] but now can retain information about tissue architecture via spatial transcriptomics [9]. New light microscopy techniques based on structured illumination permit deeper imaging with improved temporal resolution and reduced phototoxicity [10]. Fluorescent protein reporters can be used for longitudinal monitoring of transcriptional state or force transduction [11]. In parallel, cells cultured within engineered 3D biomaterials experience controlled biochemical and physical cues, which can be dynamically modulated [12, 13]. The mechanical properties of single cells and local matrix architecture can be further probed at subcellular resolution [14, 15]. These early stage technologies are now being used in translational applications with primary mouse or human organoids in order to predict disease progression and therapeutic response [16].

In this chapter, we highlight recent developments in collective tumor invasion from a biological and physical perspective. We first review the essential concepts of collective cell migration and leader-follower interactions. We then examine how patterns of collective motion can be analyzed using physical concepts such as order parameters and phase transitions, as well as the interplay of metabolism with phenotypic heterogeneity. Next, we review biomaterials and the ECM, along with precision measurement 3D matrix mechanics. Finally, we explore EMT as a representation of phenotypic heterogeneity, including recent results on partial or

intermediate states. We close with our critical perspective on the field and discussion of future directions.

## 2 Collective Cell Migration and Leader-Follower Interactions

Early work on eukaryotic cell migration investigated how individual cells (e.g., fibroblasts, leukocytes) cyclically adhere and propel themselves along planar (2D) substrates, revealing physically conserved mechanisms across various cell types [17]. First, cells polarize with a leading and trailing edge, often in response to asymmetric stimuli of soluble or immobilized biochemical factors, substrate stiffness, or local topography [18]. Next, cells extend protrusions from the leading edge driven by actin polymerization, which form integrin-mediated focal adhesions with ligands on the substrate [19]. Finally, actomyosin contractility via stress fibers pulls the cell body forward and retracts the trailing edge [20]. Subsequent work using compliant substrates revealed that cell adhesion and migration were modulated by the relative strength of cell-substrate interactions and intracellular contractility [21].

In comparison, 3D matrix is a more mechanically confined environment that can impede cell migration relative to 2D substrates [22]. Migratory cells can traverse a narrow region by local remodeling of the matrix into a wider path, as well as by deforming their intracellular components to squeeze through. Thus, the increased deformability reported for cancer cells relative to normal cells may enhance invasion and metastatic dissemination [23]. Classically, individual migration phenotypes have been described in terms of contractile mesenchymal or propulsive amoeboid modes. First, mesenchymal migration phenotypes are associated with elongated, spindle-like morphologies, which extend narrow actin-driven protrusions (via RAC1 and CDC42) that apply strong cell-matrix adhesions and secrete matrix metalloproteinases to degrade and remodel the ECM [24]. Mesenchymal cells express the intermediate filament vimentin [14], which is highly stretchable (without breaking) and can protect cells undergoing large deformations [25, 26]. Second, amoeboid migration phenotypes exhibit compact, rounded morphologies, which propel themselves forward via actomyosin contractility (via RHOA) and do not require strong adhesions or matrix metalloproteinases for effective migration [27]. Weak ECM adhesion and limited remodeling allow cells utilizing amoeboid migration (e.g., immune cells) to migrate more rapidly than mesenchymal cells (e.g., fibroblasts) which tend to migrate more slowly [28, 29]. Migratory cells are further capable of switching between mesenchymal and amoeboid migration modes, depending on local ECM adhesivity and matrix remodeling capabilities [30, 31]. Further, groups of mesenchymal or amoeboid cells may migrate as multicellular “streams” without strong cell-cell adhesions in response to some asymmetric external stimulus, where contact guidance by matrix architecture is permissive for similar migration direction



and speed [32]. In the absence of these asymmetric stimuli, cells typically exhibit more random and less directed motility [18]. Interestingly, an osmotic pressure-driven propulsion mechanism has also been observed for cancer cell lines in confining microchannels, which does not require actin polymerization [33].

Within cancer cells, the nucleus is the most rigid and sizable organelle, undergoing large deformations when translocating through confined spaces [34]. Empirically, cancer cell lines cannot traverse confined spaces smaller than  $7 \mu\text{m}^2$  without matrix remodeling [35, 36], which is gauged by nuclear deformation as an intracellular “ruler” [37, 38]. In particular, nuclear stiffness is mediated in part by the nuclear envelope via nucleoskeletal protein lamin A/C [39], and lamin A has been reported to be downregulated in breast cancer cells [40]. The nucleus is mechanically coupled to the cytoskeleton via the linker of nucleoskeleton and cytoskeleton (LINC) complexes, allowing nuclear pushing or pulling via actomyosin contractility [34]. As a consequence of these large deformations, nuclear envelope ruptures can occur and drive DNA damage, which may only be partially reversed by ESCRT III [41–45] and may enhance metastatic dissemination [46]. Indeed, cells can even use the nucleus as a “piston” to compartmentalize the front and back to generate high pressure “lobopodial” protrusions within very dense matrix architectures [47, 48].

Carcinomas arise from healthy epithelial tissues, which consist of epithelial cells with strong cell-cell adhesion and apicobasal polarity organized into tightly packed layers (Fig. 1A) [49]. During tumor progression, tissues become progressively disorganized due to uncontrolled proliferation and then transition to malignant invasion via degradation of the basement membrane [50]. Groups of epithelial cells exhibit collective migration when they remain mechanically connected, sustaining cell polarization for directed motion, as well as coordinating longer ranged responses to environmental stimuli (Fig. 1B, C) [1]. Within solid tumors, the spatial organization of these groups can vary widely, from relatively compact clusters to elongated single or multi-file strands to large masses [3]. These collectives may be categorized broadly into distinct functional groups based on parameters of multicellular morphology, the degree of cell-cell adhesion, and supracellular coupling of intercellular signaling [51]. Furthermore, collective migration patterns are shaped (in part) by the surrounding ECM architecture and presence of various stromal cells.

Despite differences in spatial organization, 3D collective invasion is most often characterized by the presence of highly motile cells at the front of invasive groups, termed “leader cells” (Fig. 1C) [4]. Leader cells often exhibit actin-rich protrusions with strong cell-matrix adhesions and actomyosin contractility to locally remodel the ECM (Fig. 1C), analogous to the mesenchymal motility phenotype described previously [51]. ECM adhesion is mediated via heterodimeric surface receptors known as integrins, such as  $\alpha_2\beta_1$  for fibrillar collagen, as well as  $\alpha_V\beta_1$ ,  $\alpha_V\beta_3$ , and  $\alpha_5\beta_1$  for fibronectin, although integrins exhibit some promiscuity and context-dependent function [52]. Leader cells further generate traction forces to deform the ECM via contractility of intracellular stress fibers, which can associate with vimentin intermediate filaments in order to enhance tractions [14] (Fig. 1, i), and may occur in combination with ECM degradation via matrix metallo-

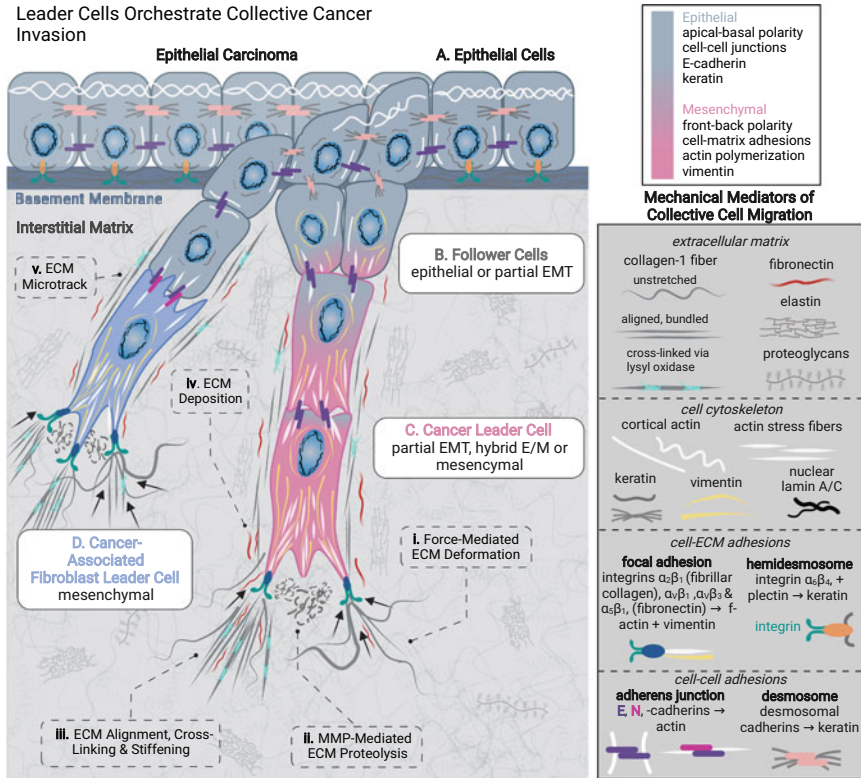


**Fig. 1** Schematic of collective cancer cell invasion. (A) Epithelial cells, (B) follower cells, (C) cancer leader cell, (D) cancer-associated fibroblast. ECM remodeling via force-mediated matrix deformations (i), MMP degradation (ii), alignment/cross-linking (iii), ECM deposition (iv), and formation of ECM microtracks (v). Created with Biorender.com

proteinases (Fig. 1, ii). Thus, through repeated protrusion-contraction-deformation events, leader cells pull on intrinsically “wavy” collagen fibers to stretch and bundle fibers into regions of aligned, stiffened ECM (Fig. 1, iii). Furthermore, collagen fibers can be cross-linked enzymatically by lysyl oxidase to locally enhance ECM stiffness and promote tumor invasion through focal adhesion kinase (FAK) signaling [53]. Finally, leader cells can deposit new ECM (Fig. 1, iv), such as fibronectin, to reinforce adhesive migratory cues [54]. Altogether, these leader cell-driven ECM remodeling activities result in the generation of ECM “microtracks” (Fig. 1, v) which are permissive for cell migration and contain aligned, bundled ECM proteins that present contact guidance cues. For the remainder of this review, we primarily focus on leader cells originating from epithelial tumors, or carcinomas, but note that leader cells may also arise from stromal cells (e.g., fibroblasts) (Fig. 1D) or immune cells (e.g., macrophages) [4]. Regardless of cell type, leader cell activity typically results in ECM architecture that is more permissive for cell migration.

Concomitant with ECM remodeling activities, leader cells may guide the migration of adjacent cells termed “followers” (Fig. 1B) along ECM microtracks. Follower cells are defined primarily by a rearward spatial position relative to leaders but may also possess migratory and ECM remodeling capabilities. Indeed, follower cells traversing wider spaces generated by leader cells encounter less mechanical resistance and can expend less energy to remodel ECM or undergo large deformations [4]. Leader cells coordinate the activity of followers through a combination of cell-cell mechanical adhesions and biochemical signaling.

First, cell-cell junctions are formed when two cells connect adhesion proteins to form a stable mechanical junction (e.g., adherens junctions and desmosomes), typically utilizing proteins in the cadherin superfamily (e.g., E-, N-, and P-cadherins or desmosomal cadherins) [55], which are intracellularly coupled to actin microfilaments or keratin intermediate filaments, respectively [56]. As a stationary sheetlike structure, epithelial cells remain tightly connected to neighboring cells via desmosome adhesions and adhere to the basement membrane via hemidesmosomes containing integrin  $\alpha_6\beta_4$  (Fig. 1A). Loss of apical-basal polarity is a common step in cancer progression, which often accompanies loss of cell-cell adhesions and acquisition of cell-ECM adhesions, which establish front-back polarity and induce cell motility (Fig. 1B). Motile follower cells may lose desmosomes and keratin expression and gain expression of vimentin IFs, which are associated with EMT. However, hybrid phenotypes expressing keratin and vimentin have been observed clinically [57]. Mesenchymal leader and followers may remain adherent through N-cadherin junctions or maintain transient adhesions that result in weak cell-cell coordination. Nonetheless, epithelial followers often retain E-cadherin to tightly coordinate migration. Finally, leader cells are connected to followers via adherens junctions. For example, cancer leader cells in partial EMT states may connect to followers via homotypic E-cadherin junctions (Fig. 1C). Leaders in later stages of EMT may express N-cadherin and adhere to followers via heterotypic E-/N-cadherin junctions, which have also been documented for fibroblast leader cells with epithelial follower cells (Fig. 1D) [58]. Overall, cell-cell adhesions maintain coherent collective motion by mechanical coupling via the cell cytoskeleton, as well as reinforcement of multicellular front-rear polarity. From a biochemical standpoint, cells in close proximity to one another may also coordinate motility by juxtacrine signaling (e.g., Notch1-Dll4 signaling) [59]. Moreover, contact-independent autocrine signaling across gap junctions may be utilized for intercellular coordination of contractility and size [60], via connexins [61, 62].

It should be noted that leader cells may not always guide collective migration, as exemplified by the diversity of collective migration behaviors in development, such as the attraction-repulsion dynamics observed in neural crest-placode migration [63]. Furthermore, followers may or may not have the potential to become leader cells. Interestingly, followers can “switch” with leaders during collective migration, which may occur if leader cells undergo cell division, and could also redistribute metabolic costs of migration. Nevertheless, the functional role and molecular definition of leader cells remain unresolved and may depend on biological context

[64]. In this chapter, we consider leader cell behavior and leader-follower dynamics in the context of epithelial cancer invasion. As discussed previously, leader cells often utilize cell-cell adhesions through proteins such as E-cadherin, which is an epithelial biomarker [65]. Thus, these leader cells may represent a hybrid or partial EMT phenotype, which we consider in detail in a subsequent section.

### 3 Analyzing Collective Migration Using Phase Transitions and Order Parameters

Healthy epithelial tissues are comprised of mechanically connected cells with limited motility, as well as uniform shape and regular geometric packing [66]. This mechanically arrested state can transition to more motile states during tumor progression, development, and wound healing [67]. For example, cells can disperse individually (e.g., gas-like), can migrate in closer proximity (e.g., fluidlike), or move in coordinated groups (e.g., active nematics with long-ranged orientational order) (Fig. 2A) [70, 71]. In these latter contexts, cells may exhibit varying cell-cell adhesion strength along with larger fluctuations in cell shape and packing. Analogous phase transitions that emerge from many interacting particles can be captured using statistical physics, assuming that the particles are relatively similar, move with constant velocity and can alter direction, interact over some distance, and are subject to “noise” of varying strength [72]. These phase transitions can be quantified based on changes in some order parameter that represents a symmetry property of the system [73]. For instance, the jamming transition describes how soft materials exhibit a liquid to solid-like response when varying control parameters of interparticle adhesion, density, or shear [74]. Fredberg proposed that a biological jamming transition could occur similarly with respect to cell-cell adhesion, cell density, or motility in 2D epithelial monolayers [75].

An intuitive order parameter for collective migration is cell velocity, and particle image velocimetry (PIV) can be used to analyze spatial and temporal correlations [76]. Early work used PIV to visualize cooperative motions within 2D epithelial monolayers. For instance, Silberzan and coworkers utilized PIV for collective migration of epithelial monolayers into unoccupied regions [77, 78]. Angelini et al. used PIV to measure how compliant substrates were deformed by epithelial monolayers, revealing characteristic length and time scales over which cells coordinate their migration, analogous to dynamic heterogeneity in a physical glass transition [79, 80]. More recently, Scita and coworkers applied PIV to reveal the onset of angular rotation and local cellular rearrangements in 3D spheroids [81, 82].

O. Ilina et al. utilized PIV to establish a physical picture of 3D collective migration based the cross talk of cell-cell adhesion with ECM confinement [83]. Multicellular spheroids were embedded within collagen matrix in varying assay geometries. When ECM porosity was sufficiently large to permit cell migra-

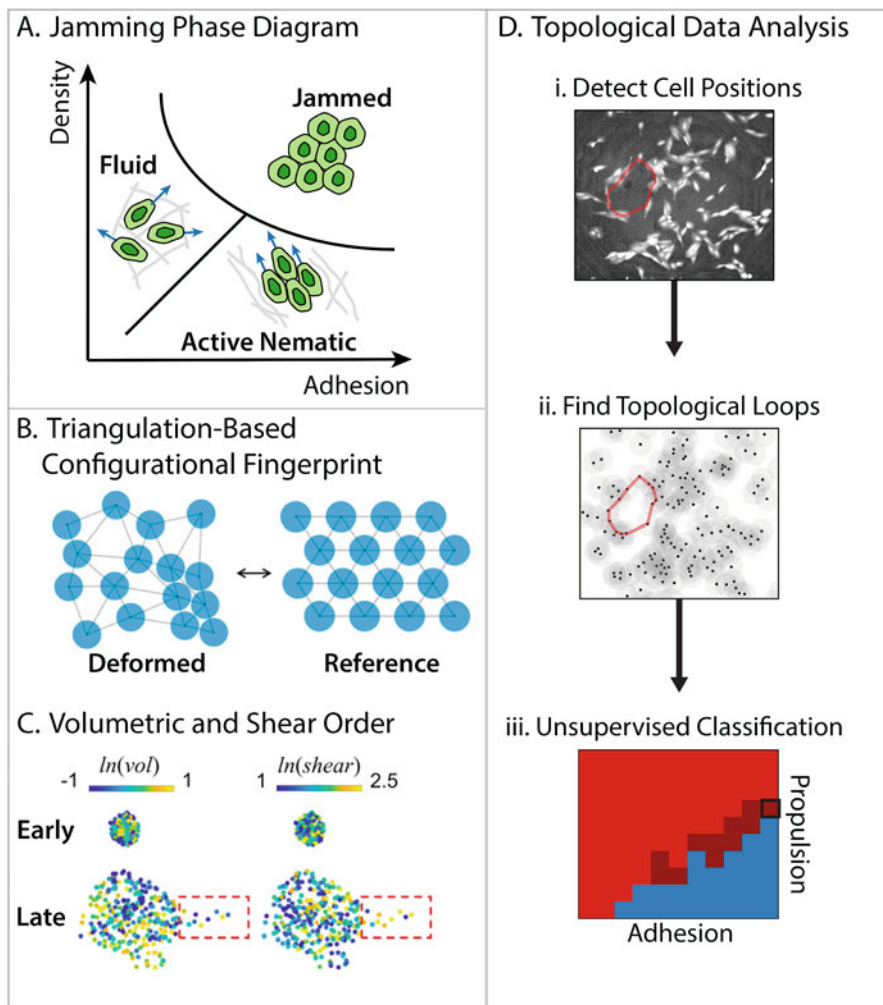


**Fig. 2** (A) “Jamming” phase diagram of individual and collective cell migration governed by cell-cell adhesion and cell density. Redrawn from [70]. (B) Triangulation-based configurational fingerprints compare deformed and (relaxed) reference states. (C) Late (invasive) spheroids exhibit increased volumetric order parameter (per cell) relative to early spheroids but comparable shear order parameters (per cell). Reproduced from [68]. (D) Topological data analysis represents discrete cell positions based on the “persistence” of topological loops at varying length scales around empty areas, which can then be mapped to computational simulations with varying adhesion and propulsion. Reproduced from [69] with permission from the Royal Society of Chemistry

tion (without ECM degradation), cells with downregulated E-cadherin typically migrated individually in a fluidlike state. As ECM porosity decreased, the increasing spatial confinement resulted in cells moving together in close proximity, despite their relatively weak cell-cell junctions. Nevertheless, higher resolution tracking

of cell velocity and spatial correlations revealed that neighboring cells within a group were locally uncorrelated when cell-cell junctions were weak. Thus, these results highlight the importance of mature cell-cell adhesions (e.g., E-cadherin) to coordinate effective group migration during tumor invasion and metastasis.

Geometric order parameters can also be defined based on cell shape or local connectivity. Historically, honeycomb-like hexagon-dominated cellular structures were observed empirically in animal and plant tissues [84]. Interestingly, proliferating cells within epithelial tissues result in a wider distribution of polygons, particularly pentagons and heptagons [85]. Bi and Manning captured these transitions based on a cell shape index (i.e., ratio of cell perimeter to area), which are indicative of shear modulus of the cell monolayer [86], effective diffusivity of single cells [87], and cellular stresses [88]. Fredberg and coworkers subsequently validated this parameter in asthmatic airway epithelium [89] and revealed that cell shape index and variability were also strongly correlated with unjamming [90, 91]. These concepts were also extended to 3D collective migration by analogy to phase transitions from solid to liquid to gas [92–94].

H. Yang et al. proposed new order parameters based on the deformation of a triangular lattice relative to an idealized equilibrium (Fig. 2B) [68]. For some spatial configuration of cells within a tissue, the cell positions (e.g., nuclei) can be connected by fictitious lines to partition the surrounding space into triangles (e.g., Delaunay triangulation). The deformation gradient can then be expressed using invariants  $vol_n = \det(\mathbf{F})$ , representing how the area of each triangle deviates from the average, along with  $shear_n = \text{tr}(\mathbf{F}^T \mathbf{F}) / \det(\mathbf{F}) - 2$ , corresponding to how a given triangle is distorted relative to an equilateral triangle. Corresponding order parameters are defined by ensemble averaging the natural logarithm of these invariants over all triangles, i.e.,  $\Phi_{vol} = \langle [\log(vol_n)]^2 \rangle$  and  $\Phi_{shear} = \langle \log(shear_n) \rangle$ . This analysis was first validated based on ventral furrow formation of the *Drosophila* germ band epithelium, which transitions from an arrested, jammed-like state towards a more motile, unjammed-like state. This macroscopic phenomenon is associated with characteristic shearing and shrinking behavior within the tissue, resulting in a sharp increase in the  $\Phi_{shear}$  and  $\Phi_{vol}$  at a characteristic timescale where this phase transitions occurs. Conversely, the proliferation of kidney epithelial cells (e.g., MDCK) first results in a suppression of density fluctuations in  $\Phi_{vol}$ , analogous to a transition from gas to liquid, followed by a further suppression of packing disorder in  $\Phi_{shear}$ , analogous to a transition from liquid to solid. Lastly, these concepts were used to analyze the collective invasion of mammary epithelial spheroids (e.g., MCF-10A). Remarkably, spheroids at earlier times with minimal invasion (e.g., acini) exhibited similar  $\Phi_{shear}$  but smaller  $\Phi_{vol}$  relative to spheroids at later time with more invasive strands (Fig. 2C). For these spheroids at later times, cells within these peripheral strands exhibited increased  $\Phi_{shear}$  relative to the interior. Although this framework does not require the reference triangles to be the same, and any experimental frames can be used as the reference, special caution should still be taken when choosing appropriate reference frames, especially when dealing with naturally heterogeneous biological systems. Indeed, Y. Han et al. observed that cells within these multicellular spheroids dynamically modulate



their size and stiffness as they shuttle between the interior and peripheral strands [61]. Remarkably, cells within the spheroid core tended to be smaller and stiffer, while cells along invasive strands were appreciably larger and softer. Cells often switched positions between the spheroid core and periphery and could dynamically regulate their volume and stiffness by fluid exchange through gap junctions. Further investigations will help to establish the validity of this approach across different biological systems.

D. Bhaskar et al. utilized topological data analysis to visualize the “shape” of a tissue based on discrete cell positions [69]. Different spatial configurations of cells can be compared by computing the “cost” of rearranging topological features (i.e., persistence homology). Briefly, the spatial connectivity between cell positions is now sampled across varying length scales, generating a topological signature (“barcode”) that emphasizes features that are present across multiple length scales. For pairwise connected components (i.e., dimension 0 homology), this analysis will be skewed by population sizes, making it challenging to compare biological specimens with different numbers of cells. Instead, Bhaskar et al. considered how nuclei can be linked as connected loops around an empty area (i.e., dimension 1 homology), which is less sensitive to population size and also samples larger scale spatial structure. This unsupervised machine learning approach correctly classified experimental data of cell positions in individual, compact clusters, or branching phases (Fig. 2D). Further, this approach could classify distinct phases and identify phase transitions for simulated self-propelled particles with varying motility and adhesion strength. The success of this approach can be explained by mapping discrete data points to a continuous shape (i.e., manifold), which remains highly effective even with relatively sparse sampling, as well as variability in the position of data points. Indeed, different phases could be successfully distinguished even when 80% of the cells were randomly removed. Ongoing research is extending this approach to multiple cell types.

Order parameters represent a powerful approach to understand nonliving physical systems, particularly in soft matter [73]. From a reductionist perspective, it is appealing to think that these approaches could also describe collective migration [67, 71], although these are living systems that are far from thermodynamic equilibrium. Indeed, groups of cancer cells are likely to be quite heterogeneous and in smaller numbers (than in soft matter systems), and the nature of biological “noise” remains poorly understood. For instance, a given population of cancer cells may be comprised of distinct subpopulations with “epithelial” or “mesenchymal” states, associated with distinct motility and adhesion phenotypes [95]. Thus, some care is warranted when using order parameters that average biological behaviors across populations and time. An intriguing possibility is that unsupervised machine learning could be used to classify spatiotemporal patterns of cell migration and infer new order parameters [96]. Although so-called deep learning is computationally expensive and typically requires extensive training data, constraining convolutional neural networks with some physical principles (e.g., physics-informed machine learning [97]) could be highly effective for smaller experimental datasets.

## 4 Metabolic Heterogeneity and Mechanobiological Phenotype

Tumor cells reprogram their metabolic activity in order to sustain proliferation and invasion in dysregulated microenvironments, an emerging hallmark of cancer [98]. Indeed, it has been hypothesized that cancer cells may optimize their metabolic activity to “go or grow,” depending on local microenvironmental conditions [99]. Ordinarily, when ample oxygen is available, normal cells utilize mitochondrial oxidative phosphorylation and glycolysis in the cytoplasm to produce chemical energy in the form of ATP (Fig. 3A). Oxidative phosphorylation converts glucose to glycolysis intermediate products to pyruvate, which is oxidized in the mitochondria under aerobic conditions to produce 36 ATP (per glucose molecule) (Fig. 3A, i). In comparison, glycolysis occurs under anaerobic conditions to produce lactate and 2 ATP (per glucose molecule) (Fig. 3A, ii). There exists a metabolic trade-off whereby oxidative phosphorylation results in higher yield of ATP per glucose molecule with slower kinetics, while glycolysis results in lower yield of ATP per glucose molecule with considerably faster kinetics. Cancer cells often encounter hypoxic conditions and may activate glycolysis via hypoxia-inducible factor 1 $\alpha$  (HIF-1 $\alpha$ ). This induces downstream transcription of glycolytic enzymes like hexokinase and lactate dehydrogenase [100], as well as enhanced expression of GLUT glucose transporters (Fig. 3A). Indeed, cancer cells benefit from using glycolysis to fulfil their metabolic requirements even when abundant oxygen is available. In particular, abundant ATP is advantageous for the near-continuous cytoskeletal reorganization associated with directed cell migration [101]. Furthermore, enhanced lactate excretion via glycolysis by cancer cells acidifies the extracellular space (Fig. 3A, ii), which has been linked to the production of matrix metalloproteinases that facilitate migration through the ECM [102]. Moreover, uncontrolled proliferation also requires glycolytic intermediates necessary for synthesis of nucleic acids, proteins, and lipids, as well as lactate which crucially maintains the NAD<sup>+</sup>/NADH redox balance [103]. Cell metabolism, morphology, and migration are intimately linked, and thus targeting cell metabolism may present a novel strategy to inhibit cellular energy production fueling collective cancer invasion.

J.S. Park et al. investigated how the metabolism of individual human bronchial epithelial cells was modulated by soft or stiff planar substrates [104]. Morphologically, cells on stiff substrates exhibited larger footprints with extensive actomyosin stress fibers, while cells on soft substrates had smaller footprints with weak contractility. Consequently, cells on soft substrates showed reduced expression of all phosphofructokinase (PFK) enzymes, which catalyze a rate-limiting step of glycolysis by phosphorylating fructose 6-phosphate and thereby determine the overall glycolytic rate (Fig. 3B, i). Loss of the PFK isoform PFKP on soft substrates could be attributed to degradation by the proteasome, specifically by the E3 ubiquitin ligase TRIM21. Indeed, TRIM21 associates with stress fibers and remains inactive when bound, thus maintaining PFKP activity. Remarkably, PFKP expression is elevated in patients with lung cancer, which could explain



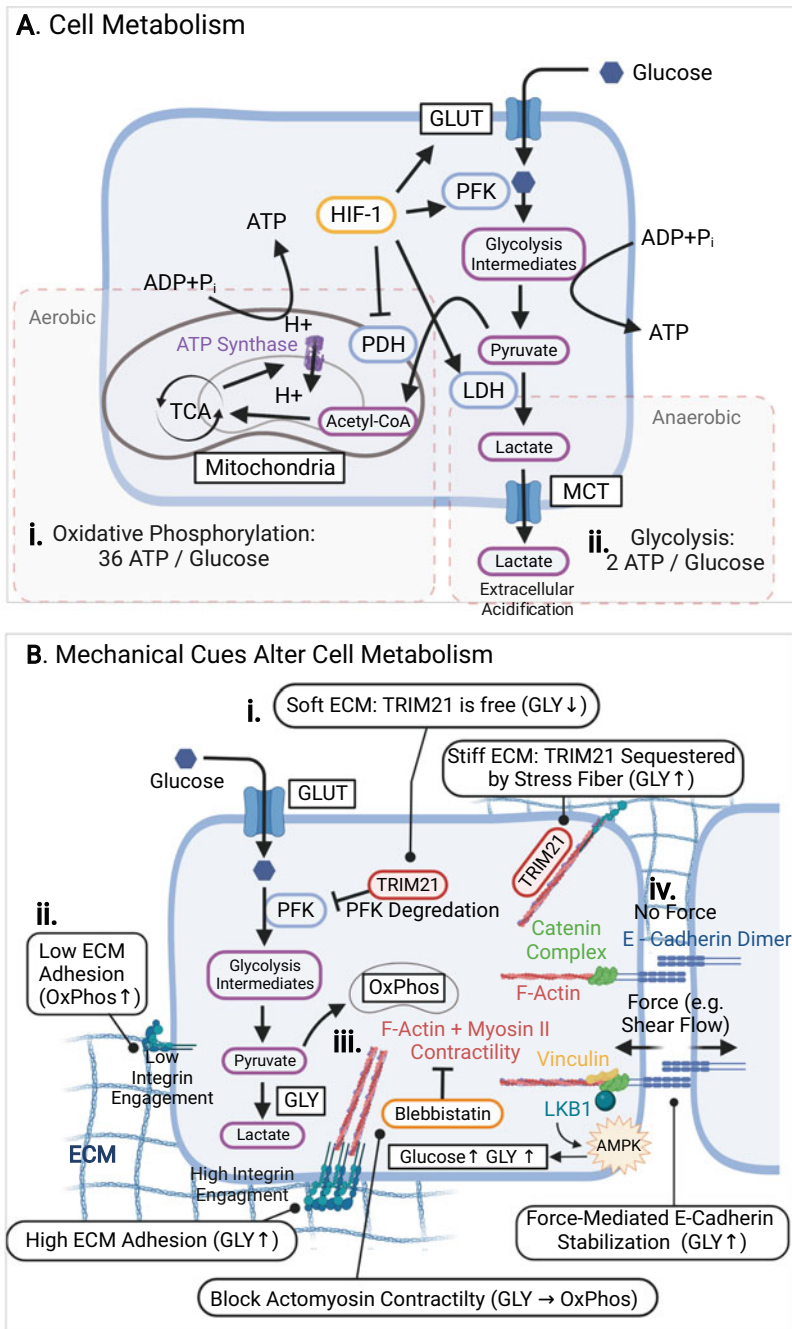


**Fig. 3** (A) Cell metabolism converts glucose to ATP via oxidative phosphorylation (i) or glycolysis (ii), depending on oxygen availability. (B) Mechanical cues alter cell metabolism via substrate stiffness and TRIM 21 (i), weak cell-matrix adhesion (ii), strong cell-matrix adhesion with actomyosin contractility (iii), or force-mediated E-cadherin stabilization (iv). Created with Biorender.com

why tumors exhibit abnormally high levels of glycolysis. Genetic manipulation of these bronchial epithelial cells with a KRAS mutation resulted in consistently high PFK levels, which became insensitive to substrate stiffness. It should be noted that metabolic activity in breast cancer cell lines exhibit varying sensitivity when cultured over planar collagen hydrogels of varying density, thus modulating cytoskeletal activity (Fig. 3B, ii–iii) [105]. Shear forces acting on cell-cell junctions can also increase glucose uptake, driving increased ATP production and glycolysis through AMPK activity (Fig. 3B, iv) [106].

S.J. Decamp et al. showed that epithelial monolayers of canine kidney cells (e.g., MDCK II) exhibit spatially varying metabolic activity at collective fronts moving to occupy empty areas (Fig. 4A) [107]. Indeed, collectively migrating cells at the front exhibited higher traction forces, elongated morphologies, and faster migration compared to cells towards the rear with small aspect ratios and low tractions. Moreover, cells at the collective front also display decreased  $\text{NAD}^+/\text{NADH}$  ratio, reduced NADH lifetime, and increased glucose uptake, which suggests a shift towards glycolysis. Interestingly, cells at the rear also displayed a decrease in NADH lifetime and enhanced glucose uptake, indicating a shift towards glycolysis. However, these rearward cells showed an elevated cytoplasmic  $\text{NAD}^+/\text{NADH}$  ratio, which differs from cells at the collective front. This long-distance signaling could be mediated through mechanical deformation of the compliant substrate, priming rearward cells for increased proliferation and migration. It should be noted that cell migration and proliferation into empty regions on top of planar substrates are relatively unimpeded and could differ significantly from metabolic behaviors in 3D extracellular matrix.

Reinhart-King's group utilized a ratiometric fluorescent reporter of ATP:ADP ratio (PercevalHR) to elucidate how cellular energetics are regulated during individual and collective migration in 3D collagen matrix. First, highly metastatic breast adenocarcinoma cells (MDA-MB-231) expressing the PercevalHR construct invaded individually through narrow bifurcating channels in collagen I [110]. Cells exhibited greater glucose uptake and ATP:ADP ratio as they migrated through narrower channels, indicating that increased cell deformation was associated with higher energetic cost. Indeed, pharmacological treatment to perturb cytoskeletal stiffness and cell deformability was sufficient to modulate cell energetic state. Further, increasing matrix stiffness also increased energy costs, since cells required enhanced contractility to deform the matrix and enter confined spaces. When cells were presented with a choice of bifurcating into a wide or narrow channel, their decision-making was shown to be biased by the relative energetic cost of these two choices. Thus, cells were more likely to choose the narrower channel when the cells themselves or the matrix were more compliant.

In a complementary study, this lab also investigated how these same cells invaded collectively from multicellular spheroids, revealing that leader and follower cells invading in 3D matrix can dynamically switch their roles (Fig. 4B) [108] (Fig. 4B, i). Collective invasion was also impeded by denser 3D matrix with greater mechanical resistance, in qualitative agreement with the previous study using individual cells [110]. Nevertheless, collective invasion was associated with cooperative behaviors

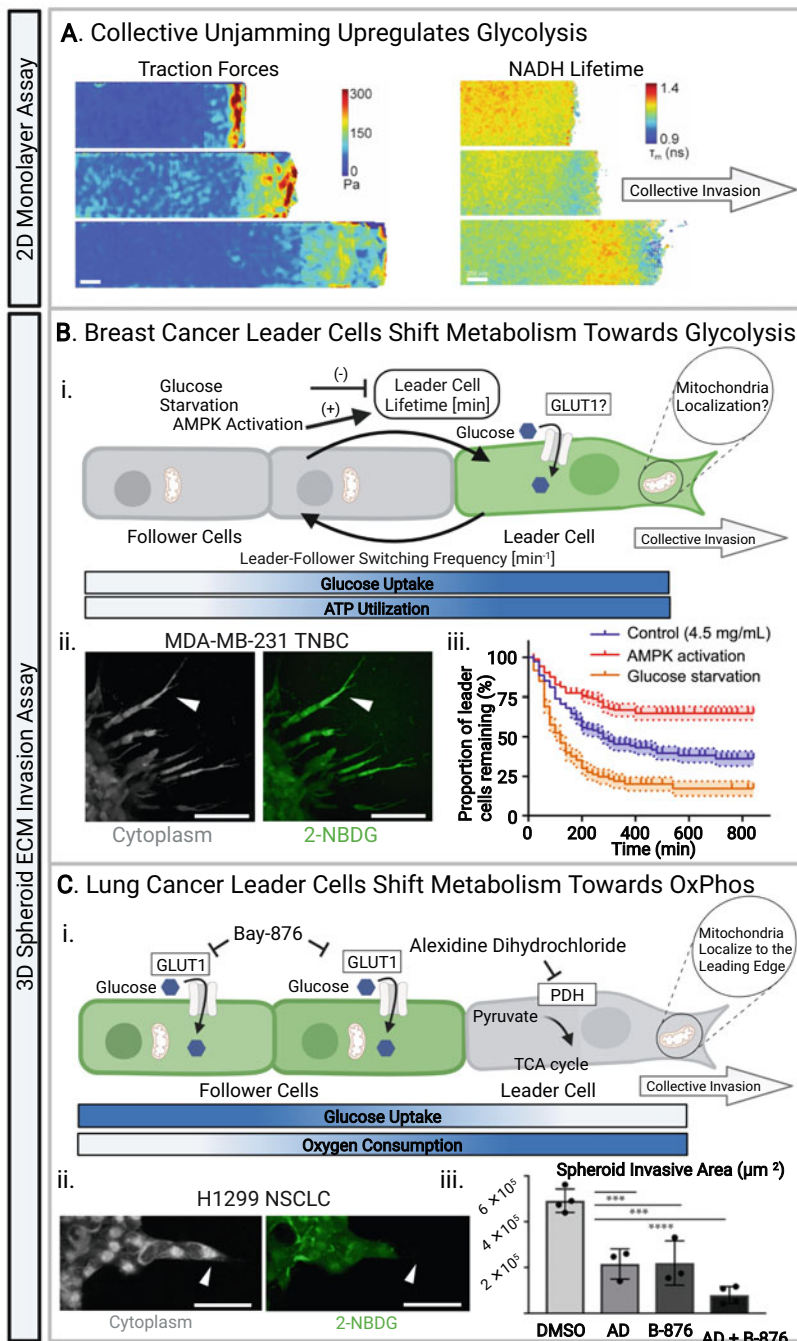


**Fig. 4** (A) Collective unjamming of epithelial monolayers reveals increase of traction forces and metabolic activity near invasion front. Reproduced from [107] under Creative Commons CC-BY. (B) Breast cancer leader cells exhibit increased glycolysis but switch places regularly with followers. Reproduced from [108]. (C) Lung cancer leader cells exhibit increased oxidative phosphorylation, and invasion can be suppressed by targeting both pyruvate dehydrogenase and glucose uptake. Reproduced from [109] under Creative Commons CC-BY

where leaders exhibited higher glucose uptake and energy consumption relative to followers. Once a leader cell exhausted its available ATP, it would switch with a follower, and this switching frequency increased in denser matrix. Moreover, expression of a fluorescent cell cycle reporter (e.g., CycleTrak) revealed that leader and follower cells exhibited behaviors consistent with the “grow-or-go” hypothesis [99], whereby leader cells were less proliferative than follower cells, which was also observed using breast tumor organoids (e.g., MMTV-PyMT mice).

In contrast, Commander et al. also observed metabolic heterogeneity in leader and follower cells invading from a different spheroid model but concluded that followers exhibit higher glucose uptake than leaders (Fig. 4C ii) [109]. Briefly, a non-small cell lung cancer line (H1299) was sorted for leaders and followers by photoswitching of a fluorescent label, followed by FACS [111]. Interestingly, followers maintained distinct morphological and invasive phenotypes for several passages before reverting to the parental phenotype, while leader cells retained their phenotype indefinitely. Metabolic analysis based on extracellular flux (e.g., Seahorse Bioscience) revealed that follower cells typically exhibited increased glucose uptake, glycolysis, and decreased oxidative phosphorylation (Fig. 4C i). Instead, leader cells exhibited mitochondrial respiration and a pyruvate dehydrogenase dependency, which could be therapeutically targeted with alexidine dihydrochloride (Fig. 4C iii). A combination drug treatment against both pyruvate dehydrogenase and glucose uptake was effective at suppressing leader cell invasion and follower cell proliferation, respectively. It should be noted that this study utilized a different cell line (H1299) than Reinhart-King’s investigations (MDA-MB-231), with varying degrees of phenotypic plasticity. Moreover, subtle differences in spheroid formation and matrix embedding procedures could result in very different phenotypic outcomes [112].

An advantage of using engineered biomaterials is that cancer cells encounter highly consistent and homogeneous mechanical cues, so that the effect of stiffness or other matrix properties on metabolic activity can be systematically elucidated. However, it should be noted that cancer cells *in vivo* may exhibit very different metabolic states as they migrate through varying mechanical and biochemical microenvironments. Further, these cancer cells may interact dynamically with other stromal and immune cells, which could further act to enhance or suppress tumor progression. Thus, additional work is needed to understand how phenotypic plasticity of metabolic and migratory phenotypes is regulated in the context of mechanical cues from the surrounding microenvironment.

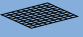
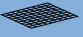
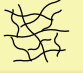
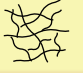


## 5 The Extracellular Matrix and Engineered Biomaterials

The extracellular matrix (ECM) is a complex structural network of proteins, glycoproteins, proteoglycans, and polysaccharides that mechanically supports tissues while presenting instructive and permissive cues [113]. ECM is continually being remodeled by a combination of protein deposition, posttranslational chemical mod-

ifications, proteolytic degradation, as well as mechanically driven reorganization [54]. These myriad processes are tightly regulated in normal tissues to maintain homeostasis but become increasingly dysregulated during aging, fibrosis, and cancer progression [114]. Moreover, alterations in ECM structure, mechanics, and composition may regulate dormancy or metastatic colonization at distant tissue sites (i.e., the premetastatic niche) [115]. We briefly review relevant features of the ECM in the context of collective migration and refer interested readers to more comprehensive reviews elsewhere [54, 113, 114].

The basement membrane is a sheetlike structure that encloses epithelial tissues, comprised of laminin and collagen IV, linked through bridging proteins such as nidogen and perlecan (Fig. 5A, i) [116]. Indeed, laminin is more prominently displayed on the inner (epithelial-facing) side and instructs epithelial phenotype, while collagen IV may be more localized on the outer (stromal-facing) side to provide more structural support [117]. Altogether, these ECM proteins are assembled with a netlike architecture that is relatively thin (hundreds of nanometers) with small pores (tens to hundreds of nanometers) (Fig. 5A, ii). Since the basement membrane is chemically cross-linked, high density, with very low porosity (Fig. 5A, iii–v), it is not permissive for epithelial cell migration [50]. Thus, enzymatic or mechanical remodeling of the basement membrane is crucial for carcinoma cells to invade into the surrounding stroma [118]. Historically, reconstituted basement membrane (e.g., Matrigel) has been widely used as a compliant biomaterial that mimics the protein composition of native basement membrane [119]. However, it should be noted that Matrigel is not of human origin and is derived from mouse sarcoma cells (e.g., Engelbreth-Holm-Swarm) which exhibits appreciable batch-to-batch variability [120].

The interstitial matrix is a three-dimensional fibrous network comprised of fibrillar collagens (I, III, V), fibronectin, elastin, proteoglycans, glycosaminoglycans, and

	i. Composition	ii. Topography	iii. Crosslinking	iv. Density	v. Porosity	vi. Stiffness	vii. Viscosity
<b>A. Basement Membrane:</b> Laminin, Collagen IV, Nidogen, Perlecan, ...			Chemical	High	Very Low	High?	High?
<b>B. Interstitial Matrix:</b> Fibrillar Collagens (I, III, V) Fibronectin, Elastin, PG...			Physical	Moderate	Moderate	Low	Low
<b>C. Tumor / Fibrotic Matrix:</b> Fibrillar Collagens (I, III, V) ↑ Fibronectin ↑, Elastin ↑ + HA, PG, Matrisome...			Chemical	High	High	High	High

**Fig. 5** Comparison of basement membrane (A), interstitial matrix (B), and tumor/fibrotic matrix (C) based on composition (i), topography (ii), cross-linking (iii), density (iv), porosity (v), stiffness (vi), and viscosity (vii). Abbreviations: HA, hyaluronic acid; PG, proteoglycans

others (Fig. 5B, i) [121]. In particular, collagen I is organized as randomly oriented fibers that are physically entangled at moderate density and porosity (Fig. 5B, ii–v) [122]. Further, Keely and coworkers observed that these fibers exhibited a wavy (“crimped”) conformation [123], which has recently been reported to impede cell polarization [124] and enhance dormancy [125]. The interstitial matrix is occupied by stromal cells (e.g., fibroblasts), which play a crucial role in depositing and organizing ECM proteins [126]. It should be noted that the interstitial matrix can be spatially and mechanically nonuniform due to the presence of cell-sized spaces surrounded by denser matrix. Nevertheless, the typical pore structure of healthy interstitial matrix impedes cell migration without significant remodeling [122]. A biomimetic model for these fibrous architectures is to reconstitute collagen I from rat tail or bovine skin, which can be tuned based on collagen concentration, polymerization temperature, and pH (see reviews in [127, 128]).

Pathological states such as fibrosis and tumor progression are associated with aberrant deposition of collagens, fibronectin, elastin, laminin, hyaluronic acid, proteoglycans (e.g., versican, syndecan, glypican, etc.), and other matrisome proteins (e.g., tenascin C, periostin, osteopontin, SPARC, thrombospondin) (Fig. 5C, i) [114]. Structurally, tumor-associated collagen I is increasingly dense, straight, and aligned, with cell-sized tracks leading into the stroma (Fig. 5C, ii–v) [123, 129, 130]. Indeed, collagen I can be further strengthened by chemical cross-linking by lysyl oxidase and transglutaminase (Fig. 5C, iii) [53], which has been recently linked to the inflammatory activity of tumor-associated macrophages [131].

The stiffness of tumor associated ECM is dramatically higher than healthy ECM, an indicator of aberrant ECM composition and architecture (Fig. 5B, vi; C, vi) [114]. For any solid material, these mechanical properties can be quantified based on a reversible deformation in response to an applied stress (i.e., elasticity), which is typically linear for small deformations (i.e., strains) [132]. Interestingly, fibrous materials often exhibit a nonlinear elasticity, so that they can stiffen at increasing strain, attributed to the increasing difficulty of reorienting fibers, or the cost of straightening and stretching fibers [133]. For sufficiently large deformations, this structural reorientation may be permanent (i.e., plastic) and will not be reversible after the stress is removed. Finally, it should be noted that biomaterials incorporate significant (viscous) fluid, resulting in a time-dependent mechanical response as some energy is dissipated via viscoelastic or poroelastic mechanisms [134]. An unresolved question is the stiffness and viscosity of the basement membrane, which varies across tissues and also is challenging to probe due to its small thickness and tight integration with surrounding tissue (Fig. 5A, vi–vii). Interestingly, H. Li et al. recently reported that cell-deposited basement membranes exhibit nonlinear strain stiffening, which has not been observed using other mechanical measurements that operate in the linear regime [135].

Synthetic hydrogels can be prepared with comparable stiffness as ECM using flexible polymers with tunable cross-links and ligand density, resulting in spatially uniform materials with nanoscale pores [12, 13]. For example, polyethylene glycol and polyacrylamide have been widely explored to elucidate how cancer cells respond *in vitro* to linear elastic material properties (see review in [21]). In particu-



lar, polyethylene glycol permits systematic control of ligand density, cross-linking, and degradability to investigate cancer cell invasion [136–139]. Alternatively, alginate is a seaweed-derived polysaccharide where viscoelasticity (e.g., stress relaxation) can be tuned using reversible ionic cross-links or by molecular weight [140]. Furthermore, synthetic hydrogels with spatially anisotropic architectures are able to mimic ECM cues, such as the aligned topographical features of collagen fibers [141]. Such “designer biomaterials” may permit improved control over distinct mechanical and biochemical features of the cell microenvironment. For example, aligned ECM cues can be patterned within a homogeneous matrix using magnetic nanoparticle self-assembly, allowing for hydrogels with modulated alignment cues while maintaining comparable elastic moduli and ligand densities [142, 143].

## 6 Precision Measurement of Cell and ECM Mechanics

Invading cancer cells both sense and respond to the structure and composition of the ECM, a bidirectional interaction known as dynamic reciprocity [144]. Fluorescence imaging of cell morphology is widely used to elucidate how cells are shaped by the local ECM properties [145]. However, visualizing how cells act on the surrounding ECM remains challenging, particularly in 3D geometries [146]. Seminal work by Legant et al. visualized how fibroblasts applied mechanical tractions within a synthetic 3D hydrogel (e.g., polyethylene glycol diacrylate, PEGDA) by tracking the motion of microscale tracer particles relative to an undeformed reference state (e.g., traction force microscopy) [147]. It should be noted that PEGDA is a purely elastic material, with a well-established constitutive equation that permits the cell-generated stresses to be quantitatively extracted from the matrix strain field. Nevertheless, naturally derived biomaterials exhibit a more complex rheological response that is nonlinear as well as viscoelastic, and can be irreversibly remodeled by cell secreted factors [148].

Both J. Steinwachs et al. and M. Hall et al. measured tractions exerted by single breast cancer cells invading within reconstituted collagen I matrix labeled with fluorescent microparticles [149, 150]. These breast cancer cells (e.g., MDA-MB-231) mechanically interact with discrete collagen fibers, which become aligned along the cell axis to locally stiffen the matrix. This nonlinear strain-stiffening response suggests that cells within these fibrillar materials can mechanically interact over longer distances than in more homogeneous materials that exhibit a linear elastic response. In order to compute cell-generated stresses, both groups formulated constitutive equations optimized for random fiber networks, validated using bulk rheology of cell-free collagen I matrix. Interestingly, recent work by van Oosten et al. shows that these strain-stiffening fiber networks switch to strain-*softening* behavior in the presence of cell-sized inclusions, reminiscent of the architecture and mechanics of living tissues [151]. Thus, nonuniformity of the ECM at multiple length scales is likely to impact cellular mechanobiology.

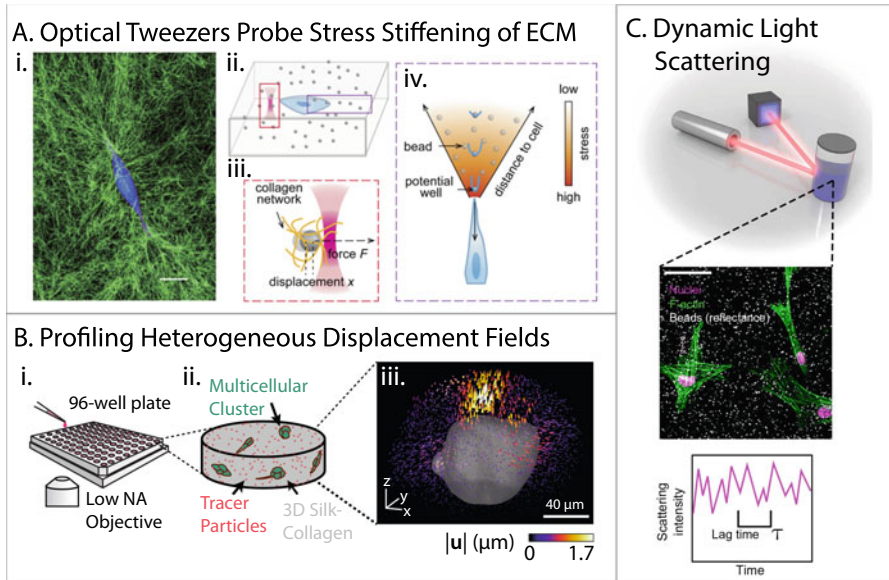


**Fig. 6** (A) Direct measurement of ECM stress stiffening using optical tweezers. (i) MDA-MB-231 cell (blue) in a 3D collagen network (green). (Scale bar, 10  $\mu\text{m}$ .) (ii)–(iv) Schematics of the force-displacement measurement using optical tweezers, and the relation between matrix stiffening (blue potential wells) and the cell-generated stress field along the cell axis. Reproduced from [152]. (B) High-throughput confocal imaging on a 96-well plate (i), visualizing multicellular clusters (green) and tracer particles (red) embedded in 3D silk collagen matrix (ii). Representative displacement field exhibits spatially nonuniform regions of local outward (yellow) and inward (purple) displacement (iii). Reproduced from [153]. (C) Dynamic light scattering based on cells encapsulated within 3D collagen/Matrigel, readout via fluctuations in scattering intensity over varying lag times. Reproduced from [154] under Creative Commons CC-BY

Y. Han et al. sought to directly measure matrix mechanical properties in the neighborhood of single cells using optical tweezers [152] (Fig. 6A, i, ii). In these experiments, microparticles entangled within a collagen I matrix were perturbed under a controlled displacement  $x$ , and the resulting force  $F$  was optically measured, which is a readout of the local matrix stiffness (Fig. 6A, iii). This approach mapped the spatial variation in stiffness to a nonlinear stress profile Fig. 6A, iv). Notably, matrix stiffness was strongly elevated near cancer cells (e.g., MDA-MB-231) as the fibrillar matrix was plastically deformed into more aligned architectures, which was also observed for reconstituted basement membrane and fibrin. Although this method is a very sensitive and localized measurement of matrix rheology, it is relatively time and labor intensive since microparticles are probed one at a time.

Multicellular clusters in 3D matrix may coordinate their tractions to facilitate collective migration, which adds additional complexity to be explored. S. Leggett et al. investigated how mammary epithelial acini (e.g., MCF-10A) transitioned towards invasion after controlled induction of EMT via the master regulator Snail [153]. Cells were embedded within composite silk-collagen matrix [155] in a 96-



well plate, enabling increased experimental throughput to evaluate drug response (Fig. 6B). Using optimized topology-based particle tracking, localized patterns of protrusive and contractile matrix displacement could be resolved with submicron resolution [156]. Notably, epithelial clusters were usually compact and exhibited several regions of local protrusion or contraction. Induction of a transitory EMT state results in clusters with extended protrusions with more regions of local contraction, indicative of outgrowth and invasion. Finally, fully mesenchymal states were associated with spindle-like morphologies with only a few localized contractile regions and minimal protrusions. These results show that collective migration and EMT are associated with spatially nonuniform patterns of matrix displacement, which can be used as a mechanophenotypic “signature” of cell state. This platform is scalable for a broader range of cell types and biomaterials, which is particularly relevant for clinical translation using patient-derived cells and drug screening.

In order to longitudinally probe matrix viscoelasticity over a wide frequency range, B. Krajina et al. utilized dynamic light scattering to measure fluctuations of dilute microparticles within a biomaterial (Fig. 6C) [154]. Based on correlations in scattering intensity, an ensemble averaged mean square displacement can be extracted and converted to a frequency-dependent shear modulus using the generalized Stokes-Einstein relation [157]. In principle, this approach could resolve both thermally driven motion as well as actively driven motion due to cell-generated forces. For instance, mammary epithelial spheroids (e.g., MCF-10A) embedded in composites of collagen I and Matrigel drove considerable changes in shear modulus over 6 days. With the addition of TGF- $\beta$  to drive invasion and EMT, there was an effective increase in matrix stiffness at high frequencies and matrix fluidization at low frequencies, which was explained based on elevated matrix degradation as well as cellular contractility. This dynamic light-scattering approach promises to provide new insights into how biomaterials are altered over extended durations in response to cellular activity, although it will likely require complementary measurements with conventional fluorescence microscopy to map back to cell morphology and migratory behaviors.

Finally, Adie and coworkers utilized optical coherence tomography for label-free imaging of cells and collagen fibers [158]. As a case study, mammary epithelial spheroids (e.g., MCF-10A) were characterized with or without co-culture with adipose stem cells [159]. Notably, mammary epithelial spheroids only remained relatively localized with limited matrix deformation. In comparison, the addition of adipose stem cells from obese mice resulted in extensive collective invasion as well as matrix remodeling, which could be rescued by pharmacological inhibition of matrix degradation or Rho kinase activity. This technique has great potential since it can be scaled to larger imaging volumes in highly scattering media, directly imaging biomaterial deformations with minimal phototoxicity.

Emerging technologies to visualize bidirectional interactions between cancer cells and 3D matrix will enable new insights into collective invasion and drug response. It should be noted that cell mechanics are challenging to measure deep inside 3D matrix, since most characterization techniques require direct contact with the cell (e.g., micropipette aspiration, atomic force microscopy, etc.). Nevertheless,

techniques such as particle tracking microrheology or optical tweezers can directly probe intracellular rheology in 3D, as we have recently reviewed elsewhere [160]. We also envision future explorations that utilize patient-derived organoids, as well as stromal and immune cells. Thus far, these early proof of concepts have investigated cell-generated tractions in relatively simplified biomaterials such as collagen I or reconstituted basement membrane (e.g., Matrigel). As the composition and architecture of biomaterials increase in complexity to mimic the *in vivo* environment, an improved fundamental understanding of these material properties will be needed to understand how cancer cells are affected. Lastly, these biophysical measurements all require specialized equipment and training for optimal results, and further work is needed to translate these techniques into conventional biomedical settings.

## 7 Epithelial-Mesenchymal Plasticity and Collective Cell Migration

Classically, EMT has been understood as a phenotypic switch in which adherent cells lose epithelial biomarkers (e.g., E-cadherin) and gain mesenchymal biomarkers (e.g., vimentin) in order to disseminate individually for embryonic development and wound healing [161]. EMT is often observed at tumor invasion fronts, mediated by tumor-stromal interactions and the interstitial matrix [162]. More recently, epithelial-mesenchymal plasticity (EMP) has been proposed to represent a broader spectrum of intermediate or hybrid cell states that may exhibit some mixture of epithelial and mesenchymal features [5]. Functionally, EMP is associated with a decrease in differentiated features (e.g., apicobasal polarity, strong cell-cell adhesions), resulting in reorganization of the cytoskeleton and cell-matrix adhesions towards front-back polarity and invasion across the basement membrane, which may or may not be captured by certain biomarkers or classical EMT transcription factors (e.g., Snail, Twist, ZEB, etc.) [5]. These morphological phenotypes often exhibit appreciable variability at the single-cell level, even for relatively controlled induction of transcription factors [163]. Nevertheless, the mechanistic role of EMT in human tumor metastasis remains unresolved, partially due to the difficulty of measuring a rare and dynamic process at the single-cell level (within patients) [164]. For instance, if EMT occurs transiently as tumor cells disseminate from the primary site and they revert back to an epithelial state (MET) at a secondary metastatic site, measurements of the primary and metastatic site will most likely yield epithelial cells [165]. Several recent papers have combined live cell imaging with deep molecular profiling in order to better elucidate the potential role of EMP.

I. Pastushenko et al. utilized fluorescence-activated cell sorting (FACS) and single-cell RNA-seq to map an EMT landscape in genetically engineered mouse models of skin squamous cell carcinoma (KRas<sup>LSL-G12D</sup>p53<sup>fl/fl</sup>) and breast cancer (MMTV-PyMT) that overexpressed fluorescent proteins [166, 167]. They defined an epithelial state based on high expression of keratin 14 (K14) with

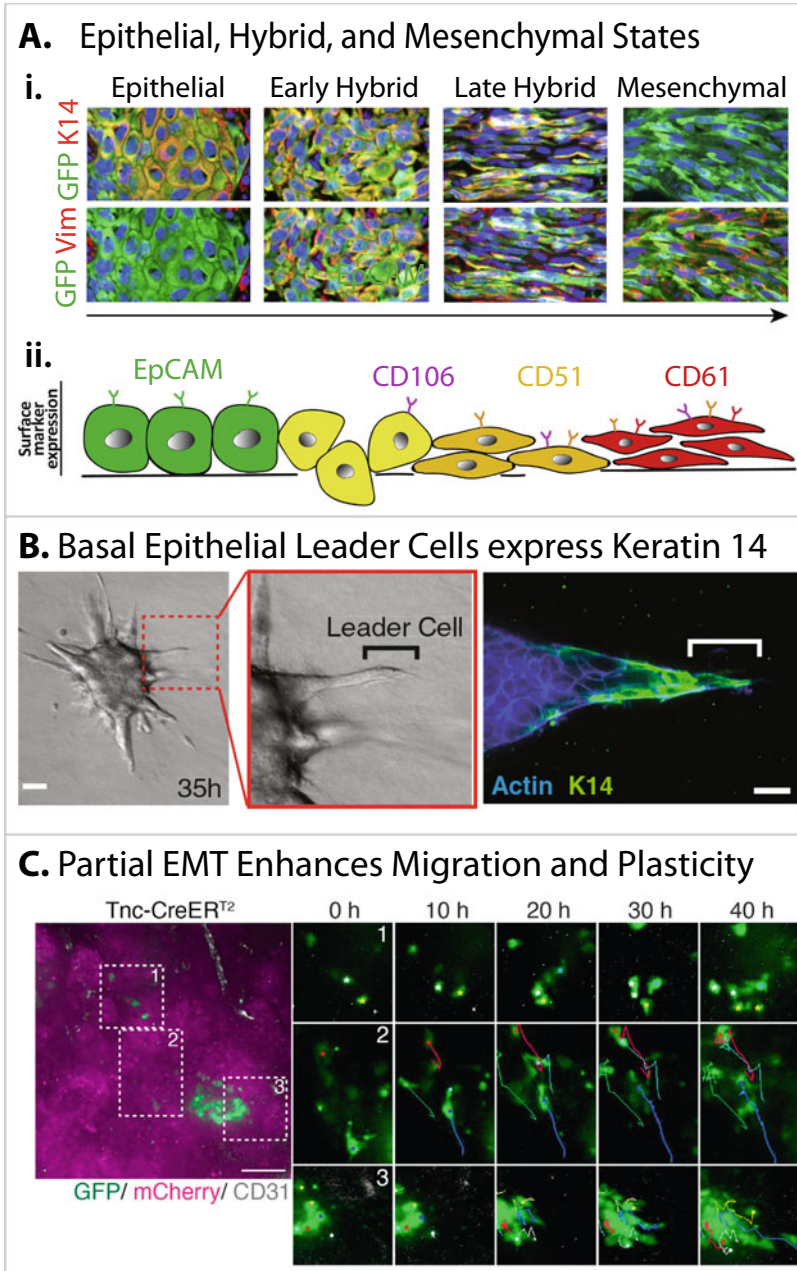


**Fig. 7** (A) Immunofluorescence staining of keratin 14 (K14) and vimentin (Vim) (red) expression in tumor cells (GFP) across epithelial, early/late hybrid, and mesenchymal states (i), corresponding to changes in EpCAM, CD106/Vcam1, CD51/Itgav, and CD61/Itgb3 (ii). Reproduced from [166] with permission from Elsevier. (B) Leader cells in MMTV-PyMT breast tumor organoids exhibit a basal epithelial phenotype with high keratin 14 expression. Reproduced from [168] with permission from Elsevier. (C) Lineage tracing of partial EMT via Tenascin C gene expression reveals enhanced migration and plasticity relative to late EMT. Reproduced from [169] under Creative Commons CC-BY

no vimentin expression, which exhibited a compact cell morphology and (high E-cadherin expression) (Fig. 7A, i). Further, hybrid states were observed which co-expressed K14 and vimentin with partially elongated morphology (and low E-cadherin expression), associated with collective migration. Finally, mesenchymal states expressed vimentin with no K14 (or E-cadherin) and exhibited a fully elongated morphology. The epithelial state also expressed high EpCAM, which was absent in hybrid and mesenchymal states (Fig. 7A, ii). Instead, an “early hybrid” state was defined based on the absence of CD106 (Vcam1), CD51 (Itgav), and CD61 (Itgb3), whereas a “hybrid state” was associated with CD106 expression only. Next, a “late hybrid” state was associated with expression of CD51 and/or CD106. A mesenchymal state was associated with co-expression of CD51 and CD61 or CD51, CD106, and CD61. Functionally, epithelial cells proliferated faster than cells in hybrid or mesenchymal states. However, hybrid or mesenchymal cells exhibited much higher tumor initiating potential than epithelial cells when implanted at successively smaller dilutions and displayed increased invasion. Nevertheless, hybrid cells exhibited the most plasticity to transition to other states, as well as the greatest metastatic potential. These hybrid or mesenchymal states were also promoted by the local microenvironment, including blood and lymphatic vessels as well as macrophages.

Instead, K.J. Cheung et al. demonstrated that epithelial cells expressing K14 from genetically engineered mouse models of breast cancer (MMTV-PyMT) act as leader cells for collective migration (Fig. 7B) [168]. Mouse tumors were isolated and digested into fragments, which were then embedded in 3D collagen I matrix. Leader cells were associated with basal markers (e.g., p63, P-cadherin, and keratin 5) but did not express common EMT biomarkers (e.g., vimentin, Snail, Twist). Further, these leader cells maintained E-cadherin expression and were mechanically connected to their followers, which were K14 negative. Indeed, K14-positive leader cells were preferentially localized at the tumor periphery and in lung metastases in mouse models, as well as in organoids and histology slides from human patients. Interestingly, K14-positive cells were present but did not function as leaders when these organoids were cultured in Matrigel. Re-transplantation of these organoids from Matrigel to collagen I rescued the K14-positive leader cell phenotype and aggressive invasion.

F. Löönd et al. developed a dual recombinase fluorescence reporter construct to lineage trace breast tumor cells that had undergone an EMT (reversible or irreversible) [169]. Briefly, a first reporter labeled epithelial cells with mCherry but irreversibly switched to GFP expression when early EMT (e.g., Tenascin C, Tnc) was induced with tamoxifen treatment. A second reporter similarly labeled epithelial cells but irreversibly switched to GFP expression during late EMT (e.g., N-cadherin, Cdh2), also under tamoxifen treatment. Live cell imaging of primary tumor slices revealed that some early (partial) EMT cells exhibited an elongated morphology as individuals with directional migration (Fig. 7C, 1,2). Other early (partial) EMT cells associated with multicellular “colonies,” which maintained cell-cell contacts, although cells at the periphery of these colonies were elongated and motile (Fig. 7C, 3). In comparison, late (full) EMT cells were also elongated but

remained localized in perivascular regions near capillaries. Moreover, early (partial) EMT cells invaded collectively and aggressively as leader cells when seeded on collagen I matrix, while late (full) EMT cells invaded individually. Further, early (partial) EMT cells were enriched in lung metastases, while late (full) EMT cells were enriched in response to chemotherapy. Other recent reports corroborate that partial EMT is associated with collective invasion and plasticity [170], as well as enhanced metastatic potential [171].

## 8 Perspective and Future Directions

The statistician G.E.P. Box famously commented that “*all models are wrong; the practical question is how wrong do they have to be to not be useful.*” [172] This aphorism is relevant in the context of cancer biology, where modeling refers to in vitro or in vivo experimental systems that represent key features of patient tumors [173], as well as the physical sciences, where modeling refers to theoretical and computational approaches [174]. In both instances, an unresolved question is how a group of cancer cells with significant (intratumoral) heterogeneity are able to coordinate robust behaviors [2]. As presented here, physical science approaches offer promising tools to elucidate generalized principles of collective invasion, given that cancer has common set of requirements for metastasis despite high intratumoral heterogeneity. We argue that such collective processes are crucial for invasion and metastasis as well as therapy resistance, which are ultimately responsible for most cancer-related fatalities in human patients [175]. Thus, in this chapter, we have considered new biological and engineering approaches that have the potential for useful insights, given the ethical and practical limits on direct experimental access to human patient tumors.

Modern single-cell omics enable unprecedented insights into molecular signaling pathways that regulate cellular behavior [8]. However, such deep phenotyping typically requires the removal and destruction of cells at an endpoint, making it difficult for dynamic measurements. In comparison, live cell imaging and fluorescent reporters can visualize how cells migrate and proliferate with unprecedented spatiotemporal resolution [10, 11]. Typically, these imaging techniques are limited to a few fluorescence channels, so that only a few signaling pathways or cellular features can be monitored. This mismatch makes it challenging to elucidate how myriad molecular signaling pathways are integrated into mechanobiological phenotypes such as cell migration and proliferation. The connectivity map approach has proven quite powerful to computationally link gene expression profiles to drug response [176]. An intriguing possibility is to further couple such molecular analyses with cellular-scale computational models that account for the mechanobiology of the cytoskeleton, cell-matrix adhesions, etc. [177] This could make testable predictions about therapeutic regimens that could inhibit invasion or proliferation. Given interpatient heterogeneity and the challenges of drug development, even predicting which treatments may *not* work would be useful to inform clinical practice.

Aberrant metabolism represents a promising target to inhibit both collective migration and uncontrolled proliferation. Leader cells represent an intriguing target, either via inhibition of glycolysis (e.g., 2-deoxyglucose) or oxidative phosphorylation (e.g., metformin). Given the observed phenotypic plasticity and heterogeneity of leader and follower cells, it may be necessary to target both glycolysis and oxidative phosphorylation. It should also be noted that various FDA-approved drugs that inhibit metabolism can in turn mitigate aggressive EMT features of tumors [178]. For example, when activated by excess glucose, the polyol metabolic pathway can induce EMT through autocrine TGF- $\beta$  stimulation [179], which is known to potentiate tumor aggressiveness. The polyol pathway inhibitor epalrestat, used in the treatment of diabetic neuropathy, is under a Phase II clinical trial to evaluate its potential to inhibit triple-negative breast cancer [180]. Thus, an improved fundamental understanding of how metabolism and mechanobiology are mechanistically coupled may inform the design of targeted therapies, likely acting in combination on different hallmarks of cancer.

Although visualizing cell morphology and migration with fluorescence microscopy is relatively straightforward, quantification of cell-cell interactions remains challenging and is often indirectly inferred from qualitative readouts. For instance, physics-inspired analyses based on PIV or order parameters are sufficient to reveal when groups of cells migrate with similar speed and direction [83] but provide limited quantitative information on how these cells interact. One promising approach for analyzing multicellular configurations is to analyze the mechanical cost of rearrangements relative to some idealized reference state [68]. Alternatively, the topological differences between different multicellular architectures can be compared using persistence homology [69]. It would be intriguing to develop a hybrid machine learning approach that accounts for the mechanical cost of cell reorganization but does not assume a reference state. However, it should be noted that tumor cells are intrinsically heterogeneous, and approximating them as identical agents with exactly the same cell-cell and cell-matrix adhesions may not be valid. Establishing meaningful readouts of heterogeneity and cooperative behavior may nevertheless be useful as a therapeutic target (beyond cell viability) that can be perturbed. Moreover, understanding when groups of cells exhibit more homogeneous behaviors may provide insight into how “noise” is regulated by homeostasis in normal epithelial tissues.

Similarly, elucidating reciprocal mechanical interactions between cells and ECM is experimentally difficult [146]. Early groundbreaking work utilized planar 2D substrates with controlled biochemical ligand density and stiffness, which were non-cell-degradable and exhibited a well-defined linear elastic response [21]. Subsequent experiments using 3D biomaterials are based on a similar premise—that cells should exhibit relatively similar behaviors when cultured within (relatively) reproducible and spatially homogeneous mechanical environments [16]. Nevertheless, cells also exhibit the capability to substantially remodel biomaterials, so that the local architecture and rheology may vary considerably at later times. Thus, recent technology development seeks to mechanically probe alterations of ECM [152, 154, 158], although there remain trade-offs in spatial and temporal resolution.



Alternatively, spatially heterogeneous patterns of forces may be sufficient to infer distinct cell states [153]. Thus, we envision that dynamic, stimuli-responsive biomaterials will be increasingly used to reveal dynamic cell responses [181]. Moreover, it should be noted that ECM *in vivo* is spatially *inhomogeneous* in composition and structure, particularly during fibrosis or tumor progression. Highly tunable biomaterials capable of recapitulating desmoplastic ECM architectures in the tumor microenvironment [141] will be needed to understand why current therapies, such as CAR-T immunotherapy, often fail to penetrate immunosuppressive solid tumors [182]. High-resolution mapping of local ECM architecture *in vivo*, combined with a physical understanding of how cells migrate collectively in different homogeneous biomaterials *in vitro*, could also predict how cell might invade inhomogeneous microenvironments *in vivo* [183]. Indeed, robust biomaterial-based models serve as an important first step in elucidating collective invasion mechanisms in a controlled environment relative to *in vivo* models, where mechanisms can be further corroborated.

Finally, tumor cells exhibit not only phenotypic heterogeneity but also phenotypic plasticity, which can be a relatively rare event. Thus, it remains challenging to test the role of epithelial-mesenchymal plasticity in human patients without complete single-cell information at high temporal resolution [5]. Indeed, it is conceivable that tumor cells could adapt their phenotype as they encounter different microregions of the primary tumor and colonize the secondary metastatic site or in response to therapeutic treatments [184]. Recent advances in biofabrication and microfluidics enable compartmentalized engineered tissues, where soluble signaling conditions can be rapidly switched [185]. This capability to rapidly and sharply switch microenvironmental cues is likely to be quite powerful to directly observe how cells respond. Further, improvements in epigenetic profiling will be useful to understand when cells mechanically adapt or retain a “memory” of prior phenotypes [186]. An ongoing translational challenge may be to understand how patient tumor cells individually and collectively adapt to changing microenvironmental conditions via leader cells or EMP and to limit heterogeneity in an evolutionary context [187].

In conclusion, we have considered how the mechanobiology of cell-cell and cell-matrix interactions mediate how tumor cells collectively invade into 3D matrix. We highlight how these coordinated behaviors with leader-follower interactions and epithelial-mesenchymal plasticity represent a caricature of embryonic development, as tumor cells repurpose the associated molecular signaling and biophysical machinery. We also highlight emerging technologies in *ex vivo* measurements of cell migration based on 3D biomaterials with live cell imaging. In combination, these technologies can quantify how groups of cells cooperate mechanically or metabolically with each other and to remodel the surrounding ECM. These exquisitely sensitive measurements of single-cell dynamics will enable new physical models that could be integrated with molecular profiling to predict how patient cells respond to targeted treatments, revealing new fundamental insights and accelerating clinical translation. Ultimately, we envision that the integration of new bioengineering assays with physical modeling represents a highly “useful” representation of human tumors to address unresolved questions of intratumoral and interpatient heterogeneity in cancer progression.

**Acknowledgments** We apologize to authors whose work could not be included due to space constraints. This work was supported by the National Institute of General Medical Sciences (R01GM140108, P20GM109035).

## References

1. Rørth P (2009) *Annu Rev Cell Dev Biol* 25:407
2. Tabassum DP, Polyak K (2015) *Nat Rev Cancer* 15(8):473
3. Friedl P, Locker J, Sahai E, Segall JE (2012) *Nat Cell Biol* 14(8):777
4. Vilchez Mercedes SA, Bocci F, Levine H, Onuchic JN, Jolly MK, Wong PK (2021) *Nat Rev Cancer* 21(9):592
5. Yang J, Antin P, Berx G, Blanpain C, Brabletz T, Bronner M, Campbell K, Cano A, Casanova J, Christofori G, Dedhar S, Derynck R, Ford HL, Fuxe J, García de Herreros A, Goodall GJ, Hadjantonakis AK, Huang RYJ, Kalcheim C, Kalluri R, Kang Y, Khew-Goodall Y, Levine H, Liu J, Longmore GD, Mani SA, Massagué J, Mayor R, McClay D, Mostov KE, Newgreen DF, Nieto MA, Puisieux A, Runyan R, Savagner P, Stanger B, Stemmler MP, Takahashi Y, Takeichi M, Theveneau E, Thiery JP, Thompson EW, Weinberg RA, Williams ED, Xing J, Zhou BP, Sheng G, E.M.T. International Association (2020) *Nat Rev Mol Cell Biol* 21(6):341
6. Trepats X, Sahai E (2018) *Nat Phys* 14(7):671
7. Nia HT, Munn LL, Jain RK (2020) *Science* 370(6516):eaaz0868
8. Stuart T, Satija R (2019) *Nat Rev Genet* 20(5):257
9. Rao A, Barkley D, França GS, Yanai I (2021) *Nature* 596(7871):211
10. Lemon WC, McDole K (2020) *Curr Opin Cell Biol* 66, 34
11. Specht EA, Braselmann E, Palmer AE (2017) *Annu Rev Physiol* 79:93
12. Leggett SE, Khoo AS, Wong IY (2017) *Biomaterials Sci* 5(8):1460
13. Beri P, Matte BF, Fattet L, Kim D, Yang J, Engler AJ (2018) *Nat Rev Mater* 3(11):418
14. Leggett SE, Hruska AM, Guo M, Wong IY (2021) *Cell Commun Signal* 19(1):32
15. Li Y, Tang W, Guo M (2021) *Matter* 4(6):1863
16. LeSavage BL, Suhar RA, Broguiere N, Lutolf MP, Heilshorn SC (2022) *Nat Mater* 21, 143–159
17. Lauffenburger DA, Horwitz AF (1996) *Cell* 84(3):359
18. SenGupta S, Parent CA, Bear JE (2021) *Nat Rev Mol Cell Biol* 22:1–19
19. Ridley AJ, Schwartz MA, Burridge K, Firtel RA, Ginsberg MH, Borisy G, Parsons JT, Horwitz AR (2003) *Science* 302(5651):1704
20. Levayer R, Lecuit T (2012) *Trends Cell Biol* 22(2):61
21. Janmey PA, Fletcher DA, Reinhart-King CA (2020) *Physiol Rev* 100(2):695
22. Yamada KM, Sixt M (2019) *Nat Rev Mol Cell Biol* 20(12):738
23. Alibert C, Goud B, Manneville JB (2017) *Biol Cell* 109(5):167
24. Yilmaz M, Christofori G (2009) *Cancer Metastasis Rev* 28(1):15
25. Hu J, Li Y, Hao Y, Zheng T, Gupta SK, Parada GA, Wu H, Lin S, Wang S, Zhao X, Goldman RD, Cai S, Guo M (2019) *Proc Natl Acad Sci USA* 116(35):17175
26. Pattenon AE, Vahabikashi A, Pogoda K, Adam SA, Mandal K, Kittisopikul M, Sivagurunathan S, Goldman A, Goldman RD, Janmey PA (2019) *J Cell Biol* 218(12):4079
27. Paluch EK, Aspalter IM, Sixt M (2016) *Annu Rev Cell Dev Biol* 32, 469
28. Liu YJ, Le Berre M, Lautenschlaeger F, Maiuri P, Callan-Jones A, Heuzé M, Takaki T, Voituriez R, Piel M (2015) *Cell* 160(4):659
29. Ruprecht V, Wieser S, Callan-Jones A, Smutny M, Morita H, Sako K, Barone V, Ritsch-Marte M, Sixt M, Voituriez R, Heisenberg CP (2015) *Cell* 160(4):673
30. Wolf K, Mazo I, Leung H, Engelke K, von Andrian UH, Deryugina EI, Strongin AY, Bröcker EB, Friedl P (2003) *J Cell Biol* 160(2):267
31. Sahai E, Marshall CJ (2003) *Nat Cell Biol* 5(8):711



32. Roussos ET, Condeelis JS, Patsialou A (2011) *Nat Rev Cancer* 11(8):573
33. Stroka KM, Jiang H, Chen SH, Tong Z, Wirtz D, Sun SX, Konstantopoulos K (2014) *Cell* 157(3):611
34. Kalukula Y, Stephens AD, Lammerding J, Gabriele S (2022) *Nat Rev Mol Cell Biol* 23, 583–602
35. Wolf K, Te Lindert M, Krause M, Alexander S, Te Riet J, Willis AL, Hoffman RM, Figdor CG, Weiss SJ, Friedl P (2013) *J Cell Biol* 201(7):1069
36. Davidson PM, Denais C, Bakshi MC, Lammerding J (2014) *Cell Mol Bioeng* 7(3):293
37. Renkawitz J, Kopf A, Stopp J, de Vries I, Driscoll MK, Merrin J, Hauschild R, Welf ES, Danuser G, Fiolka R, Sixt M (2019) *Nature* 568(7753):546
38. Lomakin AJ, Cattin CJ, Cuvelier D, Alraies Z, Molina M, Nader GPF, Srivastava N, Sáez PJ, Garcia-Arcos JM, Zhitnyak IY, Bhargava A, Driscoll MK, Welf ES, Fiolka R, Petrie RJ, De Silva NS, González-Granado JM, Manel N, Lennon-Duménil AM, Müller DJ, Piel M (2020) *Science* 370(6514):eaba2894
39. Harada T, Swift J, Irianto J, Shin JW, Spinler KR, Athirasala A, Diegmiller R, Dingal PC, Ivanovska IL, Discher DE J (2014) *Cell Biol* 204(5):669
40. Bell ES, Shah P, Zuela-Sopilniak N, Kim D, McGregor AL, Isermann P, Davidson PM, Elacqua JJ, Lakins JN, Vahdat L, Weaver VM, Smolka MB, Span PN, Lammerding J, bioRxiv (2022) *Oncogene* 41, 4211–4230. <https://doi.org/10.1101/2021.07.12.451842>
41. Denais CM, Gilbert RM, Isermann P, McGregor AL, te Lindert M, Weigel B, Davidson PM, Friedl P, Wolf K, Lammerding J (2016) *Science* 352(6283):353
42. Raab M, Gentili M, de Belly H, Thiam HR, Vargas P, Jimenez AJ, Lautenschlaeger F, Voituriez R, Lennon-Duménil AM, Manel N, Piel M (2016) *Science* 352(6283):359
43. Irianto J, Xia Y, Pfeifer CR, Athirasala A, Ji J, Alvey C, Tewari M, Bennett RR, Harding SM, Liu AJ, Greenberg RA, Discher DE (2017) *Curr Bio* 27(2):210
44. Xia Y, Ivanovska IL, Zhu K, Smith L, Irianto J, Pfeifer CR, Alvey CM, Ji J, Liu D, Cho S, Bennett RR, Liu AJ, Greenberg RA, Discher DE (2018) *J Cell Biol* 217(11):3796
45. Shah P, Hobson CM, Cheng S, Colville MJ, Paszek MJ, Superfine R, Lammerding J (2021) *Curr Biol* 31(4):753
46. Fanfone D, Wu Z, Mammi J, Berthenet K, Neves D, Weber K, Halaburkova A, Virard F, Bunel F, Jarnard C, Hernandez-Vargas H, Tait SWG, Hennino A, Ichim G (2022) *Elife* 11, e73150
47. Petrie RJ, Koo H, Yamada KM (2014) *Science* 345(6200):1062
48. Petrie RJ, Harlin HM, Korsak LI, Yamada KM (2017) *J Cell Biol* 216(1):93
49. Rodriguez-Boulant E, Nelson WJ (1989) *Science* 245(4919):718
50. Kelley LC, Lohmer LL, Hagedorn EJ, Sherwood DR (2014) *J Cell Biol* 204(3):291
51. Mayor R, Etienne-Manneville S (2016) *Nat Rev Mol Cell Biol* 17(2):97
52. Hamidi H, Ivaska J (2018) *Nat Rev Cancer* 18(9):533
53. Levental KR, Yu H, Kass L, Lakins JN, Egeblad M, Erler JT, Fong SF, Csiszar K, Giaccia A, Weninger W, Yamauchi M, Gasser DL, Weaver VM (2009) *Cell* 139(5):891
54. Winkler J, Abisoye-Ogunniyan A, Metcalf KJ, Werb Z (2020) *Nat Commun* 11(1):5120
55. Cavallaro U, Christofori G (2004) *Nat Rev Cancer* 4(2):118
56. Jacob JT, Coulombe PA, Kwan R, Omary MB (2018) *Cold Spring Harbor Perspectives Biology* 10(4):a018275
57. Thomas PA, Kirschmann DA, Cerhan JR, Folberg R, Seftor EA, Sellers TA, Hendrix MJ (1999) *Clin Cancer Res* 5(10):2698
58. Labernadie A, Kato T, Brugués A, Serra-Picamal X, Derzsi S, Arwert E, Weston A, González-Tarragó V, Elosegui-Artola A, Albertazzi L, Alcaraz J, Roca-Cusachs P, Sahai E, Trepas X (2017) *Nat Cell Biol* 19(3):224
59. Riahi R, Sun J, Wang S, Long M, Zhang DD, Wong PK (2015) *Nat Commun* 6, 6556
60. Aasen T, Leithe E, Graham SV, Kameritsch P, Mayán MD, Mesnil M, Pogoda K, Taberner A (2019) *Oncogene* 38(23):4429
61. Han YL, Pegoraro AF, Li H, Li K, Yuan Y, Xu G, Gu Z, Sun J, Hao Y, Gupta SK, Li Y, Tang W, Tang X, Teng L, Fredberg JJ, Guo M (2020) *Nat Phys* 16(1):101
62. Khalil AA, Ilina O, Vasaturo A, Venhuizen JH, Vullings M, Venhuizen V, Bilos A, Figdor CG, Span PN, Friedl P (2020) *J Cell Biol* 219(10):e201911120

63. Theveneau E, Steventon B, Scarpa E, Garcia S, Trepats X, Streit A, Mayor R (2013) *Nat Cell Biol* 15(7):763
64. Theveneau E, Linker C (2017) *F1000Research* 6:1899
65. Leggett SE, Neronha ZJ, Bhaskar D, Sim JY, Perdikari TM, Wong IY (2019) *Proc Natl Acad Sci USA* 116(35):17298
66. Guillot C, Lecuit T (2013) *Science* 340(6137):1185
67. Oswald L, Grosser S, Smith DM, Käs JA (2017) *J Phys D Appl Phys* 50(48):483001
68. Yang H, Pegoraro AF, Han Y, Tang W, Abeyaratne R, Bi D, Guo M (2021) *Proc Natl Acad Sci USA* 118(44):e2109168118
69. Bhaskar D, Zhang WY, Wong IY (2021) *Soft Matter* 17:4653
70. La Porta CAM, Zapperi S (2020) *Nat Rev Phys* 2(10):516
71. Fredberg JJ (2022) *Soft Matter* 18, 2346
72. Vicsek T, Zafeiris A (2012) *Phys Rep* 517(3-4):71
73. Chaikin PM, Lubensky TC (2000) *Principles of condensed matter physics*. Cambridge University Press, Cambridge
74. Liu AJ, Nagel SR (2010) *Annu Rev Condens Matter Phys* 1:347
75. Sadati M, Taheri Qazvini N, Krishnan R, Park CY, Fredberg JJ (2013) *Differentiation* 86(3):121
76. Adrian RJ (2005) *Experiments Fluids* 39(2):159
77. Poujade M, Grasland-Mongrain E, Hertzog A, Jouanneau J, Chavrier P, Ladoux B, Buguin A, Silberzan P (2007) *Proc Natl Acad Sci USA* 104(41):15988
78. Petitjean L, Reffay M, Grasland-Mongrain E, Poujade M, Ladoux B, Buguin A, Silberzan P (2010) *Biophys J* 98(9):1790
79. Angelini TE, Hannezo E, Trepats X, Fredberg JJ, Weitz DA (2010) *Phys Rev Lett* 104(16):168104
80. Angelini TE, Hannezo E, Trepats X, Marquez M, Fredberg JJ, Weitz DA (2011) *Proc Natl Acad Sci USA* 108(12):4714
81. Palamidessi A, Malinverno C, Frittoli E, Corallino S, Barbieri E, Sigismund S, Beznoussenko GV, Martini E, Garre M, Ferrara I, Tripodo C, Ascione F, Cavalcanti-Adam EA, Li Q, Di Fiore PP, Parazzoli D, Giavazzi F, Cerbino R, Scita G (2019) *Nat Mater* 18(11):1252
82. Cerbino R, Villa S, Palamidessi A, Frittoli E, Scita G, Giavazzi F (2021) *Soft Matter* 17(13):3550
83. Iliina O, Gritsenko PG, Syga S, Lippoldt J, La Porta CAM, Chepizhko O, Grosser S, Vullings M, Bakker GJ, Staruß J, Bult P, Zapperi S, Käs JA, Deutsch A, Friedl P (2020) *Nat Cell Biol* 22(9):1103
84. Thompson DW (1968) *On growth and form*. Cambridge University Press, Cambridge
85. Gibson MC, Patel AB, Nagpal R, Perrimon N (2006) *Nature* 442(7106):1038
86. Bi D, Lopez JH, Schwarz JM, Manning ML (2015) *Nat Phys* 11(12):1074
87. Bi D, Yang X, Marchetti MC, Manning ML (2016), *Phys Rev X* 6(2):021011
88. Yang X, Bi D, Czajkowski M, Merkel M, Manning ML, Marchetti MC (2017) *Proc Natl Acad Sci USA* 114(48):12663
89. Park JA, Kim JH, Bi D, Mitchel JA, Qazvini NT, Tantisira K, Park CY, McGill M, Kim SH, Gweon B, Notbohm J, Steward R, Burger S, Randell SH, Kho AT, Tambe DT, Hardin C, Shore SA, Israel E, Weitz DA, Tschumperlin DJ, Henske EP, Weiss ST, Manning ML, Butler JP, Drazen JM, Fredberg JJ (2015) *Nat Mater* 14(10):1040
90. Atia L, Bi D, Sharma Y, Mitchel JA, Gweon B, Koehler SA, DeCamp SJ, Lan B, Kim JH, Hirsch R, Pegoraro AF, Lee KH, Starr JR, Weitz DA, Martin AC, Park JA, Butler JP, Fredberg JJ (2018) *Nat Phys* 14(6):613
91. Mitchel JA, Das A, O'Sullivan MJ, Stancil IT, DeCamp SJ, Koehler S, Ocaña OH, Butler JP, Fredberg JJ, Nieto MA, Bi D, Park JA (2020) *Nat Commun* 11(1):5053
92. Wong IY, Javaid S, Wong EA, Perk S, Haber DA, Toner M, Irimia D (2014) *Nat Mater* 13(11):1063
93. Kang W, Ferruzzi J, Spatarelu CP, Han YL, Sharma Y, Koehler SA, Mitchel JA, Khan A, Butler JP, Roblyer D, Zaman MH, Park JA, Guo M, Chen Z, Pegoraro AF, Fredberg JJ (2021) *iScience* 24(11):103252

94. Grosser S, Lippoldt J, Oswald L, Merkel M, Sussman DM, Renner F, Gottheil P, Morawetz EW, Fuhs T, Xie X, Pawlizak S, Fritsch AW, Wolf B, Horn LC, Briest S, Aktas B, Manning ML, Käs JA (2021) *Phys Rev X* 11(1):011033
95. Gamboa Castro M, Leggett SE, Wong IY (2016) *Soft Matter* 12(40):8327
96. Cichos F, Gustavsson K, Mehlig B, Volpe G (2020) *Nat Mach Intell* 2:94
97. Karniadakis GE, Kevrekidis IG, Lu L, Perdikaris P, Wang S, Yang L (2021) *Nat Rev Phys* 3(6):422
98. Pavlova NN, Thompson CB (2016) *Cell Metab* 23(1):27
99. De Donatis A, Ranaldi F, Cirri P (2010) *Cell Commun Signal* 8:20
100. Semenza GL (2013) *J Clin Invest* 123(9):3664
101. DeWane G, Salvi AM, DeMali KA (2021) *J Cell Sci* 134(3):jcs248385
102. Romero-Garcia S, Moreno-Altamirano MMB, Prado-Garcia H, Sánchez-García FJ (2016) *Front Immunol* 7:52
103. Lunt SY, Vander Heiden MG (2011) *Annu Rev Cell Dev Biol* 27:441
104. Park JS, Burckhardt CJ, Lazcano R, Solis LM, Isogai T, Li L, Chen CS, Gao B, Minna JD, Bachoo R, DeBerardinis RJ, Danuser G (2020) *Nature* 578(7796):621
105. Mah EJ, Lefebvre AEYT, McGahey GE, Yee AF, Digman MA (2018) *Sci Rep* 8(1):17094
106. Bays JL, Campbell HK, Heidema C, Sebbagh M, DeMali KA (2017) *Nat Cell Biol* 19(6):724
107. DeCamp SJ, Tsuda VMK, Ferruzzi J, Koehler SA, Giblin JT, Roblyer D, Zaman MH, Weiss ST, Kılıç A, De Marzio M, Park CY, Ogassavara NC, Mitchel JA, Butler JP, Fredberg JJ (2020) *Sci Rep* 10(1):18302
108. Zhang J, Goliwas KF, Wang W, Taufalele PV, Bordeleau F, Reinhart-King CA (2019) *Proc Natl Acad Sci USA* 116(16):7867
109. Commander R, Wei C, Sharma A, Mouw JK, Burton LJ, Summerbell E, Mahboubi D, Peterson RJ, Konen J, Zhou W, Du Y, Fu H, Shanmugam M, Marcus AI (2020) *Nat Commun* 11(1):1533
110. Zanutelli MR, Rahman-Zaman A, VanderBurgh JA, Taufalele PV, Jain A, Erickson D, Bordeleau F, Reinhart-King CA (2019) *Nat Commun* 10(1):4185
111. Konen J, Summerbell E, Dwivedi B, Galior K, Hou Y, Rusnak L, Chen A, Saltz J, Zhou W, Boise LH, Vertino P, Cooper L, Salaita K, Kowalski J, Marcus AI (2017) *Nat Commun* 8:15078
112. Peirman A, Blondeel E, Ahmed T, Anckaert J, Audenaert D, Boterberg T, Buzas K, Carragher N, Castellani G, Castro F, Dangles-Marie V, Dawson J, De Tullio P, De Vlieghere E, Dedeyne S, Depypere H, Diosdi A, Dmitriev RI, Dolznig H, Fischer S, Gespach C, Goossens V, Heino J, Hendrix A, Horvath P, Kunz-Schughart LA, Maes S, Mangodt C, Mestdagh P, Michlíková S, Oliveira MJ, Pampaloni F, Piccinini F, Pinheiro C, Rahn J, Robbins SM, Siljamäki E, Steigemann P, Sys G, Takayama S, Tesei A, Tulkens J, Van Waeyenberge M, Vandesompele J, Wagemans G, Weindorfer C, Yigit N, Zablowsky N, Zanoni M, Blondeel P, De Wever O (2021) *Nat Methods* 18(11):1294
113. Cox TR (2021) *Nat Rev Cancer* 21(4):217
114. Piersma B, Hayward MK, Weaver VM (2020) *Biochim Biophys Acta Rev Cancer* 1873(2):188356
115. Peinado H, Zhang H, Matei IR, Costa-Silva B, Hoshino A, Rodrigues G, Psaila B, Kaplan RN, Bromberg JF, Kang Y, Bissell MJ, Cox TR, Giaccia AJ, Erler JT, Hiratsuka S, Ghajar CM, Lyden D (2017) *Nat Rev Cancer* 17(5):302
116. Pozzi A, Yurchenco PD, Iozzo RV (2017) *Matrix Biol* 57-58:1
117. Halfter W, Oertle P, Monnier CA, Camenzind L, Reyes-Lua M, Hu H, Candiello J, Labilloy A, Balasubramani M, Henrich PB, Plodinec M (2015) *FEBS J* 282(23):4466
118. Chang J, Chaudhuri O (2019) *J Cell Biol* 218(8):2456
119. Benton G, Arnaoutova I, George J, Kleinman HK, Koblinski J (2014) *Adv Drug Deliv Rev* 79-80:3
120. Aisenbrey EA, Murphy WL (2020) *Nat Rev Mater* 5(7):539
121. Gritsenko PG, Ilina O, Friedl P (2012) *J Pathol* 226(2):185

122. Wolf K, Alexander S, Schacht V, Coussens LM, von Andrian UH, van Rheenen J, Deryugina E, Friedl P (2009) *Semin Cell Dev Biol* 20(8):931
123. Provenzano PP, Eliceiri KW, Campbell JM, Inman DR, White JG, Keely PJ (2006) *BMC Med* 4(1):38
124. Fischer RS, Sun X, Baird MA, Hourwitz MJ, Seo BR, Pasapera AM, Mehta SB, Losert W, Fischbach C, Fourkas JT, Waterman CM (2021) *Proc Natl Acad Sci USA* 118(22):e2021135118
125. Di Martino JS, Nobre AR, Mondal C, Taha I, Farias EF, Fertig EJ, Naba A, Aguirre-Ghiso JA, Bravo-Cordero JJ (2021) *Nature Cancer*. <https://doi.org/10.1038/s43018-021-00291-9>
126. Plikus MV, Wang X, Sinha S, Forte E, Thompson SM, Herzog EL, Driskell RR, Rosenthal N, Biernaskie J, Horsley V (2021) *Cell* 184(15):3852
127. Hapach LA, Vanderburgh JA, Miller JP, Reinhart-King CA (2015) *Phys Biol* 12(6):061002
128. Sapudom J, Pompe T (2018) *Biomater Sci* 6(8):2009
129. Provenzano PP, Inman DR, Eliceiri KW, Knittel JG, Yan L, Rueden CT, White JG, Keely PJ (2008) *BMC Med* 6:11
130. Conklin MW, Eickhoff JC, Riching KM, Pehlke CA, Eliceiri KW, Provenzano PP, Friedl A, Keely PJ (2011) *Am J Pathol* 178(3):1221
131. Maller O, Drain AP, Barrett AS, Borgquist S, Ruffell B, Zakharevich I, Pham TT, Grusso T, Kuasne H, Lakins JN, Acerbi I, Barnes JM, Nemkov T, Chauhan A, Gruenberg J, Nasir A, Bjarnadottir O, Werb Z, Kabos P, Chen YY, Hwang ES, Park M, Coussens LM, Nelson AC, Hansen KC, Weaver VM (2021) *Nat Mater* 20(4):548
132. Fung YC, Tong P (2001) *Classical and computational solid mechanics*. World Scientific, Singapore
133. Broedersz C, MacKintosh F (2014) *Rev Mod Phys* 86(3):995
134. Chaudhuri O, Cooper-White J, Janmey PA, Mooney DJ, Shenoy VB (2020) *Nature* 584(7822):535
135. Li H, Zheng Y, Han YL, Cai S, Guo M (2021) *Proc Natl Acad Sci USA* 118(11):e2022422118
136. Gill BJ, Gibbons DL, Roudsari LC, Saik JE, Rizvi ZH, Roybal JD, Kurie JM, West JL (2012) *Cancer Res* 72(22):6013
137. Beck JN, Singh A, Rothenberg AR, Elisseff JH, Ewald AJ (2013) *Biomaterials* 34(37):9486
138. Singh S, Schwartz M, Tokuda E, Luo Y, Rogers R, Fujita M, Ahn N, Anseth K (2015) *Sci Rep* 5:17814
139. Pradhan S, Slater JH (2019) *Biomaterials* 215:119177
140. Chaudhuri O (2017) *Biomater Sci* 5(8):1480
141. Prince E, Kumacheva E (2019) *Nat Rev Mater* 4(2):99
142. Kim J, Staunton JR, Tanner K (2016) *Adv Mater* 28(1):132
143. Paul CD, Hruska A, Staunton JR, Burr HA, Daly KM, Kim J, Jiang N, Tanner K (2019) *Biomaterials* 197:101
144. Xu R, Boudreau A, Bissell MJ (2009) *Cancer Metastasis Rev* 28(1–2):167
145. Driscoll MK, Danuser G (2015) *Trends Cell Biol* 25(12):749
146. Polacheck WJ, Chen CS (2016) *Nat Methods* 13(5):415
147. Legant WR, Miller JS, Blakely BL, Cohen DM, Genin GM, Chen CS (2010) *Nat Methods* 7(12):969
148. Hall MS, Long R, Feng X, Huang Y, Hui CY, Wu M (2013) *Exp Cell Res* 319(16):2396
149. Steinwachs J, Metzner C, Skodzek K, Lang N, Thievensen I, Mark C, Münster S, Aifantis KE, Fabry B (2016) *Nat Methods* 13(2):171
150. Hall MS, Alisafaei F, Ban E, Feng X, Hui CY, Shenoy VB, Wu M (2016) *Proc Natl Acad Sci U S A* 113(49):14043
151. van Oosten ASG, Chen X, Chin L, Cruz K, Patteson AE, Pogoda K, Shenoy VB, Janmey PA (2019) *Nature* 573(7772):96
152. Han YL, Ronceray P, Xu G, Malandrino A, Kamm RD, Lenz M, Broedersz CP, Guo M (2018) *Proc Natl Acad Sci USA* 115(16):4075
153. Leggett SE, Patel M, Valentin TM, Gamboa L, Khoo AS, Williams EK, Franck C, Wong IY (2020) *Proc Natl Acad Sci USA* 117(11):5655

154. Krajina B.A., LeSavage B.L., Roth J.G., Zhu A.W., Cai P.C., Spakowitz A.J., Heilshorn S.C., *Sci Adv* 7(8):eabe1969 (2021)
155. Khoo AS, Valentin TM, Leggett SE, Bhaskar D, Bye EM, Benmelech S, Ip BC, Wong IY (2019) *ACS Biomater Sci Eng* 5(9):4341
156. Patel M, Leggett SE, Landauer AK, Wong IY, Franck C (2018) *Sci Rep* 8(1):5581
157. Squires TM, Mason TG (2010) *Annu Rev Fluid Mech* 42(1):413
158. Mulligan JA, Feng X, Adie SG (2019) *Sci Rep* 9(1):4086
159. Ling L, Mulligan JA, Ouyang Y, Shimpi AA, Williams RM, Beeghly GF, Hopkins BD, Spector JA, Adie SG, Fischbach C (2020) *Adv Funct Mater* 30(48):1910650
160. Li Y, Wong IY, Guo M (2022) *Small* 18(36):2107305. <https://doi.org/10.1002/sml.202107305>. <https://onlinelibrary.wiley.com/doi/abs/10.1002/sml.202107305>
161. Nieto MA, Huang RY, Jackson RA, Thiery JP (2016) *Cell* 166(1):21
162. Christofori G (2006) *Nature* 441(7092):444
163. Leggett SE, Sim JY, Rubins JE, Neronha ZJ, Williams EK, Wong IY (2016) *Integr Biol* 8(11):1133
164. Diepenbruck M, Christofori G (2016) *Curr Opin Cell Biol* 43:7
165. Brabletz T (2012) *Nat Rev Cancer* 12(6):425
166. Pastushenko I, Blanpain C (2019) *Trends Cell Biol* 29(3):212
167. Pastushenko I, Brisebarre A, Sifrim A, Fioramonti M, Revenco T, Boumahdi S, Van Keymeulen A, Brown D, Moers V, Lemaire S, De Clercq S, Minguijón E, Balsat C, Sokolow Y, Dubois C, De Cock F, Scozzaro S, Sopena F, Lanas A, D'Haene N, Salmon I, Marine JC, Voet T, Sotiropoulou PA, Blanpain C (2018) *Nature* 556(7702):463
168. Cheung KJ, Gabrielson E, Werb Z, Ewald AJ (2013) *Cell* 155(7):1639
169. Lüönd F, Sugiyama N, Bill R, Bornes L, Hager C, Tang F, Santacroce N, Beisel C, Ivanek R, Bürglin T, Tiede S, van Rheenen J, Christofori G (2021) *Dev Cell* 56(23):3203
170. Aiello NM, Maddipati R, Norgard RJ, Balli D, Li J, Yuan S, Yamazoe T, Black T, Sahmoud A, Furth EE, Bar-Sagi D, Stanger BZ (2018) *Dev Cell* 45(6):681
171. Simeonov KP, Byrns CN, Clark ML, Norgard RJ, Martin B, Stanger BZ, Shendure J, McKenna A, Lengner CJ (2021) *Cancer Cell* 39(8):1150
172. Box GEP, Draper NR (1987) *Empirical model-building and response surfaces*. Wiley, Hoboken
173. Ben-David U, Beroukhi R, Golub TR (2019) *Nat Rev Cancer* 19(2):97
174. Altrock PM, Liu LL, Michor F (2015) *Nat Rev Cancer* 15(12):730
175. Weiss F, Lauffenburger D, Friedl P (2022) *Nat Rev Cancer* 22:157–173
176. Lamb J, Crawford ED, Peck D, Modell JW, Blat IC, Wrobel MJ, Lerner J, Brunet JP, Subramanian A, Ross KN, Reich M, Hieronymus H, Wei G, Armstrong SA, Haggarty SJ, Clemons PA, Wei R, Carr SA, Lander ES, Golub TR (2006) *Science* 313(5795):1929
177. Buttenschön A, Edelstein-Keshet L (2020) *PLoS Comput Biol* 16(12):e1008411
178. Ramesh V, Brabletz T, Ceppi P (2020) *Trends Cancer* 6(11):942
179. Schwab A, Siddiqui A, Vazakidou ME, Napoli F, Böttcher M, Menchicchi B, Raza U, Saatci Ö, Krebs AM, Ferrazzi F, Rapa I, Dettmer-Wilde K, Waldner MJ, Ekici AB, Rasheed SAK, Mougiakakos D, Oefner PJ, Sahin O, Volante M, Greten FR, Brabletz T, Ceppi P, *Cancer Res* 78(7):1604 (2018)
180. Wu X, Li X, Fu Q, Cao Q, Chen X, Wang M, Yu J, Long J, Yao J, Liu H, Wang D, Liao R, Dong C (2017) *J Exp Med* 214(4):1065
181. Uto K, Tsui JH, DeForest CA, Kim DH (2017) *Prog Polym Sci* 65:53
182. Pires A, Burnell S, Gallimore A (2021) *Curr Opin Immunol* 74:32
183. Madsen CD, Hooper S, Tozluoglu M, Bruckbauer A, Fletcher G, Erler JT, Bates PA, Thompson B, Sahai E (2015) *Nat Cell Biol* 17(1):68
184. Gupta GP, Massagué J (2006) *Cell* 127(4):679
185. Ayuso JM, Park KY, Virumbrales-Muñoz M, Beebe DJ (2021) *APL Bioeng* 5(1):010902
186. Nemeč S, Kilian KA (2021) *Nat Rev Mater* 6(1):69
187. Gatenby RA, Brown JS (2020) *Nat Rev Clin Oncol* 17(11):675

# Collective Cellular Phase Transitions in Cancer



Adrian F. Pegoraro, Thien-Khoi N. Phung, and Jennifer A. Mitchel

**Abstract** The growth and metastasis of tumors are increasingly recognized to be an inherently collective, multiscale problem, wherein understanding at the genetic and molecular level is necessary but is not sufficient; the mechanical response of cells must also be accounted for to understand collective behavior in cancer. Like glassy, granular, and colloidal materials, cells exist in a fundamentally crowded and disordered environment and are capable of undergoing collective phase transitions between states resembling the material phases of solid, liquid, and gas. By mapping concepts from material science to cell motion, it becomes possible to better predict and understand how macroscopic properties of the cellular system – fluidity and rigidity – emerge from physical cellular-scale interactions. These cellular interactions, though enormously complex and variable from a biological standpoint, can be abstracted to generalized state variables, including density, cell shape constraints, and fluctuations, which allow phase diagrams to be constructed to aid in predicting behavior. In this chapter, we review both experimental evidence and theoretical frameworks toward understanding multicellular collectives as material systems, exploring both the power and the limitations of comparisons between biological and non-living soft matter systems. We conclude with how these lessons are being applied to develop a more holistic understanding of how physical constraints affect collective migration and invasion in cancer.

**Keywords** Cell rheology · Dynamic heterogeneity · Emergence · Flocking · Glass transition · Jamming · Phase transition · Soft matter

---

A. F. Pegoraro

Nanoscale measurement, Metrology Research Center, National Research Council, Ottawa, ON, Canada

T.-K. N. Phung

Department of Environmental Health, Harvard T.H. Chan School of Public Health, Boston, MA, USA

J. A. Mitchel (✉)

Department of Biology, Wesleyan University, Middletown, CT, USA

e-mail: [jmitchel@wesleyan.edu](mailto:jmitchel@wesleyan.edu)

© The Author(s), under exclusive license to Springer Nature Switzerland AG 2023

I. Y. Wong, M. R. Dawson (eds.), *Engineering and Physical Approaches to Cancer*, Current Cancer Research, [https://doi.org/10.1007/978-3-031-22802-5\\_2](https://doi.org/10.1007/978-3-031-22802-5_2)

# 1 Introduction

Cancer is not one disease but a range of conditions which are characterized by aberrant, uncontrolled growth. Tumor growth can occur in any organ and leads to cell populations that are highly heterogeneous [1]. Tumor growth and eventual spreading through metastasis involve changes in cell mechanics, cell signaling, drug resistance, and a host of other properties measured at the single-cell level [2–4]. Understanding these changes is important for diagnosis and treatment of cancer, but measurements of single-cell properties alone are insufficient to understand cancer behavior. Tumor cells necessarily interact with each other and their environment, and understanding these interactions is needed for a holistic picture of disease progression [5].

Recent approaches to understanding the mechanics of cellular collectives have established that physical models can both aid interpretation and predict behaviors and properties of these collectives, many of which are not apparent at the single-cell level. Instead of focusing on individual cells, these frameworks treat the collective as a *material system* and aim to predict average behavior [6–9]. While it is possible to point to examples of different material phases in the body – including solids in the form of bones and cartilage, liquids in the form of blood and lymph, and gas in the lungs – the majority of our cell and tissue systems are better described as disordered materials. In everyday life, disordered materials are everywhere, from glass in our windows to pastes and colloids like toothpaste and yogurt to granular materials like coffee beans in a dispenser or sand on the beach. These diverse systems share the ability to behave either as a solid or liquid, or, in some cases, a gas. These systems exist in metastable states far away from a thermodynamic equilibrium, yet we can still make predictions about their behavior and mechanics.

The distinguishing feature of these systems is their lack of order at both the local and long-range scale. This has made it challenging to develop straightforward metrics to characterize local behavior, although ongoing developments in machine learning may allow the determination of such metrics [10–13]. Nonetheless, average behavior does change in predictable ways in disordered systems; for example, as a glass cools from a melted, viscous state, particle motion slows down and eventually arrests, and the glass transitions from a fluid to a solid material. This slowing and eventual arrest are accompanied by a change in the mechanical properties of the bulk system. The macroscopic stiffening, or solidification, corresponds at the microscopic level to an increase in molecular coordination, as the individual constituents of the glass coordinate their motion over longer time and length scales. That molecular coordination gives rise to bulk stiffness is an example of an *emergent mesoscopic phenomenon* (see Box 1). Emergent phenomena occur across all scales of life and embody the notion that “more is different”: that is, one cannot understand the behavior of the group by investigating the individual in ever-higher detail, while at each level of increasing scale or complexity, entirely new and unpredictable properties emerge [14–16]. While biological systems are more complex than inert materials, due to the presence of energy consumption,

biochemical signaling, biological coordination, and heterogeneity, through adapting our understanding of the physics of disordered media it becomes possible to relate the measurement of single-cell properties to many types of collective behavior.

### **Box 1: Terms and Concepts Originating in Physics and Materials Science**

When describing cell collectives as a material, it is natural to draw upon the language of material science, but the correspondence of ideas is not exact. The concepts and terms are used as analogies, or behavior is described as being *like* a material phase. It is thus helpful to understand what a term means both in reference to inert material and in reference to living systems. Some of the most commonly used terms in the description of collective cell motion are:

**Active matter:** Material where each constituent particle consumes energy [203]. While this energy consumption is often tied to motility, it is not necessarily so. For example, motors in the cellular cytoskeleton consume energy and change the behavior of the cellular interior. Active matter systems are by definition not in thermal equilibrium; however, they can reach a meta-stable state.

**Adhesion:** This is the tendency of cells to attach to other materials. This can include adhesion to the substrate or extracellular matrix, but in the context of collective cell motion often refers to cell–cell adhesion. Cell–cell adhesion is controlled by a raft of proteins collectively referred to as the adhesome [204]. When compared to inert materials, adhesion is somewhat akin to the binding energy or attractive potential [6].

**Agitation:** Refers to the forces which tend to disturb the collective. In inert materials like glasses, this property is dominated by thermal fluctuations and is measured in units of  $k_B T$  where  $k_B$  is Boltzmann’s Constant and  $T$  is temperature [60, 205]. For granular materials where the constituent particles are large, thermal forces are insufficient to displace the particles. Instead, external forces such as gravity or shear moves the particles; this is why granular systems are said to be athermal [29]. Despite this, by analogy with the effect of temperature in molecular systems, we can define an effective temperature for granular materials which reflects the degree to which agitation displaces the constituent particles [206]. Similarly, for active systems, which include self-propelled particles and cells, we can also define an effective temperature [207]. In this case, however, the effective temperature is related to the self-motility of the constituents and not related to external forces.

**Attractive energy:** When discussing the phase behavior of inert, particulate matter, this describes the tendency of particles to attract or repel each other. For a system of attractive solid particles to fluidize, the amount of agitation must be sufficient to overcome this barrier [30]. In cellular systems, the

(continued)



attractive energy is determined by balance of cell adhesion and contractility [41].

**Colloidal systems:** Inert materials where one insoluble phase is dispersed in another. The insoluble phase is small and remains dispersed in the supporting medium. A commonly used system is polymer microspheres dispersed in solution. In this system, the colloids are used as model atoms to help understand standard bulk materials [208]. Similarly, analogies are made between cellular systems and colloidal suspensions [209].

**Contractility:** The cytoskeleton of a cell is contractile. When a cell adheres to an outside material, it then pulls on its surroundings. The ability of a cell to contract is resisted by both its own compressibility and its adhesion to its surroundings. When combined with adhesion, contractility can be used to define an effective binding energy of a cell with its neighbors [41, 66].

**Density:** For a traditional condensed phase material, density is understood in the standard thermodynamic sense. In jamming parlance, density is better understood in terms of volume fraction; that is, the portion of free space taken up by the particles [31, 32]. In cell systems, density more typically refers to number density [33]. A confluent cell monolayer can cover all free space yet can still accommodate new cells when divisions occur; this changing number density can affect behavior [33, 85].

**Dynamic heterogeneity:** As a glass cools, transitioning from a liquid to a solid, it undergoes structural rearrangements [61]. The distribution of these rearrangements is non-Gaussian with very long tails. Practically speaking, this means that for particles to move, they must coordinate with their neighbors. As the system cools further, the length scale of this coordination becomes longer. The presence of dynamic heterogeneity in a system is considered a hallmark of glassy dynamics [60, 61, 205]. In cellular systems, both the distribution shape and an increasing length scale of collective phenomena have been used to identify dynamic heterogeneity in cells [33, 85].

**Elastic:** Materials which are elastic store energy when they are deformed from their resting state. This energy can be recovered if the force deforming them is removed. This is in contrast to viscoelastic materials.

**Equilibrium:** When discussing changes in material state, equilibrium can mean either a thermodynamic equilibrium or, as is more typical in disordered material, a local metastable equilibrium. The term equilibrium is also used to refer to different scale objects in the same system. For example, a monolayer that is in equilibrium typically means that large scale motion has arrested, but is not referring to internal cellular activity.

**Flocking:** A collective transition where groups of particles or cells move as a cohort [136]. Flocking effects can be seen in self-propelled systems, including cells [121, 144].

(continued)

**Fluid versus solid:** In inert materials, the distinction between these phases is obvious. In cell systems, the distinction is less clear and is partly dependent on the time-scale of observation [72]. In many cases, a relative comparison is more apt with cell collectives being described as more fluid-like or more solid-like in comparison to another grouping of cells. The character of the collective can be described in terms of order parameters or dynamic measurements of rearrangements. It is worth noting that in soft matter systems, which are condensed phases, that “fluid” is often synonymous with “liquid” despite the fact that gasses are also fluids. Because many of the concepts of soft matter have been adopted to discuss collective cellular motion, fluid is often used to describe systems which are flowing even if they are strictly speaking behaving more like a liquid state.

**Fragile glasses:** When a glass melts from a solid to a liquid, it can either change its viscosity rapidly or slowly, in which case it is called either fragile (rapid change) or strong (slow change) [210]. For molecular systems, evidence suggests these changes in macroscopic behavior are related to the underlying structure [211]. For colloidal glasses where the glass formers are particles themselves, instead the behavior of the glass being either fragile or strong is related to the stiffness of the colloids, with stiff particles forming fragile glasses and soft particles forming strong glasses [48, 212]. In biological systems, isolated cells appear to undergo a glass transition when being osmotically compressed that is consistent with soft particles forming a strong glass [209], although this may be dependent on metabolic activity as well [213]. It has also been proposed that collective cell behavior is consistent with the formation of strong glasses made of deformable particles [6, 214].

**Glass transition:** For inert materials, glass formation and jamming have some commonalities, but also differences, with the primary difference being that jamming occurs in athermal systems, whereas glass transitions happen in thermal ones [60]. In cellular systems, these terms are occasionally used interchangeably to describe the transition from a more fluid-like configuration to a more solid-like one.

**Glassy material:** As an amorphous liquid cools, it can solidify by undergoing crystallization. Glasses, however, solidify while remaining amorphous. This temperature-driven transition is accompanied by slowing dynamics yet increasing dynamic heterogeneity [60, 61, 205]. Both cell collectives and the interior of a cell can be described as glassy materials [33, 209].

**Granular material:** A collection of macroscopic particles that are big enough that they do not move due to thermal motion [29]. Common examples of granular material are sand, coffee beans, or rice. Energy dissipation in these systems is often due to friction. Jamming transitions were first

(continued)

hypothesized for granular systems where arrest is largely due to geometric confinement [31, 32]. Because it is easy to visualize granular material and its jamming transition, the language used to describe cell collectives has borrowed extensively from these concepts [6].

**Emergent phenomenon:** Broadly defined, emergent phenomena are behaviors that cannot be predicted solely by looking at individual units of a whole [215]. Collectivity or collective behavior connote similar ideas. In disordered media, there are many such phenomena. For example, a glass transition where disordered particles transition from a liquid to a solid is an emergent property; looking at any one particle, it would not be possible to predict whether this system is solid-like and only by looking at the collective can this property be determined. An example from living material is flocking; the motion of a single cell may look persistent, but when compared to its neighbors, it becomes more obviously collective behavior. Conveniently, in reference to both inert and living materials, emergent maintains a consistent definition.

**Jamming transition:** A collective effect that helps explain how disordered systems transition from fluid-like to solid-like behavior, it was initially proposed as a potential explanation for behavior in a wide range of systems such as glasses, colloids, and particles [30, 31]. It is possible to develop a rigorous definition of jamming, which is due to geometric confinement and occurs in the absence of any activity or agitation [60]. In practice, however, jamming is often used to describe the emergence of a range of collective phenomena in disordered materials and used to describe systems ranging from microscopic particles to traffic jams. For many systems, a jamming transition is associated with the transition from a fluid-like state to a solid-like state where the material resists deformation. Somewhat confusingly, some of the same language is used to describe flocking formation as well [216]. When discussing cells, the term jamming transition is used to describe both types of behavior in cells; jamming is used to describe motion arrest [33] and flock formation [121, 144].

**Mesoscale:** A “middle” length scale where the actual length scale is dependent on the system being studied. Weather patterns [217], cell motion [7, 218], and individual polymers [219] all have an effective mesoscale. In some sense, the mesoscale of a system is related to emergent phenomena and collectivity; it is a length scale that spans multiple individual units and where new physics may appear. Like emergent phenomena, the definition of mesoscale is maintained for inert and living systems.

**Order parameter:** An order parameter is any system parameter which can be used to distinguish an ordered phase from a disordered one. It describes the long-range order of a material. It can be structural, such as density or crystallographic phase, or thermodynamic, such as magnetic or dielectric

(continued)

susceptibility [220]. Because order parameters are used to distinguish phases of material, there is not an exhaustive list of them and new ones, such as recent ones proposed for some disordered materials [10–12, 221], can be developed over time to help better understand material properties.

**Percolation:** Given a series of nodes, it is possible to form links between them, be they fluid channels, electrical connections, bonds, or some other connection. As links are randomly added, the network can grow rapidly at a critical density of links, and the network spans the extent of the system. Under these conditions, macroscopic changes in system behavior can occur. In both inert [222] and cellular [40] systems, percolation refers to the formation of system spanning networks which give rise to changing material properties.

**Phase transition:** For transitions where order parameters change, such as solid to liquid, a phase transition is a clear change in the state of matter. For disordered materials, the transition from a fluid to a solid is less clear. For jamming and glass transitions, these transitions are often not associated with a distinct change in an order parameter and are instead identified by changing correlation lengths and time scales and might more correctly be described as kinetic arrest [32]. Flock formation, however, is more akin to freezing with the nucleation and growth of a flock behaving solid freezing in a liquid bath yet the system remains disordered [136, 216].

**Rigidity transition:** Rigidity transitions can be ascribed to numerous causes, but are characterized by a change in the macroscopic material properties of the system being studied. In cell systems, the term rigidity transition is used to describe both resistance to neighbor swapping [66] and changes to the elastic modulus of a tissue [40, 202]. The opposite of the rigidity transition is the yielding transition, a term which is more frequently used in reference to condensed matter systems [223, 224].

**Soft matter:** Broadly defined as systems where interparticle bond strength is on the same order as thermal energy.

**Strong glasses:** See fragile glasses.

**Viscoelastic:** Materials which are viscoelastic dissipate some of the energy used to deform them. If a force is applied and then removed, the system does not return completely to its original state. Nonetheless, some energy is stored by these materials and can be recovered. Many soft matter systems, and biological systems, are viscoelastic.

One of the most commonly described, and intuitively accessible, collective emergent phenomena is **jamming**, a concept simply illustrated (and best characterized) with inert materials. Imagine a box containing a relatively low number of spheres. These spheres are free to move around if the box is tilted or jostled. As more

and more spheres are placed in the box, their ability to roll freely is restricted. Eventually, as a critical number of spheres is added, the system becomes crowded and motion stops; this is a jamming transition from a fluid-like state where motion can occur to a solid-like state where motion stops. As discussed in this chapter, in cell systems, a similar type of transition occurs despite the fact that cells are active, soft particles which can replicate and adapt to their environment. By recognizing this parallel between inert, disordered materials and cellular collectives – because cellular collectives exhibit transitions between collectively mobile and immobile states that are reminiscent of transitions between fluid-like and solid-like states in inert materials – we can apply the insights from materials science and soft matter physics to understand complex biological phenomena, including cancer. Of course, there are differences between the collective transitions observed in simple inert matter systems and in cells. Nonetheless, the overall concept – motion changing in response to neighbors – has led to much of the terminology of jamming, and phase transitions more broadly, being adapted to cellular systems. Definitions of terms and concepts which originated in the world of materials science, and which have since been adopted for use in describing cellular systems, are presented in Box 1, which covers how the different terms are used at the intersection of these different fields.

There are three core ideas underpinning the experimental results and theoretical frameworks discussed in the rest of the chapter. First, as was highlighted with the example of spheres in a box, density, defined as the number of particles in a given space, can affect whether or not those particles are free to move. This is true for both inert materials and living systems. Second, how those particles interact also affects behavior. Returning to spheres in a box, we can imagine the behavior of the system will be different if the particles stick to each other after a collision or bounce off one another like billiard balls. In inert systems, this behavior is described as an inter-particle attraction (or repulsion). For living systems, “particle-particle,” or more accurately, “cell–cell” adhesion is determined by an array of proteins, collectively called the adhesome [17]. Because cell–cell adhesion is controlled by the cells themselves and changes over time, it is a critical parameter in understanding collective cell motion, especially in the context of cancer where adhesome changes may drive cancer progression [18]. The third key axis for understanding collective material transitions is agitation. In our example of spheres in a box, the box is tilted and shaken to impart energy to the particles. This is an example of a granular system in which external energy is needed to move the particles, in contrast to soft matter systems, where thermal energy is sufficient to displace the particles, like in the example of cooling glass. In living systems, it is clear that thermal agitation is not the main driver of cell motion. Instead, agitation comes from the cells themselves which exist out of thermal equilibrium and expend energy to migrate, grow, and rearrange their environment. In the language of soft matter/jamming, cells are active matter that consumes energy. Despite all the differences, these systems all exhibit similar behavior at transition points where the collective material physics changes between fluid-like and solid-like or vice versa. Said another way, when density, particle interactions, and agitation balance, emergent collective phenomena appear

across a diverse range of systems that nonetheless bear a striking similarity to one another.

Within the framework of phase transitions of cellular systems, when cells jam, collective motion slows (i.e., becomes more solid-like) with reduced ability for cells to rearrange themselves, whereas when they unjam, collective motion increases (i.e., becomes more fluid-like) with more frequent rearrangements. By recognizing the existence of these material phases in cellular systems, solid-like versus fluid-like (using the terminology of soft matter and jamming) and solid versus liquid versus gas (if using the terminology of traditional condensed matter), it is possible to construct phase diagrams to describe cellular behavior. Many such phase diagrams have been constructed as theoretical and experimental predictions and evidence have evolved (Fig. 1). Each phase diagram is not definitive, but instead is a tool for thought that aids in the interpretation of experimental data and making predictions about how changes at the single-cell level will be reflected in the behavior of the collective. The evolution of the proposed phase diagrams depicted in Fig. 1 also highlights that cellular jamming occurs in a multidimensional space. Early phase diagrams focused on specific state parameters, while later ones have transitioned to classes of state parameters which encompass several different cellular and environmental properties. To understand how these concepts apply to cancer, it is first necessary to understand how these concepts apply to cellular systems in general, both in terms of the underlying physics and the experimental evidence to support these models. It is only thus armed that it is possible to discuss how aberrant processes in cancer fit into this framework.

## 2 Cell Jamming: From Sand to Cells

In cell systems, many experiments have shown that both motion and rate of division slow as cell density increases, through the phenomena of contact inhibition of locomotion and contact inhibition of proliferation, respectively [19–21]. While the role of biochemical signaling has long been recognized in these processes [22–25], the role of cell mechanics and physical forces has only more recently been explored. Experimental evidence demonstrates that mechanical forces could play an important role in determining behavior in collective systems [26], with several different models from soft matter physics being used to help explain collective cell properties [27, 28]. The related phenomena of jamming and glass transitions, which are collective phase transitions between motile and arrested states, offered new possibilities for understanding both contact inhibition and cell motion [29–32]. A hallmark of classical jamming transitions – kinetic arrest over time as the density of the constituent particles rises – has been observed in living systems *in vitro* [33–38] and *in vivo* [39, 40].

In each of these diverse examples, the cellular collective can transition between two states: a lower-density state, where cells collectively behave in a gas-like or liquid-like manner and a higher density state, where cells collectively behave in

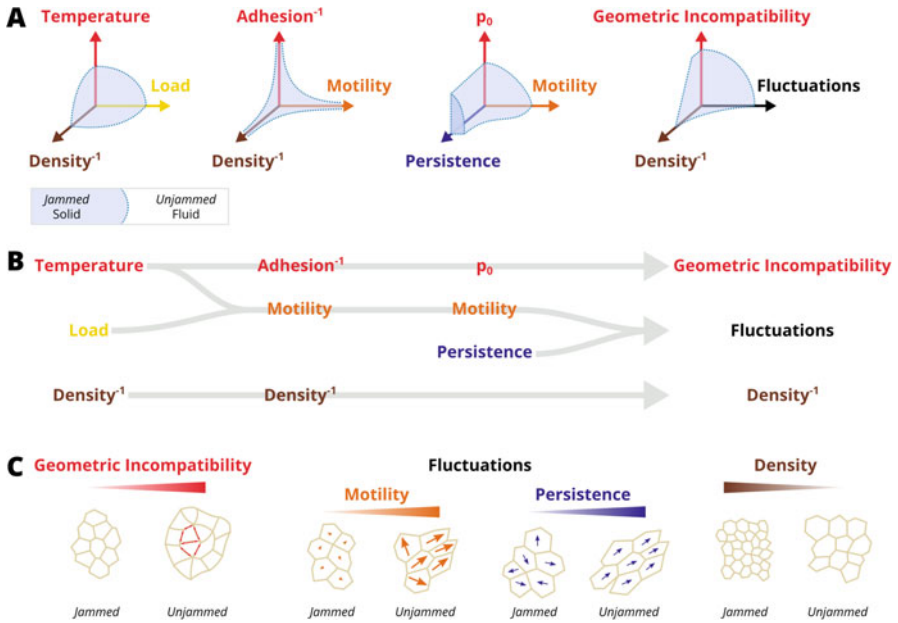


**Fig. 1 Evolution of phase diagrams for living systems.** (A) Phase diagrams for cell jamming were adapted from established work in soft matter physics (left-most panel), where close to the origin the system is solid-like (shaded in blue) and beyond the phase boundary the system is fluid-like [30, 31]. Proposed diagrams for cells introduced analogous variables describing more complex cell behaviors. A first proposed phase diagram for cell jamming (second panel) added inherent cell motility as a possible state variable [6]. At constant density, cell motility can be further decomposed into inherent motility and directional persistence, while adhesion is subsumed into a preferred shape parameter  $p_0$  (third panel) [41]. Because many cell parameters can contribute to collective cell motion, it has been proposed to recast the cell jamming phase diagram in terms of broad classes of parameters to facilitate predictions of collective motion (right-most panel) [42]. (B) Through-lines connecting the state variables for cell jamming. In inert materials, temperature and interparticle attraction are in opposition, so a natural evolution of that variable is cell–cell adhesion. External loads for inert materials can in turn be replaced by internal forcing, as can be caused by active, motile particles. Motility itself can be decomposed into different components such as absolute speed and its persistence, that is, the tendency of cells to continue migrating in a given direction. Adhesion, in turn, can be viewed as a component of intercellular force balance which can be represented as a preferred shape parameter. (C) The evolution of the cell jamming phase diagram has resulted in generalized parameters which encompass several different cell properties. Geometric incompatibility accounts for force balance between cells due to contractility, cell–cell adhesion, cytoskeletal elasticity, and related parameters. Fluctuations account for active cellular processes and its derivatives such as inherent motility, persistence, and others. Density for cell systems typically reflects number density, since area fraction is often unity

a solid-like manner. In the low-density state, cells are less constrained by their neighbors and may have less contact with them, thus allowing greater freedom to move; and, by contrast, cells in the high-density state have greater contact with their neighbors, restricting the ability of single cells to move. A multicellular system



that is increasing in density over time, for example due to the proliferation of the constituent cells, has thus been hypothesized to undergo a *jamming transition*, analogous to the observation of an increase in viscosity with increased particle density observed in granular, colloidal, or glassy materials (Box 1, Fig. 1). In some cases, density, per se, may not be increasing, but rather the contact between neighboring cells increasing [40] or extracellular space between them decreasing [39]; in all of these closely related, but physically distinct, situations, individual cells are increasingly constrained or caged by their neighbors.

As will become clear, many of the hallmarks of cell jamming arise from making analogies to inert materials. It is thus not surprising that early proposed phase diagrams for cell jamming [6] (Fig. 1A, second panel) drew upon already established work in soft matter physics (Fig. 1A, left panel) [30, 31]. However, as the field of collective cell jamming has matured, it has become clear that while the concept of phase transitions and state variables holds, the details are quite different between inert and living matter. Cells have active machinery to maintain their shape and can engage in persistent directed motion as opposed to random thermal motion of inert materials (Fig. 1A, third panel) [41]. More generally, cells are active matter which consume energy and can agitate their surroundings while simultaneously resisting changes due to their external environment (Fig. 1A, right panel) [42]. The recognition of this more complex behavior is reflected in the evolution of the proposed phase diagrams and state variables for cell jamming (Fig. 1B) resulting in general classes of variables as opposed to focusing on specific parameters (Fig. 1C). However, certain through-lines have remained, in particular that cell density is important, and also that developing metrics to recognize and characterize a change in phase is needed to establish that the material state has changed. Thus it is necessary to be familiar with the various changes in motion and mechanics that accompany changes in collective cell phase.

While the arrest of motion is the most easily recognizable feature of a cellular system undergoing a phase transition from a more fluid-like state toward a more solid-like state, several other system properties are expected to, and indeed have been observed to, change during this transition and impact biological function. In addition to the arrest of motion, these include changes in bulk rheology, dynamic heterogeneity, and structural changes; evidence of each of these in cellular systems is discussed below. Beyond that, we discuss how these hallmarks of phase transitions manifest in living systems in response to changing biologically relevant variables.

## 2.1 *Hallmarks of Collective Cellular Phase Transitions*

### 2.1.1 **Arrest of Motion**

In 2011, Angelini and colleagues demonstrated that, as cell density rises in a confluent layer of model epithelial cells (see Fig. 2A), the average migration speed of cells within the layer decreases in a manner that is consistent with a jamming or



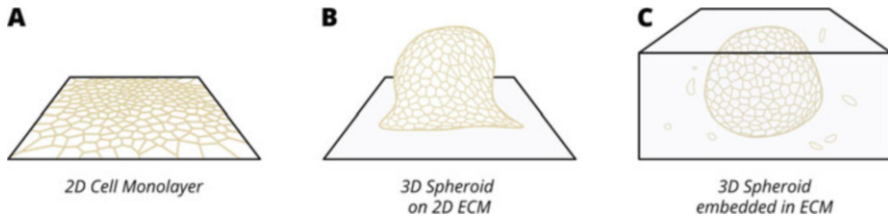


**Fig. 2 In vitro models for studying phase transitions.** Collective cellular phase transitions have been most commonly studied using (A) 2D monolayer cell culture. However, more complex 3D models have also been developed to study migration phase transitions. For example, spheroids can be used to study changes in cell phase by (B) placing them on 2D ECM [27, 28, 163], or (C) embedding them in 3D ECM [121, 130, 131]

glass transition [33]. In this experiment, all available surface area of the substrate was filled with cells – that is, observation of the system began at area fraction 1; subsequently, the number density of cells increased as cells proliferated (Fig. 1). As the number density of cells increased over time, individual cells necessarily decreased in their cross-sectional area (Fig. 1C, right panel, “density”). The authors drew parallels between the observed slowing of movements within the cellular collective with the behavior of a particulate system as it becomes increasingly crowded and approaches a glassy, or jamming, transition [33]. This seminal study was performed using the Madin-Darby Canine Kidney (MDCK) model epithelial line. The observation that system dynamics slow toward the total arrest of motion as cellular crowding increases due to the proliferation of cells in a confluent monolayer has since been shown in MDCK cells [37, 43, 44], immortalized and primary human bronchial epithelial cells (HBECs) [34, 45], and in cell lines derived from epithelial breast cancers [38, 46].

This density-dependent phase transition – relatively slower motions at relatively higher cell number densities – was later demonstrated to be due directly to differences in cell density and not a confounding effect occurring due to aging of the system such as depletion of nutrients. Saraswathibhatla and colleagues directly compared confluent monolayers of MDCK cells seeded at low versus high densities [36]. Consistent with previous reports in systems where cell density differences resulted from proliferation, here the low-density cell layers were considerably more motile than the high-density layers; therefore, the higher-density cell layers are interpreted to be closer to a jammed, solid-like state.

Changes in cell density giving rise to system-slowing toward arrest have also been observed in vivo during developmental processes [47]. During axis elongation in the developing zebrafish embryo, a solid-to-fluid transition was observed in the extending end of the axial tissue [39]. In this system, the posterior end of the embryo elongates, and cells at the mesodermal progenitor zone – the extending tip – initially display fluid-like movements; as elongation continues, these cells become incorporated into the presomitic mesoderm, which is more solid-like. The transition between the fluid-like and solid-like states is correlated with a gradient in the activity

of N-cadherins, such that increases in cell–cell adhesion gives rise to a decrease in extracellular space, solidifying the presomitic mesoderm. This change in behavior is confirmed both by observing cellular rearrangements and measuring the change in yield stress of the tissue.

### 2.1.2 Changes in Bulk Rheology

The change in yield stress measured during axis elongation of the developing zebra fish [39] highlights another key expectation of cell jamming transitions: if a phase change occurs, we expect to observe changes in bulk rheology of the system. In both jamming and glass transitions for inert materials, as the system becomes more solid-like, the viscosity increases and a bulk rigidity emerges [29–31, 48]. In 2D cell systems, measuring bulk rheology has been challenging, as the majority of the available techniques for measuring cell mechanics were developed to probe molecular or cellular-level properties. Local cellular mechanics can be measured using techniques such as AFM [49], optical tweezers [50], magnetic twisting cytometry [51, 52], Brillouin scattering [53], and more. Single-cell stiffness measurements may reveal evidence of dynamic heterogeneity [54], as discussed below, but bulk measurements are more traditional hallmarks of phase transitions. Though experiments have been limited in 2D contexts, Nnetu and colleagues showed that, for an expanding monolayer, the local elastic modulus of cells in lower-density areas was lower compared to in high-density areas, with the relationship between density and elastic modulus scaling as a weak offset power law [46]. Recent works have demonstrated that it is possible to directly measure the mechanics of cellular sheets by removing them from the underlying substrate [55], although it is unclear if a fluid-like layer could survive the process or how cell migration would proceed after removal.

Measurements of changing bulk rigidity have instead largely been used with 3D geometries (see Fig. 2B for an example system). For model spheroid systems, multiple techniques take advantage of the relatively large size and ease of handling to measure bulk rheology of the entire tissue [28]. These techniques include, amongst others, parallel-plate compression, micropipette aspiration, aggregate centrifugation, aggregate fracture, aggregate fusion, and laser ablation [28]. Micropipette aspiration in particular has found success in measuring collective phase changes in 3D cell systems [40, 56]. In micropipette aspiration, suction is applied to a material and its subsequent displacement through the pipette tip can be used to infer its mechanical properties. By changing the size of the pipette opening and pressure applied, it is possible to measure the mechanical properties of a range of living systems, from soft cells, which can have stiffness on the order of a few Pa [57], to tissues with stiffness up to the order of 10s of kPa [58]. When applied to a developing embryo, the Hannezo and Heisenberg groups find that the blastoderm undergoes fluidization and solidification by directly measuring the changes in bulk rheology that occur during this process using micropipette aspiration [56]. This collective transition is found to be driven by changes in cell–cell connectivity:

initially, cell–cell junctions are disrupted and the volume of the interstitial space increases, reducing the packing fraction of cells while the tissue fluidizes. As junctions reform and the interstitial volume is reduced, the tissue solidifies. Modeled as a rigidity percolation transition akin to what occurs in granular material [40], this provides clear evidence that collective transitions occur in biological systems.

That bulk rheology is tuned by interstitial volume in developing tissues had previously been found by measuring the local yield stress in the mesodermal progenitor zone [39] through the technique of ferrofluid deformation [59]. By implanting a force actuator inside the tissue, the authors were able to measure local yield stresses and found that the tissues with lower yield stresses had larger interstitial volume. Interestingly, this change in yield stress was correlated with changes in cellular motion, which is in contrast to the change in stiffness observed by micropipette aspiration of the developing blastoderm, where there was no obvious correlation with motion. This difference highlights that collective cell phase transitions are complex and can demonstrate some, but not all, features of glassy transitions, depending on the underlying mechanism which drives the transition.

### 2.1.3 Dynamic Heterogeneity

As inert systems undergo a density-dependent jamming transition – as the volume becomes more packed and each particle becomes caged by its neighbors – they exhibit dynamic heterogeneity, large fluctuations, and collectivity [32, 60–62]. These physical hallmarks have been observed in epithelial monolayer forces, stresses, migration patterns, and structure [6, 37]. Dynamic heterogeneity refers to the spatial correlations of dynamic properties; typically this has been applied to motion and velocity, but can also be applied to forces in cellular systems (see Box 1). Velocities are straightforward to measure in many cases but revealing the forces at work is more challenging. To measure the forces exerted by the cells on their matrix, traction force microscopy can be used. If the cell layer is confluent and assumed to be roughly uniform, it can be treated like a continuous material and forces inside the monolayer can also be calculated [63, 64]. Interestingly, dynamic heterogeneities in cellular systems can be observed using either forces [63, 64] or velocities [33], indicating the broad relevance of this physical hallmark in multicellular phase transitions.

Early evidence of dynamic heterogeneities of forces in cells was collected by Trepap and colleagues using MDCK cells on soft substrates [63]. The traction forces within an advancing monolayer are highly dynamic with large fluctuations that are not related to the structure of the underlying substrate or the presence of leader cells [63]. Interestingly, when the strength of these fluctuations is observed over time, they are found to not be normally distributed as is expected for random fluctuations but instead show evidence of exponentially decaying tails, a feature often associated with jamming behavior and dynamic heterogeneity. To further explore this behavior, the traction forces can be integrated in space; because the monolayer is not accelerating across the substrate, any unbalanced forces are necessarily balanced by

stress in the monolayer itself. Calculation of this monolayer stress reveals that cell monolayers primarily exist in a state of constant tension [63] that varies dramatically in time and space [64]. Indeed, these variations are remarkably similar to those observed in other glassy systems where spatial correlations spontaneously arise and fall within the layer. Here, Tambe and colleagues found that not only do packs form when looking at spatial correlations of the forces but also the average size of these packs grows as the system approaches arrest, as would be expected for glassy systems.

That monolayer stress demonstrates evidence of dynamic heterogeneity was a beautiful complement to the work by Angelini and colleagues discussed above [33]. In that study, beyond showing that MDCK cells arrested motion as density increased, they also showed the formation of packs of cells by segmenting based on velocity. By looking at the distribution of the fastest 20% of cells, they found that as cell density increased, the fast cells tended to cluster into packs; however, these packs were not tied to specific structural changes and were instead simply transient grouping that formed. Together these studies provided compelling initial evidence that dynamic heterogeneities occur in living systems [65].

Dynamic heterogeneity has also been observed in cell stiffness when Fujii and colleagues used AFM to study cell stiffness in an MDCK monolayer near the jamming transition [54]. Despite variations in individual cell stiffness, stiffness was correlated over long ranges among neighboring cells. These correlated mechanical properties depended on a long range actin filament network that formed within the collective. Interestingly, the length scale of the correlation in cellular stiffness was quite different from what had been observed when looking at monolayer stress. The formation of more permanent bonds via a long-range actin network raises questions as to whether these stiffness networks meet the traditional definition of dynamic heterogeneity in inert materials. Determining how these networks evolve in time will help clarify this in the future.

#### **2.1.4 Structural Changes**

Historically, hallmarks of jamming transitions relied on dynamic measurements because single snapshots in time were not thought to provide sufficient information to predict the material state. As mentioned above, recent works using machine learning have revealed that this is not necessarily the case. By testing a wide range of inert materials systems and simulations of collective material, the Liu group revealed that structural parameters could be derived which predict where particle rearrangements will occur [10–13]. Known as the “softness parameter,” this metric is based using many structural measurements and multidimensional fits. Interestingly, recent work has shown that this same parameter can be applied to models of cellular monolayers [13]. The vertex model, and the closely related Voronoi model, have been used extensively to model cellular monolayers by treating cells as space-filling polygons where each unit incurs an energy cost as it departs from its preferred perimeter and area [26, 41, 66, 67]. By applying their machine

learning approach to an *in silico* model of cells, Tah and coworkers were able to show that rearrangements and “cellular” motion can be predicted solely by looking at stationary images of the system.

Interestingly, the vertex model itself has been used to predict structural changes in living cell monolayers that are indicative of jamming in cell systems. For example, Bi et al. used the vertex model to predict that as cell shape, as measured by the cell shape parameter  $q$ , defined as the ratio of cell perimeter to the square root of cell area, decreases toward the cell shape of a pentagon ( $q \sim 3.81$ ), energy barriers to motion would arise and cell monolayers would jam (Fig. 1A) [66]. The importance of the pentagonal cell shape comes from the shape change required for a T1 transition: while hexagonal cells ( $q \sim 3.72$ ) *cannot* undergo a T1 transition, those cells which adopt a more elongated shape are able to rearrange freely. The vertex model predictions by Bi and colleagues rely on the assumption that cells have a preferred value of their cell shape, denoted  $p_0$ , and that rearrangements will occur as cells attempt to adopt this  $p_0$ ; experimentally, we can attempt to estimate  $p_0$  by measuring  $q$ . This prediction was subsequently confirmed in primary asthmatic cells in culture [45]. Subsequent works have demonstrated that in more complex systems – with active propulsion of the cells [41], heterogeneity of the constituents [68], or active fluctuations caused by cell division [44] – the absolute prediction of the critical shape index can change, but the overall trend that as the shape index decreases, cells become more jammed, holds.

The success of the shape index in marking transitions in collective cell motion inspired other structural markers of behavior to be investigated such as cellular aspect ratio [69]. Much like shape index, the average aspect ratio of the cells in a collective monolayer decreases as the cells approach jamming. While not necessarily directly predictive for comparisons across cell types, changes in aspect ratio are predictive of cell jamming across a range of systems, including inert materials [69], asthmatic and healthy lung cells [70], and cell lines of different metastatic potential [38]. Beyond aspect ratio, other order parameters have been shown to be indicative of collective cell behavior as well, with changes in cell volume indicating transitions from gas-like to liquid-like behavior and changes in cell shear indicating transitions from liquid-like to solid-like behavior [43].

The length scale over which different order parameters are predictive of cell behavior remains unclear. For example, in 3D model tumors (Fig. 2C), cell shape changes from the core to the periphery [71] and appears to be predictive of how dynamic, or fluid-like, the cells are [72]. This suggests that changes in structural parameters could be used to assess mesoscopic shifts in material phase on the length scale of several cells. However, these measurements, as with the others highlighted here for living cells, largely quantify average as opposed to local behavior and are often best understood as characterizing relative changes in state. Softness measurements can predict local behavior but have not yet been applied to living cell systems, only model ones where the individual constituents are homogeneous [13]. Whether local behavior is universally predictable from structural measurements in living systems remains unclear.

## 2.2 *Understanding Collective Cell Dynamics Through Phase Transitions*

In the jamming phase diagram of inert materials, changing the density or effective volume fraction is a conceptually straightforward method of affecting system behavior with clear spatial signatures of the change, yet it is not the only route to inducing a jamming/unjamming transition [30, 31]. In particular, temperature or agitation, along with applied or external load, have been suggested as two important control parameters for inert materials (Fig. 1A, left panel). Similarly, we expect in cell systems that it should be possible to induce fluidization and solidification by changing system parameters other than cell density. Indeed, the first proposed phase diagram for cell jamming was made by analogy to the ones for inert materials and suggested that cell–cell adhesion and cell motility could be alternative control parameters for cell jamming (Fig. 1A, second panel) [6]. As will be illustrated below, these parameters and many others can be used to describe cell jamming in what is effectively a multi-dimensional phase space [42, 72]. Despite the increase in complexity of working with biological systems, it is still possible to make predictions about collective cell behavior using effective phase diagrams and measurements of cellular properties.

### 2.2.1 **The Complex Roles of Cell Density, Division, and Maturation**

The most intuitive instance of multicellular phase transitions occurs when increasing cell number leads to arrest of motion, in an easily recognizable analogy to jamming of inert materials [6, 73]. However, the role of density and the impacts of cell crowding have been shown to be much more complicated than initially predicted. While the intuitive conception, in which an increase in cell number leads to arrest of motion, is a powerful framework for interpreting and predicting cellular phase transitions, it is also context-dependent, such that studies have shown an unexpected relationship between the phase state of the system and parameters, including density, cell division, and system maturation. For cellular systems, density can change in two distinct ways: first, volume fraction can change, as cells transition between a sub-confluent state, in which gaps between cells exist, to a confluent state, in which there are no gaps between cells (illustrated in Fig. 3A); second, a confluent layer of cells can change in density as cells divide and die, with cells modulating their volume and spread area to maintain coverage of the surface (illustrated in Fig. 1C).

At low density, where cells are sub-confluent, the interactions between cells can be broadly understood to fall into one of two categories: contact inhibition of locomotion (CIL), or cell–cell adhesion or aggregation [74, 75]. During CIL, cells make an initial contact which actively repolarizes the motility machinery such that cells reverse direction and migrate away from each other [74]; a sped-up time-lapse movie of two cells undergoing CIL is reminiscent of two billiard balls colliding. Importantly, the molecular mechanisms at play in CIL – namely, the collapse of

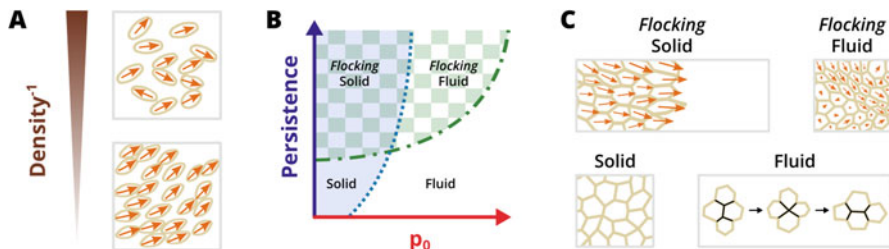


**Fig. 3 Flocking phase transitions.** (A) Increasing density of cells can trigger a kinetic phase transition, such that while cells at lower densities migrate individually, at higher densities they migrate as a collective cluster or flock [8, 137, 139]. (B) At constant density, varying cell preferred perimeter ( $p_0$ ) or directional persistence leads to solid-fluid transitions with or without flocking behavior [121, 144]. (C) Solid-like cellular collectives do not feature motion or rearrangements, while fluid-like collectives exhibit prominent local rearrangements characterized by T1 transitions throughout the system. Flocking solids and flocking fluids exhibit large-scale movement of collective clusters; however, flocking fluids include local rearrangement of individual cells whereas solid flocks do not demonstrate neighbor swapping

the leading-edge of a migrating cell in response to meeting a neighboring cell – are essential for guidance of collective migration in morphogenetic processes such as migration of the neural crest [74–78]. However, many epithelial cells will not undergo CIL when meeting; rather, they will aggregate together, forming cell–cell junctions [75, 79]. This process appears reminiscent of two soap bubbles meeting. Therefore, the nature of the transition from sub-confluent to confluent may depend in part on the inherent properties of the constituent cells: whether they are individualistic cells that will tend to undergo CIL vs. inherently communicable cells that will tend to aggregate. Cells which undergo CIL are able to form “supercells,” in which only the cells at the leading edge of the cell cluster have lamellipodia, and thus exhibit a fascinating and rich form of emergent collective behavior [80].

Regardless of whether cells tend to undergo CIL or adhere to their neighbors upon collisions, as groups of cells transition from sub-confluent to confluent, whether by proliferation, migration, or confinement, emergent multi-cellular phenomena occur. In cells that are inherently individualistic, such as sarcoma or mesenchymal cells, crowding can cause cells to behave as a collective [6, 81–83]. Friedl and colleagues demonstrated that melanoma and fibrosarcoma cells will switch from individual to collective migration when confined by their extracellular environment [81], despite the lack of cell–cell adhesion machinery expressed by these cells. The effect of confinement on collective migration in cancer is discussed below (Sect. 3.1). Similarly, cells with inherent tendency to aggregate (epithelial cells) also become increasingly collective under confinement or as density shifts from sub-confluent to confluent [34, 35, 84]. At subconfluent densities, epithelial cells can move freely and motion tends to be diffusive, indicating gas-like behavior, but as they become more crowded, they become caged by their neighbors and eventually transition from gas-like to liquid-like motion [34]. Further, as cell density increases, epithelial cells tend to cluster into ever-larger groups [43], where



intermediate densities and cluster sizes exhibit the fastest overall migration [35]. The transition from gas-like to liquid-like as epithelial cells proliferate from sub-confluent to confluent is captured by a volumetric order parameter [43].

Once a cell layer is confluent, such that there is no free space between neighboring cells, cell density can change considerably, generally on the order of ~2- to 4-fold from “low” to “high” density, all while maintaining confluence and intact intercellular junctions [33, 36, 37, 43, 44, 69, 85, 86]. As described above (Sect. 2.1.1), a hallmark of increasing cell density through proliferation within a confluent monolayer is arrest of motion and a transition from a fluid-like to a solid-like state. Another hallmark of phase transitions that occurs in systems with variable density is emergence of cooperative groups of cells, referred to as clusters, packs, or flocks; these are discussed in detail below (Sect. 2.2.4). Importantly, changes in density concur with structural changes, as cells become less elongated and variable in shape and become more rounded and isotropic in shape [36, 37, 43, 44, 69].

Depending on the experiment performed and the outcome measured, studies have reported both gradual and sharp changes in motion, correlation, structural signature, or material properties of the collective as a function of crowding and cell–cell contact [34, 40, 43, 45, 56, 69]. Importantly, in these experiments where cell density changes, whether the changes are moderate or extreme, other control parameters are observed to change in tandem. During growth in culture systems or during morphogenesis in development, cellular collectives mature and individual cells differentiate. During these processes, cell–substrate and cell–cell contacts mature, and cells change their expression profiles and cellular identities; these processes are occurring concurrently with cell division and arrest of motion [34, 45, 69]. Importantly, maturation and differentiation of epithelial layers have received attention as being drivers of a jamming transition, such that delayed maturation in the case of diseased cells corresponds to a delay in the jamming transition [45, 69]. Another control parameter predicted to play an important role in cellular phase transitions is active motility [41, 66, 70], or “cell jiggling,” [8] which can take the form of fluctuations at the cell–cell interface or be generated by traction forces exerted by cells (Fig. 1). As cell density increases or as cell–cell contacts increase, the concurrent arrest of motion may in some cases be due to a reduction in generation of active movements by the cells [39, 44]. While some progress has been made in teasing out the relative contributions of density changes in tandem with active force generation and system maturation, this remains a complex area with many open questions.

Though many studies have demonstrated the arrest of cell motion and other hallmarks of a jamming transition with increasing cell density or cell–cell contact, there are fewer studies investigating the inverse process. That is, how do collective properties such as motion, rheology, heterogeneity, and local coordination change when cell density or cell–cell contact are *reduced* throughout an initially jammed multicellular collective? There are limited studies relevant to this scenario, but the expectation is that reduced density or reduced cell–cell contact would cause an unjamming transition or tissue-level fluidization.



Mitotic rounding during cell divisions, extrusion of cells due to crowding, and loss of cells due to apoptosis can all disrupt cell–cell contacts or reduce the number of cells in a crowded monolayer. Though cell division, and the concomitant increase in cell number, tends to be associated with tissue solidification and jamming, cell division has also been shown to drive local rearrangements during normal gastrulation [87]. The stresses associated with these events have been predicted by physical models [88] and found experimentally [44] to induce local fluidization. During gastrulation in the chick embryo, a model of amniote morphogenesis, cell division is in fact necessary for cell movement, such that inhibition of cell division stabilizes the tissue, keeping it in a solid-like state without local movements [87]. The effect of reduced cell–cell contact without large changes in cell density has been investigated as well. During epiboly in the developing zebrafish, cells in the central blastoderm experience a loss of cell–cell contact that causes a sharp decrease in tissue viscosity; tissue-level fluidization is spatially restricted to this region [40, 56]. Together these data indicate that while in many circumstances, increases in cell number will promote collective arrest, cell divisions themselves can introduce active fluctuations which can fluidize a group of cells, pointing toward the complexity of understanding the role of even the most seemingly straightforward control parameters.

Cell extrusion is a widespread phenomenon used by both developing and homeostatic systems to maintain proper cell density. Cell extrusion and concomitant reduction in cell density occur when individual cells in the layer undergo apoptosis; in this case, the dying cell signals to its neighbors to contract around it, thus preventing disruption of monolayer integrity [89]. Cell extrusion can also occur in response to overcrowding in an apoptosis-independent manner, in which a fraction of cells undergo a progressive loss of junctions and are pushed out of the epithelium [90]. Importantly, extrusion of single cells or small groups promotes migration of nearby cells [91]. The effect of large-scale apoptosis on monolayer integrity and dynamics was recently investigated through use of an inducible-apoptosis system, in which epithelial cells expressing an inducible apoptosis-inducing construct were mixed with wild-type cells [92]. In this study, large-scale defects occurred, as one-third of the cells present in the monolayer expressed the apoptosis-inducing construct. In response to this large-scale disruption, cells spread out and exhibited migratory dynamic heterogeneities and structural hallmarks of an unjamming transition. Further work is needed to fully illuminate the behavior of density-dependent fluidization, to determine how reduction in cell numbers or contacts results in a solid-to-fluid phase transition across a wide variety of systems and circumstances.

### 2.2.2 Phase Transitions at Boundaries

In the examples discussed up to this point, cell density has changed relatively gradually, for example, through cell proliferation. These experiments logically lead to a related question: what happens when cell density changes dramatically or

suddenly, for example, in response to the creation of a wound or the removal of a barrier? It has been recognized for over a century that epithelial sheets will migrate into an empty space in an attempt to re-epithelialize and heal a perceived wound [93]. Collective movement of a group of cells into an open space or across a boundary occurs in the context of wound healing, development, and cancer.

Injury of the epithelium causes the formation of a free, unconstrained edge. The resulting asymmetry in both mechanical constraints and in engagement of mechanosensitive junctional complexes of cells at the wound boundary induces the formation of a leading edge [94]. Cells at the leading edge of a wound quickly adopt a front-back polarization, including the formation of a lamellipodium – a flat, spread cellular structure filled with branched actin and typically associated with cellular motility [95]. Though wounds *in vivo* involve a range of molecular and cellular mechanisms, including cell death and the release of damage-associated molecular patterns and reactive oxygen species [96], studies *in vitro* have revealed that the presence of a free edge itself, for example, created by removal of an inert, non-adhesive barrier, is sufficient to trigger leading edge repolarization and subsequent migration into the free space [97–99]. As the leading edge cells detect and begin to migrate into the newly open space, leader cells or leader groups (sometimes called fingers) can emerge [99]. In many cases these leader cells are designated by the environment, as geometry can determine where leader cells emerge, with areas of high curvature promoting formation of leader cells in a cytoskeletal tension-dependent manner [100], and leader cells can be “selected” by followers, with regions of high stress behind the leading edge preceding the emergence of a leader cell [101].

In response to the creation of a wound or gap, the initial movement of the cell monolayer occurs only at the wound boundary, with the first row of cells beginning to move and the bulk of monolayer remaining immobile [98]. Because these leading edge cells are mechanically and biochemically coupled to their neighbors [94], cellular movement begins to penetrate progressively deeper into the layer as each row of cells pulls on those behind them. This process manifests as a wave of movement that travels back into the layer from the front, where the initiation and propagation of these waves require both intact intercellular junctions and formation of cellular structures essential to migration such as lamellipodia [98, 102, 103]. After many rows of cells become migratory and begin to travel into the wound as a coordinated group, continuous mechanochemical waves of cell-stretching and contraction function to polarize the cell collective in the direction of movement [103, 104]. The migrating monolayer has characteristics of a glassy or fluid-like system, including spatial dynamic heterogeneity [37, 105], and can vary in density significantly from the leading edge into the bulk [102, 106, 107]. Importantly, changes in self-propulsion or alignment have also been found to be sufficient to unjam the leading edge of a wound, independent of density changes [108]. Together these data support a framework in which the advancing front of a monolayer can be understood to be fluid-like, whereas the immobile bulk of the collective remains solid-like, thus indicating that wound-healing can occur as a wave of unjamming.

As wounds heal, the two epithelial layers meet, whereupon barrier function and layer integrity can be restored. When these two cell sheets meet, they can either mix, with cells from each side crossing the collision line into the other layer, or a boundary can form, with each cell remaining adjacent to its original neighbors and not crossing that line. Mesenchymal cells readily mix following monolayer collision, while epithelial cells tend to form stable, long-lived boundaries [105, 109–111]. When two migratory epithelial monolayers collide, and do not mix, this is a form of a jamming transition [105] and indeed, just as a wave of unjamming propagates in response to a wound, a wave of jamming occurs in response to the collision with a dense monolayer [109]. Interestingly, in heterotypic collisions between epithelial monolayers of different densities, higher-density layers are able to displace lower-density layers with a speed proportional to the density gradient, moving the boundary until a new equilibrium is reached [110].

### 2.2.3 Density-Independent Phase Transitions

We have extensively discussed the evidence for, and circumstances leading to, phase transitions in multicellular systems in which cell density changes and thus drives the behavior of the system. However, in a vast array of biological systems, proliferation is balanced with apoptosis and extrusion, such that homeostatic balance is maintained [90, 112–114]. Both theoretical predictions [26, 115, 116] and experiments [90, 113] support the model that mechanical stresses essentially monitor cell density, orchestrating cell division when cells are too large or are stretched [117–119], and on balance, triggering extrusion of dead or living cells when cells are too compressed [89, 90, 112, 113, 119]. These observations therefore prompt the question: in these crowded cellular systems where overall density does not change, is it possible to see phase transitions between fluid-like and solid-like behaviors?

First theoretically, and then confirmed experimentally, such transitions have been found for cell layers. Theoretical models largely derive from the vertex model and subsequent improvements [26, 41, 66, 67]. To picture cell rearrangements, imagine that cells are randomly distributed in a layer, yet attached to their neighbors; these cells may be far from their preferred shape  $p_0$ , due to being either stretched or compressed. As cells begin to move toward their ideal shape, they necessarily push and pull on their neighbors; this push and pull is determined by the elasticity of the cell itself, by the strength and fluidity of its adhesions to its neighbors, and its ability to contract and pull against those constraints. As the strain increases on a cell–cell junction, it becomes energetically favorable to swap neighbors instead of maintaining the current neighbors. This neighbor swap is known as a T1 transition in the parlance of soft matter physics and is also known as intercalation in the language of developmental biology (see Fig. 3C). Intercalation is recognized as being critical to embryonic development and is controlled by the cytoskeletal structural machinery of the cells; moreover, in these developmental systems, intercalations can occur at constant density and lead to large scale rearrangements of the cell layer [120]. In

terms of fluid-like versus solid-like behavior, neighbor swapping facilitates motion toward a ground state where cells are able to better match their preferred shape. As the cells approach this ground state, the question of whether motion continues then becomes a question of energy balance. For example, if the density is low, cell–cell junctions are strained and it is easier to swap neighbors, whereas at high density the strain on cell–cell junctions is reduced and it requires more energy to swap neighbors. This balance of forces and striving toward a preferred shape is an intuitive reason why cell shape itself has emerged as a useful predictor of cell jamming dynamics in a wide range of systems.

With this physical picture in mind, it then becomes possible to investigate neighbor swapping both theoretically and experimentally to see how changes to cell properties can lead to transitions between fluid-like and solid-like states at nearly constant density. The phase diagram proposed for a constant-density system has evolved over time [45, 66, 67]; a popular, and as shown below, useful version uses axes of preferred cell shape, motility, and persistence (Fig. 1A) [41, 70, 121]. Preferred shape, denoted  $p_0$  and discussed in Sect. 2.1.4 above, is hypothesized to be set by a ratio between the cell-intrinsic properties of adhesion and contractility [26]. Experimental evidence for the role of these parameters individually in cell shape determination has shown that adhesion between neighboring cells tends to elongate cell boundaries, not unlike the lengthening that occurs when two strips of Velcro meet; cortical tension or contractility, on the other hand, has been shown to shorten cell–cell contact boundaries, as individual cells tend to become more rounded [26, 122–124]. Motility, or self-propulsion, is also hypothesized as a control parameter, as is directional persistence, or the tendency of an individual cell the move in a given direction [41].

One of the first demonstrations of the success of this framework, and in particular of the utility of measuring cell shape, came from studying primary human bronchial epithelial cells (HBECs) where cell motion slowed and cells approached a more uniform preferred shape over time [45, 69]. Interestingly, in this same cell system using well-differentiated HBECs, solid-like to fluid-like transitions can be provoked at constant density, triggered by the application of mechanical compression or exposure to ionizing radiation [45, 69, 70, 125, 126]. The biophysical characteristics of this collective fluidization were shown to be consistent with predictions from theoretical models in which cells that have a higher motility can more easily overcome energy barriers to rearrangements [41, 70]. Importantly, when these cells are triggered to unjam by either ionizing radiation or mechanical compression, they concurrently remodel their basal actin stress fibers [126], a process hypothesized to generate the propulsive forces responsible for the higher cellular motility that allows these cells to overcome the energy barriers to rearrangement [36, 127]. Furthermore, in this system, the HBEC layers fluidize without the characteristic weakening of cell–cell junctions that is observed in the epithelial-to-mesenchymal transition [70, 125].

The biochemical signals that initiate fluidization in cell collectives are still under investigation and may be disease or cell-type specific. For example, recent studies have found that in idiopathic pulmonary fibrosis, activation of EGFR,

Yap, and IL-6 can all promote collective fluidization in differentiated, previously stationary airway epithelial cells [128, 129]. However, these same studies found these pathways did not appear to be active in fluidization related to chronic obstructive pulmonary disease. Density-independent collective fluidization of an intact epithelial cell layer has been found to occur in other cell types, as well. For example, in MCF10A breast epithelial cells, overexpression of the small GTPase Rab5a, a regulator of endocytosis, induces collective fluidization in both 2D cell layers and 3D spheroids (Fig. 2A, C) [121, 130, 131]. Further, pharmacological activation of the GTPase RhoA fluidizes high-density confined monolayers of MDCK cells through reorganization of the actin cytoskeleton and generation of elevated tractions [36]. Importantly, the theoretical models utilized here essentially rely on force balance and, as such, we would expect to see changes in monolayer stress associated with changes in cell motion if the models of cell jamming hold. While not measured for all cellular systems where jamming/unjamming occurs at constant density, several of the systems highlighted here have had cell forces measured directly, or have examined a proxy for cellular forces, and they do indeed change dramatically through the observed phase transition [36, 121, 126, 130]. Together, current theoretical and experimental evidence supports the conclusion that, when cell density is roughly constant, it is through changes in cell force balance that cells can transition from one material state to another.

The variety of biological details across these studies demonstrates the usefulness of a unifying jamming framework, while also raising questions about its limits. Multiple distinct triggers – compression, ionizing radiation, elevated expression of Rab5a, and activation of RhoA, EGFR, YAP, or IL-6 – all result in qualitatively similar behaviors: initially jammed layers of epithelial cells become fluidized, wherein cells migrate in cooperative multicellular packs and swirls, while maintaining constant density. While it is unknown whether this range of triggers activates a common set of targets or converges on a single pathway, multiple studies have established a role for EGFR and ERK signaling in collective fluidization [70, 121, 129, 130], which have also been found to be essential in coordinated cell migration in other contexts [103, 132, 133].

Recently, it has been proposed that the density-dependent and density-independent phase diagrams could be unified into a single phase diagram where both density and cell-intrinsic properties are represented as control parameters (Fig. 1A, right panel) [42]. Here, motility and persistence, along with other forms of active movement such as tension fluctuations, are collapsed into the parameter “fluctuations,” while the constituent elements of preferred cell shape, adhesion, and cortical tension, are generalized to geometric incompatibility [134]. Future studies will have to explicitly explore this phase space, to understand how collective phase transitions depend on complex changes across multiple axes.

### 2.2.4 Local Coordination and Flocking

Emergent collective behavior is exemplified by dynamic heterogeneities of motion, characterized by transient clustering of cells into flocks or packs (Fig. 3). Coordinated motion within groups is found at all scales of life, from bacteria to cells of the neural crest during development or from cancer invasion to schools of fish and flocks of birds and beasts [135, 136]. Experimental and theoretical results suggest that three simple physical rules are sufficient to predict and interpret collective motions across multiple scales: first, individuals cannot occupy the same space as each other and therefore exhibit some degree of repulsion when close together; second, individuals are attracted to come close together when far apart or exhibit some degree of cohesion when in close proximity to each other; and third, neighboring individuals exhibit some degree of alignment with each other. This framework has been used to understand collective motions in both active matter and living systems [135]. Within the context of phase transitions in multicellular systems, phase space variables hypothesized or experimentally tested to control flocking in crowded multicellular systems include density, alignment, persistence, motile force, and cell–cell interactions. Though experimental details vary widely between studies, the emerging physical picture is one in which cellular crowding and the resulting physical constraint from neighboring cells causes cells to self-coordinate into locally aligned, locally cooperative, and locally coordinated migratory packs [33, 35–38, 70, 121, 137]. In practice, this has been measured by tracking cellular motions in a crowded system and measuring clusters of cells grouped by speed [33] or orientation [38, 70, 85], or by measuring the difference between each cell’s displacement and that of its nearest neighbors [36, 138].

Collective or cooperative motions in crowded multicellular systems have been explored both as a consequence of increased density, and also within constant-density confluent systems as a function of multiple control parameters (Fig. 3A, B). Multiple terms have been used to describe this transient clustering of cells and their usage is not always consistent across the literature. For our purposes, coordinated or collective movement refers to similarity in trajectory between neighboring cells, while cooperative movement connotes common purpose or an effect on behavior beyond what would occur in the absence of these clusters. Therefore, inert materials can exhibit collective behaviors, as multiple units act together through purely physical means, but it is only in living systems where we observe truly cooperative behaviors, as physical interactions are reinforced by biological responses. For example, groups of cells can form an actin-based superstructure across multiple cells, and groups of cells can behave as “supercells.” [80] Importantly, though cellular groupings are cooperative over the time scale that such a superstructure exists, membership in the group can change over time and therefore the group also remains dynamic. Further, in cellular systems where processes are not necessarily reversible, and a spontaneously formed grouping may not dissipate with the same kinetics as its formation, the difference between collective and cooperative could become meaningful.

Cooperativity has been observed, where beyond the emergence of clusters themselves, the group appears to work together as a cohesive whole. For example, several papers have found that the formation of clusters leads to higher migration speeds than would occur in the absence of clustering [37, 38, 70]. More broadly, whether the formation of clusters is determined by looking at the monolayer stress [37], velocity alignment [38, 70], or velocity magnitude [33], their presence seems to enhance the ability of cells to migrate in a dense environment (see Sect. 2.2.3). Moreover, as these clusters increase in size, the effect becomes more pronounced, wherein larger clusters lead to greater migration [38, 70].

In a foundational study published in 1995, Vicsek and colleagues theoretically explored emergent self-ordered motions characteristic of a kinematic phase transition in a system of self-propelled particles [139]. By modeling particles moving with a constant velocity, which align their direction of motion to neighboring particles within a certain radius, the authors found a strong role for both persistence (in the form of stochastic reorientation of the velocity vector) and for density. The result from this work with the largest impact on understanding cellular collectives was the observation that, at high density, the particles spontaneously formed flocks that moved collectively. This prediction was directly tested a decade later when different densities of highly migratory keratocytes were observed over time. Primary fish keratocytes have been shown to migrate with fast and highly persistent motion [140] and are classically used as a model to understand individual cell motion. As density was increased from sparse to crowded, a sharp transition from random motility to collective migration of clusters of cells was observed (Fig. 3A) [137].

Classic Vicsek style systems are different from those considered previously because they lack cell–cell adhesion and collective motion is, instead, largely driven by orientational coordination as opposed to direct force contact. Given the similarity of these collective packs to groups of animals, they are often called flocks and the transition is known as a flocking transition [141–143]. Interestingly, flocking transitions have recently been identified in epithelial layers as well, where cell adhesion does play a role [121]. In these types of transition, the preference of cells to orient with their neighbors helps control the overall phase. In work by Giavazzi et al., the authors extended existing self-propelled Voronoi models to include a preference of neighbors to mutually align; under these conditions, alignment preference, along with factors such as density and preferred cell shape, can define new types of phases of collective motion [144]. Interestingly, under these conditions, cells can form a *flocking solid* where the entire assembly moves as one unit, but neighbor exchange is rare or a *flocking liquid* where a subset of the cells form a flock, but still exchange neighbors with those cells outside of the flock (Fig. 3B, C). These types of orientationally induced alignment are part of a broad category of geometric constraints, also called topological constraints, which lead to collective phenomena in a broad range of soft matter, and in particular active matter, systems [145].

Though the overarching picture established above, wherein cellular crowding and resulting physical constraints promote the emergence of cell clusters, holds across many systems, the relationship between changing densities and details



of flock characteristics varies between systems. For example, increasing density due to proliferation can lead to larger, slower packs, as might be expected by analogy to glassy dynamics [6, 33, 34]. However, in other systems, higher density corresponds to smaller, slower packs [36] and reduced correlations in movement [46]. Similarly, increasing maturity and differentiation of the system, which can occur with relatively small increases in cell density, also results in packs that are smaller and slower [34, 45]. Therefore, while density increases or system maturation can both result in a jamming transition, as characterized by arrest of motion, the precise nature of the dynamic packs that form and dissipate during this process varies across experimental systems.

In addition to the emergence of collective and cooperative behaviors as a function of density changes, clusters of coordinated cells can form in already-crowded systems at a constant density (Fig. 3B, C) [45, 70, 121, 125, 130]. In epithelial or endothelial cell layers where cell–cell adhesion is present, cell migration within a crowded multicellular system can occur by multiple distinct regimes, as follows: (1) as local rearrangements (the simplest form being intercalation, also known as a T1 transition [146]); (2) as larger scale motions characterized by dynamic heterogeneity and formation of cooperative but temporary packs of coordinated cells; (3) as large scale motions where coordination is longer-lived and local rearrangements are rare or non-existent. Large-scale motile packs can form in the presence or absence of orientational effects and, as such, are referred to as dynamics heterogeneity, swirls, packs, or flocks, depending on the model used to describe the motion. One framework for comparing these distinct forms of motion is to construct a phase diagram that distinguishes between a flowing solid (also known as a flocking solid) and flowing fluid in addition to solid-like and fluid-like phases [121, 144]. In this conception, fluids have no barrier to local rearrangements and exhibit local T1 transitions freely, while flowing solids and flowing fluids both exhibit large-scale movement, with flowing solids moving as a bulk system with no local rearrangements, while flowing fluids exhibit packs and dynamic heterogeneities. A phase transition from solid-like to a flowing fluid has been demonstrated in multiple constant-density systems, as described above (Sect. 2.2.3) [45, 70, 121, 125, 128]. As with density-dependent phase transitions, the nature of dynamic packs can be variable. In particular, in differentiated primary human bronchial epithelial cells, which undergo a density-independent fluidization in response to mechanical compression [45, 69, 70], over time, packs of cells were observed to grow larger and move more quickly [70]. Experimental and theoretical work suggests that, in constant-density systems, cells can move more efficiently if they do so in groups, in a manner reminiscent of a peloton [38, 70].

### 3 Phase Transitions in Cancer

In recent years, it has become apparent that collective cellular movements play essential roles in cancer, during both invasion and dissemination. Histological evidence shows multicellular invasive strands and streams in cancers of both



mesenchymal and epithelial origin [147–155], and recent experiments with tissue explants and organoids directly demonstrate invasive dynamics of cancer cell collectives extending from the tumor mass into the surrounding ECM or stroma [72, 156, 157]. In addition to collective invasion, cellular collectives have been demonstrated to both exist in circulation and to be more effective than single cells at initiating metastases [158, 159]. Although the relationship between collective invasion from tumors and circulating tumor cell clusters has not been entirely elucidated, current evidence suggests that rather than forming by aggregation in circulation, that tumor cell clusters both leave the original tumor and subsequently seed a metastatic tumor through collective migration [159–161].

Together, these experiments paint a picture wherein collective cellular movements are central to cancer invasion, dissemination, and metastasis, and raise important questions about the role of phase transitions in cancer. How does the presence of the ECM change collective cell behavior? Or phrased another way, what is the role of soft or variable confinement as opposed to the hard barriers typically used in studies of collective motion. Another question is how do the phenotypic changes of individual cancer cells affect collective behavior? For example, if cells undergo either full or partial EMT, can we still apply the lessons of collective cell motion and jamming to these systems? Assuming phase transitions are occurring, what is their role in cancer? Beyond that, we can also ask what insights we can gain by applying the metrics and perspectives of physical phase transitions to studying, diagnosing, and treating cancer. Recent progress toward answering these questions is addressed in the following sections.

### ***3.1 Tumor Invasion: Force Balance***

Three-dimensional models of tumor invasion, including tissue explants, spheroids, and organoids, have been used as *in vitro* models that recapitulate many aspects of *in vivo* tumor formation and invasion. Though details vary across a range of experimental systems, these methods generally consist of a multicellular aggregate, which is capable of self-organization that can be precisely manipulated to adopt a particular spatial organization [162]. These multicellular aggregates are generally embedded in a 3D extracellular matrix, where their invasive behavior can be studied with greater temporal and spatial resolution than is possible with *in vivo* cancer models. In recent years, the lens of phase transitions has been applied to understand the invasion of cells from a tumor into the surrounding matrix. Taking together evidence from multiple studies, discussed below, a picture has emerged wherein tumors are composed of a core that exists in a solid-like phase, while the phase state of the periphery depends on the surrounding environment.

The structure, composition, and organization of the ECM around a spheroid play a significant role in determining the phase of the peripheral cells of a spheroid. One of the clearest demonstrations of this effect is from spheroids dropped on a flat surface as opposed to embedded in a matrix (Fig. 2B, C). In a series of papers

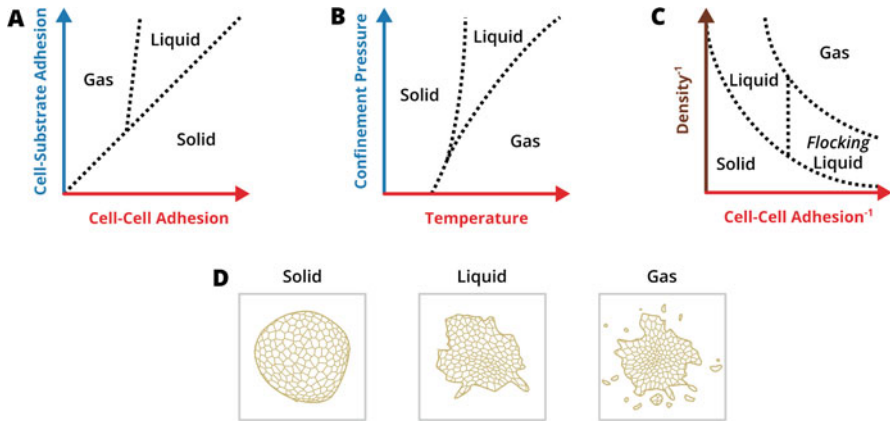


**Fig. 4 Phase transitions in cancer.** (A) For a spheroid on top of a 2D substrate, interactions between cell–cell adhesions and cell–substrate adhesions govern the solid, liquid, and gas phases describing the invasion of cells into the substrate [28]. (B) For spheroids embedded in 3D ECM, confinement pressure and temperature (encompassing structural, migratory, mechanical, and metabolic factors) govern the phase transitions [72]. (C) In vivo, the role of cell density has been shown to govern the phase transitions of collective invasion [82]. (D) A solid-like phase features no invasion. A liquid-like phase features tracks of cells collectively migrating away from the spheroid. And a gas-like phase features individual cells migrating and escaping from the spheroid

from the Brochard-Wyart group [27, 28, 163], spheroids of different cell types were placed on substrates of varying physical properties. By varying substrate stiffness or surface chemistry, it was then possible to change the resultant spheroid spreading on the surface and observe solid-like (no spreading), liquid-like (monolayer spreading) or gas-like (individual cell escape) behavior (Fig. 4A, D). The phase transition at the interface of the spheroid and the substrate depended on the force balance between cell–cell and cell–substrate adhesion. If cell–substrate adhesion was weak, then the cells remained as a solid-like collective and did not spread. If cell–substrate interactions supported adhesion of cells onto the substrate, then spreading could occur. In this case, whether the phase of the motile cells spreading at the interface was liquid-like (migrating collectively) or gas-like (migrating individually) was determined by the difference between cell–substrate and cell–cell adhesion; liquid-like monolayer spreading occurred if cell–cell adhesion was dominant whereas gas-like individual cell escape was dominant if cell–substrate adhesion was dominant.

For spheroids which are embedded in a 3D ECM, the fundamental concept of force balance between cell–substrate and cell–cell adhesion remains a powerful framework for predicting and interpreting cellular behaviors. However, in 3D, additional complications can arise. Even at the single-cell level, migration speed of cells through collagen matrices is controlled by parameters including cell tractions, cell stiffness, collagen density, and proteolytic capacity [157, 164, 165]. These same single-cell parameters in turn can affect collective migration. For example, the role of collagen properties has been studied by several groups [72, 82, 166]. Valencia et

al. [166] found that changing the collagen density surrounding a spheroid changed the rate at which cells infiltrated the ECM from a spheroid. Low-density collagen was more permissive to invasion, while higher-density collagen slowed the rate of invasion. While this study showed this effect using a single-cell type, Kang et al. [72] showed that by varying both the cell type comprising the spheroid and the collagen concentration, it was possible to observe solid-like, liquid-like, and gas-like phases in the embedded spheroid and surrounding invasion front (Fig. 4B). Importantly, in this 3D study, the cells behaved in a manner that is consistent with the lessons learned from the Brochard-Wyart group's work at the 3D/2D interface. A similar balance of cell–cell adhesion and confinement effects was observed by Ilina and colleagues, even for *in vivo* measurements (Fig. 4C) [82]. However, unlike in the studies led by Valencia and Kang where the collagen matrix was homogeneous, Ilina et al. observed invasion in collagen-based systems that were structured to match those found *in vivo*, as well collagen seeded with fibroblasts. When fibroblasts were embedded in the collagen, they oriented collagen fibers and created micro-tracks through the collagen. Strikingly, they observed that invasion occurred along the structural features of collagen in a manner very reminiscent of their *in vivo* findings. Interestingly, they also found that invasion can arrest depending on ECM structure and lead the cells to “rejam” in a new location, even if the cells are highly invasive and non-epithelial in character. This is consistent with previous findings from the same group [81] and highlights the diverse effects that the ECM can have on directing and controlling collective cell motion in cancer.

Beyond the structure of collagen itself, cancer cells can remodel their surrounding ECM in a manner which changes the collective cellular phase. For example, Carey et al. [167] found that when spheroids of MCF10A cells were embedded in collagen, they did not invade and remained relatively stationary and solid-like, whereas MDA-MB-231 cells would degrade and remodel collagen and thus were able to invade and migrate into the surrounding ECM. Interestingly, when the two cell types were co-cultured in a spheroid, the MCF10A cells became “invasive” because they were able to migrate along the tracks formed by the MDA-MB-231 cells. In a follow-up study [168], the same authors demonstrated that there are also signaling changes that occur during this invasion process; as epithelial cells transit from the epithelial compartment to the stromal compartment, the change in their local ECM promotes biochemical changes which lead to the epithelial cells adopting a more invasive phenotype. Moreover, when the stromal ECM was stiffened, such as might occur by cellular remodeling during cancer, this invasive phenotype was further reinforced, highlighting how changes in the collagen network can lead to complex cell–cell interactions. Beyond single-cell effects, the ECM can also be deformed by collective cellular effects. If cells within a relatively stationary spheroid embedded in collagen begin to overexpress Rab5a, large-scale collective motion can be triggered at the surface of the spheroid [130]. This motion in turn deforms the collagen matrix due to the applied stress of the motile spheroid. Ilina et al. [82] similarly observed that, invasion can more easily proceed along structured as opposed to randomly oriented ECM.

### 3.2 *Cell Jamming as Cell Phenotype Changes*

As was illustrated above with the changing invasiveness of co-cultured versus mono-cultured spheroids in Carey et al. [167], the phenotype of the cells which comprise a spheroid or tumor can dramatically change the collective phase. Interestingly, recent results have demonstrated that the jamming process itself may contribute to new phenotypes arising spontaneously in the system. Building on their work showing that overexpression of Rab5a can fluidize the outer monolayer of a spheroid and subsequently rearrange the surrounding collagen [130], the Scita group has demonstrated that the resultant stresses on the cells provoke changes in nuclear properties such as increased nuclear stiffening and DNA damage [131]. In this system, when the cells continue to be subjected to mechanical stresses, they take on traits of malignant cells, suggesting that mechanically driven phenotype changes can contribute to cancer development.

The impact of collective mechanics and jamming on cell phenotypes has also been investigated by Han et al. [71], where the authors grew spheroids in situ in a collagen matrix. As the spheroids evolved over time, a solid core developed while cell motion was more fluid-like in the invasive protrusions. Additionally, the cells in the invasive front were softer and more active, and, as such, had a phenotype more consistent with cancerous cells. Interestingly, the phenotype was not a permanent change in cell behavior and instead was due to geometric location; if cells swapped places with neighbors, they swapped phenotypes as well. The authors hypothesized that intratumor stress was driving fluid flow from core cells to peripheral ones, which in turn led to changes in phenotype.

While the role of mechanically induced changes in phenotype is a relatively new concept, the most commonly cited change in cell behavior during cancer is EMT. EMT, the epithelial-to-mesenchymal transition, is a transcriptionally driven process whereby epithelial cells progressively lose epithelial characteristics, including apical-basal polarity and barrier function, while simultaneously progressively gaining mesenchymal characteristics, including front-back polarity and individual migratory capacity [169, 170]. EMT was initially conceptualized to explain a phenotypic switch from epithelial to mesenchymal, whereupon single cells could be generated and gain the ability to migrate long distances [171–173], and gained wide recognition for its potential to explain cancer invasion and metastasis [174]. However, both understanding of underlying mechanisms and recognition of the nuance of this process have vastly increased in recent years, and EMT is now viewed as a dynamic process used by a range of cell types to interact with and respond to their environment. Importantly, there exists a spectrum of hybrid epithelial–mesenchymal states with a range of phenotypes, migratory capacity, adhesion, and collectivity [175–177]. As our understanding of EMT has evolved, it has become widely recognized that partial EMT allows collective cell migration without full individualization to mesenchymal cells [178–180], and has thus become a central framework for understanding collective phase transitions in development, wound healing, and cancer [177]. As such, early theoretical identification of cellular phase

transitions came with speculation that collective fluidization might be explained biologically by the EMT [41, 66].

The relationship between collective phase transitions and EMT remains an active area of investigation with many open questions, including around the role of adhesion in general and E-cadherin in particular. During EMT, as cells transition from epithelial to mesenchymal phenotypes, they change their adhesion protein profiles, with a notable loss of E-cadherin. Under such conditions, individual cell migration becomes more likely, and confinement of the collective is reduced. The hypothesis that loss of adhesion is critical for cancer migration is supported by evidence showing that diminished E-cadherin is associated with increased metastasis [181, 182]. However, E-cadherin is not solely responsible for cell–cell adhesion, while the loss of it leads to a host of downstream transcriptional changes, pointing toward a complex role in cancer [181, 182]. Moreover, recent evidence has found that both the presence of E-cadherin and the lack of observed EMT may not be barriers to the development of metastases [183–185]. That collective motion is not dependent on the loss of E-cadherin or initiation of an EMT program has also recently been confirmed in healthy tissues. For example, in the developing embryo, a fluid-like state with local rearrangements through T1 transitions can occur without evidence of EMT and with maintenance of intact junctions [186–188], while *in vitro* studies have shown that unjamming transitions can be triggered without EMT by multiple stimuli [70, 125]. Therefore, it has been suggested that the unjamming transition and the epithelial-mesenchymal transition are two distinct but complementary gateways to collective migration through fluidization [70, 125, 189–191]. Whether, and how, these transitions act together, in cooperation or in opposition, remains an open question.

### ***3.3 What Is the Role of the Jammed State in Cancer?***

The physics of cell jamming and collective cell phases changes appear to be universal; current evidence indicates that, all cells can undergo some degree of jamming behavior. For example, Kim et al. investigated collective cell motion in 2D for a panel of breast cancer cells that included both epithelial and mesenchymal lines as well as ones that could and could not metastasize in live mice; in all cases the cells became more collective over time and demonstrated evidence of jamming [38]. In 3D samples, mesenchymal cells have been found to jam if collagen density is sufficiently high to confine motion [72, 81, 82]. The question then arises, what predictive power does jamming provide in terms of understanding, diagnosing, or treating cancer?

In terms of providing new understanding, the development of phase diagrams and models can provide a framework for interpreting how interventions at the cellular level can result in changes of collective cell dynamics (Figs. 1 and 4). Weaver et al. [192] had previously demonstrated that interventions targeting cell–cell adhesion led to changes of the 3D structure of healthy and cancerous cells; these

changes were later reinterpreted by Oswald et al. [193] as evidence for the role of jamming in cancer and its ability to shape tissue structure. While this particular example uses retrospective reasoning, it is now becoming increasingly clear that some behaviors in cancer cannot be understood without taking jamming into context such as those highlighted in Sect. 3.1. Going forward, it is possible that jamming may be needed to help resolve ongoing problems in understanding cancer. For example, EMT is thought to be critical to cancer development [194], but recent studies have questioned whether it is strictly necessary [82, 183–185]. While it was illustrated in Sect. 3.2 that EMT and unjamming are both routes to collective motion, it has also been demonstrated that mixtures of mesenchymal and epithelial cells are more likely to unjam [35]. Given that recent works have shown that unjamming increases metastasis in vivo [195], and that unjamming can precipitate damage to the cell nucleus [131], could EMT and unjamming work in concert to promote metastatic behavior? This is an open and ongoing area of investigation.

Despite the fact that the mechanism of unjamming in cancer remains unclear, the evidence that unjamming is associated with increased invasiveness can already provide new tools for diagnosing cancer. Cell shape, nuclear shape, and other morphological parameters are used to grade the severity of tumor biopsies; using tools from collective cell motion it should be now possible to better understand how these changes arose and whether or not they are predictive of cell migration and possible escape; indeed recent works have already found that unjamming in cancer models is associated with changes in cell shape [196]. This could be particularly attractive in the assessment of tumor margins where using cell shape to predict where, and to what degree, unjamming has occurred could prove predictive of disease state. Beyond shape indicators, cell stiffness is known to decrease during cancer development. This change was first identified in isolated cells [197, 198], and has recently been confirmed in patient samples [199]. While measurements of cell stiffness have already been proposed as a clinical marker of cancer [200], these measurements could similarly be incorporated into models of collective cell motion to better predict motile regions of tumors.

If unjamming is associated with increased metastasis and increased DNA damage, could the jammed state be tumor suppressive, as some authors suggest? [131] And if so, could inducing jamming help treat cancer? The answers to these questions are currently unclear, but a broad-based treatment that induces jamming is unlikely to be viable given that unjamming is critical in normal biological processes like wound healing. Moreover, it is unclear how jamming is related to the establishment of secondary metastasis. To date, experiments have focused on the primary tumor and those changes which lead to cell escape, but it is plausible that jamming could play a role in the establishment of metastases. For example, when discussing the role of EMT in the spread of cancer, the simplest description of EMT is that it leads to cell escape, while the reverse process, the mesenchymal to epithelial transition (MET), plays a role in the establishment of a new cancer site [201]. Is it possible that analogous processes could be described for cell jamming? If unjamming leads to cell escape, then does jamming lead to the establishment of metastases? Given that changes in the local environment can cause mesenchymal, invasive cells to rejam

[82], it is at least conceivable. A global description of the role of jamming in cancer is still lacking, but that does not preclude a more limited application of these ideas to treatment. For example, low levels of irradiation, such as might be experienced at the periphery of a target tumor, can induce unjamming in cell systems [125]. Would pharmacological treatment to induce local jamming mitigate some immediate term damage of treatment in healthy tissue? While such questions are still open, it is exciting to consider them and will undoubtedly lead to further research in this area.

## 4 Perspective for the Future

Cells exist in a crowded environment surrounded by extracellular matrices and other cells. These systems are typically highly regulated in terms of their biological function and tissue-level organization, yet are highly disordered at a local multicellular scale, exhibiting a structure reminiscent of disordered glassy or granular materials. This disordered structure could be treated as inevitable noise and changes in cell motion ascribed only to biochemical signaling effects, but, as we have highlighted in the chapter, cells undergo collective transitions that are highly reminiscent of those found in disordered materials. Moreover, transitions in both inert and living materials can be described using similar key state variables: density, cell shape constraints, and agitation. This new framework of treating tissues and cells as a collective material phase is still a relatively recent development but is already leading to new understanding in biological function [202]. In healthy tissues, operating near a jamming or critical transition allows for large-scale changes in tissue properties with relatively small local-scale changes [189]. In cancer, where normal cell processes are disrupted, these types of phase transitions still occur and can still be modeled using concepts from material science, but the role of such phase transitions remains less clear in terms of biological function or clinical implications. Future research will continue to explore if, for example, inducing jamming in a primary tumor could suppress metastasis in the short term? This line of thinking leads to further questions, including whether there would be long-term consequences if/when cells break free? Because it is clear that changes in the collective phase of multicellular systems play a crucial role in the development and progression of cancer, work toward answering these questions is active and ongoing.

## References

1. Dagogo-Jack I, Shaw AT (2018) Tumour heterogeneity and resistance to cancer therapies. *Nat Rev Clin Oncol* 15:81–94
2. Byun S et al (2013) Characterizing deformability and surface friction of cancer cells. *Proc Natl Acad Sci* 110:7580–7585
3. Vogelstein B et al (2013) Cancer genome landscapes. *Science* 339:1546–1558

4. McGranahan N, Swanton C (2015) Biological and therapeutic impact of Intratumor heterogeneity in cancer evolution. *Cancer Cell* 27:15–26
5. Anderson NM, Simon MC (2020) The tumor microenvironment. *Curr Biol* 30:R921–R925
6. Sadati M, Taheri Qazvini N, Krishnan R, Park CY, Fredberg JJ (2013) Collective migration and cell jamming. *Differentiation* 86:121–125
7. Pegoraro AF, Fredberg JJ, Park J-A (2016) Problems in biology with many scales of length: cell-cell adhesion and cell jamming in collective cellular migration. *Exp Cell Res* 343:54–59
8. Lenne P-F, Trivedi V (2022) Sculpting tissues by phase transitions. *Nat Commun* 13:664
9. Blauth E, Kubitschke H, Gottheil P, Grosser S, Käs JA (2021) Jamming in embryogenesis and cancer progression. *Front Phys* 9:666709
10. Schoenholz SS, Cubuk ED, Sussman DM, Kaxiras E, Liu AJ (2016) A structural approach to relaxation in glassy liquids. *Nat Phys* 12:469–471
11. Cubuk ED et al (2017) Structure-property relationships from universal signatures of plasticity in disordered solids. *Science* 358:1033–1037
12. Schoenholz SS, Cubuk ED, Kaxiras E, Liu AJ (2017) Relationship between local structure and relaxation in out-of-equilibrium glassy systems. *Proc Natl Acad Sci* 114:263–267
13. Tah I, Sharp TA, Liu AJ, Sussman DM (2021) Quantifying the link between local structure and cellular rearrangements using information in models of biological tissues. *Soft Matter* 17:10242–10253
14. Ellis GFR, Kopel J (2019) The dynamical emergence of biology from physics: branching causation via biomolecules. *Front Physiol* 9:1966
15. Anderson PW (1972) More Is Different. *Science* 177:393–396
16. Strogatz S et al (2022) Fifty years of ‘More is different’. *Nat Rev Phys* 4:508–510
17. Zaidel-Bar R (2013) Cadherin adhesome at a glance. *J Cell Sci* 126:373–378
18. Janiszewska M, Primi MC, Izard T (2020) Cell adhesion in cancer: beyond the migration of single cells. *J Biol Chem* 295:2495–2505
19. Castor LN (1968) Contact regulation of cell division in an epithelial-like cell line. *J Cell Physiol* 72:161–172
20. Abercrombie M (1970) Contact inhibition in tissue culture. *In Vitro* 6:128–142
21. Martz E, Steinberg MS (1972) The role of cell-cell contact in “contact” inhibition of cell division: a review and new evidence. *J Cell Physiol* 79:189–210
22. Huttenlocher A et al (1998) Integrin and cadherin synergy regulates contact inhibition of migration and motile activity. *J Cell Biol* 141:515–526
23. Halbleib JM, Nelson WJ (2006) Cadherins in development: cell adhesion, sorting, and tissue morphogenesis. *Genes Dev* 20:3199–3214
24. Takai Y, Miyoshi J, Ikeda W, Ogita H (2008) Nectins and nectin-like molecules: roles in contact inhibition of cell movement and proliferation. *Nat Rev Mol Cell Biol* 9:603–615
25. Zeng Q, Hong W (2008) The emerging role of the hippo pathway in cell contact inhibition, organ size control, and cancer development in mammals. *Cancer Cell* 13:188–192
26. Farhadifar R, Röper J-C, Aigouy B, Eaton S, Jülicher F (2007) The influence of cell mechanics, cell-cell interactions, and proliferation on epithelial packing. *Curr Biol* 17:2095–2104
27. Douezan S et al (2011) Spreading dynamics and wetting transition of cellular aggregates. *Proc Natl Acad Sci U S A* 108:7315–7320
28. Gonzalez-Rodriguez D, Guevorkian K, Douezan S, Brochard-Wyart F (2012) Soft matter models of developing tissues and tumors. *Science* 338:910–917
29. Behringer RP, Chakraborty B (2019) The physics of jamming for granular materials: a review. *Rep Prog Phys* 82:012601
30. Trappe V, Prasad V, Cipelletti L, Segre PN, Weitz DA (2001) Jamming phase diagram for attractive particles. *Nature* 411:772–775
31. Liu AJ, Nagel SR (1998) Jamming is not just cool any more. *Nature* 396:21–22
32. Liu AJ, Nagel SR (2010) The jamming transition and the marginally jammed solid. *Annu Rev Cond Matter Phys* 1:347–369



33. Angelini TE et al (2011) Glass-like dynamics of collective cell migration. *Proc Natl Acad Sci* 108:4714–4719
34. Garcia S et al (2015) Physics of active jamming during collective cellular motion in a monolayer. *Proc Natl Acad Sci* 112:15314–15319
35. Castro MG, Leggett SE, Wong IY (2016) Clustering and jamming in epithelial–mesenchymal co-cultures. *Soft Matter* 12:8327–8337
36. Saraswathibhatla A, Notbohm J (2020) Traction and stress fibers control cell shape and rearrangements in collective cell migration. *Phys Rev X* 10:011016
37. Vishwakarma M, Thurakkal B, Spatz JP, Das T (2020) Dynamic heterogeneity influences the leader–follower dynamics during epithelial wound closure. *Philos Trans R Soc Lond B Biol Sci* 375:20190391
38. Kim JH et al (2020) Unjamming and collective migration in MCF10A breast cancer cell lines. *Biochem Biophys Res Commun* 521:706–715
39. Mongera A et al (2018) A fluid-to-solid jamming transition underlies vertebrate body axis elongation. *Nature* 561:401–405
40. Petridou NI, Corominas-Murtra B, Heisenberg C-P, Hannezo E (2021) Rigidity percolation uncovers a structural basis for embryonic tissue phase transitions. *Cell* 184:1914–1928.e19
41. Bi D, Yang X, Marchetti MC, Manning ML (2016) Motility-driven glass and jamming transitions in biological tissues. *Phys Rev X* 6:021011
42. Lawson-Keister E, Manning ML (2021) Jamming and arrest of cell motion in biological tissues. *Curr Opin Cell Biol* 72:146–155
43. Yang H et al (2021) Configurational fingerprints of multicellular living systems. *Proc Natl Acad Sci* 118:e2109168118
44. Devany J, Sussman DM, Yamamoto T, Manning ML, Gardel ML (2021) Cell cycle-dependent active stress drives epithelia remodeling. *Proc Natl Acad Sci* 118:e1917853118
45. Park J-A et al (2015) Unjamming and cell shape in the asthmatic airway epithelium. *Nat Mater* 14:1040–1048
46. Nnetu KD, Knorr M, Pawlizak S, Fuhs T, Käs JA (2013) Slow and anomalous dynamics of an MCF-10A epithelial cell monolayer. *Soft Matter* 9:9335–9341
47. Hannezo E, Heisenberg C-P (2019) Mechanochemical feedback loops in development and disease. *Cell* 178:12–25
48. Mattsson J et al (2009) Soft colloids make strong glasses. *Nature* 462:83–86
49. Viljoen A et al (2021) Force spectroscopy of single cells using atomic force microscopy. *Nat Rev Methods Primer* 1:1–24
50. Zhang H, Liu K-K (2008) Optical tweezers for single cells. *J R Soc Interface*. <https://doi.org/10.1098/rsif.2008.0052>
51. Wang N, Butler JP, Ingber DE (1993) Mechanotransduction across the cell surface and through the cytoskeleton. *Science* 260:1124–1127
52. Puig-De-Morales M et al (2001) Measurement of cell microrheology by magnetic twisting cytometry with frequency domain demodulation. *J Appl Physiol* 91:1152–1159
53. Prevedel R, Diz-Muñoz A, Ruocco G, Antonacci G (2019) Brillouin microscopy: an emerging tool for mechanobiology. *Nat Methods* 16:969–977
54. Fujii Y et al (2019) Spontaneous spatial correlation of elastic modulus in jammed epithelial monolayers observed by AFM. *Biophys J* 116:1152–1158
55. Efremov YM et al (2021) Mechanical properties of cell sheets and spheroids: the link between single cells and complex tissues. *Biophys Rev* 13:541–561
56. Petridou NI, Grigolon S, Salbreux G, Hannezo E, Heisenberg C-P (2019) Fluidization-mediated tissue spreading by mitotic cell rounding and non-canonical Wnt signalling. *Nat Cell Biol* 21:169–178
57. Hochmuth RM (2000) Micropipette aspiration of living cells. *J Biomech* 33:15–22
58. Aoki T, Ohashi T, Matsumoto T, Sato M (1997) The pipette aspiration applied to the local stiffness measurement of soft tissues. *Ann Biomed Eng* 25:581–587
59. Serwane F et al (2017) In vivo quantification of spatially varying mechanical properties in developing tissues. *Nat Methods* 14:181–186

60. Berthier L, Flenner E, Szamel G (2019) Glassy dynamics in dense systems of active particles. *J Chem Phys* 150:200901
61. Berthier L (2011) Dynamic heterogeneity in amorphous materials. *Physics* 4:42
62. Lu (陸述義) PJ, Weitz DA (2013) Colloidal particles: crystals, glasses, and gels. *Annu Rev Condens Matter Phys* 4:217–233
63. Trepats X et al (2009) Physical forces during collective cell migration. *Nat Phys* 5:426–430
64. Tambe DT et al (2011) Collective cell guidance by cooperative intercellular forces. *Nat Mater* 10:469–475
65. Garrahan JP (2011) Dynamic heterogeneity comes to life. *Proc Natl Acad Sci* 108:4701–4702
66. Bi D, Lopez JH, Schwarz JM, Manning ML (2015) A density-independent rigidity transition in biological tissues. *Nat Phys* 11:1074–1079
67. Bi D, Lopez JH, Schwarz JM, Manning ML (2014) Energy barriers and cell migration in densely packed tissues. *Soft Matter* 10:1885–1890
68. Li X, Das A, Bi D (2019) Mechanical heterogeneity in tissues promotes rigidity and controls cellular invasion. *Phys Rev Lett* 123:058101
69. Atia L et al (2018) Geometric constraints during epithelial jamming. *Nat Phys* 14:613–620
70. Mitchel JA et al (2020) In primary airway epithelial cells, the unjamming transition is distinct from the epithelial-to-mesenchymal transition. *Nat Commun* 11:5053
71. Han YL et al (2020) Cell swelling, softening and invasion in a three-dimensional breast cancer model. *Nat Phys* 16:101–108
72. Kang W et al (2021) A novel jamming phase diagram links tumor invasion to non-equilibrium phase separation. *iScience* 24:103252
73. Henkes S, Fily Y, Marchetti MC (2011) Active jamming: self-propelled soft particles at high density. *Phys Rev E* 84:040301
74. Roycroft A et al (2018) Redistribution of adhesive forces through Src/FAK drives contact inhibition of locomotion in neural crest. *Dev Cell* 45:565–579.e3
75. Mayor R, Carmona-Fontaine C (2010) Keeping in touch with contact inhibition of locomotion. *Trends Cell Biol* 20:319–328
76. Roycroft A, Mayor R (2016) Molecular basis of contact inhibition of locomotion. *Cell Mol Life Sci* 73:1119–1130
77. Carmona-Fontaine C et al (2008) Contact inhibition of locomotion in vivo controls neural crest directional migration. *Nature* 456:957–961
78. Khataee H, Czirok A, Neufeld Z (2021) Contact inhibition of locomotion generates collective cell migration without chemoattractants in an open domain. *Phys Rev E* 104:014405
79. Fagotto F (2014) The cellular basis of tissue separation. *Development* 141:3303–3318
80. Shellard A, Mayor R (2019) Supracellular migration – beyond collective cell migration. *J Cell Sci* 132:jcs226142
81. Haeger A, Krause M, Wolf K, Friedl P (2014) Cell jamming: collective invasion of mesenchymal tumor cells imposed by tissue confinement. *Biochim Biophys Acta BBA Gen Subj* 1840:2386–2395
82. Iliina O et al (2020) Cell–cell adhesion and 3D matrix confinement determine jamming transitions in breast cancer invasion. *Nat Cell Biol* 22:1103–1115
83. Szabó A et al (2016) In vivo confinement promotes collective migration of neural crest cells. *J Cell Biol* 213:543–555
84. Xi W, Sonam S, Beng Saw T, Ladoux B, Teck Lim C (2017) Emergent patterns of collective cell migration under tubular confinement. *Nat Commun* 8:1517
85. Angelini TE, Hannezo E, Trepats X, Fredberg JJ, Weitz DA (2010) Cell migration driven by cooperative substrate deformation patterns. *Phys Rev Lett* 104:168104
86. Nehls S, Nöding H, Karsch S, Ries F, Janshoff A (2019) Stiffness of MDCK II cells depends on confluency and cell size. *Biophys J* 116:2204–2211
87. Firmino J, Rocancourt D, Saadaoui M, Moreau C, Gros J (2016) Cell division drives epithelial cell rearrangements during gastrulation in Chick. *Dev Cell* 36:249–261
88. Ranft J et al (2010) Fluidization of tissues by cell division and apoptosis. *Proc Natl Acad Sci* 107:20863–20868

89. Rosenblatt J, Raff MC, Cramer LP (2001) An epithelial cell destined for apoptosis signals its neighbors to extrude it by an actin- and myosin-dependent mechanism. *Curr Biol* 11:1847–1857
90. Marinari E et al (2012) Live-cell delamination counterbalances epithelial growth to limit tissue overcrowding. *Nature* 484:542–545
91. Moitrier S et al (2019) Local light-activation of the Src oncoprotein in an epithelial monolayer promotes collective extrusion. *Commun Phys* 2:1–11
92. Yuan Y et al (2022) Recovery of structural integrity of epithelial monolayer in response to massive apoptosis-induced defects. 2022.08.08.503238 Preprint at <https://doi.org/10.1101/2022.08.08.503238>
93. Ruth ES (1911) Cicatrization of wounds in vitro. *J Exp Med* 13:422–424
94. Mayor R, Etienne-Manneville S (2016) The front and rear of collective cell migration. *Nat Rev Mol Cell Biol* 17:97–109
95. Krause M, Gautreau A (2014) Steering cell migration: lamellipodium dynamics and the regulation of directional persistence. *Nat Rev Mol Cell Biol* 15:577–590
96. Enyedi B, Niethammer P (2015) Mechanisms of epithelial wound detection. *Trends Cell Biol* 25:398–407
97. Klarlund JK, Block ER (2011) Free edges in epithelia as cues for motility. *Cell Adhes Migr* 5:106–110
98. Serra-Picamal X et al (2012) Mechanical waves during tissue expansion. *Nat Phys* 8:628–634
99. Poujade M et al (2007) Collective migration of an epithelial monolayer in response to a model wound. *Proc Natl Acad Sci* 104:15988–15993
100. Rausch S et al (2013) Polarizing cytoskeletal tension to induce leader cell formation during collective cell migration. *Biointerphases* 8:32
101. Vishwakarma M et al (2018) Mechanical interactions among followers determine the emergence of leaders in migrating epithelial cell collectives. *Nat Commun* 9:3469
102. Tlili S et al (2018) Collective cell migration without proliferation: density determines cell velocity and wave velocity. *R Soc Open Sci* 5:172421
103. Hino N et al (2020) ERK-mediated Mechanochemical waves direct collective cell polarization. *Dev Cell* 53:646–660.e8
104. Boockock D, Hino N, Ruzickova N, Hirashima T, Hannezo E (2021) Theory of mechanochemical patterning and optimal migration in cell monolayers. *Nat Phys* 17:267–274
105. Nnetu KD, Knorr M, Käs J, Zink M (2012) The impact of jamming on boundaries of collectively moving weak-interacting cells. *New J Phys* 14:115012
106. DeCamp SJ et al (2020) Epithelial layer unjamming shifts energy metabolism toward glycolysis. *Sci Rep* 10:18302
107. Nnetu KD, Knorr M, Strehle D, Zink M, Käs JA (2012) Directed persistent motion maintains sheet integrity during multi-cellular spreading and migration. *Soft Matter* 8:6913–6921
108. Chepizhko O et al (2018) From jamming to collective cell migration through a boundary induced transition. *Soft Matter* 14:3774–3782
109. Rodríguez-Franco P et al (2017) Long-lived force patterns and deformation waves at repulsive epithelial boundaries. *Nat Mater* 16:1029–1037
110. Heinrich MA, Alert R, Wolf AE, Košmrlj A, Cohen DJ (2022) Self-assembly of tessellated tissue sheets by expansion and collision. *Nat Commun* 13:4026
111. Heine P, Lippoldt J, Reddy GA, Katira P, Käs JA (2021) Anomalous cell sorting behavior in mixed monolayers discloses hidden system complexities. *New J Phys* 23:043034
112. Fernandez-Gonzalez R, Zallen JA (2012) Feeling the squeeze: live-cell extrusion limits cell density in epithelia. *Cell* 149:965–967
113. Eisenhoffer GT et al (2012) Crowding induces live cell extrusion to maintain homeostatic cell numbers in epithelia. *Nature* 484:546–549
114. Lohani S et al (2022) A novel role for PRL in regulating epithelial cell density by inducing apoptosis at confluence. *J Cell Sci* 135:jcs258550
115. Halter M, Elliott JT, Hubbard JB, Tona A, Plant AL (2009) Cell volume distributions reveal cell growth rates and division times. *J Theor Biol* 257:124–130

116. Puliafito A, Primo L, Celani A (2017) Cell-size distribution in epithelial tissue formation and homeostasis. *J R Soc Interface* 14:20170032
117. Puliafito A et al (2012) Collective and single cell behavior in epithelial contact inhibition. *Proc Natl Acad Sci U S A* 109:739–744
118. Tzur A, Kafri R, LeBleu VS, Lahav G, Kirschner MW (2009) Cell growth and size homeostasis in proliferating animal cells. *Science* 325:167–171
119. Gudipaty SA et al (2017) Mechanical stretch triggers rapid epithelial cell division through Piezo1. *Nature* 543:118–121
120. Walck-Shannon E, Hardin J (2014) Cell intercalation from top to bottom. *Nat Rev Mol Cell Biol* 15:34–48
121. Malinverno C et al (2017) Endocytic reawakening of motility in jammed epithelia. *Nat Mater* 16:587–596
122. Bertet C, Sulak L, Lecuit T (2004) Myosin-dependent junction remodelling controls planar cell intercalation and axis elongation. *Nature* 429:667–671
123. Otani T, Ichii T, Aono S, Takeichi M (2006) Cdc42 GEF Tuba regulates the junctional configuration of simple epithelial cells. *J Cell Biol* 175:135–146
124. Franke JD, Montague RA, Kiehart DP (2005) Nonmuscle Myosin II generates forces that transmit tension and drive contraction in multiple tissues during dorsal closure. *Curr Biol* 15:2208–2221
125. O’Sullivan MJ et al (2020) Irradiation induces epithelial cell unjamming. *Front Cell Dev Biol* 8:21
126. Phung T-KN, Mitchel JA, O’Sullivan MJ, Park J-A (2022) In airway epithelium, basal stem cells and their stress fibers remodel during the unjamming transition. 2022.08.18.504453 Preprint at <https://doi.org/10.1101/2022.08.18.504453>
127. Saraswathibhatla A, Henkes S, Galles EE, Sknepnek R, Notbohm J (2021) Coordinated tractions increase the size of a collectively moving pack in a cell monolayer. *Extreme Mech Lett* 48:101438
128. Stancil IT et al (2022) Interleukin-6–dependent epithelial fluidization initiates fibrotic lung remodeling. *Sci Transl Med* 14:eabo5254
129. Stancil IT et al (2021) Pulmonary fibrosis distal airway epithelia are dynamically and structurally dysfunctional. *Nat Commun* 12:4566
130. Palamidessi A et al (2019) Unjamming overcomes kinetic and proliferation arrest in terminally differentiated cells and promotes collective motility of carcinoma. *Nat Mater* 18:1252–1263
131. Frittoli E et al (2022) Tissue fluidification promotes a cGAS/STING-mediated cytosolic DNA response in invasive breast cancer. *Nature Mat.* <https://doi.org/10.1038/s41563-022-01431-x>
132. Aoki K et al (2017) Propagating wave of ERK activation orients collective cell migration. *Dev Cell* 43:305–317.e5
133. Matsubayashi Y, Ebisuya M, Honjoh S, Nishida E (2004) ERK activation propagates in epithelial cell sheets and regulates their migration during wound healing. *Curr Biol* 14:731–735
134. Moshe M, Bowick MJ, Marchetti MC (2018) Geometric frustration and solid-solid transitions in model 2D tissue. *Phys Rev Lett* 120:268105
135. Shellard A, Mayor R (2020) Rules of collective migration: from the wildebeest to the neural crest. *Philos Trans R Soc Lond B Biol Sci* 375:20190387
136. Vicsek T, Zafeiris A (2012) Collective motion. *Phys Rep* 517:71–140
137. Szabó B et al (2006) Phase transition in the collective migration of tissue cells: experiment and model. *Phys Rev E* 74:061908
138. Lin S-Z, Ye S, Xu G-K, Li B, Feng X-Q (2018) Dynamic migration Modes of collective cells. *Biophys J* 115:1826–1835
139. Vicsek T, Czirók A, Ben-Jacob E, Cohen I, Shochet O (1995) Novel type of phase transition in a system of self-driven particles. *Phys Rev Lett* 75:1226–1229
140. Lacayo CI et al (2007) Emergence of large-scale cell morphology and movement from local actin filament growth dynamics. *PLoS Biol* 5:e233

141. Toner J, Tu Y (1995) Long-range order in a two-dimensional dynamical XY model: how birds fly together. *Phys Rev Lett* 75:4326–4329
142. Toner J, Tu Y (1998) Flocks, herds, and schools: a quantitative theory of flocking. *Phys Rev E* 58:4828–4858
143. Toner J, Tu Y, Ramaswamy S (2005) Hydrodynamics and phases of flocks. *Ann Phys* 318:170–244
144. Giavazzi F et al (2018) Flocking transitions in confluent tissues. *Soft Matter* 14:3471–3477
145. Shankar S, Souslov A, Bowick MJ, Marchetti MC, Vitelli V (2022) Topological active matter. *Nat Rev Phys* 4:380–398
146. Duclut C, Paijmans J, Inamdar MM, Modes CD, Jülicher F (2022) Active T1 transitions in cellular networks. *Eur Phys J E* 45:29
147. Clark AG, Vignjevic DM (2015) Modes of cancer cell invasion and the role of the microenvironment. *Curr Opin Cell Biol* 36:13–22
148. Friedl P, Gilmour D (2009) Collective cell migration in morphogenesis, regeneration and cancer. *Nat Rev Mol Cell Biol* 10:445–457
149. Reymond N, d'Água BB, Ridley AJ (2013) Crossing the endothelial barrier during metastasis. *Nat Rev Cancer* 13:858–870
150. Friedl P (2004) Preshcification and plasticity: shifting mechanisms of cell migration. *Curr Opin Cell Biol* 16:14–23
151. Wicki A et al (2006) Tumor invasion in the absence of epithelial-mesenchymal transition: Podoplanin-mediated remodeling of the actin cytoskeleton. *Cancer Cell* 9:261–272
152. Vignjevic D et al (2007) Fascin, a novel target of  $\beta$ -catenin-TCF signaling, is expressed at the invasive front of human colon cancer. *Cancer Res* 67:6844–6853
153. Tarin D (2005) The fallacy of epithelial mesenchymal transition in neoplasia. *Cancer Res* 65:5996–6001
154. Wang X, Enomoto A, Asai N, Kato T, Takahashi M (2016) Collective invasion of cancer: perspectives from pathology and development. *Pathol Int* 66:183–192
155. Friedl P, Locker J, Sahai E, Segall JE (2012) Classifying collective cancer cell invasion. *Nat Cell Biol* 14:777–783
156. Cheung KJ, Gabrielson E, Werb Z, Ewald AJ (2013) Collective invasion in breast cancer requires a conserved basal epithelial program. *Cell* 155:1639–1651
157. Nguyen-Ngoc K-V et al (2012) ECM microenvironment regulates collective migration and local dissemination in normal and malignant mammary epithelium. *Proc Natl Acad Sci* 109:E2595–E2604
158. Cheung KJ, Ewald AJ (2016) A collective route to metastasis: seeding by tumor cell clusters. *Science* 352:167–169
159. Amintas S et al (2020) Circulating tumor cell clusters: united we stand divided we fall. *Int J Mol Sci* 21:2653
160. Cheung KJ et al (2016) Polyclonal breast cancer metastases arise from collective dissemination of keratin 14-expressing tumor cell clusters. *Proc Natl Acad Sci* 113:E854–E863
161. Maddipati R, Stanger BZ (2015) Pancreatic cancer metastases harbor evidence of polyclonality. *Cancer Discov* 5:1086–1097
162. Gunti S, Hoke ATK, Vu KP, London NR (2021) Organoid and spheroid tumor models: techniques and applications. *Cancers* 13:874
163. Douezan S, Dumond J, Brochard-Wyart F (2012) Wetting transitions of cellular aggregates induced by substrate rigidity. *Soft Matter* 8:4578–4583
164. Wolf K et al (2013) Physical limits of cell migration: control by ECM space and nuclear deformation and tuning by proteolysis and traction force. *J Cell Biol* 201:1069–1084
165. Córdor M et al (2019) Breast cancer cells adapt contractile forces to overcome steric hindrance. *Biophys J* 116:1305–1312
166. Valencia AMJ et al (2015) Collective cancer cell invasion induced by coordinated contractile stresses. *Oncotarget* 6:43438–43451

167. Carey SP, Starchenko A, McGregor AL, Reinhart-King CA (2013) Leading malignant cells initiate collective epithelial cell invasion in a three-dimensional heterotypic tumor spheroid model. *Clin Exp Metastasis* 30:615–630
168. Carey SP, Martin KE, Reinhart-King CA (2017) Three-dimensional collagen matrix induces a mechanosensitive invasive epithelial phenotype. *Sci Rep* 7:42088
169. Nieto MA, Huang RY-J, Jackson RA, Thiery JP (2016) EMT: 2016. *Cell* 166:21–45
170. Yang J et al (2020) Guidelines and definitions for research on epithelial–mesenchymal transition. *Nat Rev Mol Cell Biol* 21:341–352
171. Scarpa E et al (2015) Cadherin switch during EMT in neural crest cells leads to contact inhibition of locomotion via repolarization of forces. *Dev Cell* 34:421–434
172. Hay ED (2005) The mesenchymal cell, its role in the embryo, and the remarkable signaling mechanisms that create it. *Dev Dyn* 233:706–720
173. Hay ED (1995) An overview of epithelio-mesenchymal transformation. *Cells Tissues Organs* 154:8–20
174. Kalluri R, Weinberg RA (2009) The basics of epithelial-mesenchymal transition. *J Clin Invest* 119:1420–1428
175. Friedl P, Mayor R (2017) Tuning collective cell migration by cell–cell junction regulation. *Cold Spring Harb Perspect Biol* 9:a029199
176. Campbell K, Casanova J (2016) A common framework for EMT and collective cell migration. *Development* 143:4291–4300
177. Barriga EH, Mayor R (2019) Adjustable viscoelasticity allows for efficient collective cell migration. *Semin Cell Dev Biol* 93:55–68
178. Revenu C, Gilmour D (2009) EMT 2.0: shaping epithelia through collective migration. *Curr Opin Genet Dev* 19:338–342
179. Jolly MK et al (2015) Implications of the hybrid epithelial/mesenchymal phenotype in metastasis. *Front Oncol* 5:155
180. Aiello NM et al (2018) EMT subtype influences epithelial plasticity and mode of cell migration. *Dev Cell* 45:681–695.e4
181. Onder TT et al (2008) Loss of E-cadherin promotes metastasis via multiple downstream transcriptional pathways. *Cancer Res* 68:3645–3654
182. Bruner HC, Derksen PWB (2018) Loss of E-cadherin-dependent cell–cell adhesion and the development and progression of cancer. *Cold Spring Harb Perspect Biol* 10:a029330
183. Fischer KR et al (2015) Epithelial-to-mesenchymal transition is not required for lung metastasis but contributes to chemoresistance. *Nature* 527:472–476
184. Zheng X et al (2015) Epithelial-to-mesenchymal transition is dispensable for metastasis but induces chemoresistance in pancreatic cancer. *Nature* 527:525–530
185. Padmanaban V et al (2019) E-cadherin is required for metastasis in multiple models of breast cancer. *Nature* 573:439–444
186. Sutherland A, Keller R, Lesko A (2020) Convergent extension in mammalian morphogenesis. *Semin Cell Dev Biol* 100:199–211
187. Tada M, Heisenberg C-P (2012) Convergent extension: using collective cell migration and cell intercalation to shape embryos. *Development* 139:3897–3904
188. Wang X et al (2020) Anisotropy links cell shapes to tissue flow during convergent extension. *Proc Natl Acad Sci* 117:13541–13551
189. Fredberg JJ (2022) On the origins of order. *Soft Matter* 18:2346–2353
190. Atia L, Fredberg JJ, Gov NS, Pegoraro AF (2021) Are cell jamming and unjamming essential in tissue development? *Cells Dev* 168:203727
191. La Porta CAM, Zapperi S (2020) Phase transitions in cell migration. *Nat Rev Phys* 2:516–517
192. Weaver VM et al (1997) Reversion of the malignant phenotype of human breast cells in three-dimensional culture and in vivo by integrin blocking antibodies. *J Cell Biol* 137:231–245
193. Oswald L, Grosser S, Smith DM, Käs JA (2017) Jamming transitions in cancer. *J Phys D Appl Phys* 50:483001
194. Brabletz T, Kalluri R, Nieto MA, Weinberg RA (2018) EMT in cancer. *Nat Rev Cancer* 18:128–134

195. Käs J et al (2022) Cancer cell motility through unjamming impacts metastatic risk. Preprint at <https://doi.org/10.21203/rs.3.rs-1435523/v1>
196. Grosse S et al (2021) Cell and nucleus shape as an indicator of tissue fluidity in carcinoma. *Phys Rev X* 11:011033
197. Guck J et al (2005) Optical deformability as an inherent cell marker for testing malignant transformation and metastatic competence. *Biophys J* 88:3689–3698
198. Cross SE, Jin Y-S, Rao J, Gimzewski JK (2007) Nanomechanical analysis of cells from cancer patients. *Nat Nanotechnol* 2:780–783
199. Fuhs T et al (2021) Rigid tumors contain soft cancer cell. Preprint at <https://doi.org/10.21203/rs.3.rs-1114106/v1>
200. Cross SE, Jin Y-S, Rao J, Gimzewski JK (2020) Nanomechanical analysis of cells from cancer patients. In: *Nano-enabled medical applications*. Jenny Stanford Publishing
201. Bakir B, Chiarella AM, Pitarresi JR, Rustgi AK (2020) EMT, MET, plasticity, and tumor metastasis. *Trends Cell Biol* 30:764–776
202. Hannezo E, Heisenberg C-P (2022) Rigidity transitions in development and disease. *Trends Cell Biol* 32:433–444
203. Das M, Schmidt CF, Murrell M (2020) Introduction to active matter. *Soft Matter* 16:7185–7190
204. Bazellères E et al (2015) Control of cell–cell forces and collective cell dynamics by the intercellular adhesome. *Nat Cell Biol* 17:409–420
205. Berthier L, Biroli G (2011) Theoretical perspective on the glass transition and amorphous materials. *Rev Mod Phys* 83:587–645
206. Makse HA, Kurchan J (2002) Testing the thermodynamic approach to granular matter with a numerical model of a decisive experiment. *Nature* 415:614–617
207. Loi D, Mossa S, Cugliandolo LF (2008) Effective temperature of active matter. *Phys Rev E* 77:051111
208. Manoharan VN (2015) Colloidal matter: packing, geometry, and entropy. *Science* 349:1253751
209. Zhou EH et al (2009) Universal behavior of the osmotically compressed cell and its analogy to the colloidal glass transition. *Proc Natl Acad Sci* 106:10632–10637
210. Angell CA (1985) Spectroscopy simulation and scattering, and the medium range order problem in glass. *J Non-Cryst Solids* 73:1–17
211. Mauro NA, Blodgett M, Johnson ML, Vogt AJ, Kelton KF (2014) A structural signature of liquid fragility. *Nat Commun* 5:4616
212. Angell CA, Ueno K (2009) Soft is strong. *Nature* 462:45–46
213. Universal glass-forming behavior of in vitro and living cytoplasm | Scientific Reports. <https://www.nature.com/articles/s41598-017-14883-y>
214. Hakim V, Silberzan P (2017) Collective cell migration: a physics perspective. *Rep Prog Phys* 80:076601
215. Artime O, De Domenico M (2022) From the origin of life to pandemics: emergent phenomena in complex systems. *Philos Trans R Soc Math Phys Eng Sci* 380:20200410
216. Geyer D, Martin D, Tailleur J, Bartolo D (2019) Freezing a flock: motility-induced phase separation in polar active liquids. *Phys Rev X* 9:031043
217. Orlandi I (1975) A rational subdivision of scales for atmospheric processes. *Bull Am Meteorol Soc* 56:527–530
218. Blanchard GB, Fletcher AG, Schumacher LJ (2019) The devil is in the mesoscale: mechanical and behavioural heterogeneity in collective cell movement. *Semin Cell Dev Biol* 93:46–54
219. Galeotti G et al (2020) Synthesis of mesoscale ordered two-dimensional  $\pi$ -conjugated polymers with semiconducting properties. *Nat Mater* 19:874–880
220. Kleman M, Laverntovich OD (2003) *Soft matter physics: an introduction*. Springer
221. Tong H, Tanaka H (2019) Structural order as a genuine control parameter of dynamics in simple glass formers. *Nat Commun* 10:5596
222. Thorpe MF (1983) Continuous deformations in random networks. *J Non-Cryst Solids* 57:355–370

223. Lin J, Lerner E, Rosso A, Wyart M (2014) Scaling description of the yielding transition in soft amorphous solids at zero temperature. *Proc Natl Acad Sci* 111:14382–14387
224. Leishangthem P, Parmar ADS, Sastry S (2017) The yielding transition in amorphous solids under oscillatory shear deformation. *Nat Commun* 8:14653



# Biophysical and Biochemical Mechanisms Underlying Collective Cell Migration in Cancer Metastasis



Ushasi Roy, Tyler Collins, Mohit K. Jolly, and Parag Katira

**Abstract** Multicellular collective migration is an ubiquitous strategy of cells to translocate spatially in diverse tissue environments to accomplish a wide variety of biological phenomena, viz., embryonic development, wound healing, and tumor progression. Diverse cellular functions and behaviors, for instance, cell protrusions, active contractions, cell-cell adhesion, biochemical signaling, remodeling of tissue microenvironment, etc., play their own role concomitantly to have a single concerted consequence of multicellular migration. Thus unveiling the driving principles, both biochemical and biophysical, of the inherently complex process of collective cell migration is an insurmountable task. Mathematical and computational models, in tandem with experimental data, help in shedding some light on it. Here we review different factors influencing collective cell migration in general and then specific to cancer. We present a detailed discussion on different mathematical and computational modeling frameworks—discrete, hybrid, and continuum—which helps in revealing different aspects of multicellular migration. Finally, we discuss the applications of these modeling frameworks specific to cancer.

**Keywords** Agent-based model · Cell-cell interactions · Cellular Potts model · Machine learning · Ordinary differential equations · Phase-field model · Vertex model

---

U. Roy (✉) · M. K. Jolly

Centre for BioSystems Science and Engineering, Indian Institute of Science, Bangalore, India  
e-mail: [ushasiroy@iisc.ac.in](mailto:ushasiroy@iisc.ac.in)

T. Collins

Department of Mechanical Engineering, San Diego State University, San Diego, CA, USA

P. Katira

Department of Mechanical Engineering, San Diego State University, San Diego, CA, USA

Computational Science Research Centre, San Diego State University, San Diego, CA, USA

e-mail: [pkatira@sdsu.edu](mailto:pkatira@sdsu.edu)

© The Author(s), under exclusive license to Springer Nature Switzerland AG 2023

I. Y. Wong, M. R. Dawson (eds.), *Engineering and Physical Approaches to Cancer*,  
Current Cancer Research, [https://doi.org/10.1007/978-3-031-22802-5\\_3](https://doi.org/10.1007/978-3-031-22802-5_3)

## 1 Introduction: Collective Cell Migration

Migrating cells come in a variety of flavors that may be broadly binned into amoeboid (cells migrating by bleb formation and squeezing of cell body through pores) and mesenchymal (cells migrating by extending contractile elements into the surroundings and pulling themselves along these extensions) but mostly somewhere in between [1]. The migration phenotype depends significantly on the tissue of origin of the cell, the differentiation state of the cell, and the extracellular signals triggering and directing cell migration. For example, epithelial cells, which are cells that line the interface between organs of the body and the outside environment, may migrate as sheets during tissue regeneration and wound healing, but when altered due to mutations, dedifferentiation as during cancer metastasis, or extracellular signals, may migrate as mesenchymal cells with elongated spindle-like morphology or as amoeboid cells with rounded morphology. These cells can also migrate individually, or together in clusters, as strands or sheets in an environment and developmental or disease state dependent manner. Collective migration has been well investigated in scenarios of embryonic developmental and wound healing and has recently garnered attention in cancer metastasis as well, which has been largely thought of as driven by individual carcinoma cells undergoing an epithelial-mesenchymal transition (EMT). *In vivo* observations about clusters of circulating tumor cells (CTCs) being the main drivers of metastasis [2] have driven much interest in investigating the biophysical and biochemical modes of formation of these clusters [3] prior to dissemination from primary tumor, and their ability to traverse through capillary-sized vessels [4]. CTC clusters can contain cells of varying phenotypes—ranging from more epithelial or more mesenchymal—but hybrid epithelial/mesenchymal (E/M) cells seem to be better positioned to form clusters [5]. These clusters can contain not only cancer cells but also various stromal ones and platelets [6] which may aid in immune evasion through the journey. Both homotypic and heterotypic CTC clusters are highly metastatic and often correlate with worse patient outcomes across cancer types, as compared to the individual CTCs. Biochemically, these clusters have been interrogated at transcriptomic and methylation levels [7], while biophysical models have attempted to explain the size distribution of such CTC clusters [5] as experimentally reported in cancer patients. These models have endorsed earlier observations of how intermediate cell-cell adhesion may maximize the chances of collective cell migration [8]. Further, a conceptual overlap of hybrid E/M phenotype(s) (moderate cell-cell adhesion levels) and collective cell migration (including the CTC clusters) is now being substantiated by identification of their underlying molecular basis [9].

In diverse contexts where collective migration has been probed further, questions on leader-follower traits have taken importance [9]. It has been shown that leader and follower cells can often exchange their positions, revealing complex interplay at biochemical and biophysical levels within the cell population [10]—intercellular force transduction, energetic coordination, etc. Thus, it becomes imperative to understand how various factors crosstalk to enable cells to behave collectively at

multicell length scale in epithelial monolayers and/or sheet migration. Not only epithelial cells but also mesenchymal cells can undergo collective migration [11]. For instance, in mesoderm—a mesenchymal tissue—cells migrate together with endodermal cells during gastrulation. Similarly, neural crest cells can migrate throughout the embryo by involving mesenchymal or hybrid E/M phenotypes [11], involving contact inhibition of locomotion (CIL). Further, cells can often switch and back between collective and individual modes of migration too, including a switch to an amoeboid phenotype—cells that are deformable and soft and often migrate without remodeling the extracellular matrix (ECM) by proteolysis [12]. Thus, cells undergoing collective-to-amoeboid transition (CAT) and vice versa amoeboid-to-collective transition (ACT) have been reported [13], besides the switch from mesenchymal to amoeboid and/or epithelial and vice versa: mesenchymal-amoeboid transition (MAT) and amoeboid-mesenchymal transition (AMT) [14], as well as EMT and its reverse mesenchymal-epithelial transition (EMT). There are significant overlaps and subtle differences in the underlying regulatory networks, molecular pathways, and proximate physical mechanisms of cell migration across biological processes, such that discussion of these mechanisms observed in contexts beyond cancer, such as in migration of neural crests or during wound healing, is still relevant to understand the fundamentals of collective cell migration during cancer metastasis [15].

Together, given the complexity and plasticity of cell migration modes, decoding the multiscale emergent dynamics of collective cell migration—characterized in its broadest sense by multicellular groups migrating with a high degree of spatial and temporal correlation in direction—remains an active area of investigation in multiple biological systems, including cancer metastasis. This chapter aims to introduce the reader to the underlying, multiscale biological and biophysical factors that can influence collective cell migration, the myriad of mathematical modeling approaches used to describe and explain collective cell migration, and some of the key open questions that still need to be answered to truly understand and manipulate biological processes dependent on collective cell migration, cancer metastasis being foremost of these. Ultimately, the chapter hopes to direct the reader's thoughts to questions such as the following: (a) How clusters of cancer cells navigate dense, labyrinthine tissue environments and survive dynamical force to colonize distant sites within the body? (b) What mechanical and biochemical changes within these cells allow the cells to adapt individually or collectively to the changing environmental conditions as they metastasize? (c) How mechanistic insights and multiscale biochemical and biophysical interactions can be integrated using computational models to accurately predict collective cell migration events driving cancer metastasis? (d) How intra- and intercellular mechanisms be hijacked to prevent collective cell migration and mitigate distant metastasis with potential preventive and therapeutic interventions?

## 2 Factors Influencing Collective Cell Migration

At the individual level, there are two main mechanisms by which cells migrate on 2D substrates and through 3D environments [16, 17]. 2D substrates can be stiff substrates such as the bottom of polystyrene culture plates, or elastic, viscoelastic nanoporous polymers coated to which the cell can bind and generate forces against. 3D environments are commonly cross-linked hydrogels of biopolymers such as collagen, fibronectin, and laminin with micron-sized pores; the cells can easily squeeze through, or synthetic biocompatible polymers, with nano-sized pores that cells extensively remodel to migrate through [18, 19]. The first commonly described cell migration mode is the mesenchymal mode of migration whose hallmarks are cell protrusions containing aligned actin-myosin fibers that extend, bind, and contract against the 2D substrate, or along fibers of the 3D biopolymer matrix [16, 20–23]. The cell protrusions are transient and can be extended from the cell in different directions. The direction, frequency, and length of these protrusions are a function of a variety of cellular and extracellular biochemical and mechanical factors, which can be clubbed into a singular governing aspect of cell polarity. Depending on the amount of force generated by the actin-myosin fibers within the protrusions, the strength and amount of adhesions between the cell protrusions and the substrate, and the mechanical properties of the substrate itself, the cell can pull itself along these protrusions. The second, commonly observed mode of migration is the amoeboid migration, where active decoupling of the actin-myosin cortex from the cell membrane causes the cell periphery to bleb. The actin polymerization and actin-myosin cortex recoupling with the cell-membrane within the bleb generates directional cortical tension pulling the cell body towards the bleb [24, 25]. This motion also requires transient attachments between the cells and the substrate and can be equally fast as the mesenchymal mode of migration [26]. Cells have been shown to migrate using either mesenchymal or amoeboid or a combination of both these mechanisms [27]. They can also switch between these two mechanisms based on the mechanical and biochemical signals within the environment [28]. Beyond these two common mechanisms, there are a few other lesser-known mechanisms which have also been shown to drive individual cell migration such as osmotic pressure difference at the anterior and posterior regions of the cell, or asymmetric cell squeezing through undulating spaces [29, 30]. These mechanisms have been shown to be independent of cell-substrate adhesions; however, active forces within the cells are still known to play a role. Migrating cells also show a ventral-dorsal polarity, where the ventral region is dominated by increased actin polymerization and cell protrusion activity, while the dorsal region has increased adhesion turnover and actin depolymerization. This polarity, and the mechanisms and time scales over which it switches within individual cells, has significant impact on cell persistence and mobility [31, 32]. Further details on mechanisms of individual cell migration and models describing them can be found in several recent reviews [23, 33–35]. Spatarelu et al. [35] primarily focus on cancer, summarize various experimental

methods, and discuss about “unjamming transition” in context with epithelial-mesenchymal transitions.

The most pertinent question with regard to collective cell migration that arises is how do individual cells that can migrate independently via the above-described mechanisms interact with other cells in close proximity to synchronize their speed and direction of migration to give rise to collective migration. To understand this question, we will focus on the various ways by which neighboring cells interact with each other.

## ***2.1 Direct Cell-Cell Mechanical Interactions***

When two migrating cells collide with each other, they can either reverse direction/bounce away, go past each other, or begin to migrate together in the same direction [36–40]. The precise outcome of any such cell-cell interaction is hard to predict but is shown to depend on cell-cell adhesion type, adhesion strength, cell migration speed, cell-substrate adhesion strength, cell actin-myosin contractility, cell polarity, and the angle of approach between the cells among other factors [41]. A number of these factors themselves might be interrelated. For example, cell-cell adhesion is a function of the type of cell adhesion molecules present on the cell surface, the actin-myosin cortex tension, availability of other junction proteins, as well as upstream intracellular signaling. On the other hand, cell polarity is dynamic and can change as a result of cell-cell collisions and interactions.

Mechanically, when two or more cells come into contact, they can form a number of stable or transient bonds depending on the cell type [42, 43]. For example, epithelial cells generally form stable adhesions that permit the transmission of active contractile forces generated by the actomyosin cytoskeleton across the interacting cells. On the other hand, mesenchymal cells are known to form more transient bonds that may only weakly transmit the cytoskeletal forces generated by one cell to another [44]. Partially transformed epithelial cells would then have a combination of stable and transient interactions with each other, allowing transmission of active cytoskeletal forces up to certain threshold values, and above which the cells can transit past each other and exchange neighbors or even migrate individually [45].

Beyond cell-cell mechanical adhesions, a direct mechanical interaction between two cells can result in the repolarization of the cell. Migrating cells show a front-back polarity where the front end of the cell has faster actin polymerization, cell-substrate bond maturation, focal adhesion complex formation, and increased recruitment of actin-myosin stress fibers, while the rear end of the cell has increased dissolution of cell-substrate adhesions and increased actin depolymerization [46, 47]. A direct mechanical interaction between two cells can lead to a change/reversal of polarity within these migrating cells causing them to migrate away from each other. This phenomenon is known as contact inhibition of locomotion (CIL) [48, 49]. CIL in conjunction with transient cell-cell adhesion has been indicated in a variety

of collective cell migration behaviors such as flocking, rotation of cellular clusters within confinement, and even cells chasing or following each other [50–52].

When cells mechanically interact with each other, there are a few nonspecific cell interactions as well that can play important role in directing the dynamics of collective cell migration. For example, there can be a weak repulsion between cells due to the steric interactions between cell membranes and the exclusion of cellular volumes [45]. Depending on the mechanical properties of the cell membrane, the actin-myosin cortex, the cell cytoskeleton, and even the nucleus, these steric forces can lead to changes in cell shape and consequently changes in cell motility as well as proliferation. Additionally, nonspecific interactions between membrane coating polymers such as the glycocalyx of interacting cells can dictate intercellular friction and alter the rates of cell migration within the collectives [53, 54].

## ***2.2 Direct Cell-Cell Biochemical Interactions***

Beyond direct mechanical interactions, the contact between two cells can trigger a cascade of biochemical signaling within the interacting cells. For example, active force transmission across cell-cell adhesion can result in triggering the  $\beta$ -catenin-Wnt signaling pathway which can trigger transcriptional changes driving stem cell/cancer cell-like behavior in epithelial cells [55, 56]. Another example is the cell-cell interaction area-dependent changes in Notch signaling which is critical in a variety of cell differentiation and boundary formation processes in tissues as well as tumor cell migration and invasion [57].

The abovementioned mechanical interactions between cells are also not independent of associated biochemical signaling. A key example of this is CIL, where the repolarization of interacting cells is associated with Eph/ephrin interactions at cell-cell interfaces which trigger downstream RhoA activation and Rac inhibition [58, 59]. Rac inhibition suppresses f-actin assembly and drives repolarization of the cell away from the cell-cell contact. Adhered cells can also communicate via gap junctions that transmit electrical signals as well as small molecules and effectors such IP3 and Ca<sup>2+</sup> ions which act as secondary messengers for a variety of biochemical pathways that can promote or restrict collective cell migration [60].

## ***2.3 Indirect Cell-Cell Interactions via the Environment***

In the context of collective cell migration, the focus is primarily on direct cell-cell interactions and communication via mechanical and biochemical pathways. However, cells can also alter their immediate environment, and the sensing of these changes by neighboring cells can drive coordination and collective behavior between these cells. For example, contractile cells can strain the immediate extracellular matrix fibers [61]. This strain can be sensed by other cells in the

vicinity triggering strain sensitive migration and synchronization of contractile activity in these cells [62]. Alternatively, certain migrating cells can restructure the extracellular matrix via the action of matrix degrading enzymes or by depositing and cross-linking new matrix material. This active restructuring of the extracellular environment can create tracks or open spaces for other cells to follow, promoting collective migration and invasion of the extracellular environment [63, 64].

Paracrine signals secreted by certain cells in the environment can also induce synchronization and collective cell migration of neighboring cells [9]. An important example of this is the secretion of VEGF signals by chondrocytes that trigger collective cell migration of endothelial cells to form new vasculature [65]. Cancer-associated fibroblasts also can release such paracrine signals such as cytokines and chemokines triggering collective invasion of cancer cells into the surrounding stroma [66].

## ***2.4 Collective Cell Migration Beyond Cell-Cell Interactions***

While the common assumption is that synchronization of cell motility directions and speeds is an outcome of direct or indirect cell-cell interactions, it is also possible that the main drivers of collective motility are factors not affected by cell-cell interactions. One such scenario is the migration of cells under the influence of a chemical gradient [67]. While each cell individually senses and moves towards or away from the chemical source, there does not have to be any cell-to-cell communication for the cells to move collectively. Similarly, cells migrating in confined spaces, along patterned substrates, along gradients of cell-substrate adhesion molecules, or along gradients in substrate stiffness, all of these can cause collective cell migration independently of cell-cell interactions [68]. However, there are also scenarios where the presence of a cellular collective rather than individual, disconnected cells promotes such directional migration along chemical and physical cues. For example, there is experimental evidence that collectives of cells can be better at recognizing and migrating along biochemical gradients than individual cells in a specific environment [69]. Under which conditions individual cell behavior dominates vs collective cell interactions dominate the directional migration of cells is not completely understood.

Ultimately, it is naïve to assume collective cell migration is an outcome of just one of the above interactions. In any given collective cell migration scenario, more than one of the above interactions can be influencing cell migration behaviors. Additionally, the above list of interactions is in no way exhaustive. We have just focused on some of the more commonly described phenomena known to drive collective cell migration. The combination of these cell-cell and cell-environment interactions occurring over a wide range of spatial and temporal scales results in the various collective cell migration phenomena observed in biological systems. These include migration of small cell clusters, migration of large cell clusters, migration of cell strands (single file), migration of cell streams (multiple cells wide), migration of



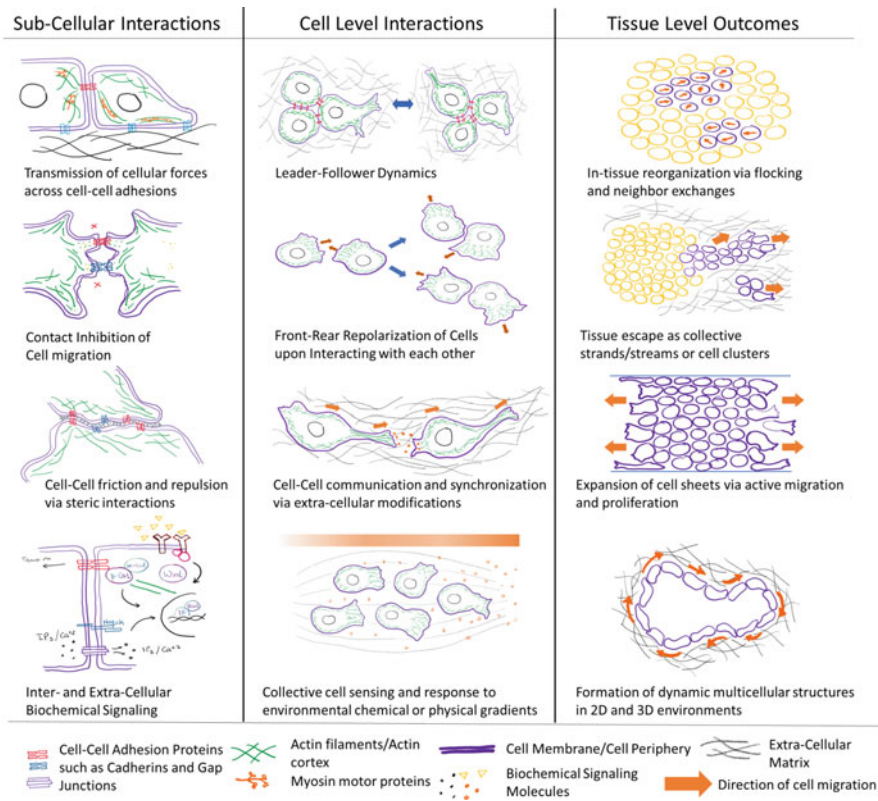


**Fig. 1** Multiscale interactions and common outcomes of collective cell migration phenomena

cell sheets, rotation of cell clusters in confined environments, rotation of entire multicellular organoids, and migration of cell along chemical gradients (chemotaxis), along stiffness gradients (durotaxis), along adhesion gradients (haptotaxis), along strain gradients (plithotaxis), herding via multiple leader cells, following a single or a small group of leader cells, flocking, jamming to unjamming transitions, and many others. Figure 1 summarizes the multiscale nature of collective cell migration and highlights some of the key interactions and outcomes of cell-cell interactions and collective cell migration. Section 4 gives us a detailed discussion on how biophysical and mathematical models can be employed to understand some of these processes.

### 3 Collective Cell Migration in Cancer

In some scenarios, cells of a primary tumor undergo epithelial-to-mesenchymal transition (EMT), become motile and invasive, and intravasate through blood stream. At a distant secondary site, the cells undergo extravasation forming micrometastases,



which is known as mesenchymal-to-epithelial transition (MET). This property of cells to switch phenotypes is well known as epithelial-mesenchymal plasticity (EMP). But the role of EMT in cancer progression remains controversial—it has not been established that EMT/MET is a requirement for metastatic dissemination and colonization.

Over the last two decades, epithelial-mesenchymal transition (EMT) has been recognized as an essential, highly regulated and mostly employed mechanism in normal embryological development and in migration of epithelial-derived cells in morphogenesis. Of late, *in vitro* and *in vivo* studies in tandem with that in *in silico* studies have suggested that EMT may also play an important role in cancer metastasis in various cancer systems. Recently, the production of fibroblast cells from epithelial precursors in fibrotic diseases has been recognized as bearing the hallmarks of EMT [70]. The biological and pharmacological importance of EMT in cancer has now achieved much attention and recognition. Problems in multicellular systems can only be understood if we have a holistic view of its overall biological activities, viz., interaction, motion, growth, division, and death, and as a result of all these, multifarious tissue-scale dynamics evolve.

It has been suggested recently that mechanically heterogeneous cancer tumors are composed of soft (exhibit mesenchymal markers) and stiff (exhibit epithelial markers) cells. The soft/fluidlike cells are known to unjam and migrate easily towards the primary tumor boundary compared to the stiff/solid-like cells—manifestation of the phenomena of tumor invasiveness or cancer metastasis [71]. In cancer metastasis, EMT at the primary site causes sedentary epithelial cells to change their phenotype to become less confluent and more migratory (akin to a solid  $\rightarrow$  fluid or jamming  $\rightarrow$  unjamming transition (UJT)). During UJT, cells lose apicobasal polarity and epithelial markers, while they concurrently gain front-back polarity and mesenchymal markers. And during MET at secondary site, epithelial cells change their phenotype to become more confluent and loses motile behavior (akin to a fluid  $\rightarrow$  solid or unjamming  $\rightarrow$  jamming transition). In a mixture of both epithelial and mesenchymal cells, when only a fraction of the cells has transitioned to the second phenotype, the tissue achieves a frustrated jamming state [72]. But recently, subtle differences between EMT and UJT have been pointed out in primary airway epithelial cells [73]. The claim is that the collective epithelial migration can take place through UJT with or without EMT or partial EMT.

In experimental models for cancer metastases, it has been observed that in lung cancer [74, 75], tumor cells survive in clusters in the blood stream and generate lung metastases, and in inflammatory breast cancer associated with lymphatic metastasis, multicellular strands travel through the lymphatic vessels [75]. A balance between EMT/UJT, collective cell migration either as clusters of strands, and MET/JT at specific invasion sites might hold the key to accurately predict disease outcomes in many cancers. Additionally, biochemical and mechanical factors triggering these collective cell phenomena are of extreme interest as potential diagnostic markers or therapeutic targets.

How decisions by an individual cell influence the collective dynamics at the population level? In multicellular systems, the variational principle of the generic,

phenomenological model of least microenvironmental uncertainty principle (LEUP) [76, 77] might be employed to understand mathematically the phenotypic decision-making of a cell, considered as the Bayesian decision-makers under energetic constraints, based on the phenotypes of the neighboring cells. LEUP minimizes the uncertainty in the measurement of microenvironmental entropy of a cell, without the exact mechanistic knowledge of the complex intercellular interactions and the precise and complete dynamics of chemomechanical factors influencing cell migration, such as biochemical signaling pathways, substrate sensing, etc.. Within the mathematical framework of the information theoretic approach of LEUP, it is assumed that the phenotypic switching of each cell happens based on its microenvironmental entropy. During cancer metastasis, cells travel as individual units and as multicellular clusters of circulating tumor cells (CTCs) through the blood stream to a distant secondary organ. While in transit, the cells are in a dynamically evolving microenvironment in which it changes its phenotype multiple times. In future, in the combined framework of LEUP and mechanistic models of collective cell migration, the phenomenological properties such as entropy, cell migration velocity, phase separation, and nonequilibrium structure formation could be mapped to other phenotypic markers, thus bridging the gap between computational models, *in vitro/in vivo* experiments, and clinical data.

## 4 Discrete, Continuum, and Hybrid Models

The complexity of collective cell migration phenomena, as described in previous sections, can be better understood with the help of computational models that allow the modeler to focus on a narrow set of interaction rules between cells and their environment at any given time and a limitless control over the parameter space. However, this means the models also have to make assumptions and simplifications regarding all the other interactions rules and properties not directly probed by the model system. Traditionally, computational complexity and costs have placed the largest constraints on the number of interactions incorporated within a model and the size of the parameter space. Geometry of the system also plays a great role in collective cell migration. Cells in native biological tissues can move along one-dimensional (1D) fibers, or two-dimensional (2D) planar substrates, or across three-dimensional (3D) matrix. The computational cost becomes manifold when collective cell migration is modeled in 3D, compared to other spatial dimensions. However, with advances in high-performance computing, current models describing collective cell migration are highly integrated and incorporate a large variety of interactions and effects ranging from subcellular to tissue level in length scales and milliseconds to days in time scales. Models can be classified into discrete, continuum, and hybrid models. “Continuum systems” are described by off-lattice models and their canonical description can be mathematically depicted with nonlinear continuous ordinary differential equations (ODEs) or partial differential equations (PDEs) having multiple terms, each describing a biological process (*viz.*,

birth, death (apoptosis/necrosis), nutrient consumption, etc.). But, in contrast, there is no well-defined way for describing interactions of discrete objects, particularly interacting and migrating discrete biological cells. In order to study the impact of the dynamics of an individual cell on multicellular cluster migration, and cell-cell interactions on tissue behavior, space- and time-dependent on- or off-lattice agent-based models (ABMs) need to be developed. Sometimes we need to couple continuum and discrete, agent-based approaches and come up with a hybrid model to unleash the maximum knowledge about the relevant system with optimum computational effort. In the following sections, we discuss some of the current computational models for collective cell migration.

### 4.1 Isotropic Active Particles Model

A standard minimal way of representation of interacting biological cells in a collective is by isotropic particles—all cells are of same circular/spherical shape in two/three dimension, and they interact in a similar fashion. The governing dynamics for the center of mass of the overdamped (moving towards equilibrium) cell  $i$  is given by the Newton's law with zero acceleration

$$F_{\text{friction}}^i + F_{\text{active}}^i + F_{\text{cell-cell}}^i = 0 \quad (1)$$

where  $F_{\text{friction}}^i = -\gamma \frac{d\mathbf{x}_i(t)}{dt}$ ,  $F_{\text{active}}^i = -\frac{\partial x_i}{\partial t}$ , and  $F_{\text{cell-cell}}^i = -\frac{\partial}{\partial x_i} U(\mathbf{x}_1, \dots, \mathbf{x}_N)$  where  $U = \frac{1}{2} \sum_{i \neq j} |V_i - V_j|$ . The first term  $F_{\text{friction}}^i$  corresponds to the frictional drag of cells against substrate or extracellular matrix (corresponding to flow at low Reynold's number regime). This mathematical form expresses frictional force proportional to the velocity of a particular cell relative to a fixed background. It can also be modeled alternatively, which will depend on the relative velocities of cells in contact, e.g.,  $|v_i - v_j|$  [78, 79], or in a more complicated form based on dissipative particle dynamics [80]. The second term represents the motility force, in the direction of the polarity of the cell.  $U$  in the third term corresponds to a pair-wise interaction potential with  $V$  having long-range attraction and short-range repulsion between  $i$ th and  $j$ th cells. The effective long-range attraction represents adhesion of cells to their neighbors, while short-range repulsion arises from an exclusion of the overlaps between different cells. However, cadherin-mediated physical attraction is relatively short range.

Herding, flocking, schooling, and swarming are different nomenclatures for the phenomena of interactive collective behavior, specific to animals, birds, fishes, and bacteria (or aggregate of any physical entities in general), respectively, and isotropic particle model has been employed to understand such phenomena.. Over the duration of the last 25 years, several self-propelled particle (SPP) models, which falls in the specific class of individual-based model (IBM), have been introduced, studied, and analyzed, in one dimension [81] and in higher dimensions [82–84], with

more biologically relevant interaction rules [82, 85–89]. Isotropic active particle is a simple minimal model which fails to predict certain aspects of tissue mechanics: coupling between cellular shape and cell behavior, cell-cell adhesion, and density which are important near unjamming transitions in confluent monolayers [90, 91].

## 4.2 Deformable Particle Model

The next natural extension is to include cell shape variability (in terms of small deviations from circularity/sphericity) in addition to its isotropic property. Cells were considered deformable ellipsoids of constant volume in models of *Dictyostelium* [92]. Complex cell-cell interactions can be considered in these models. The authors [78, 93] have considered the interactions between the ellipsoidal cells as a function of the distance between cell surfaces—a natural generalization of the central forces applied in simple isotropic cell models. These models are valuable to study the coupling between shape and motility of cells. These models are most interesting when studying experiments that include both subconfluent and confluent layers of cells, rather than for purely confluent tissues which are better understood by Vertex/Voronoi models (described in Sect. 4.4).

The net force experienced by each cell is given by

$$F_{\text{Net}}^i = F_{\text{Active}}^i + \sum_{j \in N(i)} F_{\text{Passive}}^{ij} \quad (2)$$

During the contraction phase of a cell, the force generated equals  $F_{\text{Active}}^i$ .  $F_{\text{Passive}}^{ij}$  is the passive force vector between cell  $i$  and  $j$ . It has two origins, viz., compression, which is repulsive in nature that arises from a cell's resistance to deformation, and adhesion, which is attractive, and the magnitude depends on their proximity, because it determines the number of adhesion molecules which can bind. Adding the property of shape deformations (cells as ellipsoids instead of spheres) does not suffice to explain the jamming transitions [90, 91]. These models can interestingly explain experimental results [94] which have both confluent and subconfluent layers of tissues. Vertex and Voronoi models, described in the following subsection, can model tissues which have only confluent layers in a much better fashion. The advantages of this model are as follows: (i) precise cell position and size of each individual cell are tracked and can be gradually changed (no upper length scale), and complex deformations of cell shapes can be represented; (ii) movement, division, and death of cells are captured; and (iii) mechanical stresses in the cell can be computed to subcellular level. But, since the computation time is long, parameter sensitivity analysis of this method is very constrained. Thus the parameter inference is stepwise and very tedious [95].

### 4.3 Subcellular Element Models

Biological cell is considered as the smallest unit in most models, which does not possess the capacity to capture detailed intracellular characteristics, e.g., actomyosin contractions, cell morphology, cell polarization, cell size, cell division, etc. To resolve this drawback, subcellular element model does not consider each cell as the smallest unit; instead, it has internal structures or subunits interacting among themselves [80, 96–98]. In multicellular systems, this framework primarily computes the dynamics of large number of three-dimensional deformable cells. Each cell can be represented by a collection of elastically coupled elements, interacting with one another via short-range potentials. The dynamics of each element is updated using overdamped Langevin dynamics. Mathematically, it is necessary to have two terms describing the intercellular  $U_{inter}(r)$  and intracellular  $U_{intra}(r)$  interaction potential of elements. Various models have tackled the scenario in different ways taking into account different aspects of interactions, for instance, by considering simple motility forces [80], or differential rates of breaking and reforming of intracellular connections at the cell front/back [97], or modeling the interior and the cell membrane separately [98].

The simplest subcellular element model is comprised of two subcellular elements or units, representing a single cell. The two units stand for the front and back end of the cell [99]. Using a two-subcellular element model, the role of the supracellular actomyosin cable around the wound during healing of a wound can be successfully deciphered [100]. The overdamped dynamics of each element is mathematically computed as follows

$$\xi v = f_{SP} + f_C + f_{R/A} \quad (3)$$

where  $f_{SP}$  is the self-propulsion force which is subjected to contact inhibition of locomotion (CIL) [99] and balances the intracellular contraction  $f_C$  between the front and the rear unit.  $f_{R/A}$  is the interparticle force of different cells, which is repulsive in nature in short distances and attractive at long distances and vanishes further away. This term depicts the volume exclusion and intercellular adhesions. Studying systems through these models is a natural starting point for investigating mechanical behaviors of aggregates of cells and tissues and single-cell (power-law) rheology [92, 97].

### 4.4 Active Network Models: Vertex/Voronoi Models

Network models describe epithelial tissues as networks of polygonal cells. Vertex models play an important role in gaining deeper understanding of how forces generated inside cells affect the morphology of the cells and hence the shape and mechanics of epithelial sheets [101, 102]. In the vertex model, a cell is characterized

by a set of vertices at the intersection of three or more neighboring cells. The positions of the vertices further specify the cell interfaces and volumes.

Vertex models may be categorized into 2D and 3D apical vertex models, 2D lateral vertex models, and 3D vertex models, based on the geometrical representation of the cells and how the forces act on the cells [103]. In flat epithelium, forces are usually generated in parallel to the apical surfaces and apical vertex models can be employed in understanding this phenomena, while 2D lateral vertex models are appropriate when the main forces act to deform the tissue in the plane of the cross section. The tissue shape approximately remains the same under in-plane translation, and topological rearrangements do not play a role. 3D vertex models can be applied in a larger class of instances, viz., multicellular morphogenesis with undulation, tubulation, and branching [104] and epithelial shape changes characterized by out-of-plane mechanics and three-dimensional effects, such as bending, cell extrusion, delamination, or invagination [103].

Contrastingly, the Voronoi model is based on Voronoi construction [105], in which a cell is defined by its center and any point within the region of this cell is closer to this cell's center than any other cell's center. A Voronoi diagram is quite similar to the Wigner-Seitz cell [106] description in solid-state physics. The key difference between the vertex and the Voronoi model is tracking the forces at the vertices versus energy tracking of whole cell based on shape and size. To investigate the collective behavior, a term for mechanical energy, having the cell's area and perimeter, for each cell is included. Further insights on intercellular adhesion can be obtained from this energy. A self-propelled Voronoi model was developed [71, 90] to demonstrate glassy dynamics and jamming transition from a solid-like state to a fluidlike state in a confluent biological tissue. The total energy  $E$  of both the vertex and Voronoi model systems can be expressed in the following (or similar) form in terms of the area, and perimeter of each cell, positioned at  $r$ , is given by

$$E = \sum_{i=1}^N \left[ K_A (A_{r_i} - A_0) + K_P (P_{r_i} - P_0) \right] \quad (4)$$

where  $K_A$  and  $K_P$  are the area and perimeter moduli and  $A_{r_i}$  and  $P_{r_i}$  are the cross-sectional area and perimeter of the  $i$ th cell whose center of mass is positioned at  $r_i$  and which tends to relax to the preferred area and perimeter of  $A_0$  and  $P_0$ , respectively [101, 102]. The cell shape is defined by the Voronoi tessellation of all cell positions. This has provided a good representation of epithelia of real biological systems, for instance, the blastoderm of the red flour beetle *Tribolium castaneum* and the fruit fly *Drosophila melanogaster* [107, 108].

#### 4.4.1 Key Insights: Transitions in Epithelia

A generalized mechanical inference method [108] has been developed by employing self-propelled Voronoi (SPV) model of epithelia that connects mechanical stresses

of cells to cell shape fluctuations and cell motility and deduce information regarding the rheology of the tissue. The interaction stress is generated from cell shape fluctuations due to actomyosin contractility and intercellular adhesion while cell motility determines the swim stress that is generically present in all self-propelled systems. “Cellular jamming” is the collective arrest of cell movements and formation of a dense tissue. This phenomenon is very similar to the process of “solidification” or “rigidification” in physical sciences—collective arrest of particle or molecular motion. Diverse physical mechanisms such as tension-driven rigidity and reduction in fluctuations driven by biological features like cell-cell interaction, cell-substrate interaction, differential adhesion (for instance, increased cell-cell adhesion can arrest collective motion), cell division, and cell differentiation can lead to cellular jamming or crowding—and one or more of these can simultaneously operate to have a “phase transition” in a biological tissue [108].

## 4.5 Cellular Automata

Cellular automata (CA) models can be viewed as ensembles of entities (cells) interacting with one another and the environment by phenomenological local rules, describing biological processes. This is capable of modeling a huge range of biological examples ranging from bacteria, slime, amoeba, embryonic tissues, and tumors. Cellular automata models are basically developed on a lattice which models interactions with other cells and the ECM.

Classical lattice gas-based cellular automata (LGCA) model, originally developed in 1973 by Hardy, Passis, and Pomeau (HPP models) to model ergodicity-related problems to describe ideal gases and fluids, has been extended and widely applied to model self-driven biological cells [109]. LGCA are relatively simpler CA models, in which entities (cells) select one from a discrete set of allowed rules. LGCA is capable of modeling a wide range of phenomena with different length and time scales [110].

### 4.5.1 BioLGCA

The BioLGCA model is a lattice-based agent-based cellular automata model class for a spatially extended system of interacting cells. BioLGCA models can be applied to homogeneous cell populations (cells having the same phenotype and don't change their behavior). However, the BioLGCA can be expanded to model heterogeneous populations and environments, with cells dynamically regulating their adhesivities and/or interactions with a heterogeneous noncellular environment. Several biological processes, for example, angiogenesis [111], bacterial rippling [112], active media [113], epidemiology [114], and various aspects of tumor progression [110, 115–119], have been studied by employing BioLGCA models. In BioLGCA, apart from biophysical laws for individual cell migration, update

rules for cell-cell and cell-environment interactions can also be derived from experimental data of cell migration [120], unlike update rules in classical LGCA which are mostly ad hoc. This model combines mathematically rigorous analysis and computationally efficient simulations of collective cell migration, which has a scope to build rules based on experimental data. Thus it is capable of capturing complex multiscale behavior of collective cell migration. BioLGCA does not have cell shape as a model feature; hence, it is apt for modeling cellular behaviors at low and moderate cell densities, unlike epithelial tissue. BioLGCA minimizes model artefacts by optimizing their computational efficiency and their synchronicity and explicit velocity consideration, compared to other different categories of cellular automata models. The dynamics of the BioLGCA model, as described by the authors in [120], comprises of propagation  $\mathcal{P}$ , reorientation  $\mathcal{O}$ , phenotypic switch  $\mathcal{S}$ , and birth/death operators  $\mathcal{R}$ , all of which follows conservation laws maintained by operator dynamics. The modeling strategy is based on multiple biophysical interaction rules (random walk, alignment, attraction, contact guidance, chemotaxis, haptotaxis) for individual-based and/or collective migration of cells [120]. Interaction rules can be derived mathematically from Langevin equation of self-propelled particle and the steady-state distribution from its associated Fokker-Planck equation. A mean field analysis of the BioLGCA aggregation model may be performed to predict the formation of cluster patterns. The results show four distinct regions in parameter space, viz., (i) diffusive or gas-like phase, cells moving around freely as individual units; (ii) collective motion (active nematic), cells in collection move with an overall directionality; (iii) aggregate phase, cells are in static clusters forming cellular patterns; and (iv) jammed or glass-like, cells cannot move collectively or form patterns, and all the cellular dynamics are frozen similar to a crystalline solid [120].

#### 4.5.2 Cellular Potts Model

A more sophisticated version of cellular automata (CA) is cellular Potts model (CPM) which considers individual cells as extended entities of variable shape [109]. The concept is borrowed from the q-state Potts model in statistical physics. Anderson, Grest, Sahni, and Srolovitz studied the cellular pattern coarsening in metallic grains in the early 1980s by employing q-state Potts model. CPM numerically captures the migration of multicellular clusters in two dimensions [121]. The CPM can model realistic features of cells during migration, such as changes in cell shape and size (due to internal cytoskeletal processes, such as actin polymerization and cortical myosin contraction, intercellular adhesion, and processes regulating cell volume) [122], rearrangement of cells within a cluster, and the dynamic segregation or reaggregation of subclusters. Diverse biological phenomena like chemotaxis, cell sorting, endothelial cell streaming, morphological development, and tumor progression have been modeled using the CPM [123–125].

Each cell having the same polarization/orientation is represented by multiple lattice sites  $x$  with the same integral values for their lattice labels  $\sigma(x) > 0$  in



a discrete two-dimensional lattice. Lattice label  $\sigma(x) = 0$  represents the empty lattice sites corresponding to the extracellular matrix (ECM), which provides an environment through which the cells migrate. The energy of the whole system  $E_{CPM}$  can be expressed as

$$E_{CPM} = \sum_{\langle x, x' \rangle} J_{\sigma(x), \sigma(x')} + \sum_{i=1}^N \lambda_A (\delta A_i)^2. \quad (5)$$

It has contributions from two factors: the first term denotes the adhesion while the second one is the area restriction term. The adhesion energy term  $J_{\sigma(x), \sigma(x')}$  is given by

$$J_{\sigma(x), \sigma(x')} = \begin{cases} 0 & \sigma(x)\sigma(x') \geq 0 \text{ within ECM or same cell,} \\ \alpha & \sigma(x)\sigma(x') = 0 \text{ cell-ECM contact,} \\ \beta & \sigma(x)\sigma(x') > 0 \text{ cell-cell contact.} \end{cases}$$

where  $\alpha$  is the interaction strength of adhesion of any cell with its environment while cell-cell adhesiveness is characterized by  $\beta$ . A migrating cell undergoes fluctuations in size  $\delta A_i$  around its equilibrium area  $A_0$  ( $\delta A_i \equiv A_i(t) - A_0$ ). The second term, i.e., the area restriction term in Eq. (5), controls a migrating cell from growing or shrinking to unphysical sizes, as well as branching or stretching into intangible shapes. A perimeter restriction term, in addition to the area restriction term, has also been included in many works [92, 121, 126, 127]. But this might be omitted for simplicity since sufficiently large  $\alpha$  and  $\beta$  constrain perimeter by cell-ECM or cell-cell contact. Two cells in contact with each other will have an adhesion energy cost of  $\beta$ , while if the two edges of these cells are exposed to the ECM, they will have an energy cost of  $2\alpha$ . Thus we have two regimes: adhesion energy satisfying the condition  $\beta < 2\alpha$  would promote cell scattering, while  $\beta > 2\alpha$  will promote clustering. In between, there lies the optimum regime of  $\beta \approx 2\alpha$  which corresponds to the transitional state between a fully connected cluster and multiple disconnected clusters the optimal migration velocity corresponds. In this regime, the multicellular cluster attains the maximum effective migration velocity [8].

CPMs has been frowned upon since this model assumes cellular mechanics/motility results from cell boundary fluctuations, which may not be realistic always [92, 128]. The other limitations of these models are dynamics processes like migration, division, death, and pushing which are modeled by a jump-type stochastic process. The dynamics is computed by Monte Carlo sampling since a given multicellular configuration can have a huge number of possible neighbor configurations which might lead to unnatural distortions of time scale. [95]

## 4.6 Phase-Field Model

Another approach developed by many research groups [40, 92, 129–131] is to model shape variability of cells during collective motion with space- and time-dependent phase fields  $\phi(\mathbf{r}, t)$ . This model can simulate relatively small (<100) collections of cells but can capture the scenario of simultaneous couplings among the biochemistry, cell shape, and mechanics. The minimization of the Hamiltonian  $\mathcal{H}$ , with added active terms representing the motility of the cell, gives rise to the equations of motion for the phase field, which can be expressed in the following form

$$\frac{\partial}{\partial t}\phi(\mathbf{r}, t) + \mathbf{v}_{active} \cdot \nabla\phi = -\frac{1}{\zeta\epsilon} \frac{\delta\mathcal{H}}{\delta t} \quad (6)$$

Here  $\mathbf{v}_{active}$  is the velocity due to active driving at the boundary. The driven active velocity may be constant and in a direction parallel to the cell's polarity, or to be normally outward, with a magnitude set by biochemical polarity within the cell.  $\zeta$  is the friction coefficient and  $\epsilon$  width of the phase field. The Hamiltonian  $\mathcal{H}$  in the above Eq. 6 has contributions from two terms:  $\mathcal{H} = H_{single} + H_{cell-cell}$ . The first term for the single-cell energies is given by the Canham-Helfrich energies (widely applied for the deformed fluid membrane) [132] as follows

$$\begin{aligned} H_{single} &= \gamma \times [\text{cell perimeter}] + \kappa \times [\text{curvature integrated over membrane}] \\ &= \gamma \int d^2\mathbf{r} \left[ \frac{\epsilon}{2} |\nabla\phi|^2 + \frac{G(\phi)}{\epsilon} \right] + \kappa \int d^2\mathbf{r} \frac{1}{2\epsilon} \left[ \epsilon \nabla^2\phi - \frac{G'(\phi)}{\epsilon} \right]^2 \end{aligned} \quad (7)$$

where  $\epsilon$  is the free parameter characterizing the width of the interface of the phase field and  $\gamma$  is the tension. And the second term corresponds to the bending energy of the membrane computed by the integral over the mean curvature of the membrane

$$H_{cell-cell} = \sum_{i \neq j} \int d^2\mathbf{r} \frac{\sigma}{2} \phi^{(i)}(\mathbf{r}, t) \phi^{(j)}(\mathbf{r}, t) - \frac{\sigma\epsilon^3}{4} |\phi^{(i)}(\mathbf{r}, t)|^2 |\phi^{(j)}(\mathbf{r}, t)|^2 \quad (8)$$

where  $\kappa$  is the bending modulus of the membrane. Camley et al. investigated the effect of various cell polarity mechanisms on the rotation motion of a pair of mammalian cells, including contact inhibition of locomotion, alignment of position, or velocity with neighboring cells [40] that can be experimentally observed [133]. They showed that the persistent rotational motion is promoted by the velocity alignment robustly. Lober et al. came up with an alternative phase-field model to simulate hundreds of cells [130]. Phase-field models have the advantage that they can model higher-order nonlinear terms like the bending energy of the membrane and can be readily integrated with reaction-diffusion mechanisms. However, they have a high computational cost, since the dynamics of each cell would follow

a different partial differential equation which needs to be numerically solved. Kulawiak et al. [134] described the shape and motility dynamics of a single phase-field cell by a minimal model for Rac signaling [135].

#### 4.7 Finite Element Immersed Boundary Models

This biomechanical model for a single fully deformable cell accounts for the interactions/couplings between the fluid flow of the viscous incompressible cytoplasm and the structural deformations of the elastic cell [136]. It is postulated that the fluid flow is governed by the Navier-Stokes equation, given by Batchelor and Batchelor [137]

$$\begin{aligned} \rho \nabla \cdot \mathbf{u} &= s \\ \rho \left( \frac{\partial \mathbf{u}}{\partial t} + (\mathbf{u} \cdot \nabla) \mathbf{u} \right) &= -\nabla \mathbf{p} + \mu \Delta \mathbf{u} + \frac{\mu}{3\rho} \Delta s + \mathbf{f} \end{aligned} \quad (9)$$

Here,  $\rho$ ,  $u$ , and  $s$  denote the constant fluid density, fluid velocity, and fluid source distribution, respectively, and  $\mu$  is the constant fluid viscosity,  $p$  the fluid pressure, and  $\mathbf{f}$  the external force density. This is a description of the balance of momentum and the mass in a viscous incompressible fluid with distributed sources. In this model, the fluid is assumed to be incompressible except at the sources which are representative of positions indicating cell growth. Hence, on the whole fluid domain  $\Omega$  except at the isolated point sources, the local fluid expansion rate  $\nabla \cdot \mathbf{u}$  and the source distribution  $s$  are identically equal to zero. The force density  $f$  defined by the forces  $F(l, t)$  at the elastic immersed boundaries of all cells  $X(l, t)$  can be expressed in the following way

$$\mathbf{f} = \int_{\Gamma} F(l, t) - \delta(x - X(l, t)) dl \quad (10)$$

The  $\delta$  is the Dirac delta function, and  $\Gamma$  represents the finite collection of immersed boundary of all cells (the external force  $\mathbf{f}$  vanishes away from  $\Gamma$ ). The elastic cell membranes can be defined by the curvilinear coordinates  $X(l, t)$  where  $l$  denotes the position along the cell boundaries. The boundary forces  $F(l, t)$  have a contribution from three different types of forces, viz., the adjacent forces  $F_{adj}$ , the intercellular adhesion forces  $F_{adh}$ , and the contractile forces, and are determined by the boundary configuration, the assumed elastic properties of the cell membranes, and the undergoing cell processes. This model has been applied to track morphology of the cell membrane during cytokinesis [136], a single axisymmetric cell growth and division [138], blood flow and shear stresses in cerebral vessels, and aneurysms [139].

Dynamic finite element cell model (dFEMC) has been employed to study the dynamics of the formation of tissue patterns considering the different realistic features such as change in cell shape, geometry and topology, cell growth and shrinkage, cell birth and death, and cell division and fusion during the process [140]. To overcome the limitations of the existing models, dynamic cellular finite element model (DyCellFEM) has been developed to model the complete range of cellular migration of individual cells to collectives, cell proliferation, and tissue patterning in response to biochemical and mechanical cues [141].

## 4.8 Hydrodynamic Models

During embryonic development of an organism, mechanical stresses in a biological tissue develop due to cell division, cell apoptosis, and other factors to maintain tissue homeostasis, which play a significant role in tissue growth and hence final tissue morphology [142]. The hydrodynamic models systematically study the effects of fields on tissue dynamics. The dynamics of a thick polar epithelial tissue subjected to the action of both an electric field and a flow field in a planar geometry is theoretically studied [143]. A generalized continuum hydrodynamic description is developed to describe the tissue as a two-component fluid system—the cells and the interstitial fluid. A biological tissue in a continuum limit may be characterized by a cell number density  $n$  which obeys the following equation to balance the cell number

$$\partial_t n + \partial_\alpha (n v_\alpha) = (k_d - k_a) n \quad (11)$$

where  $v_\alpha$ ,  $k_d$ , and  $k_a$  are the velocity, division rate, and apoptosis rate for a characteristic cell in the tissue [142]. A “polar” and planar thick epithelial tissue, permeated by interstitial fluid flows in the presence of an electric field with cells able to generate electric currents and fluid flow, will follow conservation laws for volume, charge and momentum, symmetry considerations, and cell number balance equations [143]. This predicts that the domain of stability of the epithelial tissue of finite thickness is rather small. Tissue proliferation or tissue collapse can be caused due to simple dc electric current or a fluid flow, without any requirement for genetic mutation. These models have been used to analyze motility of various cell types [144–146].

Jeon et al. have developed a phenomenologically realistic and bio-/physically relevant **off-lattice hybrid discrete-continuum (OLHDC)** model of tumor growth, tumor morphology, and invasion [147] in which fingerlike shapes (characteristic of invasive tumor) are observed. Aspects of microenvironmental components such as matrix-degrading enzymes, nutrients or oxygen, and extracellular matrix (ECM) concentrations are captured by the continuum part of the OLHDC model, whereas the discrete portion (modeled by persistent random walk using Langevin equation) represents individual cell behavior such as cell cycle, cell-cell and cell-ECM

interactions, and cell motility. This could reproduce the experimentally observed superdiffusive behavior (at short timescales) of mammalian cells. Coupled hybrid continuum-discrete models have been explored to unveil the connection between angiogenesis and tumor growth and identify the three regions of a tumor as necrotic, semi-necrotic, and well vascularized [148] and to understand the interplay among glioma invasion, vascularity, and necrosis [149]. The *in silico* hybrid multiscale cancer model employs the representative averaging volume (RAV) technique (integrating two open-source numerical analysis platforms: FEB3 [150, 151] and BioDynaMo [152]) to couple the macroscopic tissue biomechanics (using the finite element mesh representing the tissue) and the microscopic cellular mechanics (using agent based methods) [149].

## 4.9 Simulation Platforms

Recently numerous software have been developed to capture *in silico* this inherently complex collective behavior of cells. Efficient computational agent-based multiscale models are developed to understand the underlying complexities at different levels.



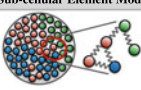
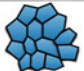
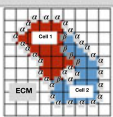
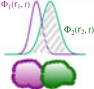
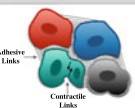
BioFVM is an efficient diffusive transport solver, written in C++ with parallelization in OpenMP, for solving systems of partial differential equations (PDEs) in 3D for release, uptake, decay, and diffusion of multiple substrates in multicellular systems [153]. PhysiCell—physics-based multicellular simulator, an open-source agent-based simulator—is an ideal *in silico* “virtual laboratory” that is capable of modeling many mechanically and biochemically interacting cells in dynamic biochemical tissue microenvironments [154]. Markovian Boolean Stochastic Simulator (MaBoSS) is a C++ software for the stochastic simulation continuous/discrete time Markov processes by employing Monte Carlo kinetic algorithm (or Gillespie algorithm), applied on a Boolean network, to compute global and semi-global characterizations of the whole system. A Python interface for the MaBoSS software, called pyMaBoSS, is also available [155]. PhysiBoSS is an open-source software and a multiscale agent-based modeling framework, which integrates multicellular behavior using agent-based modeling (PhysiCell) and intracellular signaling using Boolean modeling (MaBoSS) [156]. CompuCell3D is another open-source multiscale multicellular computational modeling environment based on cellular Potts model, which can handle a wide variety of problems including angiogenesis, bacterial colonies, cancer, embryogenesis, evolution, the immune system, tissue engineering, toxicology, and even noncellular soft materials [157]. Morpheus [158] is a graphical user interface (GUI)-based simulation environment for modeling multiscale, multicellular systems through coupled ODEs, PDEs, and CPM in 2D and 3D, which has been used to model collective motion [159], cell fate decisions (transdifferentiation and pattern formation in the pancreas using coupled ODEs) [160], vascular using a coupled reaction-diffusion/CPM model [161, 162], and also microscopy image-based models from liver tissues. One can explore executable Morpheus .xml files for figures given in [163]. Chaste (cancer, heart, and soft

tissue environment) [164, 165] is an open-source C++ simulation package aimed at multiscale (tissue and cell level electrophysiology, discrete tissue modeling, and soft tissue modeling) problems in biology and physiology. Some of the major distinct applications of the software include (i) continuum modeling of cardiac electrophysiology (cardiac chaste) [166]; (ii) individual agent-based modeling of populations of cells (cell-based chaste) [167, 168] applied to study tissue homeostasis and cancer, and (iii) a reduced dimensional modeling (structure, dynamics, and function) of ventilation in the human (healthy and diseased) lungs (lung chaste).

Thus, this section gives a detailed overview of most of the important mathematical and computational models to study various aspects of collective cell migration. Figure 2 illustrates different models of collective cell migration through simple schematics, highlighting their assumptions/interaction rules, governing equations, and applications.

#### ***4.10 Machine Learning-Based Techniques***

Apart from the mechanistic models (as described in previous sections), how different machine learning techniques are deployed to study cell motility and morphodynamics in the phenotypically heterogeneous environment, from live cell microscopy imaging data with high spatiotemporal resolutions/computer vision analyses, has been reviewed in [169]. When multiple phenotypes coexist in the same condition, it is difficult to decipher the mechanism of cellular dynamics of each cell type. In static configuration, a phenotype might be characterized by morphology, protein abundance, and localization, but these characteristics spatiotemporally evolve during migration with different timescales. Different machine learning (ML) approaches (such as autocorrelation function (ACF) [170], autoencoder (AE) [171], density peak clustering, generative adversarial network (GAN) [172], recurrent neural network (RNN) [173], support vector machine (SVM) [174], hidden Markov model (HMM) [175]) perform this nontrivial task of extracting information/features at different spatiotemporal time scales and learning the same. Hou et. al [176] employed deep reinforcement learning technique to study the effect of stimulation signal on the dynamics of follower cells. The migration speed of the follower cells got enhanced, and hence the motion of the collection of cells gets accelerated as a whole. Deep attention networks are developed which can detect, learn, and reveal distinct patterns of influence, attention, and rules of collective migration specific to each model tissue—epithelial, endothelial, and mesenchymal metastatic breast cancer cells [177]. They are also capable of detecting the changes in these rules depending on various biophysical contexts like cellular crowding or the location of the particular cell within the tissue, by analyzing cell trajectories. Mencattini et al. [178] developed a novel method to achieve a universal, massive, and fully automated analysis of cellular motility using single-cell trajectory data and pre-trained deep learning convolutional neural network architecture to study the behaviors of breast

Models	Assumptions / Interaction-rules	Governing Equations	Applications
<b>Isotropic Particle Model</b> 	Discrete, off-lattice Cells: circular/spherical in shape in 2D/3D Minimal model for collective cell behavior	$F_{\text{Friction}}^i + F_{\text{Active}}^i + F_{\text{Cell-cell}}^i = 0$ Sec. 3.1	Herding, flocking, schooling, swarming Self-propelled particle (SPP) model Individual-based models (IBM) [61 - 72]
<b>Deformable Particle Model</b> 	Discrete, off-lattice Cells: deformable ellipsoids of constant volume (cell-shape variability)	$F_{\text{Net}}^i = F_{\text{Active}}^i + \sum_{j \in N(i)} F_{\text{Passive}}^{ij}$ Sec. 3.2	Coupling between shape and motility of cells Model sub-confluent and confluent layers of cells [61, 73, 74]
<b>Sub-cellular Element Model</b> 	Discrete, off-lattice Each cell has interacting internal structures or subunits, models intracellular features along with intercellular ones.	$\xi v = f_{SP} + f_C + f_{RIA}$ Sec. 3.3	Acto-myosin contractions, cell morphology, cell polarization, cell size, cell division [63, 75 - 79]
<b>Vertex/Voronoi Model</b> 	Discrete, off-lattice Cells: polygonal, constructed from Voronoi tessellation of variable sizes	$E = \sum_{i=1}^N [K_A(A_i - A_0) + K_P(P_i - P_0)]$ Sec. 3.4	Effect of intracellular forces on the morphology of cells Epithelial tissue generation Cellular rearrangement Jamming/Unjamming [80 - 88]
<b>Cellular Potts Model</b> 	Discrete, on-lattice Cells: extended entities of variable shape, Cell-cell adhesion	$E_{CPM} = \sum_{\langle x,x' \rangle} J_{\sigma(x),\sigma(x')} + \sum_{i=1}^N \lambda_A (\delta A_i)^2$ Sec. 3.5.2	Segregation and re-aggregation of sub-clusters Multicellular cluster migration Chemotaxis, cell-sorting, Endothelial cell-sorting, Wound-healing Morphological development Tumor progression [73, 89, 101 - 106]
<b>Phase Field Model</b> 	Continuous, off-lattice Cells: space- and time-dependent phase fields	$\frac{\partial}{\partial t} \phi(\mathbf{r}, t) + v_{\text{active}} \cdot \nabla \phi = - \frac{1}{\zeta \epsilon} \frac{\delta \mathcal{H}}{\delta t}$ Sec. 3.6	Simultaneous couplings among the biochemistry, cell shape, and mechanics [31, 73, 107 - 111]
<b>Finite-element Immersed Boundary Model</b> 	Continuous, off-lattice Coupling between the fluid flow of the viscous incompressible cytoplasm and the structural deformations of the elastic cell	$\mathbf{f} = \int_{\Gamma} F(l, t) - \delta(x - X(l, t)) dl$ Sec. 3.7	Tracks morphology of the cell membrane during Cytokinesis, Blood flow and shear stresses in cerebral vessels and aneurysms. [112 - 115]

**Fig. 2** Various mathematical and computational models of collective cell migration: The key features of each model is highlighted along with the governing equations and applications

cancer cells treated with an immunotherapy drug and prostate cancer cells on the treatment of chemotherapy drugs.

## 5 Biochemical Models

Most efforts towards biochemical understanding of collective cell migration have focused on intracellular networks related to EMT, particularly those connected to hybrid E/M phenotypes. EMT has been reported in various contexts: embryogenesis

(type I EMT), wound healing and tissue homeostasis (type II EMT), and cancer metastasis and fibrosis (type III EMT) [179]. It has been largely thought of as “all-or-none” binary process, but recent observations—both computational and experimental—have unraveled that cells can acquire stably one or more hybrid E/M phenotype(s) with distinct biochemical and/or biophysical signatures [180]. Collective migration and EMT in mammary epithelia and breast cancer cell lines have been observed [44]. Here, we discuss different modeling strategies that have been adopted to elucidate EMT dynamics.

## 5.1 ODE-Based Models

Mathematical modeling of underlying biological networks has been instrumental in driving the appreciation of EMT from a binary process to a multistep one. Both the initial models on EMT signaling were ODE-based and modeled a set of experimentally identified interactions through coupled ODEs [181, 182]. Despite slightly different formalisms and parameter values used, they both predicted that cells can stably acquire a hybrid E/M phenotype. Both the models captured the dynamics of coupled feedback loops among the families of EMT and MET regulators: EMT-driving transcription factors ZEB and SNAIL and MET-drivers microRNAs miR-200 and miR-34. Other ODE models that have expanded these networks to incorporate additional nodes have shown that more than one hybrid E/M states may exist and that some molecules can act as “phenotypic stability factors” (PSFs) for hybrid E/M phenotype(s) such as GRHL2, OVOL1/2, NRF2, and NFATc [183, 184]. Interestingly, knockdown of these molecules—one at a time—in H1975 lung cancer cells (that display hybrid E/M phenotype stably in vitro for multiple passages) can push them to a more mesenchymal phenotype, as detected based on morphological and molecular changes. Thus, these PSFs can be thought of as “molecular brakes” on EMT and can increase the residence times of cells in hybrid E/M phenotype(s) [182].

More recent ODE-based models for EMT have incorporated additional contextualization, for instance, hypoxia-driven EMT such as HIF1 $\alpha$  [185] which includes SNAIL, TWIST, and miR-210, and suggest that number of positive feedback loops in a regulatory network determines the number of steady states related to EMT seen. This observation is a reminiscence of analysis of many EMT networks across a wide range of parameter values, showing that the number of positive feedback loops correlates strongly with the propensity of acquiring multistability [186].

## 5.2 Boolean Models

As the network size grows, it becomes increasingly difficult to estimate the different kinetic parameters needed to simulate an ODE model. Thus, often, a parameter-free



approach such as discrete/Boolean/logical modeling is used to decode the qualitative emergent network dynamics. In this formalism, each node in the network can be either ON (1) or OFF (0), and the levels of each node at a given time can be decided by other nodes that can either activate or inhibit it. For instance, if A inhibits B, then  $B(t+1) = \text{OFF}$  when  $A(t) = \text{ON}$ . This framework facilitates investigating the dynamics of larger networks, as has been in the case of EMT models too, and can identify different “attractors” a system can eventually converge to. Boolean models of EMT networks have also indicated coexistence of many hybrid E/M phenotypes, each defined by a set of specific nodes that are ON and others that are OFF [187–189].

ODE models are appropriate to simulate small-scale networks (see Fig. 3). Figure 3 (top left) depicts the transcription factors (TF) (ZEB and SNAIL) and microRNAs (miR-34 and miR-200) based regulatory network, identified as the molecular mechanism for the phenotype of cluster migration. The bifurcation diagram shown in the bottom left shows the coexistence of multiple phenotypes. Epithelial and mesenchymal phenotypes correspond to low and high expression levels of ZEB, respectively, while an intermediate level of ZEB has the characteristic of both phenotypes and is called a hybrid E/M state [182]. The cells in the hybrid state have ability to both adhere and migrate and potentially give rise to collective cell migration. Simulating large-scale networks is computationally heavy since they involve numerous parameters. So for a first approximation, Boolean formalism works very well to model large-scale networks (see Fig. 3). For multistable (coexistence of multiple phenotypes) networks, results from Boolean and ODE models have been shown to be consistent [190].

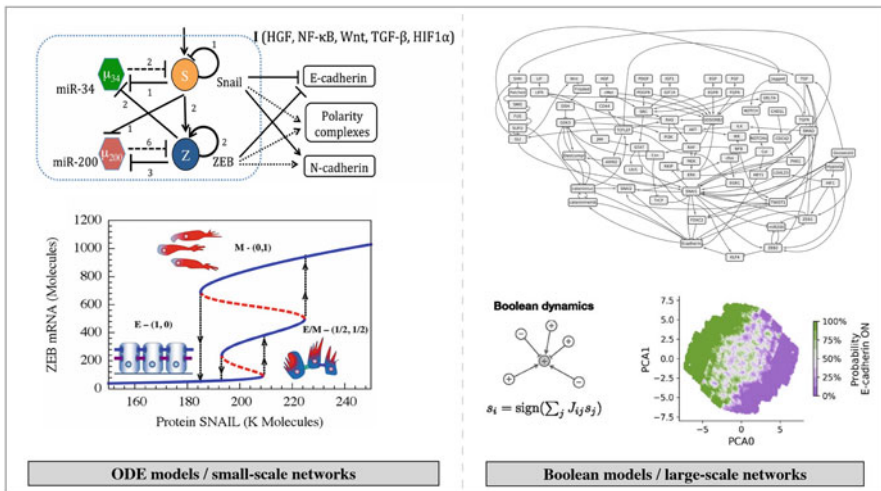


**Fig. 3** Illustrations for the ordinary differential equations (ODE)-based models for small-scale networks [182] and the Boolean models for large-scale networks [188]

## 6 Conclusions and Future Directions

Individual biochemical and biophysical models have been instrumental in decoding the mechanisms of collective cell migration, with important implications in unraveling metastasis. An integrated unique framework that combines the essential features of both the biophysical and biochemical aspects would help us understand the phenomena of cancer metastasis in a more concrete manner [191, 192]. Various aspects of mechanochemical coupling have begun to be unearthed in various contexts of collective cell migration [193–195], and the next class of mathematical models shall benefit from incorporating those latest details [196, 197].

Figure 4 shows how various computational models can recreate experimentally and clinically relevant collective cell migration phenomena ranging from cell sorting (Fig. 4A), cluster cell migration (Fig. 4B, D), collective cell migration as sheets and strands (Fig. 4C), and invasion of neighboring tissue by collectively migrating cells (Fig. 4E), to name a few. These modeling efforts show that similar underlying physics can be incorporated into different modeling frameworks, which can then be employed based on other model requirements as well as the computational and physical scale of the system being modeled. (For example, Fig. 4A and C show cell sorting and leader-follower dynamics during wound healing driven by differential adhesion as captured by different modeling approaches.) On the other hand, similar biological phenomena can be recapitulated in models using different underlying mechanisms and physical principles. For example, in Fig. 4B, collective cell migration is achieved via contact inhibition (top tiles), or via cellular crowding due to interaction with the environment (bottom panel), and in Fig. 4D via collective chemosensing and chemotaxis. Similarly, Fig. 4E shows fingerlike invasion of surrounding healthy tissue by cancer cell collectives driven by tensional instabilities at the interface between cancer and health tissue and migration by leader cells (top panel) and invasion driven by differences in mechanosensitive cell death and division rates between the two tissues (bottom panel). These are only a small sample of all possible modeling methods and underlying physical, chemical, or phenomenological mechanisms that have been combined to describe various collective cell migration phenomena. The choice of modeling method and underlying mechanisms is usually dictated by the focus of the primary research question. While each of these modeling results adds individually towards a larger puzzle, a comprehensive understanding of collective cell migration driving critical processes such as cancer metastasis will require bridging of gaps and filling of missing pieces via new modeling approaches.

One challenge that needs to be overcome is connecting diverse length and time scales: subcellular (intracellular components), cellular, supracellular/tissue scale, and eventually multi-organ level (during cancer metastasis) and organism level (during embryonic development). The length scales can broadly be stratified in the following way: (i) intracellular signaling (molecular scale), (ii) single-cell level behavior (cellular scale), and (iii) multicell/tissue-level behavior (multicellular scale). How can we bridge these different scales? How does each of these length

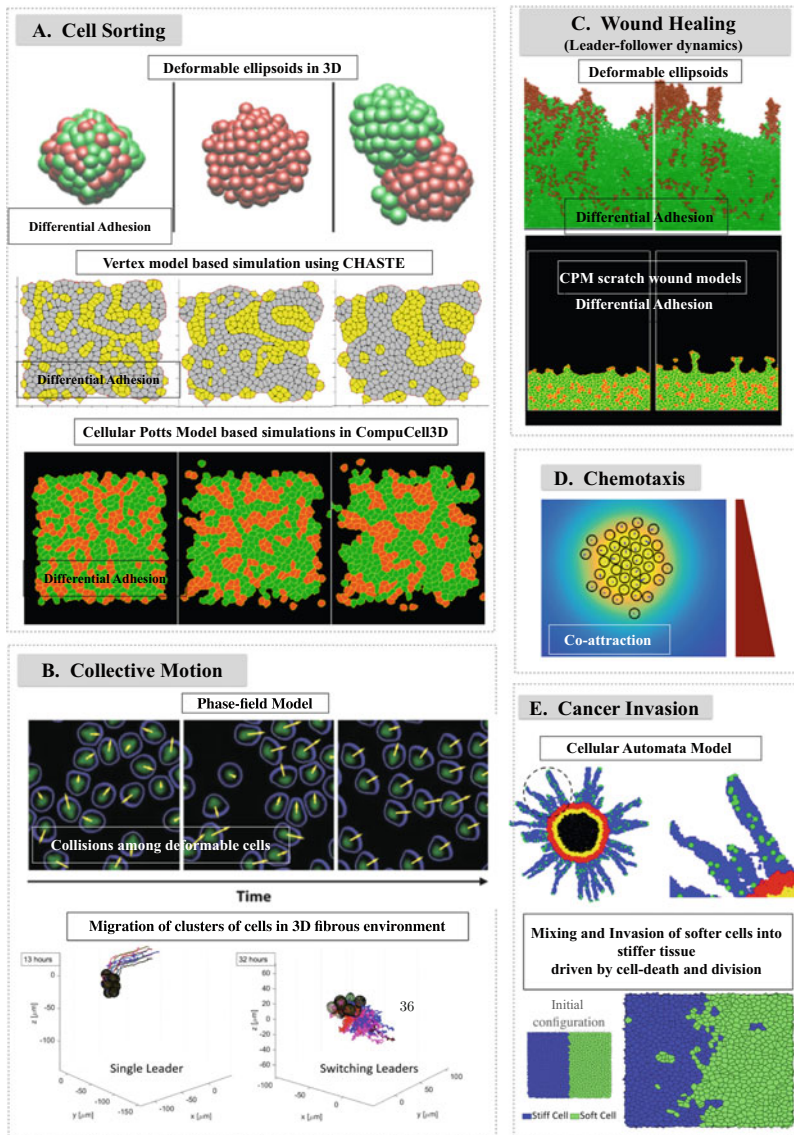


**Fig. 4** Representative simulation outcomes illustrating different biological phenomena from various models and underlying biophysical mechanisms. **(A) Cell sorting** via differential intercellular adhesion between two cell types (top) from deformable ellipsoids in three dimensions, (middle) vertex model-based simulations using chaste, and (bottom) cellular Potts model (CPM)-based simulations using CompuCell3D [198]. **(B) Collective motion** (top) using phase-field model with the underlying physical principle of contact inhibition of locomotion [130, 199] and (bottom) via cellular crowding due to interactions with the environment [200] **(C) Wound healing** via differential intercellular adhesion between two cell types using (top) deformable ellipsoids and (bottom) cellular Potts model (CPM) [198]. **(D) Chemotaxis** of a multicellular cluster bound by co-attraction (secreted co-attraction field shown in yellow) [92, 201]. **(E) Cancer invasion** (top) in a multicellular tumor spheroid (cells in black, necrotic; red, proliferative; green, invasive tumor; blue, degraded ECM; yellow, quiescent; white, ECM) using cellular automata (CA) model driven by tensional instabilities [35, 202] and (bottom) driven by differences in mechanosensitive cell death and division rates between stiff (blue) and soft (green) cells [203] (figures are adapted from the references mentioned above)

scales contribute in their own way to the emergent dynamics of collective migration? There are two distinct ways of modeling these phenomena—highly detailed and conceptually minimal. The former involves more parameters and might be more close to comparison with experiments, while the latter actin dynamics contributes to the mechanosensing and behavior, relating the molecular and cellular scale. Another aspect that needs attention is the granularity with which we model this phenomenon. Cells migrating collectively cannot be simply thought of as isotropic active particles following the exactly same generic principles. While this approximation can be a good minimal model to start with, various other factors need to be incorporated for biological realism: short-range and long-range communication via physical contact and/or diffusing biochemical molecules [204–206], change in microenvironment due to spatiotemporal variations in signaling molecules [207, 208], etc. Thus, within a mean field theory framework, a stochastic term that encapsulates many of these differences to represent cell-to-cell variability would be an important consideration. A multiscale agent-based framework can offer a good compromise in terms of granularity and usefulness of the model. For example, a multiscale model often incorporates many timescales set by rate of biochemical reactions and those set by diffusivity of various sensory as well as cell-cell communication molecules [209]. Models for tissue-level patterning that encapsulates intracellular biochemical signaling with intercellular communication have been well investigated, but most of this this work has been in static scenarios [210]. Thus, coupling these frameworks with cell motility (through, say, vertex models) at individual and cohort levels, as seen during morphogenesis, can be a first step [211] towards an integrated understanding of the multiscale dynamics of collective cell migration.

## References

1. Friedl P (2004) Preshpecification and plasticity: shifting mechanisms of cell migration. *Current Opinion Cell Biol* 16:14–23
2. Aceto N et al (2014) Circulating tumor cell clusters are oligoclonal precursors of breast cancer metastasis. *Cell* 158:1110–1122
3. Boareto M et al (2016) Notch-Jagged signalling can give rise to clusters of cells exhibiting a hybrid epithelial/mesenchymal phenotype. *J R Soc Interface* 13:20151106
4. Au SH et al (2016) Clusters of circulating tumor cells traverse capillary-sized vessels. *Proc Natl Acad Sci* 113:4947–4952
5. Bocci F, Jolly MK, Onuchic JN (2019) A biophysical model uncovers the size distribution of migrating cell clusters across cancer types. *Cancer Res* 79:5527–5535
6. Lim M et al (2021) Circulating tumor cell clusters are cloaked with platelets and correlate with poor prognosis in unresectable pancreatic cancer. *Cancers* 13:5272
7. Gkoutela S et al (2019) Circulating tumor cell clustering shapes DNA methylation to enable metastasis seeding. *Cell* 176:98–112
8. Roy U, Mugler A (2021) Intermediate adhesion maximizes migration velocity of multicellular clusters. *Phys Rev E* 103:032410
9. Vilchez Mercedes SA et al (2021) Decoding leader cells in collective cancer invasion. *Nat Rev Cancer* 21:592–604

10. Vishwakarma M, Spatz JP, Das T (2020) Mechanobiology of leader–follower dynamics in epithelial cell migration. *Current Opinion Cell Biol* 66:97–103
11. Theveneau E, Mayor R (2013) Collective cell migration of epithelial and mesenchymal cells. *Cellular Molecular Life Sci* 70:3481–3492
12. Wu J-s et al (2021) Plasticity of cancer cell invasion: Patterns and mechanisms. *Translat Oncol* 14:100899
13. Huang B et al (2015) Modeling the transitions between collective and solitary migration phenotypes in cancer metastasis. *Sci Rep* 5:1–13
14. Talkenberger K, Cavalcanti-Adam EA, Voss-Böhme A, Deutsch A (2017) Amoeboid-mesenchymal migration plasticity promotes invasion only in complex heterogeneous microenvironments. *Sci Rep* 7:1–12
15. Gallik KL et al (2017) Neural crest and cancer: divergent travelers on similar paths. *Mech Develop* 148:89–99
16. Lauffenburger DA, Horwitz AF (1996) Cell migration: a physically integrated molecular process. *Cell* 84:359–369
17. Brábek J, Mierke CT, Rösel D, Veselý P, Fabry B (2010) The role of the tissue microenvironment in the regulation of cancer cell motility and invasion. *Cell Commun Sign* 8:1–8
18. Chang SS, Guo W-h, Kim Y, Wang Y-l (2013) Guidance of cell migration by substrate dimension. *Biophys J* 104:313–321
19. Vu LT, Jain G, Veres BD, Rajagopalan P (2015) Cell migration on planar and three dimensional matrices: a hydrogel-based perspective. *Tissue Eng Part B Rev* 21:67–74
20. Bear JE, Haugh JM (2014) Directed migration of mesenchymal cells: where signaling and the cytoskeleton meet. *Current Opinion Cell Biol* 30:74–82
21. Zaman MH et al (2006) Migration of tumor cells in 3D matrices is governed by matrix stiffness along with cell-matrix adhesion and proteolysis. *Proc Natl Acad Sci* 103: 10889–10894
22. Mak M, Spill F, Kamm RD, Zaman MH (2016) Single-cell migration in complex microenvironments: mechanics and signaling dynamics. *J Biomech Eng* 138:021004
23. Yamada KM, Sixt M (2019) Mechanisms of 3D cell migration. *Nat Rev Molecular Cell Biol* 20:738–752
24. Lim FY, Koon YL, Chiam K-H (2013) A computational model of amoeboid cell migration. *Comput Methods Biomech Biomed Eng* 16:1085–1095
25. Charras GT, Coughlin M, Mitchison TJ, Mahadevan L (2008) Life and times of a cellular bleb. *Biophys J* 94:1836–1853
26. Cox CD et al (2016) Removal of the mechanoprotective influence of the cytoskeleton reveals PIEZO1 is gated by bilayer tension. *Nat Commun* 7:1–13
27. Tyson RA, Zatulovskiy E, Kay RR, Bretschneider T (2014) How blebs and pseudopods cooperate during chemotaxis. *Proc Natl Acad Sci* 111:11703–11708
28. Bravo-Cordero JJ, Hodgson L, Condeelis J (2012) Directed cell invasion and migration during metastasis. *Current Opinion Cell Biol* 24:277–283
29. Lämmermann T et al (2008) Rapid leukocyte migration by integrin-independent flowing and squeezing. *Nature* 453:51–55
30. Petrie RJ, Koo H, Yamada KM (2014) Generation of compartmentalized pressure by a nuclear piston governs cell motility in a 3D matrix. *Science* 345:1062–1065
31. Campanale JP, Sun TY, Montell DJ (2017) Development and dynamics of cell polarity at a glance. *J Cell Sci* 130:1201–1207
32. Davey CF, Moens CB (2017) Planar cell polarity in moving cells: think globally, act locally. *Development* 144:187–200
33. Conway JR, Jacquemet G (2019) Cell matrix adhesion in cell migration. *Essays Biochem* 63:535–551
34. PrahL LS, Odde DJ (2018) Modeling cell migration mechanics. *Biomech Oncol* 1092:159–187
35. Spatarelu C-P et al (2019) Biomechanics of collective cell migration in cancer progression: experimental and computational methods. *ACS Biom Sci Eng* 5:3766–3787

36. Scarpa E et al (2013) A novel method to study contact inhibition of locomotion using micropatterned substrates. *Biol Open* 2:901–906
37. Davis JR et al (2012) Emergence of embryonic pattern through contact inhibition of locomotion. *Development* 139:4555–4560
38. Desai RA, Gopal SB, Chen S, Chen CS (2013) Contact inhibition of locomotion probabilities drive solitary versus collective cell migration. *J R Soc Interface* 10:20130717
39. Milano DF, Ngai NA, Muthuswamy SK, Asthagiri AR (2016) Regulators of metastasis modulate the migratory response to cell contact under spatial confinement. *Biophys J* 110:1886–1895
40. Camley BA et al (2014) Polarity mechanisms such as contact inhibition of locomotion regulate persistent rotational motion of mammalian cells on micropatterns. *Proc Natl Acad Sci* 111: 14770–14775
41. Singh J, Pagulayan A, Camley BA, Nain AS (2021) Rules of contact inhibition of locomotion for cells on suspended nanofibers. *Proc Natl Acad Sci* 118:e2011815118
42. Peter Friedl RM (2017) Tuning collective cell migration by cell–cell junction regulation. *Cold Spring Harbor Perspect Biol* 9:a029199
43. Mayor R, Etienne-Manneville S (2016) The front and rear of collective cell migration. *Nat Rev Molecular Cell Biol* 17:97–109
44. Wong IY et al (2014) Collective and individual migration following the epithelial–mesenchymal transition. *Nat Mat* 13:1063–1071
45. Xi W, Saw TB, Delacour D, Lim CT, Ladoux B (2019) Material approaches to active tissue mechanics. *Nat Rev Mat* 4:23–44
46. Verkhovsky AB, Svitkina TM, Borisy GG (1999) Self-polarization and directional motility of cytoplasm. *Current Biol* 9:1–20
47. Bosgraaf L, Van Haastert PJ (2009) Navigation of chemotactic cells by parallel signaling to pseudopod persistence and orientation. *PLoS ONE* 4(8):1–11
48. Mayor R, Carmona-Fontaine C (2010) Keeping in touch with contact inhibition of locomotion. *Trends Cell Biol* 20: 319–328
49. Abercrombie M (1979) Contact inhibition and malignancy. *Nature* 281:259–262
50. Stramer BMR (2017) Mechanisms and in vivo functions of contact inhibition of locomotion. *Nat Rev Molecular Cell Biol* 18:43–55
51. George M, Bullo F, Campás O (2017) Connecting individual to collective cell migration. *Sci Rep* 7:9720
52. Lin S-Z, Ye S, Xu G-K, Li B, Feng X-Q (2018) Dynamic migration modes of collective cells. *Biophys J* 115:1826–1835
53. Sabri S et al (2000) Glycocalyx modulation is a physiological means of regulating cell adhesion. *J Cell Sci* 113:1589–1600
54. Yao Y, Rabodzey A, Dewey Jr CF (2007) Glycocalyx modulates the motility and proliferative response of vascular endothelium to fluid shear stress. *Amer J Physiol-Heart Circul Physiol* 293:H1023–H1030
55. Brembeck FH, Rosário M, Birchmeier W (2006) Balancing cell adhesion and Wnt signaling, the key role of  $\beta$ -catenin. *Current Opinion Genetics Develop* 16. *Oncogenes and 960 cell proliferation*, 51–59
56. Bienz M (2005)  $\beta$ -Catenin: a pivot between cell adhesion and Wnt signalling. *Current Biol* 15:R64–R67
57. Shaya O et al (2017) Cell-cell contact area affects notch signaling and notch-dependent patterning. *Develop Cell* 40:505–511
58. Batson J, Astin J, Nobes C (2013) Regulation of contact inhibition of locomotion by Ephrephrin signalling. *J Micro* 251:232–241
59. Astin JW et al (2010) Competition amongst Eph receptors regulates contact inhibition of locomotion and invasiveness in prostate cancer cells. *Nat Cell Biol* 12:1194–1204
60. Haeger A, Wolf K, Zegers MM, Friedl P (2015) Collective cell migration: guidance principles and hierarchies. *Trends Cell Biol* 25:556–566

61. Sapir L, Tzliil S (2017) Talking over the extracellular matrix: How do cells communicate mechanically? In *Seminars in cell & developmental biology* vol 71, pp 99–105
62. Sopher RS et al (2018) Nonlinear elasticity of the ECM fibers facilitates efficient intercellular communication. *Biophys J* 115:1357–1370
63. Kumar S, Kapoor A, Desai S, Inamdar MM, Sen S (2016) Proteolytic and non-proteolytic regulation of collective cell invasion: tuning by ECM density and organization. *Sci Rep* 6:1–17
64. Van Helvert S, Storm C, Friedl P (2018) Mechanoreciprocity in cell migration. *Nat Cell Biol* 20:8–20
65. Apte RS, Chen DS, Ferrara N (2019) VEGF in signaling and disease: beyond discovery and development. *Cell* 176:1248–1264
66. Bachelder RE, Wendt MA, Mercurio AM (2002) Vascular endothelial growth factor promotes breast carcinoma invasion in an autocrine manner by regulating the chemokine receptor CXCR4. *Cancer Res* 62:7203–7206
67. Roussos ET, Condeelis JS, Patsialou A (2011) Chemotaxis in cancer. *Nat Rev Cancer* 11:573–587
68. Roca-Cusachs P, Sunyer R, Trepat X (2013) Mechanical guidance of cell migration: lessons from chemotaxis. *Current Opinion Cell Biol* 25:543–549
69. Camley BA, Zimmermann J, Levine H, Rappel W-J (2016) Emergent collective chemotaxis without single-cell gradient sensing. *Phys Rev Lett* 116:098101
70. Kalluri R et al (2009) EMT: when epithelial cells decide to become mesenchymal-like cells. *J Clin Invest* 119:1417–1419
71. Bi D, Yang X, Marchetti MC, Manning ML (2016) Motility-driven glass and jamming transitions in biological tissues. *Phys Rev X* 6:021011
72. Castro MG, Leggett SE, Wong IY (2016) Clustering and jamming in epithelial–mesenchymal co-cultures. *Soft Mat* 12:8327–8337
73. Mitchel JA et al (2020) In primary airway epithelial cells, the unjamming transition is distinct from the epithelial-to-mesenchymal transition. *Nat Commun* 11:1–14
74. Liotta LA, Kleinerman J, Saidel GM (1974) Quantitative relationships of intravascular tumor cells, tumor vessels, and pulmonary metastases following tumor implantation. *Cancer Res* 34:997–1004
75. Küsters B et al (2007) Micronodular transformation as a novel mechanism of VEGF-A-induced metastasis. *Oncogene* 26:5808–5815
76. Barua A, Nava-Sedeño JM, Meyer-Hermann M, Hatzikirou H (2020) A least microenvironmental uncertainty principle (LEUP) as a generative model of collective cell migration mechanisms. *Sci Rep* 10:1–13
77. Pujar AA et al (2021) Lattice-based microenvironmental uncertainty driven phenotypic decisionmaking: a comparison with Notch-Delta-Jagged signaling. *bioRxiv* 11:468748
78. Palsson E, Othmer HG (2000) A model for individual and collective cell movement in *Dictyostelium discoideum*. *Proc Natl Acad Sci* 97:10448–10453
79. Hoehne S, Drasdo D (2010) A cell-based simulation software for multi-cellular systems. *Bioinformatics* 26:2641–2642
80. Basan M, Elgeti J, Hannezo E, Rappel W-J, Levine H (2013) Alignment of cellular motility forces with tissue flow as a mechanism for efficient wound healing. *Proc Natl Acad Sci* 110:2452–2459
81. Czirók A, Barabási A-L, Vicsek T (1999) Collective motion of self-propelled particles: Kinetic phase transition in one dimension. *Phys Rev Lett* 82:209
82. Couzin ID, Krause J, James R, Ruxton GD, Franks NR (2002) Collective memory and spatial sorting in animal groups. *J Theor Biol* 218:1–11
83. Cucker F, Smale S (2007) Emergent behavior in flocks. *IEEE Trans Autom Control* 52: 852–862
84. Vicsek T, Czirók A, Ben-Jacob E, Cohen I, Shochet O (1995) Novel type of phase transition in a system of self-driven particles. *Phys Rev Lett* 75:1226

85. AOKI I (1982) A simulation study on the schooling mechanism in fish. *NIPPON SUISAN GAKKAISHI* 48:1081–1088
86. Gazi V, Passino KM (2004) A class of attractions/repulsion functions for stable swarm aggregations. *Int J Control* 77:1567–1579
87. Huth A, Wissel C (1992) The simulation of the movement of fish schools. *J Theor Biol* 156:365–385
88. Mogilner A, Edelstein-Keshet L, Bent L, Spiros A (2003) Mutual interactions, potentials, and individual distance in a social aggregation. *J Math Biol* 47:353–389
89. Reynolds CW (1987) Flocks, herds and schools: a distributed behavioral model. In: Proceedings of the 14th annual conference on computer graphics and interactive techniques, pp 25–34
90. Bi D, Lopez J, Schwarz JM, Manning ML (2015) A density-independent rigidity transition in biological tissues. *Nat Phys* 11:1074–1079
91. Park J-A et al (2015) Unjamming and cell shape in the asthmatic airway epithelium. *Nat Mat* 14:1040–1048
92. Camley BA, Rappel W-J (2017) Physical models of collective cell motility: from cell to tissue. *J Phys D Appl Phys* 50:113002
93. Palsson E (2001) A three-dimensional model of cell movement in multicellular systems. *Future Gener Comput Sys* 17:835–852
94. Vedel S, Tay S, Johnston DM, Bruus H, Quake SR (2013) Migration of cells in a social context. *Proc Natl Acad Sci* 110:129–134
95. Van Liedekerke P, Palm M, Jagiella N, Drasdo D (2015) Simulating tissue mechanics with agent-based models: concepts, perspectives and some novel results. *Comput Part Mech* 2:401–444
96. Sandersius SA, Newman TJ (2008) Modeling cell rheology with the subcellular element model. *Phys Biol* 5:015002
97. Sandersius S, Weijer CJ, Newman TJ (2011) Emergent cell and tissue dynamics from subcellular modeling of active biomechanical processes. *Phys Biol* 8:045007
98. Gardiner BS et al (2015) Discrete element framework for modelling extracellular matrix, deformable cells and subcellular components. *PLoS Comput Biol* 11:e1004544
99. Zimmermann J, Camley BA, Rappel W-J, Levine H (2016) Contact inhibition of locomotion determines cell–cell and cell–substrate forces in tissues. *Proc Natl Acad Sci* 113: 2660–2665
100. Yang Y, Levine H (2018) Role of the supracellular actomyosin cable during epithelial wound healing. *Soft Matter* 14:4866–4873
101. Yang Y, Jolly MK, Levine H (2019) Computational modeling of collective cell migration: mechanical and biochemical aspects. In: *Cell Migrations: Causes and Functions*. Springer, Cham, pp 1–11
102. La Porta CA, Zapperi S (2019) *Cell Migrations: Causes and Functions*. Advances in Experimental Medicine and Biology. Springer, Cham.
103. Alt S, Ganguly P, Salbreux G (2017) Vertex models: from cell mechanics to tissue morphogenesis. *Philosoph Trans R Soc B Biol Sci* 372:20150520
104. Okuda S, Miura T, Inoue Y, Adachi T, Eiraku M (2018) Combining turing and 3D vertex models reproduces autonomous multicellular morphogenesis with undulation, tubulation, and branching. *Sci Rep* 8:1–15
105. Honda H (1978) Description of cellular patterns by Dirichlet domains: the two-dimensional case. *J Theor Biol* 72:523–543
106. Wigner E, Seitz F (1933) On the constitution of metallic sodium. *Phys Rev* 43:804
107. Vazquez-Faci T, van Dronghen R, van der Zee M, Idema T (2017) Mechanics of epithelial tissue formation in early insect embryos. Preprint arXiv:1705.06205
108. Yang X et al (2017) Correlating cell shape and cellular stress in motile confluent tissues. *Proc Natl Acad Sci* 114:12663–12668
109. Alber MS, Kiskowski MA, Glazier JA, Jiang Y (2003) On cellular automaton approaches to modeling biological cells. In: *Mathematical systems theory in biology, communications, computation, and finance*. Springer, Berlin, pp 1–39



110. Hatzikirou H, Brusch L, Schaller C, Simon M, Deutsch A (2010) Prediction of traveling front behavior in a lattice-gas cellular automaton model for tumor invasion. *Comput Math Appl* 59:2326–2339
111. Mente C, Prade I, Brusch L, Breier G, Deutsch A (2011) Parameter estimation with a novel gradient-based optimization method for biological lattice-gas cellular automaton models. *J Math Biol* 63:173–200
112. Alber MS, Jiang Y, Kiskowski MA (2004) Lattice gas cellular automation model for rippling and aggregation in myxobacteria. *Phys D Nonlinear Phenomena* 191:343–358
113. Syga S, Nava-Sedeño JM, Brusch L, Deutsch A (2019) A lattice-gas cellular automaton model for discrete excitable media. In: *Spirals and vortices*. Springer, Cham, pp 253–264
114. Fuks H, Lawniczak AT (2001) Individual-based lattice model for spatial spread of epidemics. *Discrete Dyn Nat and Soc* 6:191–200
115. Iliina O et al (2020) Cell-cell adhesion and 3D matrix confinement determine jamming transitions in breast cancer invasion. *Nat Cell Biol* 22:1103–1115
116. Moreira J, Deutsch A (2002) Cellular automaton models of tumor development: a critical review. *Adv Comp Sys* 5:247–267
117. Reher D, Klink B, Deutsch A, Voss-Böhme A (2017) Cell adhesion heterogeneity reinforces tumour cell dissemination: novel insights from a mathematical model. *Biol Direct* 12:1–17
118. Böttger K et al (2015) An emerging Allee effect is critical for tumor initiation and persistence. *PLoS Comput Biol* 11:e1004366
119. Tektonidis M et al (2011) Identification of intrinsic in vitro cellular mechanisms for glioma invasion. *J Theor Biol* 287:131–147
120. Deutsch A, Nava-Sedeño JM, Syga S, Hatzikirou H (2021) BIO-LGCA: a cellular automaton modelling class for analysing collective cell migration. *PLOS Comput Biol* 17:e1009066
121. Graner F, Glazier JA (1992) Simulation of biological cell sorting using a two-dimensional extended Potts model. *Phys Rev Lett* 69:2013
122. Magno R, Grieneisen VA, Marée AF (2015) The biophysical nature of cells: potential cell behaviours revealed by analytical and computational studies of cell surface mechanics. *BMC Biophys* 8:1–37
123. Szabó A et al (2010) Collective cell motion in endothelial monolayers. *Phys Biol* 7:046007
124. Thüroff F, Goychuk A, Reiter M, Frey E (2019) Bridging the gap between single-cell migration and collective dynamics. *Elife* 8:e46842
125. Kabla AJ (2012) Collective cell migration: leadership, invasion and segregation. *J R Soc Interface* 9:3268–3278
126. Glazier JA, Graner F (1993) Simulation of the differential adhesion driven rearrangement of biological cells. *Phys Rev E* 47:2128
127. Varennes J, Han B, Mugler A (2016) Collective chemotaxis through noisy multicellular gradient sensing. *Biophys J* 111:640–649
128. Voss-Böhme A (2012) Multi-scale modeling in morphogenesis: a critical analysis of the cellular Potts model. *PLoS ONE* 7(9):e42852
129. Nonomura M (2012) Study on multicellular systems using a phase field model. *PloS one* 7:e33501
130. Löber J, Ziebert F, Aranson IS (2015) Collisions of deformable cells lead to collective migration. *Sci Rep* 5:1–7
131. Palmieri B, Bresler Y, Wirtz D, & Grant M, Multiple scale model for cell migration in monolayers: Elastic mismatch between cells enhances motility. *Sci Rep* 5:1–13 (2015)
132. Brown FL, Elastic modeling of biomembranes and lipid bilayers. *Annu. Rev. Phys. Chem.* 59: 685–712 (2008)
133. Segerer FJ, Thüroff F, Alberola AP, Frey E, Rädler JO (2015) Emergence and persistence of collective cell migration on small circular micropatterns. *Phys Rev Lett* 114:228102
134. Kulawiak DA, Camley BA, Rappel W-J (2016) Modeling contact inhibition of locomotion of colliding cells migrating on micropatterned substrates. *PLoS Comput Biol* 12:e1005239
135. Camley BA, Zhao Y, Li B, Levine H, Rappel W-J (2013) Periodic migration in a physical model of cells on micropatterns. *Phys Rev Lett* 111:158102

136. Rejniak KA (2007), An immersed boundary framework for modelling the growth of individual cells: an application to the early tumour development. *J Theor Biol* 247:186–204
137. Batchelor CK, Batchelor G (2000) An introduction to fluid dynamics. Cambridge University Press, Cambridge
138. Li Y, Yun A, Kim J (2012) An immersed boundary method for simulating a single axisymmetric cell growth and division. *J Math Biol* 65:653–675
139. Mikhal J, Geurts BJ (2013) Development and application of a volume penalization immersed boundary method for the computation of blood flow and shear stresses in cerebral vessels and aneurysms. *J Math Biol* 67:1847–1875
140. Zhao J et al (2013) Dynamic mechanical finite element model of biological cells for studying cellular pattern formation. In: 2013 35th Annual international conference of the IEEE engineering in medicine and biology society (EMBC), pp 4517–4520
141. Zhao J, Cao Y, DiPietro LA, Liang J (2017) Dynamic cellular finite-element method for modelling large-scale cell migration and proliferation under the control of mechanical and biochemical cues: a study of re-epithelialization. *J R Soc Interface* 14:20160959
142. Delarue M, Joanny J-F, Jülicher F, Prost J (2014) Stress distributions and cell flows in a growing cell aggregate. *Interface Focus* 4:20140033
143. Sarkar N, Prost J, Jülicher F (2019) Field induced cell proliferation and death in a model epithelium. *New J Phys* 21:043035
144. Marth W, Voigt A (2016) Collective migration under hydrodynamic interactions: a computational approach. *Interface Focus* 6:20160037
145. Marth W, Praetorius S, Voigt A (2015) A mechanism for cell motility by active polar gels. *J R Soc Interface* 12:20150161
146. Löber J, Ziebert F, Aranson IS (2014) Modeling crawling cell movement on soft engineered substrates. *Soft Matter* 10:1365–1373
147. Jeon J, Quaranta V, Cummings PT (2010) An off-lattice hybrid discrete-continuum model of tumor growth and invasion. *Biophys J* 98:37–47
148. Lyu J, Cao J, Zhang P, Liu Y, Cheng H (2016) Coupled hybrid continuum-discrete model of tumor angiogenesis and growth. *PLoS one* 11:e0163173
149. de Montigny J et al (2021) An in silico hybrid continuum-/agent-based procedure to modelling cancer development: interrogating the interplay amongst glioma invasion, vascularity and necrosis. *Methods* 185:94–104
150. Wijeratne PA, Hipwell JH, Hawkes DJ, Stylianopoulos T, Vavourakis V (2017) Multiscale biphasic modelling of peritumoural collagen microstructure: The effect of tumour growth on permeability and fluid flow. *PLoS one* 12:e0184511
151. Anderson AR, Chaplain MA, Newman EL, Steele RJ, Thompson AM (2000) Mathematical modelling of tumour invasion and metastasis. *Comput Math Methods Med* 2:129–154
152. Bauer R et al (2017) Advanced research on biologically inspired cognitive architectures. IGI Global, Pennsylvania, pp 117–125
153. Ghaffarizadeh A, Friedman SH, Macklin P (2016) BioFVM: an efficient, parallelized diffusive transport solver for 3-D biological simulations. *Bioinformatics* 32:1256–1258
154. Ghaffarizadeh A, Heiland R, Friedman SH, Mumenthaler SM, Macklin P (2018) PhysiCell: An open source physics-based cell simulator for 3-D multicellular systems. *PLoS Comput Biol* 14:e1005991
155. Stoll G et al (2017) MaBoSS 2.0: an environment for stochastic Boolean modeling. *Bioinformatics* 33:2226–2228
156. Letort G et al (2019) PhysiBoSS: a multi-scale agent-based modelling framework integrating physical dimension and cell signalling. *Bioinformatics* 35:1188–1196
157. Swat MH et al (2012) Multi-scale modeling of tissues using CompuCell3D. *Methods Cell Biol* 110:325–366
158. Starrau J, De Back W, Brusch L, Deutsch A (2014) Morpheus: a user-friendly modeling environment for multiscale and multicellular systems biology. *Bioinformatics* 30:1331–1332
159. Starrau J, Bley T, Søggaard-Andersen L, Deutsch A (2007) A new mechanism for collective migration in *Myxococcus xanthus*. *J Statist Phys* 128:269–286

160. de Back W, Zhou JX, Brusch L (2013) On the role of lateral stabilization during early patterning in the pancreas. *J R Soc Interface* 10:20120766
161. Köhn-Luque A et al (2011) Early embryonic vascular patterning by matrix-mediated paracrine signalling: a mathematical model study. *PLoS One* 6:e24175
162. Köhn-Luque A et al (2013) Dynamics of VEGF matrix-retention in vascular network patterning. *Phys Biol* 10:066007
163. Mulberry N, Edelstein-Keshet L (2020) Self-organized multicellular structures from simple cell signaling: a computational model. *Phys Biol* 17:066003
164. Pitt-Francis J et al (2009) Chaste: a test-driven approach to software development for biological modelling. *Comput Phys Commun* 180:2452–2471
165. Mirams GR et al (2013) Chaste: an open source C++ library for computational physiology and biology. *PLoS Comput Biol* 9:e1002970
166. Pathmanathan P, Bernabeu M, Niederer S, Gavaghan D, Kay D (2012) Computational modelling of cardiac electrophysiology: explanation of the variability of results from different numerical solvers. *Int J Numer Methods Biomed Eng* 28:890–903
167. Dunn S-J, Näthke IS, Osborne JM (2013) Computational models reveal a passive 1228 mechanism for cell migration in the crypt. *PLoS one* 8:e80516
168. Davit Y, Osborne JM, Byrne H, Gavaghan D, Pitt-Francis J (2013) Validity of the Cauchy-Born rule applied to discrete cellular-scale models of biological tissues. *Phys Rev E* 87:042724
169. Choi HJ et al (2021) Emerging machine learning approaches to phenotyping cellular motility and morphodynamics. *Phys Biol* 18:041001
170. Montero P, Vilar JA (2015) TSclust: an R package for time series clustering. *J Statist Softw* 62:1–43
171. Kramer MA (1991), Nonlinear principal component analysis using autoassociative neural networks. *AIChE J* 37:233–243
172. Goodfellow I et al (2014) Generative adversarial nets. In: *Advances in neural information processing systems*, vol 27
173. LeCun Y, Bengio Y, Hinton G (2015) Deep learning. *Nature* 521:436–444
174. Cortes C, Vapnik V (1995) Support-vector networks. *Mach Learn* 20:273–297
175. Durbin R, Eddy SR, Krogh A, Mitchison G (1998) *Biological sequence analysis: probabilistic models of proteins and nucleic acids*. Cambridge University Press, Cambridge
176. Hou H et al (2019) Using deep reinforcement learning to speed up collective cell migration. *BMC Bioinf* 20:1–10
177. LaChance J, Suh K, Clausen J, Cohen DJ (2022) Learning the rules of collective cell migration using deep attention networks. *PLoS Comput Biol* 18:e1009293
178. Mencattini A et al (2020) Discovering the hidden messages within cell trajectories using a deep learning approach for in vitro evaluation of cancer drug treatments. *Sci Rep* 10:1–11
179. Kalluri R, Weinberg RA et al (2009) The basics of epithelial-mesenchymal transition. *J Clin Invest* 119:1420–1428
180. Subbalakshmi AR, Ashraf B, Jolly MK (2022) Biophysical and biochemical attributes of hybrid epithelial/mesenchymal phenotypes. *Phys Biol* 19:025001
181. Tian X-J, Zhang H, Xing J (2013) Coupled reversible and irreversible bistable switches underlying TGF $\beta$ -induced epithelial to mesenchymal transition. *Biophys J* 105:1079–1089
182. Lu M, Jolly MK, Levine H, Onuchic JN, Ben-Jacob E (2013) MicroRNA-based regulation of epithelial–hybrid–mesenchymal fate determination. *Proc Natl Acad Sci* 110:18144–18149
183. Subbalakshmi AR et al (2020) NFATc acts as a non-canonical phenotypic stability factor for a hybrid epithelial/mesenchymal phenotype. *Front Oncol* 10:1794
184. Jolly MK et al (2016) Stability of the hybrid epithelial/mesenchymal phenotype. *Oncotarget* 7:27067
185. Hang-Yu Wang, Xiao-Peng Zhang, Wei Wang (2022) Regulation of epithelial-to-mesenchymal transition in hypoxia by the HIF-1 $\alpha$  network. *FEBS Lett.* 596(3): 338–349
186. Hari K et al (2020) Identifying inhibitors of epithelial–mesenchymal plasticity using a network topology-based approach. *NPJ Syst Biol Appl* 6:1–12

187. Steinway SN et al (2015) Combinatorial interventions inhibit TGF $\beta$ -driven epithelial-to-mesenchymal transition and support hybrid cellular phenotypes. *NPJ Syst Biol Appl* 1:1–12
188. Font-Clos F, Zapperi S, La Porta CA (2018) Topography of epithelial–mesenchymal plasticity. *Proc Natl Acad Sci* 115:5902–5907
189. Silveira DA, Gupta S, Mombach JCM (2020) Systems biology approach suggests new miRNAs as phenotypic stability factors in the epithelial–mesenchymal transition. *J R Soc Interface* 17:20200693
190. Hari K, Ram U, Jolly MK (2021) Identifying “more equal than others” edges in diverse biochemical networks. *Proc Natl Acad Sci* 118:e2103698118
191. Shatkin G, Yeoman B, Birmingham K, Katira P, Engler AJ (2020) Computational models of migration modes improve our understanding of metastasis. *APL Bioeng* 4:041505
192. Deng Y, Chakraborty P, Jolly MK, Levine H (2021) A theoretical approach to coupling the epithelial-mesenchymal transition (EMT) to extracellular matrix (ECM) stiffness via LOXL2. *Cancers* 13:1609
193. Hino N et al (2020) ERK-mediated mechanochemical waves direct collective cell polarization. *Develop Cell* 53:646–660
194. Bui J, Conway DE, Heise RL, Weinberg SH (2019) Mechanochemical coupling and junctional forces during collective cell migration. *Biophys J* 117:170–183
195. Murad HY et al (2019) Mechanochemical disruption suppresses metastatic phenotype and pushes prostate cancer cells toward apoptosis. *Molecular Cancer Res* 17:1087–1101
196. Hirway SU, Lemmon CA, Weinberg SH (2021) Multicellular mechanochemical hybrid cellular Potts model of tissue formation during epithelial-mesenchymal transition. *Comput Syst Oncol* 1:e1031
197. Boockock D, Hino N, Ruzickova N, Hirashima T, Hannezo E (2021) Theory of mechanochemical patterning and optimal migration in cell monolayers. *Nat Phys* 17:267–274
198. Buttenschön A, Edelstein-Keshet L (2020) Bridging from single to collective cell migration: A review of models and links to experiments. *PLoS Comput Biol* 16:e1008411
199. Alert R, Trepast X (2020) Physical models of collective cell migration. *Ann Rev Condensed Matter Phys* 11:77–101
200. Collins TA, Yeoman BM, Katira P (2020) To lead or to herd: optimal strategies for 3D collective migration of cell clusters. *Biomech Modeling Mechanobiol* 19:1551–1564
201. Camley BA, Zimmermann J, Levine H, Rappel W-J (2016) Collective signal processing in cluster chemotaxis: Roles of adaptation, amplification, and co-attraction in collective guidance. *PLoS Comput Biol* 12:e1005008
202. Jiao Y, Torquato S (2011) Emergent behaviors from a cellular automaton model for invasive tumor growth in heterogeneous microenvironments. *PLoS Comput Biol* 7:e1002314
203. Reddy GA, Katira P (2022) Differences in cell death and division rules can alter tissue rigidity and fluidization. *Soft Matter* 18:3713–3724
204. Labernadie A et al (2017) A mechanically active heterotypic E-cadherin/N-cadherin adhesion enables fibroblasts to drive cancer cell invasion. *Nat Cell Biol* 19:224–237
205. VanderVorst K et al (2019) Wnt/PCP signaling contribution to carcinoma collective cell migration and metastasis. *Cancer Res* 79:1719–1729
206. Wyckoff J et al (2004) A paracrine loop between tumor cells and macrophages is required for tumor cell migration in mammary tumors. *Cancer Res* 64:7022–7029
207. Bocci F et al (2019) Toward understanding cancer stem cell heterogeneity in the tumor microenvironment. *Proc Natl Acad Sci* 116:148–157
208. Carmona-Fontaine C et al (2013) Emergence of spatial structure in the tumor microenvironment due to the Warburg effect. *Proc Natl Acad Sci* 110:19402–19407
209. Yaron T, Cordova Y, Sprinzak D (2014) Juxtacrine signaling is inherently noisy. *Biophys J* 107:2417–2424
210. Bocci F, Onuchic JN, Jolly MK (2020) Understanding the principles of pattern formation driven by notch signaling by integrating experiments and theoretical models. *Front Physiol* 11:929
211. Bajpai S, Prabhakar R, Chelakkot R, Inamdar MM (2021) Role of cell polarity dynamics and motility in pattern formation due to contact-dependent signalling. *J R Soc Interface* 18:20200825

# Hallmarks of an Aging and Malignant Tumor Microenvironment and the Rise of Resilient Cell Subpopulations



Carolina Mejia Peña, Amy H. Lee, Mateo F. Frare, Deepraj Ghosh,  
and Michelle R. Dawson

**Abstract** Intratumor heterogeneity, which includes intrinsic differences in cancer cells and morphological differences in the tissue architectures, represents a major challenge in understanding and treating cancer. Additionally, physical and molecular interactions between cancer cells and their surrounding tumor microenvironment, with its diversity in cell types and matrix mechanics, play a critical role in directing tumor growth and cancer progression. This chapter discusses how physical and molecular aspects of hallmark cancer traits and the tumor microenvironment have contributed to our understanding of cancer cell behavior. We discuss how the evolution of a malignant tumor microenvironment can protect, foster, and even prime stromal and cancer populations against future therapy-associated stress. Specifically, we highlight the development of senescent stromal populations and polyploid giant cancer cells – resilient subpopulations contributing to chemoresistance and disease recurrence. We summarize key studies used to profile cell forces, cytoskeletal mechanics, and a number of other cell variables (i.e., morphology, migration, proliferation) that are important in cancer progression. These physical approaches are combined with molecular analysis to systematically examine tumor microenvironment conditions that control cell

---

Authors Carolina Mejia Peña and Amy H. Lee have equally contributed to this chapter.

---

C. Mejia Peña · D. Ghosh

Department of Molecular Biology, Cell Biology and Biochemistry, Brown University,  
Providence, RI, USA

A. H. Lee · M. F. Frare

Center for Biomedical Engineering, Brown University, Providence, RI, USA

M. R. Dawson (✉)

Department of Molecular Biology, Cell Biology and Biochemistry, Brown University,  
Providence, RI, USA

Center for Biomedical Engineering, Brown University, Providence, RI, USA

e-mail: [michelle\\_dawson@brown.edu](mailto:michelle_dawson@brown.edu)

behavior, prime against therapeutic interventions, and contribute to the inherent heterogeneity in tumor microenvironments.

## 1 Introduction: Hallmark Physical and Molecular Cancer Traits

Cancer is a heterogeneous disease characterized by rapid growth of mutated cells that develop hallmark features of malignancy that contribute to cancer progression. In their seminal paper, Douglas Hanahan and Robert Weinberg described six essential hallmarks of cancer: (1) replicative immortality; (2) resistance to apoptosis; (3) autonomy in growth signaling; (4) evasion of growth suppressors; (5) tissue invasion and metastasis; and (6) sustained angiogenesis [1]. Recently, emerging cancer traits were added to this list, including: (7) tumor-promoting inflammation; (8) alterations in metabolism; (9) immune suppression; and (10) genomic instability [2], and even more recently, (11) senescent cells; (12) polymorphic microbiomes; (13) epigenetic reprogramming; and (14) phenotypic plasticity were added to this list of cancer hallmarks [3].

Many of the hallmark cancer traits, including unlimited replicative potential, apoptotic evasion, and tissue invasion and metastasis, can be directly linked to the abnormal cytoskeletal dynamics of cancer cells [4]. Thus, an increasing number of studies have focused on understanding how the biomechanical properties of cells and tissues influence these hallmark cancer traits and cancer progression [5, 6]. Atomic force microscopy [7], traction force microscopy [8], and multiple particle tracking microrheology [9] have been used to quantitatively study biomechanical changes in cells and tissues under pathological and treatment stress. These studies have demonstrated how the balance in cellular forces and matrix rigidity is disrupted in cancer [10] and the critical role of the tumor microenvironment (TME) in cancer progression [11].

The TME describes the complex milieu of tumor cells, stromal cells (such as fibroblasts, immune cells, endothelial cells), and blood and lymphatics vessels, and secreted factors (including cytokines, growth factors, and matrix proteins) present in the tumor. As cancer progresses, the TME is under a great deal of solid stress from rapidly growing and evolving tumors, extracellular matrix (ECM) remodeling, tissue stiffening, and vessel compression, which leads to high interstitial fluid pressures [6]. The stressful conditions in the TME can also select for cells capable of surviving in these harsh conditions. Furthermore, cells within complex three-dimensional (3D) TMEs are under varying levels and kinds of stress, depending on their location in the 3D structure (e.g., at the center or periphery of the tumor) and proximity to blood vessels (that provide nutrients and oxygen to the tumor).

The spatial variation in tumor architecture and variability in stress conditions lead to intratumor heterogeneity within cancer cells populations [12]. Since metastasis is a highly selective process with less than 0.1% of tumor cells capable of forming metastatic tumors [13], it is critical to understand how the spatial heterogeneity

in cancer cells contributes to metastasis. Importantly, cancer cells are thought to metastasize to specific microenvironments that are preconditioned by tumor-secreted soluble factors which promote their colonization and proliferation [14]. Thus, it is critical to understand how diversity in soluble growth factors affect TME development [15].

In addition to molecular and spatial contributions of the TME, intrinsic factors such as cell state can also dramatically impact cancer cell heterogeneity and malignancy. Almost 30% of patients diagnosed with cancer are age 65 or older, and the population of senior citizens (age 65 and older) is predicted to double within 40 years; thus, understanding how aging and accumulating senescent cells affect TME conditions that contribute to cancer progression is critical [16]. A major cause of age-dependent diseases, such as cancer, is senescence. Senescence constitutes a stress response triggered by genomic instability, oxidative stress, and telomere attrition, which are primary aging hallmarks. Importantly, senescence is largely characterized by stable growth arrest. Numerous types of cells in the primary TME can undergo senescence and Senescent cells that accumulate in aging tissues develop a pro-inflammatory senescence associated secretory phenotype (SASP) that profoundly alters the surrounding tissue to promote cancer [17]. For example, we previously showed that senescent stromal cells can remodel 3D collagen networks to promote breast cancer cell migration [18].

In addition, chemotherapy and radiation, which are widely used to treat cancer, can cause therapy-induced senescence and polyploidy. Polyploidy in cancer cells and stromal cells can be a result of mitotic slippage, endoreplication, and cell fusion [19]. We have subsequently described the physical and molecular alterations after therapy-induced senescence in stromal cells and the resilient subpopulation of polyploid giant cancer cells (PGCCs) [18, 20, 21].

Overall, this chapter discusses the key molecular and physical components of an evolving TME and how such a TME promotes the generation of resilient stromal and cancer cell populations, in the face of anticancer therapies (Fig. 1).

## 2 Tumor Microenvironment

Tumorigenesis and cancer progression are greatly influenced by the local tissue environment surrounding pre-malignant and malignant cells, which is referred to as the TME [22]. The TME consists of tumor cells, local and recruited stromal cells, and the soluble factors and matrices that are present within these environments [23]. In response to tumor-secreted factors like growth factors, cytokines, and exosomes, stromal cells (e.g., fibroblasts, immune cells, endothelial cells, and stem cells) are recruited from the local tissue, blood, and bone marrow into the tumor. For example, we have previously shown how large numbers of bone marrow derived cells are recruited to primary and metastatic tumor tissues using a bone marrow transplant mouse models with GFP positive bone marrow derived cells (Fig. 2) [24].

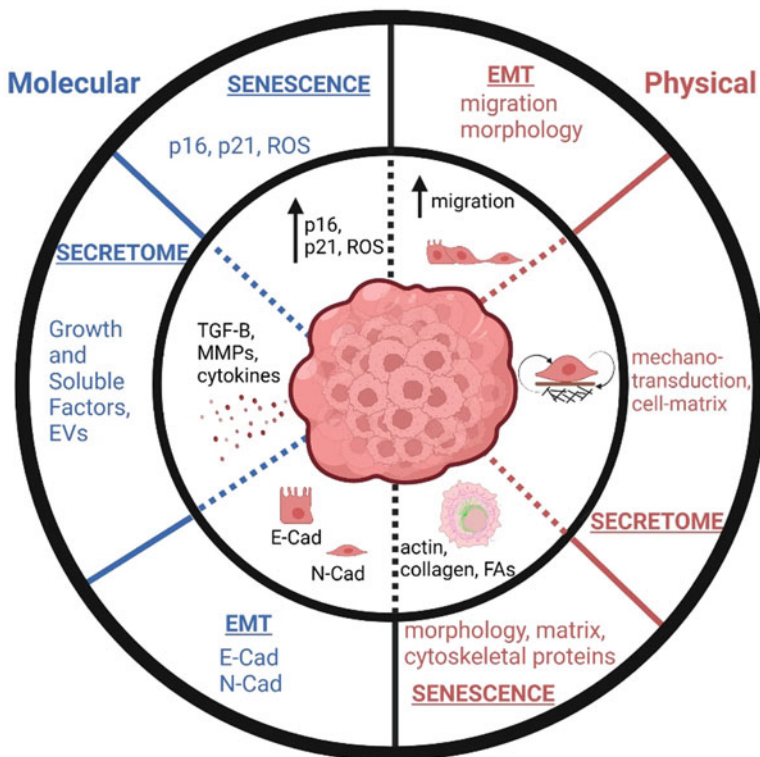


**Fig. 1** Molecular and physical hallmarks of cancer. This figure illustrates how the microenvironment of a solid tumor contributes to key alterations in the hallmark features of the tumor pathology

These recruited cells play critical roles in tumor growth and metastasis [25] and can even prime the secondary tissue sites prior to metastasis [26]. Stephen Paget’s nineteenth century “seed and soil” hypothesis first highlighted the pivotal role of the TME in metastasis [27]. The theory states that tumor cells metastasize to specific environments that can support their growth [27]. However, this idea of TME-specific metastasis was ignored for many years, with cancer research largely focusing on differences in tumor cells [28], until the seminal work from Isaiah Fidler, which demonstrated that tumor cells undergo site-specific metastasis [29]. Since then, research on the TME has clearly shown that crosstalk between tumor and stromal cells, through direct cell–cell interactions and soluble factor exchange [23], are critical to cancer progression.



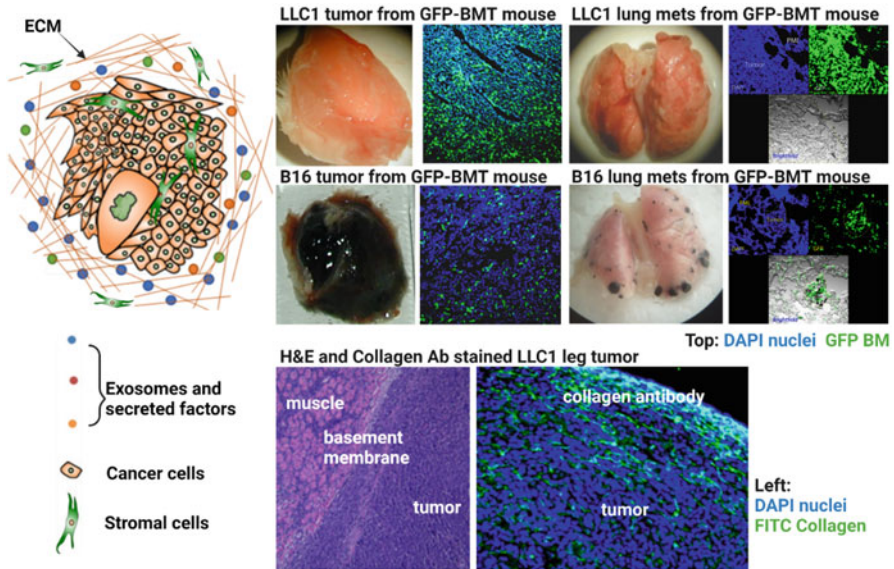


**Fig. 2** Role of stromal cells in the tumor microenvironment. **(Left)** Cartoon illustrating the cells, soluble factors, and extracellular matrix proteins that are present in solid tumors. **(Right)** Images of primary mouse tumors (grown in lower leg) and metastatic lung tumors from GFP-positive bone marrow transplant (BMT) mice (top 2 rows) and wild type (WT) mice (bottom row). Images from BMT mice illustrate that solid tumors (at the primary and secondary sites) contain large numbers of non-malignant cells that are derived directly from the bone marrow. The H&E image shows LLC1 tumor cells having crossed the collagen-rich basement membrane to invade the surrounding muscle. The image on the right shows an isolated LLC1 tumor that has been stained for Collagen Type I, demonstrating the dense collagen staining at the periphery of the tumor. (These images are adapted from Dawson et al. PLOS ONE 4(9): e6525 (2009))

### 2.1 Overview of Cell Types in the Tumor Microenvironment

Multiple cell types reside in the microenvironment of solid tumors, including tumor infiltrating immune cells, endothelial cells, adipocytes, and fibroblasts – all affecting tumor progression [30]. Tumor infiltrating immune cells within the TME include immunosuppressive cells, such as tumor-associated macrophages (TAMs) [31], myeloid-derived suppressor cells (MDSCs) [32], and regulatory T cells (T-reg) [33], as well as tumor-fighting cells, such as cytotoxic CD8 positive T-cells, CD4 positive helper T-cells (Th1), and natural killer (NK) cells [34]. Cytotoxic T-cells contribute to immune surveillance, and immunosuppressive T-reg cells and macrophages promote tumor growth and progression [35], while the role of dendritic cells and NK cells remains less clear [36]. Furthermore, adipocytes that reside in the tumor and nearby tissues have been shown to provide fatty acids and lipid signaling molecules that accelerate tumor growth. Endothelial cells and pericytes recruited to the tumor have also been shown to promote tumor persistence and growth via

angiogenesis [37]. Fibroblasts, specifically cancer-associated fibroblasts (CAFs), also play a key role in tumor maintenance [38], as they contribute greatly to the formation of matrix components and the supply of soluble factors in the tumor [39]. Signals conferred by fibroblasts have been shown to increase tumor growth and metastasis by altering the architecture of the tissue and altering the tumor immune response [40]. Mesenchymal stem cells (MSCs) are also recruited to the TME from nearby tissue and bone marrow [41] in response to tumor-secreted soluble factors that promote cell migration [42–44]. In normal tissues, MSCs largely reside in a quiescent state, where they primarily function in the replacement and turnover of aging somatic cells [45]. However, in the tumor, MSCs can differentiate into CAFs [41] that promote tumor inflammation [46], tumor growth, matrix remodeling, and angiogenesis [2]. We will now cover specific tumor-associated cell types in more detail, as well as non-cellular components of the TME.

## ***2.2 Tumor-Infiltrating Immune Cells***

Understanding the composition and level of activation of immune cells that infiltrate the tumor is critical in diagnosing and treating cancer. Single cell RNA sequencing studies have revealed that similar cancer types may have vastly different immune cell profiles; this strategy was used to cluster approximately 400 triple negative breast cancer (TNBC) tissues into three phenotypes, including immune cell deficient phenotype (tumors with low immune cell infiltration), innate immune inactivated phenotype (tumors with mostly inactive innate immune cells and immune stromal cells), and immune-inflamed phenotype (tumors with high levels of active innate and adaptive immune cells) [47]. Based on the abundance of immune cells in the last phenotype, immune-inflamed tumors are referred to as “hot tumors”; whereas, the other phenotypes are considered “cold tumors.” Since “hot tumors” are more likely to respond to immunotherapy, many current studies are focused on therapeutic strategies for “firing up the tumor microenvironment by turning cold tumors into hot tumors.” [48] Thus, studies aimed at increasing our understanding of the immunosuppressive aspects of the TME are critical in overcoming the setbacks in clinical trials for cancer immunotherapy [49].

## ***2.3 Tumor-Associated Fibroblasts***

Fibroblasts have a variety of functions and are known to play key roles in the TME via deposition and remodeling of the ECM as well as their effects on cell migration, differentiation, and inflammation [39]. Fibroblasts migrating in 3D collagen gels also alter the local mechanical properties of the collagen network by increasing the density of collagen fibers surrounding cells; at high cell densities, this matrix-stiffening effect may lead to global changes in the collagen network,

including mechanical loading of stretched fibers and collagen contraction [50, 51]. Collagen cross-linking is an important mechanism of ECM remodeling in cancer, which results in tissue stiffening in tumors [52]. In tumors, fibroblasts often develop into CAFs, which are highly contractile matrix producing cells that contribute to TME development and malignant progression [53]. CAFs promote tumor growth and matrix invasion by: (1) increasing matrix deposition, cross-linking, and bundling for increased tumor stiffness [54]; (2) generating force and protease-mediated tracks that allow cancer cells to escape during metastasis [55]; and (3) activating mechanosensitive signaling pathways that promote disease progression [56]. Multiple clinical studies have shown that cancer patients with higher CAF activity have more aggressive tumors with increased infiltration by tumor-associated macrophages and more metastasis, suggesting that CAFs may affect tumor inflammation and cancer cell escape during metastasis [57, 58].

## 2.4 *Tumor-Associated ECM*

The extracellular matrix (ECM) is a dynamic network of structural proteins that includes fibrous collagen proteins, glycoproteins such as periostin, proteoglycans like decorin and aggrecan, and polysaccharides such as hyaluronic acid [59]. Physical properties of the ECM (e.g., stiffness and porosity) provide structural support for the TME and biochemical features (e.g., specific integrins in the ECM) anchor cells to the network and control numerous cell behaviors [60]. The ECM also sequesters growth factors and proteinases that dictate tumor growth, angiogenesis, and metastasis, and even control cellular metabolism [61]. The ECM imparts these mechanical and biochemical cues on surrounding malignant and non-malignant cells, which can alter the development of tumor tissues [62]. Thus, cancer-related effects are greatly influenced by the content and structure of the ECM. Generally, the collagen proteins provide structural integrity, glycoproteins promote cell to matrix adhesion, and proteoglycans facilitate cell signaling [52]. Molecular pathways that regulate ECM remodeling are highly dysregulated in cancer, and key proteins involved in matrix stiffening are often upregulated; this includes proteins such as lysyl oxidase, periostin, transglutaminase, and multiple collagen isoforms. ECM stiffness is a microenvironmental parameter that influences cancer progression, as stiffer surrounding matrices have been associated with more invasive breast cancer phenotypes [63]. Similarly, the organization of different collagen types can affect cell polarity and the epithelial-mesenchymal transition, a process in which epithelial cancer cells develop more invasive mesenchymal cell phenotypes, which are important in metastasis [64]. The ECM can be altered by a variety of enzymes such as matrix metalloproteinases which degrade ECM proteins, or lysyl oxidases which promote collagen crosslinking and maturation [65].

Stromal cell populations of the TME are capable of altering the physical and molecular aspects of the TME by activating TGF $\beta$  or Rho-Rock signaling pathways. Forces from the external environment activate the Rho/ROCK signaling pathway

that regulates the actin cytoskeleton and cytoskeleton tension. Actin bundling (i.e.,  $\alpha$ -actinin, fascin) and crosslinking proteins (i.e., filamin) give rise to actin stress fibers that link the cytoskeleton to focal adhesions and actin networks that modulate intracellular stiffness. The cytoskeletal networks respond dynamically to soluble or mechanical cues from the tumor ECM and is directly connected to canonical signal transduction pathways important in cancer. Chemical and physical stimuli alter cell shape and cytoskeletal organization by activating cytoskeletal mediators like Rho GTPases (RhoA, Rac1, and Cdc42) and actin binding proteins (ABPs) that regulate actin filament length through capping, branching, and severing processes. We have previously showed the intrinsic expression of cell contractility molecules contributes to the optimal production of matrix for cell function; this has implications in understanding the tropism of metastatic cancer.

## 2.5 *Tumor Angiogenesis*

Judah Folkman's pioneering work demonstrated that tumor growth beyond a few millimeters in size required endothelial cell recruitment and neovascularization through the process of angiogenesis [66]. Angiogenesis occurs naturally in development and healing processes and is fundamental in transforming benign, or indolent tumors, into malignant cancers. Folkman hypothesized that tumors secreted soluble molecules (factors), like fibroblast growth factor (FGF) [67] and vascular endothelial growth factor (VEGF) [68], to trigger endothelial cell recruitment into the tumor and angiogenesis. His work showed that non-vascularized tumors can remain dormant for long periods until they undergo an angiogenic switch, which transforms indolent tumors into malignant cancers [69]. In tumor angiogenesis, increased levels of angiogenic molecules result in the creation of disorganized, structurally abnormal, highly permeable, and immature blood vessels. These blood vessels are leaky, which result in high tumor interstitial fluid pressures that impede the delivery of cancer drugs and facilitate tumor cell extravasation and metastasis. In addition, impaired blood flow in tumor vessels leads to the formation of localized and transient regions of hypoxia, which cause tumor cells to enter a quiescent state that is associated with reduced sensitivity to radiation and chemotherapy. Folkman's pioneering work led to the discovery of the first angiogenesis inhibitors (endostatin and angiostatin), which targeted angiogenesis by inducing apoptosis in endothelial cells, and the idea of using anti-angiogenic therapy to treat cancer [70]. In 2004, which was more than 10 years after Judah Folkman discovered anti-angiogenic therapy, the first angiogenesis inhibitor (bevacizumab or Avastin) was FDA-approved for the treatment of advanced stage colon cancers; Avastin is a monoclonal antibody that works by targeting VEGF [71]. Anti-angiogenic therapies like Avastin restore the balance in pro- and anti- angiogenic molecules in the tumor, which stabilizes tumor blood vessels by pruning abnormal structures [72]. Vessel normalization is a critical treatment strategy in the arsenal to fight cancer [73]. Treatment with antiangiogenic agents has been shown to normalize tumor blood

vessels by pruning immature blood vessels, increasing perivascular coverage, and reducing interstitial fluid pressure. Vascular normalization also improves treatment outcomes by increasing the transport of cancer-killing drugs into the tumor [74].

## 2.6 *Tumor-Secreted Soluble Factors*

The recruitment of stromal cells into the tumor is critical in mediating tumor growth and cancer progression [44]. This process is mediated by tumor secretion of pro-angiogenic growth factors and chemokines that enter the blood circulation and travel throughout the body to mobilize cells into the circulation and into the tumor [75]. Thus, paracrine factors involved in cell–cell communication play a key role in the TME, with many paracrine factors and signaling molecules involved in cancer progression. For example, CAFs in the breast cancer tumor microenvironment have been shown to communicate with tumor cells with an array of different paracrine factors, such as insulin-like growth factor, which encourages cell proliferation and migration and thus enhances tumor growth and matrix invasion [76]. The TME is also hypoxic, in part to the rapid growth of tumors that often lack functional blood vessels that deliver oxygen and nutrients to the tumor [77]. Hypoxia is associated with increased expression of hypoxia inducible factor 1 alpha (HIF1a) transcription factor, a key regulator of proangiogenic chemokines involved in cell recruitment processes [78]. Increased expression of VEGF by cells in hypoxic regions of the tumor has been implicated in the early stages of angiogenesis [68], and SDF-1 (CXCL12) secretion (also driven by hypoxia) by fibroblasts in the tumor stroma has been linked to breast tumor growth and angiogenesis. Heregulin (HRG) is a soluble growth factor ligand for epidermal growth factor (ErbB) receptors that are often overexpressed in tumors; HRG is a potent angiogenic factor that is implicated in cell proliferation, differentiation, invasion, and survival in human cancers [79].

Drugs that target growth factor signaling pathways involved in cancer are another critical tool in the arsenal against cancer [80, 81]. Sunitinib malate is an oral tyrosine kinase inhibitor that has activity against multiple ligands that are expressed by stromal cells, including VEGF, PDGF, and KIT ligands; Sunitinib has been shown to have antitumor and antiangiogenic activity against multiple cancer types [82]. Imatinib, also known as Gleevec, is a tyrosine kinase inhibitor with activity against ABL, BCR-ABL, PDGFRA, and c-KIT [83]. Gleevec was considered a magic bullet in the treatment of chronic myeloid leukemias and gastrointestinal tumors [83]. Imatinib has also been effective in blocking Akt signaling in PDGFR positive ovarian cancers [84]. LY2109761, a selective kinase inhibitor, was previously shown to suppress the migration and metastasis of pancreatic tumor cells by blocking TGF $\beta$ R1 and TGF $\beta$ R2 [85]. Targeted therapies against PDGF and TGF $\beta$ 1 ligands are extremely important in mediating stromal cell behavior; thus, they have been used in cancer therapies that target the TME and in regulating the cross talk between tumor and stromal cells [86].

## 2.7 Tumor Exosomes

Exosomes are membrane-bound nanosized particles that play critical roles in cancer signaling by mediating intercellular communication [87]. In recent studies, it was also shown that exosomes can direct cancer cells to form organ-specific metastases [88]. Exosomes have cholesterol-rich membranes that protect signaling molecules (mRNA, miRNA, proteins) from enzymatic degradation; thus, they are capable of transferring sensitive proteins and RNAs throughout the body [87]. Cells secrete exosomes through endosomal budding into extracellular spaces to direct paracrine and autocrine signaling processes [87]. Internal cargo can include proteins, DNAs, RNAs, and miRNAs – most of which highly mirrors the parent cell. Interestingly, more current work demonstrates that exosomes can possess content that is unique from parent cell populations [89]. Exosome exchange can lead to the transferring of various biomaterials and recipient cells taking on unique physical and molecular behaviors [90]. This exchange can also lead to the recipient cell exhibiting characteristics similar to the cell that is secreting exosomes. A number of studies have highlighted the importance of exosomes as the secreted factors that mediate metastatic tumor growth (local and distal) and preference for certain tissues through “seed and soil” behavior [91, 92]. In the TME, multiple cell types are readily secreting exosomes, which contributes to the heterogeneity in tumor exosome populations. Hallmark TME conditions, such as low pH, hypoxia, physical or chemical stress, or treatment-related side effects, can significantly alter exosome secretion [93, 94] (Fig. 3). Many studies have examined the heterogeneity in tumor exosomes from different parent cell sources; however, our recent studies showed that even a single cell line can secrete different exosome populations under different culture conditions, which likely contributes to the tumor exosome heterogeneity [90]. Exosome heterogeneity is critical in mediating heterogeneous cell–cell communication as they can serve as paracrine and autocrine signaling molecules that help reprogram recipient cells to promote or suppress cancer [95]. Our recent study showed that changes in extracellular calcium levels can lead to the release of unique exosome population that we referred to as chelation-induced exosomes [90]. These exosomes possess unique miRNA content and induce differential physical changes in the recipient cells during exosome exchange [90]. Many of the miRNAs that were altered targeted mechanotransduction pathways important in physical aspects of cancer [90]. Exosome heterogeneity can ultimately reveal unique exosome contents that may serve as targets for invasive cancers that form under TME stress.

## 3 Intratumor Heterogeneity

As we have just covered, the diversity of both cell types and ECMs generate a complex, dynamic, and protective TME. Such complexity is also found within the



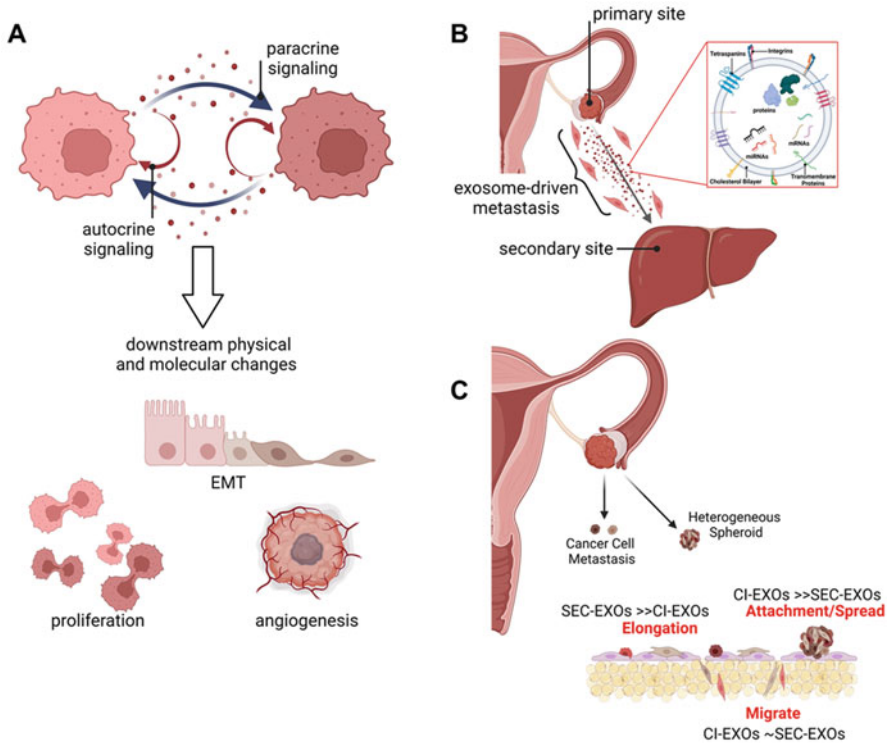


**Fig. 3** Exosome exchange directs physical and molecular alterations in the TME. Exosomes are important paracrine and autocrine factors that mediate local (A) and distal (B) TME phenotypes. Several local changes that exosomes influence include EMT induction, enhanced proliferation, and angiogenic development. These local changes can propel subsequent metastasis at the secondary site. (C) Specifically, we report that changes in extracellular calcium concentration release a unique population of chelation-induced exosomes (CI-EXOs) in addition to naturally secreted exosomes (SEC-EXOs). Different exosome populations played more “prominent” roles in inducing critical phenotypes for metastatic progression. SEC-EXOs activated cell elongation; CI-EXOs led to greater cell adhesion and spread (i.e., attachment to secondary sites); while both CI- and SEC-EXOs increased cell migration (i.e., migration from primary site or invading deeper into secondary sites)

tumor – among the cancer cell population. One major challenge to understanding and targeting cancer cells is the genotypic and phenotypic heterogeneity in cancer cell populations across the tumor landscape. The heterogeneity in primary tumor cells arises from intrinsic differences in cancer cells, along with extrinsic host-selection pressures in the developing tumor. Indeed, in addition to inherent differences in the genome [96], chromosome number, and DNA content [97], differences in plasticity and cell state can account for an evolving and dynamic cancer cell population over the course of disease progression [98].

Spatial heterogeneity describes the diversity of environmental niches present in a tumor landscape as the TME is shaped both by a growing cancer population and a reactive stromal population. The local environment of a cancer cell can vary both in physical and biochemical composition as mechanical and nutrient gradients are formed due to tumor expansion and the rise of diffusion limitations. Resilient cancer cells will cope with the specific pressures they experience thus leading to differentially primed subpopulations [99, 100].

Resilient cancer cell subpopulations will have to continuously cope with environmental stress as the TME develops over time. As the TME grows in volume and complexity, cancer cells will experience a range of extrinsic stressors (e.g., nutrient deprivation, hypoxia, and an increasing mechanical load) which will vary both in kind and magnitude depending on their physical location in the tumor and local TME. The combination of a nonuniform distribution of environmental stress and inherent genomic heterogeneity differentially primes cancer cell subpopulations to endure environmental and therapeutic stress. For these reasons, it is imperative to consider how heterogeneous subpopulations arise in the tumor as a consequence of nonuniform environmental cues and bidirectional communication with neighboring cells. We will now discuss how heterogeneity in the physical environment can lead to heterogeneity in cellular phenotype, with an emphasis on senescent stromal cells and PGCCs.

### ***3.1 Heterogeneity in Tumor Mechanics***

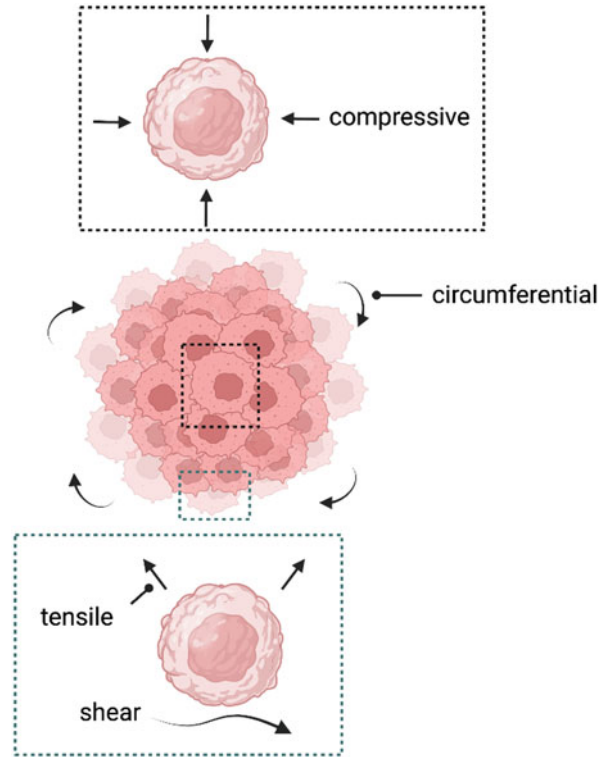
As the tumor mass grows, cancer cells in the center, at the periphery, and in between experience vastly different mechanical loads. Compressive stress is felt throughout the tumor to varying degrees as the surrounding tissue resists tumor growth. In addition to external compressive forces, compressive force is also generated within the tumor as a result of cancer cell proliferation, matrix stiffening, and high interstitial fluid pressure [101]. Cells in the center of the tumor experience radial and circumferential compressive forces, while cells at the periphery experience both compressive and tensile forces, that drive invasive cell migration (Fig. 4) [102]. Tumors are also exposed to fluid shear stress either at the surface of the tumor or within the tumor from vascular flow and interstitial fluid movement [103]. Each of these mechanical cues have been shown to elicit specific responses in cancer cells.

A common attribute of solid tumors is the gradual stiffening of the ECM. Stiffer substrates have been shown to increase proliferation and promigratory signals in cancer cells often through the induction of the epithelial-to-mesenchymal transition (EMT) [63, 104]. Cancer cells will lose their epithelial qualities via a downregulation of cadherin and integrins which compromise cell–cell junctions and cell-matrix adhesions, thus promoting dissemination from the primary site, invasion into local tissues, and, eventually, metastasis.

Fluid shear stress is another mechanical cue that can potently impact cancer cell behavior. Cancer cells can experience fluid shear stress within the TME through



**Fig. 4** Illustration of forces acting on cancer cells in the tumor microenvironment. In the tumor microenvironment, cells are under solid stress from rapidly proliferating tumor cells that are growing in a constrained environment. At the tumor center, cells are under compression from the surrounding tissue and at the periphery of the tumor, cells experience shear forces that eventually contribute to dissemination



the flow of interstitial fluid or along the periphery of the tumor if exposed to fluid (e.g., EOC is exposed to the flow of peritoneal ascites) (Fig. 4) [105]. Additionally, circulating tumor cells will experience fluid shear stress from blood as they navigate the vasculature to the target tissue. Fluid shear stress can induce EMT, promoting not only proliferative and migratory properties but also a stem cell-like phenotype [106]. Collectively, these properties have been shown to confer chemoresistance prior to the exposure of any therapeutic. Yet, it has also been postulated that metastasizing cancer cells will intravasate into low fluid shear regions (e.g., into the lymphatics instead of the vasculature) because high fluid shear stress can induce cell death [107]. Furthermore, it's been shown that invasive cancer cells and cancer-associated stromal cells that are less mechanosensitive due to decreased activity of the mechanosensor TRPM7 can endure higher shear forces and will not inhibit migration [108]. Once again, both mutational differences and magnitude of a physical cue dictate the resulting cancer cell phenotype.

### 3.2 *Heterogeneity in Cell Phenotype*

While homogenous tumor populations are responsive to initial treatments, tumors with multiple subpopulations of cancer cells are unlikely to be uniformly responsive to cancer treatments. Rather, cancer cell populations that endure mechanical and therapeutic stress will often emerge with unique adaptations that prime them for future stressful conditions. A primary example of such a phenomenon is therapy-induced senescence (TIS). In response to intracellular stress (e.g., DNA damage, oxidative and metabolic stress) elicited by chemotherapies or radiation, both stromal and cancer cell populations can become senescent as a mechanism to evade further damage and even advance a pro-tumorigenic environment [109, 110].

We have used quantitative single cell analysis to look at the underlying structural differences in pre-senescent and senescent cells. For these studies, we used 15 Gy irradiation to induce senescence in bone marrow derived mesenchymal stem cells (MSCs). We showed senescent MSCs were larger and less motile with dense actin stress fibers and focal adhesions throughout (Fig. 5A). Intracellular particle tracking was used to determine the local mechanical properties of the cytoplasm from the thermal displacements of particles embedded in the cell based on our previously established protocols [44, 111]. Here we only show the ensemble averaged MSDs for  $t = 1$  s, which were comparable between pre-senescent and senescent MSCs, indicating similarity in their bulk mechanical properties (Fig. 5B); however, the reduced heterogeneity in individual particle MSDs for senescent MSCs suggests that the microstructure of the cytoskeletal network is more homogeneous after senescence. The cytoskeletal network comprises highly dynamic networks of filamentous proteins that undergo coordinated polymerization, depolymerization, and crosslinking at different intracellular locations. Loss in the structural dynamics of this network was associated with reduced cell motility, with reductions in both mean and directional cell velocities, which were also more homogeneous in senescent cells (Fig. 5C–D). Cell biophysical properties are important in ECM remodeling and disease [8, 10, 112]. Thus, physical changes in senescent cells can modify their interactions with the ECM, contributing to tumor-promoting conditions *in vivo*.

### 3.3 *Senescent Stromal Cells*

Cellular senescence is a state of irreversible growth arrest that occurs due to the accumulation of DNA damage and is implicated in age-related tissue decline and disease. Genotoxic stress from environmental toxins, radiation, or chemotherapy can also damage resident stromal cells causing premature senescence and accelerated aging. The risk for TIS also increases with age, in part to the cumulative effects of mitochondrial dysfunction, oxidative stress, and tissue degeneration – all characteristics of senescent cells [113, 114]. Growth arrest attributed to TIS had

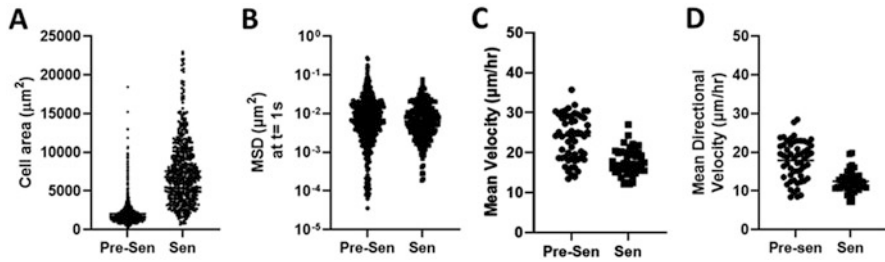


**Fig. 5** Single cell analysis of pre-senescent and senescent MSC populations shows radiation-induced senescence is associated with larger and less motile cell phenotypes. **(A)** Radiation-induced senescent MSCs (Sen) were significantly larger than the pre-senescent MSCs (Pre-sen) with more heterogeneity in their cell areas, which may be in part due to high metabolic activity in Sen cells. **(B)** To probe cytosolic dynamics of single cells, cells were injected with 200 nm probe particles and the thermal energy driven fluctuations in the particle motions were monitored to calculate ensemble averaged mean square displacements (MSDs). The distribution in MSD values was reduced for Sen MSCs relative to pre-Sen MSCs. This suggests that the induction of senescence in stromal cells leads to a more mechanically homogenous cytosol. **(C–D)** Functionally, senescent cells were less migratory than the pre-senescent cells. Both mean and directional velocities were reduced in Sen MSCs. For both parameters, we also observed more homogeneous velocities for senescent cells. At least three replicates with >200 measurements per group

largely been considered a positive treatment outcome [115]; however, senescent cells remain metabolically active and develop a senescence-associated secretory phenotype (SASP), which can promote cancer progression [116]. In addition, a small number of cancer cells are able to escape TIS, which is associated with recurrent and resistant disease [110]. Polyploid giant cancer cells (PGCCs) are a novel and understudied subpopulation of dormant and multinucleated giant cancer cells that exhibit multiple features of TIS [117, 118]. Although PGCCs share many characteristics with senescent cells, including their large size, arrested cell cycle, and SASP, they also differ from senescent cells in their ability to escape TIS by undergoing amitotic budding to form new tumors [119, 120]. Senescent cells develop a unique SASP that is characterized by increased secretion of pro-inflammatory cytokines and growth factors that can attract immune cells and cause chronic inflammation, which is a hallmark of age-related diseases. Although senescence is a tumor suppressor mechanism that halts the proliferation of damaged cells, senescent cells that build up in tissues ultimately cause inflammation and aging, which can alter the tissue microenvironment to promote malignancy.

Our recent study showed that senescent MSCs deposit and crosslink matrix proteins which alter the architecture and mechanics of the surrounding collagen-rich environment (Fig. 6) [3]. MSCs are stromal cells that are recruited to developing tissues and tumors. The senescence-associated ECM remodeling effect was associated with increased proliferation and motility of breast cancer cells [3]. ECM remodeling for increased tissue stiffness has been shown to induce malignant phenotypes in epithelial cells [10] and carcinoma-associated fibroblasts [56] to promote tumor progression [52]. In addition, senescence also increased the number and altered the

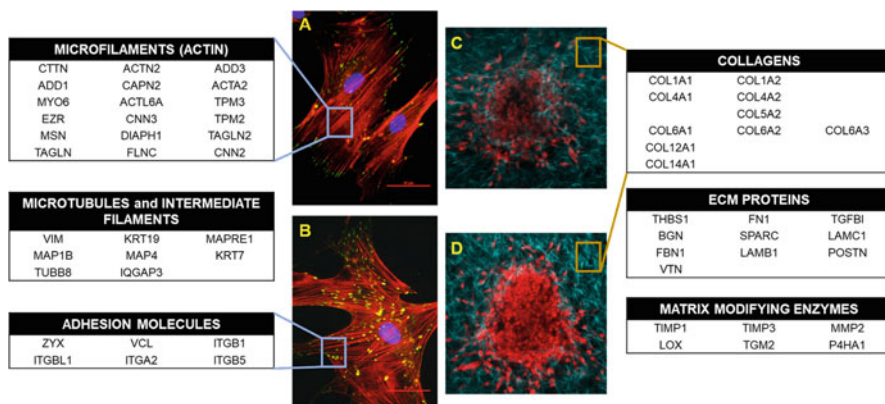


**Fig. 6** Pre and senescent MSCs express and deposit aberrant levels of collagen and matrix proteins. Left: Pre-senescent (**A**) and senescent (**B**) MSCs stained for DAPI (blue), filamentous actin (red) and vinculin, a focal adhesion protein (green). Proteomics revealed that senescence development altered MSC cytoskeleton protein activity. Right: 3D spheroids of pre-senescent (**C**) or senescent (**D**) MSCs (red) were embedded into collagen matrices. Senescent MSCs deposited elevated levels of collagen (cyan) compared to pre-senescent MSC spheroids. Second harmonic generation images corroborated an increase in the abundance of collagens and other ECM proteins found in our proteomics results

content of secreted exosomes [8], which are potent SASP factors that can transfer proteins, mRNAs, and miRNAs to other cells to mediate disease progression [9]. Previous studies have shown senescence-associated exosomes can activate nearby fibroblasts promoting ECM remodeling through activation of the TGF- $\beta$  signaling pathway [9, 10]. TGF $\beta$  is a pleiotropic cytokine that plays a critical role in ECM remodeling, tissue stiffening, and fibrosis [121]. It mediates actin cytoskeletal reorganization to alter cell contractility and the interaction with the ECM through myocardin-related transcription factor (MRTF) [122]. MRTF is a mechanosensitive signaling molecule that induces myofibroblast differentiation, cell contractility, and pro-fibrotic ECM modifications. Our recent study showed TGF $\beta$  signaling is highly dysregulated in senescent cells. We also demonstrated the critical role of TGF $\beta$  in actin cytoskeletal reorganization to alter cell contractility and ECM remodeling, critical steps in the development of fibrotic tissues and tumors [111, 123, 124]. These biophysical alterations may contribute to further ECM remodeling and tissue stiffening in part to the transfer of intracellular mechanical forces on the local environment.

Previous work on age-related disease has focused on developing senolytic agents to clear senescent cells [125–127]. These treatment strategies are promising [128]; however, senolytic drugs have been associated with off-target toxicities, serious side effects, and low potency [125, 129], which could limit their potential as anti-cancer drugs. Also, while senescent cells and their SASP create tumor-promoting microenvironments, they also participate in normal aging, wound healing, and tissue inflammation, which are critical processes that occur in normal tissues [125]. Thus,

strategies for targeting molecules in the SASP, such as TGF $\beta$ , to limit the ECM remodeling phenotype may serve as alternatives to senolytic drugs.

### 3.4 *Polyloid Giant Cancer Cells*

Polyploidy, or the harboring of more than 2 complete sets of chromosomes, is a common feature in cancer cells which are under genomic stress and genomic instability. Polyploidy has been reported in many aggressive tumor types, most often in the form of polyloid giant cancer cells (PGCCs), which are thought to play a critical role in maintenance, growth, and recurrence of tumors [130]. As the name implies, PGCCs have multiple copies of DNA which often manifest in large fragmented nuclei [131]. PGCCs are formed through mitotic slippage [133], endoreplication, and cell fusion [19, 134] and later revert to diploid cancer cell phenotypes through amitotic budding to form daughter cells [137]. PGCCs have atypical, heterogeneous karyotypes, which can also be passed down to daughter cells during budding [132], adding to the genetic diversity in cancer cells. Additionally, PGCCs exhibit qualities characteristic of stem cells, such as their ability to differentiate along different cell lineages and their expression of cancer stem cell genes, such as ALDH1, OCT4, and NANOG, which are associated with stemness [20, 135].

PGCCs exhibit multiple features of senescent cells, including their large size, arrested cell cycle, oxidative stress response, and pro-inflammatory secretory phenotype (SASP) [116]. In part to their apparent senescence, PGCCs were once considered dead end cells [120, 136]; however, their ability to escape senescence and give rise to new tumors is now more widely recognized [117]. Their arrested cell state may also aid PGCCs in their ability to evade cancer treatments that target mitotically active cells [20]. Our previous studies showed that MDA-MB-231 cells treated with high-concentration (500 nM) of paclitaxel (PTX) for 18 h initially enrich for PGCCs up to 7 days, and then the percentage of PGCCs begins to drop over 14-day period due to budding and generation of daughter cells (illustrated in Fig. 7). PGCCs constitute a growing field of research due to their ability to recover from dormancy, which may contribute to tumor recurrence in vivo.

In part to their duplicated genomes, PGCCs also have an evolutionary advantage in adapting to stress. These extra gene copies make PGCCs more resistant to DNA-damaging agents such as ionizing radiation and chemotherapy. In terms of their drug resistance, articles from multiple labs [137–141] have extensively documented the ability of PGCCs to resist conventional chemotherapeutics, including doxorubicin, vinblastine, and paclitaxel. Furthermore, PGCC's unique chromosomal organization leads to genetic alterations in their progenitor cells, which may contribute to therapy resistance in vivo.

Despite PGCCs' ability to contribute to drug resistance and relapse, few studies had investigated their heterogeneous biophysical properties. Since multiple cancer

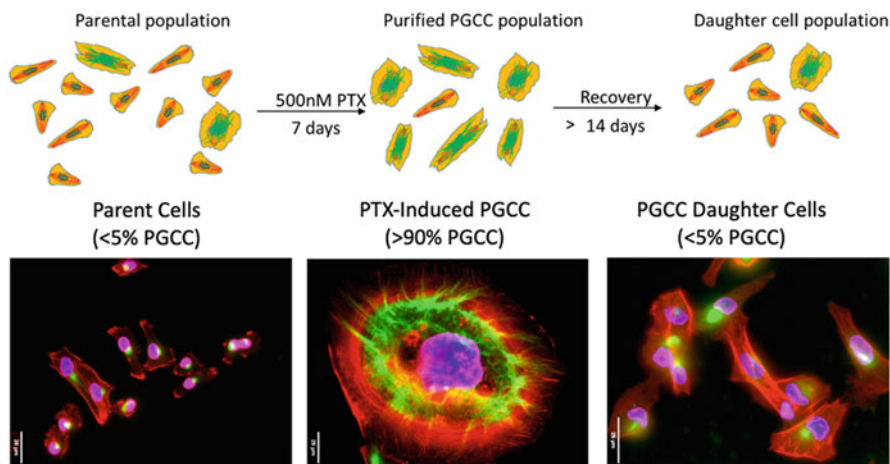


**Fig. 7** Chemotherapeutic paclitaxel (PTX) enriches for PGCCs capable of generating chemoresistant daughter cells. (Top) Schematic depicting the enrichment of PGCCs after PTX treatment and subsequent budding to form PGCC daughter cells. (Bottom) MDA-MB-231 parent cells, PGCCs, and PGCC daughter cells stained before and after PTX treatment for F-actin using Phalloidin (red), vimentin (green), and nuclei (fuchsia). MDA-MB-231 cells were treated with 500 nM PTX for 18 h to induce polyploidy, and subsequently allowed to recover for 7 days, which resulted in high-purity of PTX-induced PGCCs. After an additional 14 days, the majority of PGCCs have undergone budding to form PGCC daughter cells with highly abnormal nuclear structure

hallmarks are linked to abnormal biophysical parameters, we performed single cell biophysical analysis of PGCCs to learn more about this unique cell type. One of the most distinct features of PGCCs is their giant size; thus, one of the first properties we looked at was cell area. We showed PGCCs had a six-fold increase in average cell area compared to non-PGCCs (Fig. 8A). Next we showed particle transport in PGCCs was reduced in both cytoplasmic and nuclear compartments, indicating that PGCCs have stiffer mechanics compared to non-PGCCs (Fig. 8B). We also showed that PGCCs have dramatic differences in their actin cytoskeletal organization, including longer and thicker actin stress fiber bundles and a perinuclear actin cap, which were regulated through the RhoA-ROCK1 pathway. While PGCCs moved more slowly, their motion was more persistent, allowing them to move longer distances over time (Fig. 8C–D). We showed the directional migration of PGCCs was associated with a highly deformable nuclear structure, characterized by a unique softening of the nucleus during periods of migration. In summary, this study showed that PGCCs exhibit a unique actin cytoskeletal organization that contributes to elevated stiffness and migratory persistence, which is likely critical in promoting their aggressive cell phenotype [20].

These findings prompted us to further examine vimentin intermediate filaments that act as shock absorbers in the cell, protecting cells from compressive loads [143, 144]. Based on this, we postulated that PGCCs have unique adaptations in their vimentin structure to help support their enlarged morphology and to drive

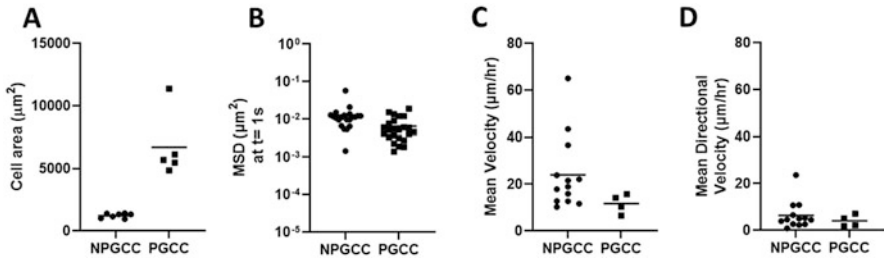


**Fig. 8** Single cell analysis of untreated MDA-MB-231 breast cancer non-PGCC (NPGCC) and PGCC subpopulations. (A) Cell area distributions were determined for NPGCCs and PGCCs (defined as having >2.5-fold increased DNA content compared to NPGCCs) that were stained with Phalloidin (for F-actin) and DAPI (for nuclei) ( $n = 5$  with >5000 total cells). (B) Particle tracking measurements of the ensemble averaged MSDs of 200 nm particles at  $t = 1$  s in the cell cytoplasm. Particle motion was decreased in PGCCs compared to NPGCCs, indicating that PGCCs were stiffer than NPGCCs. Variation in MSD was also increased, revealing increased heterogeneity in PGCCs (>200 particles per group). (C–D) Cell motion was determined for PGCCs versus NPGCCs during a 12-hr migration period ( $n = 5$  with >50 cells). Random migration of PGCCs was reduced compared to NPGCCs; however, PGCCs moved more directionally, which resulted in similar directional velocities in NPGCC and PGCC populations

their persistent migration. Indeed, we showed that PGCCs had increased levels of cytoplasmic vimentin and evenly distributed vimentin intermediate filaments compared to non-PGCCs. This dispersed network of VIFs often polarized at the leading edge during migration, and was necessary for the PGCC phenotype, as disruption of vimentin intermediate filaments decreased PGCC volume and blocked PGCC migratory persistence [142]. In sum, PGCCs display a distinctively altered and dysregulated biophysical phenotype, which is governed by alterations in actin and vimentin cytoskeletal organization.

## 4 Concluding Remarks

The exposure to mechanical and biochemical cues in the TME and reciprocal phenotypic changes in cancer cells are highly dependent on the physical location of a given cancer cell in a tumor. It is also important to remember that the physical, chemical, and cellular compositions of local niches are not stagnant and will develop over time. Thus, the heterogeneity in cancer cell phenotype is governed both spatially and temporally.

We highlighted two unique heterogeneous subpopulations (senescent cells and PGCCs) that are prominent across primary TMEs and play critical roles in subsequent metastasis. It is well accepted that both subpopulations exhibit physical, molecular, and secretory phenotypes that contribute to tumorigenesis. Several of these features overlap and are unique to each subpopulation – i.e., differential cell/nuclear volume, secretome, and migratory profiles. However, less is known



regarding how the direct interplay between these two subpopulations perpetuate drug-resistant phenotypes and cancer progression. Senescent cells PGCCs constitute a small percentage of the cells that make-up the primary TME. Therefore, it is critical to understand how these cells work jointly with each other to alter the TME. Having the ability to experimentally recapitulate both would enable us to more comprehensively examine how intratumor heterogeneity is developed, contributes to disease progression, and impacts treatment efficacy.

## References

1. Hanahan D, Weinberg RA (2000) The hallmarks of cancer. *Cell* 100:57–70
2. Hanahan D et al (2011) Hallmarks of cancer: the next generation. *Cell* 144:646–674
3. Hanahan D (2022) Hallmarks of cancer: new dimensions. *Cancer Discov* 12:31–46
4. Mierke CT (2013) Physical break-down of the classical view on cancer cell invasion and metastasis. *Eur J Cell Biol* 92:89–104
5. Pickup MW, Mouw JK, Weaver VM (2014) The extracellular matrix modulates the hallmarks of cancer. *EMBO Rep* 15
6. Nia HT et al (2016) Solid stress and elastic energy as measures of tumour mechanopathology. *Nat Biomed Eng* 1
7. Xu W et al (2012) Cell stiffness is a biomarker of the metastatic potential of ovarian cancer cells. *PLoS One* 7:e46609–e46609
8. Butcher DT, Alliston T, Weaver VM (2009) A tense situation: forcing tumour progression. *Nat Rev Cancer* 9:108–122
9. Mierke CT (2013) Invasive cancer cells and metastasis. *Phys Biol* 10:60301
10. Paszek MJ et al (2005) Tensional homeostasis and the malignant phenotype. *Cancer Cell* 8:241–254
11. Joyce JA, Pollard JW (2009) Microenvironmental regulation of metastasis. *Nat Rev Cancer* 9:239–252
12. Stanta G, Bonin S (2018) Overview on clinical relevance of intra-tumor heterogeneity. *Front Med* 5. Preprint at <https://doi.org/10.3389/fmed.2018.00085>
13. Fidler IJ (1978) Tumor heterogeneity and the biology of cancer invasion and metastasis. *Cancer Res* 38:2651–2660
14. Kaplan RN, Rafii S, Lyden D (2006) Preparing the “soil”: the premetastatic niche. *Cancer Res* 66:11089–11093
15. Quail DF, Joyce JA (2013) Microenvironmental regulation of tumor progression and metastasis. *Nat Med* 19:11 19, 1423–1437
16. Morales-Valencia J, David G (2021) The contribution of physiological and accelerated aging to cancer progression through senescence-induced inflammation. *Front Oncol* 11:747822
17. Campisi J (2013) Aging, cellular senescence, and cancer. *Annu Rev Physiol* 75:685–705
18. Ghosh D et al (2020) Senescent mesenchymal stem cells remodel extracellular matrix driving breast cancer cells to a more-invasive phenotype. *J Cell Sci* 133:jcs232470
19. Ganem NJ, Storchova Z, Pellman D (2007) Tetraploidy, aneuploidy and cancer. *Curr Opin Genet Dev* 17:157–162
20. Xuan B, Ghosh D, Cheney EM, Clifton EM, Dawson MR (2018) Dysregulation in actin cytoskeletal organization drives increased stiffness and migratory persistence in polyploid giant cancer cells. *Sci Rep* 8:11935
21. Xuan B, Ghosh D, Dawson MR (2022) Contributions of the distinct biophysical phenotype of polyploid giant cancer cells to cancer progression. *Semin Cancer Biol* 81:64–72
22. Arneith B (2020) Tumor microenvironment. *Medicina* 56



23. Mcmillin DW, Negri JM, Mitsiades CS (2013) The role of tumour-stromal interactions in modifying drug response: challenges and opportunities. *Nat Rev Drug Discov* 12:217–228
24. Dawson MR, Duda DG, Chae S-SS, Fukumura D, Jain RK (2009) VEGFR1 activity modulates myeloid cell infiltration in growing lung metastases but is not required for spontaneous metastasis formation. *PLoS One* 4:e6525
25. Jain RK (2013) Normalizing tumor microenvironment to treat cancer: bench to bedside to biomarkers. *J Clin Oncol* 31. Preprint at <https://doi.org/10.1200/JCO.2012.46.3653>
26. Psaila B, Lyden D (2009) The metastatic niche: adapting the foreign soil. *Nat Rev Cancer* 9:285–293
27. Langley RR, Fidler IJ (2011) The seed and soil hypothesis revisited—the role of tumor-stroma interactions in metastasis to different organs. *Int J Cancer* 128:2527–2535
28. Wirtz D (2009) Particle-tracking microrheology of living cells: principles and applications. *Annu Rev Biophys* 38:301–326
29. Hart IR, Fidler IJ (1980) Role of organ selectivity in the determination of metastatic patterns of B16 melanoma. *Cancer Res* 40:2281–2287
30. Whiteside TL (2008) The tumor microenvironment and its role in promoting tumor growth. *Oncogene* 27:5904–5912
31. Franklin RA et al (2014) The cellular and molecular origin of tumor-associated macrophages. *Science* 344:921–925
32. Lindau D, Gielen P, Kroesen M, Wesseling P, Adema GJ (2013) The immunosuppressive tumour network: myeloid-derived suppressor cells, regulatory T cells and natural killer T cells. *Immunology* 138:105–115
33. Bos PD, Plitas G, Rudra D, Lee SY, Rudensky AY (2013) Transient regulatory T cell ablation deters oncogene-driven breast cancer and enhances radiotherapy. *J Exp Med* 210:2435–2466
34. Barry KC et al (2018) A natural killer–dendritic cell axis defines checkpoint therapy–responsive tumor microenvironments. *Nat Med* 24:1178–1191
35. Shiao SL, Preethi Ganesan A, Rugo HS, Coussens LM (2011) Immune microenvironments in solid tumors: new targets for therapy. *Genes Dev* 25:2559–2572
36. Balkwill FR, Capasso M, Hagemann T (2012) The tumor microenvironment at a glance. *J Cell Sci* 125:5591–5596
37. Corn KC, Windham MA, Rafat M (2020) Lipids in the tumor microenvironment: from cancer progression to treatment. *Prog Lipid Res* 80:101055
38. Kojima Y et al (2010) Autocrine TGF- $\beta$  and stromal cell-derived factor-1 (SDF-1) signaling drives the evolution of tumor-promoting mammary stromal myofibroblasts. *Proc Natl Acad Sci USA* 107:20009–20014
39. Luo H, Tu G, Liu Z, Liu M (2015) Cancer-associated fibroblasts: a multifaceted driver of breast cancer progression. *Cancer Lett* 361:155–163. Preprint at <https://doi.org/10.1016/j.canlet.2015.02.018>
40. Truffi M, Sorrentino L, Corsi F (2020) Fibroblasts in the tumor microenvironment. *Undefined* 1234:15–29
41. Kidd S et al (2012) Origins of the tumor microenvironment: quantitative assessment of adipose-derived and bone marrow-derived stroma. *PLoS One* 7:e30563
42. Ferrara N, Kerbel RS (2005) Angiogenesis as a therapeutic target. *Nature* 438:967–974
43. McGrail DJ, McAndrews KM, Dawson MR (2013) Biomechanical analysis predicts decreased human mesenchymal stem cell function before molecular differences. *Exp Cell Res* 319:684–696
44. McGrail DJ, Ghosh D, Quach ND, Dawson MR (2012) Differential mechanical response of mesenchymal stem cells and fibroblasts to tumor-secreted soluble factors. *PLoS One* 7:e33248. <https://doi.org/10.1371/journal.pone.0033248>
45. Hass R, Kasper C, Böhm S, Jacobs R (2011) Different populations and sources of human mesenchymal stem cells (MSC): a comparison of adult and neonatal tissue-derived MSC. *Cell Commun Signal* 9:12
46. Erez N et al (2010) Cancer-associated fibroblasts are activated in incipient neoplasia to orchestrate tumor-promoting inflammation in an NF-kappaB-dependent manner. *Cancer Cell* 17:135–147

47. Xiao Y et al (2019) Multi-omics profiling reveals distinct microenvironment characterization and suggests immune escape mechanisms of triple-negative breast cancer. *Clin Cancer Res* 25:5002–5014
48. Duan Q, Zhang H, Zheng J, Zhang L (2020) Turning cold into hot: firing up the tumor microenvironment. *Trends Cancer* 6:605–618
49. Bonaventura P et al (2019) Cold Tumors: a therapeutic challenge for immunotherapy. *Front Immunol* 10:168
50. Grinnell F (2003) Fibroblast biology in three-dimensional collagen matrices. *Trends Cell Biol* 13:264–269
51. Tamariz E, Grinnell F (2002) Modulation of fibroblast morphology and adhesion during collagen matrix remodeling. *Mol Biol Cell* 13:3915–3929
52. Levental KR et al (2009) Matrix crosslinking forces tumor progression by enhancing integrin signaling. *Cell* 139:891–906
53. Kalluri R, Zeisberg M (2006) Fibroblasts in cancer. *Nat Rev Cancer* 6:392–401
54. Räsänen K, Vaheri A (2010) Activation of fibroblasts in cancer stroma. *Exp Cell Res* 316:2713–2722. Academic Press
55. Carey SP, Martin KE, Reinhart-King CA (2017) Three-dimensional collagen matrix induces a mechanosensitive invasive epithelial phenotype. *Sci Rep* 7
56. Calvo F et al (2013) Mechanotransduction and YAP-dependent matrix remodelling is required for the generation and maintenance of cancer-associated fibroblasts. *Nat Cell Biol* 15:637–646
57. Costa A et al (2018) Fibroblast Heterogeneity and Immunosuppressive Environment in Human Breast Cancer. *Cancer Cell* 33:463–479.e10
58. Barrett R, Puré E (2020) Cancer-associated fibroblasts: key determinants of tumor immunity and immunotherapy. *Curr Opin Immunol* 64:80–87
59. Wolf K, Friedl P (2011) Extracellular matrix determinants of proteolytic and non-proteolytic cell migration. *Trends Cell Biol* 21:736–744. Preprint at <https://doi.org/10.1016/j.tcb.2011.09.006>
60. Egeblad M, Rasch MG, Weaver VM (2010) Dynamic interplay between the collagen scaffold and tumor evolution. *Curr Opin Cell Biol* 22:697–706
61. Wolf K et al (2007) Multi-step pericellular proteolysis controls the transition from individual to collective cancer cell invasion. *Nat Cell Biol* 9:893–904
62. Oskarsson T (2013) Extracellular matrix components in breast cancer progression and metastasis. *Breast* 22(Suppl 2):S66–S72
63. Acerbi I et al (2015) Human breast cancer invasion and aggression correlates with ECM stiffening and immune cell infiltration. *Integr Biol* 7:1120–1134
64. Thiery JP, Acloque H, Huang RYJ, Nieto MA (2009) Epithelial-mesenchymal transitions in development and disease. *Cell* 139:871–890
65. Lu P, Weaver VM, Werb Z (2012) The extracellular matrix: a dynamic niche in cancer progression. *J Cell Biol* 196:395–406. Preprint at <https://doi.org/10.1083/jcb.201102147>
66. Folkman J (1971) Tumor angiogenesis: therapeutic implications. *N Engl J Med* 285:1182–1186
67. Humar R, Kiefer FN, Berns H, Resink TJ, Battegay EJ (2002) Hypoxia enhances vascular cell proliferation and angiogenesis in vitro via rapamycin (mTOR)-dependent signaling. *The FASEB J* 16:771–780
68. Carmeliet P (2005) VEGF as a key mediator of angiogenesis in cancer. *Oncology* 69:4–10. Preprint at <https://doi.org/10.1159/000088478>
69. Holmgren L, O'Reilly MS, Folkman J (1995) Dormancy of micrometastases: balanced proliferation and apoptosis in the presence of angiogenesis suppression. *Nat Med* 1:149–153
70. Folkman J (2006) Angiogenesis. *Annu Rev Med* 57:1–18
71. Ferrara N, Hillan KJ, Gerber H-P, Novotny W (2004) Discovery and development of bevacizumab, an anti-VEGF antibody for treating cancer. *Nat Rev Drug Discov* 3:391–400
72. Goel S, Wong AH-K, Jain RK (2012) Vascular normalization as a therapeutic strategy for malignant and nonmalignant disease. *Cold Spring Harb Perspect Med* 2:a006486–a006486

73. Vasudev NS, Reynolds AR (2014) Anti-angiogenic therapy for cancer: current progress, unresolved questions and future directions. *Angiogenesis* 17:471–494
74. Chauhan VP et al (2012) Normalization of tumour blood vessels improves the delivery of nanomedicines in a size-dependent manner. *Nat Nanotechnol* 7:383–388
75. Peinado H, Lavotshkin S, Lyden D (2011) The secreted factors responsible for pre-metastatic niche formation: old sayings and new thoughts. *Semin Cancer Biol* 21:139–146
76. Fridman AL, Tainsky MA (2008) Critical pathways in cellular senescence and immortalization revealed by gene expression profiling. *Oncogene* 27:5975–5987
77. Semenza GL (2009) Regulation of cancer cell metabolism by hypoxia-inducible factor 1. *Semin Cancer Biol* 19:12–16
78. Semenza G, Targeting L (2003) HIF-1 for cancer therapy. *Nat Rev Cancer* 3:721–732
79. Palmieri D et al (2007) Her-2 overexpression increases the metastatic outgrowth of breast cancer cells in the brain. *Cancer Res* 67:4190–4198
80. Yap TA, Carden CP, Kaye SB (2009) Beyond chemotherapy: targeted therapies in ovarian cancer. *Nat Rev Cancer* 9:167–181
81. Chen F et al (2015) New horizons in tumor microenvironment biology: challenges and opportunities. *BMC Med* 13
82. Chow LQM, Eckhardt SG (2007) Sunitinib: from rational design to clinical efficacy. *J Clin Oncol* 25:884–896
83. Shah NP et al (2004) Overriding imatinib resistance with a novel ABL kinase inhibitor. *Science (New York, N.Y.)* 305:399–401
84. Matei D et al (2008) Imatinib mesylate in combination with docetaxel for the treatment of patients with advanced, platinum-resistant ovarian cancer and primary peritoneal carcinomatosis: a Hoosier Oncology Group trial. *Cancer* 113:723–732
85. Melisi D et al (2008) LY2109761, a novel transforming growth factor receptor type I and type II dual inhibitor, as a therapeutic approach to suppressing pancreatic cancer metastasis. *Mol Cancer Ther* 7:829–840
86. Takai K et al (2016) Targeting the cancer-associated fibroblasts as a treatment in triple-negative breast cancer. *Oncotarget* 7:82889–82901
87. Kalluri R (2016) The biology and function of exosomes in cancer 126:1208–1215
88. Hoshino A et al (2015) Tumour exosome integrins determine organotropic metastasis. *Nature* 527:329–335
89. Doyle LM, Wang MZ (2019) Overview of extracellular vesicles, their origin, composition, purpose, and methods for exosome isolation and analysis. *Cell* 8:727
90. Lee AH, Ghosh D, Quach N, Schroeder D, Dawson MR (2020) Ovarian cancer exosomes trigger differential biophysical response in tumor-derived fibroblasts. *Sci Rep* 10:8686
91. Costa-Silva B et al (2015) Pancreatic cancer exosomes initiate pre-metastatic niche formation in the liver. *Nat Cell Biol* 17:816–826
92. Le MTN et al (2014) miR-200-containing extracellular vesicles promote breast cancer cell metastasis. *J Clin Invest* 124:5109–5128
93. Logozzi M, Spugnini E, Mizzoni D, Di Raimo R, Fais S (2019) Extracellular acidity and increased exosome release as key phenotypes of malignant tumors. *Cancer Metastasis Rev* 38:93–101
94. Chen X et al (2017) Exosomes derived from hypoxic epithelial ovarian cancer deliver microRNA-940 to induce macrophage M2 polarization. *Oncol Rep* 38:522–528
95. Han L, Lam EW-F, Sun Y. Extracellular vesicles in the tumor microenvironment: old stories, but new tales. <https://doi.org/10.1186/s12943-019-0980-8>
96. McGranahan N, Swanton C (2015) Biological and therapeutic impact of intratumor heterogeneity in cancer evolution. *Cancer Cell* 27:15–26
97. Kreso A et al (2013) Variable clonal repopulation dynamics influence chemotherapy response in colorectal cancer. *Science (New York, N.Y.)* 339:543–548
98. Wu P-H et al (2015) Evolution of cellular morpho-phenotypes in cancer metastasis. *Sci Rep* 5:18437

99. Lee AH, Mejia Peña C, Dawson MR (2022) Comparing the secretomes of chemorefractory and chemoresistant ovarian cancer cell populations. *Cancers* 14:1418
100. Zhang K et al (2022) Longitudinal single-cell RNA-seq analysis reveals stress-promoted chemoresistance in metastatic ovarian cancer. *Sci Adv* 8:eabm1831
101. Jain RK, Martin JD, Stylianopoulos T (2014) The role of mechanical forces in tumor growth and therapy. *Annu Rev Biomed Eng* 16:321–346
102. Northcott JM, Dean IS, Mouw JK, Weaver VM (2018) Feeling stress: the mechanics of cancer progression and aggression. *Front Cell Dev Biol* 6:17
103. Mitchell M, King M (2013) Computational and experimental models of cancer cell response to fluid shear stress. *Front Oncol* 3
104. Rice AJ et al (2017) Matrix stiffness induces epithelial–mesenchymal transition and promotes chemoresistance in pancreatic cancer cells. *Oncogenesis* 6:e352–e352
105. Novak C, Horst E, Mehta G (2018) Review: Mechanotransduction in ovarian cancer: shearing into the unknown. *APL Bioeng* 2:031701
106. Bregenzler ME et al (2019) The role of cancer stem cells and mechanical forces in ovarian cancer metastasis. *Cancers (Basel)* 11:1008
107. Chiang SPH, Cabrera RM, Segall JE (2016) Tumor cell intravasation. *Am J Physiol Cell Physiol* 311:C1–C14
108. Yankaskas CL et al (2021) The fluid shear stress sensor TRPM7 regulates tumor cell intravasation. *Sci Adv* 7:eabh3457
109. Erenpreisa J, Cragg MS (2013) Three steps to the immortality of cancer cells: senescence, polyploidy and self-renewal. *Cancer Cell Int* 13:92
110. Saleh T, Tyutyunyk-Massey L, Gewirtz DA (2019) Tumor cell escape from therapy-induced senescence as a model of disease recurrence after dormancy. *Cancer Res* 79:1044–1046
111. Ghosh D et al (2014) Integral role of platelet-derived growth factor in mediating transforming growth factor- $\beta$ 1-dependent mesenchymal stem cell stiffening. *Stem Cells Dev* 23:245–261
112. Kumar S, Weaver VM (2009) Mechanics, malignancy, and metastasis: the force journey of a tumor cell. *Cancer Metastasis Rev* 28:113–127
113. Thomas TS et al (2020) Advancing age and the risk of bleomycin pulmonary toxicity in a largely older cohort of patients with newly diagnosed Hodgkin Lymphoma. *J Geriatr Oncol* 11:69–74
114. Pan J et al (2017) Inhibition of Bcl-2/xl with ABT-263 selectively kills senescent type II Pneumocytes and reverses persistent pulmonary fibrosis induced by ionizing radiation in mice. *Int J Radiat Oncol \*Biology\* Physics* 99:353–361
115. Ewald JA, Desotelle JA, Wilding G, Jarrard DF (2010) Therapy-induced senescence in cancer. *JNCI: J Nat Cancer Inst* 102:1536–1546
116. Coppé J-P, Desprez P-Y, Krtolica A, Campisi J (2010) The senescence-associated secretory phenotype: the dark side of tumor suppression. *Annu Rev Pathol* 5:99–118
117. White-Gilbertson S, Voelkel-Johnson C (2020) Giants and monsters: unexpected characters in the story of cancer recurrence. *Adv Cancer Res* 148:201–232
118. Song Y, Zhao Y, Deng Z, Zhao R, Huang Q (2021) Stress-induced polyploid giant cancer cells: unique way of formation and non-negligible characteristics. *Front Oncol* 11:724781
119. Murray D, Mirzayans R (2020) Cellular responses to platinum-based anticancer drugs and UVC: role of p53 and implications for cancer therapy. *Int J Mol Sci* 21
120. Wang Q et al (2013) Polyploidy road to therapy-induced cellular senescence and escape. *Int J Cancer* 132:1505–1515
121. Jin J et al (2019) Pirfenidone attenuates lung fibrotic fibroblast responses to transforming growth factor- $\beta$ 1. *Respir Res* 20:119
122. Shi Y, Massague J (2003) Mechanisms of TGF- $\beta$  signaling from cell membrane to the nucleus. *Cell* 113:685–700
123. Ghosh D, McGrail DJDJ, Dawson MRMR (2017) TGF- $\beta$ 1 pretreatment improves the function of mesenchymal stem cells in the wound bed. *Front Cell Dev Biol* 5

124. McAndrews KM, McGrail DJ, Ravikumar N, Dawson MR (2015) Mesenchymal stem cells induce directional migration of invasive breast cancer cells through TGF- $\beta$ . *Sci Rep*. <https://doi.org/10.1038/srep16941>
125. He Y et al (2019) Cellular senescence and radiation-induced pulmonary fibrosis. *Transl Res J Lab Clin Med* 209:14–21
126. Justice JN et al (2019) Senolytics in idiopathic pulmonary fibrosis: results from a first-in-human, open-label, pilot study. *EBioMedicine* 40:554–563
127. Li M, You L, Xue J, Lu Y (2018) Ionizing radiation-induced cellular senescence in normal, non-transformed cells and the involved DNA damage response: A mini review. *Front Pharmacol*. Preprint at <https://doi.org/10.3389/fphar.2018.00522>
128. Kirkland JL, Tchkonja T (2015) Clinical strategies and animal models for developing senolytic agents. *Exp Gerontol* 68:19–25
129. Malavolta M et al (2018) Inducers of senescence, toxic compounds, and senolytics: the multiple faces of Nrf2-activating phytochemicals in cancer adjuvant therapy. *Mediat Inflamm* 2018:4159013
130. Amend SR et al (2019) Polyploid giant cancer cells: unrecognized actuators of tumorigenesis, metastasis, and resistance. *Prostate* 79:1489–1497
131. Zhang S, Zhang D, Yang Z, Zhang X (2016) Tumor budding, micropapillary pattern, and polyploidy Giant cancer cells in colorectal cancer: current status and future prospects. *Stem Cells Int* 2016:4810734
132. Mirzayans, R., Andrais, B. & Murray, D. (2018) Roles of polyploid/multinucleated giant cancer cells in metastasis and disease relapse following anticancer treatment. *Cancers* 10. Preprint at <https://doi.org/10.3390/cancers10040118>
133. Cheng B, Crasta K (2017) Consequences of mitotic slippage for antimicrotubule drug therapy. *Endocr Relat Cancer* 24:T97–T106
134. Bastida-Ruiz D, Van Hoesen K, Cohen M (2016) The dark side of cell fusion. *Int J Mol Sci* 17:E638
135. Pirsko V et al (2019) Alterations of the stem-like properties in the breast cancer cell line MDA-MB-231 induced by single pulsed doxorubicin treatment. *Proceedings of the Latvian Academy of Sciences. Section B. Natural, Exact, and Applied Sciences* 73:89–99
136. Sasai K et al (2004) Aurora-C kinase is a novel chromosomal passenger protein that can complement Aurora-B kinase function in mitotic cells. *Cell Motility and the Cytoskeleton* 59:249–263
137. Niu N et al (2016) Linking genomic reorganization to tumor initiation via the giant cell cycle. *Oncogenesis* 5:e281
138. Niu N, Mercado-Uribe I, Liu J (2017) Dedifferentiation into blastomere-like cancer stem cells via formation of polyploid giant cancer cells. *Oncogene* 36:4887–4900
139. Zhang S et al (2014) Generation of cancer stem-like cells through the formation of polyploid giant cancer cells. *Oncogene* 33:116–128
140. Lopez-Sánchez LM et al (2014) CoCl<sub>2</sub>, a mimic of hypoxia, induces formation of polyploid giant cells with stem characteristics in colon cancer. *PLoS One* 9
141. Fei F et al (2015) The number of polyploid giant cancer cells and epithelial-mesenchymal transition-related proteins are associated with invasion and metastasis in human breast cancer. *J Exp Clin Cancer Res* 34:1–13
142. Xuan B, Ghosh D, Jiang J, Shao R, Dawson MR (2020) Vimentin filaments drive migratory persistence in polyploid cancer cells. *Proc Natl Acad Sci USA* 117
143. Mendez MG, Restle D, Janmey PA (2014) Vimentin enhances cell elastic behavior and protects against compressive stress. *Biophys J* 107:314–323
144. Hu J et al (2019) High stretchability, strength, and toughness of living cells enabled by hyperelastic vimentin intermediate filaments. *Proc Natl Acad Sci* 116:17175–17180

# Physical Regulations of Cell Interactions and Metabolism in Tumor Microenvironments



Hydari Masuma Begum, Jeong Min Oh, Diane S. Kang, Min Yu, and Keyue Shen

**Abstract** Despite the advances in cancer therapeutics over the recent years, cancer remains the second leading cause of death in the United States, with metastasis accounting for over 90% of cancer-associated mortality. Elucidating the process of tumor progression in the primary tumor is important to the understanding of the sequence of events that gives rise to late stage/metastatic cancer. The primary tumor microenvironment (TME) is a dynamic, heterogeneous, and evolving “ecosystem” comprising numerous cell types and noncellular factors that each play a crucial role

---

Authors Hydari Masuma Begum and Jeong Min Oh have equally contributed to this chapter.

---

H. M. Begum · J. M. Oh

Department of Biomedical Engineering, Viterbi School of Engineering, University of Southern California, Los Angeles, CA, USA

D. S. Kang

Department of Stem Cell Biology and Regenerative Medicine, University of Southern California, Los Angeles, CA, USA

M. Yu

Department of Stem Cell Biology and Regenerative Medicine, University of Southern California, Los Angeles, CA, USA

Norris Comprehensive Cancer Center, Keck School of Medicine, University of Southern California, Los Angeles, CA, USA

Present Address: Department of Pharmacology, University of Maryland School of Medicine, Baltimore, MD, USA

e-mail: [Min.Yu@som.umaryland.edu](mailto:Min.Yu@som.umaryland.edu)

K. Shen (✉)

Department of Biomedical Engineering, Viterbi School of Engineering, University of Southern California, Los Angeles, CA, USA

Norris Comprehensive Cancer Center, Keck School of Medicine, University of Southern California, Los Angeles, CA, USA

USC Stem Cell, Keck School of Medicine, University of Southern California, Los Angeles, CA, USA

e-mail: [keyue.shen@usc.edu](mailto:keyue.shen@usc.edu)

© The Author(s), under exclusive license to Springer Nature Switzerland AG 2023

I. Y. Wong, M. R. Dawson (eds.), *Engineering and Physical Approaches to Cancer*, Current Cancer Research, [https://doi.org/10.1007/978-3-031-22802-5\\_5](https://doi.org/10.1007/978-3-031-22802-5_5)

in driving tumor progression. The focus on tumor heterogeneity was previously centered around aberrant mutations in tumor cells and biochemical signaling between different TME cell types. However, it is now evident that biophysical cues imposed by the TME also play an important role in tumor progression as the physical traits of the tumor undergo drastic changes and exert abnormal physical restraints and forces that consequently hinder the efficacy of tumor therapeutics. Therefore, understanding the causes of biophysical abnormalities of tumors and the functional consequences will be beneficial for developing new therapeutic strategies. More specifically, we focused on the regulation of metabolism (i.e., metabolic reprogramming) as the primary consequence of the biophysical abnormalities in the TME. Metabolic reprogramming is one of the emerging hallmarks of cancer and is an important regulator of cell fate. In this chapter, we describe the interrelationship between tumor–stromal interactions and altered physical cues such as stiffness, solid stress, and shear stress, and how these ultimately regulate cell metabolism within the TME.

## 1 Introduction

Despite advances in cancer therapeutics over the recent years, cancer remains the second leading cause of death in the United States [77], with metastasis accounting for over 90% of cancer-associated mortality [17]. While a causal link between primary and metastatic tumors remains elusive, it is generally accepted that the metastatic cascade initiates from the primary tumor sites [73]. Elucidating the process of tumor progression in the primary tumors is thus important to the understanding of the sequence of events that give rise to late stage/metastatic cancer. In addition to the dynamic heterogeneity that exists within the primary tumor cells, the primary tumor microenvironment (TME) is also a dynamic, heterogeneous, and evolving “ecosystem” [74] comprising numerous cell types and noncellular factors that each play a crucial role in tumor initiation, progression, and metastasis [63]. The focus on tumor heterogeneity was previously centered around aberrant mutations in tumor cells [63] and biochemical signaling between different TME cell types [21]. However, it is now evident that biophysical cues imposed by the TME also play an important role in tumor progression [54].

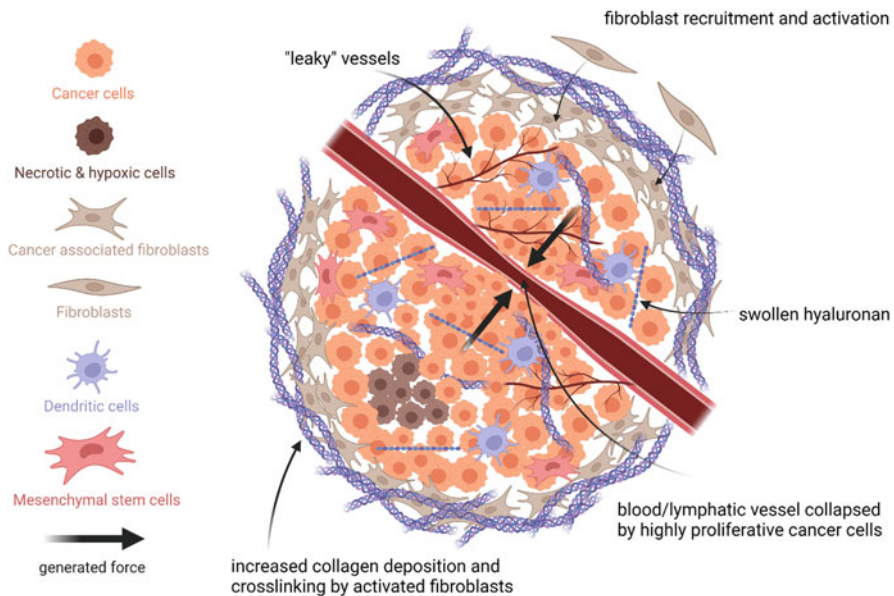
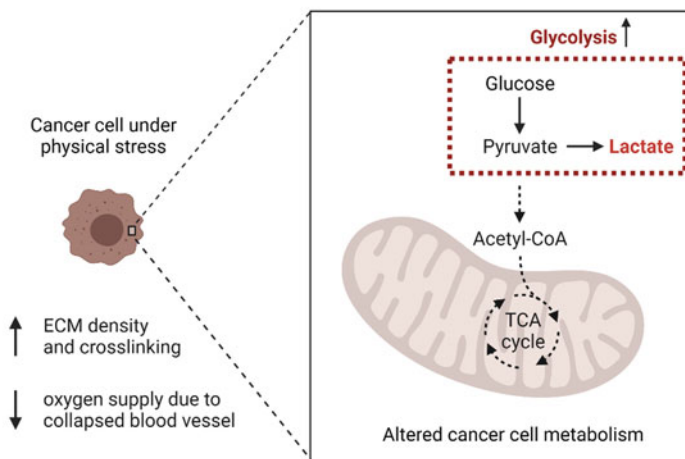
From the transformation of the normal tissue, on through the early stages of tumorigenesis, local invasion, dissemination, and metastasis, the physical traits of the tumor undergo drastic changes [55]. For example, one of the most tangible and best-recognized physical abnormalities associated with tumor progression is stiffness, which has been used as an independent prognostic marker for many cancers [26, 54]. In addition to the altered tissue stiffness, tumors can also generate physical forces (referred to as solid stresses), disrupt fluid homeostasis, and alter the architecture and behavior of intratumoral constituents (e.g., tumor cells, fibroblasts, and dendritic cells) [29]. These physical forces exerted by proliferating tumors and the resulting consequences lead to anatomical changes that hinder the efficacy of tumor therapeutics [11, 28, 37, 57]. Therefore, understanding the causes of biophysical abnormalities of tumors and the functional consequences will be beneficial for developing new therapeutic strategies.

Biophysical abnormalities of tumors are driven by the interactions between the numerous cell types and noncellular factors in the TME. The presence of the mutated cancer cells initiates the changes that alter their adjacent stroma to form a supportive environment for tumor progression [32, 52]. A key functional consequence of these biophysical abnormalities is metabolic reprogramming. Metabolic reprogramming is one of the emerging hallmarks of cancer cells [22] and is an important regulator of cell fate in the TME [60]. Cancer cells frequently display deregulated metabolism to support demands of excessive proliferation. The most notable metabolic reprogramming observed in cancer cells is the “Warburg effect,” where it was found that cancer cells preferentially utilize glycolysis over mitochondrial oxidative phosphorylation (OXPHOS) even in the presence of oxygen [41]. It was later found that this metabolic rewiring increases glycolytic flux, thereby allowing cancer cells to utilize glycolytic intermediates for biosynthesis reactions to meet increased proliferation demands [60]. Metabolic reprogramming seen during tumorigenesis is also observed in the cells undergoing epithelial–mesenchymal transition (EMT) of the metastatic process, where glycolysis and glycolytic enzymes are enhanced in these cells [69]. Therefore, therapies that inhibit these metabolic reprogramming will serve as a promising strategy to target both primary and metastatic tumor cells. A common approach to examining glycolytic and oxidative metabolism of cancer cells *in vitro* is by measuring their oxygen consumption rate (OCR; indicative of mitochondrial metabolism) and extracellular acidification rate (ECAR, indicative of glycolysis). The use of these techniques to investigate changes in cancer cell metabolism in response to physical cues such as stiffness will be discussed in the following sections. In this chapter, we will explore the interrelationship between tumor–stromal interactions and altered physical cues such as stiffness, solid stress, and shear stress, and how these ultimately regulate cell metabolism within the TME (Fig. 1).

## 2 Effect of Stiffness on Tumor–Stromal Interaction and Metabolism in the TME

Tissue stiffness is generally defined as the resistance of its deformation in response to an applied force [23], which is an intrinsic material property of the tissue. Increased tissue stiffness is one of the most commonly observed physical abnormalities of solid tumors, including breast [79], pancreatic [51], and colorectal cancers [4]. Observation of increased stiffness has been extensively studied in breast cancer because altered stiffness and ECM density are key to its detection [51]. Studies have reported that breast cancer tissues exhibit an elastic modulus (a measure of stiffness) that is around ten-fold stiffer than normal breast tissue and that the altered stiffness drives malignant transformation in the breast [9, 37]. In nature, the stiffness of biological tissue is highly dynamic and complex as it shows a strong nonlinear stiffening response (i.e., strain stiffening) [43]. Therefore, the effect of stiffness on tumor–stromal interactions and metabolism in the TME is dissected by examining both *in vitro* and *in vivo* tumor models.



**A****B**

**Fig. 1** Approaching tumor progression from a physical point-of-view. **(A)** Schematic showing the physical changes of the tumor microenvironment (TME) that occur with tumor progression. These physical changes generate stresses that further drive the physical abnormalities of the TME, e.g., collapsed blood and lymphatic vessels. **(B)** Illustrating the altered cancer cell metabolism as a response to the generated physical stresses within the TME. (Created with [BioRender.com](#))

## Positive Feedback Loop of Tumor Stiffening

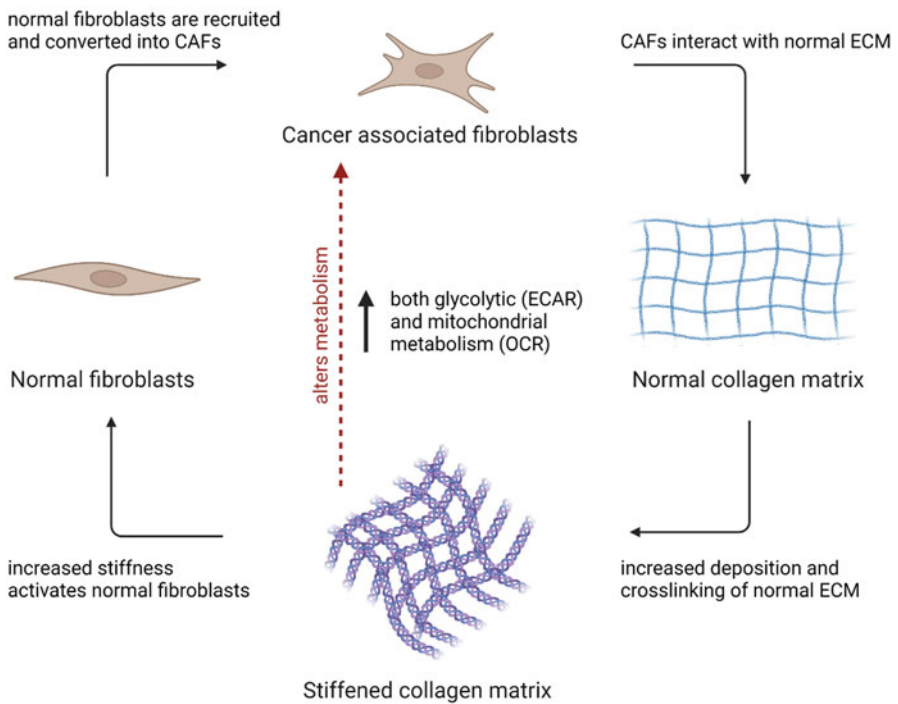


**Fig. 2** Positive feedback loop of tumor stiffening and altered CAF metabolism. Schematic showing how the interaction between stromal cells (cancer-associated fibroblasts; CAFs) and the extracellular matrix (ECM) drives tumor stiffening. CAFs interact with the existing collagen matrix by depositing additional collagen, crosslinking them together, and remodeling the overall ECM structure. The increased net quantity and crosslinking of the collagen matrix increases its stiffness. This increased stiffness, in turn, activates fibroblasts of the surrounding tissue to become CAFs, initiating the positive feedback loop. The stiffened matrix has been reported to increase both glycolytic and oxidative metabolism in CAFs [7]. (Created with [BioRender.com](#))

Tissue stiffening often occurs over months to years and involves many complex processes [51]. A primary cause of tissue stiffening is the increased net quantity and crosslinking of matrix proteins in the tumor microenvironment due to the disrupted balance between deposition, cross-linking, and degradation of ECM. The disruption of balance is driven by a positive feedback loop created between the stromal cells and the ECM. Among the stromal cells, cancer-associated fibroblasts (CAFs), which are differentially identified from normal fibroblasts by high  $\alpha$ -SMA expression, have the most significant impact on ECM remodeling. CAFs deposit ECM proteins, such as collagen and fibronectin, and exert high contractile forces that remodel and stiffen the ECM (a process described as strain stiffening) [81]. The increased stiffness, in turn, activates normal fibroblasts in the surrounding tissue to become CAFs, initiating the positive feedback loop (Fig. 2). CAFs also create paths of rearranged

ECM for the cancer cells to follow, promoting tumor invasion into the surrounding tissue [47]. The stiffened ECM matrix has been reported to alter the metabolism of CAFs. For instance, it was observed that increased stiffness (8 kPa) was associated with an increase in both glycolytic and oxidative, or mitochondrial, metabolism in CAFs as measured by the extracellular acidification rate (ECAR) and oxygen consumption rate (OCR), respectively (Fig. 2) [7].

Substrate stiffness significantly impacts the metabolism of dendritic cells (DCs), which are immune cells present in the stromal component of the TME [36]. Specifically, DCs cultured on stiffer substrates (50 kPa) have both enhanced glycolysis (measured by ECAR) as well as mitochondrial metabolism (measured by OCR) compared to those cultured on softer substrates (2 kPa) [10]. Consistent with the enhanced glycolytic phenotype, DCs cultured on stiffer substrates are also found to have increased glucose uptake and lactate secretion. YAP/TAZ are “universal mechanotransducers” [58] that read diverse biomechanical signals and transduce them into biological signals and outcomes, including cell proliferation [18], differentiation [13], and mitochondrial activity [6]. Of these, the transcriptional coactivator TAZ was found to regulate glycolysis in response to stiffness in these DCs, with TAZ knockdown preventing stiffness-mediated increase in glucose uptake [10]. In patient-derived xenograft (PDX) models of ovarian cancer, stroma derived from stiff tumors were found to have upregulation in glycolysis-related genes, whereas those derived from soft tumors have upregulation in genes associated with oxidative phosphorylation (OXPHOS), indicative of a potential stiffness-induced metabolic switch in the tumor stroma of ovarian cancers [48]. To summarize, increased ECM stiffness is a characteristic of many tumors, and it has been shown to upregulate glycolysis in several stromal cell types and models. The integrin-FAK pathway, YAP/TAZ transcriptional coactivators, Rho-ROCK actin cytoskeleton and AMPK pathway [27] are some of the potential downstream effector pathways that could transduce the mechanical properties of the ECM (stiffness) into intracellular changes in glucose metabolism [20].

In addition to the stiffness-induced changes in the stromal compartment of the TME, ECM stiffness can also regulate the metabolism of cancer cells. In some types of cancer cells such as A549 lung cancer and MDA-MB-231 breast cancer cells, it was found that culturing them on softer substrates (0.15–0.3 kPa) led to a more quiescent metabolism with longer cell cycles, and a reduction in intracellular ATP and protein synthesis, relative to cells grown on stiffer (>10 kPa) substrates. Moreover, the protein expression of phosphofructokinase (PFK), a key glycolytic enzyme, was found to be downregulated in A549 cells cultured on the softer substrates [71]. Mah et al. used fluorescence lifetime imaging microscopy (FLIM) to investigate the metabolic shift (as determined by changes in the ratios of enzyme-bound to free NADH) in MDA-MB-231 breast cancer cells, which were cultured on collagen monolayers of different densities (and thus different stiffnesses). They found that cells cultured on denser/stiffer collagen substrates showed higher glycolysis (higher ratio of free to bound NADH) compared to those cultured on softer collagen substrates [46]. This is in line with previous studies that report a downregulation of glycolysis in cancer cells cultured on softer substrates. Another

study performed with squamous cell carcinoma cells (SCC12) found that culturing them on stiffer matrices (8 kPa) increased glycolysis compared to cells cultured on softer matrices (1 kPa) [7]. Hepatocellular carcinoma cells (HepG2 and MHCC97L) cultured on stiffer collagen-coated PA gels (54 kPa) were found to have increased glucose consumption and lactate secretion, along with increased mRNA expression of glycolytic enzymes Glut-1, Hexokinase-II, and lactate dehydrogenase-A (LDHA) [44]. Furthermore, in PDX models of ovarian cancer, researchers found that stiffer tumors had upregulation in the expression of glycolysis-related genes compared to softer tumors, in line with several other studies that report enhanced glycolysis in cancer cells cultured on stiffer substrates *in vitro* [48]. To summarize, in several cancer cell types and in both *in vitro* and *in vivo* models, increased substrate stiffness is associated with enhanced glycolysis, indicated by increased ECAR rates, upregulation of glycolytic enzymes, lactate secretion, increase in the ratio of free to bound NADH measured by FLIM.

While several studies have reported on the effects of stiffness on glycolysis, whether and how stiffness regulates mitochondrial metabolism and activity is not clearly understood. In a recent study, Tharp et al. reported that increased ECM stiffness (~60 kPa; physiological stiffness of breast tumors) is associated with increased lactate levels (in line with previously reported results), as well as the induction of toroidal mitochondrial morphology and lower abundance of several mitochondrial electron transport chain (ETC) subunits in mammary epithelial cells (MECs) compared to those cultured on 400 Pa substrates (physiological breast stiffness) [70]. It is noteworthy that in normal somatic cells, there have been reports of stiffness-induced changes in mitochondrial oxygen consumption in cardiac myocytes [45] and mitochondrial membrane potential ( $\Delta\Psi_m$ ) and cluster size in vascular smooth muscle cells [2]. Together, these studies strongly suggest that stiffness mediated cues can regulate not only glycolysis but also mitochondrial metabolism in the TME.

### 3 Effect of Solid Stress on Tumor–Stromal Interaction and Metabolism in the TME

Solid stress refers to the mechanical forces (compressive and tensile) induced and transmitted by solid and elastic elements of the ECM and cellular components of the tumor [54]. Malignant and normal cells directly respond to the mechanical forces through mechanosensitive machinery (e.g., cell-to-ECM and cell-to-cell adhesions and stretch-sensitive ion channels) [42]. Solid stress in tumor is generated through multiple mechanisms that can be broadly categorized into the following: (1) tumor growth, (2) contraction, (3) swelling, and (4) externally applied forces (Fig. 3). Tumor growth-mediated stress arises primarily due to cell growth, recruitment, and motility [67]. Tumor and stromal cells proliferate, expand, and deposit additional matrix to their surroundings. The added volume exerts solid stress on collagen fibers and displaces existing matrix structures inside and outside of the tumor

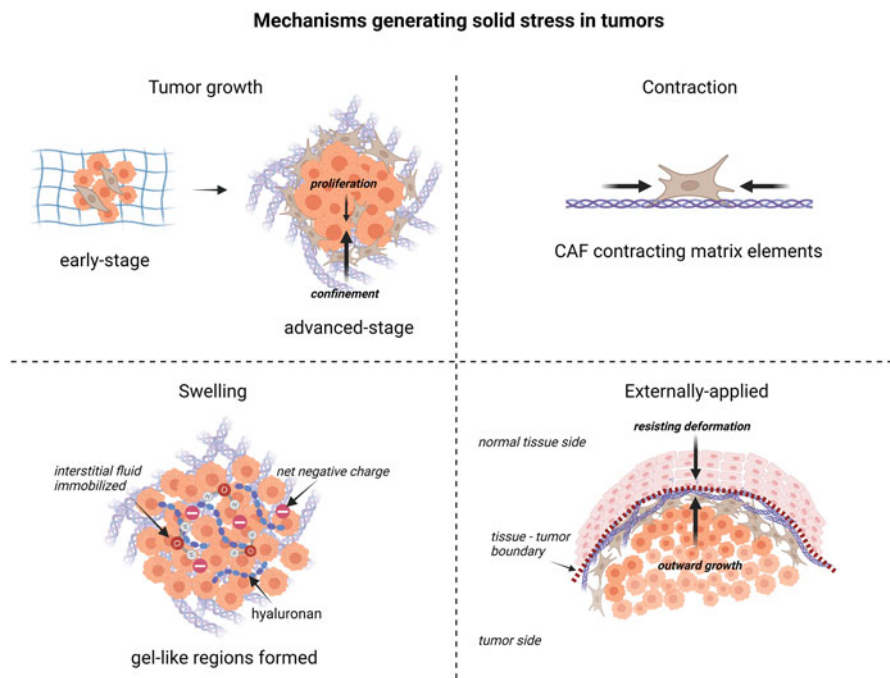


**Fig. 3** Mechanisms generating solid stress in tumors. Solid stress-generating mechanisms are broadly categorized into the following four groups: tumor growth, contraction, swelling, and externally applied. (Created with [BioRender.com](https://www.bio-render.com))

[75]. Growth-mediated solid stress also increases due to stromal cells (e.g., CAFs) contracting and adding tensile stress directly to the collagen-rich tumor ECM [61]. Tumor growth may be hindered by its surrounding stroma, and cancer cells become physically confined within dense ECM [55]. Solid stresses observed in such growth-confined condition has been modeled mathematically, and its predictions were validated using in vivo tumor models [67]. In the study, they were able to confirm that the stress in the interior of growth-confined tumor was compressive, and this compressive stress was balanced by tensile stress at the circumference of the tumor periphery [67]. It is also important to note that the compressive force observed in this physical confined tumor (illustrated by “Tumor growth” of Fig. 3) is distinct from the compressive stress that might be exerted on the tumor by the resistance of the normal tissue to the expansion of the tumor (illustrated by “Externally applied” of Fig. 3). The compressive stress that is exerted by an external source may be better recapitulated using an in vivo compression device shown in the study by [53]. Continued buildup of solid stress can compress and even collapse blood and lymphatic vessels of the tumor [57], preventing effective nutrient and oxygen delivery and waste removal as well as inhibiting the delivery and efficacy of tumor therapies [64]. Tumors rich in hyaluronan hold a high net-negative charge due

to the negatively charged groups in hyaluronan [76]. These negative charges hold interstitial fluid within the tumor and form gel-like regions, which generate solid stress. As solid stress increases at the tumor site, surrounding host tissue balances this load by exerting an equal and opposite force [75], which further exacerbates the physical abnormality observed at the tumor site.

In vitro studies recapitulating tumor-compressive stresses found that the continuous application of moderate levels of compressive stress on breast cancer cells leads to an increase in their migratory ability and is associated with the remodeling of their actin cytoskeleton (formation of stress fibers) [72]. On the other hand, application of higher levels of compressive stress led to apoptosis in these cancer cells. This suggests that the presence of a moderate level of compressive stress within the tumors plays an important role in the initiation and enhancement of cancer cell motility/invasion. Compressive forces induce cytoskeletal rearrangements, which are associated with an altered metabolic phenotype in cancer cells [15]. In tumor spheroid models of breast and colon cancer, it was found that the application of compressive stress leads to a reversible decrease in tumor spheroid proliferation and growth [14]. Compression also induces enhanced migration in H4 glioma cells and is associated with an increase in the levels of phosphorylated Erk1/2 [33], which is a known regulator of cancer cell metabolism [59]. In ovarian cancer cells, the application of a compressive stress of ~5.2 kPa leads to enhanced proliferation and chemoresistance [56]. The effect of compressive stress on metabolism is potentially highly cell-type dependent. For example, luminal MCF-7 breast cancer cells showed a downregulation in glycolysis-related genes upon the application of compressive stress, whereas basal MDA-MB-231 breast cancer cells and cancer-associated fibroblasts showed an increase in the expression of glycolysis-related genes when compressed [34].

To summarize, the compressive stress accumulated during tumor growth may play an important role in tumor progression by regulating proliferation, invasion, and ultimately, cancer and stromal cell (glycolytic) metabolism. However, our understanding of the effect of compressive stresses on mitochondrial activity and metabolism is unclear. A study performed on rat primary nucleus pulposus (NP) cells reports that the application of a compressive stress (1 MPa) leads to a loss of  $\Delta\Psi_m$  indicative of mitochondrial damage and necroptosis in these cells [12]. Several solid tumors show necrotic cores, and interestingly, the presence of a necrotic tumor core is associated with poor prognosis as well as with increased lung metastasis in a mouse model of breast cancer [31]. Collectively, these studies indicate that the buildup of compressive stresses in tumor cores could regulate mitochondrial activity and the activation of necrosis in cancer cells, and further research elucidating these mechanisms is needed.

As highlighted above, biophysical cues such as compressive forces play an important role in regulating cancer cell growth and metabolism. Uncontrolled proliferation of cancer cells in the primary tumor within a confined stromal matrix increases cell density [30], which is associated with increased solid (compressive) stress [25]. In our lab, we recapitulated stromal confinement of the tumor island using the micropatterned tumor–stromal assay ( $\mu$ TSA) [65]. When MCF-7 breast



cancer cells are micropatterned in tumor islands surrounded by bone marrow stromal cells (BMSCs) (Fig. 4A, E), we found that there was a spatial distribution of cancer cell density within the tumor micropattern showing high cell densities at the micropattern center (recapitulative of the tumor core) and lower cell densities at the micropattern edges where the tumor island is in contact with the stromal cells (recapitulative of the tumor margins) [6] (Fig. 4C). When stromal confinement of the tumor island was increased in the form of increased stromal cell density, the overall area of the micropatterned tumor island decreased (Fig. 4B), whereas the cancer cell density at the micropattern edges increased (Fig. 4C). These findings were in line with previous studies by Helmlinger et al., modeling the effect of confinement *in vitro* by culturing tumor spheroids in different concentrations of agarose gels. They found that culturing tumor spheroids in conditions of high confinement (increased agarose gel concentration) led to reduced tumor spheroid diameter while increasing cell packing density [25]. Interestingly, we found that within these tumor micropatterns, the spatial distribution of cell density correlated with the  $\Delta\Psi_m$  of cancer cells, suggesting that confinement-induced biophysical cues can regulate mitochondrial activity. When the level of stromal confinement surrounding the micropatterned tumor island was modulated, the spatial distribution of  $\Delta\Psi_m$  within the tumor island was also altered, with increased stromal confinement leading to an increase in the area of the low- $\Delta\Psi_m$  cells at the micropatterned tumor core. RNA-seq analysis of cancer cells extracted from the centers and edges of these micropatterns showed an upregulation of OXPHOS and mitochondrial ETC-related gene sets at the micropattern edges, relative to the micropattern centers (Fig. 4E, F). These results suggest that TME-mediated confinement cues can sensitively regulate cancer cell mitochondrial metabolism. Furthermore, nuclear YAP localization corresponded to the high- $\Delta\Psi_m$  regions at micropattern edges [6], whereas high intercellular E-cadherin expression was associated with the low- $\Delta\Psi_m$  tumor core [5]. These findings strongly suggest that YAP and E-cadherin adhesion-mediated downstream signaling can regulate cancer cell  $\Delta\Psi_m$  in the context of the TME.

Note on tensile stresses: While the effect of tensile stress on cancer cell metabolism is not widely studied, a few studies investigating the effect of stretch *in vitro* suggest that tensile stresses can also influence metabolism in the TME. Ansaryan et al. report that subjecting breast cancer cells (MCF-7, MDA-MB-231) to 15% static stretch for 12 hours is associated with an increase in their lactate levels, suggestive of increased glycolysis in response to the stretching stimulus [1]. Further studies are needed to investigate the detailed mechanisms by which tensile stresses can regulate cancer cell metabolism. Studies performed on different non-cancer cell types suggest the possibility of mitochondrial metabolism change in response to stretching stimuli. In cardiomyocytes, the application of 20% stretch leads to a reduction in  $\Delta\Psi_m$  as soon as 4 h after stretching [40]. On the other hand, in bovine aortic smooth muscle cells, the application of a stretching stimulus for 4 h leads to an increase in  $\Delta\Psi_m$  [3]. These studies suggest that the  $\Delta\Psi_m$  (and thus mitochondrial activity) is responsive to tensile stresses and cell-type dependent.

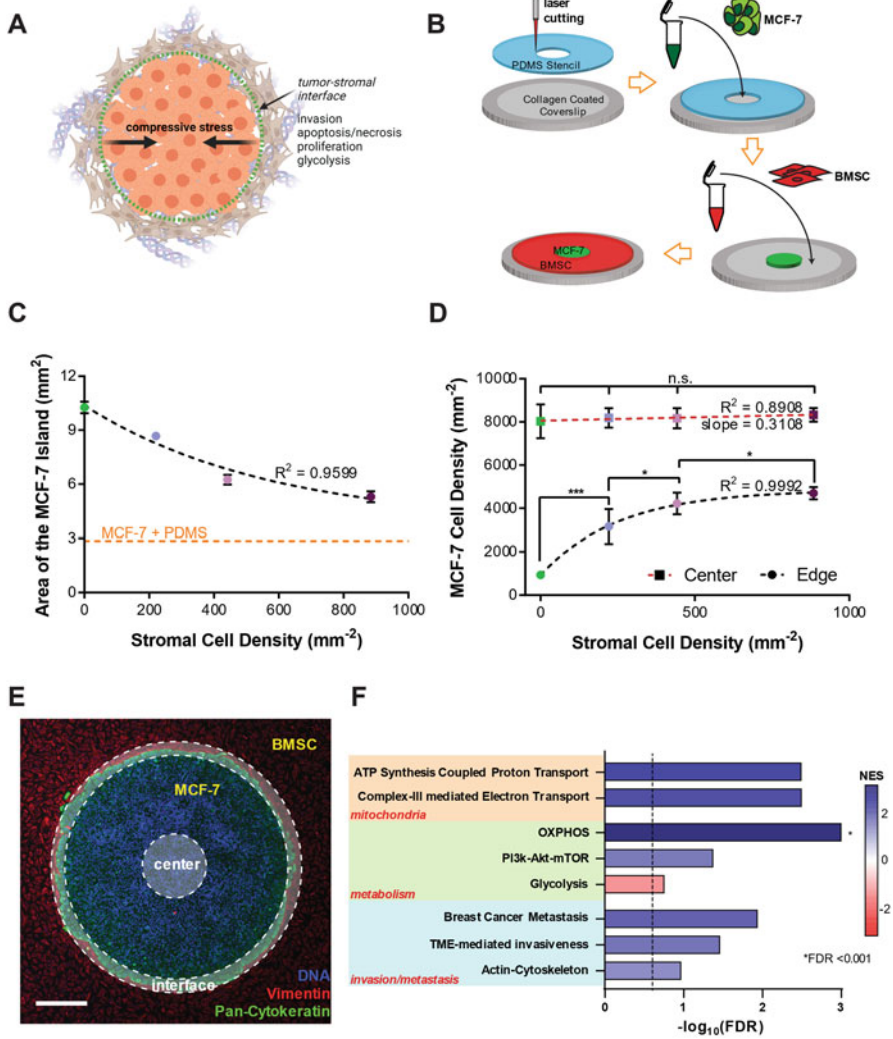


**Fig. 4** Effect of confinement on cancer cell metabolism. (A) Schematic showing build-up of compressive stress within the TME (Created with BioRender.com). (B) Micropatterned tumor-stromal assay ( $\mu$ TSA). (C) Area of the micropatterned tumor island (MCF-7 breast cancer cells) as a function of the density of surrounding stromal cells in the  $\mu$ TSA. MCF7 + PDMS represents complete confinement when stroma is replaced by a layer of PDMS surrounding the tumor island. (D) MCF-7 cell density at the centers and edges of the  $\mu$ TSA as a function of surrounding stromal density. (E) Immunostaining of an MCF-7-BMSC  $\mu$ TSA (green: Pan-cytokeratin; red: vimentin; blue: DNA); dashed white areas: extracted by laser capture microdissection for RNA-sequencing). Scale bar: 100  $\mu\text{m}$ . (F) Gene set enrichment analysis of MCF-7 cells at the interface vs. those at the tumor island center. (B–F from Begum et al. [6], reproduced under the Creative Commons Attribution 4.0 International License)



## 4 Effect of Shear Stress on Tumor–Stromal Interaction and Metabolism in the TME

Fluid homeostasis observed in normal tissue is disturbed near the solid tumor by “leaky” blood vessels and compressed blood and lymphatic vessels [54] (Fig. 5). As a combined effect of hyperpermeable blood vessels and compromised lymphatic drainage system, the interstitial fluid pressure (IFP) of most solid tumor is increased [24]. CAFs are also thought to contribute to elevated tumor IFP by exerting contractile forces on the interstitial matrix and preventing homeostatic response to the elevated IFP [24]. The tumor IFP is uniform at the tumor core and drops sharply at the periphery [24]. This IFP gradient generates fluid flow outward from the center of the tumor toward the surrounding normal tissue [62]. This interstitial flow applies shear stress directly to the tumor and stromal cells. Shear stress and fluid flow can increase transforming growth factor- $\beta$  (TGF $\beta$ ) expression and activation on the stromal cells, activate fibroblasts, regulate immunity, activate YAP/TAZ downstream pathways [68]. For instance, it was reported that the interplay of flow-induced shear stress and altered ECM composition increased cell invasion and expression of mesenchymal-like markers in a HUVEC and breast cancer cell co-culture model [49]. Fluid flow also modulates endothelial sprouting, which affects the formation of new blood and lymphatic vessels [66]. The generated interstitial convective flow also facilitates tumor invasion and growth into the surrounding normal tissue [19]. Tumor cells can also adopt a mesenchymal phenotypic motility and move against the direction of the generated flow by using the ECM scaffold [19]. Overall, elevated IFP subjects various cells in the tumor microenvironment (cancer cells, endothelial cells, immune cells) to shear forces and thereby alters their

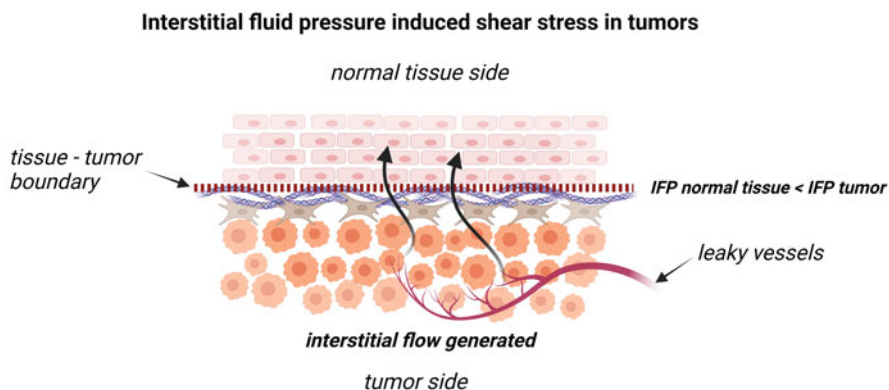


**Fig. 5** *Shear stress generated in the tumors.* Fluid homeostasis is disturbed by leaky blood vessels and compromised lymphatic drainage system in the tumor. As a result, interstitial fluid pressure (IFP) in the tumor is increased. The elevated tumor IFP generates fluid flow outward toward the surrounding normal tissue and applies shear stress directly to the tumor and stromal cells. (Created with [BioRender.com](https://www.biorender.com) )

biology [54]. In this section, we will summarize the effects of elevated shear stress on tumor–stromal interactions and metabolism of different types of cells found in the tumor microenvironment.

The direct effects of shear stress on cancer cells have been studied mainly in the context of circulating tumor cells (CTCs), which will be discussed in detail in the next chapter. In addition to regulating CTC survival and mitochondrial activity [38], there is evidence for shear stress-mediated regulation of stromal cell metabolism. Exertion of a continuous shear stress of 2.3 dynes/cm<sup>2</sup> leads to an increase in levels of phosphorylated ERK and phosphorylated p38 (MAPK) in bone marrow stromal cells (BMSCs), a cell type commonly found in the TME [35]. ERK and MAPK are known regulators of cellular metabolism [59]. Exposure to shear stress can thus alter stromal cell metabolism. In endothelial cells, the application of a shear stress was found to decrease their glucose uptake and mitochondrial DNA content through the expression of KLF-2 (pro-quiescence signal) [16, 39]. In human umbilical vein endothelial cells (HUVECs), the application of a 12 dynes/cm<sup>2</sup> shear stress leads to an increase in their  $\Delta\Psi_m$  [8, 78] and ATP production [78]. Furthermore, in human aortic endothelial cells, the application of a shear stress (15 dynes/cm<sup>2</sup>) was found to significantly increase mitochondrial ATP levels, indicating that shear stress not only regulates glycolysis but also mitochondrial metabolism in endothelial cells [80]. In conclusion, the shear stress experienced by cancer and stromal cells within the TME can regulate their metabolism, thereby influencing cell fate in the process of tumor progression.

## 5 Conclusion

Recent evidence has shed light on the important role of biophysical cues in the TME in directing tumor progression and metastasis [54]. Altered cell metabolism is an important hallmark of cancer cells in the TME [22], and over the past several years, there has been an emergence of studies reporting how biophysical cues regulate cell metabolism. Increased stiffening is a characteristic of several tumors and, as discussed earlier, several studies have reported how increased stiffness is associated with increased glycolysis in both cancer and stromal cell types. Stiffness-induced changes in mitochondrial activity and metabolism, however, is not clear in the context of cancer/stromal cells in the TME. While there are some reports of stiffness regulating the mitochondrial activity [45] and morphology [70] in non-cancer cell types, further studies are required to delineate how local stiffness can regulate mitochondrial metabolism in the TME.

Another important biophysical cue in the TME is the solid stress that builds up resulting from resistance offered by the surrounding stromal tissue as the tumor undergoes uncontrolled proliferation and growth. While some studies have reported how compressive stress (an important component of solid stress) leads to changes in cell migration, proliferation and glycolytic metabolism, the biological response to compressive forces seems to be highly cell-type dependent [34] as well as dependent

**Table 1** Summary of studies investigating the effects of physical stresses on metabolism of tumor/stromal cells

Type of physical stress	Cell type/model system	Change in metabolism	Mechanism	References
Increased stiffness	Cancer-associated fibroblasts (CAFs)	Increase in both glycolytic (ECAR) and mitochondrial metabolism (OCR)	YAP/TAZ dependent glutamate/aspartate cross talk	[7]
Increased stiffness	SCC12 (human squamous carcinoma cell line)	Increase in glycolysis (ECAR)	YAP/TAZ-dependent glutamate/aspartate cross talk	[7]
Increased stiffness	Dendritic cells (DCs)	Increase in both glycolytic (ECAR) and mitochondrial metabolism (OCR)	Hippo signaling (TAZ), Ca <sup>2+</sup> ion channel PEIZOI	[10]
Increased stiffness	Stroma derived from stiff tumors in PDX models of ovarian cancer	Upregulation in genes related to OXPHOS	Potentially MEK	[48]
Decreased stiffness	A549 lung cancer cells MDAD-MB-231 breast cancer cells	Quiescent metabolism (longer cell cycles and reduction in ATP and protein synthesis)	Potentially PFK, several differentially expressed proteins between cells cultured on soft vs. stiff substrates identified by mass spectrometry	[71]
Increased stiffness and collagen density	MDA-MB-231 breast cancer cells	Increased glycolysis	ROCK	[46]
Increased stiffness	Hepatocellular carcinoma cells (HepG2 and MHCC97L)	Increased glycolysis	MAPK-YAP signaling	[44]
Compressive stress	Spheroid models of breast and colon cancer	Reversible decrease in spheroid growth and proliferation	p27 <sup>Kip1</sup>	[14]
Compressive stress	H4 glioma cells	Increase in phosphorylated Erk1/2	Erk1/2	[33]
Compressive stress	Ovarian cancer cells	Enhanced proliferation	CDC42	[56]
Compressive stress	MCF7 breast cancer cells	Downregulation in expression of glycolysis related genes	List of differentially expressed genes in compressed vs. uncompressed cells identified	[34]
Compressive stress	MDA-MB-231 breast cancer cells, cancer-associated fibroblasts (CAFs)	Increase in expression of glycolysis related genes	Metabolic genes <i>ENO2</i> , <i>HK2</i> , <i>PFKFB3</i>	[34]
Static stretch	MCF-7, MDA-MB-231 breast cancer cells	Increased glycolysis (lactate levels)	Expression of MnSOD through activation of H-Ras	[1]
Shear stress	Bone marrow stromal cells (BMSCs)	Increase in phosphorylated ERK and MAPK	ERK/MAPK	[35]

on the level of compressive stress applied [72]. In our own studies, we recapitulated stromal confinement of the tumor island in an in vitro micropatterned tumor model and found that nuclear YAP corresponded to the high- $\Delta\Psi_m$  region at the tumor-edge, and that cytoplasmic YAP corresponded to the low- $\Delta\Psi_m$  micropatterned tumor core [6]. These results suggest that YAP could be an important downstream effector of biophysical cues and call for further studies investigating the role of YAP mediating metabolism changes in response to different compressive stresses in the TME. Furthermore, we have also found that increased intercellular E-cadherin adhesions (found at the center of the tumor micropatterns, in the same region that corresponds to the cytoplasmic YAP and low- $\Delta\Psi_m$ ) negatively regulate cancer cell  $\Delta\Psi_m$  [5]. Overexpression of E-cadherin in MCF-7 cells led to a decrease in  $\Delta\Psi_m$  at both the centers and edges of the tumor micropatterns, whereas a knockdown of E-cadherin led to an increase of  $\Delta\Psi_m$  at the micropattern centers [5]. These results suggest that E-cadherin mediated adhesions can also serve as downstream effectors of biophysical cues and thus sensitively regulate cancer cell metabolism. Further studies investigating how different levels of compressive stresses can regulate E-cadherin-mediated mitochondrial metabolism changes in different cell types would help shed light on how metabolism is regulated in the TME. Increased interstitial fluid pressure is another important biophysical cue in the TME, and while the effects of shear stress on apoptosis [50] and anoikis resistance [38] have been reported by some research groups, an understanding of how increased interstitial fluid pressure affects glycolytic and mitochondrial metabolism of cancer cells remains lacking (Table 1).

## References

1. Ansaryan S, Khayamian MA, Saghafi M, Shalileh S, Nikshoar MS, Abbasvandi F, Mahmoudi M, Bahrami F, Abdollahad M (2019) Stretch induces invasive phenotypes in breast cells due to activation of aerobic-glycolysis-related pathways. *Adv Biosyst* 3:e1800294
2. Bartolak-Suki E, Imsirovic J, Nishibori Y, Krishnan R, Suki B (2017) Regulation of mitochondrial structure and dynamics by the cytoskeleton and mechanical factors. *Int J Mol Sci* 18
3. Bartolak-Suki E, Imsirovic J, Parameswaran H, Wellman TJ, Martinez N, Allen PG, Frey U, Suki B (2015) Fluctuation-driven mechanotransduction regulates mitochondrial-network structure and function. *Nat Mater* 14:1049–1057
4. Bauer J, Emon MAB, Staudacher JJ, Thomas AL, Zessner-Spitzenberg J, Mancinelli G, Krett N, Saif MT, Jung B (2020) Increased stiffness of the tumor microenvironment in colon cancer stimulates cancer associated fibroblast-mediated prometastatic activin a signaling. *Sci Rep* 10:50
5. Begum HM, Mariano C, Zhou H, Shen K (2021) E-cadherin regulates mitochondrial membrane potential in cancer cells. *Cancers* 13
6. Begum HM, Ta HP, Zhou H, Ando Y, Kang D, Nemes K, Mariano CF, Hao J, Yu M, Shen K (2019) Spatial regulation of mitochondrial heterogeneity by stromal confinement in micropatterned tumor models. *Sci Rep* 9:11187
7. Bertero T, Oldham WM, Grasset EM, Bourget I, Boulter E, Pisano S, Hofman P, Bellvert F, Meneguzzi G, Bulavin DV, Estrach S, Feral CC, Chan SY, Bozec A, Gaggioli C (2019) Tumor-stroma mechanics coordinate amino acid availability to sustain tumor growth and malignancy. *Cell Metab* 29(124–140):e10

8. Breton-Romero R, Acin-Perez R, Rodriguez-Pascual F, Martinez-Molledo M, Brandes RP, Rial E, Enriquez JA, Lamas S (2014) Laminar shear stress regulates mitochondrial dynamics, bioenergetics responses and PRX3 activation in endothelial cells. *Biochim Biophys Acta* 1843:2403–2413
9. Butcher DT, Alliston T, Weaver VM (2009) A tense situation: forcing tumour progression. *Nat Rev Cancer* 9:108–122
10. Chakraborty M, Chu K, Shrestha A, Revelo XS, Zhang X, Gold MJ, Khan S, Lee M, Huang C, Akbari M, Barrow F, Chan YT, Lei H, Kotoulas NK, Jovel J, Pastrello C, Kotlyar M, Goh C, Michelakis E, Clemente-Casares X, Ohashi PS, Engleman EG, Winer S, Jurisica I, Tsai S, Winer DA (2021) Mechanical stiffness controls dendritic cell metabolism and function. *Cell Rep* 34:108609
11. Chauhan VP, Jain RK (2013) Strategies for advancing cancer nanomedicine. *Nat Mater* 12:958–962
12. Chen S, Lv X, Hu B, Zhao L, Li S, Li Z, Qing X, Liu H, Xu J, Shao Z (2018) Critical contribution of RIPK1 mediated mitochondrial dysfunction and oxidative stress to compression-induced rat nucleus pulposus cells necroptosis and apoptosis. *Apoptosis* 23:299–313
13. Cosgrove BD, Mui KL, Driscoll TP, Caliri SR, Mehta KD, Assoian RK, Burdick JA, Mauck RL (2016) N-cadherin adhesive interactions modulate matrix mechanosensing and fate commitment of mesenchymal stem cells. *Nat Mater* 15:1297–1306
14. Delarue M, Montel F, Vignjevic D, Prost J, Joanny JF, Cappello G (2014) Compressive stress inhibits proliferation in tumor spheroids through a volume limitation. *Biophys J* 107:1821–1828
15. Dewane G, Salvi AM, Demali KA (2021) Fueling the cytoskeleton – links between cell metabolism and actin remodeling. *J Cell Sci* 134
16. Doddaballapur A, Michalik KM, Manavski Y, Lucas T, Houtkooper RH, You X, Chen W, Zeiher AM, Potente M, Dimmeler S, Boon RA (2015) Laminar shear stress inhibits endothelial cell metabolism via KLF2-mediated repression of PFKFB3. *Arterioscler Thromb Vasc Biol* 35:137–145
17. Fares J, Fares MY, Khachfe HH, Salhab HA, Fares Y (2020) Molecular principles of metastasis: a hallmark of cancer revisited. *Signal Transduct Target Ther* 5:28
18. Feng X, Liu P, Zhou X, Li MT, Li FL, Wang Z, Meng Z, Sun YP, Yu Y, Xiong Y, Yuan HX, Guan KL (2016) Thromboxane A2 activates YAP/TAZ protein to induce vascular smooth muscle cell proliferation and migration. *J Biol Chem* 291:18947–18958
19. Follain G, Herrmann D, Harlepp S, Hyenne V, Osmani N, Warren SC, Timpson P, Goetz JG (2020) Fluids and their mechanics in tumour transit: shaping metastasis. *Nat Rev Cancer* 20:107–124
20. Ge H, Tian M, Pei Q, Tan F, Pei H (2021) Extracellular matrix stiffness: new areas affecting cell metabolism. *Front Oncol* 11:631991
21. Hanahan D, Coussens LM (2012) Accessories to the crime: functions of cells recruited to the tumor microenvironment. *Cancer Cell* 21:309–322
22. Hanahan D, Weinberg RA (2011) Hallmarks of cancer: the next generation. *Cell* 144:646–674
23. Handorf AM, Zhou Y, Halanski MA, Li W-J (2015) Tissue stiffness dictates development, homeostasis, and disease progression. *Organogenesis* 11:1–15
24. Heldin C-H, Rubin K, Pietras K, Östman A (2004) High interstitial fluid pressure — an obstacle in cancer therapy. *Nat Rev Cancer* 4:806–813
25. Helmlinger G, Netti PA, Lichtenbeld CH, Melder RJ, Jain RK (1997) Solid stress inhibits the growth of multicellular tumor spheroids. *Nat Biotechnol* 15
26. Huang J, Zhang L, Wan D, Zhou L, Zheng S, Lin S, Qiao Y (2021) Extracellular matrix and its therapeutic potential for cancer treatment. *Signal Transduct Target Ther* 6:153
27. Hupfer A, Brichkina A, Koeniger A, Keber C, Denkert C, Pfefferle P, Helmprobst F, Pagenstecher A, Visekruna A, Lauth M (2021) Matrix stiffness drives stromal autophagy and promotes formation of a protumorigenic niche. *Proc Natl Acad Sci U S A* 118

28. Jain RK, Baxter LT (1988) Mechanisms of heterogeneous distribution of monoclonal antibodies and other macromolecules in tumors: significance of elevated interstitial pressure. *Cancer Res* 48:7022–7032
29. Jain RK, Martin JD, Stylianopoulos T (2014) The role of mechanical forces in tumor growth and therapy. *Annu Rev Biomed Eng* 16:321–346
30. Jayatilaka H, Umanson FG, Shah V, Meirson T, Russo G, Starich B, Tyle P, Lee JSH, Khatau S, Gil-Henn H, Wirtz D (2018) Tumor cell density regulates matrix metalloproteinases for enhanced migration. *Oncotarget* 9
31. Jiao D, Cai Z, Choksi S, Ma D, Choe M, Kwon HJ, Baik JY, Rowan BG, Liu C, Liu ZG (2018) Necroptosis of tumor cells leads to tumor necrosis and promotes tumor metastasis. *Cell Res* 28:868–870
32. Junttila MR, DE Sauvage FJ (2013) Influence of tumour micro-environment heterogeneity on therapeutic response. *Nature* 501:346–354
33. Kalli M, Voutouri C, Minia A, Pliaka V, Fotis C, Alexopoulos LG, Stylianopoulos T (2019) Mechanical compression regulates brain cancer cell migration through MEK1/Erk1 pathway activation and GDF15 expression. *Front Oncol* 9:992
34. Kim BG, Sung JS, Jang Y, Cha YJ, Kang S, Han HH, Lee JH, Cho NH (2019) Compression-induced expression of glycolysis genes in CAFs correlates with EMT and angiogenesis gene expression in breast cancer. *Commun Biol* 2:313
35. Kreke MR, Sharp LA, Lee YW, Goldstein AS (2008) Effect of intermittent shear stress on mechanotransductive signaling and osteoblastic differentiation of bone marrow stromal cells. *Tissue Eng Part A* 14:529–537
36. Lei X, Lei Y, Li J-K, Du W-X, Li R-G, Yang J, Li J, Li F, Tan H-B (2020) Immune cells within the tumor microenvironment: biological functions and roles in cancer immunotherapy. *Cancer Lett* 470:126–133
37. Levental KR, Yu H, Kass L, Lakins JN, Egeblad M, Ertler JT, Fong SF, Csiszar K, Giaccia A, Weninger W, Yamauchi M, Gasser DL, Weaver VM (2009) Matrix crosslinking forces tumor progression by enhancing integrin signaling. *Cell* 139:891–906
38. Li S, Chen Y, Zhang Y, Jiang X, Jiang Y, Qin X, Yang H, Wu C, Liu Y (2019a) Shear stress promotes anoikis resistance of cancer cells via caveolin-1-dependent extrinsic and intrinsic apoptotic pathways. *J Cell Physiol* 234:3730–3743
39. Li X, Sun X, Carmeliet P (2019b) Hallmarks of endothelial cell metabolism in health and disease. *Cell Metab* 30:414–433
40. Liao XD, Wang XH, Jin HJ, Chen LY, Chen Q (2004) Mechanical stretch induces mitochondria-dependent apoptosis in neonatal rat cardiomyocytes and G2/M accumulation in cardiac fibroblasts. *Cell Res* 14
41. Liberti MV, Locasale JW (2016) The Warburg effect: how does it benefit cancer cells? *Trends Biochem Sci* 41:211–218
42. Lim C-G, Jang J, Kim C (2018) Cellular machinery for sensing mechanical force. *BMB Rep* 51:623–629
43. Liu K, Wiendels M, Yuan H, Ruan C, Kouwer PHJ (2022) Cell-matrix reciprocity in 3D culture models with nonlinear elasticity. *Bioactive Mater* 9:316–331
44. Liu QP, Luo Q, Deng B, Ju Y, Song GB (2020) Stiffer matrix accelerates migration of hepatocellular carcinoma cells through enhanced aerobic glycolysis via the MAPK-YAP signaling. *Cancers (Basel)* 12
45. Lyra-Leite DM, Andres AM, Petersen AP, Ariyasinghe NR, Cho N, Lee JA, Gottlieb RA, McCain ML (2017) Mitochondrial function in engineered cardiac tissues is regulated by extracellular matrix elasticity and tissue alignment. *Am J Physiol Heart Circ Physiol* 313:H757–H767
46. Mah EJ, Lefebvre A, Mccahey GE, Yee AF, Digman MA (2018) Collagen density modulates triple-negative breast cancer cell metabolism through adhesion-mediated contractility. *Sci Rep* 8:17094
47. Micalet A, Moendarbary E, Cheema U (2021) 3D in vitro models for investigating the role of stiffness in cancer invasion. *ACS Biomater Sci Eng*

48. Mieulet V, Garnier C, Kieffer Y, Guilbert T, Nemati F, Marangoni E, Renault G, Chamming's F, Vincent-Salomon A, Mechta-Grigoriou F (2021) Stiffness increases with myofibroblast content and collagen density in mesenchymal high grade serous ovarian cancer. *Sci Rep* 11:4219
49. Mina SG, Huang P, Murray BT, Mahler GJ (2017) The role of shear stress and altered tissue properties on endothelial to mesenchymal transformation and tumor-endothelial cell interaction. *Biomicrofluidics* 11:044104–044104
50. Mitchell MJ, King MR (2013) Fluid shear stress sensitizes cancer cells to receptor-mediated apoptosis via trimeric death receptors. *New J Phys*:15
51. Mohammadi H, Sahai E (2018) Mechanisms and impact of altered tumour mechanics. *Nat Cell Biol* 20:766–774
52. Mueller MM, Fusenig NE (2004) Friends or foes — bipolar effects of the tumour stroma in cancer. *Nat Rev Cancer* 4:839–849
53. Nia HT, Datta M, Seano G, Zhang S, Ho WW, Roberge S, Huang P, Munn LL, Jain RK (2020a) In vivo compression and imaging in mouse brain to measure the effects of solid stress. *Nat Protoc* 15:2321–2340
54. Nia HT, Munn LL, Jain RK (2020b) Physical traits of cancer. *Science* 370
55. Northcott JM, Dean IS, Mouw JK, Weaver VM (2018a) Feeling stress: the mechanics of cancer progression and aggression. *Front Cell Dev Biol* 6
56. Novak CM, Horst EN, Lin E, Mehta G (2020) Compressive stimulation enhances ovarian cancer proliferation, invasion, chemoresistance, and mechanotransduction via CDC42 in a 3D bioreactor. *Cancers (Basel)* 12
57. Padera TP, Stoll BR, Tooredman JB, Capen D, Tomaso ED, Jain RK (2004) Cancer cells compress intratumour vessels. *Nature* 427:695–695
58. Panciera T, Azzolin L, Cordenonsi M, Piccolo S (2017) Mechanobiology of YAP and TAZ in physiology and disease. *Nat Rev Mol Cell Biol* 18:758–770
59. Papa S, Choy PM, Bubicic C (2019) The ERK and JNK pathways in the regulation of metabolic reprogramming. *Oncogene* 38:2223–2240
60. Pavlova NN, Thompson CB (2016) The emerging hallmarks of cancer metabolism. *Cell Metab* 23:27–47
61. Perentes JY, Mckee TD, Ley CD, Mathiew H, Dawson M, Padera TP, Munn LL, Jain RK, Boucher Y (2009) In vivo imaging of extracellular matrix remodeling by tumor-associated fibroblasts. *Nat Methods* 6:143–145
62. Piotrowski-Daspit AS, Tien J, Nelson CM (2016) Interstitial fluid pressure regulates collective invasion in engineered human breast tumors via snail, vimentin, and E-cadherin. *Integr Biol* 8:319–331
63. Quail DF, Joyce JA (2013) Microenvironmental regulation of tumor progression and metastasis. *Nat Med* 19:1423–1437
64. Schaaf MB, Garg AD, Agostinis P (2018) Defining the role of the tumor vasculature in antitumor immunity and immunotherapy. *Cell Death Dis* 9:115
65. Shen K, Luk S, Hicks DF, Elman JS, Bohr S, Iwamoto Y, Murray R, Pena K, Wang F, Seker E, Weissleder R, Yarmush ML, Toner M, Sgroi D, Parekkadan B (2014) Resolving cancer-stroma interfacial signalling and interventions with micropatterned tumour-stromal assays. *Nat Commun* 5:5662
66. Song JW, Munn LL (2011) Fluid forces control endothelial sprouting. *Proc Natl Acad Sci* 108:15342–15347
67. Stylianopoulos T, Martin JD, Chauhan VP, Jain SR, Diop-Frimpong B, Bardeesy N, Smith BL, Ferrone CR, Hornicek FJ, Boucher Y, Munn LL, Jain RK (2012) Causes, consequences, and remedies for growth-induced solid stress in murine and human tumors. *Proc Natl Acad Sci* 109:15101–15108
68. Swartz MA, Lund AW (2012) Lymphatic and interstitial flow in the tumour microenvironment: linking mechanobiology with immunity. *Nat Rev Cancer* 12:210–219
69. Tarragó-Celada J, Cascante M (2021) Targeting the metabolic adaptation of metastatic cancer. *Cancers* 13:1641

70. Tharp KM, Higuchi-Sanabria R, Timblin GA, Ford B, Garzon-Coral C, Schneider C, Muncie JM, Stashko C, Daniele JR, Moore AS, Frankino PA, Homentcovschi S, Manoli SS, Shao H, Richards AL, Chen KH, Hoeve JT, Ku GM, Hellerstein M, Nomura DK, Saijo K, Gestwicki J, Dunn AR, Krogan NJ, Swaney DL, Dillin A, Weaver VM (2021) Adhesion-mediated mechanosignaling forces mitohormesis. *Cell Metab* 33:1322–1341 e13
71. Tilghman RW, Blais EM, Cowan CR, Sherman NE, Grigera PR, Jeffery ED, Fox JW, Blackman BR, Tschumperlin DJ, Papin JA, Parsons JT (2012) Matrix rigidity regulates cancer cell growth by modulating cellular metabolism and protein synthesis. *PLoS One* 7:e37231
72. Tse JM, Cheng G, Tyrrell JA, Wilcox-Adelman SA, Boucher Y, Jain RK, Munn LL (2012) Mechanical compression drives cancer cells toward invasive phenotype. *Proc Natl Acad Sci U S A* 109:911–916
73. Valastyan S, Weinberg RA (2011) Tumor metastasis: molecular insights and evolving paradigms. *Cell* 147:275–292
74. Valkenburg KC, DE Groot AE, Pienta KJ (2018) Targeting the tumour stroma to improve cancer therapy. *Nat Rev Clin Oncol* 15:366–381
75. Vella A, Eko EM, Del Río Hernández A (2018) The emergence of solid stress as a potent biomechanical marker of tumour progression. *Emerging Topics in Life Sciences* 2:739–749
76. Voutouri C, Polydorou C, Papageorgis P, Gkretsi V, Stylianopoulos T (2016) Hyaluronan-derived swelling of solid Tumors, the contribution of collagen and cancer cells, and implications for cancer therapy. *Neoplasia (New York, NY)* 18:732–741
77. Wang H, Naghavi M, Allen C, Barber RM, Bhutta ZA, Carter A, Casey DC, Charlson FJ, Chen AZ, Coates MM, Coggeshall M, Dandona L, Dicker DJ, Erskine HE, Ferrari AJ, Fitzmaurice C, Foreman K, Forouzanfar MH, Fraser MS, Fullman N, Gething PW, Goldberg EM, Graetz N, Haagsma JA, Hay SI, Huynh C, Johnson CO, Kassebaum NJ, Kinfu Y, Kulikoff XR, Kutz M, Kyu HH, Larson HJ, Leung J, Liang X, Lim SS, Lind M, Lozano R, Marquez N, Mensah GA, Mikesell J, Mokdad AH, Mooney MD, Nguyen G, Nsoesie E, Pigott DM, Pinho C, Roth GA, Salomon JA, Sandar J, Silpakit N, Sliigar A, Sorensen RJD, Stanaway J, Steiner C, Teepie S, Thomas BA, Troeger C, Vanderzanden A, Vollset SE, Wanga V, Whiteford HA, Wolock T, Zoeckler L, Abate KH, Abbafati C, Abbas KM, Abd-Allah F, Abera SF, Abreu DMX, Abu-Raddad LJ, Abyu GY, Achoki T, Adelekan AL, Ademi Z, Adou AK, Adsuar JC, Afanvi KA, Afshin A, Agardh EE, Agarwal A, Agrawal A, Kiadaliri AA, Ajala ON, Akanda AS, Akinyemi RO, Akinyemiju TF, Akseer N, Lami FHA, Alabed S, Al-Aly Z, Alam K, Alam NKM, Alasfoor D, Aldhahri SF, Aldridge RW, Alegretti MA, Aleman AV, Alemu ZA, Alexander LT et al (2016) Global, regional, and national life expectancy, all-cause mortality, and cause-specific mortality for 249 causes of death, 1980–2015: a systematic analysis for the Global Burden of Disease Study 2015. *Lancet* 388:1459–1544
78. Wu LH, Chang HC, Ting PC, Wang DL (2018) Laminar shear stress promotes mitochondrial homeostasis in endothelial cells. *J Cell Physiol* 233:5058–5069
79. Wullkopf L, West A-KV, Leijnse N, Cox TR, Madsen CD, Oddershede LB, Erler JT (2018) Cancer cells' ability to mechanically adjust to extracellular matrix stiffness correlates with their invasive potential. *Mol Biol Cell* 29:2378–2385
80. Yamamoto K, Nogimori Y, Imamura H, Ando J (2020) Shear stress activates mitochondrial oxidative phosphorylation by reducing plasma membrane cholesterol in vascular endothelial cells. *Proc Natl Acad Sci U S A* 117:33660–33667
81. Zhang J, Reinhart-King CA (2020) Targeting tissue stiffness in metastasis: mechanomedicine improves cancer therapy. *Cancer Cell* 37:754–755



# Biophysical Regulation of TGF $\beta$ Signaling in the Tumor Microenvironment



Chinmay S. Sankhe, Jessica L. Sacco, and Esther W. Gomez

**Abstract** Transforming growth factor (TGF)- $\beta$  is a multifunctional cytokine that contributes to epithelial–mesenchymal transition, tumor development, and metastasis. The tumor microenvironment experiences dynamic changes in composition and mechanical properties, including alignment of matrix components and variations in the stiffness of the stroma, during cancer progression and recent studies have started to elucidate how these changes govern TGF $\beta$  signaling. This chapter describes the impact of matrix mechanical properties and cell-generated forces on the activation of TGF $\beta$  by cancer-associated fibroblasts and tumor cells. It further reports TGF $\beta$ -induced signaling cascades that respond to biophysical cues and that regulate epithelial–mesenchymal transition and tumor progression. Finally, it highlights approaches for targeting biophysical properties of the tumor microenvironment and mechanoresponsive signaling molecules as strategies to block TGF $\beta$ -induced tumor progression and metastasis.

**Keywords** Mechanics · Cancer · Epithelial–mesenchymal transition · Myocardin related transcription factor · Cancer-associated fibroblast · Extracellular matrix

---

Authors Chinmay S. Sankhe and Jessica L. Sacco have equally contributed to this chapter.

---

C. S. Sankhe · J. L. Sacco

Department of Chemical Engineering, The Pennsylvania State University, University Park, PA, USA

E. W. Gomez (✉)

Department of Chemical Engineering, The Pennsylvania State University, University Park, PA, USA

Department of Biomedical Engineering, The Pennsylvania State University, University Park, PA, USA

e-mail: [ewg10@psu.edu](mailto:ewg10@psu.edu)

© The Author(s), under exclusive license to Springer Nature Switzerland AG 2023

I. Y. Wong, M. R. Dawson (eds.), *Engineering and Physical Approaches to Cancer*, Current Cancer Research, [https://doi.org/10.1007/978-3-031-22802-5\\_6](https://doi.org/10.1007/978-3-031-22802-5_6)

## 1 Introduction

Tumors are surrounded by a complex microenvironment, where cancer cells interact with matrix components, soluble cues such as growth factors and cytokines, and stromal cells that together influence tumor growth, invasion, and metastasis (Fig. 1). Stromal cells, including fibroblasts, cancer-associated fibroblasts (CAFs), endothelial cells, and immune cells, among others, influence the chemical and physical signals within the tumor microenvironment and crosstalk between these cells and tumor cells contributes to tumor cell invasiveness and malignancy [1, 2]. Throughout cancer progression, the mechanical landscape of tumors evolves with changes in tissue structure accompanied by alterations in the mechanics of cellular and matrix components [3]. Indeed, changes in the biophysical properties of tumors are attributed to shifts in cell mechanics and mechanotransduction, changes in the deposition of extracellular matrix (ECM) components, and remodeling of the matrix by tumor cells and stromal cells. Transforming growth factor (TGF)- $\beta$ , a critical cytokine within the tumor microenvironment, serves as both a tumor suppressor and tumor promoter and many recent studies have revealed valuable insights into how mechanical stimuli regulate TGF $\beta$  bioavailability and signal transduction in the context of cancer.

The purpose of this chapter is to review the role of TGF $\beta$  in cancer and to discuss how the biophysical properties of the tumor microenvironment, including matrix stiffness, promote activation of TGF $\beta$  and mediate TGF $\beta$ -induced development and function of CAFs, regulation of epithelial–mesenchymal transition (EMT), and metastasis of tumor cells. The chapter also highlights mechanoresponsive signaling molecules and their role in mediating CAF and tumor cell response to TGF $\beta$  and mechanical cues. Lastly, the chapter provides a summary of strategies to target TGF $\beta$  signaling and tumor mechanics to inhibit cancer cell growth, invasion, and metastasis, thereby improving cancer outcomes.

## 2 Dynamic Changes in Tumor Mechanics Accompany Cancer Progression

Tissues are composed of a variety of cell types and ECM molecules that together contribute to the mechanical properties of the tissue. During disease progression, tissues can experience dynamic changes in the number and types of cells, changes in cell phenotype, and matrix remodeling through ECM deposition, degradation, and reorganization [4], which together lead to modulation of tissue mechanics. In the case of cancer, cells are subjected to alterations in solid stress, matrix stiffness, interstitial fluid flow, and geometry and topology of the ECM [2, 3]. For example, the stiffness (i.e., Young's or elastic modulus) of a tumor can change during tumor development (Table 1), and tissues oftentimes stiffen as cancer progresses. These mechanical changes are specific to different tissue types

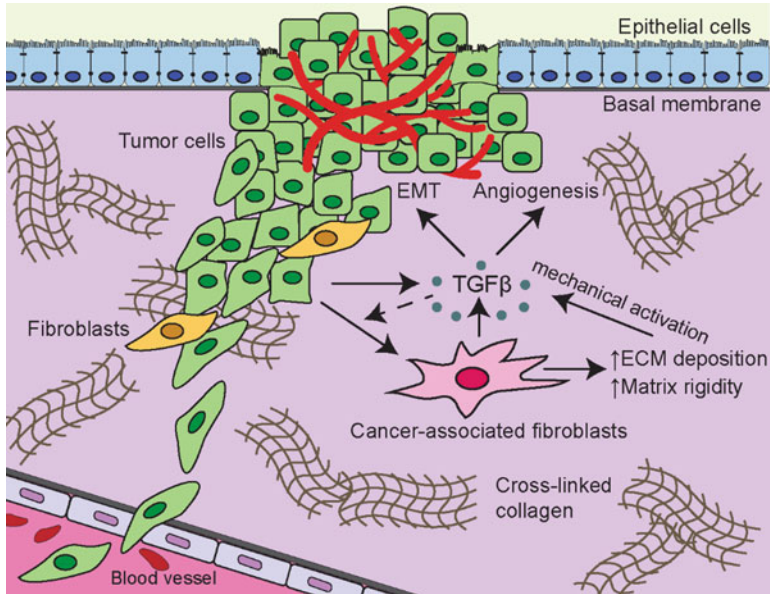


**Fig. 1** Schematic depicting transforming growth factor (TGF)- $\beta$  signaling in the context of the tumor microenvironment. TGF $\beta$ , a pleiotropic cytokine, controls cell growth, differentiation, inflammation, and angiogenesis in the tumor microenvironment. Cancer-associated fibroblasts and tumor cells produce latent TGF $\beta$ , which is deposited to the matrix, and activate TGF $\beta$  from its latent complex via mechanical forces. Resident cells of the tumor microenvironment respond to and remodel the matrix composition and mechanical properties of the tumor microenvironment

and tumor microenvironments. It is challenging to decouple the impact of tissue mechanical properties from other factors *in vivo*, and thus it can be difficult to decipher how mechanical properties regulate TGF $\beta$  signaling and cancer. As such, *in vitro* cell culture platforms that enable precise control of mechanical properties are needed and these platforms can provide complementary information to *in vivo* tumor models.

To mimic the *in vivo* properties of the tumor microenvironment, hydrogel platforms, with tunable chemical and mechanical properties, have been developed and used to examine the effect of defined chemical and physical signals on cellular behaviors *in vitro*. For example, polyacrylamide hydrogels are a common platform for investigating the effect of substrate stiffness on cell signaling and phenotype [21–23]. Polyacrylamide hydrogels are formed via a free-radical polymerization reaction, where acrylamide monomers are crosslinked with bis-acrylamide. By modulating the relative concentrations of acrylamide and bis-acrylamide, the stiffness (i.e., elastic modulus) of the hydrogels can be varied while keeping the surface chemical properties constant. In order to facilitate cell attachment, the surface of the polyacrylamide hydrogel is functionalized with extracellular matrix proteins [24]. Researchers have also developed and used a variety of other matrices (as reviewed

**Table 1** Young's modulus for physiological and diseased states of tissues

Tissue	Young's modulus (kPa)	Reference
Bladder (human)		
Normal	4.7	[5]
Urothelial carcinoma	13.5	
Breast/Mammary Gland (human)		
Normal	1.3	[6]
Invasive ductal carcinoma	3.2	
Breast/Mammary Gland (mouse)		
Normal	0.17, 0.4	[7, 8]
Tumor	1.2–4	
Kidney (human)		
Normal	5–10, 19.2	[5, 9]
Renal cell carcinoma	13	[5]
Liver (human)		
Normal	2.5–5	
Hepatocellular carcinoma	55	[10]
Metastatic tumor	66.5	
Cholangiocellular carcinoma	75	
Lung (human)		[11]
Normal	2	
Idiopathic pulmonary fibrosis	17	
Ovary (human)		
Reproductive age	3.2	
Menopausal	7.2	
Mature Teratoma	14	[12, 13]
Serous tumor	1.6	
Mucinous tumor	3.5	
Endometriosis	2.1	
Pancreas (human)		
Normal	1, 3.5	
Pancreatitis	2.2	[14, 15]
Tumor	5.5, 44.8	
Pancreas (mouse)		
Normal	4.2	
Fibrotic	5.5	[15]
Tumor	11.3	
Prostate (human)		
Normal	10–20	[16–18]
Tumor	45–90	
Thyroid (human)		
Normal	9	[19, 20]
Tumor	45	

in [25]), with moduli spanning that of normal and diseased tissue, to evaluate the effect of matrix stiffness on cellular response and disease progression. Furthermore, other bioengineering approaches, such as soft lithography and electrospinning of fibers, can also be used to control cell and tissue geometry and ECM topology in culture [26, 27]. In the following sections, we will highlight *in vivo* tumor models as well as *in vitro* studies that have utilized biomaterials with defined mechanical properties to examine TGF $\beta$  activation and signaling.

### 3 TGF $\beta$ Signaling in Cancer

TGF $\beta$  is a multifunctional cytokine that regulates development, homeostasis, proliferation, and differentiation, and dysregulation of this pathway can lead to pathologies, including fibrosis and cancer [28–30]. TGF $\beta$  is secreted in a latent form by many cell types found in the tumor microenvironment including macrophages, stromal fibroblasts, CAFs, immune cells, and cancer cells [30, 31]. Activation of TGF $\beta$  from the latent complex is mediated by proteolysis, integrin engagement, and physical forces exerted by myofibroblasts and tumor cells, thus enabling its bioactivity [32, 33]. Many studies have revealed that high levels of TGF $\beta$  in the tumor microenvironment are correlated with advanced clinical stages of human tumors of the pancreas [34], colon [35], skin [36], lung, ovary [37], prostate [38], breast [39–41], brain, and bone [42]. For example, primary tumors and lymph node metastases of breast carcinomas show enhanced deposition of TGF $\beta$ 1 within the tumor stroma [39], and high levels of TGF $\beta$ 1 are positively correlated with breast cancer progression [41]. Furthermore, enhancement of TGF $\beta$  signaling has been correlated with more aggressive breast tumors and poor survival [40, 41].

TGF $\beta$  regulates multiple, complex processes within the tumor microenvironment, many of which are dependent upon the biochemical and physical properties of the tumor and surrounding stroma. TGF $\beta$  can suppress tumorigenesis through regulation of apoptosis of pre-malignant cells and by inhibition of cancer cell proliferation. In contrast, during late stages of cancer, TGF $\beta$  can act as a tumor promoter by facilitating EMT [43–45], enhancing invasion [46], and promoting stem cell-like properties [47, 48] in tumor cells. TGF $\beta$  also mediates the development of CAFs from other cell types and facilitates crosstalk between CAFs and tumor cells [49]. In addition, apoptosis, cell proliferation, EMT, and cell migration are regulated by physical properties, including matrix stiffness [21, 22, 50], and thus tissue mechanics can impact cancer progression in a variety of ways. The following sections will describe how CAFs and tumor cells respond to and mediate TGF $\beta$  signaling within the tumor microenvironment and highlight the impact of TGF $\beta$  on EMT and genomic instability.

### 3.1 *Cancer-Associated Fibroblasts Respond to and Mediate TGF $\beta$ Signaling*

CAFs have been identified as residents of the tumor microenvironment in cancers derived from prostate, lung, breast, gastric, colorectal, and pancreatic tissues as well as others [49]. These fibroblast populations are heterogeneous and can express a variety of protein markers including  $\alpha$ -smooth muscle actin ( $\alpha$ SMA), vimentin, podoplanin (PDPN), fibroblast-specific protein 1 (FSP1/S100A4), fibroblast-activated protein (FAP), platelet-derived growth factor receptor (PDGFR)- $\alpha/\beta$ , tenascin-C, neuron glial antigen (NG2), desmin, CD90/THY1, and caveolin-1 [51, 52], but these protein markers are not selectively expressed by CAFs, nor are they expressed by all CAFs [53]. For pancreatic cancer, CAFs that are in close proximity to the tumor cells exhibit higher  $\alpha$ SMA expression, and hence have been termed myofibroblastic CAFs, whereas CAFs far away from tumor cells have low  $\alpha$ SMA expression and higher levels of inflammatory cytokines such as interleukin 6, and have been termed inflammatory CAFs [54]. Transcriptomic analysis, such as single-cell RNA sequencing, has also been used to characterize gene expression patterns in CAFs for esophageal squamous cell carcinoma [55], pancreatic cancer [56], breast cancer [57], and head and neck squamous cell carcinoma [58]. These studies found that a subset of CAFs express high levels of  $\alpha$ SMA along with genes contributing to contractility such as tropomyosin and myosin-light chain kinase, while another subset of CAFs express high levels of cytokines such as *Cxcl12*, *Il6* and *Ccl2*, but have reduced expression of  $\alpha$ SMA [56, 57]. These findings suggest that there are multiple populations of CAFs within the tumor microenvironment which may serve unique roles in regulating tumor properties and progression.

Studies have shown that CAFs can arise from a variety of cell sources, including tissue-resident fibroblasts, mesenchymal stem cells, and pericytes, and through transdifferentiation of epithelial and endothelial cells [59, 60]. For example, in breast cancer, single cell RNA sequencing revealed that CAF subpopulations have distinct gene expression patterns that suggest they arise from fibroblasts, perivascular cells, and malignant tumor cells [61], while CAFs are derived from stromal fibroblasts and myofibroblasts in head and neck tumors [58]. CAFs are also thought to develop from bone marrow derived mesenchymal stem cells in gastric [62], breast [63, 64], and pancreatic [65] cancers. Normal fibroblasts, through interaction with cancer cells and cytokines such as TGF $\beta$  that are secreted in the tumor microenvironment, can also convert into tumor-promoting CAFs during cancer progression [66, 67]. Indeed, TGF $\beta$  found within the tumor microenvironment has been shown to mediate recruitment of stromal fibroblasts to tumor sites, promote activation to myofibroblast and CAF phenotypes, and regulate CAF proliferation and behavior [49, 68, 69].

CAFs secrete a variety of growth factors that enhance tumor development, angiogenesis, and directional migration of tumor cells [49, 70–72]. Media conditioned by co-cultures of normal murine dermal fibroblasts and metastatic breast

cancer cells enhances scattering and migration of breast cancer cells in vitro [73]. Furthermore, when breast cancer cells are cultured in conditioned media from CAFs, the breast cancer cells acquire a more aggressive phenotype with higher migration and invasion [74]. CAFs also physically interact with cancer cells via N-cadherin-E-cadherin adhesion junctions, and this interaction facilitates collective cancer cell migration and invasion [75]. CAFs can deposit fibronectin into parallel fibers in the tumor stroma, and prostate cancer cells can directionally migrate along these fibers [76]. Similar behaviors have been observed in squamous cell carcinoma, where the tumor cells collectively invaded into the matrix with the help of fibroblast-generated tracks [77]. In addition, interaction of gastric carcinoma cells with gastric fibroblasts induces higher expression of Snail, vimentin, and matrix metalloproteinases (MMPs) with lower levels of E-cadherin in the cancer cells, suggesting activation of EMT-like characteristics in the tumor cells [78]. Similar findings have been observed for non-small cell lung cancer cells co-cultured with CAFs [79].

While many residents of the tumor microenvironment can secrete TGF $\beta$ , myofibroblasts and CAFs have been identified as major sources of TGF $\beta$  [66, 74, 80–82] and also as important contributors to the activation of TGF $\beta$  from its latent complex, as discussed in a later section of this chapter. Downregulation of key TGF $\beta$ -signaling molecules or treatment with a TGF $\beta$  function-blocking antibody reduces CAF-mediated tumor cell motility, which suggests that crosstalk between CAFs and tumor cells via TGF $\beta$  may promote a more aggressive migratory phenotype of gastric carcinoma cells [83]. Furthermore, TGF $\beta$ 1, expressed by both gastrointestinal tumor cells and CAFs, promotes the development of CAFs from resident fibroblasts and enhances tumor cell migration in vitro and tumor metastasis in vivo [67].

During tumor progression, the stroma undergoes remodeling in both its composition and mechanical properties. CAFs contribute to this process through TGF $\beta$ -mediated secretion of matrix proteins, including collagen, fibronectin, and tenascin-C, which they deposit into the tumor microenvironment [49, 84, 85], as well as by secretion of lysyl oxidase (LOX), which catalyzes crosslinking of collagen, thereby contributing to increased stiffness of the matrix [86–88]. Increased tissue stiffness is associated with tumor progression in the liver [10], mammary gland [7, 8, 89], and prostate [16–18]. ECM deposited by CAFs shows more alignment and organization than that deposited by normal fibroblasts [90]. Furthermore, CAFs exhibit increased contractility in comparison to fibroblasts [91], which enables remodeling of the matrix and further promotes increased stiffness of the tumor stroma [92]. Later sections of this chapter will discuss how increased tissue stiffness promotes activation of TGF $\beta$  from its latent complex and enhances mechanoresponsive signaling through TGF $\beta$ -induced cascades.



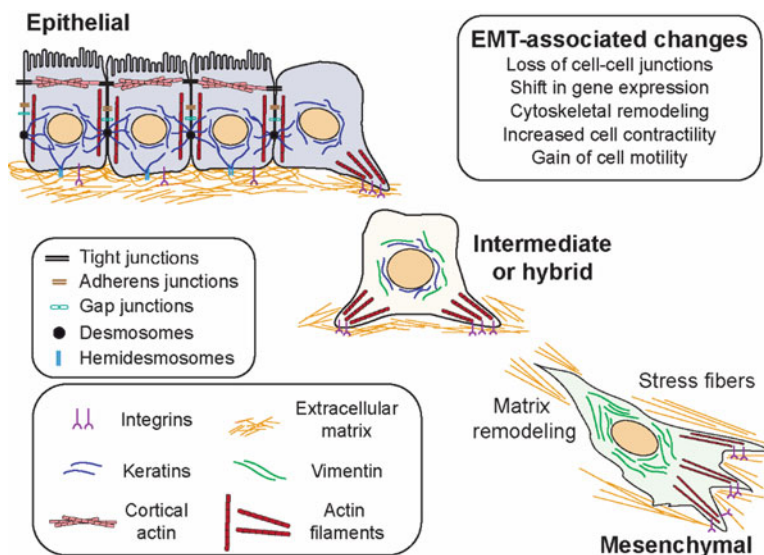


**Fig. 2** Phenotypic changes that occur during epithelial-mesenchymal transition (EMT). Epithelial cells display cell–cell contacts, including tight junctions, adherens junctions, gap junctions and desmosomes, and tethering to the basement membrane using hemidesmosomes and integrins. During EMT, epithelial cells lose cell–cell contacts and apicobasal polarity and exhibit remodeling of the cytoskeleton to acquire a mesenchymal phenotype. Mesenchymal cells remodel the extracellular matrix through deposition of matrix proteins and by exertion of forces and exhibit increased motility. Cells can also exhibit an intermediate cell state, where the cells have attributes of both epithelial and mesenchymal cells

### 3.2 *TGF $\beta$ Induces Epithelial–Mesenchymal Transition*

Epithelial–mesenchymal transition (EMT) is associated with loss of epithelial features, including cell–cell contacts and apicobasal polarity, and acquisition of migratory and invasive behaviors (Fig. 2). During TGF $\beta$ -induced EMT, the expression of epithelial markers, including E-cadherin and ZO-1, are downregulated and cells upregulate the expression of mesenchymal markers such as N-cadherin and  $\alpha$ SMA and matrix proteins, including collagen and fibronectin [93, 94]. Furthermore, following induction of EMT by TGF $\beta$ , cells also experience dramatic cytoskeletal remodeling, where the cortical actin structure typical of epithelial cells transitions to a filamentous stress fiber architecture [95, 96]. Changes in the expression of genes related to actin crosslinking and cell contractility during EMT are accompanied by cytoskeletal softening and an increase in traction forces exerted by cells [21, 97]. TGF $\beta$ -induced actin remodeling regulates EMT and facilitates the gain of invasive and migratory properties in cells [98, 99].

The composition and levels of intermediate filaments, including cytokeratins and vimentin, are also modulated during EMT. Cytokeratins are important for cell–cell



adhesion and maintaining an epithelial phenotype [100], while vimentin contributes to cell-matrix adhesion and cell migration [95, 101, 102]. Different cancer cell types exhibit varying expression levels of keratins and vimentin. For example, in hepatocellular carcinoma, high keratin 19 expression is correlated with increased tumor size, cancer cell invasion, and metastasis [103]. In contrast, knockdown of keratin 8/18 promotes increased motility and invasion of breast cancer cells in vitro [104]. Furthermore, cytokeratin 20 and 7 expression is higher in colorectal cancer tissue than in normal tissue [105]. Vimentin expression is correlated with high motility for prostate cancer cells [106] and vimentin filament polarization enhances migratory persistence in polyploid breast cancer cells [107]. Moreover, overexpression of vimentin has been correlated to enhanced metastatic potential and poor patient survival in breast cancer, cervical cancer, melanoma, prostate cancer, renal cell carcinoma, and hepatocellular carcinoma [106, 108–111].

EMT is thought to mediate dissociation of cancer cells from a primary tumor to facilitate metastasis; however, the role of EMT in cancer and metastasis is not fully understood. While many studies support a role for EMT in the spread of cancer cells from the primary tumor site (as reviewed in [112]), some recent reports suggest that EMT may be dispensable for metastasis, but does contribute to chemoresistance [113, 114]. Nevertheless, tumor cells can exhibit a full EMT or intermediate hybrid epithelial and mesenchymal phenotypes [115, 116]. Cells with an intermediate phenotype may co-express epithelial and mesenchymal markers (for example, cytokeratins and vimentin) and oftentimes there is heterogeneity in epithelial and mesenchymal characteristics amongst cancer cells from the same tumor [117]. TGF $\beta$  has been shown to promote aspects of EMT in cancer cells derived from different tissues, including pancreas [43], lung [118], stomach [119], ovary [120], and mammary gland [45, 47, 121], as well as others. In addition, evidence supports a role for TGF $\beta$  and an intermediate EMT state in priming cells to acquire cancer stem cell-like properties [45, 47, 116]. Gain of cancer stem cell properties in tumor cells allows for them to self-renew and differentiate into heterogeneous progenies with enhanced properties such as drug resistance [122].

### **3.3 TGF $\beta$ Induces Genomic Instability**

TGF $\beta$ -induced EMT has also been linked to genomic instability, a common trait of cancer cells characterized by variations in chromosome structure and number, abnormal mitoses, and DNA mutations. Circulating mesenchymal-like tumor cells from metastatic breast cancer patients have elevated binucleation and micronuclei, which is a protrusion of a chromosome that is not incorporated into the daughter cells during division and suggests chromosomal instability [123]. Multinucleation can arise if abscission, the last step of cytokinesis when the parent cell separates into two daughter cells, is disrupted. Multinucleation results in genomic instability that can lead to cancer progression; more than one third of tumors exhibit multinucleation [124]. Studies have shown that TGF $\beta$ 1-induced EMT is associated with

genomic instability. Inability to arrest cell proliferation in MCF10A and SKBR3 breast cancer cells during TGF $\beta$ -induced EMT prevents cytokinesis, resulting in mitotic abnormalities and aneuploidy, as well as nuclear blebbing and reduced nuclear circularity [123]. Removal of TGF $\beta$  reverses these mitotic defects, but the resulting genomic abnormalities, such as chromosome number variation, remain and promote an increase in tumorigenic phenotypes.

Polypoidal giant cancer cells (PGCCs), which have been observed in late-stage cancers, exhibit differential biophysical phenotypes from other cancer cells. These differences include an enlarged cell size and higher levels of actin bundling as well as longer and thicker actin stress fibers [125]. Furthermore, vimentin is upregulated in PGCCs in comparison to non-PGCCs, with cells exhibiting extensive vimentin networks that span throughout the cell [107]. These changes in cytoskeletal properties are accompanied by an increase in cell stiffness, higher traction forces exerted by the cells, and by a higher rate of migratory persistence. Together, these biophysical properties may contribute to the ability of these cells to withstand increased mechanical stress within the tumor microenvironment.

Studies also reveal that increased matrix stiffness can promote TGF $\beta$ -induced multinucleation. In normal murine mammary gland (NMuMG) epithelial cells cultured on 4 kPa substrata mimicking the stiffness of an average breast tumor, but not on 0.13 kPa substrata mimicking healthy breast tissue, Snail overexpression increases septin-6, anillin, and Mklp1 expression, which are proteins involved in abscission that allow daughter cells to separate from one another [126]. Overexpression of these proteins leads to multinucleation. Ectopic expression of Mklp1 in cells cultured on tumor mimicking 4 kPa substrates resulted in multinucleation, while cells on healthy tissue mimicking 0.13 kPa substrates were protected from multinucleation, even in the presence of increased Mklp1 and septin-6. Increasing focal adhesion engagement with a  $\beta$ 1-integrin mutant in cells cultured on 0.13 kPa substrates resulted in EMT and induction of multinucleation. Furthermore, TGF $\beta$  treatment promotes multinucleation in SCp2 mouse mammary epithelial cells when cultured on 4 kPa substrates, but not on 0.13 kPa substrates. In addition, Snail and septin-6 levels are increased in breast metaplastic carcinoma from human breast tumor samples, specifically in tumor regions with high levels of collagen. Culture of SCp2 cells on 0.13 kPa substrata prevented Snail-induced septin-6 expression and reduced multinucleation [127]. Thus, the combined effects of TGF $\beta$  and matrix stiffness can impact genomic stability in cancer cells. Later sections of this chapter will further describe mechanoresponsive signaling cascades that are activated by TGF $\beta$  in epithelial cells and tumor cells to regulate EMT.

## 4 Mechanical Activation of TGF $\beta$

TGF $\beta$  is stored in a latent form attached to the extracellular matrix and it is activated by cells through both proteolysis and mechanical processes. The TGF $\beta$  protein is synthesized from a large precursor molecule that contains a signal peptide, a shorter

carboxy-terminal fragment (the mature peptide), and a longer amino-terminal fragment called the latency associated peptide (LAP) [128]. An endoprotease, furin, cleaves the precursor, and the LAP and mature peptide reassemble by non-covalent associations to form a homodimer linked by disulfide bonds. This complex is called the small latent complex because the associated LAP homodimer prevents the mature peptide from binding to its receptors rendering it inactive [129]. The small latent complex forms a disulfide bond with the cysteine residue in the latent TGF $\beta$  binding protein (LTBP) to form the large latent complex (LLC) which attaches to extracellular matrix proteins such as fibronectin and fibrillin, where latent TGF $\beta$  is stored until it is released by biological and mechanical stimuli [130]. Alterations in the mechanics of the tumor microenvironment and in the contractility of CAFs and tumor cells during cancer progression play an important role in mechanical activation of latent TGF $\beta$  through mechanisms described below.

Integrins, proteins that mediate cell-extracellular matrix adhesions, enable cells to sense the mechanical properties of their environment and allow for cell exerted forces to be transmitted to the surrounding matrix. Several integrins, including  $\alpha\text{v}\beta 5$  and  $\alpha\text{v}\beta 6$ , have been implicated in mechanical activation of TGF $\beta$  [32, 33]. In rat myofibroblasts, thrombin treatment induces cell contraction, which leads to an increase in latent TGF $\beta 1$  activation, and use of a function-blocking antibody targeting  $\alpha\text{v}\beta 5$  prevents cell contraction-induced TGF $\beta 1$  activation [33]. To confirm activation via cell contraction rather than through proteolysis, cytoskeletons and matrix proteins were examined following extraction from myofibroblasts. Treatment with ATP leads to contraction of the extracted myofibroblast cytoskeleton and increased activation of TGF $\beta 1$ , which is reduced by treatment with an  $\alpha\text{v}\beta 5$  function-blocking antibody. These findings suggest that cytoskeletal tension and mechanical force are key factors that can mediate the bioavailability of active TGF $\beta$ .

Integrin  $\alpha\text{v}\beta 6$  is weakly expressed in normal epithelia, but upregulated in cervical squamous, esophageal, skin, head and neck squamous, non-small cell lung, and breast carcinomas [131–135]. Expression of  $\alpha\text{v}\beta 6$  correlates with decreased patient survival, while blocking  $\alpha\text{v}\beta 6$  reduces tumor growth in breast, colon, cervical, esophageal, and head and neck cancers [131, 132, 135–137], and  $\alpha\text{v}\beta 6$  expression positively correlates with TGF $\beta 1$  levels in cervical squamous carcinoma cells [131]. Furthermore,  $\alpha\text{v}\beta 6$  overexpression in normal myoepithelial cells promotes activation of TGF $\beta 1$  and increased MMP9 levels, while inhibiting TGF $\beta 1$  or MMP9 prevents  $\alpha\text{v}\beta 6$ -positive myoepithelial cells from promoting breast cancer invasion [133]. TGF $\beta$  activation from its latent complex by  $\alpha\text{v}\beta 6$  is mediated by force and actin/myosin cytoskeletal contractility. LAP is a ligand for  $\alpha\text{v}\beta 6$ ; however, LAP binding to  $\alpha\text{v}\beta 6$  is not sufficient to activate latent TGF $\beta 1$  and an intact cytoskeleton is required for  $\alpha\text{v}\beta 6$ -mediated TGF $\beta 1$  activation [138]. Treatment of primary human bronchial epithelial cells with sphingosine 1-phosphate (S1P) induces cortical actin structures, cell contraction, and  $\alpha\text{v}\beta 6$ -mediated TGF $\beta$  activation [32]. Treatment with the cell contractility inhibitors, Y27632 and blebbistatin, reveals that  $\alpha\text{v}\beta 6$ -mediated TGF $\beta$  activation requires ROCK and non-muscle myosin II signaling. Furthermore, culture of bronchial epithelial cells on substrata of increasing stiffness demonstrated that treatment with S1P can promote activation of TGF $\beta$  on

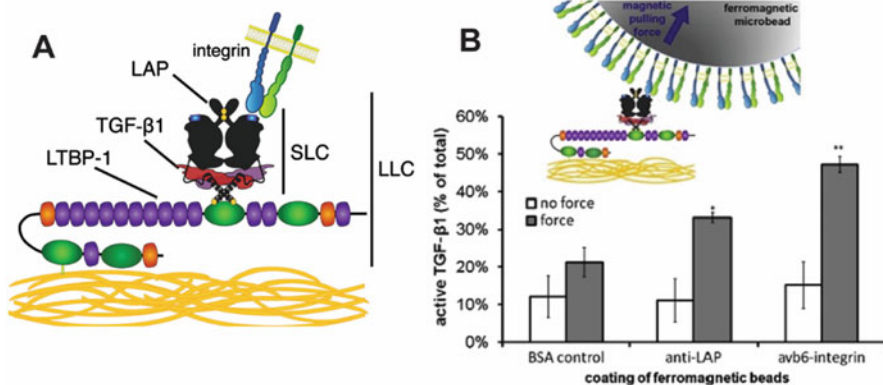


**Fig. 3** Mechanical activation of TGF $\beta$ 1 is mediated by integrins. **(A)** Schematic of the latent TGF $\beta$ 1 complex depicting the latency-associated peptide (LAP), small latent complex (SLC), large latent complex (LLC), latent TGF- $\beta$ -binding protein-1 (LTBP-1), TGF- $\beta$ 1, and integrin interaction. **(B)** Ferromagnetic microbeads coated with LAP antibodies, integrin  $\alpha$ v $\beta$ 6, or a bovine serum albumin (BSA) control adsorbed to the ECM containing large latency complexes (LLC) and force was applied using a magnetic field. The ECM was obtained by performing a deoxycholate (DOC) extraction of Chinese hamster ovary cells, which resulted in extraction of ECM components, including LLC. Beads coated with LAP antibodies or recombinant integrin  $\alpha$ v $\beta$ 6 that were subjected to force application release 1.7–2.2-fold higher amounts of active TGF $\beta$ 1 compared to the BSA control with force application. All three treatments in the no force condition had low levels of active TGF $\beta$ 1 as measured with a mink lung reporter cell assay. (Reprinted from *Current Biology*, Vol 21, Buscemi, L., Ramonet, D., Klingberg, F., Formey, A., Smith-Clerc, J., Meister, J.J., Hinz, B., The single-molecule mechanics of the latent TGF- $\beta$ 1 complex, Pages 2046–2054, Copyright 2011, with permission from Elsevier)

stiff substrata (0.2% polyacrylamide hydrogels), where cell-generated force can be transmitted to the bound latent complex, but not on soft substrata (0.025% polyacrylamide hydrogels).

Several studies have examined how force mechanistically releases TGF $\beta$  from the latent complex [139–141]. Using force spectroscopy, it was determined that mechanical forces, like pulling, induce conformational changes in LAP, which lead to unfolding of the  $\alpha$ 1 helix and latency lasso to release TGF $\beta$  from LAP. When TGF $\beta$  is bound to LTBP-1 in the extracellular matrix, TGF $\beta$  can be released by mechanical forces as small as what a single integrin can transmit [139]. In additional studies, ferromagnetic microbeads coated with LAP antibodies, recombinant integrin  $\alpha$ v $\beta$ 6, or bovine serum albumin (BSA) were allowed to interact with extracellular matrix, and TGF $\beta$ 1 activation was measured in response to force which was applied using a magnetic field. As shown in Fig. 3, when zero force is applied to the bead, all three conditions show low levels of active TGF $\beta$ 1. In contrast, when force is exerted on the bead complex, beads coated with LAP antibodies or  $\alpha$ v $\beta$ 6 integrin have a 1.7–2.2-fold increase in the release of TGF $\beta$ 1 compared to the BSA control [139]. Structural characterization and molecular dynamics

simulations of force-dependent activation reveal that integrin  $\alpha\beta6$  regulates TGF $\beta$  activation by binding to the TGF $\beta$  prodomain, which alters its conformation, and via actin-generated forces applied through the integrin  $\beta$ -subunit to release TGF $\beta$  from latency [140]. Another study found that tensile force is required to break the disulfide bonds that maintain the LLC in order to activate TGF $\beta$  from the  $\alpha\beta6$ -prodomain complex [141]. Together, these findings support a model whereby mechanical forces promote conformational changes in the LAP/prodomain complex to release TGF $\beta$ .

Fibroblasts and primary human bronchial epithelial cells can use contractile forces to activate latent TGF $\beta$  on stiff, but not soft, substrates [32, 33]. Matrix stiffness has also been found to contribute to TGF $\beta$  activation by cell tension generated through a  $\beta1$  integrin-FAK-Rho GTPase signaling axis in hepatocellular carcinoma cells [142]. Upregulation of  $\beta1$  expression, enhanced pFAK and pSmad2 levels, and increased levels of active TGF $\beta$  in culture media were observed when hepatocellular carcinoma cells were cultured on 10 kPa substrates, all of which decreased upon treatment with RGD blocking peptides, Y27632 and blebbistatin [142]. On 32 kPa polyacrylamide hydrogel substrates, increased cell contractility results in  $\alpha\beta6$ -mediated TGF $\beta$  activation and EMT induction in primary alveolar epithelial and rat lung epithelial T-antigen negative (RLE-6TN) cells [143]. As shown in Fig. 4, increased matrix stiffness promotes EMT in primary alveolar type II (ATII) cells as characterized by actin cytoskeletal rearrangements, increased  $\alpha$ SMA expression, and decreased E-cadherin expression. Fibronectin (Fn)- or laminin (Ln)- coated glass slides or tissue culture polystyrene (TCP) were used for control experiments, since it has been shown that ATII cells undergo EMT on Fn-coated surfaces, but maintain an epithelial phenotype on Ln-coated surfaces [144]. Increased EMT induction with increasing matrix stiffness is mediated by higher levels of TGF $\beta$  activation by cells cultured on 24 and 32 kPa substrata. Indeed, TGF $\beta$  activation by RLE-6TN cells increases as substrate stiffness increases, and stiffness-induced TGF $\beta$ -activation by cells cultured on 32 kPa substrata can be prevented by TGF $\beta$ - and  $\alpha\beta6$ -neutralizing antibodies [143].

Increased matrix stiffness and changes in cytoskeletal organization and signaling within cells that accompany cancer can promote changes in force generation by cells. Traction force microscopy experiments have revealed that metastatic breast, lung, and prostate cancer cells exert larger traction forces on the underlying substratum in comparison to normal cells derived from the same tissues [145]. As shown in Fig. 5, metastatic MDA-MB-231 breast cancer cells exert larger tractions and higher net forces on 5 kPa collagen I-coated substrata than normal MCF10A mammary epithelial cells. These findings suggest that as cancer progresses, some cancer cells may gain the ability to exert larger forces on the surrounding matrix and these increased traction forces may promote increased activation of latent TGF $\beta$  as well as reorganization of the matrix.

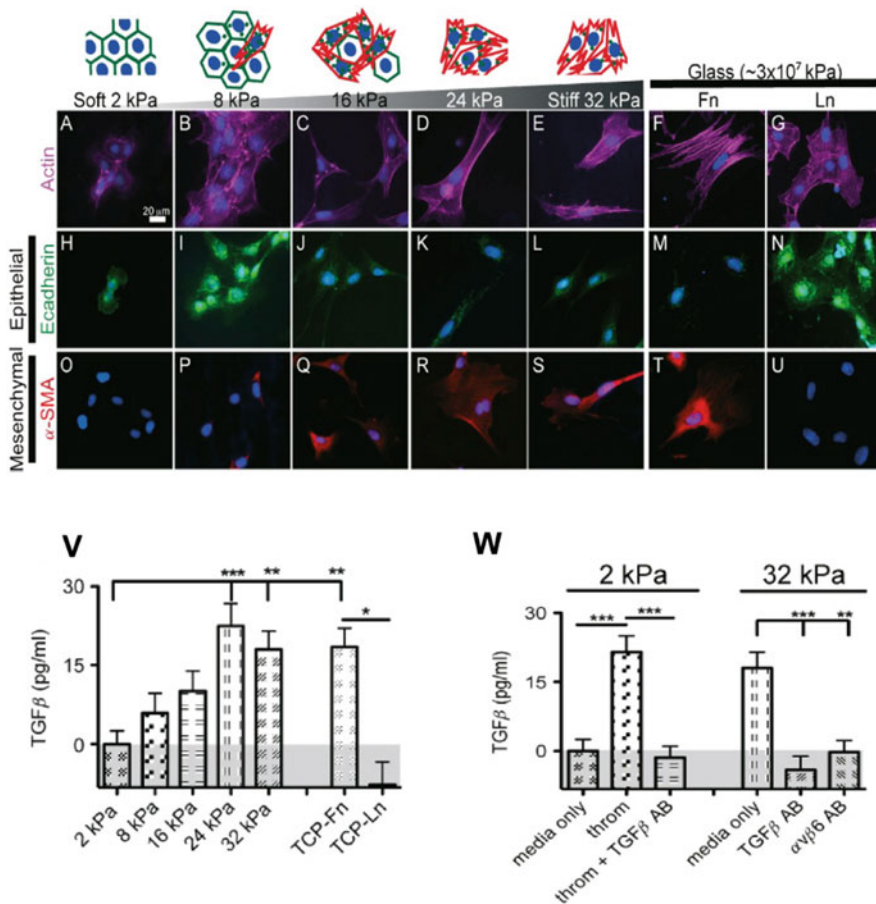


**Fig. 4** Cell contraction and integrin-mediated TGF $\beta$  activation drives stiffness-mediated EMT in lung epithelial cells. (A–U) Increased stiffness induces EMT in primary alveolar type II cells. Cells were cultured on fibronectin (Fn)-coated polyacrylamide gels of varying stiffness or on Fn- (F, M, T) or laminin (Ln)-coated (G, N, U) glass slides. Immunofluorescence staining reveals actin organization (magenta), E-cadherin expression (green), and  $\alpha$ SMA expression (red). (V) RLE-6TN cells increase TGF $\beta$  activation as substrate stiffness increases. Cells were cultured on polyacrylamide hydrogel substrates of increasing stiffness, or Fn- or Ln-coated tissue culture polystyrene (TCP) as control experiments, and TGF $\beta$  activation was monitored using a mink lung epithelial reporter cell (MLEC) bioluminescence co-culture assay. (W) TGF $\beta$  activation in response to stiffness, cell contractility, and integrin  $\alpha$ v $\beta$ 6 was analyzed using a MLEC bioluminescence co-culture assay. RLE-6TN cells were cultured on 2 kPa or 32 kPa polyacrylamide hydrogels and treated with thrombin (a contractility agonist), TGF $\beta$ -neutralizing antibodies, integrin  $\alpha$ v $\beta$ 6-neutralizing antibodies, or a media only control. Cells cultured on the 2 kPa substrates with thrombin treatment activated TGF $\beta$  more than in the absence of thrombin. TGF $\beta$ -neutralizing antibodies prevent the increased TGF $\beta$  activation promoted by thrombin. Cells cultured on 32 kPa substrates with TGF $\beta$  neutralizing antibodies or  $\alpha$ v $\beta$ 6 neutralizing antibodies show decreased TGF $\beta$  activation. (Figure adapted with permission from Brown, A.C., Fiore, V.F., Sulchek, T.A., & Barker, T.H. (2013), Physical and chemical microenvironmental cues orthogonally control the degree and duration of fibrosis-associated epithelial-to-mesenchymal transition. *Journal of Pathology*, 229(1), 25–35. Copyright © 2012 Pathological Society of Great Britain and Ireland. Published by John Wiley & Sons, Ltd)

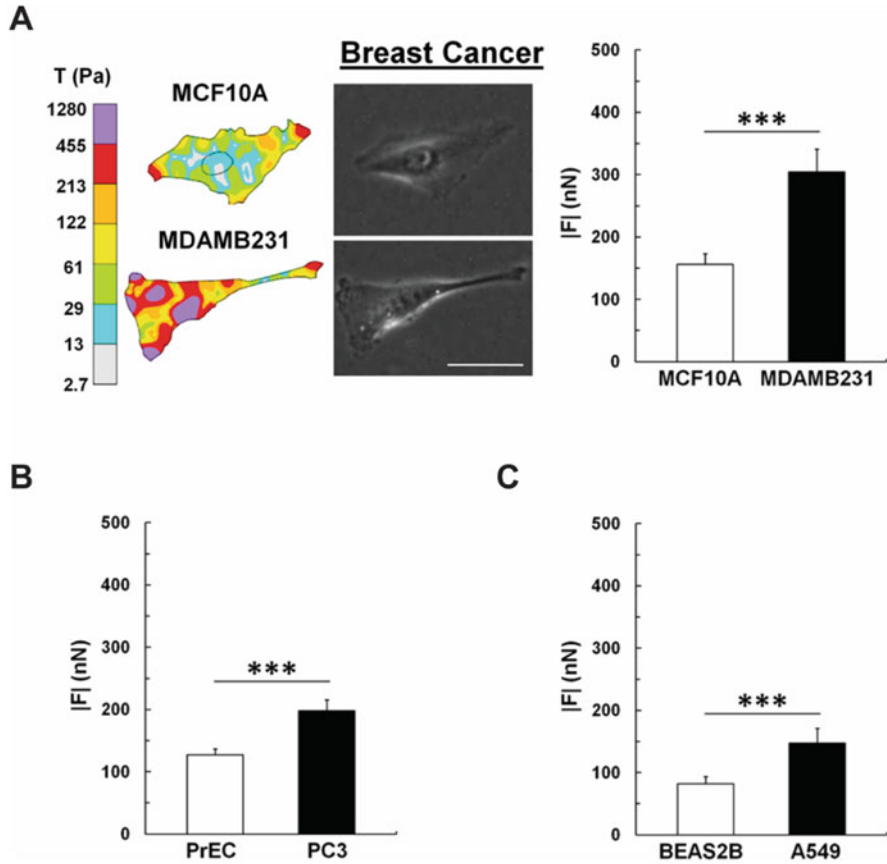


**Fig. 5** Metastatic cancer cells exert higher traction forces than their healthy counterparts. (A) Traction stress maps, phase images, and net traction forces exerted by normal MCF10A mammary epithelial cells and MDA-MB-231 breast cancer cells. Net traction forces exerted by (B) normal prostate cells (PrEC) and metastatic prostate cells (PC3), and (C) normal bronchial epithelial cells (BEAS2B) and metastatic lung cancer cells (A549). All cells were seeded on polyacrylamide substrates with a Young's Modulus (denoted by  $E$ ) of 5 kPa and type I collagen concentration of 0.1 mg/mL. Scale bar: 50  $\mu$ m. Data represents mean  $\pm$  s.e.m.; \*\*\*indicates  $p < 0.001$ . (Figures adapted with permission from Kraning-Rush, C.M., Califano, J.P., Reinhart-King C.A. (2012) Cellular traction stresses increase with increasing metastatic potential. PLoS One. 7(2): e32572)

## 5 Mechanical Regulation of TGF $\beta$ -Induced Signaling Cascades

TGF $\beta$  receptors, which mediate activation of intracellular signaling cascades, are expressed in a wide variety of tissues, and mutations in TGF $\beta$  receptors are associated with cancer of the colon, stomach, and brain [146]. Expression of a dominant-negative type II TGF $\beta$  receptor (TGF $\beta$ RII-dn) in EpRas cells and



in highly metastatic mouse CT26 colon carcinoma cells blocks TGF $\beta$  receptor signaling and inhibits cancer cell invasiveness and metastasis [147]. TGF $\beta$  binding to its cell surface receptors leads to signal transduction by canonical Smad and non-canonical Smad-independent pathways. TGF $\beta$ -induced Smad signaling is initiated by the interaction between the TGF $\beta$  ligand and TGF $\beta$  receptors I and II, which leads to phosphorylation of TGF $\beta$  receptor I and subsequent phosphorylation of Smad2/3. Smad2/3 form a heterotrimeric complex with Smad4, and this complex translocates to the nucleus to regulate gene expression [148]. TGF $\beta$  also activates signaling pathways, including extracellular signal-regulated kinase (Erk) [149], phosphoinositide 3-kinase (PI3K)-Akt [118, 150], focal adhesion kinase (FAK) [151], p38 mitogen-activated protein kinase (p38MAPK) [152, 153], RhoA/ROCK [154], integrin linked kinase (ILK) [155], myocardin-related transcription factors (MRTFs) [156], Yes-associated protein (YAP), and transcriptional coactivator with PDZ binding motif (TAZ), among others (Fig. 6). This section will focus on how mechanical signals from the tumor microenvironment regulate TGF $\beta$ -induced signaling cascades.

### ***5.1 EMT-Associated Transcription Factors***

EMT is orchestrated by a variety of transcription factors, including Snail, Slug, Twist1/2, and Zeb1/2, that play important roles in regulation of epithelial and mesenchymal genes [116, 157]. Multiple reports have demonstrated that TGF $\beta$ 1-induced expression of Snail increases in mammary epithelial cells that are cultured on substrata with moduli greater than 5 kPa in comparison to cells cultured on substrata with moduli less than 1 kPa [21, 50]. Recent evidence also supports a role for matrix stiffness in the regulation of TGF $\beta$ 1-induced Smad2/3 and Twist1 signaling [158, 159]. Twist1 was found to predominantly localize to the nucleus when normal breast epithelial cells were cultured on 3 kPa substrata mimicking the mechanical properties of a breast tumor and to localize to the cytoplasm when cells were cultured on 0.1 kPa substrata mimicking the mechanical properties of normal breast tissue [158]. In addition, phosphorylated Smad2/3 was found to localize to the nucleus when cells were seeded on 3 kPa substrata and Smad2/3 nuclear localization was inhibited on 3 kPa substrata when cells were treated with the TGF $\beta$  receptor inhibitor Galunisertib [158]. Knockdown of Twist1 in human mammary epithelial cells blocks EMT in response to TGF $\beta$ 1 when the cells are cultured on 5.7 kPa substrata suggesting a role for Twist1 in the mechanical regulation of EMT [159]. Indeed, Twist1 remains in the cytoplasm bound to its cytoplasmic binding partner Ras GTPase-activating protein-binding protein 2 (G3BP2) when cells are cultured on 0.15 kPa substrata, and culture of cells on stiffer 5.7 kPa substrata promotes release of Twist1 from G3BP2, thereby facilitating its nuclear translocation. Downregulation of G3BP2 leads to Twist1 nuclear localization in cells cultured on both 0.1 kPa and 5.7 kPa substrata, thereby enabling EMT across all matrix stiffnesses examined. Thus, matrix mechanical properties regulate TGF $\beta$ -induced transcription factor signaling to control EMT.



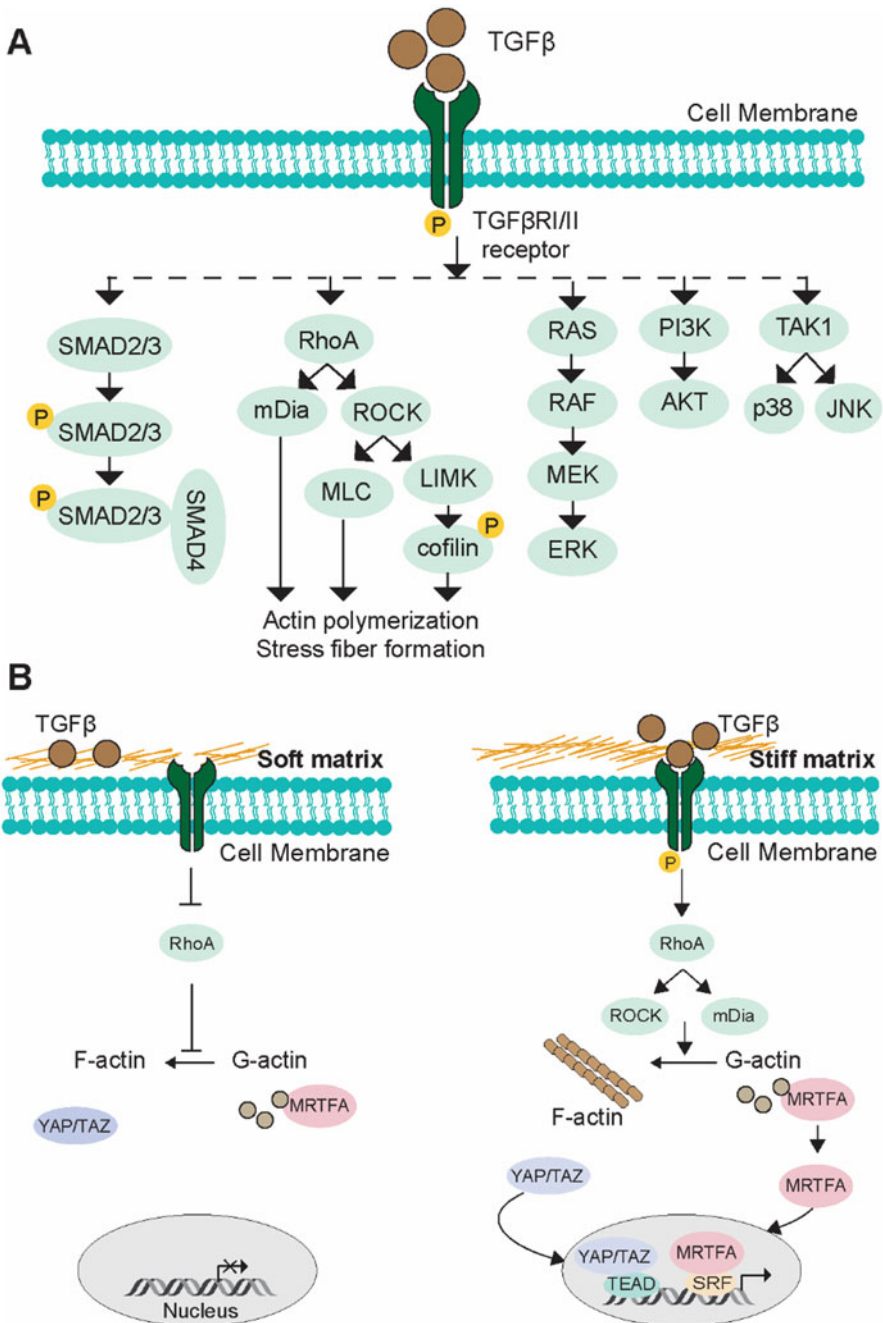


**Fig. 6** Schematic of TGFβ-induced signaling cascades. **(A)** TGFβ ligand interacts with TGFβ receptors I and II to promote activation of SMAD, Ras homolog family member A (RhoA), extracellular signal regulated kinase (ERK), phosphoinositide 3-kinase (PI3K)-Akt, p38 mitogen-activated protein kinase (p38 MAPK), and JUN N-terminal kinase (JNK). **(B)** Matrix stiffness regulates cytoskeletal organization and the subcellular localization and activity of myocardin-related transcription factor (MRTF)-A, Yes-activated protein (YAP), and transcriptional coactivator with PDZ binding motif (TAZ)

## 5.2 *RhoA/ROCK*

Rho GTPase signaling regulates cytoskeletal organization and cellular processes, including adhesion, motility, and transcription factor translocation [160]. Misregulation of Rho GTPase signal transduction occurs in cancer and is associated with metastasis and chemoresistance [161, 162]. TGF $\beta$ 1 treatment increases RhoA and Rho kinase activity in normal murine mammary gland (NMuMG) and MCF10CA1h cells, as well as Cdc42-GTP activity in PC-3U human prostate cancer cells [153, 154, 163]. Following treatment with TGF $\beta$ 1, mouse mammary epithelial cells lose cortical actin structures and exhibit an increase in the number, width, and length of actin filaments [96]. Expression of a dominant negative RhoA prevents TGF $\beta$ 1-induced cytoskeletal rearrangements, morphology changes, and gene expression changes, suggesting that RhoA is required for TGF $\beta$  to induce EMT [154]. Studies have also shown that treatment of mouse embryonic fibroblasts with Y27632, a ROCK inhibitor, prevents the cells from undergoing TGF $\beta$ -induced oncogenic transformation [164]. Furthermore, in PC-3U human prostate cancer cells, TGF $\beta$ 1 treatment induces actin reorganization and stress fiber formation, both of which are blocked by treatment with Y27632 or HA-1077 [163]. Together, these findings suggest that RhoA/ROCK signaling plays an essential role in mediating cytoskeletal rearrangements and gene expression changes in response to TGF $\beta$ .

Changes in the mechanical properties of the tumor microenvironment can be sensed by cells and can promote changes in cytoskeletal signaling pathways including RhoA/ROCK signaling. Figure 7 shows human colonic fibroblasts that were cultured on 4.3 kPa or 28 kPa polyacrylamide substrates to mimic normal or fibrotic intestinal tissue [165]. Cells cultured on the 28 kPa, but not the 4.3 kPa, substrates form actin stress fibers and exhibit mature focal adhesions. Y27632 treatment prevents actin stress fiber and mature focal adhesion formation in cells cultured on both 4.3 kPa and 28 kPa substrates. Y27632 treatment also prevents stiffness-induced increase in myosin light chain kinase (MLCK; MYLK) gene expression, suggesting that RhoA/ROCK signaling and cytoskeletal reorganization are sensitive to mechanical cues [165]. Furthermore, human lung fibroblasts, cultured on 21 kPa substrates, have higher F-actin levels, increased production of RhoA, increased activity of RhoA/ROCK, and higher levels of phosphorylated MLC compared to cells cultured on 0.52 kPa substrates [166]. Y27632 treatment decreased F-actin levels in cells cultured on 21 kPa substrates down to the levels seen on 0.52 kPa substrates and prevented  $\alpha$ SMA-containing stress fiber formation. These findings suggest that increases in the stiffness of the microenvironment that are associated with tumor progression mediate changes in gene expression and increased contractility of fibroblasts.

Rho/ROCK signaling during TGF $\beta$ -induced EMT is also regulated by the mechanical properties of the microenvironment. Mouse mammary epithelial cells cultured on 6.3 kPa substrata that mimic the mechanical properties of an average breast tumor, undergo EMT in response to TGF $\beta$ 1 and exhibit a decrease in the expression of the epithelial marker E-cadherin and an increase in stress fiber

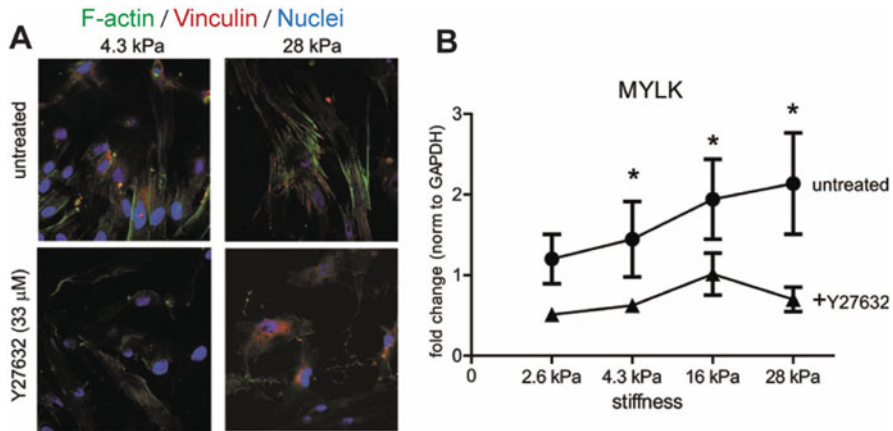


**Fig. 7** RhoA/ROCK signaling and matrix stiffness regulate stress fiber formation and gene expression in human colonic fibroblasts. Human colonic fibroblasts were cultured on soft (4.3 kPa) polyacrylamide substrates to mimic normal intestinal tissue or stiff (28 kPa) substrates to mimic fibrotic intestine. **(A)** Y27632 (33  $\mu$ M) treatment prevents mature focal adhesion formation and actin stress fiber formation as visualized by staining for vinculin (red) and with phalloidin (green), respectively. Cell nuclei are shown in blue. **(B)** Myosin light chain kinase (MYLK) mRNA expression in fibroblasts increases as a function of the stiffness of the microenvironment. Treatment of cells with Y27632 attenuates MYLK gene expression changes. (Johnson, Laura A.; Rodansky, Eva S., Novel Rho/MRTF/SRF inhibitors block matrix-stiffness and TGF- $\beta$ -induced fibrogenesis in human colonic myofibroblasts, *Inflammatory Bowel Diseases*, 2013, 20, 1, 154–165, by permission of Oxford University Press)

formation and the expression of mesenchymal markers including  $\alpha$ SMA [21]. In contrast, cells cultured on 0.3 kPa substrata that mimic the mechanical properties of normal breast tissue, maintain cortical actin architecture and are refractive to TGF $\beta$ 1. Treatment of cells cultured on 6.3 kPa substrata with Y27632 attenuates stress fiber formation and blocks gene expression changes associated with TGF $\beta$ 1-induced EMT [21]. Similar results have also been observed for alveolar type II cells and kidney epithelial cells [50, 143, 167]. The above findings highlight the close cooperation between mechanics, TGF $\beta$ , and RhoA/ROCK signaling that together regulate cytoskeletal reorganization and EMT.

### 5.3 Integrin-Linked Kinase

Integrin-linked kinase (ILK), an intracellular protein that interacts with the cytoplasmic domains of integrins  $\beta$ 1 and  $\beta$ 3 [168], is a key signaling molecule in cancer. PINCH1, an adaptor protein, binds to ILK, facilitating its localization to focal adhesions where ILK can also interact with the actin cytoskeleton to mediate cell-extracellular matrix communication and mechanotransduction [169]. PINCH1

and ILK regulate cell behaviors that are often influenced by ECM mechanics, including cell growth and motility, as well as cancer progression [170, 171]. Indeed, ILK expression and activity have been associated with tumor cell proliferation and invasion and shorter survival in cancer [172–177].

Studies have demonstrated that TGF $\beta$ 1 can promote upregulation of the expression of ILK in some cell types, including melanoma and lung cancer cells, and that ILK plays an important role in the regulation of TGF $\beta$ 1-induced EMT [155, 178–180]. In A549 lung carcinoma cells, TGF $\beta$ 1 upregulates ILK expression through a Smad2/3-dependent mechanism and downregulation of ILK attenuates TGF $\beta$ 1-induced expression of vimentin, but does not restore E-cadherin expression [180]. In normal mammary epithelial cells, ILK inhibition prevents TGF $\beta$ 1-induced EMT and cell migration, while in MDA-MB-231 breast cancer cells, which exhibit high metastatic potential, ILK inhibition reduces cell migration and  $\alpha$ SMA expression and partially rescues E-cadherin expression [155]. ILK also mediates TGF $\beta$ 1-induced alterations in matrix properties. In renal tubular epithelial cells, overexpression of ILK upregulates fibronectin, PAI-1, MMP-2, and  $\alpha$ v $\beta$  integrins, which are important for promoting latent TGF $\beta$ 1 activation and for remodeling of the ECM [181].

ILK also regulates the secretion of latent TGF $\beta$  by fibroblasts, which are one of the major sources of TGF $\beta$  in the tumor microenvironment. ILK-deficient mouse fibroblasts produce lower levels of total and active TGF $\beta$ 1 and exhibit reduced  $\alpha$ SMA levels compared to fibroblasts containing ILK [182]. Decreased extracellular TGF $\beta$ 1 levels are not attributed to differences in transcription, but arise due to decreased secretion of TGF $\beta$ 1. Exogenous TGF $\beta$ 1 was found to restore  $\alpha$ SMA expression and Smad2 phosphorylation in ILK-deficient cells. Further studies have also shown that silencing of ILK in human fibroblasts results in reduced secretion of TGF $\beta$ 1, which is mediated in part by RhoA/ROCK signaling [183]. Disruption of ILK reduces its interactions with and the activity of the RhoGAP ARHGAP26, which catalyzes Rho-GTP hydrolysis. Inhibiting ARHGAP26 reduces TGF $\beta$ 1 secretion, suggesting that ARHGAP26 and ILK both play important roles in TGF $\beta$ 1 secretion by fibroblasts.

Given that ILK associates with focal adhesions, it can act as a mechanotransducer to relay microenvironmental mechanical cues to the cell nucleus to regulate TGF $\beta$ -induced EMT. Recent studies show that stiff and hypoxic microenvironments, which are characteristic of tumors, promote the development of breast cancer stem-cells through regulation of ILK [184]. Human and mouse mammary carcinoma cells cultured on 4 kPa substrata had enhanced expression of  $\beta$ 1 integrin and ILK in comparison to cells cultured on 0.13 kPa substrata, with hypoxic conditions further enhancing the expression. Depleting ILK abrogated the formation of breast cancer stem cell properties for cells on stiff substrates and under hypoxic conditions. It was determined that the activation of the PI3K/Akt signaling pathway is necessary for the ILK-dependent acquisition of breast cancer stem cell properties. ILK has also been found to regulate the switch between apoptosis and EMT in response to TGF $\beta$ 1 and matrix stiffness [185]. Normal murine mouse mammary gland (NMuMG) epithelial cells cultured on polyacrylamide substrates with elastic moduli greater

than 5 kPa undergo EMT following TGF $\beta$ 1 treatment, while cells cultured on 0.4 and 1.0 kPa polyacrylamide substrates undergo apoptosis [50]. ILK knockdown results in apoptosis in cells cultured on both 0.13 and 4 kPa substrata following TGF $\beta$ 1 stimulation [185]. ILK knockdown also promotes a decrease in focal adhesions and an increase in cell–cell adhesions in this system, suggesting a mechanism by which ILK regulates cell fate downstream of TGF $\beta$ 1.

#### ***5.4 Myocardin-Related Transcription Factors***

The myocardin-related transcription factors, MRTF-A (MKL1) and MRTF-B (MKL2), play a critical role in transducing mechanical signals through the cell cytoplasm to the nucleus and in activating serum response factor (SRF)-dependent transcription [186]. The activity and nuclear localization of MRTF-A is regulated in part by its association with monomeric G-actin. MRTF-A localizes predominantly to the cytoplasm when the level of G-actin is high in cells, which can be promoted by several conditions, including by inhibiting RhoA, by treatment with an actin depolymerizing drug latrunculin, or by culture of cells on soft substrata. In contrast, actin polymerization leads to disruption of the interaction between MRTF-A and monomeric actin and to increased nuclear accumulation of MRTF-A where it can regulate gene expression [187, 188]. Shuttling of MRTF-A between the nucleus and the cytoplasm is also regulated by the phosphorylation state of various residues of MRTF-A [189, 190]. For example, ERK mediates phosphorylation of MRTF-A at Ser33, Ser98, and Ser454, each of which have differential impacts on MRTF-A subcellular localization [189, 191]. Phosphorylation of Ser98 promotes nuclear accumulation of MRTF-A, while phosphorylation of Ser33 and Ser454 promotes cytosolic localization [191]. Thus, MRTFs can be regulated by both chemical and mechanical signals from the cellular microenvironment.

MRTFs contribute to developmental processes and tissue homeostasis, including muscle cell differentiation and cardiovascular development [192, 193], and recent studies have also identified roles for MRTFs in cancer [194, 195]. Pancreatic cancer tissues show higher expression levels of MRTF-A and MRTF-B than non-neoplastic pancreas tissues, and increased MRTF-A and MRTF-B expression in pancreatic cancer cells promotes EMT, which is accompanied by a decrease in E-cadherin and an increase in vimentin, fibronectin, and N-cadherin expression and cancer stem cell-like traits [195]. Furthermore, increasing evidence suggests that MRTFs play important roles in cancer cell migration, invasion, and metastasis by controlling cytoskeletal dynamics [194]. MRTF-A expression is higher in metastatic anaplastic thyroid cancer tissues than in matched primary thyroid cancer tissues, while no differences in MRTF-A levels are detected between primary cancer tissues and normal thyroid tissues, suggesting a role for MRTF-A in metastasis [196]. Indeed, overexpression of MRTF-A in thyroid cancer cells promotes increased motility and invasion as measured by wound healing and transwell invasion assays, while knockdown of MRTF-A reduces motility and invasion. Increased MRTF-A

expression also leads to an increase in migration of MCF7 breast cancer cells [197] and promotes migration, invasion, and lung metastasis in 4T1 breast cancer cells [198]. Furthermore, knockdown of MRTF-A reduces cell migration in MDA-MB-231 breast cancer cells and B16 mouse melanoma cells in vitro and in vivo [194].

Recent evidence supports a role for MRTFs in regulation of the development of CAFs and in remodeling of the tumor microenvironment by CAFs. MRTF-A has been shown to regulate differentiation of mesenchymal stem cells (MSCs) toward a CAF phenotype in vitro and in vivo [199]. Treatment of MSCs with TGF $\beta$ 1 or tumor conditioned medium from HCT8 colorectal carcinoma cells promotes increased expression of  $\alpha$ SMA, calponin 1, and collagen 1A1, and knockdown of MRTF-A results in a decrease of  $\alpha$ SMA and calponin 1 expression in vitro. Furthermore, knockdown of MRTF-A in MSCs, which impairs their ability to fully differentiate into CAFs, promotes a reduction in tumor size in a mouse HCT8 xenograft in vivo. Knockdown of MRTF-A/B in TGF $\beta$ 1-differentiated myofibroblasts also leads to a reduction in the expression of h1-calponin,  $\alpha$ SMA, and vinculin and a decrease in contractile force generation [200]. In lung fibroblasts, MRTF-A knockdown promotes a decrease in mRNA levels of type I collagen (COL1A2), suggesting a role for MRTF-A in regulation of matrix deposition [201].

Various studies have also examined the regulation of MRTF signaling in myofibroblasts as a function of matrix stiffness, which is particularly important in the context of the tumor microenvironment because CAFs exhibit myofibroblast-like properties and modulate matrix properties. Increased matrix stiffness promotes nuclear import of MRTF-A in normal human lung fibroblasts and normal human colonic fibroblasts [165, 166]. Nuclear localization of MRTF-A in fibroblasts cultured on 21 kPa substrata correlates with higher F-actin levels in cells as well as higher expression levels of  $\alpha$ SMA in comparison to cells cultured on 0.52 kPa substrata [166]. Furthermore, primary lung fibroblasts isolated from MRTF-A knockout mice (MKL1<sup>-/-</sup>) are refractive to stiffness-induced differentiation to a myofibroblast phenotype [166]. Pharmacological inhibition of MRTF-A in colonic fibroblasts promotes cytosolic localization of MRTF-A and attenuates matrix stiffness-induced and TGF $\beta$ 1-induced  $\alpha$ SMA and type I collagen expression [165]. Cells can also experience mechanical compressive stresses within the tumor microenvironment, and a recent study demonstrated that NIH3T3 fibroblasts have a decrease in nuclear localization of MRTF-A in response to compressive force [202]. These findings suggest that mechanical cues found in the tumor microenvironment impact the subcellular localization and activity of MRTFs in myofibroblasts and CAFs and signaling through the MRTF pathway enables these cells to modulate the chemical and mechanical properties of the tumor microenvironment.

Several studies have shown that an increase in matrix stiffness, which is a hallmark of some tumor microenvironments, also regulates MRTF signaling in the context of EMT. TGF $\beta$ 1-treated mammary epithelial cells cultured on 6.3 kPa substrata, which mimic the mechanical properties of the average breast tumor, show downregulation of E-cadherin, upregulation of the mesenchymal marker  $\alpha$ SMA, enhanced filamentous actin levels, and MRTF-A localization predominantly to the



nucleus [21]. In contrast, cells cultured on 0.3 kPa substrata, which mimic the mechanical properties of normal breast tissue, are refractive to TGF $\beta$ 1-induced EMT and show cytosolic localization of MRTF-A (Fig. 8). Expression of a dominant negative MRTF-A construct, lacking the transcriptional activation domain, reduces the percentage of cells expressing  $\alpha$ SMA in response to TGF $\beta$ 1. Furthermore, when osteosarcoma MG63 cells are cultured on 34 kPa substrata, the cells exhibit higher levels of filamentous actin, enhanced nuclear accumulation of MRTF-A, and enhanced migration in comparison to when the cells are cultured on 2 kPa substrata, and inhibition of MRTF-A abrogates EMT-related behaviors on stiff substrata [203].

Cancer cells located along the invasive fronts of tumors display EMT-like properties including changes in E-cadherin expression [204, 205]. Disparities between cells located at the invasion fronts of tumors in comparison to cells located within the interior regions of tumors may arise in part due to differences in the levels of mechanical stress experienced by the cells found at different spatial locations within the tumor. Mechanical stress in tissues is propagated through cell–cell adhesions and regions of maximal stress are defined by the tissue geometry. Spatial patterning of EMT arises in two-dimensional sheets of mammary epithelial cells following treatment with TGF $\beta$ 1 [206]. As shown in Fig. 8, cells located along the edges of epithelial sheets and in regions of the tissue that experience high mechanical stress, show decreased E-cadherin expression, increased expression of mesenchymal markers including  $\alpha$ SMA, and nuclear localization of MRTF-A. In contrast, cells found within the interior region of the tissue have cytosolic localization of MRTF-A and are refractive to TGF $\beta$ 1-induced EMT. Thus, tumor geometry and gradients in mechanical stress within the tumor may impact cell response to TGF $\beta$ .

During metastasis, cancer cells migrate and invade through confined microenvironments, and cells oftentimes undergo dramatic shape changes to efficiently invade surrounding tissues [207, 208]. Examination of differences in cell shape between invasive osteosarcoma cells and their less invasive parental type demonstrates that highly metastatic cells display a more mesenchymal-like morphology characterized by increased cell elongation and aspect ratio [209]. In the context of TGF $\beta$ 1-induced EMT, cell shape can also regulate the expression of mesenchymal markers, with increased cell spreading and increased cell elongation promoting the expression of  $\alpha$ SMA [210]. Restricting cell spreading significantly decreases the percentage of TGF $\beta$ 1-treated cells with nuclear localized MRTF-A and this is accompanied by a reduction in the percentage of cells expressing mesenchymal markers  $\alpha$ SMA, caldesmon, and tropomyosin as compared to TGF $\beta$ 1-treated cells that are cultured on large protein micropatterns which allow for the cells to spread. Furthermore, knockdown of MRTF-A suppresses the expression of  $\alpha$ SMA in TGF $\beta$ 1-treated cells even when cells are permitted to spread on the underlying substratum. In summary, MRTF signaling is regulated by a combination of TGF $\beta$  and a variety of mechanical cues presented to cells.

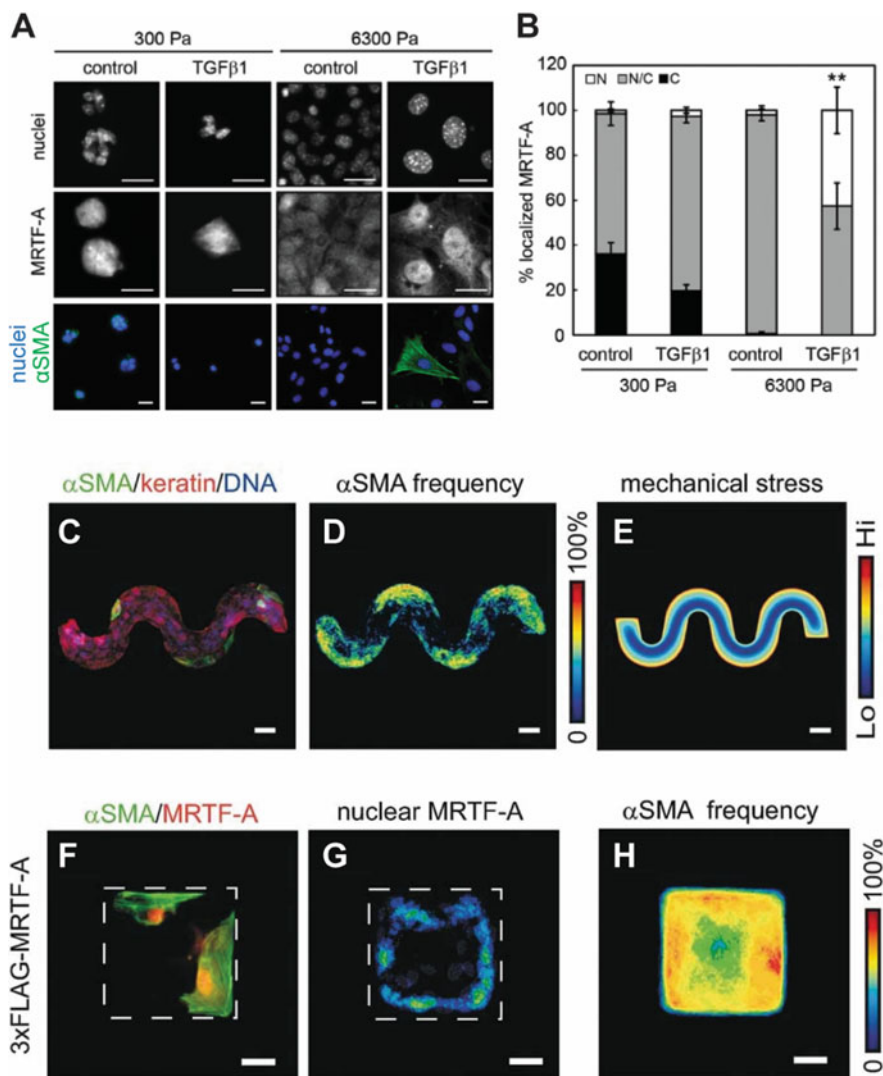


**Fig. 8** MRTF-A regulates TGFβ-induced epithelial-mesenchymal transition in response to matrix stiffness and mechanical stress gradients. **(A)** Immunofluorescence staining for nuclei, MRTF-A, and αSMA (green) in normal murine mammary gland (NMuMG) epithelial cells cultured on fibronectin-coated soft (300 Pa) and stiff (6300 Pa) polyacrylamide substrata in the presence and absence of TGFβ1. Scale bars: 20 μm. **(B)** Quantification of the percentage of cells with nuclear (N), pan-cellular (N/C), and cytoplasmic (C) MRTF-A as a function of matrix stiffness and TGFβ1 treatment reveals MRTF-A predominantly localizes to the nucleus in TGFβ1-treated cells cultured on stiff matrix.  $**p < 0.01$ . TGFβ1-induced EMT occurs in regions of tissues that exhibit high mechanical stress. **(C)** Staining for αSMA (green), cytokeratin (red), and DNA (blue) following induction of EMT by TGFβ1. **(D, E)** Frequency map shows that cells that express αSMA are located in regions of the tissue that are predicted by finite element method modeling to have higher mechanical stresses. Scale bars: 50 μm. **(F)** Staining for FLAG-tagged



## 5.5 Hippo Pathway

The Hippo pathway regulates cell growth and differentiation and dysregulation of signaling effectors of this pathway contributes to cancer progression [211, 212]. Yes-associated protein (YAP) and transcriptional coactivator with PDZ binding motif (TAZ), key coactivators of the Hippo pathway, interact with Smad transcription factors of the TGF $\beta$  signaling pathway [213, 214]. TGF $\beta$ 1-induced tumorigenic activity in MDA-MB-231 cells is mediated in part by YAP/TAZ, Smad2/3, and TEAD family transcription factors that interact to regulate genes such as NEGR1, CTGF, and UCA1 [213]. Knockdown of YAP/TAZ reduces TGF $\beta$ 1-induced mammosphere formation, cell migration, and invasion of human breast cancer cells. TGF $\beta$ 1 treatment induces TAZ nuclear localization in oral squamous carcinoma cells, and TAZ knockdown prevents TGF $\beta$ 1-induced loss of E-cadherin and gain of vimentin in Cal27 and HN6 oral cancer cells [215]. TAZ knockdown also reduces cancer stem cell colony formation in oral cancer cells. Together, these findings suggest a role for YAP/TAZ in TGF $\beta$ -induced EMT and acquisition of cancer stem cell properties.

Studies have revealed that YAP and TAZ cooperate with MRTF-A to regulate cell response to TGF $\beta$  signaling [216–218]. In fibroblasts and epithelial cells, TGF $\beta$  can induce TAZ expression [218]. TGF $\beta$ 1 treatment stimulates MRTF-A transcriptional activity, and chromatin immunoprecipitation experiments have confirmed that MRTF-A interacts with the TAZ promoter, which leads to an increase in TAZ expression [218]. TAZ has also been shown to regulate TGF $\beta$ 1-induced EMT along wound sites, where TAZ and MRTF-A colocalize to the nucleus in cells at the wound edge but to the cytoplasm in cells within the interior intact region of the tissue [217]. Downregulation of TAZ prevents TGF $\beta$ 1-induced  $\alpha$ SMA expression in cells located along the wound edge. These findings imply an important role for YAP/TAZ and MRTF-A in regulation of EMT along wound sites. Further studies are needed to determine how these transcription factors may act cooperatively to regulate behaviors of tumor cells that are located at the invasion fronts of tumors.

YAP/TAZ signaling is also regulated by mechanical cues, including confinement and matrix stiffness [219], and mechanical regulation of YAP/TAZ has implications for both tumor cells and CAFs. High expression of YAP and ILK are associated

---

←  
**Fig. 8** (continued) MRTF-A (red) and  $\alpha$ SMA (green), and frequency maps for (G) nuclear localized MRTF-A and (H)  $\alpha$ SMA reveal that the spatial distribution of  $\alpha$ SMA expression correlates with nuclear localized MRTF-A within the tissue. Scale bars: 25  $\mu$ m. (Figures adapted with permission from O'Connor, J.W., Riley, P.N., Nalluri, S.M., Ashar, P.K., & Gomez, E.W. (2015), Matrix rigidity mediates TGF $\beta$ 1-induced epithelial-myofibroblast transition by controlling cytoskeletal organization and MRTF-A localization. *Journal of Cellular Physiology*, 230(8), 1829–1839. © 2014 Wiley Periodicals, Inc. Figures adapted with permission from Gomez, E.W., Chen, Q.K., Gjorevski, N., & Nelson, C.M. (2010), Tissue geometry patterns epithelial-mesenchymal transition via intercellular mechanotransduction. *Journal of Cellular Biochemistry*, 110(1), 44–51. © 2010 Wiley-Liss, Inc)

with poor outcomes in breast cancer patients, and drug resistance correlates with YAP expression [220]. Overexpression of YAP induces EMT in MCF10A normal mammary gland cells, and promotes an increase in fibronectin, vimentin, and N-cadherin expression and a decrease in E-cadherin and occludin expression [221]. When MDA-MB-231 breast cancer cells are cultured on 38 kPa substrates, compared to 10 kPa or 57 kPa substrates, the cells show increased ILK expression, enhanced YAP nuclear localization and activity, and reduced uptake of doxorubicin, suggesting drug resistance [220]. Pharmacological inhibition of ILK revealed that ILK acts upstream of YAP to mediate matrix stiffness-regulated drug resistance. As shown in Fig. 9, pancreatic tumor cells also exhibit increased nuclear localization of YAP and TAZ with increasing matrix stiffness, and this correlates with increased EMT and chemoresistance [222]. In the context of fibroblasts, renal fibroblasts cultured on 100 kPa substrata, show increased Smad2/3 nuclear localization and Smad transcriptional activity in comparison to when the cells are cultured on 2 kPa substrata [223]. Smad2/3 nuclear localization and activity correlate with YAP/TAZ localization to the nucleus in cells cultured on the stiff substrata. YAP and TAZ also localize to the nucleus in fibroblasts derived from lung tissue when the cells are cultured on 25 kPa substrata that mimic the mechanical properties of fibrotic lung lesions, but not on 0.4 kPa substrata that mimic the mechanical properties of normal lung tissue [224]. Downregulation of YAP and TAZ attenuates stiffness-induced cell spreading, actin polymerization, collagen I expression, and traction forces exerted by lung fibroblasts. These findings together suggest that mechanical properties of the microenvironment influence YAP/TAZ signal transduction and impact tumor cell EMT and drug resistance as well as the activity of fibroblasts and their ability to remodel the matrix via protein deposition and exertion of force.

## 6 Effect of Matrix Dimension on TGF $\beta$ -Induced EMT

Most in vitro experiments investigating TGF $\beta$ -induced EMT have been performed in two-dimensional (2D) culture, but there is growing interest in three-dimensional (3D) cell culture, which better mimics properties of the tumor microenvironment. Gene expression profiling of cells from multiple types of breast cancer determined that genes that encode proteins involved in signal transduction, such as ITGB1, the gene that encodes for  $\beta$ 1-integrin which is required for TGF $\beta$ 1-induced EMT [225], are differentially expressed in cells grown in 2D compared to 3D environments, and resistance to chemotherapeutic agents is increased in 3D cultures [226]. Cells can be cultured in 3D spheroids, scaffolds, organoids, and microfluidic devices to more closely mimic the in vivo tumor environment. These 3D cultures can incorporate cell–cell and cell–ECM interactions, as well as hypoxic centers and oxygen and nutrient gradients that are present in tumors [227, 228].

A better understanding of cell behavior in 3D during mammary gland development could provide insights into how breast tumors form and progress. Hence, efforts have been made to study branching morphogenesis, a process required

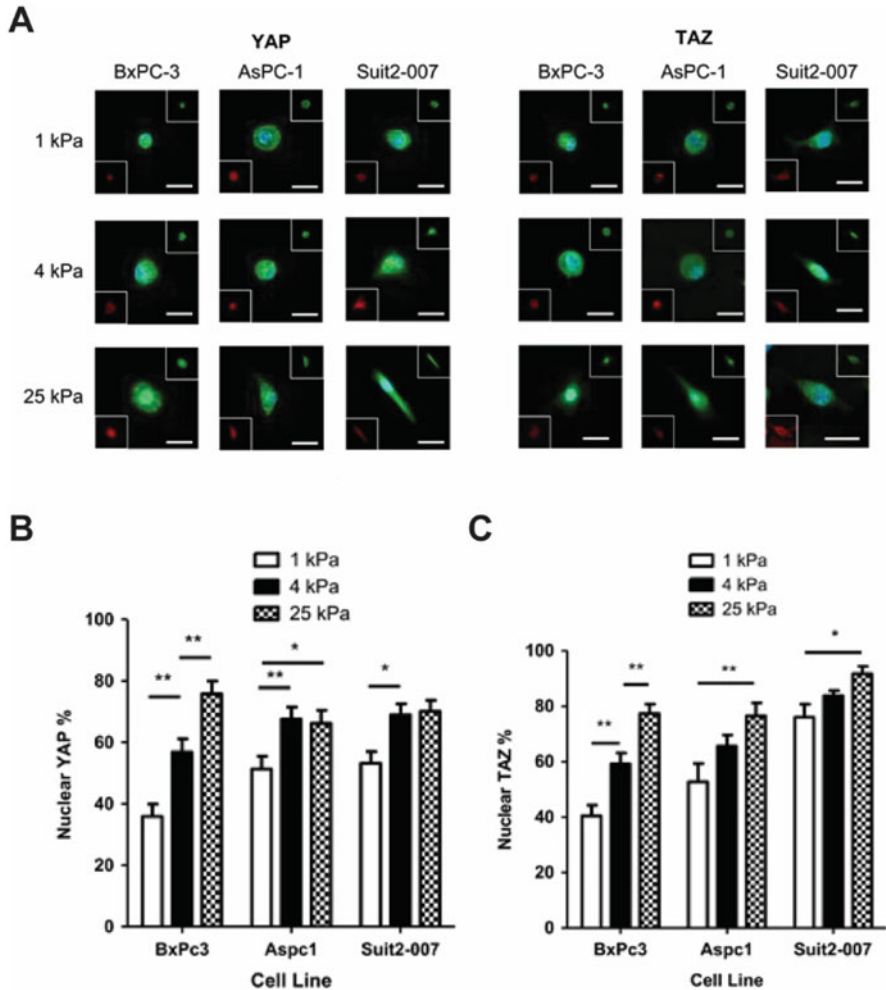


**Fig. 9** Matrix stiffness regulates YAP/TAZ nuclear localization in pancreatic cancer cells. (A) Pancreatic cancer cells, BxPC-3 (mostly epithelial), AsPC-1 (some metastases), and Suit2-007 (highly mesenchymal), were cultured on polyacrylamide hydrogels with varying stiffnesses. Localization of YAP/TAZ (green) and filamentous actin as visualized by staining with phalloidin (red). The cell nuclei are shown in blue. (B) YAP and (C) TAZ nuclear localization increases with increasing stiffness. Data represent mean  $\pm$  s.e.m. \* $p < 0.05$ , \*\* $p < 0.01$ . (Figures adapted with permission from Rice, A.J., Cortes, E., Lachowski, D., Cheung, B.C.H., Karim, S.A., Morton, J.P., & Del R o Hern andez, A. (2017). Matrix stiffness induces epithelial–mesenchymal transition and promotes chemoresistance in pancreatic cancer cells. *Oncogenesis*, 6(7), e352)

for normal mammary gland formation where EMT occurs at branch tips to enable invasion into the ECM and organ development. Geometric constraints in 3D regulate branching morphogenesis; normal mouse mammary epithelial cells (EpH4) embedded in micropatterned collagen tubules show increased vimentin gene

promoter activity in cells positioned at the tips of the microfabricated tubules where branching occurs. Branching position depends on the geometry of the tubule, and branching is promoted in regions of the tubule that experience high mechanical stress. TGF $\beta$  overexpression inhibits branching, and blocking TGF $\beta$  results in uniform branching from tubules suggesting an important role for TGF $\beta$  signaling in patterning branching morphogenesis [229].

Similar to what has been observed in 2D cell culture, mechanical cues regulate cell migration and cell signaling in 3D. MRTF-A localized to the nucleus in normal EpH4 mouse mammary epithelial cells cultured in 3D collagen matrices at the tips of micropatterned tubules, and inhibiting cell contractility reduced cell migration and MRTF-A nuclear localization [230], similar to what has been found during TGF $\beta$ -induced EMT in 2D [206, 231, 232]. Focal adhesion assembly, an event that occurs during TGF $\beta$ -induced EMT, requires a stiff matrix in both 2D and 3D; mammary epithelial cells could phosphorylate FAKpY397 and recruit vinculin to integrin adhesions when cultured on 1–2 GPa 2D tissue culture plastic and 1200 Pa 3D collagen gels, but not on 175 Pa 3D collagen gels [8]. It is not yet fully clear how cell signaling in response to mechanical changes differs, or remains similar, in 2D and 3D cell culture models and further studies are needed to determine the role of substrate dimension in regulation of cell behavior.

TGF $\beta$  signaling and EMT progression differ in 2D and 3D culture and depend on cell type. Some studies suggest that cells may undergo TGF $\beta$ -induced EMT more efficiently in 3D tumor models. For instance, TGF $\beta$  signaling is upregulated in ovarian and endometrial cancer cells when cultured in 3D compared to 2D [233–235]. Epithelial marks, such as E-cadherin, decrease and mesenchymal marks increase in SKOV3 and CAOV3 ovarian cancer and A549 non-small cell lung cancer cells cultured in 3D spheroids compared to cells cultured on 2D tissue culture plastic [233, 236]. Furthermore, when cultured in 3D collagen I scaffolds, OV-NC and OV-206 invasive ovarian cancer cells form spheroids, have decreased E-cadherin levels, and increased levels of mesenchymal markers compared to 2D. However, OV-206 cells have significantly higher levels of mesenchymal markers compared to OV-NC cultured in 3D [235]. In contrast, other studies suggest that E-cadherin reduction and stress fiber formation are more prominent in cells cultured in 2D compared to 3D. Indeed, LK1108 and LK0902 head and neck squamous carcinoma cells have higher levels of E-cadherin and lower levels of vimentin when cultured in anchorage-independent 3D spheroids compared to on 2D tissue culture plates [237]. Following TGF $\beta$  treatment, human adenocarcinoma stomach cells (MKN-1) cultured on 2D tissue culture plastic form robust actin stress fibers, while cells cultured in 3D type I collagen gels have peripheral actin filaments [238]. Thus, substrate dimension exhibits differential effects on TGF $\beta$  signaling and EMT phenotypic changes in cells from different types of tumors. While 3D cell culture models show promise in more closely mimicking the *in vivo* tumor microenvironment, further studies are needed to elucidate how the dimensionality of culture systems regulates TGF $\beta$ -induced EMT.

## 7 Targeting TGF $\beta$ -Associated Mechanoresponsive Pathways for Treatment of Cancer

Due to the critical regulatory roles of TGF $\beta$  in cancer development and metastasis, much effort has been directed toward identifying and designing novel therapies to target TGF $\beta$  signaling. However, because TGF $\beta$  is also important for tissue homeostasis and development, targeting TGF $\beta$  directly is challenging due to potential off-target effects on normal tissue functions. Investigators have developed a number of receptor kinase inhibitors, small molecule inhibitors, monoclonal antibodies, ligand traps, and antisense oligonucleotides to target the TGF $\beta$  pathway, as previously reviewed [239]. Other approaches that may prove fruitful as cancer therapies include targeting CAFs, matrix remodeling, activation of TGF $\beta$ , and TGF $\beta$ -induced mechanoresponsive signaling cascades. Indeed,  $\alpha v \beta 6$  integrin monoclonal antibodies, which block activation of TGF $\beta$  from its latent complex, have been shown to reduce tumor cell invasiveness and prevent xenograft tumor growth in vivo [240, 241]. Anti-fibrotic drugs such as Transilast and Pirfenidone have also been shown to decrease expression of collagen, leading to enhancement in the efficacy of chemotherapeutic drugs such as doxorubicin [242, 243]. Inhibition of LOX, using a LOX-blocking antibody, decreases pancreatic cancer migration, decreases fibrillar collagen levels, and abrogates metastasis in a mouse tumor model [244]. In addition, several inhibitors targeting the Rho/MRTF/SRF pathway have been developed and tested in various cancer models and have shown efficacy in blocking aspects of EMT, reducing the viability of CAFs, and in preventing cancer cell proliferation and invasion [245–248]. As such, methods to target biophysical aspects of the tumor microenvironment and cell response to these mechanical properties may prove to be viable approaches for blocking TGF $\beta$ -mediated cancer progression.

## 8 Summary

TGF $\beta$  is highly expressed in many cancers and it mediates both the development and function of resident cells of the tumor microenvironment, including CAFs and tumor cells. During cancer progression, the biochemical and physical properties of the tumor stroma change dynamically, with increases in collagen levels and alignment that are accompanied by variations in the mechanics of the tumor and surrounding matrix. These changes in mechanical properties can impact TGF $\beta$  activation by CAFs and tumor cells as well as signaling cascades downstream of TGF $\beta$  including Rho/ROCK, ILK, MRTF, and YAP/TAZ to facilitate EMT, metastasis, and chemoresistance. Future experiments using technologies such as single-cell RNA sequencing along with in vivo tumor models and biophysical characterization of cell phenotypes can assist with further defining the properties of CAFs, cancer cells, and other cell types in the tumor microenvironment. Efforts

can also be directed toward the development of biomaterials and cell culture systems that more closely mimic the *in vivo* tumor environment. Further examination of the role of biophysical properties of the tumor and surrounding stroma in the regulation of TGF $\beta$ , CAFs, and tumor cells will provide mechanistic insight into how TGF $\beta$  orchestrates tumor growth, cancer cell invasion, and therapy resistance.

**Acknowledgments** This work was supported by a grant from the National Science Foundation [CMMI-1751785].

## References

1. Whiteside TL (2008) The tumor microenvironment and its role in promoting tumor growth. *Oncogene* 27(45):5904–5912
2. Liu Q, Luo Q, Ju Y, Song G (2020) Role of the mechanical microenvironment in cancer development and progression. *Cancer Biol Med* 17(2):282–292
3. Kumar S, Weaver VM (2009) Mechanics, malignancy, and metastasis: the force journey of a tumor cell. *Cancer Metastasis Rev* 28(1-2):113–127
4. Martinez-Vidal L, Murdica V, Venegoni C, Pederzoli F, Bandini M, Necchi A et al (2021) Causal contributors to tissue stiffness and clinical relevance in urology. *Commun Biol* 4(1):1011
5. Lee JW, Lorenzo EIS, Ahn B, Oh CK, Kim H-J, Han WK et al (2011) Palpation device for the identification of kidney and bladder cancer: a pilot study. *Yonsei Med J* 52(5):768–772
6. Keller CR, Hu Y, Ruud KF, VanDeen AE, Martinez SR, Kahn BT et al (2021) Human breast extracellular matrix microstructures and protein hydrogel 3D cultures of mammary epithelial cells. *Cancer* 13(22):5857
7. Lopez JI, Kang I, You WK, McDonald DM, Weaver VM (2011) In situ force mapping of mammary gland transformation. *Integr Biol (Camb)* 3(9):910–921
8. Paszek MJ, Zahir N, Johnson KR, Lakins JN, Rozenberg GI, Gefen A et al (2005) Tensional homeostasis and the malignant phenotype. *Cancer Cell* 8(3):241–254
9. Johnson B, Campbell S, Campbell-Kyureghyan N (2021) Characterizing the material properties of the kidney and liver in unconfined compression and probing protocols with special reference to varying strain rate. *Biomechanics* 1(2):264–280
10. Masuzaki R, Tateishi R, Yoshida H, Sato T, Ohki T, Goto T et al (2007) Assessing liver tumor stiffness by transient elastography. *Hepato Int* 1(3):394–397
11. Booth AJ, Hadley R, Cornett AM, Dreffs AA, Matthes SA, Tsui JL et al (2012) Acellular normal and fibrotic human lung matrices as a culture system for *in vitro* investigation. *Am J Respir Crit Care Med* 186(9):866–876
12. Ouni E, Peaucelle A, Haas KT, Van Kerk O, Dolmans M-M, Tuuri T et al (2021) A blueprint of the topology and mechanics of the human ovary for next-generation bioengineering and diagnosis. *Nat Commun* 12(1):5603
13. Ansardamavandi A, Tafazzoli-Shadpour M, Omidvar R, Nili F (2020) An AFM-based nanomechanical study of ovarian tissues with pathological conditions. *Int J Nanomedicine* 15:4333–4350
14. Rubiano A, Delitto D, Han S, Gerber M, Galitz C, Trevino J et al (2018) Viscoelastic properties of human pancreatic tumors and *in vitro* constructs to mimic mechanical properties. *Acta Biomater* 67:331–340
15. Nabavizadeh A, Payen T, Iuga AC, Sagalovskiy IR, Desrouilleres D, Saharkhiz N et al (2020) Noninvasive Young's modulus visualization of fibrosis progression and delineation of pancreatic ductal adenocarcinoma (PDAC) tumors using Harmonic Motion Elastography (HME) *in vivo*. *Theranostics* 10(10):4614–4626

16. Cao R, Huang Z, Varghese T, Nabi G (2013) Tissue mimicking materials for the detection of prostate cancer using shear wave elastography: a validation study. *Med Phys* 40(2):022903
17. Barr RG, Memo R, Schaub CR (2012) Shear wave ultrasound elastography of the prostate: initial results. *Ultrasound Quarterly* 28(1):13
18. Zhang M, Nigwekar P, Castaneda B, Hoyt K, Joseph JV, di Sant'Agnese A et al (2008) Quantitative characterization of viscoelastic properties of human prostate correlated with histology. *Ultrasound Med Biol* 34(7):1033–1042
19. Levental I, Georges PC, Janmey PA (2007) Soft biological materials and their impact on cell function. *Soft Matter* 3(3):299–306
20. Lyshchik A, Higashi T, Asato R, Tanaka S, Ito J, Hiraoka M et al (2005) Elastic moduli of thyroid tissues under compression. *Ultrason Imaging* 27(2):101–110
21. O'Connor JW, Riley PN, Nalluri SM, Ashar PK, Gomez EW (2015) Matrix rigidity mediates TGF $\beta$ 1-induced epithelial-myofibroblast transition by controlling cytoskeletal organization and MRTF-A localization. *J Cell Physiol* 230(8):1829–1839
22. Yeung T, Georges PC, Flanagan LA, Marg B, Ortiz M, Funaki M et al (2005) Effects of substrate stiffness on cell morphology, cytoskeletal structure, and adhesion. *Cell Motil* 60(1):24–34
23. Lo C-M, Wang H-B, Dembo M, Wang Y-l (2000) Cell movement is guided by the rigidity of the substrate. *Biophys J* 79(1):144–152
24. Tse JR, Engler AJ (2010) Preparation of hydrogel substrates with tunable mechanical properties. *Curr Protocols Cell Biol* 47(1):10.6.1–10.6.6
25. Caliani SR, Burdick JA (2016) A practical guide to hydrogels for cell culture. *Nat Methods* 13(5):405–414
26. Chen S, Boda SK, Batra SK, Li X, Xie J (2018) Emerging roles of electrospun nanofibers in cancer research. *Adv Healthc Mater* 7(6):e1701024
27. Gomez EW, Nelson CM (2011) Lithographically defined two- and three-dimensional tissue microarrays. *Methods Mol Biol* 671:107–116
28. Gordon KJ, Blobel GC (2008) Role of transforming growth factor-beta superfamily signaling pathways in human disease. *Biochim Biophys Acta* 1782(4):197–228
29. Elliott RL, Blobel GC (2005) Role of transforming growth factor Beta in human cancer. *J Clin Oncol* 23(9):2078–2093
30. Massague J (2008) TGFbeta in cancer. *Cell* 134(2):215–230
31. Denney L, Byrne AJ, Shea TJ, Buckley JS, Pease JE, Herledan GMF et al (2015) Pulmonary epithelial cell-derived cytokine TGF- $\beta$ 1 is a critical cofactor for enhanced innate lymphoid cell function. *Immunity* 43(5):945–958
32. Giacomini MM, Travis MA, Kudo M, Sheppard D (2012) Epithelial cells utilize cortical actin/myosin to activate latent TGF-beta through integrin alpha(v)beta(6)-dependent physical force. *Exp Cell Res* 318(6):716–722
33. Wipff PJ, Rifkin DB, Meister JJ, Hinz B (2007) Myofibroblast contraction activates latent TGF-beta1 from the extracellular matrix. *J Cell Biol* 179(6):1311–1323
34. Friess H, Yamanaka Y, Büchler M, Ebert M, Beger HG, Gold LI et al (1993) Enhanced expression of transforming growth factor  $\beta$  isoforms in pancreatic cancer correlates with decreased survival. *Gastroenterology* 105(6):1846–1856
35. Tsuchida H, Kawata S, Tamura S, Ito N, Shirai Y, Kiso S et al (1996) High levels of transforming growth factor beta 1 in patients with colorectal cancer: association with disease progression. *Gastroenterology* 110(2):375–382
36. Moretti S, Pinzi C, Spallanzani A, Berti E, Chiarugi A, Mazzoli S et al (1999) Immunohistochemical evidence of cytokine networks during progression of human melanocytic lesions. *Int J Cancer* 84(2):160–168
37. Bristow RE, Baldwin RL, Yamada SD, Korc M, Karlan BY (1999) Altered expression of transforming growth factor- $\beta$  ligands and receptors in primary and recurrent ovarian carcinoma. *Cancer* 85(3):658–668

38. Shariat SF, Kattan MW, Traxel E, Andrews B, Zhu K, Wheeler TM et al (2004) Association of pre- and postoperative plasma levels of transforming growth factor  $\beta$ 1 and interleukin 6 and its soluble receptor with prostate cancer progression. *Clin Cancer Res* 10(6):1992–1999
39. Dalal BI, Keown PA, Greenberg AH (1993) Immunocytochemical localization of secreted transforming growth factor-beta 1 to the advancing edges of primary tumors and to lymph node metastases of human mammary carcinoma. *Am J Pathol* 143(2):381–389
40. Desruisseau S, Palmari J, Giusti C, Romain S, Martin PM, Berthois Y (2006) Determination of TGF $\beta$ 1 protein level in human primary breast cancers and its relationship with survival. *Br J Cancer* 94(2):239–246
41. Gorsch SM, Memoli VA, Stukel TA, Gold LI, Arrick BA (1992) Immunohistochemical staining for transforming growth factor-beta-1 associates with disease progression in human breast cancer. *Cancer Res* 52(24):6949–6952
42. Gold LI (1999) The role for transforming growth factor-beta (TGF-beta) in human cancer. *Crit Rev Oncog* 10(4):303–360
43. Ellenrieder V, Hendler SF, Boeck W, Seufferlein T, Menke A, Ruhland C et al (2001) Transforming growth factor  $\beta$ 1 treatment leads to an epithelial-mesenchymal transdifferentiation of pancreatic cancer cells requiring extracellular signal-regulated kinase 2 activation. *Cancer Res* 61(10):4222–4228
44. Kim BN, Ahn DH, Kang N, Yeo CD, Kim YK, Lee KY et al (2020) TGF- $\beta$  induced EMT and stemness characteristics are associated with epigenetic regulation in lung cancer. *Sci Rep* 10(1):10597
45. Morel A-P, Lièvre M, Thomas C, Hinkal G, Ansieau S, Puisieux A (2008) Generation of breast cancer stem cells through epithelial-mesenchymal transition. *PLoS One* 3(8):e2888
46. Tang B, Vu M, Booker T, Santner SJ, Miller FR, Anver MR et al (2003) TGF-beta switches from tumor suppressor to prometastatic factor in a model of breast cancer progression. *J Clin Invest* 112(7):1116–1124
47. Mani SA, Guo W, Liao M-J, Eaton EN, Ayyanan A, Zhou AY et al (2008) The epithelial-mesenchymal transition generates cells with properties of stem cells. *Cell* 133(4):704–715
48. Konge J, Leteurtre F, Goislard M, Biard D, Morel-Altmeier S, Vaurijoux A et al (2018) Breast cancer stem cell-like cells generated during TGF $\beta$ -induced EMT are radioresistant. *Oncotarget* 9(34):23519–23531
49. Kalluri R (2016) The biology and function of fibroblasts in cancer. *Nat Rev Cancer* 16(9):582–598
50. Leight JL, Wozniak MA, Chen S, Lynch ML, Chen CS (2012) Matrix rigidity regulates a switch between TGF-beta 1-induced apoptosis and epithelial-mesenchymal transition. *Mol Biol Cell* 23(5):781–791
51. Patel AK, Singh S (2020) Cancer associated fibroblasts: phenotypic and functional heterogeneity. *FBL* 25(5):961–978
52. Liu T, Han C, Wang S, Fang P, Ma Z, Xu L et al (2019) Cancer-associated fibroblasts: an emerging target of anti-cancer immunotherapy. *J Hematol Oncol* 12(1):86
53. Nurmik M, Ullmann P, Rodriguez F, Haan S, Letellier E (2020) In search of definitions: cancer-associated fibroblasts and their markers. *Int J Cancer* 146(4):895–905
54. Öhlund D, Handly-Santana A, Biffi G, Elyada E, Almeida AS, Ponz-Sarvisé M et al (2017) Distinct populations of inflammatory fibroblasts and myofibroblasts in pancreatic cancer. *J Exp Med* 214(3):579–596
55. Dinh HQ, Pan F, Wang G, Huang Q-F, Olingy CE, Wu Z-Y et al (2021) Integrated single-cell transcriptome analysis reveals heterogeneity of esophageal squamous cell carcinoma microenvironment. *Nat Commun* 12(1):7335
56. Elyada E, Bolisetty M, Laise P, Flynn WF, Courtois ET, Burkhart RA et al (2019) Cross-species single-cell analysis of pancreatic ductal adenocarcinoma reveals antigen-presenting cancer-associated fibroblasts. *Cancer Discov* 9(8):1102–1123
57. Sebastian A, Hum NR, Martin KA, Gilmore SF, Peran I, Byers SW et al (2020) Single-cell transcriptomic analysis of tumor-derived fibroblasts and normal tissue-resident fibroblasts reveals fibroblast heterogeneity in breast cancer. *Cancer* 12(5):1307



58. Puram SV, Tirosh I, Parikh AS, Patel AP, Yizhak K, Gillespie S et al (2017) Single-cell transcriptomic analysis of primary and metastatic tumor ecosystems in head and neck cancer. *Cell* 171(7):1611–24.e24
59. Zeisberg EM, Potenta S, Xie L, Zeisberg M, Kalluri R (2007) Discovery of endothelial to mesenchymal transition as a source for carcinoma-associated fibroblasts. *Cancer Res* 67(21):10123–10128
60. Kurashige M, Kohara M, Ohshima K, Tahara S, Hori Y, Nojima S et al (2018) Origin of cancer-associated fibroblasts and tumor-associated macrophages in humans after sex-mismatched bone marrow transplantation. *Commun Biol* 1:131
61. Bartoschek M, Oskolkov N, Bocci M, Lövrot J, Larsson C, Sommarin M et al (2018) Spatially and functionally distinct subclasses of breast cancer-associated fibroblasts revealed by single cell RNA sequencing. *Nat Commun* 9(1):5150
62. Quante M, Tu SP, Tomita H, Gonda T, Wang SSW, Takashi S et al (2011) Bone marrow-derived myofibroblasts contribute to the mesenchymal stem cell niche and promote tumor growth. *Cancer Cell* 19(2):257–272
63. Raz Y, Cohen N, Shani O, Bell RE, Novitskiy SV, Abramovitz L et al (2018) Bone marrow-derived fibroblasts are a functionally distinct stromal cell population in breast cancer. *J Exp Med* 215(12):3075–3093
64. Mishra PJ, Mishra PJ, Humeniuk R, Medina DJ, Alexe G, Mesirov JP et al (2008) Carcinoma-associated fibroblast-like differentiation of human mesenchymal stem cells. *Cancer Res* 68(11):4331–4339
65. Ishii G, Sangai T, Oda T, Aoyagi Y, Hasebe T, Kanomata N et al (2003) Bone-marrow-derived myofibroblasts contribute to the cancer-induced stromal reaction. *Biochem Biophys Res Commun* 309(1):232–240
66. Kojima Y, Acar A, Eaton EN, Mellody KT, Scheel C, Ben-Porath I et al (2010) Autocrine TGF- $\beta$  and stromal cell-derived factor-1 (SDF-1) signaling drives the evolution of tumor-promoting mammary stromal myofibroblasts. *Proc Natl Acad Sci* 107(46):20009–20014
67. Yoon H, Tang C-M, Banerjee S, Delgado AL, Yebra M, Davis J et al (2021) TGF- $\beta$ 1-mediated transition of resident fibroblasts to cancer-associated fibroblasts promotes cancer metastasis in gastrointestinal stromal tumor. *Oncogenesis* 10(2):13
68. Aoyagi Y, Oda T, Kinoshita T, Nakahashi C, Hasebe T, Ohkohchi N et al (2004) Overexpression of TGF-beta by infiltrated granulocytes correlates with the expression of collagen mRNA in pancreatic cancer. *Br J Cancer* 91(7):1316–1326
69. Lohr M, Schmidt C, Ringel J, Kluth M, Muller P, Nizze H et al (2001) Transforming growth factor-beta1 induces desmoplasia in an experimental model of human pancreatic carcinoma. *Cancer Res* 61(2):550–555
70. Sahai E, Atsaturov I, Cukierman E, DeNardo DG, Egeblad M, Evans RM et al (2020) A framework for advancing our understanding of cancer-associated fibroblasts. *Nat Rev Cancer* 20(3):174–186
71. Yamaguchi H, Sakai R (2015) Direct interaction between carcinoma cells and cancer associated fibroblasts for the regulation of cancer invasion. *Cancer* 7(4):2054–2062
72. Linares J, Marin-Jimenez JA, Badia-Ramentol J, Calon A (2020) Determinants and functions of CAFs secretome during cancer progression and therapy. *Front Cell Dev Biol* 8:621070
73. Stuelten CH, Busch JI, Tang B, Flanders KC, Oshima A, Sutton E et al (2010) Transient tumor-fibroblast interactions increase tumor cell malignancy by a TGF-Beta mediated mechanism in a mouse xenograft model of breast cancer. *PLoS One* 5(3):e9832-e
74. Yu Y, Xiao CH, Tan LD, Wang QS, Li XQ, Feng YM (2014) Cancer-associated fibroblasts induce epithelial-mesenchymal transition of breast cancer cells through paracrine TGF- $\beta$  signalling. *Br J Cancer* 110(3):724–732
75. Labernadie A, Kato T, Brugués A, Serra-Picamal X, Derzsi S, Arwert E et al (2017) A mechanically active heterotypic E-cadherin/N-cadherin adhesion enables fibroblasts to drive cancer cell invasion. *Nat Cell Biol* 19(3):224–237
76. Erdogan B, Ao M, White LM, Means AL, Brewer BM, Yang L et al (2017) Cancer-associated fibroblasts promote directional cancer cell migration by aligning fibronectin. *J Cell Biol* 216(11):3799–3816

77. Gaggioli C, Hooper S, Hidalgo-Carcedo C, Grosse R, Marshall JF, Harrington K et al (2007) Fibroblast-led collective invasion of carcinoma cells with differing roles for RhoGTPases in leading and following cells. *Nat Cell Biol* 9(12):1392–1400
78. Semba S, Kodama Y, Ohnuma K, Mizuuchi E, Masuda R, Yashiro M et al (2009) Direct cancer-stromal interaction increases fibroblast proliferation and enhances invasive properties of scirrhous-type gastric carcinoma cells. *Br J Cancer* 101(8):1365–1373
79. Choe C, Shin Y-S, Kim S-H, Jeon M-J, Choi S-J, Lee J et al (2013) Tumor-stromal interactions with direct cell contacts enhance motility of non-small cell lung cancer cells through the hedgehog signaling pathway. *Anticancer Res* 33(9):3715
80. Ao M, Franco OE, Park D, Raman D, Williams K, Hayward SW (2007) Cross-talk between paracrine-acting cytokine and chemokine pathways promotes malignancy in benign human prostatic epithelium. *Cancer Res* 67(9):4244–4253
81. San Francisco IF, DeWolf WC, Peehl DM, Olumi AF (2004) Expression of transforming growth factor-beta 1 and growth in soft agar differentiate prostate carcinoma-associated fibroblasts from normal prostate fibroblasts. *Int J Cancer* 112(2):213–218
82. Zhuang J, Lu Q, Shen B, Huang X, Shen L, Zheng X et al (2015) TGFβ1 secreted by cancer-associated fibroblasts induces epithelial-mesenchymal transition of bladder cancer cells through lncRNA-ZEB2NAT. *Sci Rep* 5:11924
83. Fuyuhiko Y, Yashiro M, Noda S, Matsuoka J, Hasegawa T, Kato Y et al (2012) Cancer-associated orthotopic myofibroblasts stimulates the motility of gastric carcinoma cells. *Cancer Sci* 103(4):797–805
84. Belhabib I, Zaghdoudi S, Lac C, Bousquet C, Jean C (2021) Extracellular matrices and cancer-associated fibroblasts: targets for cancer diagnosis and therapy? *Cancer* 13(14):3466
85. Takei H, Iino Y, Horiguchi J, Yokoe T (1995) Immunohistochemical fibronectin staining pattern and prognosis in invasive breast carcinoma. *Oncology* 52(2):106–111
86. Li Q, Zhu CC, Ni B, Zhang ZZ, Jiang SH, Hu LP et al (2019) Lysyl oxidase promotes liver metastasis of gastric cancer via facilitating the reciprocal interactions between tumor cells and cancer associated fibroblasts. *EBioMedicine* 49:157–171
87. Pickup MW, Laklai H, Acerbi I, Owens P, Gorska AE, Chytil A et al (2013) Stromally derived lysyl oxidase promotes metastasis of transforming growth factor-beta-deficient mouse mammary carcinomas. *Cancer Res* 73(17):5336–5346
88. Torres S, Garcia-Palmero I, Herrera M, Bartolome RA, Pena C, Fernandez-Acenero MJ et al (2015) LOXL2 is highly expressed in cancer-associated fibroblasts and associates to poor colon cancer survival. *Clin Cancer Res* 21(21):4892–4902
89. Levental I, Levental KR, Klein EA, Assoian R, Miller RT, Wells RG et al (2010) A simple indentation device for measuring micrometer-scale tissue stiffness. *J Phys Condens Matter* 22(19):194120
90. Dumont N, Liu B, Defilippis RA, Chang H, Rabban JT, Karnezis AN et al (2013) Breast fibroblasts modulate early dissemination, tumorigenesis, and metastasis through alteration of extracellular matrix characteristics. *Neoplasia* 15(3):249–262
91. Shen Y, Wang X, Lu J, Salfenmoser M, Wirsik NM, Schleussner N et al (2020) Reduction of liver metastasis stiffness improves response to bevacizumab in metastatic colorectal cancer. *Cancer Cell* 37(6):800–17.e7
92. Liu T, Zhou L, Li D, Andl T, Zhang Y (2019) Cancer-associated fibroblasts build and secure the tumor microenvironment. *Front Cell Dev Biol* 7(60)
93. O'Connor JW, Gomez EW (2014) Biomechanics of TGFβ-induced epithelial-mesenchymal transition: implications for fibrosis and cancer. *Clin Transl Med* 3(1):23
94. Kalluri R, Weinberg RA (2009) The basics of epithelial-mesenchymal transition. *J Clin Invest* 119(6):1420–1428
95. Nalluri SM, O'Connor JW, Gomez EW (2015) Cytoskeletal signaling in TGFβ-induced epithelial-mesenchymal transition. *Cytoskeleton* 72(11):557–569
96. Haynes J, Srivastava J, Madson N, Wittmann T, Barber DL (2011) Dynamic actin remodeling during epithelial-mesenchymal transition depends on increased moesin expression. *Mol Biol Cell* 22(24):4750–4764

97. McGrail DJ, Mezencev R, Kieu QMN, McDonald JF, Dawson MR (2015) SNAIL-induced epithelial-to-mesenchymal transition produces concerted biophysical changes from altered cytoskeletal gene expression. *FASEB J* 29:1280–1289
98. Gladilin E, Ohse S, Boerries M, Busch H, Xu C, Schneider M et al (2019) TGF $\beta$ -induced cytoskeletal remodeling mediates elevation of cell stiffness and invasiveness in NSCLC. *Sci Rep* 9(1):7667
99. Shankar J, Nabi IR (2015) Actin cytoskeleton regulation of epithelial mesenchymal transition in metastatic cancer cells. *PLoS One* 10(3):e0119954-e
100. Coulombe PA, Omary MB (2002) ‘Hard’ and ‘soft’ principles defining the structure, function and regulation of keratin intermediate filaments. *Curr Opin Cell Biol* 14(1):110–122
101. Gonzales M, Weksler B, Tsuruta D, Goldman RD, Yoon KJ, Hopkinson SB et al (2001) Structure and function of a vimentin-associated matrix adhesion in endothelial cells. *Mol Biol Cell* 12(1):85–100
102. Gilles C, Polette M, Zahm JM, Tournier JM, Volders L, Foidart JM et al (1999) Vimentin contributes to human mammary epithelial cell migration. *J Cell Sci* 112(24):4615–4625
103. Govaere O, Komuta M, Berkens J, Spee B, Janssen C, de Luca F et al (2014) Keratin 19: a key role player in the invasion of human hepatocellular carcinomas. *Gut* 63(4):674–685
104. Iyer SV, Dange PP, Alam H, Sawant SS, Ingle AD, Borges AM et al (2013) Understanding the role of Keratins 8 and 18 in neoplastic potential of breast cancer derived cell lines. *PLoS One* 8(1):e53532
105. Hernandez BY, Frierson HF, Moskaluk CA, Li YJ, Clegg L, Cote TR et al (2005) CK20 and CK7 protein expression in colorectal cancer: demonstration of the utility of a population-based tissue microarray. *Hum Pathol* 36(3):275–281
106. Lang SH, Hyde C, Reid IN, Hitchcock IS, Hart CA, Gordon Bryden AA et al (2002) Enhanced expression of vimentin in motile prostate cell lines and in poorly differentiated and metastatic prostate carcinoma. *Prostate* 52(4):253–263
107. Xuan B, Ghosh D, Jiang J, Shao R, Dawson MR (2020) Vimentin filaments drive migratory persistence in polyploidal cancer cells. *Proc Natl Acad Sci* 117(43):26756–26765
108. Hu L, Lau SH, Tzang C-H, Wen J-M, Wang W, Xie D et al (2004) Association of Vimentin overexpression and hepatocellular carcinoma metastasis. *Oncogene* 23(1):298–302
109. Domagala W, Striker G, Szadowska A, Dukowicz A, Harezga B, Osborn M (1994) p53 protein and vimentin in invasive ductal NOS breast carcinoma—relationship with survival and sites of metastases. *Eur J Cancer* 30a(10):1527–1534
110. Gilles C, Polette M, Piette J, Delvigne A-C, Thompson EW, Foidart J-M et al (1996) Vimentin expression in cervical carcinomas: association with invasive and migratory potential. *J Pathol* 180(2):175–180
111. Moch H, Schraml P, Bubendorf L, Mirlacher M, Kononen J, Gasser T et al (1999) High-throughput tissue microarray analysis to evaluate genes uncovered by cDNA microarray screening in renal cell carcinoma. *Am J Pathol* 154(4):981–986
112. Ye X, Weinberg RA (2015) Epithelial-mesenchymal plasticity: a central regulator of cancer progression. *Trends Cell Biol* 25(11):675–686
113. Fischer KR, Durrans A, Lee S, Sheng J, Li F, Wong ST et al (2015) Epithelial-to-mesenchymal transition is not required for lung metastasis but contributes to chemoresistance. *Nature* 527(7579):472–476
114. Zheng X, Carstens JL, Kim J, Scheible M, Kaye J, Sugimoto H et al (2015) Epithelial-to-mesenchymal transition is dispensable for metastasis but induces chemoresistance in pancreatic cancer. *Nature* 527(7579):525–530
115. Jolly MK, Boaretto M, Huang B, Jia D, Lu M, Ben-Jacob E et al (2015) Implications of the hybrid epithelial/mesenchymal phenotype in metastasis. *Front Oncol* 5:155
116. Nieto MA, Huang RY, Jackson RA, Thiery JP (2016) EMT: 2016. *Cell* 166(1):21–45
117. Huang RY, Wong MK, Tan TZ, Kuay KT, Ng AH, Chung VY et al (2013) An EMT spectrum defines an anoikis-resistant and spheroidogenic intermediate mesenchymal state that is sensitive to e-cadherin restoration by a src-kinase inhibitor, saracatinib (AZD0530). *Cell Death Dis* 4:e915

118. Chen X-F, Zhang H-J, Wang H-B, Zhu J, Zhou W-Y, Zhang H et al (2012) Transforming growth factor- $\beta$ 1 induces epithelial-to-mesenchymal transition in human lung cancer cells via PI3K/Akt and MEK/Erk1/2 signaling pathways. *Mol Biol Rep* 39(4):3549–3556
119. Zhang H, Liu L, Wang Y, Zhao G, Xie R, Liu C et al (2013) KLF8 involves in TGF- $\beta$ -induced EMT and promotes invasion and migration in gastric cancer cells. *J Cancer Res Clin Oncol* 139(6):1033–1042
120. Cao L, Shao M, Schilder J, Guise T, Mohammad KS, Matei D (2012) Tissue transglutaminase links TGF- $\beta$ , epithelial to mesenchymal transition and a stem cell phenotype in ovarian cancer. *Oncogene* 31(20):2521–2534
121. Pang MF, Georgoudaki AM, Lambut L, Johansson J, Tabor V, Hagikura K et al (2016) TGF- $\beta$ 1-induced EMT promotes targeted migration of breast cancer cells through the lymphatic system by the activation of CCR7/CCL21-mediated chemotaxis. *Oncogene* 35(6):748–760
122. Phi LTH, Sari IN, Yang Y-G, Lee S-H, Jun N, Kim KS et al (2018) Cancer Stem Cells (CSCs) in drug resistance and their therapeutic implications in cancer treatment. *Stem Cells Int* 2018:5416923
123. Comaills V, Kabeche L, Morris R, Buisson R, Yu M, Madden M et al (2016) Genomic instability is induced by persistent proliferation of cells undergoing epithelial-to-mesenchymal transition. *Cell Rep* 17(10):2632–2647
124. Zack T, Schumacher S, Carter S, Cherniack A, Saksena G, Tabak B et al (2015) Pan-cancer patterns of somatic copy-number alteration. *Nat Genet* 45(10):1134–1140
125. Xuan B, Ghosh D, Cheney EM, Clifton EM, Dawson MR (2018) Dysregulation in actin cytoskeletal organization drives increased stiffness and migratory persistence in polyploid giant cancer cells. *Sci Rep* 8:11935
126. Rabie E, Zhang S, Dunn C, Nelson C (2021) Substratum stiffness signals through integrin-linked kinase and  $\beta$ 1-integrin to regulate midbody proteins and abscission during EMT. *Mol Biol Cell* 32(18):1664–1676
127. Simi A, Anlaş A, Stallings-Mann M, Zhang S, Hsia T, Cichon M et al (2018) A soft microenvironment protects from failure of midbody abscission and multinucleation downstream of the EMT-promoting transcription factor snail. *Cancer Res* 78(9):2277–2289
128. Derynck R, Budi E (2019) Specificity, versatility, and control of TGF $\beta$  family signaling. *Sci Signal* 12(570):aav5183
129. Sheppard D (2005) Integrin-mediated activation of latent transforming growth factor  $\beta$ . *Cancer Metastasis Rev* 24:395–402
130. Taipale J, Miyazono K, Heldin C-H, Keski-Oja J (1994) Latent transforming growth factor beta 1 associates to fibroblast ECM via latent TGF- $\beta$  binding protein. *J Cell Biol* 124:171–181
131. Hazelbag S, Kenter G, Gorter A, Dreef E, Koopman L, Violette SM et al (2007) Overexpression of the  $\alpha$ v $\beta$ 6 integrin in cervical squamous cell carcinoma is a prognostic factor for decreased survival. *J Pathol* 212(3):316–324
132. Koopman Van Aarsen LA, Leone DR, Ho S, Dolinski BM, McCoon PE, LePage DJ et al (2008) Antibody-mediated blockade of integrin  $\alpha$ v $\beta$ 6 inhibits tumor progression in vivo by a transforming growth factor- $\beta$ -regulated mechanism. *Cancer Res* 68(2):561–570
133. Allen MD, Thomas GJ, Clark S, Dawoud MM, Vallath S, Payne SJ et al (2014) Altered microenvironment promotes progression of preinvasive breast cancer: myoepithelial expression of  $\alpha$ v $\beta$ 6 integrin in DCIS identifies high-risk patients and predicts recurrence. *Clin Cancer Res* 20:344–357
134. Bruess JM, Gallo J, DeLisser HM, Klimanskaya IV, Folkesson HG, Pittet JF et al (1995) Expression of the  $\beta$ 6 integrin subunit in development, neoplasia and tissue repair suggests a role in epithelial remodeling. *J Cell Sci* 108(6):2241–2251
135. Elayadi AN, Samli KN, Prudkin L, Liu Y-H, Bian A, Xie X-J et al (2007) A peptide selected by biopanning identifies the integrin  $\alpha$ v $\beta$ 6 as a prognostic biomarker for non-small cell lung cancer. *Cancer Res* 67(12):5889–5895
136. Moore K et al (2014) Therapeutic targeting of  $\alpha$ v $\beta$ 6 in breast cancer. *J Natl Cancer Inst* 106(8):dju169

137. Bates RC, Bellovin DI, Brown C, Maynard E, Wu B, Kawakatsu H et al (2005) Transcriptional activation of integrin  $\beta 6$  during the epithelial-mesenchymal transition defines a novel prognostic indicator of aggressive colon carcinoma. *J Clin Invest* 115(2):339–347
138. Munger JS, Huang X, Kawakatsu H, Griffiths MJ, Dalton SL, Wu J et al (1999) The integrin  $\alpha v$  beta 6 binds and activates latent TGF beta 1: a mechanism for regulating pulmonary inflammation and fibrosis. *Cell* 96(3):319–328
139. Buscemi L, Ramonet D, Klingberg F, Formey A, Smith-Clerc J, Meister JJ et al (2011) The single molecule mechanics of the latent TGF $\beta 1$  complex. *Curr Biol* 21(24):2046–2054
140. Dong X, Zhao B, Iacob R, Zhu J, Koksai AC, Lu C et al (2017) Force interacts with macromolecular structure in activation of TGF- $\beta$ . *Nature* 542(7639):55–59
141. Shi M, Zhu J, Wang R, Chen X, Mi L, Walz T et al (2011) Latent TGF $\beta$  structure and activation. *Nature* 474(7351):343–349
142. Pang M, Teng Y, Huang J, Yuan Y, Lin F, Xiong C (2017) Substrate stiffness promotes latent TGF- $\beta 1$  activation in hepatocellular carcinoma. *Biochem Biophys Res Commun* 483(1):553–558
143. Brown AC, Fiore VF, Sulchek TA, Barker TH (2013) Physical and chemical microenvironmental cues orthogonally control the degree and duration of fibrosis-associated epithelial-to-mesenchymal transitions. *J Pathol* 229(1):25–35
144. Kim KK, Kugler MC, Wolters PJ, Robillard L, Galvez MG, Brumwell AN et al (2006) Alveolar epithelial cell mesenchymal transition develops in vivo during pulmonary fibrosis and is regulated by the extracellular matrix. *Proc Natl Acad Sci* 103(35):13180–13185
145. Kraning-Rush CM, Califano JP, Reinhart-King CA (2012) Cellular traction stresses increase with increasing metastatic potential. *PLoS One* 7(2):e32572-e
146. Derynck R, Akhurst RJ, Balmain A (2001) TGF- $\beta$  signaling in tumor suppression and cancer progression. *Nat Genet* 29(2):117–129
147. Oft M, Heider KH, Beug H (1998) TGFbeta signaling is necessary for carcinoma cell invasiveness and metastasis. *Curr Biol* 8(23):1243–1252
148. Shi YG, Massague J (2003) Mechanisms of TGF-beta signaling from cell membrane to the nucleus. *Cell* 113(6):685–700
149. Xie L, Law BK, Chytil AM, Brown KA, Aakre ME, Moses HL (2004) Activation of the Erk pathway is required for TGF-beta1-induced EMT in vitro. *Neoplasia* 6(5):603–610
150. Bakin AV, Tomlinson AK, Bhowmick NA, Moses HL, Arteaga CL (2000) Phosphatidylinositol 3-kinase function is required for transforming growth factor beta-mediated epithelial to mesenchymal transition and cell migration. *J Biol Chem* 275(47):36803–36810
151. Cicchini C, Laudadio I, Citarella F, Corazzari M, Steindler C, Conigliaro A et al (2008) TGFbeta-induced EMT requires focal adhesion kinase (FAK) signaling. *Exp Cell Res* 314(1):143–152
152. Bhowmick NA, Zent R, Ghiassi M, McDonnell M, Moses HL (2001) Integrin beta 1 signaling is necessary for transforming growth factor-beta activation of p38MAPK and epithelial plasticity. *J Biol Chem* 276(50):46707–46713
153. Kamaraju A, Roberts A (2005) Role of Rho/ROCK and p38 MAPK kinase pathways in transforming growth factor- $\beta$ -mediated Smad-dependent growth inhibition of human breast carcinoma cells in vivo. *J Biol Chem* 280(2):1024–1036
154. Bhowmick NA, Ghiassi M, Bakin A, Aakre M, Lundquist CA, Engel ME et al (2001) Transforming growth factor-beta1 mediates epithelial to mesenchymal transdifferentiation through a RhoA-dependent mechanism. *Mol Biol Cell* 12(1):27–36
155. Serrano I, McDonald P, Dedhar S (2013) Role of integrin-linked kinase (ILK)/Rictor complex in TGF $\beta 1$ -induced epithelial-mesenchymal transition (EMT). *Oncogene* 32:50–60
156. Morita T, Mayanagi T, Sobue K (2007) Dual roles of myocardin-related transcription factors in epithelial mesenchymal transition via slug induction and actin remodeling. *J Cell Biol* 179(5):1027–1042
157. Stemmler MP, Eccles RL, Brabletz S, Brabletz T (2019) Non-redundant functions of EMT transcription factors. *Nat Cell Biol* 21(1):102–112

158. Ondeck MG, Kumar A, Placone JK, Plunkett CM, Matte BF, Wong KC et al (2019) Dynamically stiffened matrix promotes malignant transformation of mammary epithelial cells via collective mechanical signaling. *Proc Natl Acad Sci* 116(9):3502–3507
159. Wei SC, Fattet L, Tsai JH, Guo Y, Pai VH, Majeski HE et al (2015) Matrix stiffness drives epithelial-mesenchymal transition and tumour metastasis through a TWIST1-G3BP2 mechanotransduction pathway. *Nat Cell Biol* 17(5):678–688
160. Chin V, Nagrial A, Chou A, Biankin A, Gill A, Timpson P et al (2015) Rho-associated kinase signalling and the cancer microenvironment: novel biological implications and therapeutic opportunities. *Expert Rev Mol Med* 17:e17
161. Tang Y, Olufemi L, Wang MT, Nie D (2008) Role of Rho GTPases in breast cancer. *Front Biosci* 13:759–776
162. Jung H, Yoon SR, Lim J, Cho HJ, Lee HG (2020) Dysregulation of Rho GTPases in human cancers. *Cancers (Basel)* 12(5):1179–1195
163. Edlund S, Landstrom M, Heldin C, Aspenstrom P (2002) Transforming growth factor-beta-induced mobilization of actin cytoskeleton requires signaling by small GTPases Cdc42 and RhoA. *Mol Biol Cell* 13:902–914
164. Fleming Y, Ferguson G, Spender L, Larsson J, Karlsson S, Ozanne B et al (2009) TGFβ-mediated activation of RhoA signalling is required for efficient v12HaRas and v600eBRAF transformation. *Oncogene* 28:983–993
165. Johnson LA, Rodansky ES, Haak AJ, Larsen SD, Neubig RR, Higgins PDR (2014) Novel Rho/MRTF/SRF inhibitors block matrix-stiffness and TGF-beta-induced fibrogenesis in human colonic myofibroblasts. *Inflamm Bowel Dis* 20(1):154–165
166. Huang X, Yang N, Fiore V, Barker T, Sun Y, Morris S et al (2012) Matrix stiffness-induced myofibroblast differentiation is mediated by intrinsic mechanotransduction. *Am J Respir Cell Mol Biol* 47(3):340–348
167. Markowski MC, Brown AC, Barker TH (2012) Directing epithelial to mesenchymal transition through engineered microenvironments displaying orthogonal adhesive and mechanical cues. *J Biomed Mater Res A* 100(8):2119–2127
168. Hannigan GE, Leung-Hagesteijn C, Fitz-Gibbon L, Coppolino MG, Radeva G, Filmus J et al (1996) Regulation of cell adhesion and anchorage-dependent growth by a new beta1-integrin linked protein kinase. *Nature* 379:91–96
169. Li F, Zhang Y, Wu C (1999) Integrin linked kinase is localized to cell-matrix focal adhesions but not cell-cell adhesion sites and the focal adhesion localization of integrin linked kinase is regulated by the PINCH-binding ANK repeats. *J Cell Sci* 112(24):4589–4599
170. Fukuda T, Chen K, Shi X, Wu C (2003) PINCH1 is an obligate partner of integrin-linked kinase (ILK) functioning in cell shape modulation, motility, and survival. *J Biol Chem* 278(51):51324–51333
171. McDonald P, Fielding A, Dedhar S (2008) Integrin-linked kinase- essential roles in physiology and cancer biology. *J Cell Sci* 121(19):3121–3132
172. Takanami I (2005) Increased expression of integrin-linked kinase is associated with shorter survival in non-small cell lung cancer. *BMC Cancer* 5:1
173. Zhu X, Liu N, Liu W, Song S-W, Guo K-J (2012) Silencing of the integrin-linked kinase gene suppresses the proliferation, migration and invasion of pancreatic cancer cells (Panc-1). *Genet Mol Biol* 35(2):538–544
174. Xing Y, Qi J, Deng S, Wang C, Zhange L, Chen J (2013) Small interfering RNA targeting ILK inhibits metastasis in human tongue cancer cells through repression of epithelial-to-mesenchymal transition. *Exp Cell Res* 319(13):2058–2072
175. White DE, Cardiff RD, Dedhar S, Muller WJ (2001) Mammary epithelial-specific expression of the integrin linked kinase (ILK) results in the induction of mammary gland hyperplasias and tumors in transgenic mice. *Oncogene* 20(48):7064–7072
176. Troussard AA, Costello P, Yoganathan NT, Kumagai S (2000) The integrin linked kinase (ILK) induces an invasive phenotype via AP-1 transcription factor-dependent upregulation of matrix metalloproteinase 9 (MMP-9). *Oncogene* 19(48):5444–5452

177. Matsui Y, Assi K, Ogawa O, Raven PA, Dedhar S, Gleave ME et al (2012) The importance of integrin-linked kinase in the regulation of bladder cancer invasion. *Int J Cancer* 130(3):521–531
178. Kang Y, Li Y, Dai C, Kiss L, Wu C, Liu Y (2010) Inhibition of integrin-linked kinase blocks podocyte epithelial-mesenchymal transition and ameliorates proteinuria. *Kidney Int* 78:363–373
179. Janji B, Melchior C, Gouon V, Vallar L, Kieffer N (1999) Autocrine TGF- $\beta$  regulated expression of adhesion receptors and integrin-linked kinase in HT-144 melanoma cells correlates with their metastatic phenotype. *Int J Cancer* 83:255–262
180. Kavvadas P, Kypreou KP, Protapadakis E, Prodromidi E, Sideras P, Charonis AS (2010) Integrin-linked kinase (ILK) in pulmonary fibrosis. *Virchows Arch* 457(5):563–575
181. Li Y, Tan X, Dai C, Stolz D, Wang D, Liu Y (2009) Inhibition of integrin-linked kinase attenuates renal interstitial fibrosis. *J Am Soc Nephrol* 20(9):1907–1918
182. Blumbach K, Zweers MC, Brunner G, Peters AS, Schmitz M, Schulz JN et al (2010) Defective granulation tissue formation in mice with specific ablation of integrin-linked kinase in fibroblasts- role of TGF $\beta$ 1 levels and RhoA activity. *J Cell Sci* 123(22):3872–3883
183. Nüchel J, Ghatak S, Zuk AV, Illerhaus A, Mörgelin M, Schönborn K et al (2018) TGF $\beta$ 1 is secreted through an unconventional pathway dependent on the autophagic machinery and cytoskeletal regulators. *Autophagy* 14(3):465–486
184. Pang MF, Siedlik MJ, Han S, Stallings-Mann M, Radisky DC, Nelson CM (2016) Tissue stiffness and hypoxia modulate the integrin-linked kinase ILK to control breast cancer stem-like cells. *Cancer Res* 76(18):5277–5287
185. Kilinc AN, Han S, Barrett LA, Anandasivam N, Nelson CM (2021) Integrin-linked kinase tunes cell–cell and cell matrix adhesions to regulate the switch between apoptosis and EMT downstream of TGF $\beta$ 1. *Mol Biol Cell* 32(5):402–412
186. Posern G, Treisman R (2006) Actin' together: serum response factor, its cofactors and the link to signal transduction. *Trends Cell Biol* 16(11):588–596
187. Gau D, Roy P (2018) SRF'ing and SAP'ing – the role of MRTF proteins in cell migration. *J Cell Sci* 131(19):jcs218222
188. Miralles F, Posern G, Zaromytidou AI, Treisman R (2003) Actin dynamics control SRF activity by regulation of its coactivator MAL. *Cell* 113(3):329–342
189. Panayiotou R, Miralles F, Pawlowski R, Diring J, Flynn HR, Skehel M et al (2016) Phosphorylation acts positively and negatively to regulate MRTF-A subcellular localisation and activity. *elife* 5:e15460
190. Hayashi K, Murai T, Oikawa H, Masuda T, Kimura K, Muehlich S et al (2015) A novel inhibitory mechanism of MRTF-A/B on the ICAM-1 gene expression in vascular endothelial cells. *Sci Rep* 5(1):10627
191. Muehlich S, Wang R, Lee S-M, Lewis TC, Dai C, Prywes R (2008) Serum-induced phosphorylation of the serum response factor coactivator MKL1 by the extracellular signal-regulated kinase 1/2 pathway inhibits its nuclear localization. *Mol Cell Biol* 28(20):6302–6313
192. Leitner L, Shaposhnikov D, Mengel A, Descot A, Julien S, Hoffmann R et al (2011) MAL/MRTF-A controls migration of non-invasive cells by upregulation of cytoskeleton-associated proteins. *J Cell Sci* 124(24):4318–4331
193. Scharenberg MA, Chiquet-Ehrismann R, Asparuhova MB (2010) Megakaryoblastic leukemia protein-1 (MKL1): increasing evidence for an involvement in cancer progression and metastasis. *Int J Biochem Cell Biol* 42(12):1911–1914
194. Medjkane S, Perez-Sanchez C, Gaggioli C, Sahai E, Treisman R (2009) Myocardin-related transcription factors and SRF are required for cytoskeletal dynamics and experimental metastasis. *Nat Cell Biol* 11(3):257–268
195. Song Z, Liu Z, Sun J, Sun F-L, Li C-Z, Sun J-Z et al (2016) The MRTF-A/B function as oncogenes in pancreatic cancer. *Oncol Rep* 35(1):127–138
196. Zhang W-L, Lv W, Sun S-Z, Wu X-Z, Zhang J-H (2015) miR-206 inhibits metastasis-relevant traits by degrading MRTF-A in anaplastic thyroid cancer. *Int J Oncol* 47(1):133–142

197. Zhang C, Luo X, Liu L, Guo S, Zhao W, Mu A et al (2013) Myocardin-related transcription factor A is up-regulated by 17 $\beta$ -estradiol and promotes migration of MCF-7 breast cancer cells via transactivation of MYL9 and CYR61. *Acta Biochim Biophys Sin* 45(11):921–927
198. Asparuhova MB, Secondini C, Rüegg C, Chiquet-Ehrismann R (2015) Mechanism of irradiation-induced mammary cancer metastasis: a role for SAP-dependent Mkl1 signaling. *Mol Oncol* 9(8):1510–1527
199. Werner S, Lützkendorf J, Müller T, Müller LP, Posern G (2019) MRTF-A controls myofibroblastic differentiation of human multipotent stromal cells and their tumour-supporting function in xenograft models. *Sci Rep* 9(1):11725
200. Crider BJ, Risinger GM Jr, Haaksma CJ, Howard EW, Tomasek JJ (2011) Myocardin-related transcription factors A and B are key regulators of TGF- $\beta$ 1-induced fibroblast to myofibroblast differentiation. *J Invest Dermatol* 131(12):2378–2385
201. Luchsinger LL, Patenaude CA, Smith BD, Layne MD (2011) Myocardin-related transcription factor-A complexes activate type I collagen expression in lung fibroblasts. *J Biol Chem* 286(51):44116–44125
202. Damodaran K, Venkatchalapathy S, Alisafaei F, Radhakrishnan AV, Sharma Jokhun D, Shenoy VB et al (2018) Compressive force induces reversible chromatin condensation and cell geometry-dependent transcriptional response. *Mol Biol Cell* 29(25):3039–3051
203. Dai J, Qin L, Chen Y, Wang H, Lin G, Li X et al (2019) Matrix stiffness regulates epithelial-mesenchymal transition via cytoskeletal remodeling and MRTF-A translocation in osteosarcoma cells. *J Mech Behav Biomed Mater* 90:226–238
204. Jung A, Schrauder M, Oswald U, Knoll C, Sellberg P, Palmqvist R et al (2001) The invasion front of human colorectal adenocarcinomas shows co-localization of nuclear beta-catenin, cyclin D1, and p16INK4A and is a region of low proliferation. *Am J Pathol* 159(5):1613–1617
205. Brabletz T, Jung A, Reu S, Porzner M, Hlubek F, Kunz-Schughart LA et al (2001) Variable beta-catenin expression in colorectal cancers indicates tumor progression driven by the tumor environment. *Proc Natl Acad Sci U S A* 98(18):10356–10361
206. Gomez EW, Chen QK, Gjorevski N, Nelson CM (2010) Tissue geometry patterns epithelial-mesenchymal transition via intercellular mechanotransduction. *J Cell Biochem* 110(1):44–51
207. Perea Paizal J, Au SH, Bakal C (2021) Squeezing through the microcirculation: survival adaptations of circulating tumour cells to seed metastasis. *Br J Cancer* 124(1):58–65
208. Zhang X, Chan T, Mak M (2021) Morphodynamic signatures of MDA-MB-231 single cells and cell doublets undergoing invasion in confined microenvironments. *Sci Rep* 11(1):6529
209. Lyons SM, Alizadeh E, Mannheimer J, Schuamberg K, Castle J, Schroder B et al (2016) Changes in cell shape are correlated with metastatic potential in murine and human osteosarcomas. *Biology Open* 5(3):289–299
210. O'Connor JW, Gomez EW (2013) Cell adhesion and shape regulate TGF-beta1-induced epithelial-myofibroblast transition via MRTF-A signalling. *PLoS One* 8(12):e83188
211. Harvey KF, Zhang X, Thomas DM (2013) The Hippo pathway and human cancer. *Nat Rev Cancer* 13(4):246–257
212. Zanconato F, Cordenonsi M, Piccolo S (2019) YAP and TAZ: a signalling hub of the tumour microenvironment. *Nat Rev Cancer* 19(8):454–464
213. Hiemer S, Szymaniak A, Varelas X (2014) The transcriptional regulators TAZ and YAP direct transforming growth factor  $\beta$ -induced tumorigenic phenotypes in breast cancer cells. *J Biol Chem* 289(19):13461–13474
214. Varelas X, Samavarchi-Tehrani P, Narimatsu M, Weiss A, Cockburn K, Larsen BG et al (2010) The Crumbs complex couples cell density sensing to Hippo-dependent control of the TGF-beta-SMAD pathway. *Dev Cell* 19(6):831–844
215. Li Z, Wang Y, Zhu Y, Yuan C, Wang D, Zhang W et al (2015) The Hippo transducer TAZ promotes epithelial to mesenchymal transition and cancer stem cell maintenance in oral cancer. *Mol Oncol* 9:1091–1105
216. Speight P, Kofler M, Szaszi K, Kapus A (2016) Context-dependent switch in chemo/mechanotransduction via multilevel crosstalk among cytoskeleton-regulated MRTF-A and TAZ and TGF $\beta$ -regulated Smad3. *Nat Commun* 7:11642



217. Speight P, Nakano H, Kelley TJ, Hinz B, Kapus A (2013) Differential topical susceptibility to TGF $\beta$  in intact and injured regions of the epithelium: key role in myofibroblast transition. *Mol Biol Cell* 24(21):3326–3336
218. Miranda M, Bialik J, Speight P, Dan Q, Yeung T, Szaszi K et al (2017) TGF- $\beta$ 1 regulates the expression and transcriptional activity of TAZ protein via a Smad3-independent, myocardin-related transcription factor-mediated mechanism. *J Biol Chem* 292(36):14902–14920
219. Dupont S, Morsut L, Aragona M, Enzo E, Giulitti S, Cordenonsi M et al (2011) Role of YAP/TAZ in mechanotransduction. *Nature* 474(7350):179–183
220. Qin X, Lv X, Li P, Yang R, Xia Q, Chen Y et al (2020) Matrix stiffness modulates ILK-mediated YAP activation to control the drug resistance of breast cancer cells. *Biochim Biophys Acta (BBA) Mol Basis Dis* 1866(10):165625
221. Overholtzer M, Zhang J, Smolen Gromoslaw A, Muir B, Li W, Sgroi Dennis C et al (2006) Transforming properties of YAP, a candidate oncogene on the chromosome 11q22 amplicon. *Proc Natl Acad Sci* 103(33):12405–12410
222. Rice AJ, Cortes E, Lachowski D, Cheung BCH, Karim SA, Morton JP et al (2017) Matrix stiffness induces epithelial-mesenchymal transition and promotes chemoresistance in pancreatic cancer cells. *Oncogenesis* 6(7):e352
223. Szeto S, Narimatsu M, Lu M, He X, Sidiqi A, Tolosa M et al (2016) YAP/TAZ are mechanoregulators of TGF $\beta$ -Smad signaling and renal fibrogenesis. *J Am Soc Nephrol* 27(10):3117–3128
224. Liu F, Lagares D, Choi K, Stopfer L, Marinkovic A, Vrbancac V et al (2015) Mechanosensing through YAP and TAZ drives fibroblast activation and fibrosis. *Am J Physiol Lung Cell Mol Physiol* 308:344–357
225. Bhowmick N, Zent R, Ghiassi M, McDonnell M, Moses H (2001) Integrin beta 1 signaling is necessary for transforming growth factor beta activation of p38MAPK and epithelial plasticity. *J Biol Chem* 276(14):46707–46713
226. Kenny P, Lee G, Myers C, Neve R, Semeiks J, Spellman P et al (2007) The morphologies of breast cancer cell lines in three-dimensional assays correlate with their profiles of gene expression. *Mol Oncol* 1(1):84–96
227. Atat O, Farzaneh Z, Pourhamzeh M, Taki F, Abi-Habib R, Vosough M et al (2022) 3D modeling in cancer studies. *Hum Cell* 35:23–36
228. Hickman J, Graeser R, de Hoogt R, Vidic S, Brito C, Gutekunst M et al (2014) Three-dimensional models of cancer for pharmacology and cancer cell biology: capturing tumor complexity *in vitro/ex vivo*. *Biotechnol J* 9(9):1115–1128
229. Nelson C, VanDuijn M, Inman J, Fletcher D, Bissell M (2006) Tissue geometry determines sites of mammary branching morphogenesis in organotypic cultures. *Science* 314(5797):298–300
230. Gjorevski N, Piotrowski AS, Varner VD, Nelson CM (2015) Dynamic tensile forces drive collective cell migration through three-dimensional extracellular matrices. *Sci Rep* 5:11458
231. O'Connor J, Gomez E (2013) Cell adhesion and shape regulate TGF- $\beta$ 1-induced epithelial-myofibroblast transition via MRTF-A signaling. *PLoS One* 8(12):e83188
232. Zhao X, Laschinger C, Arora P, Szaszi K, Kapus A, McCulloch C (2007) Force activates smooth muscle  $\alpha$ -actin promoter activity through the Rho signaling pathway. *J Cell Sci* 120(10):1801–1809
233. Ameri W, Ahmed I, Al-Dasim F, Mohamound Y, Al-Azwani I, Malek J et al (2019) Cell-type specific TGF- $\beta$  mediated EMT in 3d and 2d models and its reversal by TGF- $\beta$  receptor kinase inhibitor in ovarian cancer cell lines. *Int J Mol Sci* 20:3568
234. Sahoo S, Quah M, Nielsen S, Atkins J, Au G, Cairns M et al (2017) Inhibition of extracellular matrix mediated TGF- $\beta$  signaling suppresses endometrial cancer metastasis. *Oncotarget* 8(42):71400–71417
235. Liu M, Zhang X, Long C, Xu H, Cheng X, Chang J et al (2018) Collagen-based three-dimensional culture microenvironment promotes epithelial to mesenchymal transition and drug resistance of human ovarian cancer *in vitro*. *The Royal Society of Chemistry* 8:8910–8919

236. Kumar M, Allison D, Baranova N, Wamsley J, Katz A, Bekiranov S et al (2013) NF- $\kappa$ B regulates mesenchymal transition for the induction of non-small cell lung cancer initiating cells. *PLoS One* 8(7):e68597
237. Melissaridou S, Wiechec E, Magan M, Jain M, Chung M, Farnebo L et al (2019) The effect of 2D and 3D cell cultures on treatment response, EMT profile and stem cell features in head and neck cancer. *Cancer Cell Int* 19:16
238. Oyanagi J, Ogawa T, Sato H, Higashi S, Miyazaki K (2012) Epithelial-mesenchymal transition stimulates human cancer cells to extend microtubule-based invasive protrusions and suppresses cell growth in collagen gel. *PLoS One* 7(12):e53209
239. Kim B-G, Malek E, Choi SH, Ignatz-Hoover JJ, Driscoll JJ (2021) Novel therapies emerging in oncology to target the TGF- $\beta$  pathway. *J Hematol Oncol* 14(1):55
240. Van Aarsen LA, Leone DR, Ho S, Dolinski BM, McCoon PE, LePage DJ et al (2008) Antibody-mediated blockade of integrin  $\alpha$  v  $\beta$  6 inhibits tumor progression in vivo by a transforming growth factor- $\beta$ -regulated mechanism. *Cancer Res* 68(2):561–570
241. Xue H, Atakilit A, Zhu W, Li X, Ramos DM, Pytela R (2001) Role of the  $\alpha$ v $\beta$ 6 integrin in human oral squamous cell carcinoma growth in vivo and in vitro. *Biochem Biophys Res Commun* 288(3):610–618
242. Papageorgis P, Polydorou C, Mpekris F, Voutouri C, Agathokleous E, Kapnissi-Christodoulou CP et al (2017) Tranilast-induced stress alleviation in solid tumors improves the efficacy of chemo- and nanotherapeutics in a size-independent manner. *Sci Rep* 7(1):46140
243. Polydorou C, Mpekris F, Papageorgis P, Voutouri C, Stylianopoulos T (2017) Pirfenidone normalizes the tumor microenvironment to improve chemotherapy. *Oncotarget* 8(15):24506–24517
244. Miller BW, Morton JP, Pinese M, Saturno G, Jamieson NB, McGhee E et al (2015) Targeting the LOX/hypoxia axis reverses many of the features that make pancreatic cancer deadly: inhibition of LOX abrogates metastasis and enhances drug efficacy. *EMBO Mol Med* 7(8):1063–1076
245. Evelyn CR, Wade SM, Wang Q, Wu M, Iniguez-Lluhi JA, Merajver SD et al (2007) CCG-1423: a small-molecule inhibitor of RhoA transcriptional signaling. *Mol Cancer Ther* 6(8):2249–2260
246. Watanabe B, Minami S, Ishida H, Yoshioka R, Nakagawa Y, Morita T et al (2015) Stereospecific inhibitory effects of CCG-1423 on the cellular events mediated by myocardin-related transcription factor A. *PLoS One* 10(8):e0136242
247. Haak AJ, Appleton KM, Lisabeth EM, Misek SA, Ji Y, Wade SM et al (2017) Pharmacological inhibition of myocardin-related transcription factor pathway blocks lung metastases of RhoC-overexpressing melanoma. *Mol Cancer Ther* 16(1):193
248. Leal AS, Misek SA, Lisabeth EM, Neubig RR, Liby KT (2019) The Rho/MRTF pathway inhibitor CCG-222740 reduces stellate cell activation and modulates immune cell populations in KrasG12D; Pdx1-Cre (KC) mice. *Sci Rep* 9(1):7072

# Bioengineering and Bioinformatic Approaches to Study Extracellular Matrix Remodeling and Cancer–Macrophage Crosstalk in the Breast Tumor Microenvironment



Youngbin Cho, Ruxuan Li, and Ioannis K. Zervantonakis

**Abstract** Tumor-associated macrophages (TAMs) are one of the most abundant cell types in the breast tumor microenvironment. TAMs are characterized by significant subpopulation heterogeneity, where subsets can exhibit either pro-tumor or anti-tumor functions. In the clinic, high TAM infiltration correlates with aggressive breast cancer; this is supported by multiple preclinical studies that demonstrate the effects of TAMs on tumor progression, metastasis, drug resistance, and tumor recurrence. Hence, there is a strong interest to therapeutically target the pro-tumor function of TAMs. The extracellular matrix (ECM) is an integral component of the tumor microenvironment; it modulates cell motility, proliferation, and survival, while also impacting transport of paracrine signaling molecules or therapeutic agents due to the physical tissue microarchitecture. Here, we describe how ECM remodeling in the breast tumor microenvironment regulates macrophage recruitment and polarization via a complex cancer cell–TAM crosstalk during tumor progression. We also introduce bioengineering approaches to precisely control cell–matrix interactions in 3D environments and study cancer–macrophage dynamics. Finally, we discuss gene-expression-based bioinformatic analyses that can enable the discovery of new regulators of cancer cell–ECM–TAM crosstalk, prognostic biomarkers, and therapeutic strategies.

**Keywords** Monocytes · Macrophages · Breast cancer · ECM · Matrix remodeling · Recruitment · Cancer–macrophage dynamics · Gene signatures

---

Y. Cho · R. Li

Department of Bioengineering, University of Pittsburgh, Pittsburgh, PA, USA

I. K. Zervantonakis (✉)

Department of Bioengineering, University of Pittsburgh, Pittsburgh, PA, USA

UPMC Hillman Cancer Center, Pittsburgh, PA, USA

e-mail: [ioz1@pitt.edu](mailto:ioz1@pitt.edu)

## 1 Introduction

Macrophages that have been recruited to the tumor microenvironment convert into tumor-associated macrophages (TAMs) and can be classified into subpopulations along a spectrum with differential effects on tumor progression [1]. On one end of the spectrum are the pro-tumorigenic “alternatively activated” TAMs (M2 like) that establish an immunosuppressive microenvironment [2], and on the other end are the anti-tumorigenic “classically activated” (M1 like) TAMs [1]. A majority of TAMs in breast tumors acquire an M2-like phenotype driven by tumor-secreted factors [3]. In the clinic, a high ratio of M2-like TAMs to M1-like TAMs has been associated with poor breast cancer patient outcomes [4]. Furthermore, TAM-rich microenvironments have been linked with increased invasion of cancer cells through ECM remodeling [5], new blood vessel formation through secretion of pro-angiogenic factors [6], impaired endothelial barrier function that supports cancer cell intravasation [7], and suppressed cytotoxic T cell function [8].

The tumor-promoting role of TAMs has motivated the development of various therapeutic approaches targeting TAM function that can be classified into the following categories: (1) blockade of TAM recruitment by targeting paracrine signals (e.g., CCL2) driving chemotaxis [9], (2) depletion of TAMs by inhibiting key survival regulators (e.g., CSF1R) [10], (3) repolarization of M2-like TAMs toward an anti-tumorigenic M1-like phenotype using pharmacological approaches (e.g., BRD4 inhibitors) [11], (4) activation of costimulatory receptor CD40 to promote macrophage-T cell immunostimulatory crosstalk [12], and (5) regulation of the CD47 phagocytic checkpoint to increase TAM tumoricidal activity [13]. A better understanding of how TAMs evolve during tumor progression and the interactions between TAM subpopulations is necessary to improve the efficacy of macrophage-targeted therapeutic approaches [14]. The heterogeneity and plasticity of TAM subpopulations that are impacted by the complexity of the biochemical and biophysical factors in the tumor microenvironment remain major challenges. Specifically, the extracellular matrix (ECM) is a key dynamic component of the tumor microenvironment that is remodeled during breast cancer progression. This remodeling includes synthesis of ECM proteins, cellular-force-mediated alignment, and expression of proteolytic enzymes that alter ECM stiffness and microstructure, while also impacting cytokine transport (diffusion and binding) [15]. The local remodeling of the ECM 3D networks regulates macrophage function including migration [16], polarization [17], proliferation [18], and phagocytic activity [19]. Despite progress in characterizing macrophage gene expression programs and changes during tumor progression, the mechanisms regulating the interactions between macrophage recruitment, conversion toward a pro-tumor TAM phenotype, and ECM matrix microarchitecture in physiologically relevant 3D breast tumor microenvironments are poorly defined.

In this chapter, we review the role of matrix remodeling in regulating TAM infiltration in breast cancer with a focus on bioengineered model systems, in vivo findings, and bioinformatic approaches. First, we present mechanisms of 3D

macrophage migration and introduce recent experimental studies on how matrix remodeling regulates cancer cell–macrophage dynamics. We also discuss *in vitro* approaches, which modulate individual structural components and enable novel measurements of biophysical cell–matrix interactions, to precisely engineer the ECM architecture and dissect the complexity of the *in vivo* matrix. Finally, we introduce bioinformatic approaches to discover ECM- and TAM-gene signatures expressed in breast tumors. In summary, these quantitative bioengineering approaches provide unique opportunities to improve our understanding of breast cancer–TAM crosstalk in a dynamically changing microenvironment, develop biomarkers of tumor progression and therapy response, and prioritize new therapeutic target development.

## 2 Macrophage Recruitment in Breast Tumors

Increased macrophage density in tumors can be driven via differentiation of monocytes trafficking from the bone marrow and/or proliferation of tissue-resident macrophages [20]. Several animal studies have shown that the major source of TAMs in solid tumors is bone marrow–derived monocytes [21, 22]. During tumor progression, circulating monocytes extravasate from blood vessels and differentiate to TAMs in the breast tumor microenvironment (Fig. 1). A number of chemokine signaling pathways have been shown to play a critical role in monocyte trafficking, including the CCL2-CCR2 [23], CCL20-CCR6 [24], CCL5-CCR5 ligand–receptor pairs [25] (The regulation and crosstalk between chemokine signaling pathways are described in detail elsewhere [9]). Elevated levels of chemokines in the tumor microenvironment promote monocyte adhesion to the endothelial barrier, integrin activation (e.g.,  $\alpha 4\beta 1$ ) to invade across the endothelial barrier [26], and subsequent migration in the 3D tissue [27]. For example, tumor-derived overexpression of the macrophage colony stimulating factor 1 (CSF1) activates CSF1R signaling to enhance monocyte infiltration, followed by subsequent macrophage differentiation and proliferation [28]. In turn, these monocyte-derived macrophages are reprogrammed toward pro-tumorigenic M2-like TAMs that are characterized by markers, including arginase-1 and secretion of IL-10 and TGF- $\beta$  (described in detail elsewhere [29]).

Compared to normal breast tissue, tumor ECM exhibits a higher density, stiffness, and fiber linearization [30]. For example, breast tumor tissue stiffness has been reported to be up to ~20 kPa depending on the tumor stage, compared to healthy breast tissue stiffness, which is ~1.83 kPa [31]. Matrix stiffness regulates cell–ECM adhesion via cell surface receptors (e.g., integrins) that activate signaling cascades (e.g., PI3K) to regulate cell survival and proliferation [32]. Furthermore, the mechanical properties of the 3D ECM can modify macrophage polarization; macrophages cultured on high stiffness substrates exhibit pro-inflammatory phenotypes compared to anti-inflammatory phenotypes on softer substrates [17]. In addition to directly stimulating intracellular signaling, ECM functions as a physical

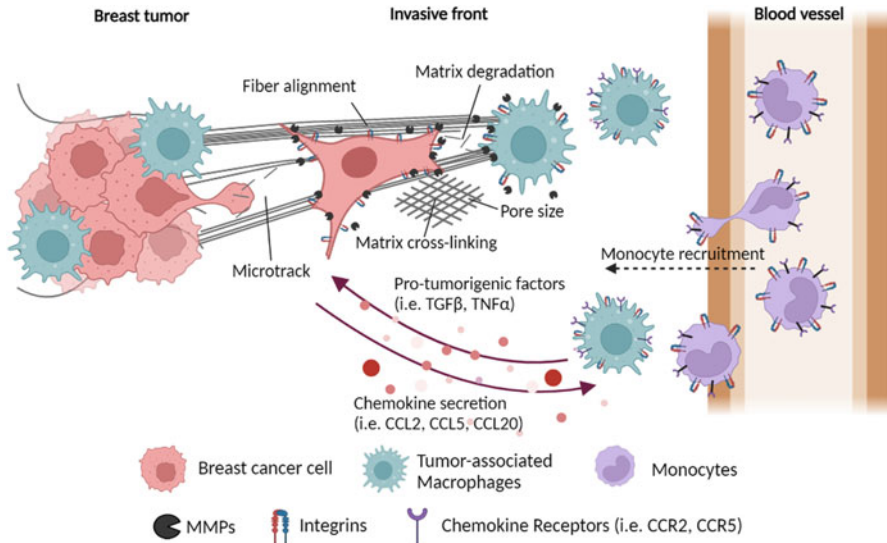


**Fig. 1** Macrophage recruitment factors in the 3D breast tumor microenvironment. Following adhesion on the blood vessel wall, monocytes are recruited in the subendothelial space via chemokines such as CCL2, CCL5, and CCL20 and subsequently differentiate into macrophages. The mechanical properties of the tumor matrix (such as ECM deposition, alignment, crosslinking, stiffness, pore size) can regulate macrophage migration, proliferation, and polarization. (Created with [BioRender.com](https://www.biorender.com))

barrier for cell migration and transport of soluble factors, including chemokines, growth factors, proteolytic enzymes, and therapeutic agents [33, 34]. Specifically, multiple features of the tumor ECM, including fiber binding properties, enzyme-mediated degradation (e.g., matrix metalloproteinases [MMPs]) crosslinking, and microstructure (e.g., alignment and pore size) need to be considered when examining the direct matrix effects on both cancer cells and TAMs and the distribution of chemokines and soluble factors that regulate cell–cell crosstalk. We illustrate this complex interplay between macrophages and cancer cells including soluble and biophysical factors that are impacted by dynamic ECM remodeling during the different steps of monocyte recruitment in Fig. 1.

### 3 Mechanisms of Macrophage Migration in 3D Environments

Macrophage migration efficiency through the 3D ECM is determined by the balance of cell–matrix adhesion, cell deformability, and remodeling of the ECM via cell-mediated contractile forces or proteolytic matrix degradation [35]. Several studies have reported the heterogeneous migration modes in 3D matrices [36].

Amoeboid migration largely depends on actomyosin contractility regulated by the Rho/ROCK pathway with low cell–matrix adhesion and matrix degradation. In this mode, macrophages do not form new migratory microtracks (Fig. 1) but instead actively navigate the 3D ECM via cellular shape changes (e.g., blebs) and utilize matrix passages with the least resistance [37]. The other type of migration mode involves cellular protrusions with strong cell–matrix adhesion and proteolytic matrix degradation. During this mode, macrophages often utilize “podosomes,” which are actin-rich structures formed at the end of long finger-like protrusions (often termed as “invadopodia”) and include complexes with vinculin and paxillin [38]. Furthermore, matrix proteolytic enzymes such as matrix metalloproteinases are enriched at podosomes and mediate localized matrix degradation [39] to form new migratory microtracks in the 3D matrix (Fig. 1). Since cells need to degrade the matrix to create these microtracks, this mode of migration exhibits slower migration speeds compared to amoeboid migration [35]. Importantly, migration modes can be plastic, where macrophages actively switch modes to achieve the most efficient migration depending on the matrix composition and architecture [16]. Interestingly, the migration mode can vary spatially inside a tumor, with TAMs exhibiting an amoeboid migration mode in the tissue periphery (connective tissue), while an MMP-mediated migration mode is engaged in the tumor core [36]. Moreover, a hybrid mode has been described that is characterized by high cell deformability, cellular contractile forces, and cell–matrix adhesion to create an aligned microtrack in the matrix without proteolytic matrix degradation [35]. Taken together, these studies highlight that local matrix architecture determines the mode of macrophage migration, with a high degree of plasticity that enables efficient navigation in the breast tumor microenvironment.

## 4 Matrix Remodeling and Cancer Cell–Macrophage Dynamics

### 4.1 Tumor ECM Composition

Compared to normal breast tissue, breast tumors exhibit alterations in ECM components, such as fibrillar collagens, fibronectin, hyaluronic acid (HA), proteoglycans, and matricellular proteins such as tenascin-C [34, 40, 41]. Critically, a high expression of these components has been associated with tumor stage and poor prognosis in breast cancer [30, 40, 42]. Furthermore, breast tumors with high levels of HA [43], tumor-derived tenascin-C [44], and collagen type I also exhibit high levels of TAMs (Table 1) [45]. For example, in the transgenic PyMT breast mouse model carrying a mutation in collagenase, an increased collagen type I density was associated with high cyclooxygenase-2 (COX-2) expression, elevated chemokine/cytokine levels (CCL2, CCL3, TNF- $\alpha$ , and IL10), and increased macrophage numbers [45]. COX-2 inhibition using celecoxib in these spontaneous

**Table 1** Matrix remodeling factors associated with macrophage recruitment and cancer cell–macrophage interactions in breast tumors

Matrix features	Key factors	Mechanism of cancer–TAM crosstalk, phenotypic outcomes, and clinical relevance	Ref.
Matrix composition	Hyaluronan	High numbers of TAMs correlate with high HA levels, HA synthases, CD44 positivity, and poor outcomes	[43]
	Tenascin-C	Tumor-derived tenascin-C polarizes TAMs toward an immunosuppressive protumor M2-like phenotype	[44]
	Collagen type I	Macrophage and neutrophil recruitment are higher in collagen type I-rich tumors	[45]
Cell–matrix adhesion	Kindlin-2, TGF $\beta$ , CSF1	Kindlin-2 deficiency in breast cancer cells reduces macrophage infiltration and CSF-1 secretion	[46]
	DAB2, integrins	DAB2 is overexpressed in tumor-infiltrating TAMs. DAB2-expressing TAMs participate in integrin recycling, ECM remodeling, and directional migration. DAB2 + macrophages promote the dissemination of cancer cells	[47]
	SPARC, integrin $\alpha_v\beta_5$	Macrophage-derived SPARC enhances cancer cell migration in a $\alpha_v\beta_5$ integrin-dependent mechanism	[48]



	CCL18, integrin $\beta_1$	TAM-secreted CCL18 promotes cancer cell invasiveness by triggering integrin clustering and enhancing adhesion to extracellular matrix	[49]
	E2f3	Ablation of E2f3 in TAMs, but not in tumor epithelial cells, attenuates lung metastasis without affecting primary tumor growth. E2f3 controls a gene expression program associated with cytoskeleton, cell migration, and adhesion to ECM	[50]
Matrix crosslinking and alignment	Collagen type I crosslinking	Cancer cell and stromal cell-secreted LOX mediates collagen crosslinking to promote the recruitment of TAMs and cancer metastasis	[51–53]
	Collagen linearization	The high number of infiltrating macrophages associates with an aligned collagen matrix.	[30, 54]
Matrix proteolytic remodeling and microtrack formation	Cleaved fibrillar collagen I, IL-4, IL-13	Cleaved fibrillar collagen type I plays a key role as a chemoattractant in macrophage recruitment	[55]
	MMP-2,-9,-10	A high expression of MMPs in both infiltrating myeloid cells and breast cancer cells contributes to 3D matrix remodeling and microtrack formation that enhances macrophage motility and cancer cell invasion	[56–59]

tumors blocked macrophage recruitment [45]. The critical role of COX-2 in macrophage function has also been shown in the 4T1 syngeneic model, where COX-2 inhibition impaired CSF1-induced M2 macrophage differentiation and promoted the anti-tumor TAM function with reduced lung metastatic burden in vivo [60].

## **4.2 Cell–Matrix Adhesion**

Cell–matrix adhesion involves multiple cell surface receptors, such as integrins, which activate downstream signaling nodes regulating cellular contractility, matrix proteolysis, migration, and proliferation [61]. Loss of integrin-regulatory protein kindlin-2, which regulates integrin-dependent cell adhesion, was shown to inhibit tumor growth and macrophage infiltration in vivo via a lower expression of cancer cell–derived CSF1 that was dependent on a kindlin-2/TGF- $\beta$ /CSF1 signaling axis (Table 1) [46]. In addition, cancer cell–secreted CSF1 has also been shown to activate the E2F3 transcription factor in TAMs that enhanced cancer progression [50]. Specifically, loss of E2F3 in TAMs led to impaired adhesion to extracellular matrix, cellular contractility, and migration [50]. In a recent elegant in vivo study employing syngeneic mouse models, activation of the YAP–TAZ mechanosensing complex was shown to regulate disabled homolog 2 mitogen-responsive phosphoprotein (DAB2) expression in macrophages [47]. Mechanistic studies highlighted the critical role of DAB2 in integrin recycling and 3D ECM remodeling that, in turn, enhanced cancer cell invasion. Furthermore, an increased number of DAB2+ macrophages were detected in breast cancer patients with a luminal B molecular subtype, and a high DAB2 expression was associated with decreased survival in invasive lobular carcinoma [47].

TAM-mediated matrix remodeling can also indirectly regulate matrix adhesion of cancer cells to induce a pro-metastatic phenotype. For example, TAM-derived secreted protein acidic and rich in cysteine (SPARC) enhanced cancer cell adhesion, migration, and metastasis via an integrin  $\beta$ 5–dependent mechanism [48]. Finally, in addition to the matrix remodeling factors, TAM-derived chemokines, such as CCL18, can also promote breast cancer invasion via integrin clustering and binding to the phosphatidylinositol transfer protein 3 (PITPNM3) receptor [49]. These studies suggest that cancer cells and macrophages employ direct or indirect mechanisms involving cell–matrix adhesion in the tumor microenvironment to regulate cell motility.

## **4.3 Matrix Crosslinking and Fiber Alignment**

Increased matrix crosslinking and fiber alignment at the tumor invasive front have been associated with breast tumor progression [30]. The lysyl oxidase (LOX) family of proteins are frequently elevated in tumors [62] and regulate matrix

crosslinking. LOX proteins modify the side chain of lysine residues in collagen and elastin precursors, leading to a highly reactive aldehyde-derived crosslinking and fibrillogenesis via stabilization of ECM proteins [63]. Furthermore, LOX-mediated collagen crosslinking increases matrix stiffness [64] and activates integrin signaling to promote cancer cell adhesion, motility, and invasion [65]. Inhibition of LOX reduces collagen crosslinking with both direct effects on enhancing transport of diffusible factors (e.g., chemokines or drugs) and downregulating integrin-mediated signaling in cancer cells to prevent cancer cell survival [66]. Interestingly, LOX secreted from cancer cells promotes the adhesion of CD11b + bone marrow-derived monocytes to the matrix and enhances their recruitment to premetastatic sites (Table 1) [52, 56]. TAMs can also stimulate LOX-mediated matrix crosslinking to stiffen the matrix resulting in a sustained cancer-TAM feedback loop that enhances metastasis via the CSF1-TGF- $\beta$ 1-LOX signaling axis [53]. Thus, both cancer- and TAM-mediated effects on matrix crosslinking need to be considered to understand the establishment of pro-metastatic breast tumor microenvironments.

In addition to crosslinking, collagen alignment in fibrils has also been associated with increased TAM recruitment. Fibrillar collagen levels have also been reported to increase during mammary gland involution, where changes in macrophage number have been documented [55]. Hence, matrix alignment plays a critical role both during tissue regeneration and malignant progression. During tumor progression, the linearization of collagen is maximum at the tumor invasive front resulting in the increased mechanical stiffness with a heterogeneous pattern of mechanotransduction pathway activation associated with focal adhesions, YAP, and growth factor receptors [30]. This spatial reorganization of matrix alignment promotes the accumulation of infiltrating macrophages at the invasive front where the mechanical stiffness was the highest [30, 54]. Matrix crosslinking and alignment have been linked with chemokine secretion, whereby CCL2 overexpression in the mammary epithelium overlaps with high collagen density, expression of LOX, and tissue inhibitor of matrix metalloproteinases 3 (TIMP3) [51]. Elevated matrix stiffness has also been shown to increase CSF1 expression in breast cancer cells and recruit more macrophages [67]. Overall, these studies suggest that the spatial matrix remodeling in the tumor microenvironment changes the mechanical ECM properties and plays a central role in TAM recruitment.

#### ***4.4 Matrix Degradation and Formation of Microtracks That Promote Cancer Cell and Macrophage Migration***

Under conditions of 3D cellular physical confinement, where cell size is large compared to matrix pore size, matrix proteolysis plays a critical role in facilitating 3D cell migration. The expression of proteolytic enzymes, such as MMPs, has been shown to be higher in metastatic cancers compared to benign tumors or matched normal breast tissue (Table 1) [68, 69]. CD11b + myeloid cells that adhere to cancer

cell-derived collagen type IV are activated to produce MMP-2 that degrades the matrix and, in turn, enhances both the recruitment of new bone marrow-derived cells and tumor cell invasion [56]. Both cancer cells and infiltrating monocytes at the invasive front express high levels of another member of the MMP family, MMP-9, which degrades fibrillar collagens [57]. Recent studies also demonstrate that cancer cell-mediated matrix degradation promotes TAM polarization toward an immunosuppressive phenotype that limits anti-tumor immunity [29]. Treatment with amino-biphosphonates has been shown to reduce MMP-9 expression, recruit macrophages in the tumor stroma, and ultimately impair tumor growth [59]. Following MMP-mediated proteolysis, the denatured non-fibrillar collagen fragments have been shown to act as a chemoattractant factor and increase macrophage motility [55]. Macrophages can, in turn, promote cancer cell invasion in an MMP-dependent mechanism by releasing TNF- $\alpha$  and TGF- $\beta$ 1 [70]. Taken together, these studies highlight the complex interplay between cancer-TAM crosstalk in a dynamically remodeled ECM and the establishment of bidirectional feedback loops with effects both on chemokines and proteolytic enzymes.

Spatial analysis of matrix remodeling has shown that local MMP-mediated matrix degradation by macrophages facilitates 3D cancer cell migration via the formation of microtracks. These are migratory passages in a dense ECM, where physical confinement dominates, and provide routes for fast and directional cell migration [58]. Real-time analysis of cancer cell-macrophage dynamics in a microfluidic device showed that macrophage-derived MMP-9 results in the formation of microtracks to subsequently promote cancer cell migration [58]. Intravital imaging of solid tumors showed that endocytic collagen degradation is highly active in the tumor and that TAMs originating from CCR2+ monocytes were driving collagen degradation [71]. Macrophages expressing DAB2, which are localized at the invasive tumor border, also contributed to this endocytic ECM degradation and promoted breast cancer cell invasion [47]. In addition to these effects on 3D cancer migration, *in vitro* and *in vivo* studies have shown that macrophage-mediated matrix remodeling contributes to multiple steps in the metastatic cascade including angiogenesis, intravasation, extravasation, and metastatic outgrowth in the secondary sites (reviewed in detail in [6, 72, 73]).

## **5 Bioengineering Approaches to Dissect Extracellular Matrix Complexity and Quantify Cancer-Macrophage Dynamics**

### ***5.1 Engineering the Extracellular Matrix Structure***

To dissect the *in vivo* complexity of the extracellular matrix, several bioengineered technologies have been developed to independently control individual matrix properties and investigate effects on cell adhesion, migration, and growth. Different

technologies that can be used to modulate matrix alignment, stiffness, and pore size are summarized in Table 2.

Fiber alignment in collagen type I hydrogels can be tuned by controlling the levels of mechanical stress during matrix polymerization. Microfluidic devices are an ideal platform to precisely control these mechanical forces using channels of varying dimensions and flow rates, with a higher shear stress promoting a greater collagen alignment [74]. Aligned collagen type I hydrogels in microfluidic chips enhanced lymphocyte migration compared to nonaligned collagen hydrogels [75]. Breast cancer cell migration was also greater in aligned matrices [79]. Cyclic stretch presents another approach to align collagen matrices using mechanical strain. Cyclic stretch has also been shown to promote cellular alignment in the direction of the applied force in a magnitude- and frequency-dependent fashion [78]. Cyclic stretch exerted on fibronectin-coated substrates induced alignment of macrophages and downregulated the expression of inflammatory genes, such as iNOS and ARG1 [89]. ECM alignment by ECM micropatterning also induced macrophage elongation and, in turn, modulated their polarization state [77]. Fibronectin micropatterning in a 20  $\mu\text{m}$  or 50  $\mu\text{m}$  wide linear pattern induced greater cell shape elongation compared to homogeneous substrates and also resulted in macrophage polarization toward an M2-like state [77]. Finally, magnetic beads embedded in collagen hydrogels under an externally controlled magnetic field [80] or electrospinning of anisotropic collagen nanofibers [76] have been employed to modulate matrix linearization and induce endothelial cell realignment.

Matrix stiffness can be controlled using various types of hydrogels such as polyacrylamide (PA) [81], gelatin methacryloyl (GelMA) [82], and fibrin [83]. In these hydrogel systems, matrix stiffening is determined by the monomer to crosslinker ratio or via UV exposure and photo-crosslinking. Matrix stiffness has been shown to play a critical role on macrophage motility. Macrophages cultured on collagen-coated polyacrylamide gels with varied stiffness exhibited amoeboid migration on soft substrates compared to contractility-driven migration on stiff substrates [17]. Matrix stiffness promoted the expression of the Piezo-1 ion channel via NF $\kappa$ B-dependent transcription that resulted in the upregulation of inflammatory markers such as INOS and ARG1 [90]. Matrix stiffness also promoted CSF1 overexpression in cancer cells and macrophage recruitment. Specifically, transwell experiments showed that a higher number of macrophages migrated toward MDA-MB-231 cells when they were cultured on a stiffer PA gel [67]. Furthermore, fibrillar matrices with tunable stiffness have been fabricated, by combining UV crosslinking and electrospinning [84]. Using this method, methacrylated dextran (DexMA) fibers with different stiffness have been aligned by electrospinning followed by exposure to varying duration of UV light [84]. Specifically, it was shown that mesenchymal stem cells locally modified the fiber stiffness with increased focal adhesion signaling and cell proliferation [84].

The matrix pore size plays a key role in determining the mode of 3D cell migration. Temperature control during collagen hydrogel polymerization has been used to control fibril size and pore size. Modulation of the freezing rate during fabrication of collagen-glycosaminoglycan scaffold in a freeze-dry process has

**Table 2** Methods for in vitro extracellular matrix engineering

ECM property	Methods	Principle	Ref.
Matrix alignment	Microfluidic devices	Modulation of collagen fiber alignment using different channel widths and shear-induced forces	[74, 75]
	Electrospinning	Electrospinning using a core-shell nozzle to form an aqueous acidic solution of collagen within a shell of polyvinylpyrrolidone (PVP). After core collagen gelation, the shell PVP was washed away using a basic ethanol solution to yield anisotropic collagen hydrogel nanofibers	[76]
	ECM micropatterning	Patterning ECM in specific topographies (e.g., $\mu\text{m}$ -wide lines or shapes) on 2D substrates	[77]
	Mechanical stretching	Highly aligned collagen fibers fabricated by mechanical stretching. For example, collagen alignment can be induced via cyclic stretching at a defined magnitude and frequency	[78]
	Magnetic field	Collagen gel embedded with streptavidin-coated magnetic beads to induce aligned gels via exposure to magnetically induced forces	[79, 80]

<p>Matrix stiffness</p>	<p>Hydrogel crosslinking</p>	<p>Polyacrylamide gels: By controlling the ratio of acrylamide (monomer) to bis-acrylamide (crosslinker), a Young's modulus in the range of ~200 pa to hundreds of kPa can be achieved. Gelatin methacryloyl (GelMA) gel: Adjust GelMA concentration to achieve ~2~180 kPa range. Fibrin gel: Photo-initiated crosslinking methods to modulate stiffness</p>	<p>[81–83]</p>
	<p>Electrospinning and UV curation</p>	<p>To control the stiffness of fibrous substrate, methacrylated dextran (DexMA) fibers are aligned by electrospinning and exposing to different levels of UV light</p>	<p>[84]</p>
<p>Pore size</p>	<p>Temperature control</p>	<p>Gelation temperatures from 22 to 37 °C are used to control the pore size of collagen matrices independent of collagen concentration</p>	<p>[85]</p>
	<p>Microfluidic devices with porous membranes</p>	<p>Porous membranes with predefined pore size are immobilized between microfluidic channels</p>	<p>[86]</p>
	<p>Electrospinning</p>	<p>Modulating protein and polymer concentration to alter the fiber diameter and pore size</p>	<p>[87]</p>
	<p>Freeze-drying method</p>	<p>The freezing rate during fabrication of collagen-glycosaminoglycan scaffolds determines the pore size due to ice nucleation and crystal growth</p>	<p>[88]</p>

also been shown to result in different scaffold pore sizes [88]. Another approach involves electrospinning of a hybrid scaffold that combines synthetic materials such as poly(3-caprolactone) (PCL) with natural materials such as gelatin, collagen, and elastin [87]. Fiber diameter and pore size can be controlled by tuning the synthetic–natural material mixture [87]. For example, culturing murine bone marrow–derived macrophages on these hybrid matrices showed a correlation between increasing scaffold pore size and expression of M2-like markers in macrophages [91]. Finally, embedding membrane inserts with a predefined pore size between two microfluidic channels has also been used to study cancer cell transmigration [92]. A subpopulation of cancer cells that transmigrated through a pore diameter of 24  $\mu\text{m}$  showed a higher cell migration speed compared to the bulk cell population [92]. These studies demonstrate that the ECM microstructure modulates the morphology, dynamics, and proliferation of multiple cell types.

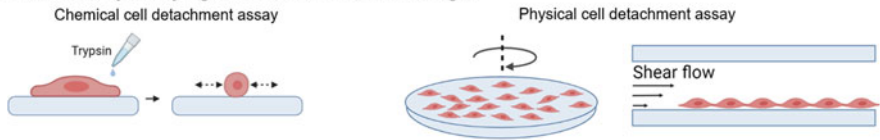
## 5.2 *Quantification of Matrix Remodeling*

Matrix remodeling involves complex processes including cell–matrix adhesion, cellular contractile force generation, matrix synthesis, and degradation [93]. Importantly, these processes can be coupled via feedback loops, where proteolytically degraded matrix components activate cellular signaling programs that further promote remodeling via cell-generated forces [94]. Thus, real-time quantification of cell–matrix interactions is critical for elucidating this complex bidirectional crosstalk. Below, we describe multiple methods to characterize cell–matrix adhesion, contractile forces, and matrix degradation (Fig. 2).

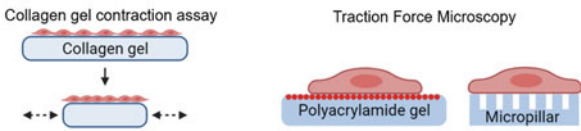
The strength of cell–matrix adhesion exhibits a biphasic relationship with cell migration. Specifically, baseline integrin expression levels in macrophages result in moderate matrix adhesion and support 3D migration, while overexpression of integrins results in strong adhesion and hinders 3D migration both *in vitro* and *in vivo* [95]. Adhesion characterization methods quantify the number of adherent cells and cellular area on a matrix-coated substrate, as a function of time following cell seeding [96]. Cell detachment assays represent another approach to measure the strength of cell–matrix adhesion. There are two types of cell detachment assays: chemically induced cell detachment [97] and mechanically induced cell detachment [98]. In chemically induced cell detachment, adherent cells are treated with enzymes to cleave their substrate adhesion (e.g., trypsin) and the temporal evolution of the cellular area that is determined by cell–matrix adhesion strength is characterized [97]. This method has been employed to monitor cancer cell adhesion strength following treatment with cytoskeletal inhibitors targeting actin, myosin-II, and microtubules [97] or adhesion strength to substrates with different geometries [99]. In the mechanically induced cell detachment assay, cells are exposed to controlled levels of shear stress using a spinning disk [98], parallel plate shear channel [100], or a micropipette [101]. The spinning disk method sorts cancer cells according to their adhesion strength, where weakly adherent cells are collected in the floating



**Methods for quantifying cell-matrix adhesion strength**



**Methods for quantifying cell contractility**



**Methods for quantifying MMP-mediated matrix degradation**

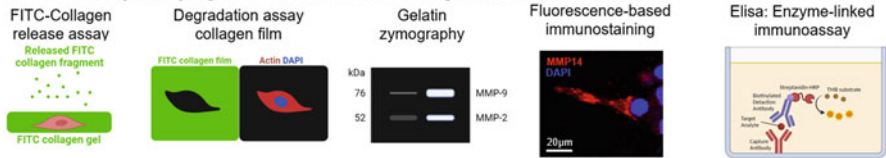


**Fig. 2** Experimental methods to quantify cell–matrix adhesion strength, cell contractility, and matrix remodeling. (Created with BioRender.com)

fraction after shearing and strongly adherent cells are collected by subsequent trypsinization of the adherent fraction [98]. Using this methodology, the weakly adherent subpopulation of MDA-MB-231 cancer cells was found to exhibit higher migration rates compared to the strongly adherent subpopulation [98, 100]. The micropipette-mediated assay has been used to show that blocking integrin CD11b in dendritic cells, macrophages, and monocytes enhances the adhesion strength to fibrinogen [96].

Cytoskeleton alignment and actomyosin-mediated contractility in TAMs can impact migration and polarization [102]. Following adhesion to the matrix, cells exert mechanical forces via actomyosin-mediated contractility [103]. These contractility-generated forces are transduced to the cell exterior via cell–matrix adhesion complexes that, in turn, remodel the extracellular environment to regulate cell migration and matrix remodeling [104]. One of the simplest methods for quantifying cellular traction forces is the gel contraction assay [105, 106]. In this method, cells are seeded inside or on top of a hydrogel (typically collagen type I hydrogel), and the hydrogel is released from the supporting culture vessel in a floating setup to observe cell-mediated contraction. Hydrogel area and shape are monitored over time. Another technique is traction force microscopy (TFM), where the cell-induced deformation of the substrate is measured using soft hydrogels of predefined stiffness [107] or an elastic micropillar array [108]. The substrate deformation field is monitored by either the displacement of embedded microbeads or the deflection of micropillars. Given a known substrate or pillar stiffness, traction forces can be calculated [109]. TFM enables high-resolution analysis

of single cells or cellular monolayers [110] and has been employed to compare cancer and normal cells [111] or macrophages with different polarization states [112]. A number of biophysical platforms have integrated TFM with control of exogenous biochemical or biophysical factors to study the interplay between cell mechanics and different tumor microenvironment factors (e.g., shear stress, mechanical compression, electric fields) [113]. Finally, recent developments in microparticle TFM have enabled visualization of subcellular force patterns throughout macrophage phagocytosis of deformable hydrogel microparticles [114].

MMP expression levels correlate with poor outcomes in breast cancer and are elevated in aggressive breast cancer subtypes compared to normal breast tissue [69, 115]. Macrophage-derived paracrine signals (TNF- $\alpha$ , TGF- $\beta$ ) enhance cancer cell migration via MMP-mediated matrix remodeling [70]. The expression level of MMPs in cancer cells or macrophages can be characterized using enzyme-linked immunoassays, immunoblotting and immunostaining assays. Functional assays to quantify the matrix remodeling activities of MMPs against specific ECM components are shown in Fig. 2. One of these assays involves quantification of fluorescence-labeled collagen monomers that are released following matrix degradation [116]. Alternatively, using a FITC-conjugated collagen I film, the spatial reorganization of matrix remodeling can be quantified [117]. Collagen degradation by cancer cells can also be visualized by staining collagen fragments derived from the MT1-MMP-mediated cleavage [116, 118]. Expression levels of gelatinases (MMP-2 and MMP-9) can also be assessed by gelatin zymography [119]. The development of the quantification methods described above has proven how cells actively remodel the matrix, in either a physical or chemical way. A combination of these techniques will unveil the strategies that cells use to accommodate to their surroundings for survival, proliferation, and invasion.

## 6 Bioinformatic Analysis of ECM- and Macrophage-Specific Gene Signatures

Gene expression analysis is a powerful tool to identify genes that are associated with cancer progression and different tumor microenvironment features (e.g., macrophages and ECM). A major application of these bioinformatic approaches is the identification of gene signatures that can stratify breast cancer patients into groups with distinct clinical characteristics, such as survival outcomes and therapy response [120]. Breakthrough molecular signature studies in the last two decades have reshaped clinical decision-making for therapy in two out of the three receptor-based subtypes. For example, Oncotype DX provides a validated prognostic signature for endocrine therapy outcomes and a predictive signature for whether chemotherapy reduces recurrence [121, 122]. In Table 3, we present landmark gene signatures with prognostic value in breast cancer, as well as ECM- and macrophage-specific gene signatures.

**Table 3** Gene signatures in breast cancer: prognostic and ECM- and TAM-related signatures

Approach used to develop signature	Number of genes	Predictive value and associations with clinical or biological variables	Ref.
DNA microarray analysis with unsupervised and supervised classification algorithms was applied to a 117-sample dataset labeled with pathology annotations	70	Predicts metastatic and BRCA1 mutation carrier for young breast cancer patients	[123, 124]
The gene expression of patients from the NSABP B20 clinical trial was evaluated with the Oncotype DX. Recurrence score (RS) was analyzed and associated with clinical outcomes	21	The RS is predictive to the recurrence of tumor after chemotherapy and the magnitude of the benefits of ER+ breast tumors. Multiple clinical outcomes associated with the RS, including survival, tumor size, tumor grade, and ER/PR status	[125]
Clustering and correlation analysis were performed based on 2 independent microarray databases with normal and tumorous breast epithelium to develop the "invasiveness gene signature" (IGS)	IGS: 182 (WR: 512)	Predicts breast tumor cell invasiveness and patient prognosis, and its performance can be further improved by combining the wound response (WR) signature	[120, 126]
The "PAM50" gene signature was developed based on microarray data with feature selection and multivariate cox regression. Hierarchical clustering was performed for subtype identification	50	The 4 intrinsic breast tumor subtypes (basal like, luminal A, luminal B, HER2 enriched) were identified, which associated with breast cancer molecular subtypes and predict patient survival	[127, 128]
Endopredict score (EP) was calculated with qPCR data of the expression of 8 genes plus nodal status and tumor size. A model with cutoff values was built and validated with 2 independent phase III clinical trial datasets with distant metastasis annotation	EP: 8	Predicts the recurrence of adjuvant endocrine therapy for ER+ breast cancer and is more predictable than all conventional clinicopathologic methods	[129]
Microarray data from 28 primary breast carcinoma with clinical annotation was analyzed with hierarchical clustering to identify a breast tumor ECM signature. The signature was validated and evaluated with independent datasets	278	The classification of breast tumor on this ECM signature associates with patient survival, nodal infiltration, and expression of ECM molecules. Genes that significantly associated with a poor clinical outcome were identified	[130]

(continued)

**Table 3** (continued)

Approach used to develop signature	Number of genes	Predictive value and associations with clinical or biological variables	Ref.
Data from the EORTC 10994 neoadjuvant trial were analyzed and stromal metagenes were evaluated for association with patient clinical phenotypes	50	The stromal metagene significantly predicts patient survival and associates with multiple histological features and signaling pathways	[131]
Single-cell RNA sequencing analysis of breast tumors identified 314 macrophage-specific genes that were, in turn, filtered using a multivariate model of overall survival in the TCGA dataset	7	Predicts 3-year and 5-year breast cancer survival in multiple independent datasets. Predictive value depends on receptor subtype (ER, PR, HER2) and signature risk score depends on age, tumor size, and lymph node status	[132]
Next-generation sequencing and microarray data were analyzed with clustering to identify a gene signature in TAMs. The association between single genes (chemokines) and macrophage and monocyte status was analyzed	37 or 2: SINGLEC1/CCL8	The gene signature associates with breast cancer clinical outcomes. Critical chemokines such as CX3CL1 and CCL8 associate with monocyte activation, tumor cell-TAM crosstalks, and patient survival	[133]

## 6.1 *Extracellular Matrix Gene Signatures*

In many solid tumors, the expression levels of ECM genes are higher compared to matched normal tissue [134]. ECM gene signature studies in breast cancer have been shown to have prognostic value (Table 3). Using hierarchical clustering of 278 ECM-related genes, breast cancer patients were classified into four groups with distinct survival outcomes [130]. The group with poor survival exhibited a high expression of integrins and metalloproteinases, while the good outcome group was enriched in protease inhibitors belonging to the serpin family [130]. Another pioneering study identified a 50-gene ECM-related signature that predicted response to chemotherapy and was associated with stroma-rich tumors [131]. In addition to chemotherapy, ECM gene signatures have been developed to predict resistance to endocrine therapy and radiotherapy [135]. Furthermore, ECM gene signatures have been shown to predict the failure of immunotherapies, such as PD-1 blockade [136], where the anti-tumor function of TAMs and immune infiltration plays a critical role. Proteomics-based ECM molecular signature studies in animal models have shown that the ECM composition differs with the tumor's metastatic potential [137]. Furthermore, single-cell RNA sequencing-based comparison of premalignant and invasive breast tumors in an immunocompetent mouse model revealed that TAM subpopulations exhibit differences in the expression of tissue remodeling gene sets [138]. Hence, the analysis of ECM signatures combined with mechanistic *in vitro* and *in vivo* studies provides an unbiased approach to identify new regulators of metastasis, stroma reaction, and therapeutic response [34].

## 6.2 *TAM-Specific Gene Expression Signatures*

TAM molecular signatures in breast cancer have been developed using both single-cell RNA sequencing [132, 139] and bulk RNA sequencing of flow-sorted macrophages [133]. A seven-gene macrophage gene signature has been developed using the tumor cancer genome atlas (TCGA) dataset that predicts patient survival in breast tumors; these seven genes are a subset of 314 differentially expressed genes in macrophages [132]. Differential expression analysis of these seven genes in normal breast tissue compared to breast tumors highlighted that ADAM9 and SERPINA1 expression was similar; CD24, CD74, and PGK1 were overexpressed in tumors; while STX11 and NFKBIA exhibited lower levels in tumors. Interestingly, the prognostic ability of this seven-gene signature was higher in the estrogen-receptor-positive breast tumor subtype, and the predicted risk was dependent on the patient cohort, highlighting the challenges with patient-to-patient heterogeneity. Macrophage heterogeneity in the breast tumor microenvironment has been elegantly demonstrated in a landmark study of transcriptomic phenotyping of macrophages in breast tumors [139]. Specifically, although a subset of TAMs exhibited a higher expression of M2-like marker genes compared to other myeloid cells,

these M2-like marker genes correlated significantly with M1-like marker genes. These results highlight that the TAM transcriptomic state in the breast tumor microenvironment does not match a discrete polarization model of M1-like and M2-like TAMs. Transcriptional analysis of monocytes, tissue resident macrophages, and TAMs in breast tumors identified a 37-gene TAM signature that was enriched in aggressive breast cancer subtypes and predicted shorter disease-free survival [133]. Mechanistic follow-up studies uncovered a positive feedback loop between cancer cells and TAMs involving CCL8-SINGLEC1 that was sustained via tumor-derived CSF1 and resulted in monocyte recruitment in the tumor. The central role of ECM on modulating immune cell function in the tumor microenvironment [140] is supported by studies that have shown overexpression of ECM gene signatures (such as collagen, lumican, LOX, PCOLCE2) in TAMs compared to normal macrophages [141] and other inflammatory cells [142]. Taken together, these bioinformatic studies highlight the association between gene signatures of ECM and TAM function.

## 7 Summary and Future Perspectives

TAMs are a major component of the tumor microenvironment and play a critical role in tumor progression, metastasis, and anti-tumor immunity. Both pathology-based and bioinformatic approaches have highlighted that high infiltration of pro-tumorigenic TAMs in the breast tumor microenvironment predicts poor patient survival. Despite the progress in understanding TAM biology, targeting TAMs remains challenging due to the presence of heterogeneous subpopulations and their phenotypic plasticity. ECM composition and architecture in the tumor microenvironment modulate multiple TAM functions, including cell–ECM adhesion, motility, cytokine secretion, and matrix remodeling that can, in turn, stimulate pro-metastatic signaling in the cancer cells. Recent studies have identified strategies to target tumor-specific ECM (e.g., HA, tenascin C) [34, 143], ECM remodeling (e.g., MMPs, LOXL2) [144, 145], and cell-mediated forces (e.g., ROCK) [146] in order to halt tumor progression and improve therapy response.

A number of key unanswered questions remain regarding fundamental mechanisms of tumor matrix–macrophage communication. Understanding the plasticity of migration modes employed by macrophages in the context of a complex tumor ECM is currently limited. The relationship between spatial heterogeneity in ECM deposition, matrix alignment, and macrophage function also needs to be further elucidated. The role of denatured ECM on macrophage recruitment also needs to be investigated. For example, there is a lack of systematic comparison of macrophage recruitment into denatured ECM versus loosely crosslinked matrix, where despite similar mechanical properties macrophage behavior can diverge due to differential cell adhesion. Furthermore, the role of tumor subtype heterogeneity on tumor cell chemokine profiles and distinct matrix-remodeling characteristics remains poorly understood. In-depth characterization of tumor-associated macrophage transcrip-

tional signatures, paired with analysis of the secretome and matrisome in the tumor microenvironment, will reveal novel cancer-specific and TAM-specific regulators of disease progression.

To this end, the development of novel *in vitro* model systems that enable spatiotemporal control of mechanical and chemical signals in bioengineered matrices combined with high-resolution, real-time imaging of intracellular and intercellular pathway activity is necessary. For example, future studies that integrate bioengineered matrices with cancer–macrophage cells expressing signaling reporters [147, 148] with microfluidic systems could provide novel insights into the interplay of chemokine and mechanotransduction regulators. Development of bioengineering and bioinformatic approaches to investigate tumor-specific matrix features in TAM-rich breast cancers will lead to the discovery of novel therapeutic targets and identification of biomarkers to personalize cancer therapies and ultimately improve patient outcomes.

**Acknowledgments** This work was supported by the US National Institutes of Health (R00 CA222554 and administrative supplement from U54CA209988 to I.K.Z.), a National Cancer Center Postdoctoral Fellowship (to Y.C), a Magee Women’s Research Institute Breast Cancer Pilot Award, and the Department of Bioengineering, School of Engineering at the University of Pittsburgh.

## References

1. Beltraminelli T, De Palma M (2020) Biology and therapeutic targeting of tumour-associated macrophages. *J Pathol* 250:573–592. <https://doi.org/10.1002/path.5403>
2. DeNardo DG, Brennan DJ, Rexhepaj E et al (2011) Leukocyte complexity predicts breast cancer survival and functionally regulates response to chemotherapy. *Cancer Discov* 1:54–67. <https://doi.org/10.1158/2159-8274.CD-10-0028>
3. Mantovani A, Sozzani S, Locati M et al (2002) Macrophage polarization: tumor-associated macrophages as a paradigm for polarized M2 mononuclear phagocytes. *Trends Immunol* 23:549–555. [https://doi.org/10.1016/S1471-4906\(02\)02302-5](https://doi.org/10.1016/S1471-4906(02)02302-5)
4. Jeong H, Hwang I, Kang SH et al (2019) Tumor-associated macrophages as potential prognostic biomarkers of invasive breast cancer. *J Breast Cancer* 22:38–51. <https://doi.org/10.4048/jbc.2019.22.e5>
5. Winkler J, Abisoye-Ogunniyan A, Metcalf KJ, Werb Z (2020) Concepts of extracellular matrix remodelling in tumour progression and metastasis. *Nat Commun* 11:1–19. <https://doi.org/10.1038/s41467-020-18794-x>
6. Riabov V, Gudima A, Wang N et al (2014) Role of tumor associated macrophages in tumor angiogenesis and lymphangiogenesis. *Front Physiol* 5:1–13. <https://doi.org/10.3389/fphys.2014.00075>
7. Zervantonakis IK, Hughes-Alford SK, Charest JL et al (2012) Three-dimensional microfluidic model for tumor cell intravasation and endothelial barrier function. *Proc Natl Acad Sci U S A* 109:13515–13520. <https://doi.org/10.1073/pnas.1210182109>
8. Peranzoni E, Lemoine J, Vimeux L et al (2018) Macrophages impede CD8 T cells from reaching tumor cells and limit the efficacy of anti–PD-1 treatment. *Proc Natl Acad Sci U S A* 115:E4041–E4050. <https://doi.org/10.1073/pnas.1720948115>



9. Argyle D, Kitamura T (2018) Targeting macrophage-recruiting chemokines as a novel therapeutic strategy to prevent the progression of solid tumors. *Front Immunol* 9:1–15. <https://doi.org/10.3389/fimmu.2018.02629>
10. Cannarile MA, Weisser M, Jacob W et al (2017) Colony-stimulating factor 1 receptor (CSF1R) inhibitors in cancer therapy. *J Immunother Cancer* 5:1–13. <https://doi.org/10.1186/s40425-017-0257-y>
11. Pathria P, Louis TL, Varner JA (2019) Targeting tumor-associated macrophages in cancer. *Trends Immunol* 40:310–327. <https://doi.org/10.1016/j.it.2019.02.003>
12. Djureinovic D, Wang M, Kluger HM (2021) Agonistic cd40 antibodies in cancer treatment. *Cancers (Basel)* 13:1–18. <https://doi.org/10.3390/cancers13061302>
13. Lecoultre M, Dutoit V, Walker PR (2020) Phagocytic function of tumor-associated macrophages as a key determinant of tumor progression control: a review. *J Immunother Cancer* 8:1–11. <https://doi.org/10.1136/jitc-2020-001408>
14. Wu K, Lin K, Li X et al (2020) Redefining tumor-associated macrophage subpopulations and functions in the tumor microenvironment. *Front Immunol* 11:1731. <https://doi.org/10.3389/fimmu.2020.01731>
15. Werb Z, Lu P (2015) The role of stroma in tumor development. *Cancer J (United States)* 21:250–253. <https://doi.org/10.1097/PPO.0000000000000127>
16. Van Goethem E, Poincloux R, Gauffre F et al (2010) Matrix architecture dictates three-dimensional migration modes of human macrophages: differential involvement of proteases and podosome-like structures. *J Immunol* 184:1049–1061. <https://doi.org/10.4049/jimmunol.0902223>
17. Sridharan R, Cavanagh B, Cameron AR et al (2019) Material stiffness influences the polarization state, function and migration mode of macrophages. *Acta Biomater* 89:47–59. <https://doi.org/10.1016/j.actbio.2019.02.048>
18. Fang JY, Yang Z, Han B (2020) Switch of macrophage fusion competency by 3D matrices. *Sci Rep* 10:1–12. <https://doi.org/10.1038/s41598-020-67056-9>
19. Tomlin H, Piccinini AM (2018) A complex interplay between the extracellular matrix and the innate immune response to microbial pathogens. *Immunology* 155:186–201. <https://doi.org/10.1111/imm.12972>
20. Ma RY, Zhang H, Li XF et al (2020) Monocyte-derived macrophages promote breast cancer bone metastasis outgrowth. *J Exp Med* 217. <https://doi.org/10.1084/JEM.20191820>
21. Chen Z, Feng X, Herting CJ et al (2017) Cellular and molecular identity of tumor-associated macrophages in glioblastoma. *Cancer Res* 77:2266–2278. <https://doi.org/10.1158/0008-5472.CAN-16-2310>
22. Franklin RA, Liao W, Sarkar A et al (2014) The cellular and molecular origin of tumor-associated macrophages. *Science* 344:921–925. <https://doi.org/10.1126/science.1252510>
23. Qian BZ, Li J, Zhang H et al (2011) CCL2 recruits inflammatory monocytes to facilitate breast-tumour metastasis. *Nature* 475:222–225. <https://doi.org/10.1038/nature10138>
24. Boyle ST, Faulkner JW, McColl SR, Kochetkova M (2015) The chemokine receptor CCR6 facilitates the onset of mammary neoplasia in the MMTV-PyMT mouse model via recruitment of tumor-promoting macrophages. *Mol Cancer* 14:1–14. <https://doi.org/10.1186/s12943-015-0394-1>
25. Frankenberger C, Rabe D, Bainer R et al (2015) Metastasis suppressors regulate the tumor microenvironment by blocking recruitment of prometastatic tumor-associated macrophages. *Cancer Res* 75:4063–4073. <https://doi.org/10.1158/0008-5472.CAN-14-3394>
26. Jin H, Su J, Garmy-Susini B et al (2006) Integrin  $\alpha 4\beta 1$  promotes monocyte trafficking and angiogenesis in tumors. *Cancer Res* 66:2146–2152. <https://doi.org/10.1158/0008-5472.CAN-05-2704>
27. An G, Wu F, Huang S et al (2019) Effects of CCL5 on the biological behavior of breast cancer and the mechanisms of its interaction with tumor-associated macrophages. *Oncol Rep* 42:2499–2511. <https://doi.org/10.3892/or.2019.7344>
28. Chockalingam S, Ghosh SS (2014) Macrophage colony-stimulating factor and cancer: a review. *Tumor Biol* 35:10635–10644. <https://doi.org/10.1007/s13277-014-2627-0>



29. Wang H, Yung MMH, Ngan HYS et al (2021) The impact of the tumor microenvironment on macrophage polarization in cancer metastatic progression. *Int J Mol Sci* 22. <https://doi.org/10.3390/ijms22126560>
30. Acerbi I, Cassereau L, Dean I et al (2015) Human breast cancer invasion and aggression correlates with ECM stiffening and immune cell infiltration. *Integr Biol (United Kingdom)* 7:1120–1134. <https://doi.org/10.1039/c5ib00040h>
31. Plodinec M, Loparic M, Monnier CA et al (2012) The nanomechanical signature of breast cancer. *Nat Nanotechnol* 7:757–765. <https://doi.org/10.1038/nnano.2012.167>
32. Legate KR, Wickström SA, Fässler R (2009) Genetic and cell biological analysis of integrin outside-in signaling. *Genes Dev* 23:397–418. <https://doi.org/10.1101/gad.1758709>
33. Huang J, Zhang L, Wan D et al (2021) Extracellular matrix and its therapeutic potential for cancer treatment. *Signal Transduct Target Ther* 6:153. <https://doi.org/10.1038/s41392-021-00544-0>
34. Henke E, Nandigama R, Ergün S (2020) Extracellular matrix in the tumor microenvironment and its impact on cancer therapy. *Front Mol Biosci* 6:1–24. <https://doi.org/10.3389/fmolb.2019.00160>
35. Yamada KM, Sixt M (2019) Mechanisms of 3D cell migration. *Nat Rev Mol Cell Biol* 20:738–752. <https://doi.org/10.1038/s41580-019-0172-9>
36. Gui P, Ben-Neji M, Belozertseva E et al (2018) The protease-dependent mesenchymal migration of tumor-associated macrophages as a target in cancer immunotherapy. *Cancer Immunol Res* 6:1337–1351. <https://doi.org/10.1158/2326-6066.CIR-17-0746>
37. Lämmermann T, Sixt M (2009) Mechanical modes of “amoeboid” cell migration. *Curr Opin Cell Biol* 21:636–644. <https://doi.org/10.1016/j.ceb.2009.05.003>
38. Wiesner C, Le-Cabec V, El Azzouzi K et al (2014) Podosomes in space: macrophage migration and matrix degradation in 2D and 3D settings. *Cell Adhes Migr* 8:179–191. <https://doi.org/10.4161/cam.28116>
39. Wiesner C, El Azzouzi K, Linder S (2013) A specific subset of RabGTPases controls cell surface exposure of MT1-MMP, extracellular matrix degradation and three-dimensional invasion of macrophages. *J Cell Sci* 126:2820–2833. <https://doi.org/10.1242/jcs.122358>
40. Oskarsson T, Acharyya S, Zhang XHF et al (2011) Breast cancer cells produce tenascin C as a metastatic niche component to colonize the lungs. *Nat Med* 17:867–874. <https://doi.org/10.1038/nm.2379>
41. Insua-Rodríguez J, Oskarsson T (2016) The extracellular matrix in breast cancer. *Adv Drug Deliv Rev* 97:41–55. <https://doi.org/10.1016/j.addr.2015.12.017>
42. Wu W, Chen L, Wang Y et al (2020) Hyaluronic acid predicts poor prognosis in breast cancer patients: a protocol for systematic review and meta analysis. *Medicine (Baltimore)* 99:e20438. <https://doi.org/10.1097/MD.00000000000020438>
43. Tiainen S, Tumelius R, Rilla K et al (2015) High numbers of macrophages, especially M2-like (CD163-positive), correlate with hyaluronan accumulation and poor outcome in breast cancer. *Histopathology* 66:873–883. <https://doi.org/10.1111/his.12607>
44. Deligne C, Murdamoothoo D, Gammage AN et al (2020) Matrix-targeting immunotherapy controls tumor growth and spread by switching macrophage phenotype. *Cancer Immunol Res* 8:368–382. <https://doi.org/10.1158/2326-6066.CIR-19-0276>
45. Esbona K, Inman D, Saha S et al (2016) COX-2 modulates mammary tumor progression in response to collagen density. *Breast Cancer Res* 18:1–15. <https://doi.org/10.1186/s13058-016-0695-3>
46. Sossey-Alaoui K, Pluskota E, Bialkowska K et al (2017) Kindlin-2 regulates the growth of breast cancer tumors by activating CSF-1-mediated macrophage infiltration. *Cancer Res* 77:5129–5141. <https://doi.org/10.1158/0008-5472.CAN-16-2337>
47. Marigo I, Trovato R, Hofer F et al (2020) Disabled homolog 2 controls prometastatic activity of tumor-associated macrophages. *Cancer Discov* 10:1758–1773. <https://doi.org/10.1158/2159-8290.CD-20-0036>

48. Sangaletti S, Di Carlo E, Gariboldi S et al (2008) Macrophage-derived SPARC bridges tumor cell-extracellular matrix interactions toward metastasis. *Cancer Res* 68:9050–9059. <https://doi.org/10.1158/0008-5472.CAN-08-1327>
49. Chen J, Yao Y, Gong C et al (2011) CCL18 from tumor-associated macrophages promotes breast cancer metastasis via P1TPNM3. *Cancer Cell* 19:541–555. <https://doi.org/10.1016/j.ccr.2011.02.006>
50. Trikha P, Sharma N, Pena C et al (2016) E2f3 in tumor macrophages promotes lung metastasis. *Oncogene* 35:3636–3646. <https://doi.org/10.1038/onc.2015.429>
51. Sun X, Glynn DJ, Hodson LJ et al (2017) CCL2-driven inflammation increases mammary gland stromal density and cancer susceptibility in a transgenic mouse model. *Breast Cancer Res* 19:1–15. <https://doi.org/10.1186/s13058-016-0796-z>
52. Joo YN, Jin H, Eun SY et al (2014) P2Y2R activation by nucleotides released from the highly metastatic breast cancer cell contributes to pre-metastatic niche formation by mediating lysyl oxidase secretion, collagen crosslinking, and monocyte recruitment. *Oncotarget* 5:9322–9334. <https://doi.org/10.18632/oncotarget.2427>
53. Maller O, Drain AP, Barrett AS et al (2021) Tumour-associated macrophages drive stromal cell-dependent collagen crosslinking and stiffening to promote breast cancer aggression. *Nat Mater* 20:548–559. <https://doi.org/10.1038/s41563-020-00849-5>
54. Esbona K, Yi Y, Saha S et al (2018) The presence of cyclooxygenase 2, tumor-associated macrophages, and collagen alignment as prognostic markers for invasive breast carcinoma patients. *Am J Pathol* 188:559–573. <https://doi.org/10.1016/j.ajpath.2017.10.025>
55. O'Brien J, Lyons T, Monks J et al (2010) Alternatively activated macrophages and collagen remodeling characterize the postpartum involuting mammary gland across species. *Am J Pathol* 176:1241–1255. <https://doi.org/10.2353/ajpath.2010.090735>
56. Erler JT, Bennewith KL, Cox TR et al (2009) Hypoxia-induced Lysyl oxidase is a critical mediator of bone marrow cell recruitment to form the premetastatic niche. *Cancer Cell* 15:35–44. <https://doi.org/10.1016/j.ccr.2008.11.012>
57. Juric V, O'Sullivan C, Stefanutti E et al (2018) MMP-9 inhibition promotes anti-tumor immunity through disruption of biochemical and physical barriers to T-cell trafficking to tumors. *PLoS One* 13:1–21. <https://doi.org/10.1371/journal.pone.0207255>
58. Kim H, Chung H, Kim J et al (2019) Macrophages-triggered sequential remodeling of endothelium-interstitial matrix to form pre-metastatic niche in microfluidic tumor microenvironment. *Adv Sci* 6. <https://doi.org/10.1002/adv.201900195>
59. Melani C, Sangaletti S, Barazzetta FM et al (2007) Amino-biphosphonate-mediated MMP-9 inhibition breaks the tumor-bone marrow axis responsible for myeloid-derived suppressor cell expansion and macrophage infiltration in tumor stroma. *Cancer Res* 67:11438–11446. <https://doi.org/10.1158/0008-5472.CAN-07-1882>
60. Na YR, Yoon YN, Son DI, Seok SH (2013) Cyclooxygenase-2 inhibition blocks M2 macrophage differentiation and suppresses metastasis in murine breast cancer model. *PLoS One* 8:e63451. <https://doi.org/10.1371/journal.pone.0063451>
61. Hannigan G, Troussard AA, Dedhar S (2005) Integrin-linked kinase: a cancer therapeutic target unique among its ILK. *Nat Rev Cancer* 5:51–63. <https://doi.org/10.1038/nrc1524>
62. Wuest M, Kuchar M, Sharma SK et al (2015) Targeting lysyl oxidase for molecular imaging in breast cancer. *Breast Cancer Res* 17:1–15. <https://doi.org/10.1186/s13058-015-0609-9>
63. Herchenhan A, Uhlenbrock F, Eliasson P et al (2015) Lysyl oxidase activity is required for ordered collagen fibrillogenesis by tendon cells. *J Biol Chem* 290:16440–16450. <https://doi.org/10.1074/jbc.M115.641670>
64. Pfeiffer BJ, Franklin CL, Hsieh FH et al (2005) Alpha 2(I) collagen deficient oim mice have altered biomechanical integrity, collagen content, and collagen crosslinking of their thoracic aorta. *Matrix Biol* 24:451–458. <https://doi.org/10.1016/j.matbio.2005.07.001>
65. Bonnans C, Chou J, Werb Z (2014) Remodelling the extracellular matrix in development and disease. *Nat Rev Mol Cell Biol* 15:786–801. <https://doi.org/10.1038/nrm3904>
66. Saatci O, Kaymak A, Raza U et al (2020) Targeting lysyl oxidase (LOX) overcomes chemotherapy resistance in triple negative breast cancer. *Nat Commun* 11:1–17. <https://doi.org/10.1038/s41467-020-16199-4>

67. Taufalele PV, Wang W, Simmons AJ et al (2022) Matrix stiffness enhances cancer-macrophage interactions and M2-like macrophage accumulation in the breast tumor microenvironment. *Acta Biomater.* <https://doi.org/10.1016/j.actbio.2022.04.031>
68. Mehner C, Hockla A, Miller E et al (2014) Tumor cell-produced matrix metalloproteinase 9 (MMP-9) drives malignant progression and metastasis of basal-like triple negative breast cancer. *Oncotarget* 5:2736–2749. <https://doi.org/10.18632/oncotarget.1932>
69. Yousef EM, Tahir MR, St-Pierre Y, Gaboury LA (2014) MMP-9 expression varies according to molecular subtypes of breast cancer. *BMC Cancer* 14:1–12. <https://doi.org/10.1186/1471-2407-14-609>
70. Li R, Hebert JD, Lee TA et al (2017) Macrophage-secreted TNF $\alpha$  and TGF $\beta$ 1 influence migration speed and persistence of cancer cells in 3D tissue culture via independent pathways. *Cancer Res* 77:279–290. <https://doi.org/10.1158/0008-5472.CAN-16-0442>
71. Madsen DH, Jürgensen HJ, Siersbæk MS et al (2017) Tumor-associated macrophages derived from circulating inflammatory monocytes degrade collagen through cellular uptake. *Cell Rep* 21:3662–3671. <https://doi.org/10.1016/j.celrep.2017.12.011>
72. Doak GR, Schwertfeger KL, Wood DK (2018) Distant relations: macrophage functions in the metastatic niche. *Trends Cancer* 4:445–459. <https://doi.org/10.1016/j.trecan.2018.03.011>
73. Deligne C, Midwood KS (2021) Macrophages and extracellular matrix in breast cancer: partners in crime or protective allies? *Front Oncol* 11:1–12. <https://doi.org/10.3389/fonc.2021.620773>
74. Lee P, Lin R, Moon J, Lee LP (2006) Microfluidic alignment of collagen fibers for in vitro cell culture. *Biomed Microdevices* 8:35–41. <https://doi.org/10.1007/s10544-006-6380-z>
75. Pruitt HC, Lewis D, Ciccaglione M et al (2020) Collagen fiber structure guides 3D motility of cytotoxic T lymphocytes. *Matrix Biol* 85–86:147–159. <https://doi.org/10.1016/j.matbio.2019.02.003>
76. Wakuda Y, Nishimoto S, Suye SI, Fujita S (2018) Native collagen hydrogel nanofibres with anisotropic structure using core-shell electrospinning. *Sci Rep* 8:1–10. <https://doi.org/10.1038/s41598-018-24700-9>
77. McWhorter FY, Wang T, Nguyen P et al (2013) Modulation of macrophage phenotype by cell shape. *Proc Natl Acad Sci U S A* 110:17253–17258. <https://doi.org/10.1073/pnas.1308887110>
78. Nam E, Lee WC, Takeuchi S (2016) Formation of highly aligned collagen nanofibers by continuous cyclic stretch of a collagen hydrogel sheet. *Macromol Biosci*:995–1000. <https://doi.org/10.1002/mabi.201600068>
79. Riching KM, Cox BL, Salick MR et al (2015) 3D collagen alignment limits protrusions to enhance breast cancer cell persistence. *Biophys J* 107:2546–2558. <https://doi.org/10.1016/j.bpj.2014.10.035>
80. Guo C, Kaufman LJ (2007) Flow and magnetic field induced collagen alignment. *Biomaterials* 28:1105–1114. <https://doi.org/10.1016/j.biomaterials.2006.10.010>
81. Tse JR, Engler AJ (2010) Preparation of hydrogel substrates with tunable mechanical properties. *Curr Protoc Cell Biol*:1–16. <https://doi.org/10.1002/0471143030.cb1016s47>
82. Zhuang Z, Zhang Y, Sun S et al (2020) Control of matrix stiffness using methacrylate-gelatin hydrogels for a macrophage-mediated inflammatory response. *ACS Biomater Sci Eng* 6:3091–3102. <https://doi.org/10.1021/acsbomaterials.0c00295>
83. Hsieh JY, Keating MT, Smith TD et al (2019) Matrix crosslinking enhances macrophage adhesion, migration, and inflammatory activation. *APL Bioeng* 3:016103. <https://doi.org/10.1063/1.5067301>
84. Baker BM, Trappmann B, Wang WY et al (2015) Cell-mediated fibre recruitment drives extracellular matrix mechanosensing in engineered fibrillar microenvironments. *Nat Mater* 14:1262–1268. <https://doi.org/10.1038/nmat4444>
85. Yang YL, Motte S, Kaufman LJ (2010) Pore size variable type I collagen gels and their interaction with glioma cells. *Biomaterials* 31:5678–5688. <https://doi.org/10.1016/j.biomaterials.2010.03.039>

86. Kühnbach C, da Luz S, Baganz F et al (2018) A microfluidic system for the investigation of tumor cell extravasation. *Bioengineering* 5. <https://doi.org/10.3390/bioengineering5020040>
87. Heydarkhan-Hagvall S, Schenke-Layland K, Dhanasopon AP et al (2008) Three-dimensional electrospun ECM-based hybrid scaffolds for cardiovascular tissue engineering. *Biomaterials* 29:2907–2914. <https://doi.org/10.1016/j.biomaterials.2008.03.034>
88. O'Brien FJ, Harley BA, Yannas IV, Gibson L (2004) Influence of freezing rate on pore structure in freeze-dried collagen-GAG scaffolds. *Biomaterials* 25:1077–1086. [https://doi.org/10.1016/S0142-9612\(03\)00630-6](https://doi.org/10.1016/S0142-9612(03)00630-6)
89. Atcha H, Meli VS, Davis CT et al (2021) Crosstalk between CD11b and Piezo1 mediates macrophage responses to mechanical cues. *Front Immunol* 12:1–14. <https://doi.org/10.3389/fimmu.2021.689397>
90. Atcha H, Jairaman A, Holt JR et al (2021) Mechanically activated ion channel Piezo1 modulates macrophage polarization and stiffness sensing. *Nat Commun* 12:1–14. <https://doi.org/10.1038/s41467-021-23482-5>
91. Garg K, Pullen NA, Oskeritzian CA et al (2013) Macrophage functional polarization (M1/M2) in response to varying fiber and pore dimensions of electrospun scaffolds. *Biomaterials* 34:4439–4451. <https://doi.org/10.1016/j.biomaterials.2013.02.065>
92. Cui X, Guo W, Sun Y et al (2017) A microfluidic device for isolation and characterization of transendothelial migrating cancer cells. *Biomicrofluidics* 11:014105. <https://doi.org/10.1063/1.4974012>
93. Poltavets V, Kochetkova M, Pitson SM, Samuel MS (2018) The role of the extracellular matrix and its molecular and cellular regulators in cancer cell plasticity. *Front Oncol* 8:1–19. <https://doi.org/10.3389/fonc.2018.00431>
94. Wang N, Tytell JD, Ingber DE (2009) Mechanotransduction at a distance: mechanically coupling the extracellular matrix with the nucleus. *Nat Rev Mol Cell Biol* 10:75–82. <https://doi.org/10.1038/nrm2594>
95. Cui K, Ardell CL, Podolnikova NP, Yakubenko VP (2018) Distinct migratory properties of M1, M2, and resident macrophages are regulated by  $\alpha\beta 2$  and  $\alpha\mu\beta 2$  integrin-mediated adhesion. *Front Immunol* 9:1–14. <https://doi.org/10.3389/fimmu.2018.02650>
96. Sándor N, Lukácsi S, Ungai-Salánki R et al (2016) CD11c/CD18 dominates adhesion of human monocytes, macrophages and dendritic cells over CD11b/CD18. *PLoS One* 11:1–17. <https://doi.org/10.1371/journal.pone.0163120>
97. Sen S, Kumar S (2009) Cell-matrix de-adhesion dynamics reflect contractile mechanics. *Cell Mol Bioeng* 2:218–230. <https://doi.org/10.1007/s12195-009-0057-7>
98. Fuhrmann A, Banisadr A, Beri P et al (2017) Metastatic state of cancer cells may be indicated by adhesion strength. *Biophys J* 112:736–745. <https://doi.org/10.1016/j.bpj.2016.12.038>
99. Lee G, Cho Y, Kim EH et al (2022) Pillar-based mechanical induction of an aggressive tumorigenic lung cancer cell model. *ACS Appl Mater Interfaces* 14:20–31. <https://doi.org/10.1021/acsami.1c12380>
100. Beri P, Popravko A, Yeoman B et al (2020) Cell adhesiveness serves as a biophysical marker for metastatic potential. *Cancer Res* 80:901–911. <https://doi.org/10.1158/0008-5472.CAN-19-1794>
101. Griffin MA, Engler AJ, Barber TA et al (2004) Patterning, prestress, and peeling dynamics of myocytes. *Biophys J* 86:1209–1222. [https://doi.org/10.1016/S0006-3495\(04\)74195-8](https://doi.org/10.1016/S0006-3495(04)74195-8)
102. Hoffmann EJ, Ponik SM (2020) Biomechanical contributions to macrophage activation in the tumor microenvironment. *Front Oncol* 10:1–11. <https://doi.org/10.3389/fonc.2020.00787>
103. Murrell M, Oakes PW, Lenz M, Gardel ML (2015) Forcing cells into shape: the mechanics of actomyosin contractility. *Nat Rev Mol Cell Biol* 16:486–498. <https://doi.org/10.1038/nrm4012>
104. Sheetz MP, Felsenfeld DP, Galbraith CG (1998) Cell migration: regulation of force on extracellular-matrix-integrin complexes. *Trends Cell Biol* 8:51–54. [https://doi.org/10.1016/S0962-8924\(98\)80005-6](https://doi.org/10.1016/S0962-8924(98)80005-6)
105. Ngo P, Ramalingam P, Phillips JA, Furuta GT (2006) Collagen gel contraction assay. *Methods Mol Biol* 341:103–109. <https://doi.org/10.1385/1-59745-113-4:103>

106. Zhang T, Day JH, Su X et al (2019) Investigating fibroblast-induced collagen gel contraction using a dynamic microscale platform. *Front Bioeng Biotechnol* 7:1–9. <https://doi.org/10.3389/fbioe.2019.00196>
107. Dembo M, Wang Y (1999) Stresses at the cell-to-substrate interface during locomotion of fibroblasts. *Biophys J* 76:2307–2316
108. Ladoux B, Nicolas A (2012) Physically based principles of cell adhesion mechanosensitivity in tissues. *Rep Prog Phys* 75:116601. <https://doi.org/10.1088/0034-4885/75/11/116601>
109. Butler JP, Tolic-Norrelykke IM, Fabry B, Fredberg JJ (2002) Traction fields, moments, and strain energy that cells exert on their surroundings. *AJP Cell Physiol* 282:C595–C605. <https://doi.org/10.1152/ajpcell.00270.2001>
110. Lekka M, Gnanachandran K, Kubiak A et al (2021) Traction force microscopy – measuring the forces exerted by cells. *Micron* 150:103138. <https://doi.org/10.1016/j.micron.2021.103138>
111. Li Z, Persson H, Adolffson K et al (2017) Cellular traction forces: a useful parameter in cancer research. *Nanoscale* 9:19039–19044. <https://doi.org/10.1039/c7nr06284b>
112. Hind LE, Lurier EB, Dembo M et al (2016) Effect of M1–M2 polarization on the motility and traction stresses of primary human macrophages. *Cell Mol Bioeng* 9:455–465. <https://doi.org/10.1007/s12195-016-0435-x>
113. Cho Y, Park EY, Ko E et al (2016) Recent advances in biological uses of traction force microscopy. *Int J Precis Eng Manuf* 17:1401–1412. <https://doi.org/10.1007/s12541-016-0166-x>
114. Vorselen D, Wang Y, de Jesus MM et al (2020) Microparticle traction force microscopy reveals subcellular force exertion patterns in immune cell–target interactions. *Nat Commun* 11:20. <https://doi.org/10.1038/s41467-019-13804-z>
115. Köhrmann A, Kammerer U, Kapp M et al (2009) Expression of matrix metalloproteinases (MMPs) in primary human breast cancer and breast cancer cell lines: new findings and review of the literature. *BMC Cancer* 9:1–20. <https://doi.org/10.1186/1471-2407-9-188>
116. Wolf K, Wu YI, Liu Y et al (2007) Multi-step pericellular proteolysis controls the transition from individual to collective cancer cell invasion. *Nat Cell Biol* 9:893–904. <https://doi.org/10.1038/ncb1616>
117. Yu X, Zech T, McDonald L et al (2012) N-WASP coordinates the delivery and F-actin-mediated capture of MT1-MMP at invasive pseudopods. *J Cell Biol* 199:527–544. <https://doi.org/10.1083/jcb.201203025>
118. Marchesin V, Castro-Castro A, Lodillinsky C et al (2015) ARF6-JIP3/4 regulate endosomal tubules for MT1-MMP exocytosis in cancer invasion. *J Cell Biol* 211:339–358. <https://doi.org/10.1083/jcb.201506002>
119. Toth M, Sohail A, Fridman R (2012) Assessment of gelatinases (MMP-2 and MMP-9) by gelatin. *Metastasis Res Protoc* 878:121–135. <https://doi.org/10.1007/978-1-61779-854-2>
120. Liu R, Wang X, Chen GY et al (2015) The prognostic role of a gene signature from tumorigenic breast-cancer cells. *N Engl J Med* 352:687–696
121. Ohnstad HO, Borgen E, Falk RS et al (2017) Prognostic value of PAM50 and risk of recurrence score in patients with early-stage breast cancer with long-term follow-up. *Breast Cancer Res* 19:1–12. <https://doi.org/10.1186/s13058-017-0911-9>
122. Perou CM, Sirlie T, Eisen MB et al (2000) Molecular portraits of human breast tumours. *Nature* 533:747–752
123. Van Veer LJ, Dai H, Van De Vijver MJ et al (2002) Gene expression profiling predicts clinical outcome of breast cancer. *Nature* 415:530–536. <https://pubmed.ncbi.nlm.nih.gov/11823860/>
124. De Vijver V, He YD, Van Veer LJ et al (2002) A gene-expression signature as a predictor of survival in breast cancer. *N Engl J Med* 347:1999–2009
125. Paik S, Tang G, Shak S et al (2006) Gene expression and benefit of chemotherapy in women with node-negative, estrogen receptor-positive breast cancer. *J Clin Oncol* 24:3726–3734. <https://doi.org/10.1200/JCO.2005.04.7985>
126. Chang HY, Nuyten DSA, Sneddon JB et al (2005) Robustness, scalability, and integration of a wound-response gene expression signature in predicting breast cancer survival. *Proc Natl Acad Sci U S A* 102:3738–3743. <https://doi.org/10.1073/pnas.0409462102>

127. Parker JS, Mullins M, Cheung MCU et al (2009) Supervised risk predictor of breast cancer based on intrinsic subtypes. *J Clin Oncol* 27:1160–1167. <https://doi.org/10.1200/JCO.2008.18.1370>
128. Wallden B, Storhoff J, Nielsen T et al (2015) Development and verification of the PAM50-based prognostic breast cancer gene signature assay. *BMC Med Genet* 8:1–14. <https://doi.org/10.1186/s12920-015-0129-6>
129. Filipits M, Rudas M, Jakesz R et al (2011) A new molecular predictor of distant recurrence in ER-positive, HER2-negative breast cancer adds independent information to conventional clinical risk factors. *Clin Cancer Res* 17:6012–6020. <https://doi.org/10.1158/1078-0432.CCR-11-0926>
130. Bergamaschi A, Tagliabue E, Sørlie T et al (2008) Extracellular matrix signature identifies breast cancer subgroups with different clinical outcome. *J Pathol* 214:357–367. <https://doi.org/10.1002/path>
131. Farmer P, Bonnefoi H, Anderle P et al (2009) A stroma-related gene signature predicts resistance to neoadjuvant chemotherapy in breast cancer. *Nat Med* 15:68–74. <https://doi.org/10.1038/nm.1908>
132. Li Y, Zhao X, Liu Q, Liu Y (2021) Bioinformatics reveal macrophages marker genes signature in breast cancer to predict prognosis. *Ann Med* 53:1019–1031. <https://doi.org/10.1080/07853890.2021.1914343>
133. Cassetta L, Fragkogianis S, Sims AH et al (2019) Human tumor-associated macrophage and monocyte transcriptional landscapes reveal cancer-specific reprogramming, biomarkers, and therapeutic targets. *Cancer Cell* 35:588–602.e10. <https://doi.org/10.1016/j.ccell.2019.02.009>
134. Provenzano PP, Inman DR, Eliceiri KW et al (2008) Collagen density promotes mammary tumor initiation and progression. *BMC Med* 6:1–15. <https://doi.org/10.1186/1741-7015-6-11>
135. Oskarsson T (2013) Extracellular matrix components in breast cancer progression and metastasis. *Breast* 22:S66–S72. <https://doi.org/10.1016/j.breast.2013.07.012>
136. Chakravathy A, Khan L, Bensler NP et al (2018) TGF- $\beta$ -associated extracellular matrix genes link cancer-associated fibroblasts to immune evasion and immunotherapy failure. *Nat Commun* 9:1–10. <https://doi.org/10.1038/s41467-018-06654-8>
137. Naba A, Clauser KR, Lamar JM et al (2014) Extracellular matrix signatures of human mammary carcinoma identify novel metastasis promoters. *elife* 2014:1–23. <https://doi.org/10.7554/eLife.01308>
138. Ibrahim AM, Moss MA, Gray Z et al (2020) Diverse macrophage populations contribute to the inflammatory microenvironment in premalignant lesions during localized invasion. *Front Oncol* 10:1–16. <https://doi.org/10.3389/fonc.2020.569985>
139. Azizi E, Carr AJ, Plitas G et al (2018) Single-cell map of diverse immune phenotypes in the breast tumor microenvironment. *Cell* 174:1293–1308.e36. <https://doi.org/10.1016/j.cell.2018.05.060>
140. Pickup MW, Mouw JK, Weaver VM (2014) The extracellular matrix modulates the hallmarks of cancer. *EMBO Rep* 15:1243–1253. <https://doi.org/10.15252/embr.201439246>
141. Finkernagel F, Reinartz S, Lieber S et al (2016) The transcriptional signature of human ovarian carcinoma macrophages is associated with extracellular matrix reorganization. *Oncotarget* 7:75339–75352. <https://doi.org/10.18632/oncotarget.12180>
142. Wei S, Lu J, Lou J et al (2020) Gastric cancer tumor microenvironment characterization reveals stromal-related gene signatures associated with macrophage infiltration. *Front Genet* 11:1–16. <https://doi.org/10.3389/fgene.2020.00663>
143. Kohli AG, Kivimäe S, Tiffany MR, Szoka FC (2014) Improving the distribution of Doxil<sup>®</sup> in the tumor matrix by depletion of tumor hyaluronan. *J Control Release* 191:105–114. <https://doi.org/10.1016/j.jconrel.2014.05.019>
144. Fields GB (2019) The rebirth of matrix metalloproteinase inhibitors: moving beyond the dogma. *Cell* 8:20–23. <https://doi.org/10.3390/cells8090984>



145. Murdocca M, De Masi C, Pucci S et al (2021) LOX-1 and cancer: an indissoluble liaison. *Cancer Gene Ther* 28:1088–1098. <https://doi.org/10.1038/s41417-020-00279-0>
146. Kim S, Kim SA, Han J, Kim IS (2021) Rho-kinase as a target for cancer therapy and its immunotherapeutic potential. *Int J Mol Sci* 22. <https://doi.org/10.3390/ijms222312916>
147. Liu L, He F, Yu Y, Wang Y (2020) Application of FRET biosensors in mechanobiology and mechanopharmacological screening. *Front Bioeng Biotechnol* 8:1–17. <https://doi.org/10.3389/fbioe.2020.595497>
148. Hoppe AD, Swanson JA (2004) Cdc42, Rac1, and Rac2 display distinct patterns of activation during phagocytosis. *Mol Biol Cell* 15:3509–3519. <https://doi.org/10.1091/mbc.E03>

# Engineering Approaches in Ovarian Cancer Cell Culture



Marcin Iwanicki, Tonja Pavlovic, and Panteha Behboodi

**Abstract** Determination of the frequency of somatic mutations, copy number variations, and the composition of single-nucleus transcriptomes in epithelial ovarian cancer (OC) biopsies have provided crucial information about the heterogeneity of cancer cell assemblies and their various tumor microenvironments (TMs). Translating this information into tumor biology for the discovery of new treatments could be accomplished by the engineering tissue culture models of OC within its TM.

**Keywords** Biomaterial · Dissemination · Endometrium · Fallopian tubes · Mesothelium · Microfluidic · Organoid · Organotypic culture

## 1 Introduction

OC remains a major health problem among women because the disease often progresses after treatment is completed [1]. Standard-of-care approaches to disease management can involve cytoreductive surgery followed by platin-/taxane-based cytotoxic therapies and targeted inhibitions of angiogenic and/or DNA repair mechanisms [2]. However, despite these aggressive interventions, tumors continue to grow [3], signifying a need to further understand disease progression after therapy.

While genomic, transcriptomic, and proteomic analysis of tumor tissues [3–9] will continue to play a major role in tracking the diversification of tumors and the identification of new therapeutic targets, these analyses will need to be supplemented with disease-relevant assays that can resolve the functional consequences of

---

M. Iwanicki (✉) · T. Pavlovic  
Departments of Chemistry, Chemical Biology, Hoboken, NJ, USA  
e-mail: [marcin.iwanicki@stevens.edu](mailto:marcin.iwanicki@stevens.edu)

P. Behboodi  
Chemical Engineering and Materials Science, Hoboken, NJ, USA



disease evolution for a better understanding of the mechanisms of OC cell growth and treatment response.

Traditional *in vitro* approaches to study OC involve cancer cell monolayers or suspended spheroid cultures of established OC cell lines or short-term cultures of patient-derived cells [10]. These tissue culture methods provide high reproducibility, but they are limited to studying tumor cells in isolation and might not preserve the heterogeneous nature of human tumors. In contrast, mouse models that are grafted with excised human tumor fragments have been used in pre-clinical studies and currently represent the most relevant platform to study tumor growth and therapy response [11]. However, these models lack components of human TMs; they are expensive and generally not applicable to discovery screens to identify new treatments for OC growth within TMs. Therefore, a need exists for methods that would fill the gap between traditional tissue culture approaches (monolayers and spheroids) and xenografts to study the disease.

Collaborations among clinicians, tumor biologists, immunologists, and bioengineers can offer a prospect to move beyond OC cell monolayers and spheroids and increase the complexity of *in vitro* OC tissue culture systems. Recently, the field has seen an advance in the engineering of cellular approaches that incorporate reconstituted basement membranes, novel growth factors, cell–cell interactions, and fluid mechanics. The intention of this book chapter, entitled *Engineering Approaches in Ovarian Cancer Cell Culture*, is to provide basic information about OC progression and present an overview of traditional and newly emerging tissue engineering culture models that are intended to mimic disease phenotypes. These evolving culture techniques might offer a unique opportunity to better understand the mechanisms of OC and provide, in addition to mouse models, an opportunity to examine more directions for the evaluation of clinical and experimental therapeutics.

## 2 OC Progression

### 2.1 Initiation

OC can originate from the epithelium of the reproductive tract including the endometrium, ovaries, and the fallopian tubes [12–14]. Based on histopathology and tumoral genetics, the disease has been classified as type I or type II cancers [15] (Table 1). Type I cancers include low-grade endometrioid, mucinous, low-grade serous, and clear cell carcinomas. Endometrioid tumors have mutations in phosphatase and tensin homology (*PTEN*) and catenin beta 1 (*CTNNB1*) genes [16–18]. In mucinous tumors, the tumor protein P53 gene (*TP53*) is highly mutated (>50%) and frequent mutations are also observed in the Kirsten rat sarcoma viral oncogene (*KRAS*) pathway [19]. Clear cell tumors are frequently associated with mutations in *KRAS*, *PTEN*, and phosphatidylinositol-4,5-bisphosphate 3-kinase catalytic subunit alpha (*PIK3CA*) [18]. Low-grade serous carcinomas are predominantly characterized by mutational activation of *KRAS* pathways [20]. The most

**Table 1** OC types and subtypes with reported mutations

OC main types	OC subtypes	Mutations	References (PMID)
Type I	Endometrioid	<i>PTEN</i> , <i>CTNNB1</i> , <i>PPP2R1<math>\alpha</math></i> , MMR deficient, <i>ARID1A</i>	[16–18], [21]
	Mucinous	<i>KRAS</i> , <i>HER-2</i> amplification	[21–26]
	Clear cell	<i>PIK3CA</i> , <i>KRAS</i> , <i>PTEN</i> , <i>ARID1A</i>	[18], [27], [21], [28–31]
	Low-grade serous	<i>BRAF</i> , <i>KRAS</i> , <i>NRAS</i> , <i>ERBB2</i>	[20], [21], [32–34]
Type II	High-grade serous	<i>TP53</i> , <i>BRCA1</i> , <i>BRCA2</i> , <i>CDK12</i>	[21], [35–39]

prevalent among women are type II OCs that include high-grade serous ovarian carcinomas (HGSOCs) [1]. These tumors are characterized by the omnipresence of *TP53* mutations, a high degree of copy number variations, and defects in DNA repair pathways [1].

Until recently, it was thought that most OCs, such as HGSOCs, initiate from the superficial single mesothelial cell layer that encloses ovaries. However, with the advancement of tissue sectioning methodologies, examination of whole fallopian tubes revealed secretory epithelial cells as a candidate site of origin for HGSOC [40]. Neoplastic fallopian tube lesions referred to as serous tubal intraepithelial carcinomas (STICs) have been identified in women carrying mutations in breast and ovarian cancer susceptibility protein 1 (*BRCA1*), and pathologic examination of STICs shows strong expression of Ki67 and p53 proteins, an indication of the loss of p53-mediated control of the cell cycle [41]. Follow-up studies [42, 43] using genomic analysis of STICs and matched disseminated HGSOCs confirmed near-ubiquitous loss of *TP53* heterozygosity and discovered additional genetic alterations that were shared between early (in the fallopian tube) and late (disseminated within peritoneal cavity) tumors, giving strong support that HGSOC can originate not only from the ovarian mesothelium but also from the fallopian tube epithelium.

Secretory epithelial cells, along with the ciliated epithelial cells, polarize to form the mucosal layer of the fallopian tube [44], and clinical observations support the idea that transformation could occur in secretory cells expressing paired box 8 (*PAX8*) transcription factor [45]. Loss of tumor suppression, through targeted disruptions of *Tp53*, *Pten*, and *Brca1* alleles in *Pax8*-positive murine fallopian tube secretory cells can evoke HGSOC development [46], highlighting the important role of secretory cell biology in tumor initiation. However, a direct comparison of tumorigenic potential between secretory epithelial cells of the fallopian tube and mesothelial cells of the ovary revealed that the same genetic manipulations can initiate HGSOC from both cell types in a genetically modified mouse model [47]. These experiments are consistent with the hypothesis that multiple and distinct tissues, upon transformation, can initiate HGSOC.

In addition to a tumor's intrinsic mutations in *TP53*, *PTEN*, and *BRCA1* genes, extrinsic microenvironmental factors, including deposition, and remodeling of extracellular matrix (ECM) have been associated with HGSOC initiation [48, 49].

Immunohistochemical and second harmonic two-photon microscopic evaluation of STICs documented the extensive presence of laminin  $\gamma 1$  [48] within carcinoma tissue and the presence of dense collagen fibers in the adjacent microenvironment [50]. Therefore, OC initiation from the fallopian tube could also be linked to the formation of at least two ECM TMs that support growth and dissemination. In contrast to mutations in tumor suppressor genes, the roles of these ECM TMs in tubal tumorigenesis are currently unknown, as new ECM-reconstituted tissue culture approaches that mimic the spatial organization of laminin  $\gamma 1$  and collagens are being developed to study the contributions of these factors. In addition to ECM, immune cell dynamics have been shown to associate with the expansion of fallopian tube epithelium [51]; however, it is not clear whether recruitment of these cell types is caused by tumor initiation, e.g., due to *BRCA1/BRCA2* alterations, or normal growth homeostasis of tubal tissue. Current *in vitro* models of fallopian tube transformation involve monolayer or ECM-reconstituted cultures that can assess the role of tumor suppressors or proto-oncogenes in tubal tumorigenesis.

## 2.2 Dissemination

Type I and type II OCs share a common metastatic site, the peritoneum [52]. Peritoneal dissemination of OCs is a result of malignant tissue detachment from primary or secondary sites (fallopian tube, ovary, omentum) and subsequent translocation of detached tumors into the peritoneal cavity [53, 54] (Fig. 1). After detachment, surviving tumor clusters can establish solid implants by intercalation into the superficial mesothelial cell layers covering nearby organs, including the ovary, bowel, and the omentum [55]. While the biological processes that promote OC detachment are unknown, the mechanism associated with the survival of detached tumor clusters and their attachment to, and intercalation into, the mesothelium is beginning to be better understood. Suspended OC cell cultures (spheroids) of established cell lines or patient-derived cells are considered to partially mimic conditions of OC tumors that float within the peritoneal cavity after detachment [56]. In contrast to monolayer cultures, spheroids display increased activation of molecular programs involved in: (a) anti-apoptotic signaling [57], (b) ECM production [58], and (c) activation of stem cell regulatory components including mesenchyme transcription [59] and enzymes involved in aldehyde metabolism [60]. Spheroids can adhere to and intercalate into mesothelial cell monolayers that enclose peritoneal organs [61]. The mechanisms associated with OC adhesion to the mesothelium have been linked to the expression of various ECM, cell–matrix, and cell–cell adhesion molecules on mesothelial and OC cells [62–64]. Mesothelial cells, in response to TGF $\beta$  secreted by tumor cells, can produce and deposit fibronectin and collagens on their lateral surfaces and engage integrins expressed on OC cells [65]. These ECM–integrin interactions mediate activation of actomyosin contractility to promote force-induced mesothelial cell displacement from beneath the intercalating spheroids [66]. In addition to integrins, cadherins [67] and hyaluronic acid receptors [68] mediate the adhesion

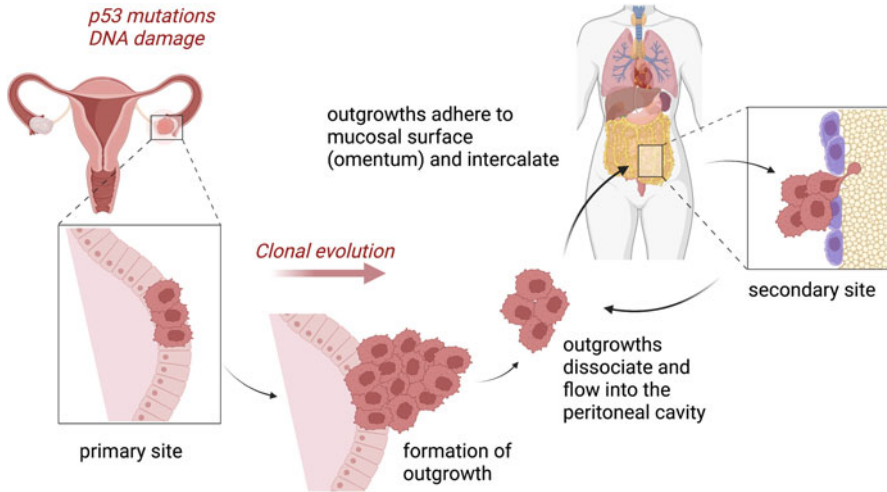


**Fig. 1** Mode of OC dissemination. Transformed epithelial cells form outgrowths at the primary site, the fallopian tube. These outgrowths eventually dissociate and translocate into the peritoneal cavity where they adhere to the surface of omentum and intercalate into mesothelial cell layers

of OC cells to mesothelial monolayers, and tetraspanins [69] contribute to integrin activation and control mesothelial intercalation. The expression of cell–matrix and cell–cell adhesion receptors that mediate OC cell adhesion to the mesothelium is largely regulated by the activity of OC-associated mesenchymal transcription factors (MTFs), and recent studies support the role of MTFs, such as ZEB, TWIST, and SNAIL in controlling mesothelial intercalation [61]. The cell culture models that examine OC spheroids’ capabilities to intercalate into mesothelium involve the co-culture of spheroids on the top of the monolayers composed of mesothelial cells expressing fluorescent proteins [70]. Under these culture conditions, fluorescent mesothelial cells contact OC spheroids and can migrate away (clear) from the initial site of spheroid attachment. The migration of mesothelial cells creates a hole in the monolayer, and the hole can be visualized by the loss of fluorescent intensity. The size of the hole is measured and correlated with the spheroid’s size to estimate the degree of intercalation.

### 2.3 OC Metastatic Microenvironment

Ovarian tumors predominantly metastasize to the mesothelial cell layer that covers the adipocyte-rich tissues of the omentum [55]. Intercalation of tumors into omental tissues results in direct contact between carcinoma and omental TMs [71]. These new interactions are important for tumor growth [52]. For instance, tumor contact with adipocytes activates lipolysis that promotes the growth of OC cells within

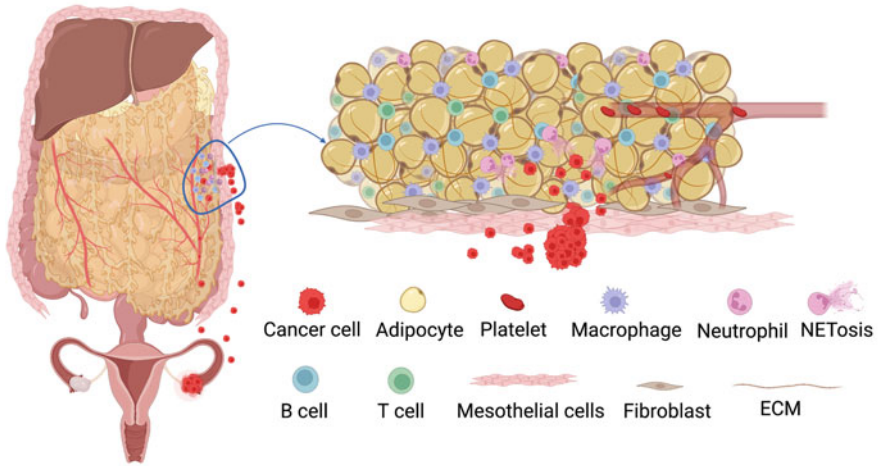


**Fig. 2** OC metastatic microenvironment. Metastasis of OC cells into the mesothelial cell layer and the omental tissue. Several cellular components and non-cellular components in the TM including adipocytes, macrophages, neutrophils, NETosis, and ECM can promote OC growth and progression

the omentum [71]. In addition to adipocytes, cancer-associated fibroblasts [72], macrophages [73], and neutrophils [74] have been implicated in supporting disease progression in the context of tumor metastasis. For instance, extravasated neutrophils that take residence within omentum, through the tumor-induced NETosis, a form of neutrophil death resulting in the formation of neutrophil extracellular traps (NETs), can support OC adhesion to the mesothelium and subsequent tumor expansion [74] (Fig. 2). Fibroblasts, mesothelial cells, and platelets in response to tumor-derived TGF $\beta$  and/or IL6 activate ECM production that can support OC cells [65, 75, 76]. Engineering cell cultures that can mimic ECM deposition by stroma in the context of tumor metastasis can provide an opportunity to test whether stroma-specific ECM programs could be exploited as a vulnerability to target disseminated OC. Recently developed organotypic models (discussed in technical detail below), which mimic ECM deposition observed in solid OC omental metastases [75, 76], began to address the possibility of targeting ECM through inhibition of cancer-associated fibroblasts or platelets. The incorporation of other cellular components including immune cells and endothelium will improve the modeling of the spectrum of OC cell interactions with nearby microenvironments.

## 2.4 Tumor Expansion After Therapy

Chemotherapy can induce genomic and transcriptomic changes in OC [8], and dissemination continues after chemotherapy because detached tumor cell assemblies

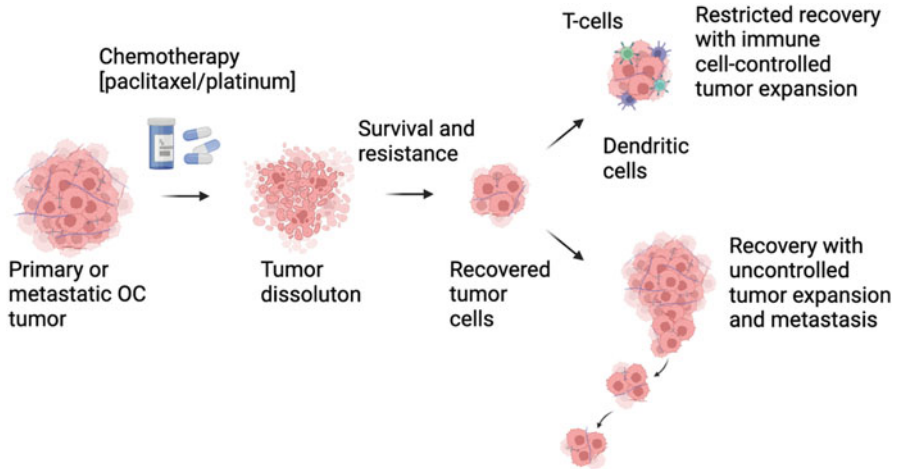


**Fig. 3** Tumor recovery after chemotherapy. Chemotherapy reduces primary and/or metastatic tumors by killing most OC cells. However, a subset of tumor cells survive and recover, resulting in recurrent disease. Recovered OC tumors can continue expanding uncontrollably, metastasizing even further. In some cases, however, tumor cells that survive initial chemotherapy face restricted growth, which can be modulated by immune cells

are detected in patients with recurrent disease [3]. While genetic-guided approaches have identified chemotherapy-induced alterations that could potentially be leveraged to sensitize OC cells to a new treatment, the role of TMs in modulating tumor recovery from chemotherapy is largely unknown. Most recent studies implicate that some residual tumors can form new metastases between or after treatment's regimens, and their evolution appears to be controlled by the dynamics of immune cell recruitment into tumors [3] (Fig. 3). OC mouse models, which are the gold standard for translational OC research [77], often lack appropriate immune components. Hence, tissue culture engineering of immune response in the context of chemotherapy could supplement mouse models to determine immune mechanisms that support or restrict the disease.

### 3 In Vitro Modeling of OC: What to Consider Before Starting the Project

The pathology-driven knowledge of tumor cell phenotypes and molecular characteristics of the disease offers enthusiasm to engineer OC culture systems. The use of appropriate OC cells has been crucial in disease modeling, since the initial finding that frequently utilized cell lines in OC research, SKOV3, and A2780, were not representative of the most prevalent type of OC, HGSOC [78]. Hence, knowing which OC cell lines represent what type of OC is key information to starting tissue

culture models. There are several resource papers that should help investigators to choose appropriate cell lines for projects [79–83]. If patient-derived tumor cells are used, the investigators usually confirm the expression of PAX8 protein, the Müllerian transcriptional factor expressed by most HGSOCS, and the presence of mutated *TP53* alleles. These two molecular markers are routinely used in pathology to diagnose HGSOCS; thus, they would represent a good confirmation of OC cells used in culture.

Tumor growth, detachment, abdominal dissemination, and establishment of solid peritoneal metastases are key biological characteristics of OC progression. To model these phenotypes, various culture approaches have been developed (described in technical details below) using adhered, suspended, ECM-reconstituted, and multicell type co-culture systems. Combining immunohistochemistry and molecular genetics became a good approach to compare in vitro engineered models with human OC biopsies. The similarities between the topographical locations of different types of cells and ECM within biopsies and engineered cultures determine the validity of the model. Below, we discuss traditional and emerging culture models of OC and its TMs.

## **4 In Vitro Culture Models of OC**

### ***4.1 Two-Dimensional (2D) Tissue Cultures***

Two-dimensional tissue cultures can provide a quick, reproducible, and high-throughput approach to evaluate OC cell culture growth, migration, and treatment response. These methods usually involve culturing monotypic cells on flat surfaces such as the bottom of culture ware (Fig. 4). Under 2D culture conditions, cells form substrate adhesion complexes that mediate cell spreading leading to the formation of flat monolayers (Fig. 4). The monolayers are artificial because they reflect the response of cells to substrates with stiffness far beyond tissues where OC develops and grows after dissemination. However, the establishment of patient-derived OC cell lines frequently involves 2D cultures, and recently, a combination of 2D cultures and defined cell culture media led to the derivation of 25 OC cell lines, which phenocopied genetic landscapes of type I or type II tumors [84]. These cell lines have been used in multiple studies [85–88] and represent well-validated and important cellular models of OC.

### ***4.2 Spheroid Cultures***

One of the characteristics of metastatic OC is the enrichment of detached tumor clusters within the peritoneal cavity. These floating cellular assemblies are often



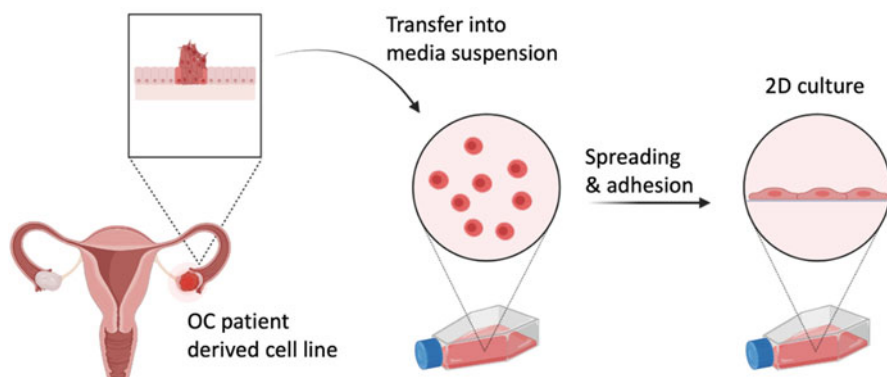


**Fig. 4** Establishment of the classic 2D culture method. Cells are extracted from an OC patient during biopsy, isolated, and transferred into specialized media. Individual cells suspended in media begin to attach and spread on the provided surface if supplied with correct growth stimulants. Some patient-derived cells can be propagated and cryopreserved

referred to as spheroids [89]. To partially mimic spheroids *in vitro*, OC cell cultures are initiated under non-adherent conditions, which can be achieved by coating adherent surfaces with adhesion blocking solutions such as poly(2-hydroxyethyl methacrylate) (pHEMA) or poloxamers including Pluronics<sup>®</sup> (Fig. 5). In these culture environments, single cells clump to form cell assemblies that can evolve into spherical structures. Spheroid cultures are frequently established using ultra-low adhesion 96-well plates, where single cells are plated to form one suspended spheroid [90]. The recent integration of spheroid cultures with quantitative imaging provided an attractive approach to studying the dynamics of spheroid formation and the role of suspended cell–cell interaction in OC survival and growth [91]. It has become apparent that, as *in vivo*, cells that make spheroids use intercellular interactions to self-organize and, as opposed to 2D cultures, form structures resembling epithelial tumors. These phenotypic characteristics appear to correlate with resistance to therapeutics and the evolution of distinct phenotypes associated with the activation of various transcriptional and epigenetic programs that contribute to tumor progression *in vivo*. Therefore, spheroids continue to be a major tissue engineering approach to studying the mechanisms of OC growth, interaction with the microenvironment, and response to therapy.

### 4.3 Organotypic OC Cultures

Organotypic OC cultures represent cellular models that incorporate carcinoma cells and components of TMs. These approaches can integrate spheroids with ECM and/or 2D or 3D cultures of other cell types [75, 92]. The establishment



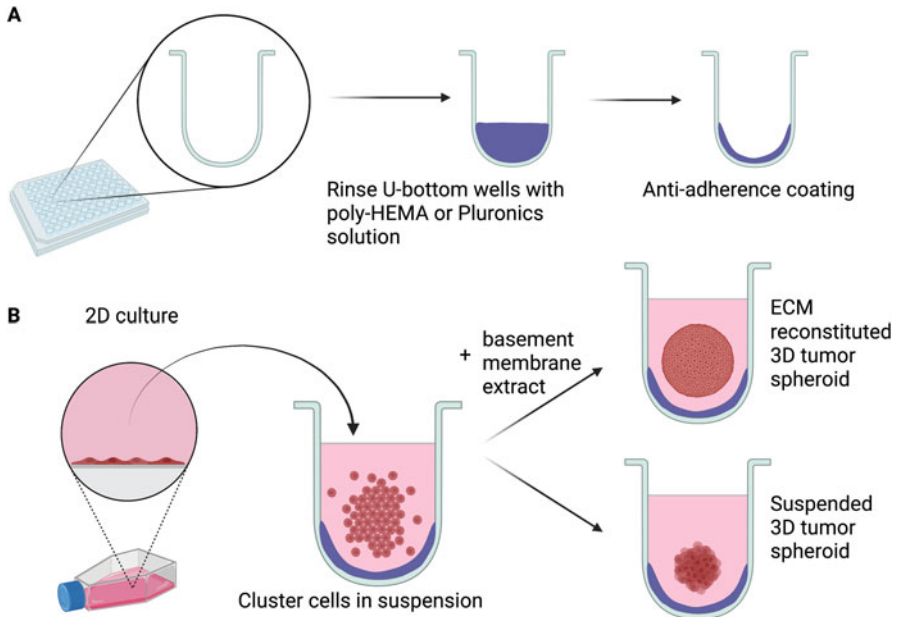


**Fig. 5** 3D tumor spheroid culture method. **(A)** 3D spheroid culture is generally started in a 96-well format (or 384-well format for high throughput) with round bottom wells. To prevent cell attachment and spreading, the bottom of each well is treated or coated with solutions to prevent adhesion. Examples of an anti-adherence surface treatment is poly-HEMA or Pluronic coating. **(B)** Method for establishing 3D spheroids from cell lines. Cells grown in 2D monolayer are detached and transferred to the round bottom wells in suspension. Suspended cells cluster at the bottom, whereas the anti-adherence surface treatment prevents cells from spreading across the surface. After formation of intercellular interactions, a 3D spheroid unit is formed. ECM components can be added to provide support and scaffolding around the 3D spheroid and thus reconstitute its specific microenvironment

of organotypic cultures is usually guided by the pathology examination of tissues that are intended to be modeled *in vitro*. For instance, a recent examination of OC outgrowths in the fallopian tubes or the ovaries revealed enrichment of laminin  $\gamma 1$  inside tumors and collagen deposition within tumor-adjacent connective tissue [48, 50, 93]. Guided by these observations, we have engineered an OC outgrowth model using suspended cultures of fallopian tube non-ciliated epithelial cells expressing mutant p53 (FNE-m-p53) reconstituted with low elasticity media containing laminin-/collagen-rich ECM [93]. This tissue mimetic was created by culturing 100 FNE-m-p53 cells as suspended 3D spheroids in single wells of an ultra-low attachment 96-well plate. Integration of this model with live cell imaging and quantitative image analysis revealed that cells forming outgrowths proliferate and translocate within the 3D structure. Outgrowths that protrude from an afflicted organ can detach and invade superficial layers of the mesothelial cells covering the omentum [94]. To model detached OC cell interaction with the omentum, the

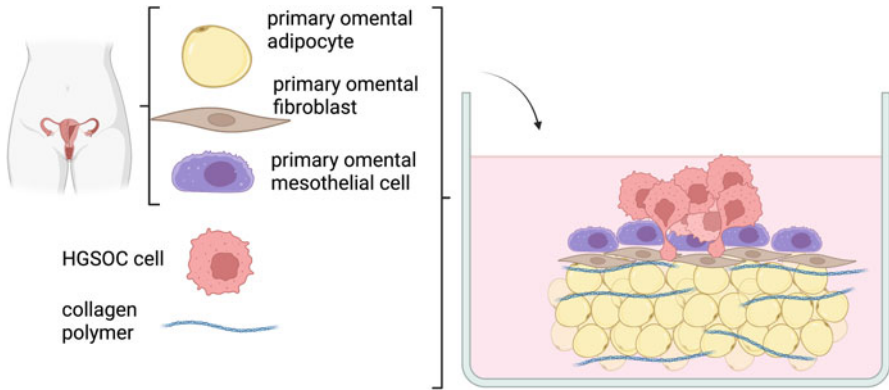


**Fig. 6** Multicellular organotypic models of human omental tissue. Primary omental adipocytes are cultured in a 3D substrate (collagen) to form a gel composed of adipocytes and collagen polymers. After addition of primary omental fibroblasts and mesothelial cells overlaying the adipocyte base, a multicellular culture recapitulates a normal omentum model. Incorporation of HGSOC cells takes the multicellular model further in mimicking the progress of omental metastasis

organotypic omental model has been engineered by integrating (into one culture system) omental mesothelial cells, omental fibroblasts, and collagen-/fibronectin-rich ECM that separates these cell types [65]. Omental fibroblasts were encapsulated within collagen-/fibronectin-rich matrices and plated on flat surfaces. Mesothelial cells were layered on top of the ECM-encapsulated fibroblasts (Fig. 6). This model has been used, in conjunction with mouse studies, to discover that detached OC cells reprogrammed mesothelial cells to self-deposit fibronectin that supported adhesion and growth of OC cells. Recently, this model has been extended to a high-throughput format to identify compounds that might target omental metastasis [95, 96]. Since the initial design, omental metastasis models have evolved significantly and now incorporate other cell types of the omentum. For instance, in a recently engineered model, omentum-derived adipocytes were embedded into collagen I gel, cultured for up to 7 days, and then integrated with carcinoma and fibroblasts that were previously reconstituted with collagen I gels. The cells and the ECM were co-cultured for additional 14 days. The resulting organotypic model of omental metastasis remarkably mimicked the architecture of omental tissue, and the cells maintained expression of molecular markers associated with carcinoma, fibroblasts, and adipocytes [75]. The same group has already extended this model to incorporate mesothelial cells and platelets and found that the addition of platelets further induced deposition of ECM by mesothelial cells [76]. These organotypic omental models currently represent the most advanced tissue engineering approaches to OC metastasis. Adaptation of these approaches to long-term culture, incorporation of immune cells and fluid flow, and integration with single-cell technologies will help to recreate OC progression and open possibilities to gain new knowledge about the mechanisms of tumor evolution in the context of TMs and response to treatment.

#### 4.4 Organoid Cultures of the Fallopian Tube and OC Cells

Organoids are broadly defined as ECM-embedded cultures of organs, tissues, or tissue-derived cells [97, 98]. Organ or tissue-specific organoid cultures involve embedding the entire cellular composition of an explant into ECM gels [99–102]. The explants can contain multiple types of cells that represent the epithelium and its microenvironment, including fibroblasts, adipocytes, and immune cells. Tissue-derived cell-type organoids are established from single cells, extracted from tissues by reconstituting with ECM [103]. The derivation of organoids from single cells depends on the clonal expansion of cells with stem-cell-like characteristics [104]. Recently, a variety of normal tissue-derived cell-type organoid models, which represents different tissue types, has been established to study cell differentiation and tissue development in vitro [97]. These include the intestines [105], liver [106], stomach [107], brain [108], breast [109], kidney [110], and fallopian tube [111]. Tissue-derived cell-type organoid cultures involve resuspension of single cells in Matrigel<sup>®</sup> (MG) or other types of ECM gels. An MG–cell suspension is positioned, in the form of domes, on the surface of the culture dish or a precast MG layer, and the domes are overlaid with a complete media containing tissue-specific growth factors, hormones, nutrients, and supplements (Fig. 7). In one of the first reports on establishing an organoid system, from single cells isolated from human fallopian tubes [111], Kessler et al. demonstrated clonal expansion and differentiation into ciliated and secretory cells forming cystic structures made of epithelial-tissue-like layer(s). The derivation of fallopian-tube-like epithelium depended on supplementation with novel growth factors activating Wnt and Notch signaling that supported expression of stem cell regulatory pathways including G-coupled protein receptor 6 (LGR6), olfactomedin 4, and the gene encoding Axin-

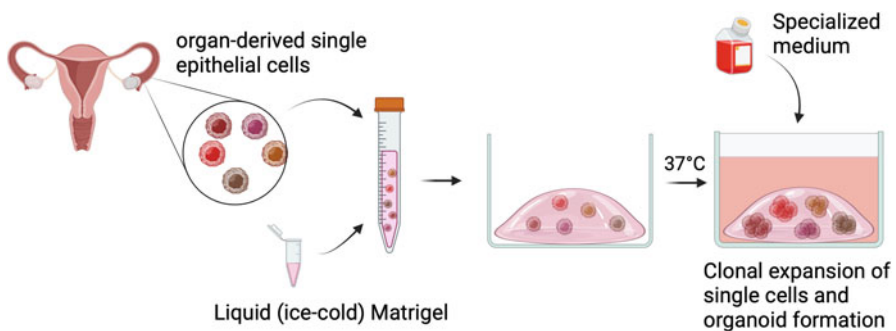


**Fig. 7** Establishment of tissue-derived cell-type organoids. Organoid cultures are established by isolation of single epithelial cells, followed by resuspension of cells in liquid (ice-cold) Matrigel<sup>®</sup> (MG). MG and cell suspension is then plated to form a liquid droplet at the bottom of the culture well. To crosslink MG, the liquid droplets are then incubated at 37° C to promote gelling and formation of domes, which tightly embed the organoids. Domes are subsequently overlaid with specialized media formulation containing specific growth factors and other supplements

related protein 2 (AXIN2) [111, 112]. In addition to studying cell differentiation and epithelial layer development, organoid culture approaches have been used as novel pre-clinical cell models to evaluate OC response to therapeutics. Using high ECM gel content and growth factors that stimulate Wnt and Notch signaling, Hill et al. demonstrated the feasibility of short-term culture of patient-derived OC organoids and their application to study response to DNA repair inhibitors [113]. The durability of patient-derived OC organoid cultures has been subsequently improved by the development of culture conditions that, through activation of bone morphogenetic protein (BMP) and the absence of Wnt signaling, supported long-term organoid propagation without loss of a tumor's genetic makeup [114, 115]. These studies provided proof of concept that OC organoids could represent an attractive, pre-clinical tissue engineering approach to study OC growth and therapy response.

#### ***4.5 OC Cultures with Natural and Synthetic Polymers***

MG reconstitution has been a preferred method of casting a natural 3D ECM scaffold to support organotypic or organoid OC cultures. However, the complexity of MG and variations among MG preparations constitute a major problem in reproducing the results and understanding the contribution of individual ECM components or a scaffold's physical characteristics to OC growth, survival, and chemotherapy resistance [116]. Non-MG-based hydrogels have recently emerged as highly reproducible 3D methods to grow OC cells in vitro [116]. Purified ECM components such as collagens [117] and laminins [118] can be used to form hydrogels and provide a controlled 3D ECM environment for cell culture. As opposed to MG, mechanical properties including viscoelasticity and porosity can be precisely tuned to mimic the mechanical characteristics of various tissues. In addition to natural ECM biomimetics, synthetic poly(ethylene glycol)-crosslinked poly(methyl vinyl ether-alt-maleic acid) hydrogels containing arginine-glycine-aspartic acid (RGD) molecules have been developed [119] to mimic ECM adhesion and study OC cell growth and chemotherapy response [120] (Fig. 8). There are several methods to fabricate ECM mimetics including freeze-drying, solvent casting, electrospinning, and 3D printing [121] to resemble the pathophysiological features of the ovarian tumor tissue (Fig. 9). Freeze-drying is a method to make a porous structure by sublimation of water ice crystals from frozen material. In the lyophilization or freeze-drying process, the material is first frozen and then placed under a high vacuum to convert the frozen water directly into vapor, finally leaving the original material in a solid state [122] (Fig. 9A). A second method is solvent casting to form a fibrous scaffold. The polymer is dissolved in an organic solvent, then salt is added to the polymeric solution, and the final dispersion is cast in silicone molds. After solvent evaporation, the sample is extracted from the mold and washed with DI water to remove the salt resulting in the formation of the final scaffold [123] (Figure 9B). Another popular method to create porous scaffolds

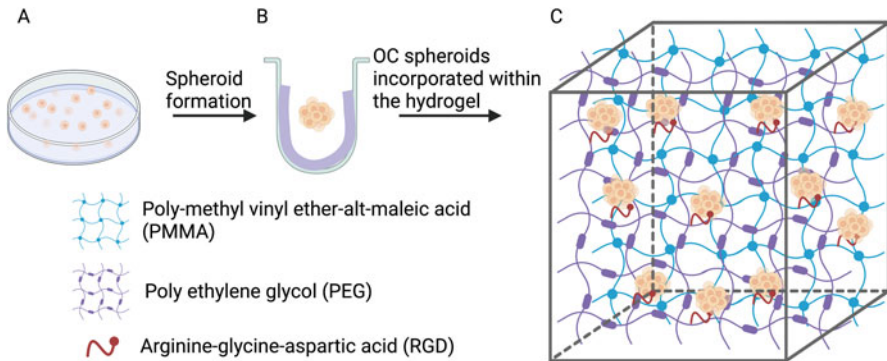


**Fig. 8** Synthetic polymer network as a scaffold for OC spheroids. (A) Monolayer of OC cells in a petri dish, (B) formation of 3D suspended spheroid in single U-shaped well, (C) embedded OC spheroids within the crosslinked networks of the poly(methyl vinyl ether-alt-maleic acid) (PMMA) and polyethylene glycol (PEG) containing arginine-glycine-aspartic acid (RGD) peptide

resembling the ECM environment is electrospinning, which utilizes electrostatic forces to make nanoporous scaffolds with a large surface-to-volume ratio. In this procedure, a high-voltage electric field passes through the polymer melt, creating an electrostatic repulsion that results in the formation of a thin jet. Eventually, the jet is directed toward a counter electrode or collection surface to form the final scaffold [124] (Figure 9C). One of the most recent methods for scaffold fabrication is 3D printing (Figure 9D). 3D printing is a precision technique that enables the making of scaffolds with accurate pore size; well-arranged, highly interconnected fibers; and high mechanical strength. Synthetic polymers like poly(ethylene glycol), diacrylate (PEGDA), poly( $\epsilon$ -caprolactone) (PCL), and poly(D, L-lactic-co-glycolic acid) (PLGA) can be used to create suitable paths for cell proliferation and differentiation [125].

#### 4.6 Integration of OC Tissue Culture with Microfluidics

OC progression is often associated with inflamed vasculature that can cause abdominal accumulation of fluids containing extravasated immune cells and platelets. Thus, OC cells that come in direct contact with eluates can be exposed to additional fluid shear stresses [126–129] and de novo cell–cell interactions [130, 131]. The relevance of fluid-mediated shear stress and stromal extravasation to OC progression has been recently evaluated using microfluidic cultures. The studies demonstrated that low levels of fluid shear force can activate chemotherapy resistance programs [132] and promote platelet extravasation to infiltrate OC monolayers and induce cancer cell growth [133]. Microfluidic culture systems usually consist of microchannels that connect cell culture chambers to produce fluid-movement-induced

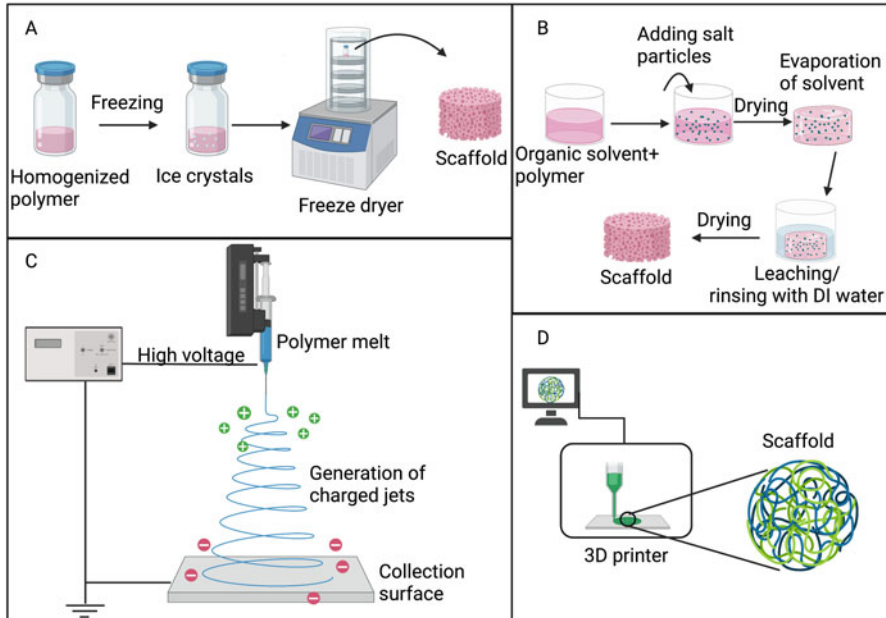


**Fig. 9** Various porous scaffold fabrication methods. (A) Freeze-drying; (B) Solvent casting; (C) Electrospinning; (D) 3D printing

tensile stresses. These micro-channels also enable the incorporation of cancer cells, ECM microenvironment, and stroma while providing a path to perfuse nutritious media and remove wastes. The main component of microfluidic devices is polydimethylsiloxane (PDMS), which is a flexible and biocompatible polymer. PDMS is easy to get patterned and bonded to glass, which makes it a convenient and inexpensive tool to make culture devices. Moreover, it is permeable to gas and transparent, which enables the integration of cell-based assays with optical observations. The conventional method for fabrication of PDMS molds, and eventually a simple microfluidic channel, is represented in Fig. 10. Soft lithography is the basic method to make an epoxy-based photoresist master mold for PDMS casting. The process is initiated by spinning the epoxy coat (SU-8) and binding it to a silicon wafer substrate. Then, the patterns of desired chambers and channels can be designed and carved, using a bio-printer, to form a photomask. PDMS is poured on the photomask pattern and cured. The resulting microfluidic device is peeled off the mold and sealed to a glass slide by plasma cleaning. Another fabrication method utilizes a biocompatible pressure-sensitive adhesive (PSA) tape to design and print various patterns using a Silhouette cutter. PSA patterns are adhered to a glass base and overlaid with PDMS containing inlet and outlet ports (Fig. 11).

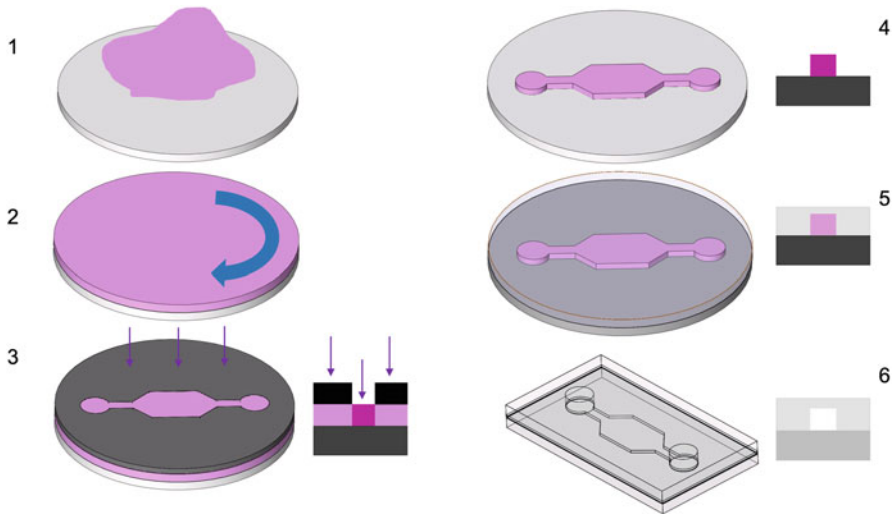


**Fig. 10** Microfluidic device fabrication. [1] SU-8 photoresist on a silicon wafer substrate; [2] spin coating and soft baking; [3] photomask alignment and exposure to UV light to harden exposed photoresist; [4] SU-8 development, baking, and rinsing; [5] PDMS casting on the SU-8 mold; [6] inlet and outlet creation, plasma treatment, and sealing the PDMS to a glass slide for final device configuration

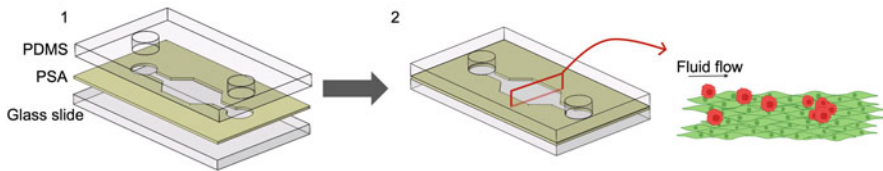


**Fig. 11** Microfluidic device fabrication with pressure-sensitive adhesive (PSA) tape. [1] Final device is made from a glass slide, PSA tape, and PDMS layer, [2] OC cells (red) on a mesothelial cell layer (green) in a hexagon-shaped microfluidic device

## 5 Concluding Remarks

Traditional methods of culturing OC cells (monolayers and spheroids) paved the way for studies addressing the mechanisms of OC growth, survival, invasion, and response to clinical or experimental drugs. These approaches are a preferred choice for many OC researchers today. However, with the increasing recognition of the important roles of various TMs in OC and profound OC cancer cell heterogeneity within tumor biopsies, new *in vitro* cell culture approaches incorporating patient-derived OC cells and TMs started to emerge. So far, these methodologies have provided evidence that supports the idea of treating OC by targeting TMs. Therefore, the utility of these models might provide an opportunity to answer outstanding



questions relating to the role of different components of OC TMs in the modulation of tumor growth and survival. However, these models are still prototypes, and they need to include vasculature and the immune system, critical components that have long been implicated in regulating tumorigenesis. The challenges ahead are also related to technological advances that standardize complex multicellular culture approaches and integrate them with image-based automated quantification of phenotypes associated with different cell types represented in the model. Collaborations among pathologists, cell biologists, immunologists, and bioengineers should be strongly encouraged to overcome these challenges by providing appropriate directions for meaningful engineering of OC cell cultures that fill the gap between standard culture approaches and animal models.

## References

1. Bowtell DD et al (2015) Rethinking ovarian cancer II: reducing mortality from high-grade serous ovarian cancer. *Nat Rev Cancer* 15:668–679. <https://doi.org/10.1038/nrc4019>
2. Matulonis UA et al (2016) Ovarian cancer. *Nat Rev Dis Primers* 2:16061. <https://doi.org/10.1038/nrdp.2016.61>
3. Jimenez-Sanchez A et al (2017) Heterogeneous tumor-immune microenvironments among differentially growing metastases in an ovarian cancer patient. *Cell* 170:927–938 e920. <https://doi.org/10.1016/j.cell.2017.07.025>
4. McPherson A et al (2016) Divergent modes of clonal spread and intraperitoneal mixing in high-grade serous ovarian cancer. *Nat Genet* 48:758–767. <https://doi.org/10.1038/ng.3573>
5. Zhang AW et al (2018) Interfaces of malignant and immunologic clonal dynamics in ovarian cancer. *Cell* 173:1755–1769 e1722. <https://doi.org/10.1016/j.cell.2018.03.073>
6. Winterhoff BJ et al (2017) Single cell sequencing reveals heterogeneity within ovarian cancer epithelium and cancer associated stromal cells. *Gynecol Oncol* 144:598–606. <https://doi.org/10.1016/j.ygyno.2017.01.015>
7. Hu Y et al (2020) Integrated proteomic and Glycoproteomic characterization of human high-grade serous ovarian carcinoma. *Cell Rep* 33:108276. <https://doi.org/10.1016/j.celrep.2020.108276>
8. Javellana M et al (2022) Neoadjuvant chemotherapy induces genomic and transcriptomic changes in ovarian cancer. *Cancer Res* 82:169–176. <https://doi.org/10.1158/0008-5472.CAN-21-1467>
9. Lee S et al (2020) Molecular analysis of clinically defined subsets of high-grade serous ovarian cancer. *Cell Rep* 31:107502. <https://doi.org/10.1016/j.celrep.2020.03.066>
10. Sheng Q et al (2010) An activated ErbB3/NRG1 autocrine loop supports in vivo proliferation in ovarian cancer cells. *Cancer Cell* 17:298–310. S1535-6108(10)00038-3 [pii]. <https://doi.org/10.1016/j.ccr.2009.12.047>
11. George E et al (2017) A patient-derived-xenograft platform to study BRCA-deficient ovarian cancers. *JCI Insight* 2:e89760. <https://doi.org/10.1172/jci.insight.89760>
12. Kurman RJ, Shih Ie M (2010) The origin and pathogenesis of epithelial ovarian cancer: a proposed unifying theory. *Am J Surg Pathol* 34:433–443. <https://doi.org/10.1097/PAS.0b013e3181cf3d79>
13. Auersperg N, Woo MMM, Gilks CB (2008) The origin of ovarian carcinomas: a developmental view. *Gynecol Oncol* 110:452–454. <https://doi.org/10.1016/j.ygyno.2008.05.031>
14. Folkins AK et al (2008) A candidate precursor to pelvic serous cancer (p53 signature) and its prevalence in ovaries and fallopian tubes from women with BRCA mutations. *Gynecol Oncol* 109:168–173. S0090-8258(08)00007-3 [pii]. <https://doi.org/10.1016/j.ygyno.2008.01.012>



15. Kim J et al (2018) Cell origins of high-grade serous ovarian cancer. *Cancers (Basel)* 10:433. <https://doi.org/10.3390/cancers10110433>
16. Zhai Y et al (2002) Role of beta-catenin/T-cell factor-regulated genes in ovarian endometrioid adenocarcinomas. *Am J Pathol* 160:1229–1238. [https://doi.org/10.1016/s0002-9440\(10\)62550-3](https://doi.org/10.1016/s0002-9440(10)62550-3)
17. McConechy MK et al (2014) Ovarian and endometrial endometrioid carcinomas have distinct CTNNB1 and PTEN mutation profiles. *Mod Pathol* 27:128–134. <https://doi.org/10.1038/modpathol.2013.107>
18. Wiegand KC et al (2010) ARID1A mutations in endometriosis-associated ovarian carcinomas. *N Engl J Med* 363:1532–1543. <https://doi.org/10.1056/NEJMoa1008433>
19. Cheasley D et al (2019) The molecular origin and taxonomy of mucinous ovarian carcinoma. *Nat Commun* 10:3935. <https://doi.org/10.1038/s41467-019-11862-x>
20. Singer G et al (2003) Mutations in BRAF and KRAS characterize the development of low-grade ovarian serous carcinoma. *J Natl Cancer Inst* 95:484–486. <https://doi.org/10.1093/jnci/95.6.484>
21. Zhou J et al (2018) The effect of histological subtypes on outcomes of stage IV epithelial ovarian cancer. *Front Oncol* 8:577. <https://doi.org/10.3389/fonc.2018.00577>
22. Vereczkey I et al (2011) Molecular characterization of 103 ovarian serous and mucinous tumors. *Pathol Oncol Res* 17:551–559. <https://doi.org/10.1007/s12253-010-9345-8>
23. Teer JK et al (2017) Mutational heterogeneity in non-serous ovarian cancers. *Sci Rep* 7:9728. <https://doi.org/10.1038/s41598-017-10432-9>
24. Cuatrecasas M, Villanueva A, Matias-Guiu X, Prat J (1997) K-ras mutations in mucinous ovarian tumors: a clinicopathologic and molecular study of 95 cases. *Cancer* 79:1581–1586. [https://doi.org/10.1002/\(sici\)1097-0142\(19970415\)79:8<1581::aid-cnrcr21>3.0.co;2-t](https://doi.org/10.1002/(sici)1097-0142(19970415)79:8<1581::aid-cnrcr21>3.0.co;2-t)
25. Lin WL et al (2011) Identification of the coexisting HER2 gene amplification and novel mutations in the HER2 protein-overexpressed mucinous epithelial ovarian cancer. *Ann Surg Oncol* 18:2388–2394. <https://doi.org/10.1245/s10434-011-1572-z>
26. Massad LS, Gao F, Hagemann I, Powell M (2016) Clinical outcomes among women with mucinous adenocarcinoma of the ovary. *Gynecol Obstet Investig* 81:411–415. <https://doi.org/10.1159/000441791>
27. Zannoni GF et al (2014) Mutational status of KRAS, NRAS, and BRAF in primary clear cell ovarian carcinoma. *Virchows Arch* 465:193–198. <https://doi.org/10.1007/s00428-014-1599-1>
28. Campbell IG et al (2004) Mutation of the PIK3CA gene in ovarian and breast cancer. *Cancer Res* 64:7678–7681. <https://doi.org/10.1158/0008-5472.CAN-04-2933>
29. Kajiyama H et al (2018) The possible existence of occult metastasis in patients with ovarian clear-cell carcinoma who underwent complete resection without any residual tumours. *Oncotarget* 9:6298–6307. <https://doi.org/10.18632/oncotarget.23921>
30. Kumar A, Gilks CB, Mar C, Santos J, Tinker AV (2013) Patterns of spread of clear cell ovarian cancer: case report and case series. *Gynecol Oncol Case Rep* 6:25–27. <https://doi.org/10.1016/j.gynor.2013.07.008>
31. Nam G, Lim YM, Cho MS, Lee J, Kim YH (2017) Skin metastases in ovarian clear cell adenocarcinoma: a case report and a review of the literature. *Obstet Gynecol Sci* 60:593–597. <https://doi.org/10.5468/ogs.2017.60.6.593>
32. Singer G et al (2005) Patterns of p53 mutations separate ovarian serous borderline tumors and low- and high-grade carcinomas and provide support for a new model of ovarian carcinogenesis: a mutational analysis with immunohistochemical correlation. *Am J Surg Pathol* 29:218–224. 00000478-200502000-00009 [pii]
33. Hunter SM et al (2015) Molecular profiling of low grade serous ovarian tumours identifies novel candidate driver genes. *Oncotarget* 6:37663–37677. <https://doi.org/10.18632/oncotarget.5438>
34. Kubo C et al (2018) Late recurrence of pStage 1 low-grade serous ovarian tumor presenting as a symptomatic bone metastasis: a case report. *Diagn Pathol* 13:43. <https://doi.org/10.1186/s13000-018-0720-1>

35. Ahmed AA et al (2010) Driver mutations in TP53 are ubiquitous in high grade serous carcinoma of the ovary. *J Pathol* 221:49–56. <https://doi.org/10.1002/path.2696>
36. Cancer Genome Atlas Research Network, Bell D (2011) Integrated genomic analyses of ovarian carcinoma. *Nature* 474:609–615. [nature10166](https://doi.org/10.1038/nature10166) [pii]. <https://doi.org/10.1038/nature10166>
37. Turner N, Tutt A, Ashworth A (2004) Hallmarks of ‘BRCAness’ in sporadic cancers. *Nat Rev Cancer* 4:814–819. <https://doi.org/10.1038/nrc1457>
38. Jazaeri AA et al (2002) Gene expression profiles of BRCA1-linked, BRCA2-linked, and sporadic ovarian cancers. *J Natl Cancer Inst* 94:990–1000. <https://doi.org/10.1093/jnci/94.13.990>
39. Reyes MC, Arnold AG, Kauff ND, Levine DA, Soslow RA (2014) Invasion patterns of metastatic high-grade serous carcinoma of ovary or fallopian tube associated with BRCA deficiency. *Mod Pathol* 27:1405–1411. <https://doi.org/10.1038/modpathol.2013.237>
40. Medeiros F et al (2006) The tubal fimbria is a preferred site for early adenocarcinoma in women with familial ovarian cancer syndrome. *Am J Surg Pathol* 30:230–236. 00000478-200602000-00012 [pii]
41. Piek JM et al (2001) Dysplastic changes in prophylactically removed fallopian tubes of women predisposed to developing ovarian cancer. *J Pathol* 195:451–456. 10.1002/path.1000 [pii]. <https://doi.org/10.1002/path.1000>
42. Labidi-Galy SI et al (2017) High grade serous ovarian carcinomas originate in the fallopian tube. *Nat Commun* 8:1093. <https://doi.org/10.1038/s41467-017-00962-1>
43. Ducie J et al (2017) Molecular analysis of high-grade serous ovarian carcinoma with and without associated serous tubal intra-epithelial carcinoma. *Nat Commun* 8:990. <https://doi.org/10.1038/s41467-017-01217-9>
44. Dinh HQ et al (2021) Single-cell transcriptomics identifies gene expression networks driving differentiation and tumorigenesis in the human fallopian tube. *Cell Rep* 35:108978. <https://doi.org/10.1016/j.celrep.2021.108978>
45. Bowen NJ et al (2007) Emerging roles for PAX8 in ovarian cancer and endosalpigeal development. *Gynecol Oncol* 104:331–337. S0090-8258(06)00696-2 [pii]. <https://doi.org/10.1016/j.ygyno.2006.08.052>
46. Perets R et al (2013) Transformation of the fallopian tube secretory epithelium leads to high-grade serous ovarian cancer in Brca;Tp53;Pten models. *Cancer Cell* 24:751–765. <https://doi.org/10.1016/j.ccr.2013.10.013>
47. Zhang S et al (2019) Both fallopian tube and ovarian surface epithelium are cells-of-origin for high-grade serous ovarian carcinoma. *Nat Commun* 10:5367. <https://doi.org/10.1038/s41467-019-13116-2>
48. Kuhn E et al (2012) The diagnostic and biological implications of laminin expression in serous tubal intraepithelial carcinoma. *Am J Surg Pathol* 36:1826–1834. <https://doi.org/10.1097/PAS.0b013e31825ec07a>
49. Visvanathan K et al (2018) Fallopian tube lesions in women at high risk for ovarian cancer: a multicenter study. *Cancer Prev Res (Phila)* 11:697–706. <https://doi.org/10.1158/1940-6207.CAPR-18-0009>
50. Rentschler EC, Gant KL, Drapkin R, Patankar M, P, J. C. (2019) Imaging collagen alterations in STICs and high grade ovarian cancers in the fallopian tubes by second harmonic generation microscopy. *Cancers (Basel)* 11:1805. <https://doi.org/10.3390/cancers11111805>
51. George SH, Milea A, Shaw PA (2012) Proliferation in the normal FTE is a hallmark of the follicular phase, not BRCA mutation status. *Clin Cancer Res* 18:6199–6207. <https://doi.org/10.1158/1078-0432.CCR-12-2155>
52. Lengyel E (2010) Ovarian cancer development and metastasis. *Am J Pathol* 177:1053–1064. <https://doi.org/10.2353/ajpath.2010.100105>
53. Meserve EEK, Brouwer J, Crum CP (2017) Serous tubal intraepithelial neoplasia: the concept and its application. *Mod Pathol* 30:710–721. <https://doi.org/10.1038/modpathol.2016.238>
54. Eckert MA et al (2016) Genomics of ovarian cancer progression reveals diverse metastatic trajectories including intraepithelial metastasis to the fallopian tube. *Cancer Discov* 6:1342–1351. <https://doi.org/10.1158/2159-8290.CD-16-0607>

55. Mitra AK (2016) Ovarian cancer metastasis: a unique mechanism of dissemination. In: Ke Xu (ed) Tumor metastasis. Intechopen. <https://doi.org/10.5772/64700>
56. Dhaliwal D, Shepherd TG (2022) Molecular and cellular mechanisms controlling integrin-mediated cell adhesion and tumor progression in ovarian cancer metastasis: a review. *Clin Exp Metastasis* 39:291–301. <https://doi.org/10.1007/s10585-021-10136-5>
57. Yang Y et al (2019) Reversing platinum resistance in ovarian cancer multicellular spheroids by targeting Bcl-2. *Onco Targets Ther* 12:897–906. <https://doi.org/10.2147/OTT.S187015>
58. Fritz JL et al (2020) A novel role for NUA1 in promoting ovarian cancer metastasis through regulation of fibronectin production in spheroids. *Cancers (Basel)* 12:1250. <https://doi.org/10.3390/cancers12051250>
59. Rafehi S et al (2016) TGFbeta signaling regulates epithelial-mesenchymal plasticity in ovarian cancer ascites-derived spheroids. *Endocr Relat Cancer* 23:147–159. <https://doi.org/10.1530/ERC-15-0383>
60. Condello S et al (2015) Beta-catenin-regulated ALDH1A1 is a target in ovarian cancer spheroids. *Oncogene* 34:2297–2308. <https://doi.org/10.1038/onc.2014.178>
61. Davidowitz RA et al (2014) Mesenchymal gene program-expressing ovarian cancer spheroids exhibit enhanced mesothelial clearance. *J Clin Invest* 124:2611–2625. <https://doi.org/10.1172/JCI69815>
62. Burlinson KM et al (2004) Ovarian carcinoma ascites spheroids adhere to extracellular matrix components and mesothelial cell monolayers. *Gynecol Oncol* 93:170–181. S0090825803009508 [pii]. <https://doi.org/10.1016/j.ygyno.2003.12.034>
63. Lessan K, Aguiar DJ, Oegema T, Siebenson L, Skubitz AP (1999) CD44 and beta1 integrin mediate ovarian carcinoma cell adhesion to peritoneal mesothelial cells. *Am J Pathol* 154:1525–1537
64. Slack-Davis JK, Atkins KA, Harrer C, Hershey ED, Conaway M (2009) Vascular cell adhesion molecule-1 is a regulator of ovarian cancer peritoneal metastasis. *Cancer Res* 69:1469–1476. 0008-5472.CAN-08-2678 [pii]. <https://doi.org/10.1158/0008-5472.CAN-08-2678>
65. Kenny HA et al (2014) Mesothelial cells promote early ovarian cancer metastasis through fibronectin secretion. *J Clin Invest* 124:4614–4628. <https://doi.org/10.1172/JCI74778>
66. Iwanicki MP et al (2011) Ovarian cancer spheroids use myosin-generated force to clear the mesothelium. *Cancer Discov* 1:144–157. <https://doi.org/10.1158/2159-8274.CD-11-0010>
67. Usui A, Ko SY, Barengo N, Naora H (2014) P-cadherin promotes ovarian cancer dissemination through tumor cell aggregation and tumor-peritoneum interactions. *Mol Cancer Res* 12:504–513. <https://doi.org/10.1158/1541-7786.MCR-13-0489>
68. Nakamura K et al (2017) Exosomes promote ovarian cancer cell invasion through transfer of CD44 to peritoneal mesothelial cells. *Mol Cancer Res* 15:78–92. <https://doi.org/10.1158/1541-7786.MCR-16-0191>
69. Medrano M et al (2017) Interrogation of functional cell-surface markers identifies CD151 dependency in high-grade serous ovarian cancer. *Cell Rep* 18:2343–2358. <https://doi.org/10.1016/j.celrep.2017.02.028>
70. Davidowitz RA, Iwanicki MP, Brugge JS (2012) In vitro mesothelial clearance assay that models the early steps of ovarian cancer metastasis. *J Vis Exp* 60:3888. <https://doi.org/10.3791/3888>
71. Nieman KM et al (2011) Adipocytes promote ovarian cancer metastasis and provide energy for rapid tumor growth. *Nat Med* 17:1498–1503. nm.2492 [pii]. <https://doi.org/10.1038/nm.2492>
72. Mitra AK et al (2012) MicroRNAs reprogram normal fibroblasts into cancer-associated fibroblasts in ovarian cancer. *Cancer Discov* 2:1100–1108. <https://doi.org/10.1158/2159-8290.CD-12-0206>
73. Yin M et al (2016) Tumor-associated macrophages drive spheroid formation during early transcoelomic metastasis of ovarian cancer. *J Clin Invest* 126:4157–4173. <https://doi.org/10.1172/JCI87252>

74. Lee W et al (2019) Neutrophils facilitate ovarian cancer premetastatic niche formation in the omentum. *J Exp Med* 216:176–194. <https://doi.org/10.1084/jem.20181170>
75. Delaine-Smith RM et al (2021) Modelling TGFbetaR and Hh pathway regulation of prognostic matrisome molecules in ovarian cancer. *iScience* 24:102674. <https://doi.org/10.1016/j.isci.2021.102674>
76. Malacrida B et al (2021) A human multi-cellular model shows how platelets drive production of diseased extracellular matrix and tissue invasion. *iScience* 24:102676. <https://doi.org/10.1016/j.isci.2021.102676>
77. Scott CL, Becker MA, Haluska P, Samimi G (2013) Patient-derived xenograft models to improve targeted therapy in epithelial ovarian cancer treatment. *Front Oncol* 3:295. <https://doi.org/10.3389/fonc.2013.00295>
78. Domcke S, Sinha R, Levine DA, Sander C, Schultz N (2013) Evaluating cell lines as tumour models by comparison of genomic profiles. *Nat Commun* 4:2126. <https://doi.org/10.1038/ncomms3126>
79. Harrington BS et al (2016) Cell line and patient-derived xenograft models reveal elevated CDCP1 as a target in high-grade serous ovarian cancer. *Br J Cancer* 114:417–426. <https://doi.org/10.1038/bjc.2015.471>
80. Thu KL et al (2017) A comprehensively characterized cell line panel highly representative of clinical ovarian high-grade serous carcinomas. *Oncotarget* 8:50489–50499. <https://doi.org/10.18632/oncotarget.9929>
81. Beaufort CM et al (2014) Ovarian cancer cell line panel (OCCP): clinical importance of in vitro morphological subtypes. *PLoS One* 9:e103988. <https://doi.org/10.1371/journal.pone.0103988>
82. Letourneau IJ et al (2012) Derivation and characterization of matched cell lines from primary and recurrent serous ovarian cancer. *BMC Cancer* 12:379. <https://doi.org/10.1186/1471-2407-12-379>
83. Kreuzinger C et al (2019) Patient-derived cell line models revealed therapeutic targets and molecular mechanisms underlying disease progression of high grade serous ovarian cancer. *Cancer Lett* 459:1–12. <https://doi.org/10.1016/j.canlet.2019.05.032>
84. Ince TA et al (2015) Characterization of twenty-five ovarian tumour cell lines that phenocopy primary tumours. *Nat Commun* 6:7419. <https://doi.org/10.1038/ncomms8419>
85. Simpkins F et al (2018) Dual Src and MEK inhibition decreases ovarian cancer growth and targets tumor initiating stem-like cells. *Clin Cancer Res* 24:4874–4886. <https://doi.org/10.1158/1078-0432.CCR-17-3697>
86. Lui GYL et al (2020) BET, SRC, and BCL2 family inhibitors are synergistic drug combinations with PARP inhibitors in ovarian cancer. *EBioMedicine* 60:102988. <https://doi.org/10.1016/j.ebiom.2020.102988>
87. Jang K et al (2017) VEGFA activates an epigenetic pathway upregulating ovarian cancer-initiating cells. *EMBO Mol Med* 9:304–318. <https://doi.org/10.15252/emmm.201606840>
88. Witt AE et al (2017) Identification of a cancer stem cell-specific function for the histone deacetylases, HDAC1 and HDAC7, in breast and ovarian cancer. *Oncogene* 36:1707–1720. <https://doi.org/10.1038/onc.2016.337>
89. Liao J et al (2014) Ovarian cancer spheroid cells with stem cell-like properties contribute to tumor generation, metastasis and chemotherapy resistance through hypoxia-resistant metabolism. *PLoS One* 9:e84941. <https://doi.org/10.1371/journal.pone.0084941>
90. Boylan KLM, Manion RD, Shah H, Skubitz KM, Skubitz APN (2020) Inhibition of ovarian cancer cell spheroid formation by synthetic peptides derived from Nectin-4. *Int J Mol Sci* 21:4637. <https://doi.org/10.3390/ijms21134637>
91. Iwanicki MP et al (2016) Mutant p53 regulates ovarian cancer transformed phenotypes through autocrine matrix deposition. *JCI Insight* 1:e86829. <https://doi.org/10.1172/jci.insight.86829>
92. Kenny HA et al (2009) Organotypic models of metastasis: a three-dimensional culture mimicking the human peritoneum and omentum for the study of the early steps of ovarian cancer metastasis. *Cancer Treat Res* 149:335–351. [https://doi.org/10.1007/978-0-387-98094-2\\_16](https://doi.org/10.1007/978-0-387-98094-2_16)

93. Alshehri S, Pavlovic T, Farsinejad S, Behboodi P, Quan L, Centeno D, Kung D, Rezler M, Lee W, Jasiński P, Dziabaszweska E, Nowak-Markwitz E, Kalyon D, Zaborowski MP, Iwanicki M (2022) Extracellular matrix levels modulate outgrowths dynamics in ovarian cancer. *bioRxiv*. <https://doi.org/10.1101/2022.01.30.478322>
94. Kenny HA, Nieman KM, Mitra AK, Lengyel E (2011) The first line of intra-abdominal metastatic attack: breaching the mesothelial cell layer. *Cancer Discov* 1:100–102
95. Kenny HA et al (2015) Quantitative high throughput screening using a primary human three-dimensional organotypic culture predicts in vivo efficacy. *Nat Commun* 6:6220. <https://doi.org/10.1038/ncomms7220>
96. Kenny HA et al (2019) Quantitative high-throughput screening using an organotypic model identifies compounds that inhibit ovarian cancer metastasis. *Mol Cancer Ther* 19(1):52–62. <https://doi.org/10.1158/1535-7163.MCT-19-0052>
97. Shamir ER, Ewald AJ (2014) Three-dimensional organotypic culture: experimental models of mammalian biology and disease. *Nat Rev Mol Cell Biol* 15:647–664. <https://doi.org/10.1038/nrm3873>
98. Simian M, Bissell MJ (2017) Organoids: a historical perspective of thinking in three dimensions. *J Cell Biol* 216:31–40. <https://doi.org/10.1083/jcb.201610056>
99. Hardman P, Klement BJ, Spooner BS (1993) Growth and morphogenesis of embryonic mouse organs on non-coated and extracellular matrix-coated biopore membrane. *Develop Growth Differ* 35:683–690. <https://doi.org/10.1111/j.1440-169x.1993.00683.x>
100. Topper RJ, Oka T, Vonderhaar BK (1975) Techniques for studying development of normal mammary epithelial cells in organ culture. *Methods Enzymol* 39:443–454. [https://doi.org/10.1016/s0076-6879\(75\)39039-3](https://doi.org/10.1016/s0076-6879(75)39039-3)
101. Aplin AC, Fogel E, Zorzi P, Nicosia RF (2008) The aortic ring model of angiogenesis. *Methods Enzymol* 443:119–136. [https://doi.org/10.1016/S0076-6879\(08\)02007-7](https://doi.org/10.1016/S0076-6879(08)02007-7)
102. Stoppini L, Buchs PA, Muller D (1991) A simple method for organotypic cultures of nervous tissue. *J Neurosci Methods* 37:173–182. [https://doi.org/10.1016/0165-0270\(91\)90128-m](https://doi.org/10.1016/0165-0270(91)90128-m)
103. Gahwiler BH, Capogna M, Debanne D, McKinney RA, Thompson SM (1997) Organotypic slice cultures: a technique has come of age. *Trends Neurosci* 20:471–477. [https://doi.org/10.1016/s0166-2236\(97\)01122-3](https://doi.org/10.1016/s0166-2236(97)01122-3)
104. Ootani A et al (2009) Sustained in vitro intestinal epithelial culture within a Wnt-dependent stem cell niche. *Nat Med* 15:701–706. <https://doi.org/10.1038/nm.1951>
105. Sato T et al (2009) Single Lgr5 stem cells build crypt-villus structures in vitro without a mesenchymal niche. *Nature* 459:262–265. <https://doi.org/10.1038/nature07935>
106. Huch M et al (2013) In vitro expansion of single Lgr5+ liver stem cells induced by Wnt-driven regeneration. *Nature* 494:247–250. <https://doi.org/10.1038/nature11826>
107. Barker N et al (2010) Lgr5(+ve) stem cells drive self-renewal in the stomach and build long-lived gastric units in vitro. *Cell Stem Cell* 6:25–36. <https://doi.org/10.1016/j.stem.2009.11.013>
108. Lancaster MA et al (2013) Cerebral organoids model human brain development and microcephaly. *Nature* 501:373–379. <https://doi.org/10.1038/nature12517>
109. Rosenbluth JM et al (2020) Organoid cultures from normal and cancer-prone human breast tissues preserve complex epithelial lineages. *Nat Commun* 11:1711. <https://doi.org/10.1038/s41467-020-15548-7>
110. Homan KA et al (2019) Flow-enhanced vascularization and maturation of kidney organoids in vitro. *Nat Methods* 16:255–262. <https://doi.org/10.1038/s41592-019-0325-y>
111. Kessler M et al (2015) The Notch and Wnt pathways regulate stemness and differentiation in human fallopian tube organoids. *Nat Commun* 6:8989. <https://doi.org/10.1038/ncomms9989>
112. Xie Y, Park ES, Xiang D, Li Z (2018) Long-term organoid culture reveals enrichment of organoid-forming epithelial cells in the fimbrial portion of mouse fallopian tube. *Stem Cell Res* 32:51–60. <https://doi.org/10.1016/j.scr.2018.08.021>
113. Hill SJ et al (2018) Prediction of DNA repair inhibitor response in short-term patient-derived ovarian cancer organoids. *Cancer Discov* 8:1404–1421. <https://doi.org/10.1158/2159-8290.CD-18-0474>

114. Hoffmann K et al (2020) Stable expansion of high-grade serous ovarian cancer organoids requires a low-Wnt environment. *EMBO J* 39:e104013. <https://doi.org/10.15252/embj.2019104013>
115. Kopper O et al (2019) An organoid platform for ovarian cancer captures intra- and interpatient heterogeneity. *Nat Med* 25:838–849. <https://doi.org/10.1038/s41591-019-0422-6>
116. Aisenbrey EA, Murphy WL (2020) Synthetic alternatives to matrigel. *Nat Rev Mater* 5:539–551. <https://doi.org/10.1038/s41578-020-0199-8>
117. Antoine EE, Vlachos PP, Rylander MN (2014) Review of collagen I hydrogels for bioengineered tissue microenvironments: characterization of mechanics, structure, and transport. *Tissue Eng Part B Rev* 20:683–696. <https://doi.org/10.1089/ten.TEB.2014.0086>
118. Barros D et al (2019) Engineering hydrogels with affinity-bound laminin as 3D neural stem cell culture systems. *Biomater Sci* 7:5338–5349. <https://doi.org/10.1039/c9bm00348g>
119. Zhou N et al (2021) Effect of RGD content in poly(ethylene glycol)-crosslinked poly(methyl vinyl ether-alt-maleic acid) hydrogels on the expansion of ovarian cancer stem-like cells. *Mater Sci Eng C Mater Biol Appl* 118:111477. <https://doi.org/10.1016/j.msec.2020.111477>
120. Yang Z, Zhao X (2011) A 3D model of ovarian cancer cell lines on peptide nanofiber scaffold to explore the cell-scaffold interaction and chemotherapeutic resistance of anticancer drugs. *Int J Nanomedicine* 6:303–310. <https://doi.org/10.2147/IJN.S15279>
121. Braccini S, Tacchini C, Chiellini F, Puppi D (2022) Polymeric hydrogels for in vitro 3D ovarian cancer modeling. *Int J Mol Sci* 23:3265. <https://doi.org/10.3390/ijms23063265>
122. Adams G (2007) The principles of freeze-drying. *Methods Mol Biol* 368:15–38. [https://doi.org/10.1007/978-1-59745-362-2\\_2](https://doi.org/10.1007/978-1-59745-362-2_2)
123. Sola A et al (2019) Development of solvent-casting particulate leaching (SCPL) polymer scaffolds as improved three-dimensional supports to mimic the bone marrow niche. *Mater Sci Eng C Mater Biol Appl* 96:153–165. <https://doi.org/10.1016/j.msec.2018.10.086>
124. Xue J, Wu T, Dai Y, Xia Y (2019) Electrospinning and electrospun nanofibers: methods, materials, and applications. *Chem Rev* 119:5298–5415. <https://doi.org/10.1021/acs.chemrev.8b00593>
125. Do AV, Khorsand B, Geary SM, Salem AK (2015) 3D printing of scaffolds for tissue regeneration applications. *Adv Healthc Mater* 4:1742–1762. <https://doi.org/10.1002/adhm.201500168>
126. Kipps E, Tan DS, Kaye SB (2013) Meeting the challenge of ascites in ovarian cancer: new avenues for therapy and research. *Nat Rev Cancer* 13:273–282. <https://doi.org/10.1038/nrc3432>
127. Novak C, Horst E, Mehta G (2018) Review: mechanotransduction in ovarian cancer: shearing into the unknown. *APL Bioeng* 2:031701. <https://doi.org/10.1063/1.5024386>
128. Ip CK et al (2016) Stemness and chemoresistance in epithelial ovarian carcinoma cells under shear stress. *Sci Rep* 6:26788. <https://doi.org/10.1038/srep26788>
129. Gotlieb WH et al (1998) Intraperitoneal pressures and clinical parameters of total paracentesis for palliation of symptomatic ascites in ovarian cancer. *Gynecol Oncol* 71:381–385. <https://doi.org/10.1006/gyno.1998.5215>
130. Zhang S et al (2021) Macrophage-mediated vascular permeability via VLA4/VCAM1 pathway dictates ascites development in ovarian cancer. *J Clin Invest* 131:1–14. <https://doi.org/10.1172/JCI140315>
131. Orellana R et al (2015) Platelets enhance tissue factor protein and metastasis initiating cell markers, and act as chemoattractants increasing the migration of ovarian cancer cells. *BMC Cancer* 15:290. <https://doi.org/10.1186/s12885-015-1304-z>
132. Rizvi I et al (2013) Flow induces epithelial-mesenchymal transition, cellular heterogeneity and biomarker modulation in 3D ovarian cancer nodules. *Proc Natl Acad Sci U S A* 110:E1974–E1983. <https://doi.org/10.1073/pnas.1216989110>
133. Saha B et al (2020) OvCa-Chip microsystem recreates vascular endothelium-mediated platelet extravasation in ovarian cancer. *Blood Adv* 4:3329–3342. <https://doi.org/10.1182/bloodadvances.2020001632>



# Biophysical Properties and Isolation of Circulating Tumor Cells



**Diane S. Kang, Aidan Moriarty, Jeong Min Oh, Hydari Masuma Begum, Keyue Shen, and Min Yu**

**Abstract** Circulating tumor cells (CTCs) are tumor cells that have entered the bloodstream. Although the vast majority do not survive the numerous stressors in the fluid environment, the small fraction of CTCs that are able to resist destruction and elimination have the potential to form metastatic colonies and can therefore be considered metastatic precursors. CTC survival in the circulatory system is dependent on a number of factors including interactions with the physical environment and intrinsic biophysical characteristics. Additionally, CTCs are highly heterogeneous due to intratumoral heterogeneity and molecular plasticity inherent

---

Authors Diane S. Kang and Aidan Moriarty have equally contributed to this chapter.

---

D. S. Kang

Department of Stem Cell Biology and Regenerative Medicine, University of Southern California, Los Angeles, CA, USA

Norris Comprehensive Cancer Center, Keck School of Medicine, University of Southern California, Los Angeles, CA, USA

A. Moriarty

Department of Stem Cell Biology and Regenerative Medicine, University of Southern California, Los Angeles, CA, USA

Department of Pharmacology, University of Maryland School of Medicine, Baltimore, MD USA

J. M. Oh · H. M. Begum

Department of Biomedical Engineering, Viterbi School of Engineering, University of Southern California, Los Angeles, CA, USA

K. Shen

Norris Comprehensive Cancer Center, Keck School of Medicine, University of Southern California, Los Angeles, CA, USA

Department of Biomedical Engineering, Viterbi School of Engineering, University of Southern California, Los Angeles, CA, USA

USC Stem Cell, Keck School of Medicine, University of Southern California, Los Angeles, CA, USA

to cancer cells. The heterogeneous nature of CTCs is essential when considering the design and implementation of techniques for the detection, isolation, and characterization of these critical metastatic precursors. However, the rarity of CTCs in the blood makes their isolation and subsequent research difficult. Improving our understanding of CTC biology and the underlying molecular and biophysical mechanisms contributing to metastasis, organotropism, and other clinically relevant parameters will generate a more accurate and comprehensive understanding of this devastating phenomenon. In this chapter, we will discuss the physical environment of circulation and its relevance in CTC biology, as well as different engineering approaches for CTC isolation.

**Keywords** Circulating tumor cell · Epithelial-mesenchymal transition · Fluid shear stress · Leukocyte · Metastatic colonization · Microfluidics · Negative selection · Platelet

## 1 Introduction

Circulating tumor cells (CTCs) are malignant cells that acquire distinct biological and physical properties that allow them to move from primary or metastatic solid tumors into the bloodstream where they then circulate and have the potential to disseminate to distant sites as “seeds” of metastasis. However, the circulatory system is a harsh physical environment drastically different from that of a solid tumor. CTC survival in circulation is dependent on numerous factors such as interactions with the physical environmental forces including shear stress forces, collisions, compression, traction, and anoikis, as well as intrinsic biophysical characteristics such as stiffness and deformability [1–3]. Therefore, only CTCs that have certain properties will survive the pressures of the vasculature to form new metastases. Understanding CTC biology and the molecular mechanisms contributing to metastasis, organotropism, and other clinically relevant parameters will generate a comprehensive knowledge of this devastating phenomenon to improve patient outcomes. One major obstacle to achieve this is the difficulty in isolating CTCs for downstream molecular analysis and ex vivo culture, due to the rarity and heterogeneity of CTCs. As a majority of CTCs originate from carcinomas, this chapter will primarily focus on the epithelial subset of solid tumors.

---

M. Yu

Department of Stem Cell Biology and Regenerative Medicine, University of Southern California, Los Angeles, CA, USA

Norris Comprehensive Cancer Center, Keck School of Medicine, University of Southern California, Los Angeles, CA, USA

Present Address: Department of Pharmacology, University of Maryland School of Medicine, Baltimore, MD, USA

e-mail: [Min.Yu@som.umaryland.edu](mailto:Min.Yu@som.umaryland.edu)



Epithelial cells have inherent apical–basal polarity, form strong cell–cell attachments through tight junctions and adherens junctions and are also anchored to the extracellular matrix (ECM) of the basement membrane by hemidesmosome structures [4–5]. Together, these properties enable epithelial organization into mono- or multi-layered epithelium, which line the various luminal spaces of the body. In epithelial cancers, however, these cell–cell adhesions and polarity are disrupted, primarily through the process of epithelial-to-mesenchymal transition (EMT). EMT is a fundamental process of embryogenesis, but it is now clear this process is also instrumental in metastasis [6–7]. During EMT, epithelial cells undergo significant molecular and biophysical changes that alter the cytoskeleton and migratory potential to resemble that of mesenchymal cells. These changes include restructuring of cellular polarity and morphology, loss of cell–cell adhesions due to decreased E-cadherin and increased N-cadherin expression, and increased expression of matrix metalloproteinases that degrade the confining ECM [4–7], all of which enables the transmigration of a tumor cell and the intravasation into circulation, at which point they are referred to as CTCs.

CTCs undergoing EMT exist on a spectrum of intermediate states [8–10], contributing additional phenotypic diversity to the high heterogeneity of CTC populations, both intratumor and between patients. Intratumoral heterogeneity is a well-established feature of solid tumors, due to genomic instability, epigenetic changes, and phenotypic plasticity intrinsic to cancer cells, which, in turn, lead to functional variation between cells [11–16]. Additionally, it has become increasingly clear that interactions with the tumor microenvironment (TME) have significant effects on tumor evolution, highlighting the effect of spatial placement on intratumoral heterogeneity as well [16, 17]. These various molecular factors translate to high diversity in biophysical features of CTCs including surface biomarker expression, size, deformability, and existence in clusters or as single cells. Engineering approaches for the detection, isolation, and characterization of CTCs should take these variations into account to generate robust, accurate representations of these rare cell populations.

In this book chapter, we will first provide an overview of the physical forces exerted on CTCs in the bloodstream and the engineering approaches to mimic these forces in the laboratory to improve our knowledge of CTC survival and metastatic potential. Secondly, we will review the various existing methods for CTC isolation and considerations for the heterogeneity of CTC populations when utilizing one technique or another.

## **2 Physical Environment of CTCs and Engineering Approaches for Research**

### ***2.1 Introduction***

The human vascular system is a highly variable and physically treacherous environment in which CTCs must survive to successfully metastasize. It encompasses

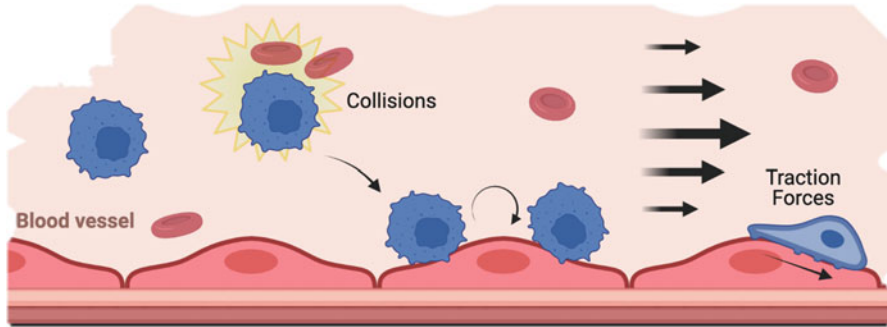


**Fig. 1** CTCs experience various physical stressors as they travel through the circulatory system. These stressors include fluid shear stress, collisions with red blood cells and the vascular endothelium, traction forces, and compressive forces. Created with [BioRender.com](https://www.biorender.com)

a large range of lumen diameters from the large aorta (2 cm) to tiny capillaries (8  $\mu\text{m}$ ), possesses different functional properties depending on whether it is an arterial or venous vessel, displays a wide range of organ-specific endothelial permeability (liver versus blood–brain barrier), and experiences different blood flow velocities depending on the amount of cardiac output at rest or during exercise. In addition to the rate of flow, there are also different types of blood flow patterns, such as disturbed, or turbulent flow in aberrant blood vessels near tumor cells, as well as undisturbed, laminar flow in healthy vessels [18]. Additionally, CTCs experience collisions with other blood cells such as red blood cells (RBCs) and white blood cells (WBCs) at the branch points of furcating blood vessels and the vessel wall. In the smallest capillaries where CTC diameter is larger than the capillary diameter, tumor cells experience compressive forces and undergo large deformations. How these forces affect CTC biology still requires further investigation. Furthermore, differences in cardiovascular anatomy and function and the development, progression, and presentation of vascular diseases are very different between men and women [19]. It is, therefore, conceivable that physiological blood flow profiles measured in men may not be applicable for *in vitro* experimentation of female breast cancer. Modeling the human vascular system is, therefore, incredibly complex and requires a more thorough description of such parameters in both healthy and disease states if we are to grasp its full impact on CTCs and the metastatic cascade (Fig. 1).

## 2.2 CTCs Experience Fluid Shear Stress

The velocity of blood in the center of a blood vessel is higher than that of blood moving closer to the vessel wall [20]. This difference in velocity generates a force vector that is parallel to the cross section of the blood vessel and is defined as fluid shear stress (FSS), whereas the frictional forces exerted by blood flowing against the

endothelial wall are specifically called the wall shear stress (WSS). While WSS has been well studied as a factor influencing remodeling of the vascular endothelium, atherosclerosis, and general health of blood vessels [21–23], the effect of FSS on CTCs or adherent cell lines grown in suspension conditions has been the most well-studied physical parameter *in vitro*. Physiological FSS in humans is reported to range from 0.5 to 4 dynes/cm<sup>2</sup> in venules and 4 to 30 dynes/cm<sup>2</sup> in the arteries [24] but can vary greatly based on the type of blood vessel, location, physical activity, and underlying health conditions.

In a peristaltic pump-based microfluidic assay where cells are continuously circulating for 4 hours, the application of high FSS of 60 dynes/cm<sup>2</sup>, associated with vigorous exercise, was found to destroy more CTCs than physiological levels of FSS that are typical of human arteries in the resting state [25]. The high FSS condition resulted in the death of 90% of CTCs within the first 4 hours of circulation and the majority of surviving cells underwent apoptosis within 24 hours. In clinical studies as well, physical activity was significantly associated with reduced CTC count among stage I–III colon cancer patients [26]. Reduced blood flow, on the other hand, was permissive for the arrest and stable adhesion to the vascular endothelium and subsequent successful extravasation in a zebra fish model [27]. Additionally, FSS plays a role in CTC interactions with other cells that typically traffic and adhere to endothelial cells of the bloodstream such as neutrophils, platelets, and monocytes [28]. The study of neutrophils in promoting metastasis has been gaining traction in recent years [29] and have particular importance in CTC behavior. For example, Chen et al. found that when tumor cells and LPS-stimulated neutrophils were subjected to shear flow conditions *in vitro*, heterotypic cell clusters between these two cell types formed and significantly increased the extravasation potential of tumor cells through interaction and modulation of endothelial cells [30]. Additionally, these researchers observed this phenomenon in an *in vivo* zebra fish model. Platelets are also well known to form complexes with CTCs and increase adhesion to endothelial cells when subjected to FSS *in vitro* [21, 31]. Similarly, another *in vitro* FSS model demonstrates that breast cancer cells under low FSS require monocyte binding to adhere to endothelial cells [32], although it should be noted these studies do not measure the combined effect of numerous hematopoietic cells that are present in patients. Together, these studies highlight the importance of blood flow velocities and shear stress in CTC survival and eventual extravasation. However, while these studies are informative, there are still many unknown parameters that make it difficult to accurately model these forces on CTCs. For example, it is unknown how much shear stress a CTC experiences and for how long in the human body. One study applying an *in vivo* flow cytometry (IVFC) approach with a highly metastatic and adherent MDA-MB-231 cell line in mouse models found that single MDA-MB-231 cells could be detected circulating in the bloodstream with a half-life of about 25–30 minutes, whereas the half-life of circulating tumor clusters was only 6–10 minutes [33].

Other groups looked at the contribution of FSS to the molecular and phenotypic characteristics of CTCs. There are various reports regarding the effect of FSS on the viability and proliferation of colon cancer CTCs [34], the induction of EMT

in breast cancer CTCs [35], induction of RhoA/actomyosin-dependent resistance to mechanical destruction [36], and CTC metabolism [37]. However, the biggest caveat of these studies is that they were performed on adherent cell lines simply grown or assayed in suspension conditions to mimic the circulatory environment and not on true CTCs. The differences in physical and molecular properties between CTCs and adherent cell lines across different cancer types have been well characterized [38–41]. Understandably, the rarity of CTCs in blood samples combined with the paucity of available CTC lines that can be cultured and expanded long term for experiments necessitates the use of CTC-like cells [42]. However, the generalization of phenomenon observed in CTC-like cells to true CTCs must be carefully considered, and the terminology used to describe CTC research needs to be more specific and rigorously defined. Despite these caveats, the experimental approaches to studying tumor cells in suspension have proven to be simple for *in vitro* approaches and provide useful insights. Future experimentation on existing CTC lines or freshly isolated patient CTCs will advance our understanding of FSS on CTC biology.

Controlled FSS can be applied to cells in various microfluidic configurations. Syringe pumps connected to microfluidic devices made of polydimethylsiloxane (PDMS) channels adhered to glass coverslips can model the effect of various shear flow conditions on cells. In a recently reported method, glass coverslips could be directly or indirectly functionalized with various ligands that mimic endothelial cell surface receptors, such as vascular cell adhesion protein 1 (VCAM1) [43]. Indirect functionalization involved embedding freely diffusible receptors in a lipid layer, thus more accurately modeling fluid cell membranes. Direct visualization of cell morphology and adhesion under various flow conditions are possible through the glass coverslip, and adhered cells can later be analyzed for transcriptional or signaling changes.

Peristaltic microfluidic devices are similar except that they are closed-loop systems where the rotational motion of various rollers pumps cell-containing fluid suspensions through the microfluidic device at desired speeds to control flow rate and shear stress in a pulsatile manner [25, 43].

Cone-and-plate shear devices [44, 45] were the earliest techniques to examine the effect of shear stress on cells and involve a rotating cone inside a flat plate filled with cells and fluid. The rotation rate of the cone can be manipulated to control the amount of shear stress applied to the sample in the plate. This technique is based on mechanical principles of non-Newtonian fluids, such as whole blood. A parallel-plate flow chamber [46, 47] is another device where a cell suspension is injected between two parallel plates with a defined gap size, and the rate lateral motion of one of the plates exerts a shear stress on the sample in the gap.

*In vivo* flow cytometry is a type of intravital microscopy method in which cells are injected into a live anesthetized animal, and fluorescently labeled cells are detected in a blood vessel that is between 20 and 50  $\mu\text{m}$  in diameter in the mouse or rat ear [48]. This method involves a complicated set up but can be used to quantitate CTC dynamics in the circulatory system over time, with the caveats being differences between the animal and human circulatory systems and

that the animal must be immobilized. Since initial invention, this technique has been further optimized for increased sensitivity and sampling rate and for detection in larger vessels [49]. Development of a different type of intravital microscopy, where a microscopic window is mounted over the dorsal skin fold to illuminate the superficial blood vessels of an awake and mobile mouse [50], removes the requirement for an animal to be immobilized and can potentially be used to examine the effect of exercise-induced increased blood flow and shear stress on CTC biology and circulatory dynamics.

### ***2.3 CTCs Experience Numerous Collisions***

CTCs can exist as clusters or as single cells. Both can also exist together with non-tumor blood components such as leukocytes and platelets. The differing configurations of CTC composition can affect their survival in circulation as they collide with surrounding RBCs, WBCs, and the vascular anatomy. For example, CTCs coated in platelets were reported to be physically shielded from destruction by natural killer cells [51, 52], which contributes to an increased potential for metastasis. In general, physical interactions between CTCs and their physical environment have been most extensively studied by *in silico* mathematical modeling. Specifically, these collisions generate wall-directed forces that change CTC trajectory and cause margination of cells from the center of a blood vessel to the periphery where fluid velocity is comparatively slower [53] and adhesive interactions can occur [26]. Computational experiments predict that tumor cells frequently adhere to microvascular bifurcations and that increasing numbers of collisions with RBCs are positively correlated with tumor adhesion to the endothelium [54].

Collisions can also result in cell rupture and death. Only cells with favorable intrinsic biophysical characteristics and cytoskeletal composition survive collision events. Intermediate filaments within the cell are responsible for modulating mechanical forces experienced by cells, and vimentin, in particular, has been shown to protect cells against nuclear rupture during migration [55]. Vimentin, an intermediate filament molecule highly expressed in mesenchymal cells, is upregulated by cancer cells undergoing EMT, and therefore, CTCs with a more mesenchymal phenotype may have greater resistance to collision forces compared to CTCs with epithelial phenotypes, although this concept requires further research. Various studies have also examined the contributions of actin and tubulin to CTC survival and metastatic propensity [56]. For example, the ratio of globular (G) to filamentous (F) actin was reported to be higher in malignant cells compared to normal cells [57], but exactly how that translates to mechanical resistance to rupture is unclear.

*In vitro* methods for studying the effect of collisions on CTCs are limited to microfluidic platforms that mimic obstacles encountered in the bloodstream. The obstacle can be on the scale of an individual cell [58] or on a much larger scale to model turbulent flow of a mixture of cells [59]. For example, one study used an *in*

vitro microfluidic device to investigate the correlation between metastatic propensity and resistance to fragmentation upon flow-induced collision at a micropillar-based bifurcation. Results showed that highly metastatic prostate cancer cells were more resistant to fragmentation compared to weakly metastatic cells [58].

## 2.4 CTCs Experience Traction Forces

Besides physical occlusion, which is a passive process, CTCs can adhere to the endothelial cell lining in an active, multi-step process that is very similar to that of leukocytes [60]. CTCs initially experience margination by collisions with RBCs. Closer to the endothelial wall, slower blood flow velocities allow marginated tumor cells to form weak adhesions and begin to roll along the endothelium. If not complexed with platelets or other endothelial interactors, this rolling motion of CTCs alone still increases the probability and strength of adhesive contacts between the cancer cell and the endothelium that eventually results in cell arrest. The continual movement of blood flow over the adhering tumor cell applies an FSS that not only impacts cell morphology but also contributes to traction forces of the cell rolling along the endothelium [61]. Traction forces of leukocytes on vascular endothelial cells were observed to facilitate the opening of junctions before transendothelial migration [62], but whether CTCs also co-opt this mechanism is yet unclear. FSS can also increase the adhesion strength of already adhered cells—according to a study that used adhered glioma cells with or without FSS exposure [63] in a novel live-single-cell extractor (LSCE) assay, which measures the amount of time it takes for a detaching cell to move a specified distance [64]. Adhesion to the endothelium is also affected by the cortical tension exhibited by CTCs. FSS can induce a higher cortical tension, which is correlated with rounded morphology and decreased deformability [63] and faster margination and prolonged time in circulation [73]. As adhesive strength between CTCs and the endothelium increases, lower cortical tension and therefore higher deformability allow for lower rolling velocities and a higher degree of cell spreading that enables the formation of firm adhesions and decreased time in circulation [65, 66]. Once adhered, metastasizing cells must continue to resist rupture under the forces experienced and achieve transendothelial migration. It has been shown that microtentacles on CTCs can facilitate the transendothelial cell migration [67, 68], but whether microtentacles can be induced by physical stresses or if they facilitate CTC survival during extravasation requires further investigation.

In addition to microfluidics-based approaches to examine CTC rolling adhesion on selectin-coated channels, traction forces can be measured using PDMS micropillars. Cells are seeded on a bed of micropillars that can bend like a spring depending on the pillar dimensions. Taking into account the size and spacing of the micropillars, traction forces can be calculated from the amount of displacement experienced by the apex of the micropillar [69].

Traction force microscopy [70] is another method that couples the amount of substrate deformation with the amount of traction force exerted by a cell on that substrate. The substrate can be a wide range of ECM components or hydrogels that are embedded with fluorescent beads. Traction forces upon the substrate causes a measurable displacement of the fluorescent beads that can be quantified and converted into a traction force.

Cortical tension measurements are typically achieved using micropipette aspiration assays, in which a vacuum is applied to the surface of the cell membrane in order to induce a membrane deformation. The amount of negative pressure applied and the amount of membrane deformation can be used to determine the cortical tension of a single cell. High-throughput micropipette aspiration arrays have been developed to assess the individual cortical tensions of a population of cells [71].

## 2.5 CTCs Experience Compressive Forces

It takes less than a minute for blood to circulate around the entire body. When CTCs enter small capillary vessels, they can either squeeze through or become trapped. The number of compressive events and the amount of force experienced by the cell depend on the circulatory half-life, the amount of time spent trapped in the blood vessel (which is related to cell deformability [72]), the size differential between the CTC and the vasculature, intermediate filament expression, and whether they exist as single cells or clusters. Many of these parameters are unknown, but some studies provide clues. At the single cell level, a recent study determined that vimentin intermediate filaments stiffen when the cell experiences compression stain, as opposed to F-actin or microtubules, which typically soften under compressive forces, and that this stiffening of vimentin filaments was also shown to protect nuclei from compression [73]. On the other hand, CTC clusters have been reported to exhibit upregulation of plakoglobin, a desmosomal protein that links the cytoskeletons of adjacent cells together and facilitates tight cell–cell adhesions [6]. These plakoglobin-enriched clusters showed greater resistance to apoptosis compared to single CTCs and had a 23–50-fold higher metastatic potential [33]. This suggests that the supracellular cytoskeletal scaffold generated by plakoglobin upregulation and enhanced desmosomal junctions is a potential mechanism by which mechanical resilience is achieved by distribution of compressive forces [74] across the CTC cluster, therefore leading to the observed phenotypes. In contrast to the idea that CTC clusters maintain their structure and organization under compression, a different study reported that individual cells within an aggregate can rearrange into single-file chain-like configurations in order to squeeze through capillary sized 5–10  $\mu\text{m}$  constrictions [75]. This indicates that each individual cell could experience the same amount of compressive forces, which is highly dependent on cluster size and shape [76]. These are merely speculations, however, and there are many unknowns that warrant further investigation.



On a cellular level, compressive forces can lead to either deformation or rupture. Individual CTCs were observed to undergo extreme physical elongation and deformation in capillaries. Tumor cells observed inside mouse capillaries had 4x increased cellular length and 1.6x greater nuclear length compared to uncompressed cells [77]. Furthermore, nuclear volume and stiffness have been inversely correlated with the ability and speed at which a cell moves through a smaller constrictive vessel [78]. This suggests that cells with nuclei that are more resistant to compressive forces remain lodged in capillary vessels for longer periods of time and can increase the probability of metastatic colonization. Nuclear flattening also results in an increased nuclear transport of the yes-associated protein 1 (YAP1) transcription co-factor that activates genes involved in cancer progression [79]. Therefore, the ability of CTCs and their nuclei to deform and resist rupture and fragmentation under compressive forces determines the rate of metastasis [80].

Indeed, highly metastatic cell lines have been reported to be softer and more deformable than less metastatic cell lines [81] and their parental, isogenic counterparts [82]. Atomic force microscopy (AFM) measurements of metastatic cancer cells isolated from the pleura of patients with lung, breast, and pancreatic cancer were also 70% softer than benign cells [83]. In a study where cell stiffness was directly manipulated by hypo- or hyperosmotic environmental conditions to induce swelling or compression, respectively, increasing the tumor cell stiffness at the periphery of a breast cancer organoid led to a significant decrease in the formation of invasive structures [84]. Furthermore, mechanical compression of brain tumor cells impairs proliferation but can induce migration via MEK1/Erk1 pathway activation [85]. Despite the evidence for the effect of compressive forces on tumor cell behavior and the biophysical characteristics related to modulation of cellular response, there are very limited studies specifically examining the effects of these forces on CTCs. As CTC survival and subsequent metastasis are likely a combination of both selective and adaptive events, future investigations are needed to further elucidate the nuance within the metastatic cascade.

Though there are many ways to apply compressive forces on adherent cells or tissues, the methods described to date for suspension cells are mainly pore or microfluidics based. Pore-based approaches involve driving cell suspensions through membranes containing micron-sized pores. However, microfluidic devices fabricated with constricted microchannels of specific dimensions can better model the anatomy of a blood capillary. A high-throughput microconstriction array has been developed that can drive cells through a constrictive channel and simultaneously provide readouts for the deformability and stiffness of each individual cell in the given population [86]. The dimensions of the microchannels still need to be optimized for different cell lines due to cell/nuclear size considerations in order to find the optimal balance between high throughput and high sensitivity.



### 3 CTC Detection and Isolation Methods

#### 3.1 Introduction

The physical forces exerted on CTCs in the bloodstream directly relate to their rarity. The rarity of CTCs presents significant challenges not only to the actualization of using CTCs as a liquid biopsy for precision medicine but also to the study of these critical metastatic precursors due to difficulties in isolation and downstream analysis. Isolation methods must also account for the heterogeneity in size, density, cluster formation, and biomarker expression of CTCs.

Molecular heterogeneity is common in CTC populations even within a single patient. One major cause of CTC heterogeneity is EMT, which is critical to the invasive and metastatic potential of CTCs [10, 33]. In addition to the previously mentioned changes to polarity, morphology, cell adhesions, and ECM remodeling that enable invasive and migratory behavior, the molecular changes involved in EMT also result in cellular changes in biomarker expression. For example, unlike EMT in development, EMT in cancer is characterized by a switch from cytokeratin expression as the major intermediate filaments to vimentin expression [87, 88]. As cytokeratin expression is often utilized as a biomarker in CTC detection methods, cells along the spectrum of EMT may not be captured and may misrepresent the CTC population. Others have suggested the importance of EMT in regard to the collective migration model, which hypothesizes that groups of heterogeneous tumor cells migrate collectively to form metastases, with a mix of mesenchymal-like cells at the “front,” which aid in ECM remodeling and motility, while partial EMT and epithelial cells that have retained their cell adhesions and proliferative properties exist to hold the cluster together and colonize metastatic sites. This model has been supported by various studies. Research by Tsuji et al. demonstrated that in a BALB/c athymic mouse model, co-injection of both non-EMT and EMT cells is necessary for the formation of metastasis [89]. Additionally, other groups have reported that CTC clusters have a 23–50-fold increased metastatic potential in mouse models [33]. While these studies largely focused on single CTCs and homotypic CTC clusters, heterotypic CTC clusters that can include neutrophils, platelets, and other cell types [90] have been reported to be more resistant to anoikis [91] and shielded from destruction by natural killer cells [92]. This molecular heterogeneity and its correlation to metastatic behavior must also be accounted for when isolating CTCs.

Beyond EMT, molecular plasticity of CTCs has been documented in the literature. In one study, 84% of CTCs analyzed from 19 HER2- breast cancer patients had acquired HER2 expression and some were observed to interconvert between HER2+ and HER2- states [93], highlighting the unique properties and molecular plasticity of CTCs. This study also exemplified that CTCs can exhibit biological characteristics distinct from that of the primary tumor, which has important implications for the molecular characterization of metastatic lesions and metastatic precursor cells.

CTCs are also reported to show a wide range of diversity in physical properties not only within a single patient but also between CTC populations of different cancer types. For example, whereas ER+/PR+ breast cancer CTCs are reported to have diameters ranging from 9 to 19  $\mu\text{m}$ , most melanoma CTC diameters are  $>12 \mu\text{m}$  [94]. However, to complicate things further, reports have shown that between melanoma patients, there is also a range of median CTC sizes, with one patient demonstrating a median CTC diameter of 16  $\mu\text{m}$ , while another had a median CTC diameter of approximately 10  $\mu\text{m}$  [94], with 10  $\mu\text{m}$  being the approximate size of the white blood cells from the same patient. Given the heterogeneity of CTC population, many groups are focusing on developing technologies that can isolate CTCs based on various combinations of molecular and biophysical properties.

As mentioned in the previous chapter, there are currently only a handful of patient-derived CTC lines that have been successfully established for long-term culture and expansion: six from luminal breast cancer patients [95], one from prostate [96], and one from colon cancer [97]. Although advanced technologies exist for the fixation, detection, and enumeration of CTCs in set volumes of patient blood, there is an urgent need for further development of techniques that can isolate live, rare CTCs for ex vivo expansion and in vitro and in vivo characterization. This was highlighted by findings from Klotz et al., in which the researchers demonstrated that CTC cell lines established from breast cancer patients generate metastases in mice with similar organotropism as observed in the individual patients from which the CTCs were derived [98]. Although technological advances for the study of CTCs are expanding rapidly, each method has particular advantages and disadvantages. In this section, we will provide an overview of the various methodologies to CTC detection and isolation, in particular, focusing on techniques that can isolate live, rare CTCs for ex vivo expansion and in vitro and in vivo characterization (Table 1).

### ***3.2 Positive Selection Approach to CTC Isolation***

Positive enrichment-based approaches to CTC isolation, meaning those that select for a tumor-associated antigen expressed on the surface of CTCs, are an attractive concept as they theoretically allow for the selective isolation of CTCs with a high specificity and reproducibility. The most common biomarker used for positive selection CTC isolation is epithelial cell adhesion molecule (EpCAM), which is highly and exclusively expressed by epithelial cells.

Currently, the only FDA-approved system for CTC detection is the CellSearch<sup>®</sup> platform, which utilizes a positive selection approach. CellSearch is specifically designed for the enumeration of CTCs but not necessarily the isolation or downstream molecular analysis of these cells. This system uses an antibody-conjugated ferromagnetic approach to first isolate all EpCAM-expressing cells in the buffy coat (thin cell fraction in an anticoagulated blood sample that contains a concentration of white blood cells and platelets after centrifugation) of a whole blood sample.

**Table 1** Examples of CTC isolation technologies

Technology	Approach	Method	Molecular analysis compatible	Cells viable	Advantages & limitations	Refs
CellSearch	Positive selection	Anti-EpCAM immunomagnetic beads	No	No	High specificity, semi-automated, substantial clinical evidence, commercially available Limited detection of heterogeneous populations.	[99–104]
HD-SCA	Positive selection	All nucleated cells plated on slides, antibody cocktail (CD45, pCK, vimentin) used for CTC detection	Yes	No	Heterogeneous CTC detection, high specificity Not compatible live cell, imaging dependent	[109, 110]
CTC-iChip	Negative selection, size based	Antibody cocktail (anti-CD45,-CD15), inertial particle focusing size depletion, & magnetic sorting of negative selection CD45+ CD15+ cells	Yes	Yes	High-throughput, automated, high sensitivity, heterogeneous CTC detection Lower specificity	[94, 95]
PIC&RUN	Negative selection, density gradient	Density depletion non-nucleated cells and immune marker antibody cocktail	Yes	Yes	Single-live-cell isolation, heterogeneous CTC detection, high viability, high sensitivity Lower specificity, long processing time	[111]
Accucyte	Density gradient	Separation of buffy coat and RBC without lysis, nucleated cells plated on slide for IF verification	Yes	No	Heterogeneous CTC detection, no pretreatment required, unbiased selection all nucleated cells Not compatible live cell, imaging dependent	[115–118]
RosetteSep	Negative selection, density gradient	Crosslinking WBCs to RBCs, then Ficoll-Paque density separation	Yes	Yes	Heterogeneous CTC detection, high viability, commercially available Low specificity, low efficiency	[96], [119], [120]

(continued)

**Table 1** (continued)

Technology	Approach	Method	Molecular analysis compatible	Cells viable	Advantages & limitations	Refs
Parsortix	Size and deformability	Captures cells with large size and low deformability compared to WBC and RBC	Yes	Yes	Antigen independent, suitable heterogeneous CTCs Low purity, no capture of smaller or highly deformable CTCs present in many patients	[123–126]
N/a	Acoustofluidic	Ultrasonic standing wave field forces cells through a channel for separation based on physical parameters (size, deformability)	Yes	Yes	High throughput, automated, antigen independent Pre-processing may result in cell loss	[15], [134–136]
ApoStream	Dielectrophoresis	Nonuniform electric forces applied to cells exploit the dielectric properties between WBCs and CTCs	Yes	Yes	High throughput, automated, antigen independent Pre-processing may result in cell loss	[137, 138]
DEParrray	Dielectrophoresis	Nonuniform electric field exerts forces on cells in suspension to create single-cell “cages.”	Yes	Yes	Single cell, high throughput, automated imaging, detection of heterogeneous populations Pre-enrichment; pre-processing may result in cell loss	[139]

These EpCAM+ cells are stained with fluorescently labeled antibodies against the epithelial markers cytokeratins 8, 18, and/or 19 (pan-cytokeratin, pCK) and the white blood cell marker CD45, aligned to a single focal plane by a magnet, and then microscopically identified as a true CTC by pCK+ and CD45- status [99–104].

The major caveat to positive antibody-based selection approaches like the CellSearch<sup>®</sup> system is that a CTC population within an individual exhibits a spectrum of gene expression along the EMT continuum that can preclude more mesenchymal-like CTCs from EpCAM-based detection [10]. These CTCs also show epithelial–mesenchymal plasticity (EMP) and can possess molecular characteristics of one or the other, or even both simultaneously [105], further complicating positive-selection-based approaches. Additionally, certain cancers like clear cell renal cell carcinoma have reduced EpCAM expression, suggesting positive selection approaches based on this marker would not be an appropriate choice in this or similar contexts [106]. Positive selection can be based on other biomarkers, such as EGFR [107] or folate receptor [108], but a similar bias will be applied as only cells expressing those markers will be captured. Other methods of tumor-antigen-based identification of CTCs, such as the high-definition single-cell analysis (HD-SCA) platform, may expand on this technique by isolating and plating all nucleated cells from a whole blood sample onto a slide and then performing immunofluorescence staining for immune cell markers and pCK and vimentin [109, 110], potentially capturing a greater range of heterogeneous CTCs. Importantly, however, these methods are still not compatible with live cell capture and ex vivo culture due to the requirements of fixation for immunofluorescence staining.

### ***3.3 Negative Selection Approach to CTC Isolation***

Given that antibody-based positive selection approaches selectively enrich for only a subset of CTCs, many groups are working on the development of negative selection approaches to CTC isolation, or those that rely on the identification and/or depletion of the leukocyte population to thereby detect and isolate CTCs. These methods often combine biomarker-based strategies with other methods that take biophysical factors such as size or density into account. For example, PIC&RUN [111] is a recently developed negative selection assay based on the AccuCyte<sup>®</sup> density-based cell separation instrument and RareCyte<sup>®</sup> robotic detection and retrieval system (reviewed more thoroughly in Sect. 3.4). In the negative selection module of the PIC&RUN protocol, all nucleate cells within the buffy coat of a blood sample are retrieved by AccuCyte<sup>®</sup>-based separation and subsequently stained with a live cell dye and an antibody cocktail detecting immune cells. The cells that are labeled with the live cell dye but negative for immune markers are thus identified as CTCs, isolated by a computer-controlled robotic needle and transferred to a cell culture vessel. Subsequent molecular and phenotypic analysis confirms these cells as CTCs.

The CTCs isolated in this antibody-agnostic, negative selection approach remained viable and were able to be expanded in culture [111].

Another negative-selection-based method is the CTC-iChip [94], a microfluidic device combining size and negative-selection-based systems. In this approach, magnetic labelling of CD45+/CD15+ WBCs in whole blood is applied prior to sample input into the microfluidic device. Nucleated cells, including CTCs and WBCs, are debulked from whole blood using deterministic lateral displacement for hydrodynamic size-dependent sorting. The smaller, non-nucleated components including RBCs, platelets, plasma proteins, and free magnetic beads are automatically discarded leaving only nucleated cells. Nucleated cells are then subjected to inertial particle focusing to create a tight row of single nucleated cells entering the collection channel, upon which magnetophoresis is applied to deflect magnetically labelled WBCs, leaving only non-labelled CTCs. This platform is responsible for the isolation of the six successfully established patient-derived CTC lines from breast cancer patients, a valuable resource for long-term culture of patient-derived CTCs [95].

Compared to antibody-based positive selection approaches, the tumor-antigen-free negative selection approaches are capable of a more heterogeneous CTC capture and thus isolate greater numbers of CTCs that may better represent a patient tumor population [111–113]. However, CTC selection without the use of antibodies is difficult and requires the integration of multiple approaches in various combinations and permutations optimized for different types of cancers. Too much cell manipulation can impact downstream viability, whereas too little can lead to impurities and contaminants that contribute to noise and obscure biological data.

### ***3.4 Density-Gradient-Based CTC Isolation***

A majority of CTCs have densities that are similar to that of the buffy coat (<1.077 g/mL) [114], although some very small CTCs and CTC clusters can have much lower or higher densities. Density-based approaches, therefore, involve mixing blood samples with solutions that are formulated to precise densities to achieve separation of red blood cells and granulocytes that have densities >1.077 g/mL from the less-dense CTC-containing buffy coat layer.

The AccuCyte<sup>®</sup> instrument and RosetteSep<sup>™</sup> procedure are both density-based CTC isolation methods that work by the same principles but differ in their approaches to the challenges of getting a clean separation of the different cell layers. The AccuCyte<sup>®</sup> by RareCyte [115] overcomes this challenge by utilizing a float with specific density in the blood collection tube, which settles between the red blood cell (RBC) layer and the buffy coat after centrifugation. A CyteSealer<sup>®</sup> device then forms a tight seal around the float to accurately and reproducibly separate the buffy coat from the RBCs without human manipulation [116]. All nucleated cells isolated from the buffy coat are then plated onto a slide for subsequent

immunofluorescence staining to differentiate CTCs from immune cells. Slides are scanned by a high-speed fluorescence scanner, the CtyeFinder<sup>®</sup> [117], and verified CTCs can then be picked using the CtyePicker<sup>®</sup> module, which utilizes a ceramic-tipped needle to extract single cells [118]. Various compatible antibody panels are available from the company depending on the cancer type being investigated. However, although the AccuCyte<sup>®</sup> technology provides an unbiased and antigen-independent isolation of all nucleated cells including CTCs, it is not compatible with downstream analyses requiring live cells. The RosetteSep<sup>™</sup> procedure, on the other hand, works by crosslinking the undesired cells (WBCs) to the RBCs before density centrifugation, thereby pelleting unwanted cells and leaving behind live CTCs for downstream analysis, including for ex vivo culture [119, 120]. Of note, the RosetteSep<sup>™</sup> procedure using CD45 depletion prior to density-based separation with Ficoll-Paque was used to successfully isolate viable CTCs from one prostate cancer patient to establish a patient-derived prostate cancer CTC line [96]. Density-gradient approaches have the advantages of unbiased CTC selection but are also limited by a lower specificity and therefore lower purity for downstream analyses.

### ***3.5 Size-/Deformability-Based CTC Isolation***

CTCs from different types of cancers are reported to be different sizes. In a study that used the CellSearch<sup>®</sup> platform to detect a total of 71,612 patient-derived CTCs from across different cancer types, the median computed diameter was reported to be 12.4  $\mu\text{m}$  in breast cancer, 10.3  $\mu\text{m}$  in prostate cancer, 7.5  $\mu\text{m}$  in colorectal cancer, and 8.6  $\mu\text{m}$  in bladder cancer [41]. Leukocytes, on the other hand, had a median computed diameter of 9.4  $\mu\text{m}$  in this study [39], whereas other groups that used different detection and measurement methods have reported diameters ranging between 7 and 20  $\mu\text{m}$  [121]. In addition to cell size, deformability is another biophysical parameter that can be exploited to isolate CTCs. Deformability is defined as the amount of change in shape under application of a defined amount of pressure without rupture. Related to deformability is the concept of cellular stiffness, which is defined as the amount of resistance to deformation under an applied force. Although a higher deformability of tumor cells is correlated with increased metastatic propensity [81, 122], they are reported to be comparatively less deformable than RBCs and WBCs [72].

The Parsortix<sup>®</sup> system takes advantage of both the size and deformability parameters of CTCs to isolate them from other blood components [123–125]. This technology involves injecting a whole blood sample through a filtration cassette that captures CTCs based on their large size and low deformability (high resistance to compressive forces) while letting other blood components pass through. Although Parsortix<sup>®</sup> can isolate significantly more mesenchymal CTCs compared to the antibody-based CellSearch<sup>®</sup> system [124], CTC sizes can overlap with some WBCs, and the deformability of different types of cancer cells compared to the surrounding

blood components is yet to be extensively studied. At the time of this writing, the Parsortix<sup>®</sup> system is under evaluation in a clinical trial that began in 2018 (NCT03427450), the results of which will provide insight into the advantages and disadvantages of the size- and deformability-based capture technique.

Inertial particle focusing is another size-based separation technique. This method takes advantage of the physics of fluid forces and particle dynamics flowing through a microchannel [125] to isolate CTCs. The first prototype was designed with a double-spiral inertial focusing configuration [128, 129], but subsequent iterations have investigated various designs to achieve improved CTC separation [130–133].

### **3.6 Acoustofluidic-Based CTC Isolation**

Acoustofluidics is a field of research that uses tunable ultrasonic acoustic waves to achieve microfluidic-based cell separation. Acoustofluidic separation of CTCs takes advantage of how acoustic waves interact with the physical properties of fluids and the particles embedded within and enables a contactless and more biocompatible approach to CTC isolation. The first proof-of-concept acoustofluidic separation of tumor cells from WBCs was developed using prostate cancer cell lines spiked into whole blood [134]. In this first-generation prototype of acoustofluidic-based tumor cell isolation from blood samples, RBCs were depleted by lysis buffers before processing the remaining WBCs and tumor fraction by acoustic focusing [134]. Since then, protocols have been optimized to detect CTCs from breast cancer [137] and metastatic castration-resistant prostate cancer patients [136]. Of note, these protocols require an RBC lysis step, which may result in loss of rare CTCs or be incompatible with downstream ex vivo culture. Furthermore, acoustofluidic-based approaches have not yet demonstrated capability for isolating viable CTCs from patient samples, thereby presenting opportunities for improvement.

### **3.7 Dielectrophoresis-Based CTC Isolation**

Dielectrophoresis (DEP) isolation approaches leverage the differences in cellular morphology and electrical conductivity between CTCs and WBCs. When a nonuniform high-frequency electrical field is applied to viable cells in a suspension media with low conductivity, a dielectrophoretic force is generated that causes cells to move directionally either toward or away from the electric field depending on their polarization state. The polarization state of a given cell will depend on its surface area and size, which will determine the accumulation of charge on the cell membrane relative to the surrounding media [135]. As cancer cells from solid tumors have been shown to have distinct dielectrical properties compared to blood cells [136], DEP-based approaches can be utilized as an antigen-independent



method for CTC separation from leukocytes. ApoStream™ is a commercially available DEP-based technology that was first developed in 2012 [139], which separates cancer cells from peripheral blood monocytes (PBMCs) and has been proven to work on patient samples [140]. DEPArray™ is a similar technology but has the ability to generate ~30,000 DEP “cages” that can each individually levitate and capture single CTCs avoiding adhesive interactions with other cells and surfaces [141]. A major advantage of DEP approaches compared to other methods utilizing the physical properties of a cell is that it relies on differences in cell surface area, which are on the nanometer scale, compared to other approaches such as size-based separation that rely on micrometer-scale properties with less variation across cell types. While DEP-based approaches are promising, particularly for the capture of heterogeneous CTC populations, further research is needed before they are firmly adopted into clinical practice as the CellSearch platform is.

### ***3.8 Caveats and Future Directions***

Different isolation methods have different downstream consequences—some methods affect cell viability and are therefore not suitable for live cell isolation. Employing singular physical approaches to CTC detection and isolation is also not recommended due to overlapping biophysical parameters. For example, employment of a size-based approach to isolating CTCs from bladder cancer would be unadvisable since they are reported to have diameters similar in range to leukocytes [39]. Moreover, some CTC isolation methods involve WBC depletion, but CTCs can exist in heterotypic cell clusters with WBCs [142] and depletion can unintentionally reduce the already low numbers of CTCs. While methods for CTC cluster isolation are being developed, such as that reported by Boya et al. for the label-free isolation of clusters in meshed microwells [143], refinement of these techniques and comparison to existing methods are needed. It is also evident that the molecular and physical properties of CTCs can vary widely between different types of cancers. Taking a singular approach to broadly capture a heterogeneous population of CTCs is unlikely. However, different approaches can be individually optimized and integrated together in various ways to improve the broad recovery of heterogeneous CTCs. For example, density-based RBC depletion with WBC crosslinking can be combined with acoustofluidic isolation to improve CTC viability, recovery, and purity. In line with both inter-patient and inter-cancer CTC heterogeneity, the standard criteria for CTC identification may require refinement based on a cancer-type or cancer-subtype basis. As such, large-scale profiling of the range of physical parameters of CTCs from different cancers will be needed in future studies to improve our knowledge of CTC biology.

## 4 Conclusions

Mechanical phenotyping of CTCs is quickly being investigated as a way to predict cancer progression. Characterization of stiffness, deformability, and fragmentability are all emerging physical approaches to generating a better understanding of measurable biophysical parameters associated with the metastatic propensity of CTCs. Despite these technological advances, the challenge of CTC rarity remains. This has prompted the use of adherent cell lines grown briefly in suspension conditions to model CTCs. However, the validity of using adherent cell lines as a model for CTCs has never been tested, and there are yet no reports comparing these two distinct biological resources. Since the establishment of the first long-term cultures of CTC lines generated from breast cancer patients [10], there have been continued efforts to develop methods compatible with the isolation of viable CTCs for cell line establishment and the generation of renewable sources of CTCs [90]. Simultaneously, there are also parallel efforts generating biophysical profiles of real CTCs from different cancer types using combinations of the detection, isolation, and mechanical phenotyping platforms described. This will allow for the accurate determination of parameters necessary for in vitro and in silico modeling of CTCs in circulation and the ability to deduce appropriate conclusions from in vivo models.

## References

1. Kumar S, Weaver VM (2009) Mechanics, malignancy, and metastasis: the force journey of a tumor cell. *Cancer Metastasis Rev* 28:113–127. <https://doi.org/10.1007/s10555-008-9173-4>
2. Maeshiro M, Shinriki S, Liu R, Nakachi Y, Komohara Y, Fujiwara Y, Ohtsubo K, Yoshida R, Iwamoto K, Nakayama H et al (2021) Colonization of distant organs by tumor cells generating circulating homotypic clusters adaptive to fluid shear stress. *Sci Rep* 11:6150. <https://doi.org/10.1038/s41598-021-85743-z>
3. Vasilaki D, Bakopoulou A, Tsouknidas A, Johnstone E, Michalakis K (2021) Biophysical interactions between components of the tumor microenvironment promote metastasis. *Biophys Rev* 13:339–357. <https://doi.org/10.1007/s12551-021-00811-y>
4. Teronen TA, Partanen JI, Saarikoski ST, Myllynen M, Marques E, Paasonen K, Moilanen A, Wohlfahrt G, Kovanen PE, Klefstrom J (2011) Faulty epithelial polarity genes and cancer. In: *Advances in cancer research*, Elsevier, pp 97–161
5. Jie X-X, Zhang X-Y, Xu C-J (2017) Epithelial-to-mesenchymal transition, circulating tumor cells and cancer metastasis: mechanisms and clinical applications. *Oncotarget* 8:81558–81571. <https://doi.org/10.18632/oncotarget.18277>
6. Thiery JP, Acloque H, Huang RYJ, Nieto MA (2009) Epithelial-mesenchymal transitions in development and disease. *Cell* 139:871–890. <https://doi.org/10.1016/j.cell.2009.11.007>
7. Hotary K, Li X-Y, Allen E, Stevens SL, Weiss SJ (2006) A cancer cell metalloprotease triad regulates the basement membrane transmigration program. *Genes Dev* 20:2673–2686. <https://doi.org/10.1101/gad.1451806>
8. Sun Y-F, Guo W, Xu Y, Shi Y-H, Gong Z-J, Ji Y, Du M, Zhang X, Hu B, Huang A et al (2018) Circulating tumor cells from different vascular sites exhibit spatial heterogeneity in epithelial and mesenchymal composition and distinct clinical significance in hepatocellular carcinoma. *Clin Cancer Res* 24:547–559. <https://doi.org/10.1158/1078-0432.CCR-17-1063>

9. Yang J, Antin P, Berx G, Blanpain C, Brabletz T, Bronner M, Campbell K, Cano A, Casanova J, Christofori G et al (2020) Guidelines and definitions for research on epithelial–mesenchymal transition. *Nat Rev Mol Cell Biol* 21:341–352. <https://doi.org/10.1038/s41580-020-0237-9>
10. Yu M, Bardia A, Wittner BS, Stott SL, Smas ME, Ting DT, Isakoff SJ, Ciciliano JC, Wells MN, Shah AM et al (2013) Circulating breast tumor cells exhibit dynamic changes in epithelial and mesenchymal composition. *Science* 339:580–584. <https://doi.org/10.1126/science.1228522>
11. Dentre SC, Leshchiner I, Haase K, Tarabichi M, Wintersinger J, Deshwar AG, Yu K, Rubanova Y, Macintyre G, Demeulemeester J et al (2021) Characterizing genetic intra-tumor heterogeneity across 2,658 human cancer genomes. *Cell* 184:2239–2254.e39. <https://doi.org/10.1016/j.cell.2021.03.009>
12. Heitzer E, Auer M, Gasch C, Pichler M, Ulz P, Hoffmann EM, Lax S, Waldispuehl-Geigl J, Mauermann O, Lackner C et al (2013) Complex tumor genomes inferred from single circulating tumor cells by array-CGH and next-generation sequencing. *Cancer Res* 73:2965–2975. <https://doi.org/10.1158/0008-5472.CAN-12-4140>
13. Lim SB, Lim CT, Lim W-T (2019) Single-cell analysis of circulating tumor cells: why heterogeneity matters. *Cancers* 11:1595. <https://doi.org/10.3390/cancers11101595>
14. Lohr JG, Adalsteinsson VA, Cibulskis K, Choudhury AD, Rosenberg M, Cruz-Gordillo P, Francis JM, Zhang C-Z, Shalek AK, Satija R et al (2014) Whole-exome sequencing of circulating tumor cells provides a window into metastatic prostate cancer. *Nat Biotechnol* 32:479–484. <https://doi.org/10.1038/nbt.2892>
15. Magnusson C, Augustsson P, Lenshof A, Ceder Y, Laurell T, Lilja H (2017) Clinical-scale cell-surface-marker independent acoustic microfluidic enrichment of tumor cells from blood. *Anal Chem* 89:11954–11961. <https://doi.org/10.1021/acs.analchem.7b01458>
16. Tirosh I, Suvà ML (2019) Deciphering human tumor biology by single-cell expression profiling. *Annu Rev Cancer Biol* 3:151–166. <https://doi.org/10.1146/annurev-cancerbio-030518-055609>
17. Grünwald BT, Devisme A, Andrieux G, Vyas F, Aliar K, McCloskey CW, Macklin A, Jang GH, Denroche R, Romero JM et al (2021) Spatially confined sub-tumor microenvironments in pancreatic cancer. *Cell* 184:5577–5592.e18. <https://doi.org/10.1016/j.cell.2021.09.022>
18. Chiu J-J, Chien S (2011) Effects of disturbed flow on vascular endothelium: pathophysiological basis and clinical perspectives. *Physiol Rev* 91:327–387. <https://doi.org/10.1152/physrev.00047.2009>
19. Huxley VH (2007) Sex and the cardiovascular system: the intriguing tale of how women and men regulate cardiovascular function differently. *Adv Physiol Educ* 31:17–22. <https://doi.org/10.1152/advan.00099.2006>
20. Tangelder GJ, Slaaf DW, Arts T, Reneman RS (1988) Wall shear rate in arterioles in vivo: least estimates from platelet velocity profiles. *Am J Phys Heart Circ Phys* 254:H1059–H1064. <https://doi.org/10.1152/ajpheart.1988.254.6.H1059>
21. Puri R, Leong DP, Nicholls SJ, Liew GYL, Nelson AJ, Carbone A, Copus B, Wong DT, Beltrame JF, Worthley SG et al (2015) Coronary artery wall shear stress is associated with endothelial dysfunction and expansive arterial remodeling in patients with coronary artery disease. *EuroIntervention* 10:1440–1448. <https://doi.org/10.4244/EIJV10I12A249>
22. Paszkowiak JJ, Dardik A (2003) Arterial Wall shear stress: observations from the bench to the bedside. *Vasc Endovasc Surg* 37:47–57. <https://doi.org/10.1177/153857440303700107>
23. Tian Y, Fopiano KA, Buncha V, Lang L, Rudic RD, Filosa JA, Dou H, Bagi Z (2022) Aging-induced impaired endothelial wall shear stress mechanosensing causes arterial remodeling via JAM-A/F11R shedding by ADAM17. *GeroScience* 44:349–369. <https://doi.org/10.1007/s11357-021-00476-1>
24. Mitchell MJ, King MR (2013) Fluid shear stress sensitizes cancer cells to receptor-mediated apoptosis via trimeric death receptors. *New J Phys* 15:015008. <https://doi.org/10.1088/1367-2630/15/1/015008>

25. Regmi S, Fu A, Luo KQ (2017) High shear stresses under exercise condition destroy circulating tumor cells in a microfluidic system. *Sci Rep* 7:39975. <https://doi.org/10.1038/srep39975>
26. Brown JC, Rhim AD, Manning SL, Brennan L, Mansour AI, Rustgi AK, Damjanov N, Troxel AB, Rickels MR, Ky B et al (2018) Effects of exercise on circulating tumor cells among patients with resected stage I-III colon cancer. *PLoS One* 13:e0204875. <https://doi.org/10.1371/journal.pone.0204875>
27. Follain G, Osmani N, Azevedo AS, Allio G, Mercier L, Karreman MA, Solecki G, Garcia León MJ, Lefebvre O, Fekonja N et al (2018) Hemodynamic forces tune the arrest, adhesion, and extravasation of circulating tumor cells. *Dev Cell* 45:33–52.e12. <https://doi.org/10.1016/j.devcel.2018.02.015>
28. Huang Q, Hu X, He W, Zhao Y, Hao S, Wu Q, Li S, Zhang S, Shi M (2018) Fluid shear stress and tumor metastasis. *Am J Cancer Res* 8:763–777
29. Szczerba BM, Castro-Giner F, Vetter M, Krol I, Gkountela S, Landin J, Scheidmann MC, Donato C, Scherrer R, Singer J et al (2019) Neutrophils escort circulating tumour cells to enable cell cycle progression. *Nature* 566:553–557. <https://doi.org/10.1038/s41586-019-0915-y>
30. Chen MB, Hajal C, Benjamin DC, Yu C, Azizgolshani H, Hynes RO, Kamm RD (2018) Inflamed neutrophils sequestered at entrapped tumor cells via chemotactic confinement promote tumor cell extravasation. *Proc Natl Acad Sci U S A* 115:7022–7027. <https://doi.org/10.1073/pnas.1715932115>
31. Jabbar AA, Kazarian T, Hakobyan N, Valentino LA (2006) Gangliosides promote platelet adhesion and facilitate neuroblastoma cell adhesion under dynamic conditions simulating blood flow. *Pediatr Blood Cancer* 46:292–299. <https://doi.org/10.1002/pbc.20326>
32. Evani SJ, Prabhu RG, Gnanaruban V, Finol EA, Ramasubramanian AK (2013) Monocytes mediate metastatic breast tumor cell adhesion to endothelium under flow. *FASEB J* 27:3017–3029. <https://doi.org/10.1096/fj.12-224824>
33. Aceto N, Bardia A, Miyamoto DT, Donaldson MC, Wittner BS, Spencer JA, Yu M, Pely A, Engstrom A, Zhu H et al (2014) Circulating tumor cell clusters are oligoclonal precursors of breast cancer metastasis. *Cell* 158:1110–1122. <https://doi.org/10.1016/j.cell.2014.07.013>
34. Fan R, Emery T, Zhang Y, Xia Y, Sun J, Wan J (2016) Circulatory shear flow alters the viability and proliferation of circulating colon cancer cells. *Sci Rep* 6:27073. <https://doi.org/10.1038/srep27073>
35. Xin Y, Li K, Yang M, Tan Y (2020) Fluid shear stress induces EMT of circulating tumor cells via JNK Signaling in favor of their survival during hematogenous dissemination. *IJMS* 21:8115. <https://doi.org/10.3390/ijms21218115>
36. Moose DL, Krog BL, Kim T-H, Zhao L, Williams-Perez S, Burke G, Rhodes L, Vanneste M, Breheny P, Milhem M et al (2020) Cancer cells resist mechanical destruction in circulation via RhoA/Actomyosin-dependent mechano-adaptation. *Cell Rep* 30:3864–3874.e6. <https://doi.org/10.1016/j.celrep.2020.02.080>
37. Park H-A, Brown SR, Kim Y (2020) Cellular mechanisms of circulating tumor cells during breast cancer metastasis. *IJMS* 21:5040. <https://doi.org/10.3390/ijms21145040>
38. Lazar DC, Cho EH, Luttgen MS, Metzner TJ, Uson ML, Torrey M, Gross ME, Kuhn P (2012) Cytometric comparisons between circulating tumor cells from prostate cancer patients and the prostate-tumor-derived LNCaP cell line. *Phys Biol* 9:016002. <https://doi.org/10.1088/1478-3975/9/1/016002>
39. Mendelaar PAJ, Kraan J, Van M, Zeune LL, Terstappen LWMM, Oomen-de Hoop E, Martens JWM, Sleijfer S (2021) Defining the dimensions of circulating tumor cells in a large series of breast, prostate, colon, and bladder cancer patients. *Mol Oncol* 15:116–125. <https://doi.org/10.1002/1878-0261.12802>
40. Park S, Ang RR, Duffy SP, Bazov J, Chi KN, Black PC, Ma H (2014) Morphological differences between circulating tumor cells from prostate cancer patients and cultured prostate cancer cells. *PLoS One* 9:e85264. <https://doi.org/10.1371/journal.pone.0085264>

41. Rao C, Chianese D, Doyle G, Miller M, Russell T, Sanders R, Terstappen L (2005) Expression of epithelial cell adhesion molecule in carcinoma cells present in blood and primary and metastatic tumors. *Int J Oncol* 27(1):49–57. <https://doi.org/10.3892/ijo.27.1.49>
42. Park JY, Jeong AL, Joo HJ, Han S, Kim S-H, Kim H-Y, Lim J-S, Lee M-S, Choi H-K, Yang Y (2018) Development of suspension cell culture model to mimic circulating tumor cells. *Oncotarget* 9:622–640. <https://doi.org/10.18632/oncotarget.23079>
43. Voyvodic PL, Min D, Baker AB (2012) A multichannel dampened flow system for studies on shear stress-mediated mechanotransduction. *Lab Chip* 12:3322. <https://doi.org/10.1039/c2lc40526a>
44. Franzoni M, Cattaneo I, Ene-Iordache B, Oldani A, Righettini P, Remuzzi A (2016) Design of a cone-and-plate device for controlled realistic shear stress stimulation on endothelial cell monolayers. *Cytotechnology* 68:1885–1896. <https://doi.org/10.1007/s10616-015-9941-2>
45. Ye C, Ali S, Sun Q, Guo M, Liu Y, Gao Y, Huo B (2019) Novel cone-and-plate flow chamber with controlled distribution of wall fluid shear stress. *Comput Biol Med* 106:140–148. <https://doi.org/10.1016/j.combiomed.2019.01.014>
46. Martines E, McGhee K, Wilkinson C, Curtis A (2004) A parallel-plate flow chamber to study initial cell adhesion on a nanofeatured surface. *IEEE Trans Nanobiosci* 3:90–95. <https://doi.org/10.1109/TNB.2004.828268>
47. Munn LL, Melder RJ, Jain RK (1994) Analysis of cell flux in the parallel plate flow chamber: implications for cell capture studies. *Biophys J* 67:889–895. [https://doi.org/10.1016/S0006-3495\(94\)80550-8](https://doi.org/10.1016/S0006-3495(94)80550-8)
48. Novak J, Georgakoudi I, Wei X, Prossin A, Lin CP (2004) In vivo flow cytometer for real-time detection and quantification of circulating cells. *Opt Lett* 29:77. <https://doi.org/10.1364/OL.29.000077>
49. Tan X, Patil R, Bartosik P, Runnels JM, Lin CP, Niedre M (2019b) In vivo flow cytometry of extremely rare circulating cells. *Sci Rep* 9:3366. <https://doi.org/10.1038/s41598-019-40143-2>
50. Saspotas LS, Gambhir SS (2014) Imaging circulating tumor cells in freely moving awake small animals using a miniaturized Intravital microscope. *PLoS One* 9:e86759. <https://doi.org/10.1371/journal.pone.0086759>
51. Palumbo JS, Talmage KE, Massari JV, La Jeunesse CM, Flick MJ, Kombrinck KW, Jirousková M, Degen JL (2005) Platelets and fibrin(ogen) increase metastatic potential by impeding natural killer cell-mediated elimination of tumor cells. *Blood* 105:178–185. <https://doi.org/10.1182/blood-2004-06-2272>
52. Burdick MM, Konstantopoulos K (2004) Platelet-induced enhancement of LS174T colon carcinoma and THP-1 monocytoïd cell adhesion to vascular endothelium under flow. *Am J Phys Cell Phys* 287:C539–C547. <https://doi.org/10.1152/ajpcell.00450.2003>
53. Secomb TW (2016) Hemodynamics. In: Terjung R (ed) *Comprehensive physiology*. Wiley, pp 975–1003
54. Wang S, Ye T, Li G, Zhang X, Shi H (2021) Margination and adhesion dynamics of tumor cells in a real microvascular network. *PLoS Comput Biol* 17:e1008746. <https://doi.org/10.1371/journal.pcbi.1008746>
55. Patteson AE, Vahabikashi A, Pogoda K, Adam SA, Mandal K, Kittisopikul M, Sivagurunathan S, Goldman A, Goldman RD, Janmey PA (2019) Vimentin protects cells against nuclear rupture and DNA damage during migration. *J Cell Biol* 218:4079–4092. <https://doi.org/10.1083/jcb.201902046>
56. Matrone MA, Whipple RA, Balzer EM, Martin SS (2010) Microtentacles tip the balance of cytoskeletal forces in circulating tumor cells. *Cancer Res* 70:7737–7741. <https://doi.org/10.1158/0008-5472.CAN-10-1569>
57. Katsantonis J, Tosca A, Koukouritaki SB, Theodoropoulos PA, Gravanis A, Stournaras C (1994) Differences in the G/total actin ratio and microfilament stability between normal and malignant human keratinocytes. *Cell Biochem Funct* 12:267–274. <https://doi.org/10.1002/cbf.290120407>

58. Kamyabi N, Vanapalli SA (2016) Microfluidic cell fragmentation for mechanical phenotyping of cancer cells. *Biomicrofluidics* 10:021102. <https://doi.org/10.1063/1.4944057>
59. Tan J, Ding Z, Hood M, Li W (2019a) Simulation of circulating tumor cell transport and adhesion in cell suspensions in microfluidic devices. *Biomicrofluidics* 13:064105. <https://doi.org/10.1063/1.5129787>
60. Rejniak KA (2016) Circulating tumor cells: when a solid tumor meets a fluid microenvironment. In: Rejniak KA (ed) *Systems biology of tumor microenvironment*. Springer, Cham, pp 93–106
61. Liu Z, Sniadecki NJ, Chen CS (2010) Mechanical forces in endothelial cells during firm adhesion and early transmigration of human monocytes. *Cell Mol Bioeng* 3:50–59. <https://doi.org/10.1007/s12195-010-0105-3>
62. Yeh Y-T, Serrano R, François J, Chiu J-J, Li Y-SJ, del Álamo JC, Chien S, Lasheras JC (2018) Three-dimensional forces exerted by leukocytes and vascular endothelial cells dynamically facilitate diapedesis. *Proc Natl Acad Sci U S A* 115:133–138. <https://doi.org/10.1073/pnas.1717489115>
63. Li W, Mao S, Khan M, Zhang Q, Huang Q, Feng S, Lin J-M (2019) Responses of cellular adhesion strength and stiffness to fluid shear stress during tumor cell rolling motion. *ACS Sens* 4:1710–1715. <https://doi.org/10.1021/acssensors.9b00678>
64. Mao S, Zhang Q, Li H, Zhang W, Huang Q, Khan M, Lin J-M (2018) Adhesion analysis of single circulating tumor cells on a base layer of endothelial cells using open microfluidics. *Chem Sci* 9:7694–7699. <https://doi.org/10.1039/C8SC03027H>
65. Bose S, Das SK, Karp JM, Karnik R (2010) A Semianalytical model to study the effect of cortical tension on cell rolling. *Biophys J* 99:3870–3879. <https://doi.org/10.1016/j.bpj.2010.10.038>
66. King MR, Phillips KG, Mitrugno A, Lee T-R, de Guillebon AME, Chandrasekaran S, McGuire MJ, Carr RT, Baker-Groberg SM, Rigg RA et al (2015) A physical sciences network characterization of circulating tumor cell aggregate transport. *Am J Phys Cell Phys* 308:C792–C802. <https://doi.org/10.1152/ajpcell.00346.2014>
67. Balzer EM, Whipple RA, Thompson K, Boggs AE, Slovic J, Cho EH, Matrone MA, Yoneda T, Mueller SC, Martin SS (2010) c-Src differentially regulates the functions of microtentacles and invadopodia. *Oncogene* 29:6402–6408. <https://doi.org/10.1038/onc.2010.360>
68. Whipple RA, Matrone MA, Cho EH, Balzer EM, Vitolo MI, Yoon JR, Ioffe OB, Tuttle KC, Yang J, Martin SS (2010) Epithelial-to-mesenchymal transition promotes tubulin detryrosination and microtentacles that enhance endothelial engagement. *Cancer Res* 70:8127–8137. <https://doi.org/10.1158/0008-5472.CAN-09-4613>
69. Coppola S, Schmidt T, Ruocco G, Antonacci G (2019) Quantifying cellular forces and biomechanical properties by correlative micropillar traction force and Brillouin microscopy. *Biomed Opt Express* 10:2202. <https://doi.org/10.1364/BOE.10.002202>
70. Mulligan JA, Bordeleau F, Reinhart-King CA, Adie SG (2018) Traction force microscopy for noninvasive imaging of cell forces. In: Dong C, Zahir N, Konstantopoulos K (eds) *Biomechanics in oncology*. Springer International Publishing, Cham, pp 319–349
71. Davidson PM, Fedorchak GR, Mondésert-Deveraux S, Bell ES, Isermann P, Aubry D, Allena R, Lammerding J (2019) High-throughput microfluidic micropipette aspiration device to probe time-scale dependent nuclear mechanics in intact cells. *Lab Chip* 19:3652–3663. <https://doi.org/10.1039/C9LC00444K>
72. Shaw Bagnall J, Byun S, Begum S, Miyamoto DT, Hecht VC, Maheswaran S, Stott SL, Toner M, Hynes RO, Manalis SR (2015) Deformability of tumor cells versus blood cells. *Sci Rep* 5:18542. <https://doi.org/10.1038/srep18542>
73. Pogoda K, Byfield F, Deptuła P, Cieśluk M, Suprewicz Ł, Skłodowski K, Shivers JL, van Oosten A, Cruz K, Tarasovets E et al (2022) Unique role of Vimentin networks in compression stiffening of cells and protection of nuclei from compressive stress. *Nano Lett* 22:4725–4732. <https://doi.org/10.1021/acs.nanolett.2c00736>
74. Green KJ, Simpson CL (2007) Desmosomes: new perspectives on a classic. *J Investig Dermatol* 127:2499–2515. <https://doi.org/10.1038/sj.jid.5701015>



75. Au SH, Storey BD, Moore JC, Tang Q, Chen Y-L, Javaid S, Sarioglu AF, Sullivan R, Madden MW, O'Keefe R et al (2016) Clusters of circulating tumor cells traverse capillary-sized vessels. *Proc Natl Acad Sci U S A* 113:4947–4952. <https://doi.org/10.1073/pnas.1524448113>
76. Khavari A, Ehrlicher AJ (2019) Nuclei deformation reveals pressure distributions in 3D cell clusters. *PLoS One* 14:e0221753. <https://doi.org/10.1371/journal.pone.0221753>
77. Yamauchi K, Yang M, Jiang P, Yamamoto N, Xu M, Amoh Y, Tsuji K, Bouvet M, Tsuchiya H, Tomita K et al (2005) Real-time *in vivo* dual-color imaging of intracapillary cancer cell and nucleus deformation and migration. *Cancer Res* 65:4246–4252. <https://doi.org/10.1158/0008-5472.CAN-05-0069>
78. Lautscham LA, Kämmerer C, Lange JR, Kolb T, Mark C, Schilling A, Strissel PL, Strick R, Gluth C, Rowat AC et al (2015) Migration in confined 3D environments is determined by a combination of adhesiveness, nuclear volume, contractility, and cell stiffness. *Biophys J* 109:900–913. <https://doi.org/10.1016/j.bpj.2015.07.025>
79. Elosegui-Artola A, Andreu I, Beedle AEM, Lezamiz A, Uroz M, Kosmalska AJ, Oria R, Kechagia JZ, Rico-Lastres P, Le Roux A-L et al (2017) Force triggers YAP nuclear entry by regulating transport across nuclear pores. *Cell* 171:1397–1410.e14. <https://doi.org/10.1016/j.cell.2017.10.008>
80. Weiss L, Nannmark U, Johansson BR, Bagge U (1992) Lethal deformation of cancer cells in the microcirculation: a potential rate regulator of hematogenous metastasis. *Int J Cancer* 50:103–107. <https://doi.org/10.1002/ijc.2910500121>
81. Ahmmed SM, Bithi SS, Pore AA, Muhtasim N, Schuster C, Gollahon LS, Vanapalli SA (2018) Multi-sample deformability cytometry of cancer cells. *APL Bioengineering* 2:032002. <https://doi.org/10.1063/1.5020992>
82. Liu Z, Lee SJ, Park S, Konstantopoulos K, Glunde K, Chen Y, Barman I (2020) Cancer cells display increased migration and deformability in pace with metastatic progression. *FASEB J* 34:9307–9315. <https://doi.org/10.1096/fj.202000101RR>
83. Cross SE, Jin Y-S, Rao J, Gimzewski JK (2007) Nanomechanical analysis of cells from cancer patients. *Nature Nanotech* 2:780–783. <https://doi.org/10.1038/nnano.2007.388>
84. Han YL, Pegoraro AF, Li H, Li K, Yuan Y, Xu G, Gu Z, Sun J, Hao Y, Gupta SK et al (2020) Cell swelling, softening and invasion in a three-dimensional breast cancer model. *Nat Phys* 16:101–108. <https://doi.org/10.1038/s41567-019-0680-8>
85. Kalli M, Voutouri C, Minia A, Pliaka V, Fotis C, Alexopoulos LG, Stylianopoulos T (2019) Mechanical compression regulates brain cancer cell migration through MEK1/Erk1 pathway activation and GDF15 expression. *Front Oncol* 9:992. <https://doi.org/10.3389/fonc.2019.00992>
86. Lange JR, Steinwachs J, Kolb T, Lautscham LA, Harder I, Whyte G, Fabry B (2015) Microconstriction arrays for high-throughput quantitative measurements of cell mechanical properties. *Biophys J* 109:26–34. <https://doi.org/10.1016/j.bpj.2015.05.029>
87. Dongre A, Weinberg RA (2019) New insights into the mechanisms of epithelial–mesenchymal transition and implications for cancer. *Nat Rev Mol Cell Biol* 20:69–84. <https://doi.org/10.1038/s41580-018-0080-4>
88. Welch DR, Hurst DR (2019) Defining the hallmarks of metastasis. *Cancer Res* 79:3011–3027. <https://doi.org/10.1158/0008-5472.CAN-19-0458>
89. Tsuji T, Ibaragi S, Shima K, Hu MG, Katsurano M, Sasaki A, Hu G (2008) Epithelial–mesenchymal transition induced by growth suppressor p12CDK2–AP1 promotes tumor cell local invasion but suppresses distant colony growth. *Cancer Res* 68:10377–10386. <https://doi.org/10.1158/0008-5472.CAN-08-1444.92>
90. Aceto N (2020) Bring along your friends: homotypic and heterotypic circulating tumor cell clustering to accelerate metastasis. *Biom J* 43:18–23. <https://doi.org/10.1016/j.bj.2019.11.002>
91. Velez J, Enciso LJ, Suarez M, Fiegl M, Grismaldo A, López C, Barreto A, Cardozo C, Palacios P, Morales L et al (2014) Platelets promote mitochondrial uncoupling and resistance to apoptosis in leukemia cells: a novel paradigm for the bone marrow microenvironment. *Cancer Microenviron* 7:79–90. <https://doi.org/10.1007/s12307-014-0149-3>

92. Nieswandt B, Hafner M, Echtenacher B, Männel DN (1999) Lysis of tumor cells by natural killer cells in mice is impeded by platelets. *Cancer Res* 59:1295–1300
93. Jordan NV, Bardia A, Wittner BS, Benes C, Ligorio M, Zheng Y, Yu M, Sundaresan TK, Licausi JA, Desai R et al (2016) HER2 expression identifies dynamic functional states within circulating breast cancer cells. *Nature* 537:102–106. <https://doi.org/10.1038/nature19328>
94. Ozkumur E, Shah AM, Ciciliano JC, Emmink BL, Miyamoto DT, Brachtel E, Yu M, Chen P, Morgan B, Trautwein J et al (2013) Inertial focusing for tumor antigen-dependent and –independent sorting of rare circulating tumor cells. *Sci Transl Med* 5:179ra47. <https://doi.org/10.1126/scitranslmed.3005616>
95. Yu M, Bardia A, Aceto N, Bersani F, Madden MW, Donaldson MC, Desai R, Zhu H, Comaills V, Zheng Z et al (2014) Ex vivo culture of circulating breast tumor cells for individualized testing of drug susceptibility. *Science* 345:216–220. <https://doi.org/10.1126/science.1253533>
96. Gao D, Vela I, Sboner A, Iaquinta PJ, Karthaus WR, Gopalan A, Dowling C, Wanjala JN, Undvall EA, Arora VK et al (2014) Organoid cultures derived from patients with advanced prostate cancer. *Cell* 159:176–187. <https://doi.org/10.1016/j.cell.2014.08.016>
97. Cayrefourcq L, Mazard T, Joosse S, Solassol J, Ramos J, Assenat E, Schumacher U, Costes V, Maudelonde T, Pantel K et al (2015) Establishment and characterization of a cell line from human circulating colon cancer cells. *Cancer Res* 75:892–901. <https://doi.org/10.1158/0008-5472.CAN-14-2613>
98. Klotz R, Thomas A, Teng T, Han SM, Iriondo O, Li L, Restrepo-Vassalli S, Wang A, Izadian N, MacKay M et al (2020) Circulating tumor cells exhibit metastatic tropism and reveal brain metastasis drivers. *Cancer Discov* 10:86–103. <https://doi.org/10.1158/2159-8290.CD-19-0384>
99. Andree KC, van Dalum G, Terstappen LWMM (2016) Challenges in circulating tumor cell detection by the CellSearch system. *Mol Oncol* 10:395–407. <https://doi.org/10.1016/j.molonc.2015.12.002>
100. Beije N, Jager A, Sleijfer S (2015) Circulating tumor cell enumeration by the CellSearch system: the clinician’s guide to breast cancer treatment? *Cancer Treat Rev* 41:144–150. <https://doi.org/10.1016/j.ctrv.2014.12.008>
101. Cristofanilli M, Hayes DF, Budd GT, Ellis MJ, Stopeck A, Reuben JM, Doyle GV, Matera J, Allard WJ, Miller MC et al (2005) Circulating tumor cells: a novel prognostic factor for newly diagnosed metastatic breast cancer. *JCO* 23:1420–1430. <https://doi.org/10.1200/JCO.2005.08.140>
102. Hayes DF, Cristofanilli M, Budd GT, Ellis MJ, Stopeck A, Miller MC, Matera J, Allard WJ, Doyle GV, Terstappen LWMM (2006) Circulating tumor cells at each follow-up time point during therapy of metastatic breast cancer patients predict progression-free and overall survival. *Clin Cancer Res* 12:4218–4224. <https://doi.org/10.1158/1078-0432.CCR-05-2821>
103. Miller MC, Doyle GV, Terstappen LWMM (2010) Significance of circulating tumor cells detected by the CellSearch system in patients with metastatic breast colorectal and prostate cancer. *J Oncol* 2010:1–8. <https://doi.org/10.1155/2010/617421>
104. Riethdorf S, Fritsche H, Müller V, Rau T, Schindlbeck C, Rack B, Janni W, Coith C, Beck K, Jänicke F et al (2007) Detection of circulating tumor cells in peripheral blood of patients with metastatic breast cancer: a validation study of the CellSearch system. *Clin Cancer Res* 13:920–928. <https://doi.org/10.1158/1078-0432.CCR-06-1695>
105. Hassan S, Blick T, Thompson EW, Williams ED (2021) Diversity of epithelial-mesenchymal phenotypes in circulating tumour cells from prostate cancer patient-derived xenograft models. *Cancers* 13:2750. <https://doi.org/10.3390/cancers13112750>
106. Maertens Y, Humberg V, Erlmeier F, Steffens S, Steinestel J, Bögemann M, Schrader AJ, Bernemann C (2017) Comparison of isolation platforms for detection of circulating renal cell carcinoma cells. *Oncotarget* 8:87710–87717. <https://doi.org/10.18632/oncotarget.21197>. <https://doi.org/10.18632/oncotarget.21197>
107. Scharpenseel H, Hanssen A, Loges S, Mohme M, Bernreuther C, Peine S, Lamszus K, Goy Y, Petersen C, Westphal M et al (2019) EGFR and HER3 expression in circulating tumor cells and tumor tissue from non-small cell lung cancer patients. *Sci Rep* 9:7406. <https://doi.org/10.1038/s41598-019-43678-6>



108. Hu Y, Chen D, Napoleon JV, Srinivasarao M, Singhal S, Savran CA, Low PS (2022) Efficient capture of circulating tumor cells with low molecular weight folate receptor-specific ligands. *Sci Rep* 12:8555. <https://doi.org/10.1038/s41598-022-12118-3>
109. Chai S, Ruiz-Velasco C, Naghdloo A, Pore M, Singh M, Matsumoto N, Kolatkar A, Xu L, Shishido S, Aparicio A et al (2022) Identification of epithelial and mesenchymal circulating tumor cells in clonal lineage of an aggressive prostate cancer case. *Npj Precis Onc* 6:41. <https://doi.org/10.1038/s41698-022-00289-1>
110. Thiele J-A, Pitule P, Hicks J, Kuhn P (2019) Single-cell analysis of circulating tumor cells. In: Murray SS (ed) *Tumor profiling*. Springer, New York, pp 243–264
111. Kamal M, Saremi S, Klotz R, Iriondo O, Amzaleg Y, Chairez Y, Tulpule V, Lang JE, Kang I, Yu M (2019) PIC&RUN: an integrated assay for the detection and retrieval of single viable circulating tumor cells. *Sci Rep* 9:17470. <https://doi.org/10.1038/s41598-019-53899-4>
112. Drucker A, Teh EM, Kostyleva R, Rayson D, Douglas S, Pinto DM (2020) Comparative performance of different methods for circulating tumor cell enrichment in metastatic breast cancer patients. *PLoS One* 15:e0237308. <https://doi.org/10.1371/journal.pone.0237308>
113. Kang H, Kim J, Cho H, Han K-H (2019) Evaluation of positive and negative methods for isolation of circulating tumor cells by lateral magnetophoresis. *Micromachines* 10:386. <https://doi.org/10.3390/mi10060386>
114. Morgan T, M. (2007) Detection and characterization of circulating and disseminated prostate cancer cells. *Front Biosci* 12:3000. <https://doi.org/10.2741/2290>
115. Ramirez AB, Bhat R, Sahay D, De Angelis C, Thangavel H, Hedayatpour S, Dobrolecki LE, Nardone A, Giuliano M, Nagi C et al (2019) Circulating tumor cell investigation in breast cancer patient-derived xenograft models by automated immunofluorescence staining, image acquisition, and single cell retrieval and analysis. *BMC Cancer* 19:220. <https://doi.org/10.1186/s12885-019-5382-1>
116. Ramirez AB, U'Ren L, Campton DE, Stewart D, Nordberg JJ, Stilwell JL, Kaldjian EP (2017) RareCyte<sup>®</sup> CTC analysis step 1: AccuCyte<sup>®</sup> sample preparation for the comprehensive recovery of nucleated cells from whole blood. In: Magbanua MJM, Park JW (eds) *Circulating tumor cells*. Springer, New York, pp 163–172
117. Werbin JL, Nordberg JJ, Tzucker J, Varshavskaya P, Stilwell JL, Kaldjian EP (2017) RareCyte<sup>®</sup> CTC analysis step 2: detection of circulating tumor cells by CyteFinder<sup>®</sup> automated scanning and Semiautomated image analysis. In: Magbanua MJM, Park JW (eds) *Circulating tumor cells*. Springer, New York, pp 173–180
118. Stilwell JL, Varshavskaya P, Werbin JL, Nordberg JJ, Ramirez AB, Quarre S, Tzucker J, Chow J, Enright B, Kaldjian EP (2017) RareCyte<sup>®</sup> CTC analysis step 3: using the CytePicker<sup>®</sup> module for individual cell retrieval and subsequent whole genome amplification of circulating tumor cells for genomic analysis. In: Magbanua MJM, Park JW (eds) *Circulating tumor cells*. Springer, New York, pp 181–192
119. Gerges N, Rak J, Jabado N (2010) New technologies for the detection of circulating tumour cells. *Br Med Bull* 94:49–64. <https://doi.org/10.1093/bmb/ldq011>
120. Kuske A, Gorges TM, Tennstedt P, Tiebel A-K, Pompe R, Preißer F, Prues S, Mazel M, Markou A, Lianidou E et al (2016) Improved detection of circulating tumor cells in non-metastatic high-risk prostate cancer patients. *Sci Rep* 6:39736. <https://doi.org/10.1038/srep39736>
121. Prinyakupt J, Pluempitwiriyawej C (2015) Segmentation of white blood cells and comparison of cell morphology by linear and naïve Bayes classifiers. *Biomed Eng Online* 14:63. <https://doi.org/10.1186/s12938-015-0037-1>
122. Hakim M, Khorasheh F, Alemzadeh I, Vossoughi M (2021) A new insight to deformability correlation of circulating tumor cells with metastatic behavior by application of a new deformability-based microfluidic chip. *Anal Chim Acta* 1186:339115. <https://doi.org/10.1016/j.aca.2021.339115>

123. Chudziak J, Burt DJ, Mohan S, Rothwell DG, Mesquita B, Antonello J, Dalby S, Ayub M, Priest L, Carter L et al (2016) Clinical evaluation of a novel microfluidic device for epitope-independent enrichment of circulating tumour cells in patients with small cell lung cancer. *Analyst* 141:669–678. <https://doi.org/10.1039/C5AN02156A>
124. Miller MC, Robinson PS, Wagner C, O'Shannessy DJ (2018) The Parsortix™ cell separation system—a versatile liquid biopsy platform. *Cytometry* 93:1234–1239. <https://doi.org/10.1002/cyto.a.23571>
125. Xu L, Mao X, Imrali A, Syed F, Mutsvangwa K, Berney D, Cathcart P, Hines J, Shamash J, Lu Y-J (2015) Optimization and evaluation of a novel size based circulating tumor cell isolation system. *PLoS One* 10:e0138032. <https://doi.org/10.1371/journal.pone.0138032>
126. Kitz J, Goodale D, Postenka C, Lowes LE, Allan AL (2021) EMT-independent detection of circulating tumor cells in human blood samples and pre-clinical mouse models of metastasis. *Clin Exp Metastasis* 38:97–108. <https://doi.org/10.1007/s10585-020-10070-y>
127. Ying Y, Lin Y (2019) Inertial focusing and separation of particles in similar curved channels. *Sci Rep* 9:16575. <https://doi.org/10.1038/s41598-019-52983-z>
128. Sollier E, Go DE, Che J, Gossett DR, O'Byrne S, Weaver WM, Kummer N, Rettig M, Goldman J, Nickols N et al (2014) Size-selective collection of circulating tumor cells using vortex technology. *Lab Chip* 14:63–77. <https://doi.org/10.1039/C3LC50689D>
129. Sun J, Li M, Liu C, Zhang Y, Liu D, Liu W, Hu G, Jiang X (2012) Double spiral microchannel for label-free tumor cell separation and enrichment. *Lab Chip* 12:3952. <https://doi.org/10.1039/c2lc40679a>
130. Abdulla A, Liu W, Gholamipour-Shirazi A, Sun J, Ding X (2018) High-throughput isolation of circulating tumor cells using cascaded inertial focusing microfluidic channel. *Anal Chem* 90:4397–4405. <https://doi.org/10.1021/acs.analchem.7b04210>
131. Lin E, Rivera-Báez L, Fouladdel S, Yoon HJ, Guthrie S, Wieger J, Deol Y, Keller E, Sahai V, Simeone DM et al (2017) High-throughput microfluidic labyrinth for the label-free isolation of circulating tumor cells. *Cell Systems* 5:295–304.e4. <https://doi.org/10.1016/j.cels.2017.08.012>
132. Smith KJ, Jana JA, Kaehr A, Purcell E, Opdycke T, Paoletti C, Cooling L, Thamm DH, Hayes DF, Nagrath S (2021) Inertial focusing of circulating tumor cells in whole blood at high flow rates using the microfluidic CTCKey™ device for CTC enrichment. *Lab Chip* 21:3559–3572. <https://doi.org/10.1039/D1LC00546D>
133. Xu X, Huang X, Sun J, Wang R, Yao J, Han W, Wei M, Chen J, Guo J, Sun L et al (2021) Recent progress of inertial microfluidic-based cell separation. *Analyst* 146:7070–7086. <https://doi.org/10.1039/D1AN01160J>
134. Augustsson P, Magnusson C, Nordin M, Lilja H, Laurell T (2012) Microfluidic, label-free enrichment of prostate cancer cells in blood based on acoustophoresis. *Anal Chem* 84:7954–7962. <https://doi.org/10.1021/ac301723s>
135. Li P, Mao Z, Peng Z, Zhou L, Chen Y, Huang P-H, Truica CI, Drabick JJ, El-Deiry WS, Dao M et al (2015) Acoustic separation of circulating tumor cells. *Proc Natl Acad Sci U S A* 112:4970–4975. <https://doi.org/10.1073/pnas.1504484112>
136. Wu M, Huang P, Zhang R, Mao Z, Chen C, Kemeny G, Li P, Lee AV, Gyanchandani R, Armstrong AJ et al (2018) Circulating tumor cell phenotyping via high-throughput acoustic separation. *Small* 14:1801131. <https://doi.org/10.1002/smll.201801131>
137. Cen EG, Dalton C, Li Y, Adamia S, Pilarski LM, Kaler KVIS (2004) A combined dielectrophoresis, traveling wave dielectrophoresis and electrorotation microchip for the manipulation and characterization of human malignant cells. *J Microbiol Methods* 58:387–401. <https://doi.org/10.1016/j.mimet.2004.05.002>
138. Gascoyne P, Shim S (2014) Isolation of circulating tumor cells by dielectrophoresis. *Cancers* 6:545–579. <https://doi.org/10.3390/cancers6010545>
139. Gupta V, Jafferji I, Garza M, Melnikova VO, Hasegawa DK, Pethig R, Davis DW (2012) ApoStream™, a new dielectrophoretic device for antibody independent isolation and recovery of viable cancer cells from blood. *Biomicrofluidics* 6:024133. <https://doi.org/10.1063/1.4731647>

140. Shim S, Stenke-Hale K, Tsimberidou AM, Noshari J, Anderson TE, Gascoyne PRC (2013) Antibody-independent isolation of circulating tumor cells by continuous-flow dielectrophoresis. *Biomicrofluidics* 7:011807. <https://doi.org/10.1063/1.4774304>
141. Di Trapani M, Manaresi N, Medoro G (2018) DEPArray™ system: an automatic image-based sorter for isolation of pure circulating tumor cells. *Cytometry* 93:1260–1266. <https://doi.org/10.1002/cyto.a.23687>
142. Cho EH, Wendel M, Lutgen M, Yoshioka C, Marrinucci D, Lazar D, Schram E, Nieva J, Bazhenova L, Morgan A et al (2012) Characterization of circulating tumor cell aggregates identified in patients with epithelial tumors. *Phys Biol* 9:016001. <https://doi.org/10.1088/1478-3975/9/1/016001>
143. Boya M, Ozkaya-Ahmadov T, Swain BE, Chu C-H, Asmare N, Civelekoglu O, Liu R, Lee D, Tobia S, Biliya S et al (2022) High throughput, label-free isolation of circulating tumor cell clusters in meshed microwells. *Nat Commun* 13:3385. <https://doi.org/10.1038/s41467-022-31009-9>

# In Vitro and In Vivo Host Models of Metastasis



Sam H. Au

**Abstract** Metastasis is a complex multi-step process that typically occurs over years, making the process challenging to accurately model in the laboratory. This chapter explores our existing animal and non-animal host model systems commonly used to study metastasis: mice, zebrafish and microfluidics. These model systems have inherent strengths and limitations, and the combined use of multiple models either through the use of parallel or integrated model systems can enable new questions to be explored and provide greater confidence to our findings.

**Keywords** Model systems · Metastasis · Mice · Rats · Zebrafish · Animals · Microfluidics

A majority of cancer-related deaths are not caused by primary tumours but are the result of the spread of cancer cells to distant organs, a process called metastasis. Patients who present with metastatic disease at diagnosis have dramatically worse prognoses. For example, patients diagnosed with localized non-metastatic breast cancer have 5-year survival odds of 99%, while those diagnosed with stage IV metastatic cancer have only a 26% chance of 5-year survival [1].

The local microenvironment provides important cues that facilitate or hinder the metastatic process. Tissue stiffness [2], interstitial fluid pressure [3], extracellular matrix pore sizes [4], microvascular confinement [5], fibroblasts [6], neutrophils [7], macrophages [8], platelets [9], extracellular vesicles [10] and inflammation [11] all appear to influence the ability of tumour cells to metastasize. Experimental model systems that accurately mimic human tumour and tissue microenvironments are therefore important for studying the metastatic process and developing inhibitory strategies against it. An instructive case study for our need for better host model

---

S. H. Au (✉)

Department of Bioengineering, Imperial College London, London, UK  
e-mail: [s.au@imperial.ac.uk](mailto:s.au@imperial.ac.uk)

Cancer Research UK Convergence Science Centre, London, UK

systems for metastasis is the example of therapies developed to inhibit matrix metalloproteinases, enzymes that promote tumour cell invasion by degrading extracellular matrix proteins. These therapeutic candidates were successful in preclinical *in vitro* and *in vivo* models but have thus far disappointingly failed clinical trials due to poor efficacy and deleterious side effects when administered to humans [12]. Host model systems that better recapitulate tumourigenesis and drug responses in humans will allow us to accelerate drug discovery and development.

Creating biologically meaningful host models of the metastatic process is particularly difficult for a number of reasons: (1) The metastatic process is very inefficient on a per cell basis. Millions of tumour cells per gram of tumour mass may disseminate into the bloodstream daily [13], yet very few of these eventually establish metastases. (2) While billions of cells may be released over the course of metastatic disease, metastases can be initiated by a single tumour cell or cluster. Experiments that model the physiological rates of metastasis, must therefore balance the requirement for high numbers of individually weakly metastatic competent cells and the challenge of deriving statistical significance from the rare cells that do succeed. (3) Tumour cells that disseminate to distant organs may take years before they establish a metastatic tumour [14, 15] because these cells can remain dormant for decades. Immunocompromised or genetically modified host organisms and transplantation of cell lines with highly aggressive metastatic propensities can accelerate our studies, but these results may be poorly representative of the metastatic process in patients (4). The metastatic process occurs in multiple organ sites and microenvironments. Tumour cells disseminate from primary tumours, intravasate into circulation and transit and extravasate into distant organs for colonization. It is particularly challenging to develop *in vitro* models that accurately represent all these landscapes, but even *in vivo* models have difficulty in this area. For instance, our models should ideally allow us to address inter-patient heterogeneity (e.g. how differences in geography, human behaviour, diet and genetics interact to drive disparate outcomes in metastasis). Advancements in this area will enable us to better explore important epigenetic influences on metastatic progression.

This chapter introduces established and emerging “*in vitro* and *in vivo*” laboratory host models used for metastasis research. Engineered *in vitro* model systems will be compared to living organisms commonly used to model the development of human metastases. Table 1 is a summary of the relative merits and weaknesses of commonly used host model systems. We do not (and may never) have perfect experimental models of human metastasis, but understanding the relative merits and weaknesses of our models may help us draw meaningful conclusions from our data and help us develop better strategies for mimicking the process in humans.

**Table 1** Comparison of strengths and limitations of host model systems for metastasis research

	Rodent	Fish	Large mammalian	Microfluidic & in vitro
Similarity to human microenvironment	+	–	++	+/-
Ease of genetic engineering	+	++	–	N/A
Ease of cellular and subcellular imaging	–	++	–	++
Multi-organ interactions	++	+	++	–
Control over biophysical parameters	–	–	–	++
Feasible throughput	–	+	–	+
Ethical considerations	–	–	–	++

## 1 Rodent Models

Mice and, to a lesser extent, rat models are the most commonly used host organisms for metastasis research. It is difficult to estimate the precise number of animals used for these purposes, but a Pubmed search for “metastasis AND mouse” reveals approximately 3000–4000 journal articles published annually. If we estimate that 8 mice are required per condition and two condition and one control arm are run per experiment, we could conservatively estimate that ~70,000 mice are used in published metastasis research yearly. The widespread use of murine models is due to their high levels of genetic and organ homology to humans, reasonable costs and ease of genetic modification.

Numerous murine models have been developed. Tumours induced by chemical carcinogens [16] and mice genetically engineered to overexpress oncogenes [17] or with inhibited expression of tumour suppressors genes [18] allow for the formation of tumours and metastases in manners that mirror spontaneous tumourigenesis in humans. These models can take up to 12 months or longer to produce detectable metastases [19], however, and by their nature, these developed tumours are not of human origin. Although there is good genetic homology between humans and mice, tumourigenicity in mouse cells differs from human counterparts. Mouse cells spontaneously immortalize in culture and can be transformed by modifying just two oncogenes [20], neither of which are true for human cells.

Xenograft models where human tumour cells are injected into rodents enable the more rapid formation of models of human metastases but require modification of host immunity to prevent cross-species immune responses. Immunodeficient *Prkdc*<sup>-/-</sup> SCID [21] and *Rag1*<sup>-/-</sup> [22] mutant models do not reject xenografts because they lack mature T and B cells, while *Foxn1*<sup>-/-</sup> nude mutants are T cell deficient but still reject xenografts. As explored later, the manner and location that tumour cells are introduced into animals can also considerably bias the results we obtain because tumour cell injections are not representative of how tumours arise and disseminate in humans.

The rodent models described above do not permit us to study the interactions between human immunity and human tumour cells. These interactions are vital for the formation and progression of metastatic tumours [7, 8]. Humanized models attempt to reconstruct human immunity through the engraftment of functioning human immune cells into animal hosts. The introduction of human hematopoietic stem cells and peripheral blood mononuclear cells into mice hosts has led to the establishment of numerous cancer models with humanized host immunity including lymphoma, glioma, breast cancer, colorectal cancer, kidney cancer and prostate tumours [23]. Human immunity in these systems is particularly useful for the development of immunotherapies. Experiments using humanized mice are the gold standard for evaluating safety, efficacy, immune response, exhaustion and persistence in chimeric antigen receptor (CAR) T and NK therapies [24]. An alternative approach to humanizing the immune system of mice is to humanize specific distant organ sites for metastatic colonization. In one example of this, the subcutaneous implantation of bone discs obtained from patients undergoing hip replacement surgery into SCID mice allowed the study of breast cancer colonization patterns into human bone [25]. These humanized models overcome many of the limitations inherent to cross-species studies of cancer, but their use must be considered within the context of the additional expertise, cost and effort required to utilize them.

There are far more details and nuances to rodent models in metastasis research than is covered here. Readers interested in this topic are encouraged to explore more comprehensive reviews elsewhere [26, 27]. Overall, rodent models of metastasis have many strengths, providing more physiological recapitulation of multi-organ interactions than non-mammalian model systems, potential for incorporation of human stromal interactions through humanized models and a lower cost with greater availability of genetically modified models than larger mammalian models. These must be balanced by acknowledging that drug candidate responses in these models may not be representative of those in humans and the ethical implications of our experiments, particularly when serious or severe procedures are required.

## 2 Fish Models

Fish may at first glance seem unlikely models for human metastases, but their use has expanded since the first xenotransplantation of human melanoma cells into zebrafish in 2005 [28]. These vertebrate model organisms have a number of attractive features including: (1) fast reproductive cycles allowing large numbers of experimental conditions to be conducted at low cost, (2) limited immune rejection in young animals since they do not have fully formed immune systems until as late as 6 weeks post fertilization [29], (3) small size meaning that few numbers of rare or precious tumour cells can be efficiently studied, (4) ease of genetic modification because fertilization occurs *in vitro* and (5) naturally transparent at young ages, which when combined with bioluminescent or fluorescent protein

expressing transgenic models allows for superior visualization of tumour cells *in vivo*.

There are some limitations to the use of zebrafish however. Beyond the most obvious reduced genetic homology to humans in comparison to mammals, zebrafish are typically maintained at 28 °C, lower than the human physiological temperature of 37 °C. Incubation at lower temperatures may not be catastrophic to tumour cell functions, however. Follain et al. found that the adhesion characteristics of melanoma cells to endothelial cells was not impaired at 28 °C [30], and Lee et al. reported that the proliferative colony formation ability of melanoma cells was retained at 31 °C on agar [28]. An alternative compromise to address this temperature mismatch may be to incubate zebrafish around 35 °C, which appears to allow normal fish development [31, 32]. Some concerns, however, remain around potential zebrafish development defects, transcriptional changes in response to hyperthermia and differential drug responses by tumour cells at non-physiological temperatures [33].

Another limitation to the use of zebrafish as metastasis models is the difference in anatomy in comparison to humans. Zebrafish lack organs such as lungs and mammarys, which limits opportunities for orthotopic transplantation. Organ systems in zebrafish are also often of a much smaller scale than that of humans, which can lead to significant differences in biomechanical parameters. For instance, the circulatory system of zebrafish 2–3 days post fertilization is comprised of ~5–10 µm diameter, one-cell thick blood vessels that are good models of human capillaries but not larger vessels [34] and have pressure drops across their circulation lower than that across human capillaries [35, 36]. When combined with fish genetically engineered to express fluorescent protein throughout their blood vessels [37], zebrafish models are exceptional platforms for studying the behaviour of circulating tumour cells (CTCs) in the micro circulation [30, 38]. Care should still be taken when translating results to humans due to anatomical differences in the vasculature. As described in more depth below, tumour cells were found to preferentially occlude in regions of zebrafish microvasculature [30] of which there is no human analog.

Transgenic models with fluorescently tagged reporter neutrophils [39] and macrophages [40] allow us to study interactions between immune cells and tumour cells at single-cell resolution over time. Studies have demonstrated a remarkable degree of conservation in tumour cells and immune cell interactions across species. Neutrophils [41] and macrophages [42] have been observed migrating to and promoting neovascularization within tumour xenografts and their micrometastases. The lack of adaptive immunity and the translatability of these findings to human disease, however, is still limiting. Recently, groups have begun to humanize zebrafish through co-injection of tumour-associated macrophage cells during xenograft transplantation [43] and the transplantation of human hematopoietic stem cells into zebrafish hosts engineered to express human hematopoietic-specific cytokines [44].

Altogether, the superior optical properties of transgenic reporter zebrafish models and their non-mammalian incubation temperatures make them potentially better suited for shorter-term studies such as exploring the transit and migration of circulating tumour cells through the vasculature.



### 3 Microfluidic and In Vitro Systems

The use of laboratory models of metastasis removes most impediments to throughput because these systems are less hindered by the high costs and ethical concerns associated with animal experimentation. Laboratory systems also benefit from superior optical properties but are often poor substitutes for the complex microenvironmental conditions present in tumours, vasculature and colonizable distant organs. This is particularly true for traditional in vitro culture systems, but historical and ongoing improvements to our model systems are closing the gap between the physiological relevance of living and non-living host models for metastasis. This subsection will explore how technological advances are helping us achieve this. Given the plethora of technologies and model systems that may be useful for studying metastasis, this will not be an exhaustive review, but rather a high-level overview of ongoing trends.

Solid tumours stiffen their local microenvironment through matrix remodelling and the deposition of extracellular matrix proteins [45]. However, tumour cells and associated matrix are still far softer than commonly used substrates for tumour cell culture. Polystyrene and glass substrates have Young's modulus values of ~3 and 50 GPa, respectively, making them approximately six orders of magnitude stiffer than human tumours [46, 47]. The stiffness of the local microenvironment is an important cue for cancer progression and metastasis by promoting proliferation [48], tumour cell dissemination [49], epithelial mesenchymal transition [50] and drug resistance [51]. Many of these effects appear to be regulated in part by Hippo pathway activation via yes-associated protein (YAP) nuclear translocation [52]. For example, YAP activation has been linked to enhanced expression of matrix metalloproteinases [53] integral to tumour cell migration, phenotypic changes that render cells more capable of resisting chemotherapy [51]. Cells and organoids can be cultured using hydrogel stiffness matched to tumours [54] to more accurately recapitulate tumour microenvironments or with hydrogels containing stiffness gradients [55] to study durotaxis and migration. Beyond stiffness, the architectural characteristics of extracellular matrices can influence tumour cell migration and speeds. The alignment and porosity of collagen fibres can be controlled by methods such as gelation temperature [56] and microfabricated devices can be engineered to provide precise control over alignment [57] and porosity [58] during migration. The advantage of in vitro hosts for these studies is the greater degree of control over microenvironmental conditions such as the extent and magnitude of a stiffness gradient, which can be used to elucidate causal relationships between biomechanical signals and cellular behaviour.

One of the most apparent disadvantages of non-living host model systems is their lack of inherent stroma. Co-culture with human stromal cells [59] or media conditioned by these cells [60] can restore some important paracrine signals. Microfluidic devices can be beneficial in these systems because of their precise spatiotemporal control over cellular organization. For instance, microfluidics can spatially organize cancer-associated fibroblasts [61, 62] or bacteria [63] to study

the influence of stromal cells and the microbiome on tumour cell phenotypes. More complex microfluidic platforms have been developed, to recapitulate organs or their subsystems. Numerous “organ-on-a-chip” devices have been developed to mimic distant organs for exploring metastatic colonization [64, 65] and the establishment of the premetastatic niche [66], blood vessels to study tumour cell transit and intravasation/extravasation in vascular endothelial cell models [38, 67–69] and tumour-on-chip platforms for exploring immune-tumour cross-talk [70]. The further development of organ-on-chip platforms may allow us to reduce the number of animals required by eliminating compounds destined to fail clinical trials.

Tumour cells are highly responsive to biomechanical factors, which drive many aspects of metastasis [71]. Microfluidic devices can provide tight control over the forces, stresses and strains that tumour cells experience at all stages of the metastatic cascade. Compliant devices featuring microactuators have been developed, capable of mechanically stimulating and compressing tumour cells [72]. Microscale features can be used to study how tissue confinement [58, 73, 74] affects tumour cell motility and fluid shear stress affects tumour cell adhesion [30, 75], vasculature transit [5, 38] and extravasation [76, 77]. The influence of the higher interstitial fluid pressure present in tumours on mass transport [78] and drug resistance [79] is also readily modelled with integrated pressure control systems. While these biomechanical cues are also present in in vivo models, the ability to precisely control and manipulate these cues in microfluidics allows us to better understand the relationship between biomechanics and metastatic progression.

## 4 Complementary Investigations Using In Vitro and In Vivo Models

One approach to addressing the relative strengths and weaknesses of various models (Table 1) is to use multiple host systems. This is most often accomplished by conducting similar experiments in parallel but using different models to provide greater functionality and give greater confidence in obtained results. Au et al. [38] used microfluidic, computational and zebrafish models to explore how CTC clusters can traverse narrow vessels far smaller than their overall diameters. The use of these three models was complementary because: (1) hydrodynamic relationships between applied pressures and vessel diameters could be determined because of precise over microfluidic channel geometries and applied pressures, (2) the impact of intercellular adhesion strengths on cluster cohesion could be easily studied in computational models and (3) the recapitulation of these behaviours in zebrafish vessels that closely mimic human microvasculature helped to give confidence to this observation. To explore how microvascular hemodynamics were permissive or inhibitory for CTC arrest, Follain et al. [30] also used three different complementary model systems: zebrafish, microfluidics and mice (Fig. 1). The majority of experiments were conducted in zebrafish models that provided superior optical

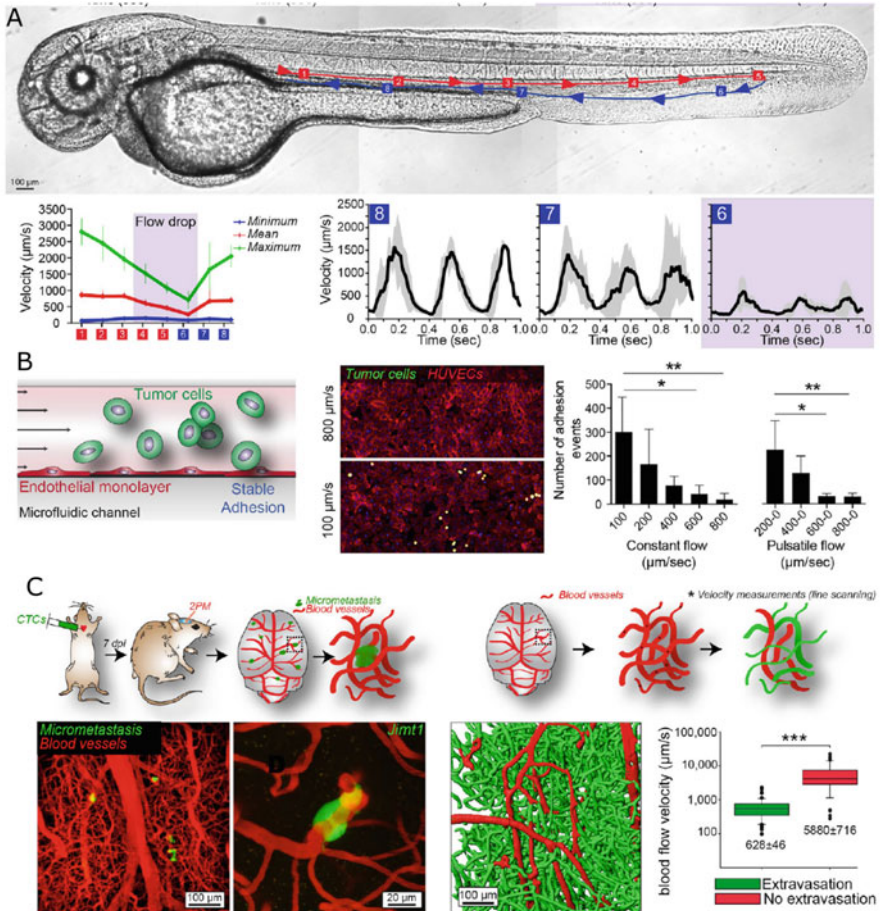


**Fig. 1** Arrest and adhesion of CTCs driven by hemodynamics in multiple model systems. (A) Blood flow velocity measurements (PIV) in the indicated region (red and blue squares 1 to 8) of the zebrafish embryo. Arrows indicate blood flow direction. Minimum, maximum and mean values of the blood flow velocity are plotted over the eight different regions ( $n = 3$  embryos). (B) Experimental setup, representative images and quantification of the microfluidic approach. CTCs (green) are perfused over a monolayer of HUVECs (ECs, red) and adhesion is quantified. (C) Experimental workflow and representative images of micrometastases in 7 days post-infection (dpi) mice injected with Jimt1-GFP cells (2 PM, two-photon microscopy). (Adapted with permission from Follain et al. [30])

and microenvironmental conditions. Studies of tumour cell adhesion on microfluidic channels conducted in parallel allowed better control over fluid velocities and applied shear stress and also permitted the interaction between human tumour cells and human endothelial cells to be explored. The use of mice helped to address the anatomical differences between fish and mammalian microvasculature. The majority of tumour cells were found to arrest in the caudal plexus of zebrafish

tails, a tightly connected meshwork of narrow vessels that experiences low blood velocity. Because we have no human analog to these networks, it can be difficult to generalize these findings to human metastases. However, the observation that CTCs preferentially arrested in regions of low flow in mouse capillary networks helped to bridge these cross-species differences. In a third example, Martínez-Pena et al. [80] compared the survival and proliferative ability of xenotransplanted CTC clusters and single CTCs in both zebrafish and mice models. Similar trends of greater survival and proliferative abilities for CTC clusters were observed in both models even though fish were incubated at 28 °C and were in good agreement with patient-derived data [81]. In a similar fashion, Paul et al. demonstrated that breast cancer tumour cells presented patterns of organ-specific homing similar to those observed in mice models [82]. These findings help validate the use of zebrafish as models for studies in metastasis. While models can be actively compared through parallel experiments such as these, we also “passively” generate useful data through the drug development process. The primary objective of clinical trials is to evaluate a drug candidate’s efficacy and safety in humans, but this data can also help us validate and refine our models through better understanding the limitations of currently deployed preclinical models [12]. For instance, this data has been used to promote the development of humanized animal models [83], change regulatory standards [83] and justify the need for more sophisticated organ-on-chip models [64].

## 5 Multiple Integrated Models

Another approach to incorporating multiple host model systems is to integrate the systems together to create hybrid systems with greater utility than what their constituent parts can provide individually. For instance, one challenge with the use of immature zebrafish is that these small organisms need to be immobilized, aligned and repositioned for imaging, microinjection and culturing purposes. These are time- and labor-intensive processes. Microfluidic devices have been developed to address all of these challenges [84]. Alignment and immobilization can be achieved using pressure traps [85], passive pumping into microscale constrictions [86] or even microstructured indentation arrays that zebrafish passively settle into [87]. When combined with automation, this can allow the automated microinjection of large numbers of zebrafish [88].

While mice are too large to fit onto microfluidic devices, these two host systems can be integrated in another manner. Hamza et al. [89] permanently cannulated mice to withdraw blood from the left carotid artery, which was then perfused through a microfluidic device that could detect and sort CTCs as desired (Fig. 2A). Unsorted blood was returned to the mice through the right jugular vein, completing a full loop. This setup allowed the continuous tracking of CTCs in circulation for up to weeks at a time. This technique was taken a step further by connecting the circulatory systems of two mice with microfluidic CTC cell counters bridging both circuits [90] (Figs. 2B–C). This double animal setup allowed the researchers to track the number of

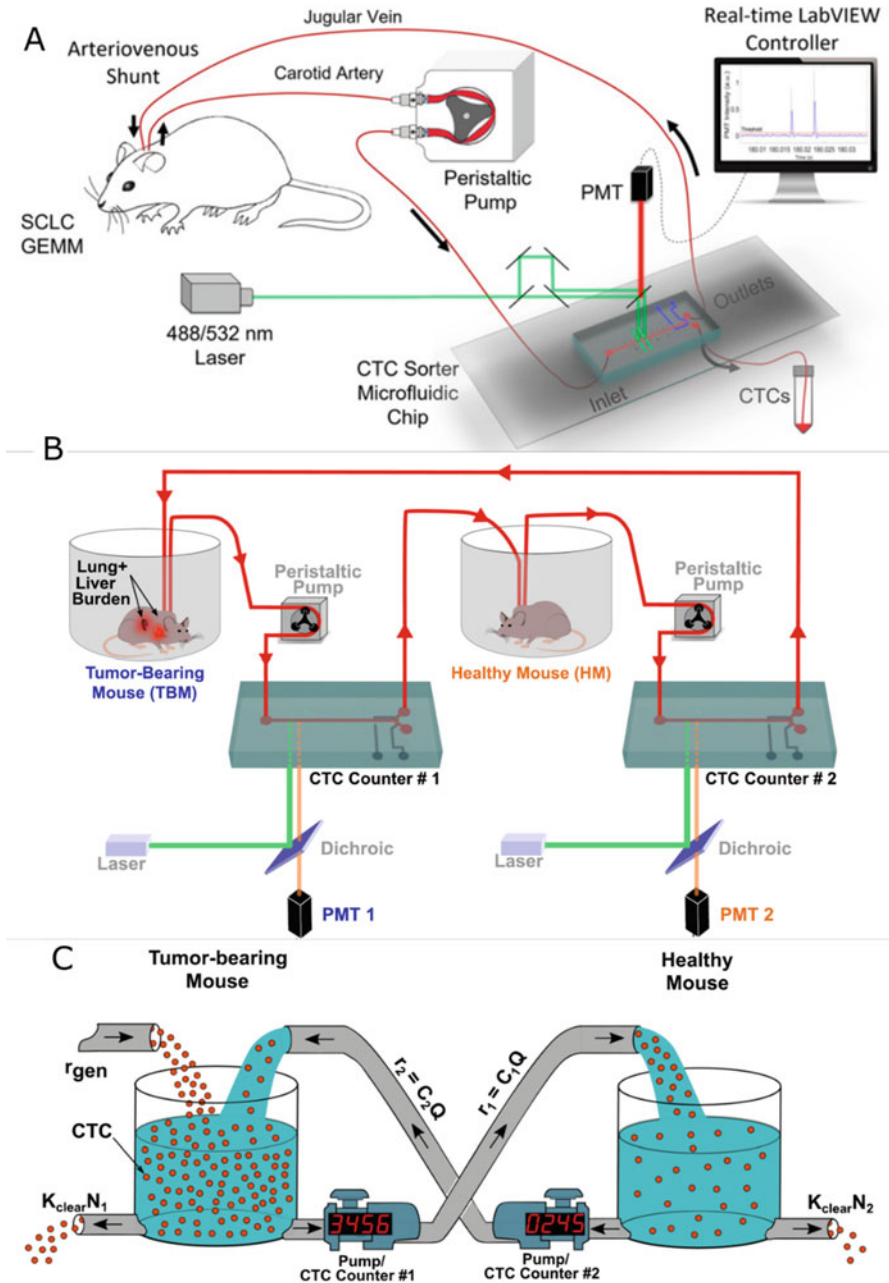


**Fig. 2** Integrated mouse and microfluidic model systems for studying vascular CTC kinetics. (A) Peristaltic pump withdraws blood from a surgically implanted cannula in the carotid artery of a genetically engineered mouse, directed into the main flow channel of the CTC sorter chip. Based on the timing of the pulses, a LabVIEW program computes

CTCs released from one tumour-laden animal and to compare that to the number of metastatic tumours seeded by these cells in the other initially tumour-free animal. This approach addresses some of the concerns around our existing experimental models of mouse metastasis. For instance, tumour cells suspensions of  $\sim 0.2$  mL [91] are routinely injected into the tail vein of mice to generate experimental models of metastasis and to measure CTC circulatory half-lives. This can be problematic because this volume is a large fraction of the  $\sim 1.5$  mL total blood volume of a  $\sim 25$  g mouse, which may cause alterations to arterial pressure and cardiac output. Furthermore, the bolus injection of tumour cells increases the probability of multiple occlusion events and intravascular clustering, and cells injected into mice tails do not encounter the same vascular environments and conditions as experienced by those released by human tumours. Finally, bolus injection protocols typically use tumour cells that have been expanded in vitro. These cells are likely phenotypically different from CTCs since they may not have undergone important processes undertaken by metastasis-competent cells such as epithelial-to-mesenchymal transition and survival adaptations against anoikis. This integrated model method allows for the study of CTCs that are more representative of human disease. Altogether, these factors have likely contributed to the extremely divergent reports of the circulating half-lives of CTCs, ranging from seconds [92] to hours [93]. At the cost of additional complexity, the integrated microfluidic mouse approach has a number of advantages for metastasis research: (1) the use of genetically engineered mice meant that tumour progression and CTC release occurred in a more physiological manner over time than experimental xenotransplantation models and (2) as little as 1.0% of the total blood volume of each animal can be withdrawn into the ex vivo space at a steady state. This reduces the likelihood of altering the hemodynamics, which we know greatly affects tumour cell arrest and colonization behaviours [30].

←

**Fig. 2** (continued) the velocity of the cells and operates computer-controlled pneumatic valves to redirect fluorescent CTCs towards a collection tube. After exiting the chip, CTC-depleted blood returns to the jugular vein of the mouse a second surgically implanted cannula. (Adapted from Hamza et al. [89] under Creative Commons CC BY-NC-ND 4.0 license). **(B)** Schematic demonstrating the blood exchange method in which the circulatory systems of two mice (one tumour-bearing mouse [TBM] and one healthy mouse [HM]) are connected in a closed-loop through two CTC counters. **(C)** A visual representation of the relevant parameters of the blood exchange technique to solve for the generation rate and the half-life time of CTCs. The circulatory system of each mouse is represented as a well-mixed container of red spheres (CTCs). In the TBM (left tank), CTCs enter the circulation from the tumour microenvironment at a rate equal to  $r_{gen}$ . CTC clearance out of the circulation is represented by a hole at the bottom of each container with a clearance rate of  $K_{clear} \times N$ . Pumps with counters represent the CTC counter systems and their peristaltic pumps that transfer the CTC-containing blood at rates equal to  $C \times Q$ .  $r$ , Rate of CTC transfer.  $C$ , concentration.  $Q$ , flow rate.  $K_{clear}$ , first-order clearance coefficient.  $N$ , total number of CTCs in each mouse. (Adapted from Hamza et al. [90] under Creative Commons CC BY license)



## 6 Summary

The complexity and long-time scales associated with the metastatic process mean we have much work ahead to arrive at an ideal in vitro, in vivo or integrated host model system. However, understanding the capabilities and limitations of our existing rodent, fish, large mammalian and microfluidic hosts for modelling human cancer metastasis will allow us to use the correct model system or systems for a given experiment. As we continue to discover the importance of immune and stromal interactions in driving tumourigenesis and metastasis, it becomes more and more imperative that we accurately model these interactions in our host systems. Further development of humanized animal models can provide us with more reliable experimental data and may improve our drug development process. The development and validation of more sophisticated organ-on-chip platforms give us the possibility of studying fully human–human tumour–stromal interactions without the burden of ethical concerns around animal experimentation.

## References

1. [Cancer.net](#). Breast Cancer: Statistics. 2017
2. Reid SE, Kay EJ, Neilson LJ, Henze A-T, Serneels J, McGhee EJ et al (2021) Tumor matrix stiffness promotes metastatic cancer cell interaction with the endothelium. *EMBO J*
3. Rofstad EK, Galappathi K, Mathiesen BS (2014) Tumor interstitial fluid pressure—a link between tumor hypoxia, microvascular density, and lymph node metastasis. *Neoplasia* (New York, NY) 16(7):586–594
4. Tien J, Ghani U, Dance YW, Seibel AJ, Karakan MÇ, Ekinci KL et al (2020) Matrix pore size governs escape of human breast cancer cells from a microtumor to an empty cavity. *iScience* 23(11):101673
5. Varotsos VA, Perea PJ, Bakal C, Au S (2021) Arresting metastasis within the microcirculation. *Clin Exp Metastasis* 38(4)
6. Kwa M, Herum K, Brakebusch C (2019) Cancer-associated fibroblasts: how do they contribute to metastasis? *Clin Exp Metastasis* 36(2)
7. Szczerba BM, Castro-Giner F, Vetter M, Krol I, Gkountela S, Landin J et al (2019) Neutrophils escort circulating tumour cells to enable cell cycle progression. *Nature* 566(7745):553
8. Sanchez L, Borriello L, Entenberg D, Condeelis J, Oktay M, Karagiannis G (2019) The emerging roles of macrophages in cancer metastasis and response to chemotherapy. *J Leukoc Biol* 106(2)
9. Lucotti S, Muschel RJ (2020) Platelets and metastasis: new implications of an old interplay. *Front Oncol* 10(1350)
10. Mo Z, Cheong JYA, Xiang L, Le MTN, Grimson A, Zhang DX (2021) Extracellular vesicle-associated organotropic metastasis – Mo – 2021 – Cell Proliferation – Wiley Online Library
11. Liu J, Lin PC, Zhou BP (2015) Inflammation fuels tumor progress and metastasis. *Curr Pharm Des* 21(21):3032–3040
12. Winer A, Adams S, Mignatti P (2018) Matrix metalloproteinase inhibitors in cancer therapy: turning past failures into future successes. *Mol Cancer Ther* 17(6):1147–1155
13. Paterlini-Brechot P, Benali NL (2007) Circulating tumor cells (CTC) detection: clinical impact and future directions. *Cancer Lett* 253(2):180–204

14. DW M, JW S, JH D (1981) Renal cell carcinoma: long-term survival and late recurrence. *J Urol* 126(1)
15. TG K, DJ F, P M (1999) Dormancy of mammary carcinoma after mastectomy. *J Natl Cancer Inst* 91(1)
16. Liu Y, Yin T, Feng Y, Cona MM, Huang G, Liu J, et al. Mammalian models of chemically induced primary malignancies exploitable for imaging-based preclinical theragnostic research (2223–4292 (Print))
17. Hooijkaas AI, Gadiot J, van der Valk M, Mooi WJ, Blank CU (2012) Targeting BRAFV600E in an inducible murine model of melanoma. *Am J Pathol* 181(3):785–794
18. Chen Z, Trotman LC, Shaffer D, Lin HK, Dotan ZA, Niki M et al (2005) Crucial role of p53-dependent cellular senescence in suppression of Pten-deficient tumorigenesis. *Nature* 436(7051):725–730
19. Fox N, Crooke R, Hwang LH, Schibler U, Knowles BB, Solter D (1989) Metastatic hibernomas in transgenic mice expressing an alpha-amylase-SV40 T antigen hybrid gene. *Science* 244(4903):460–463
20. Compere SJ, Baldacci P, Sharpe AH, Thompson T, Land H, Jaenisch R (1989) The ras and myc oncogenes cooperate in tumor induction in many tissues when introduced into midgestation mouse embryos by retroviral vectors. *Proc Natl Acad Sci U S A* 86(7):2224–2228
21. GD P-M, CW T, RA C, MH L, RT D, CS J, et al (1997) Human tumor models in the severe combined immune deficient (scid) mouse. *Cancer Chemother Pharmacol* 40(3)
22. Mombaerts P, Howard Hughes Medical Institute at the Center for Cancer Research and Department of Biology Massachusetts Institute of Technology Cambridge MU, Iacomini J, Howard Hughes Medical Institute at the Center for Cancer Research and Department of Biology Massachusetts Institute of Technology Cambridge MU, Johnson RS, Dana-Farber Cancer Institute and Department of Biological Chemistry and Molecular Pharmacology Harvard Medical School Boston MU, et al (1992) RAG-1-deficient mice have no mature B and T lymphocytes. *Cell* 68(5):869–877
23. Li Z, Zheng W, Wang H, Cheng Y, Fang Y, Wu F et al (2021) Application of animal models in cancer research: recent progress and future prospects. *Cancer Manag Res* 13
24. Mhaidly R, Verhoeven E (2020) Humanized mice are precious tools for preclinical evaluation of CAR T and CAR NK cell therapies. *Cancers* 12(7)
25. Lefley D, Howard F, Arshad F, Bradbury S, Brown H, Tulotta C et al (2019) Development of clinically relevant in vivo metastasis models using human bone discs and breast cancer patient-derived xenografts. *Breast Cancer Res* 21(1):130
26. Gómez-Cuadrado L, Tracey N, Ma R, Qian B, Brunton VG (2017) Mouse models of metastasis: progress and prospects. *Dis Model Mech* 10(9):1061–1074
27. Li Z, Zheng W, Wang H, Cheng Y, Fang Y, Wu F et al (2021) Application of animal models in cancer research: recent progress and future prospects. *Cancer Manag Res* 13:2455–2475
28. Lee L, Seftor E, Bonde G, Cornell R, Hendrix M (2005) The fate of human malignant melanoma cells transplanted into zebrafish embryos: assessment of migration and cell division in the absence of tumor formation. *Dev Dyn* 233(4)
29. Lam SH, Chua HL, Gong Z, Lam TJ, Sin YM (2004) Development and maturation of the immune system in zebrafish, *Danio rerio*: a gene expression profiling, in situ hybridization and immunological study. *Dev Comp Immunol* 28(1):9–28
30. Follain G, Osmani N, Azevedo AS, Allio G, Mercier L, Karreman MA et al (2018) Hemodynamic forces tune the arrest, adhesion, and extravasation of circulating tumor cells. *Dev Cell* 45(1):33–52.e12
31. Corkery D, Dellaire G, Berman JN (2011) Leukaemia xenotransplantation in zebrafish—chemotherapy response assay in vivo. *Br J Haematol* 153(1365–2141 (Electronic)):786
32. Haldi M, Ton C, Seng WL, McGrath P (2006) Human melanoma cells transplanted into zebrafish proliferate, migrate, produce melanin, form masses and stimulate angiogenesis in zebrafish. *Angiogenesis* 9(3):139–151
33. Cabezas-Sáinz P, Pensado-López A, Sáinz B Jr, Sánchez L (2020) Modeling cancer using zebrafish xenografts: drawbacks for mimicking the human microenvironment. *Cell* 9(9):1978



34. Isogai S, Horiguchi M, Weinstein BM (2001) The vascular anatomy of the developing zebrafish: an atlas of embryonic and early larval development. *Dev Biol* 230(2):278–301
35. Hu N, Sedmera D, Yost HJ, Clark EB (2000) Structure and function of the developing zebrafish heart. *Anat Rec* 260(2):148–157
36. Williams SA, Wasserman S, Rawlinson DW, Kitney RI, Smaje LH, Tooke JE (1988) Dynamic measurement of human capillary blood-pressure. *Clin Sci* 74(5):507–512
37. Lawson N, Weinstein B (2002) In vivo imaging of embryonic vascular development using transgenic zebrafish. *Dev Biol* 248(2)
38. Au SH, Storey BD, Moore JC, Tang Q, Chen Y-L, Javaid S et al (2016) Clusters of circulating tumor cells traverse capillary-sized vessels. *Proc Natl Acad Sci* 113(18):4947–4952
39. Renshaw SA, Loynes CA, Trushell DMI, Elworthy S, Ingham PW, Whyte MKB (2006) A transgenic zebrafish model of neutrophilic inflammation. *Blood* 108(13):3976–3978
40. Bernut A, Herrmann J-L, Kissa K, Dubremetz J-F, Gaillard J-L et al (2014) Mycobacterium abscessus cording prevents phagocytosis and promotes abscess formation. *Proc Natl Acad Sci* 111:E943–EE52
41. He S, Lamers GE, Beenakker J-WM, Cui C, Ghotra VP, Danen EH et al (2012) Neutrophil-mediated experimental metastasis is enhanced by VEGFR inhibition in a zebrafish xenograft model. *J Pathol* 227(4):431–445
42. Britto DD, Wyroba B, Chen W, Lockwood RA, Tran KB, Shepherd PR et al (2018) Macrophages enhance Vegfa-driven angiogenesis in an embryonic zebrafish tumour xenograft model. *Dis Model Mech* 11(12):dmm035998
43. Seoane S, Martinez-Ordoñez A, Eiro N, Cabezas-Sainz P, Garcia-Caballero L, Gonzalez L et al (2019) POU1F1 transcription factor promotes breast cancer metastasis via recruitment and polarization of macrophages. *J Pathol* 249(3)
44. Rajan V, Melong N, Hing WW, King B, Tong S, Mahajan N et al (2020) Humanized zebrafish enhance human hematopoietic stem cell survival and promote acute myeloid leukemia clonal diversity. *Haematologica* 105(10)
45. Emon B, Bauer J, Jain Y, Jung B, Saif T (2018) Biophysics of tumor microenvironment and cancer metastasis – a mini review. *Comput Struct Biotechnol J* 16:279–287
46. Samani A, Zubovits J, Plewes D (2007) Elastic moduli of normal and pathological human breast tissues: an inversion-technique-based investigation of 169 samples. *Phys Med Biol* 52(6):1565–1576
47. Samani A, Bishop J, Luginbuhl C, Plewes DB (2003) Measuring the elastic modulus of ex vivo small tissue samples – IOPscience. *Phys Med Biol* 48:2183
48. Tilghman RW, Cowan CR, Mih JD, Koryakina Y, Gioeli D, Slack-Davis JK et al (2010) Matrix rigidity regulates cancer cell growth and cellular phenotype. *PLoS One* 5(9):e12905-e
49. Leggett SE, Hruska AM, Guo M, Wong IY (2021) The epithelial-mesenchymal transition and the cytoskeleton in bioengineered systems. *Cell Commun Signal* 19(1):1–24
50. Matte BF, Kumar A, Placone JK, Zanella VG, Martins MD, Engler AJ et al (2019) Matrix stiffness mechanically conditions EMT and migratory behavior of oral squamous cell carcinoma. *J Cell Sci* 132(1):jcs224360
51. Joyce MH, Lu C, James ER, Hegab R, Allen SC, Suggs LJ et al (2018) Phenotypic basis for matrix stiffness-dependent chemoresistance of breast cancer cells to doxorubicin. *Front Oncol* 8(337)
52. Noguchi S, Saito A, Nagase T (2018) YAP/TAZ Signaling as a molecular link between fibrosis and cancer. *Int J Mol Sci* 19(11)
53. . !!! INVALID CITATION !!! {}
54. Stowers RS, Allen SC, Suggs LJ (2015) Dynamic phototuning of 3D hydrogel stiffness. *Proc Natl Acad Sci U S A* 112(7):1953–1958
55. Chang C-Y, Lin C-C (2021) Hydrogel models with stiffness gradients for interrogating pancreatic cancer cell fate. *Bioengineering (Basel, Switzerland)* 8(3):37
56. Taufalele PV, Vanderburgh JA, Muñoz A, Zanotelli MR, Reinhart-King CA (2019) Fiber alignment drives changes in architectural and mechanical features in collagen matrices. *PLoS One* 14(5):e0216537-e

57. Teixeira AI, Abrams GA, Bertics PJ, Murphy CJ, Nealey PF (2003) Epithelial contact guidance on well-defined micro- and nanostructured substrates. *J Cell Sci* 116(Pt 10):1881–1892
58. Raab M, Gentili M, de Belly H, Thiam HR, Vargas P, Jimenez AJ et al (2016) ESCRT III repairs nuclear envelope ruptures during cell migration to limit DNA damage and cell death. *Science* 352(6283):359–362
59. Llames S, García-Pérez E, Meana Á, Larcher F, del Río M (2015) Feeder layer cell actions and applications. *Tissue Eng Part B Rev* 21(4):345–353
60. Awaji M, Futakuchi M, Heavican T, Iqbal J, Singh RK (2019) Cancer-associated fibroblasts enhance survival and progression of the aggressive pancreatic tumor via FGF-2 and CXCL8. *Cancer Microenviron* 12(1):37–46
61. Jeong S-Y, Lee J-H, Shin Y, Chung S, Kuh H-J (2016) Co-culture of tumor spheroids and fibroblasts in a collagen matrix-incorporated microfluidic Chip mimics reciprocal activation in solid tumor microenvironment. *PLoS One* 11(7):e0159013-e
62. Kim S-A, Lee EK, Kuh H-J (2015) Co-culture of 3D tumor spheroids with fibroblasts as a model for epithelial–mesenchymal transition in vitro. *Exp Cell Res* 335(2):187–196
63. Shah P, Fritz JV, Glaab E, Desai MS, Greenhalgh K, Frchet A et al (2016) A microfluidics-based in vitro model of the gastrointestinal human–microbe interface. *Nat Commun* 7:11535
64. Sontheimer-Phelps A, Hassell BA, Ingber DE (2019) Modelling cancer in microfluidic human organs-on-chips. *Nat Rev Cancer* 19(2):65–81
65. Xu Z, Li E, Guo Z, Yu R, Hao H, Xu Y, et al. Design and construction of a multi-organ microfluidic chip mimicking the in vivo microenvironment of lung cancer metastasis. 2016
66. Kim J, Lee C, Kim I, Ro J, Kim J, Min Y et al (2020) Three-dimensional human liver-chip emulating premetastatic niche formation by breast cancer-derived extracellular vesicles. *ACS Nano* 14(11):14971–14988
67. Zervantonakis IK, Hughes-Alford SK, Charest JL, Condeelis JS, Gertler FB, Kamm RD (2012) Three-dimensional microfluidic model for tumor cell intravasation and endothelial barrier function. *Proc Natl Acad Sci U S A* 109(34):13515–13520
68. Osaki T, Sivathanu V, Kamm RD (2018) Vascularized microfluidic organ-chips for drug screening, disease models and tissue engineering. *Curr Opin Biotechnol* 52:116–123
69. Song JW, Cavnar SP, Walker AC, Luker KE, Gupta M, Tung YC et al (2009) Microfluidic endothelium for studying the intravascular adhesion of metastatic breast cancer cells. *PLoS One* 4(6)
70. Parlato S, Grisanti G, Sinibaldi G, Peruzzi G, Casciola CM, Gabriele L (2021) Tumor-on-a-chip platforms to study cancer-immune system crosstalk in the era of immunotherapy. *Lab Chip* 21(2):234–253
71. Northcott JM, Dean IS, Mouw JK, Weaver VM (2018) Feeling stress: the mechanics of cancer progression and aggression. *Front Cell Dev Biol* 6(17)
72. Onal S, Alkaisy MM, Nock V (2021) A flexible microdevice for mechanical cell stimulation and compression in microfluidic settings. *Front Phys* 9(280)
73. Paul CD, Hung W-C, Wirtz D, Konstantopoulos K (2016) Engineered models of confined cell migration. *Annu Rev Biomed Eng* 18(1):159–180
74. Denais CM, Gilbert RM, Isermann P, McGregor AL, te Lindert M, Weigelin B et al (2016) Nuclear envelope rupture and repair during cancer cell migration. *Science* 352(6283):353–358
75. Li W, Mao S, Khan M, Zhang Q, Huang Q, Feng S et al (2019) Responses of cellular adhesion strength and stiffness to fluid shear stress during tumor cell rolling motion. *ACS Sens* 4(6):1710–1715
76. Buchanan CF, Verbridge SS, Vlachos PP, Rylander MN (2014) Flow shear stress regulates endothelial barrier function and expression of angiogenic factors in a 3D microfluidic tumor vascular model. *Cell Adhes Migr* 8(5):517–524
77. Chen MB, Whisler JA, Fröse J, Yu C, Shin Y, Kamm RD (2017) On-chip human microvasculature assay for visualization and quantification of tumor cell extravasation dynamics. *Nat Protoc* 12(5):865–880
78. Avendano A, Cortes-Medina M, Song JW (2019) Application of 3-D microfluidic models for studying mass transport properties of the tumor interstitial matrix. *Front Bioeng Biotechnol* 7(6)

79. Shang M, Lim SB, Jiang K, Yap YS, Khoo BL, Han J et al (2021) Microfluidic studies of hydrostatic pressure-enhanced doxorubicin resistance in human breast cancer cells. *Lab Chip* 21(4):746–754
80. Martínez-Pena I, Hurtado P, Carmona-Ule N, Abuín C, Dávila-Ibáñez AB, Sánchez L et al (2021) Dissecting breast cancer circulating tumor cells competence via modelling metastasis in zebrafish. *Int J Mol Sci* 22(17):9279
81. Hong YP, Fang F, Zhang Q (2016) Circulating tumor cell clusters: what we know and what we expect (review). *Int J Oncol* 49(6):2206–2216
82. Paul CD, Bishop K, Devine A, Paine EL, Staunton JR, Thomas SM et al (2019) Tissue architectural cues drive organ targeting of tumor cells in zebrafish. *Cell Systems* 9(2):187–206.e16
83. Denayer T, Stöhr T, Van Roy M (2014) Animal models in translational medicine: validation and prediction. *New Horizons in Translational Medicine* 2(1):5–11
84. Yang F, Gao C, Wang P, Zhang G-J, Chen Z (2016) Fish-on-a-chip: microfluidics for zebrafish research. *Lab Chip* 16(7):1106–1125
85. Lin X, Wang S, Yu X, Liu Z, Wang F, Li WT et al (2015) High-throughput mapping of brain-wide activity in awake and drug-responsive vertebrates. *Lab Chip* 15(3):680–689
86. Bischel LL, Mader BR, Green JM, Huttenlocher A, Beebe DJ (2013) Zebrafish entrapment by restriction Array (ZEBRA) device: a low-cost, agarose-free zebrafish mounting technique for automated imaging. *Lab Chip* 13(9):1732–1736
87. Ellett F, Irimia D (2017) Microstructured devices for optimized microinjection and imaging of zebrafish larvae. *J Vis Exp* 130:56498
88. Wang W, Liu X, Gelinis D, Ciruna B, Sun Y (2007) A fully automated robotic system for microinjection of zebrafish embryos. *PLoS One* 2(9):e862-e
89. Hamza B, Ng SR, Prakadan SM, Delgado FF, Chin CR, King EM et al (2019) Optofluidic real-time cell sorter for longitudinal CTC studies in mouse models of cancer. *Proc Natl Acad Sci* 116(6):2232
90. Hamza B, Miller AB, Meier L, Stockslager M, Ng SR, King EM et al (2021) Measuring kinetics and metastatic propensity of CTCs by blood exchange between mice. *Nat Commun* 12(1):5680
91. Mohanty S, Xu L (2010) Experimental metastasis assay. *J Vis Exp* 42:1942
92. Fidler IJ (1970) Metastasis: quantitative analysis of distribution and fate of tumor emboli labeled with 125 I-5-iodo-2'-deoxyuridine. *J Natl Cancer Inst* 45(4):773–782
93. Meng S, Tripathy D, Frenkel EP, Shete S, Naftalis EZ, Huth JF et al (2004) Circulating tumor cells in patients with breast cancer dormancy. *Clin Cancer Res* 10(24):8152–8162

# Physical Sciences in Cancer: Recent Advances and Insights at the Interface



Olalekan H. Usman and Jerome Irianto

**Abstract** Within the tumor, cancer cells interact dynamically with their microenvironment via biochemical and physical mechanisms. The roles of biochemical interactions between the cancer cells and their environment and their impact on tumorigenesis have been the focus of many studies. However, the study of the effects of physical cues on cancer progression started garnering attention in the last decade. Here, to provide a glance at the current state of this research field, we summarized some of the studies associated with the National Cancer Institute–funded Physical Sciences-Oncology Network, including the use of computational modeling to study cancer biology, the use of physical science technologies in cancer studies, and the study of physical cues in cancer biology. These studies cover a wide range of topics, ranging from cancer evolution and progression to the optimization of cancer therapies, suggesting the significant contribution of physical science to studying cancer biology and to the development of more efficient therapies.

**Keywords** Computational modeling · Hydrogel · Matrix stiffness · Microfluidics · Nuclear mechanics · Therapy response · Solid stress · Tumor evolution · Tumor microenvironment

## 1 Introduction

A tumor is a complex tissue consisting of cancer cells that are in dynamic metabolic and physical interactions with immune cells, cancer-associated fibroblasts, and the extracellular matrix (ECM) in their microenvironment. Cancer is considered to be a cellular disease whose progression is driven by mutations in genes that regulate apoptosis, cell proliferation, and angiogenesis [1]. The molecular biology of cancer is relatively well studied when compared to the physical aspects of

---

O. H. Usman · J. Irianto (✉)

Department of Biomedical Sciences, College of Medicine, Florida State University, Tallahassee, FL, USA

e-mail: [jerome.irianto@med.fsu.edu](mailto:jerome.irianto@med.fsu.edu)

© The Author(s), under exclusive license to Springer Nature Switzerland AG 2023

I. Y. Wong, M. R. Dawson (eds.), *Engineering and Physical Approaches to Cancer*, Current Cancer Research, [https://doi.org/10.1007/978-3-031-22802-5\\_11](https://doi.org/10.1007/978-3-031-22802-5_11)

301

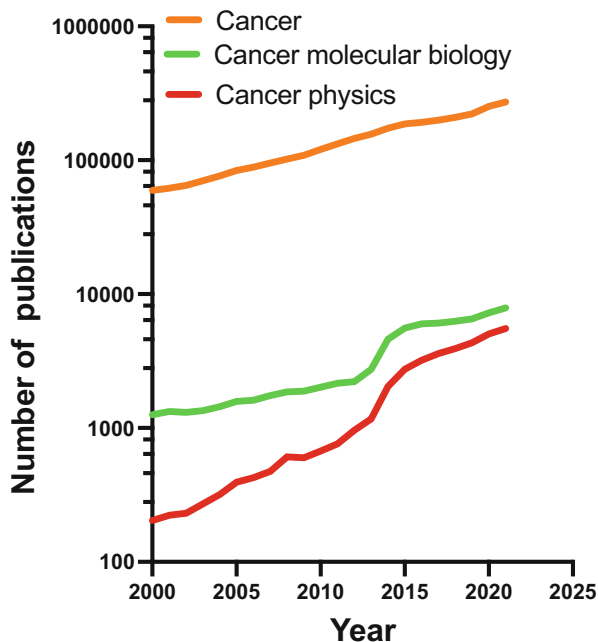


**Fig. 1** Publication counts from the year 2000 to 2022, acquired from Pubmed search with the following keywords: cancer, cancer molecular biology, and cancer physics. This plot shows the increasing publication rate of physics-related cancer studies

the disease (Fig. 1). Interestingly, the emerging studies suggest the role of these physical cues on cancer evolution, metastasis, progression, heterogeneity, and even resistance to drug treatment [2]. The recent understanding and growing appreciation of the effects of physical cues on cancer tumor development have led to the birth of a transdisciplinary field made up of cancer researchers, computational scientists, physicists, chemists, mathematicians, and engineers. The growth of this transdisciplinary field was facilitated by the creation of the Physical Sciences-Oncology Network (PS-ON) in 2009, which was funded by the National Cancer Institute. The PS-ON aims to promote the physical sciences perspective of cancer by fostering the formation of transdisciplinary research teams of physical scientists and cancer researchers. Hence, the funded projects need to: (i) establish a physical sciences perspective within the cancer research community, (ii) facilitate field convergence of physical sciences and cancer research, and (iii) collectively test physical sciences-based experimental and theoretical concepts of cancer while promoting innovative solutions of outstanding questions in cancer research. The current and past members of PS-ON and their funded projects can be found in the following website: <https://physics.cancer.gov/>. The term physical sciences can cover broad aspects of cancer, such as the study of physical properties of the tumor, like physical cues and transport phenomena, or the use of advanced imaging techniques

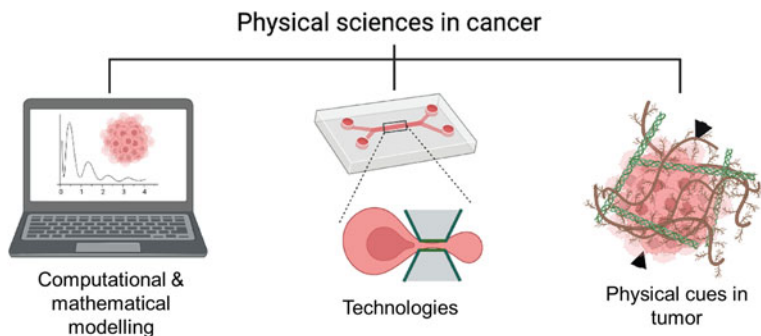


**Fig. 2** The application of physical sciences in cancer research, ranging from the use of computational and mathematical modeling; the use of physical science instrumentations, like microfluidics technology; and the studies of various physical cues from within and outside of the tumor. (Image created in [Biorender.com](https://www.biorender.com))

to study biological processes with a high degree of temporal and spatial precision. In this chapter, we provide an overview of the current state of this research field: We summarize the studies that are associated with the projects funded by the PS-ON initiative, including the use of computational modeling to study cancer biology, the use of physical science technologies in cancer studies, and the study of physical cues in cancer biology (Fig. 2). It is important to note that the members of PS-ON are only a fraction of US-based researchers in this field; hence, this chapter does not represent the whole international effort in studying the physics of cancer.

## 2 Mathematical and Computational Modeling of Cancer

Throughout disease progression, cancer cells actively interact with the surrounding biochemical and physical environment. A tumor's microenvironment is complex, and researchers often use a reductionist approach in which cancer is studied *in vitro* by decoupling different factors (e.g., interstitial pressure, oxygen diffusion, stiffness, metabolite gradient) and investigating their effects independently on tumor evolution, progression, and resistance to therapy. However, most of these factors affect the tumor simultaneously *in vivo*, and understanding how they work together in the tumor microenvironment will provide better insight to delineate tumorigenesis. To solve this limitation in wet lab research oncology, scientists developed mathematical and computational models that enable the integration of multiple inputs from experimental studies to provide insightful predictions of a complex process. In this section, we will highlight the utilization of mathematical and computational modeling to study the roles of the tumor microenvironment in cancer progression, the biological processes in cancer cell migration, and the

**Table 1** Summary of the mathematical models' inputs and outputs

Author	Input	Output
Leder et al. [31]	i. SLRC and DSC response to radiation percentage of DSC that mutate to SLRC ii. Rate at which both DSC and SLRC enter and exit the cell cycle	Optimal radiotherapy dosing schedule
Poels et al. [40]	i. Drug concentration over time ii. Patients' drug pharmacokinetics iii. Toxicity constraints iv. Tumor composition	The optimal dosage for dacomitinib–osimertinib combination therapy
Rockne et al. [42]	i. Gene expression variation with drug ii. The transition from drug sensitive to drug resistant	Drug-induced tumor evolution
Zhang et al. [44]	i. Cellular competition ii. Differences in subpopulation growth	Optimal concentration and frequency of cytotoxic agent needed for adaptive therapy
Gatenby et al. [12]	i. Rate of glycolysis ii. Diffusion rate of hydrogen ion produced by the tumor into adjacent normal cells	Acid-induced toxicity level
Chaplain et al. [11]	i. Cell growth ii. ECM production iii. ECM-degrading enzyme production	Compression-induced clonal selection
Bauer et al. [10]	i. Cell growth ii. Cell migration iii. ECM degradation iv. Cell adhesion	Effect of matrix density on angiogenesis and sprout branching
Chan and Odde [19]	i. Myosin motors ii. Number of integrins iii. Force exerted on F-actin iv. Rate of integrin binding and unbinding	Optimal substrate stiffness for cell migration

*SLRC* stemlike resistant cells, *DSC* differentiated sensitive cells, *ECM* extracellular matrix

optimization of cancer therapies. The summary of the inputs and outputs of these models can be seen in Table 1.

## 2.1 Modeling the Roles of Tumor Microenvironment

The tumor microenvironment is defined as the surrounding in which the tumor exists [3]. The cellular components of the tumor microenvironment consist of the stromal cells, which may include various immune cells, endothelial cells, and fibroblast cells in most tumors. The non-cellular part includes the soluble factors like growth

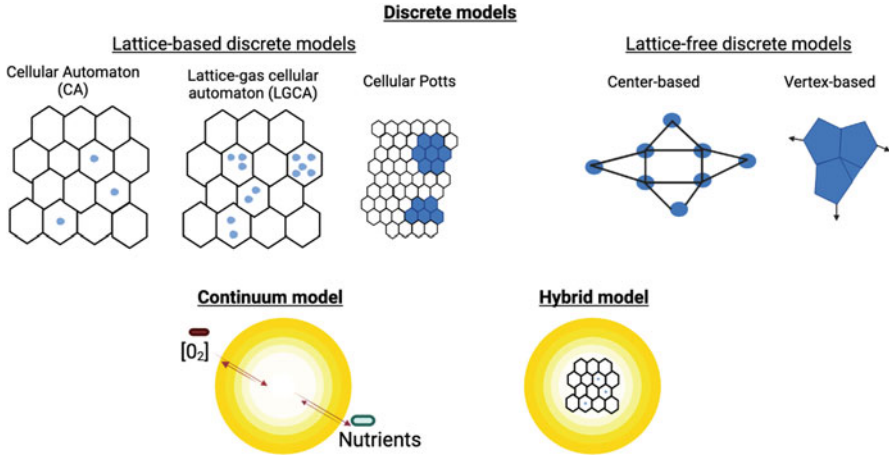


**Fig. 3** The mathematical model approaches used in modeling tumor biology. (Imaged adapted from [6, 7]. Image created in [Biorender.com](https://www.biorender.com) )

factors and nutrients and the non-soluble extracellular matrix proteins such as laminin, fibronectin, collagen, and hyaluronic acid. The cancer cells dynamically interact with the microenvironment, and the microenvironment is often modified and regulated by the cancer cells to promote cancer progression and metastasis. One example of such regulation is through cancer cells' aberrant metabolism. Under normoxic conditions, normal cells use the oxidative phosphorylation pathway to synthesize ATP. In contrast, cancer cells preferentially use glycolysis to meet their energy demands (a phenomenon known as the Warburg effect), thereby leading to an elevated level of lactic acid [4]. The acidic tumor microenvironment will then preferentially promote tumor cell growth over normal cells. Another example of tumor microenvironment modification is through the inflammation response. Tumor cells often secrete inflammation-promoting growth factors that activate the surrounding fibroblasts to produce and deposit excessive extracellular matrix (ECM) proteins in the microenvironment. This process is called fibrosis, and it leads to drastic physical alterations of the microenvironment, which enhances tissue stiffness and may also provide a path for cancer cell migration. Such excessive deposition of ECM may also alter cancer cell phenotype and metabolism through mechanotransduction pathways, reviewed in [5].

Mathematical models can integrate laws of physics and experimental data to derive the impact of the tumor microenvironment on disease progression. Mathematical modeling of the tumor can be broadly classified into three approaches (Fig. 3): discrete, continuum, and hybrid models [6]. The discrete model predicts individual cell behavior in a tumor environment by following a set of biological rules that guide the phenotype of the model. Some examples of these rules include the placement of a daughter cell in a nearby space when a cell divides, the removal of a cell from a defined space when a cell dies, or the movement of the cell to an adjacent space



for migration [7]. The discrete model can be categorized into two categories based on the rules: (i) Lattice-based models use structured or unstructured coordinates for the location where the cells are permitted to occupy. Lattice-based models can either be the cellular automaton model (one cell occupies one lattice), the lattice gas cellular automaton model (multiple cells occupy one lattice), or the cellular Potts models (single cell occupies multiple lattices) [8]. (ii) Off-lattice models, on the other hand, are not bound to coordinates and the cells are allowed to move in any distance and direction in line with the physical and biochemical processes in the study. Some of the off-lattice models track the cell position either by using their center of mass or volume (center-based models) [7] or by calculating the forces acting on the vertices of the cells represented as polygonal/polyhedral shape evolved by minimizing an energy potential (vertex-based models) [9]. Continuum models use differential equations to simulate the interaction between cells and the underlying chemical and physical processes with parameters that are represented as continuously distributed variables. Although developing parameters and simulating cellular processes with this model are easier compared to discrete models, the equations may result in simplifications, such as the assumption of continuity that do not totally mirror the biology of the process [6]. The hybrid modeling approach combines both the continuum and discrete models. To apply this model to a tumor, the cells are often modeled with discrete models while hormones, growth factors, cytokines, nutrients, and oxygen are described with the continuum model.

The hybrid mathematical model approach was used by Bauer and colleagues to study angiogenesis in tumors. In this study, the authors combined cellular Potts and continuous models to investigate the effect of inhomogeneous tumor microenvironment on tumor-induced angiogenesis. The continuous–Potts hybrid model takes into account endothelial cell growth, migration, adhesion, and extracellular matrix degradation, while the continuous model is used to describe uptake, diffusion, and the half-life of the VEGF secreted by the tumor. In this study, the authors observed that when leading endothelial cells encounter a high matrix region in the stroma, the cells redirect themselves to take the path of a lesser resistance [10], leading to blood vessel sprout branching—a process in which new capillary vessels penetrating the tumor divide into two. Meanwhile, considering the space required to accommodate cellular overgrowth in a tumor, the surrounding tumor microenvironment also physically constrains tumor growth, leading to a highly compressed environment inside the tumor. Chaplain and colleagues developed a mathematical model to understand the effect of this compressive stress on tumorigenesis. The model's inputs include cellular growth, ECM production, and the production of matrix-degrading enzymes. This model's output shows that a cell's inability to sense compression from its immediate environment can lead to a clonal selection of abnormal cells and tumor growth [11].

In another study, Gatenby and colleagues developed a mathematical model to understand acid-mediated tumor invasion [12]. This model's inputs include the glycolysis rate and diffusion rate of the hydrogen ion produced by the tumor into adjacent normal tissues. This model gives the peritumoral hydrogen concentration and the acid-induced toxicity as its output. This model predicts that due to the altered

metabolism of glucose, cancer cells can create an acidic environment that impairs the phenotype of the neighboring normal cells. Finally, they concluded that this acidic environment promotes the cancer cells' invasiveness, a process referred to as acid-mediated invasion. Furthermore, the tunability of mathematical models enabled the authors to accommodate another variable: the interactions between stromal cells and cancer cells [13]. This mathematical model, aiming to show the effect of the interactions between stromal cells and tumor cells on invasion, takes inputs that include hydrogen concentration, normal cell death induced by acidification of the tumor environment, remodeling of the extracellular matrix, metalloproteinases (MMP) density. This model predicts that optimal tumor acidity can cause matrix remodeling. Also, it predicts that the tumor-induced acidity causes stromal cell death; however, the tumor also needs the stromal cells for invasion, suggesting that very high acid levels may prevent invasion in some types of tumors. Cumulatively, these two models predict the effects of acidity on tumorigenesis and metastasis.

## ***2.2 Modeling Cancer Cell Migration***

Cell migration is crucial for various physiological and pathophysiological processes: epithelial cells migrate collectively to the site of injury during wound healing [14]. During embryonic development, cells migrate to form the germ layers, and the cells of the germ layers migrate to specific regions, forming specialized cells and tissues [15]. During metastasis, cancer cells migrate to the basement membrane and extracellular matrix to the lymphatics and the blood vessels [16]. Cell migration has been studied in 1D, 2D, and 3D. In 1D migration, cells move along a linear structure, e.g., the migration of cancer cells along collagen fibrils. One-dimensional studies have shown that invasive breast cancer cells preferentially migrate along perpendicular collagen arrays [17]. In 2D migration, cells migrate over a flat surface, while in 3D, cells are continuously surrounded by the extracellular matrix or other cells as they migrate [18]. In general, mechanistically, migration can be summarized into a cyclic process of three steps: (i) cell polarization and extension of filopodia and lamellipodia at the leading edge, driven by actin polymerization, in response to migration-inducing signals, (ii) cell adhesion and formation of focal contacts as a result of interaction between integrins and the extracellular matrix, and (iii) detachment of the rear of the cell following turnover of focal adhesion [18]. In the effort to study cancer cell migration, the utilization of mathematical modeling enables the integration of the different modalities such as substrate stiffness, ECM ligand concentration, and activities of other proteins that control migration.

Cell migration depends on the ability of a cell to adhere to the underlying substrate and to pull in the migration direction, which is driven by actomyosin contractility. With this in mind, Chan and Odde developed the motor-clutch mathematical model to simulate single-cell migration [19]. In this model, the cell migration rate depends on the force balance between the myosin contraction on the F-actin (the motor) and the cellular bond to the substrate through proteins like

integrins (the clutch). In a follow-up study, Bangasser and colleagues incorporated the compliance of the substrate into the model and predicted the optimal substrate stiffness for cell migration [20]. This model input includes the number of myosin motors (which pull the F-actin in opposite direction, thereby driving a retrograde flow), the number of clutches, the force exerted on the F-actin, and the rate at which the clutches bind and unbind F-actin. This model predicts that the stiffness optimum for retrograde flow can be shifted by changing the number of motors and clutches accordingly. To experimentally validate this, the group inhibited both myosin (motor) and integrins (clutch) in U251 glioma cells and they observed optimum stiffness reduction from  $\sim 100$  kPa to 4 kPa.

Unlike single-cell migration, the study of collective cell migration must consider the impact of the neighboring cells, including cell–cell adhesion bonds and straining effects from the neighboring cells. The normal confluent epithelial cell layer is often non-migratory and jammed, where cells rarely swap places with their neighbors and become locked in place. In contrast, the healing or remodeling confluent epithelial cell layer tends to be migratory and unjammed. Ilina et al. reported an increase in unjamming and single-cell dissemination with downregulation of cell–cell adhesion protein, E-cadherin, and low matrix density in breast cancer [21]. In a study where various adherens junction proteins were knockdown, Bazellieres and colleagues showed that the velocity of cells in a jammed phase increases with low levels of P-cadherin and  $\alpha$ - and  $\beta$ -catenin [22]. This transition between jammed and unjammed cellular behavior is in line with a widely studied physical theory for granular materials: jamming phase transition. Kim and colleagues showed that this concept of cell jamming can be used as an indicator of cancer cells' invasiveness [23]. The more invasive cells tend to have a higher degree of unjamming and larger cooperative cell packs. The authors also suggested the correlation between cellular morphology heterogeneity and the degree of unjamming. In a follow-up study, Kang and colleagues showed that the mode of collective cancer cell migration in 3D collagen I hydrogels can be predicted by a jamming phase diagram, which was a function of extracellular matrix density and cancer cell migration potential [24].

### ***2.3 Modeling Cancer Evolution and Response to Therapy***

Cancer undergoes cycles of clonal expansion, genetic diversification, and selection of adaptive clones, a process that mirrors Darwin's natural selection [25]. In a tumor, specific mutations will provide a growth advantage to some cancer cells, giving rise to the evolution of different cellular clones [26]. This evolution creates a myriad of cells within the tumor with different phenotypes and specifically responses to therapy [27]. In this section, we will summarize several studies that utilize computational modeling to develop or optimize cancer therapies, ranging from the development of the adaptive therapy regimen that is based on cancer evolution to the optimization of the radiotherapy dosing schedule.

Glioblastoma (GBM) is a malignant primary brain tumor with a low survival rate. There is a high recurrence rate of this cancer in patients treated with surgery, chemotherapy, or radiotherapy [28]. This nearly inevitable recurrence in GBM patients is partially a result of clonal evolution and dynamic heterogeneity states, which then lead to the proliferation of therapy-resistant cancer cells. Different radiotherapy dosing schedules that have been applied to treat GBM include: hypofractionated dosing of 3–6 Gy per treatment session, accelerated dosing that involves radiation with 2 Gy multiple times per day, hypofractionated dosing of 1 Gy fractions 2–3 times per day during the course of treatment [29]. However, none of these schedules has significantly improved the GBM survival rate. This is attributed to the presence of a subpopulation of cells that are resistant to radiation [30] and the plasticity of the radiosensitive cells to revert to radioresistant cells after exposure to radiation [31]. To address this problem and to identify the optimal and efficient radiation dosing schedules in glioma, Leder and colleagues developed a mathematical model that puts into consideration both the stemlike resistant cells (SLRC) and differentiated sensitive cells (DSC) in GBM [31]. The inputs for this model are the response of the SLRC and DSC to radiation, the percentage of DSC that turns to SLRC after rounds of radiation, the rate of DSC to SLRC reversion, the rate at which newly created DSC reproduces and gives rise to clonal expansion, and the rates at which both DSC and SLRC leave quiescence and enter the cell cycle. Putting these inputs together, this model predicts an optimal radiation dosing schedule to be 2 Gy radiation for 5 days as its output. To validate the application of this model, the authors performed a survival analysis using mice with glioma. They found out that glioma mice treated with a standard single dose of 10 Gy have a significantly lower survival rate compared to those treated with the optimal schedule predicted by the model. In another GBM study, Zhao and colleagues used an extensive computational model approach to combine and analyze the clinical, imaging, genomics, and transcriptomic data that were collected from 66 patients throughout their treatment with PD-1 inhibitors, nivolumab or pembrolizumab. In this study, the authors derived the tumors' molecular evolution during the anti-PD-1 therapy and characterized the genetic background of responders and non-responders to this immunotherapy [32]. Such molecular characterization of the responders and non-responders will potentially enable the derivation of a set of genetic markers that predicts the efficacy of anti-PD-1 therapy for patients with GBM, prior to the actual treatment. This insight might provide a piece of essential information for the clinical management algorithm of patients with GBM.

In addition to GBM, mathematical modeling has also broken a new ground for lung cancer, melanoma, and myeloid leukemia. Lung cancer is the leading cause of cancer-related deaths [33]. Non-small cell lung cancer (NSCLC) is a subtype of lung cancer with poor diagnosis and approximately 50% of this subtype are diagnosed at metastases [34]. About 10–50% of NSCLC patients have exon 19 deletion or missense mutation in exon 21 (L588R) of EGFR, thereby activating the receptor [35]. First-generation EGFR tyrosine kinase inhibitors (TKIs), such as erlotinib and gefitinib, inhibit the binding of ATP to the mutant EGFR in NSCLC. However, the cells become resistant over time due to the occurrence of a secondary

mutation (T790M) on the EGFR [36]. This resistance-conferring mutation is also observed with second-generation EGFR TKIs such as dacomitinib, a pan-HER inhibitor [37]. Osimertinib, a third-generation EGFR inhibitor, is effective in patients with T790M mutations [38]. However, over time, NSCLC cells acquire resistance to osimertinib due to second-site mutations at EGFR C797S, the site at which osimertinib binds EGFR [39]. To combat this series of mutation-induced resistance to treatment in NSCLC lung cancer, Poels and colleagues developed a mathematical model to identify the optimal dosing schedule for combination therapy of dacomitinib and osimertinib [40]. The inputs for this model include changes in concentrations of the drugs over time, patients' pharmacokinetics variation, changes in tumor composition over time, the probability of drug-sensitive cells becoming drug-resistant cells after division, and toxicity constraints. This model predicts the optimal combination of the two drugs. The output of the model showed that the combined therapy of lower but more frequent doses of osimertinib and higher but less frequent doses of dacomitinib significantly reduces the resistance of NSCLC to drug treatment when compared with the conventional treatment. In a study aimed at understanding the transition from drug-sensitive to drug-resistant phenotype in melanoma, Su and colleagues combined mathematical modeling and experimental methods to study the plasticity of BRAF<sup>V600E</sup> mutant melanoma cell lines [41]. The inputs for this mathematical model are gene expression variation over 2.5 months of BRAF low-dose treatment, flow cytometry plots showing the transition between melanocytic (drug-sensitive) cells, and cells displaying mesenchymal properties (drug resistant). This model predicts the drug-induced cell evolution in melanoma and free energy-like potential during the transition from drug response and tolerance as its output. Similarly, the application of the state-transition model on time-sequential transcriptomic data from an acute myeloid leukemia murine model has been reported to predict critical points in leukemia progression and evolution [42]. Put together, these models can contribute to better therapy development by helping to predict the susceptibility and response of cancer cells to the drug (as shown in the Su et al. study above) [41]. Also, they can predict the most effective dosing radiation schedules used in cancer treatment (as described by Leder et al. study) [31] and also identify the most optimal drug combination to combat drug resistance as shown in Poels et al. study [40].

Mathematical models have also played a crucial role in the birth of a new cancer therapy regimen termed adaptive therapy. Adaptive therapy takes into account tumor heterogeneity, evolution, and therapy-induced changes. It hinges on the competition between the chemosensitive and chemoresistant subclones in the tumor. Before a treatment, chemosensitive cells have a growth advantage and occupy most of the tumor space, which suppresses the growth of less fit chemoresistant cells. In this context, standard-of-care treatment of cancer is termed linear therapy because it aims at using the maximum tolerated dose administered to kill the highest possible number of cancerous cells. Upon a conventional fixed and linear therapy, most of the chemosensitive cells will be killed, leaving behind space and resources that enable the growth of the chemoresistant cells during remission. Adaptive therapy, on the other hand, aims to control the growth of chemosensitive cells while suppressing

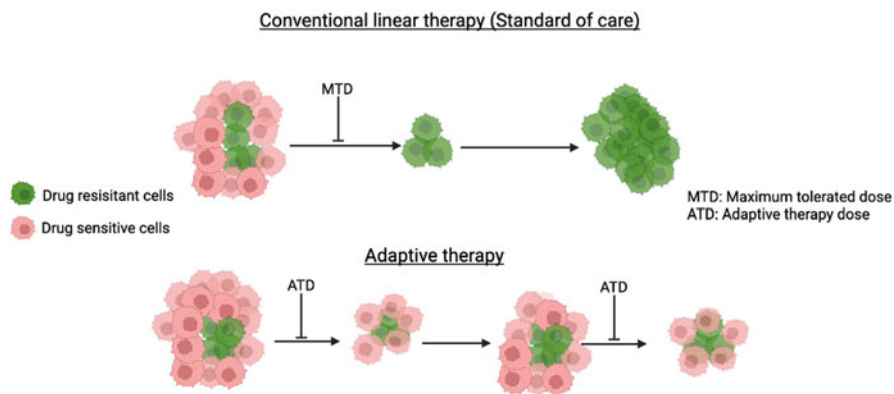


**Fig. 4** Illustration of conventional linear therapy and adaptive therapy, showing the population control of drug-sensitive cells (red) in adaptive therapy by modulating the amount of drug-resistant cells (green). (Image adapted from [47] and created in [Biorender.com](https://www.biorender.com) )

the growth of chemoresistant cells (Fig. 4) [43]. In contrast to linear therapy, adaptive therapy is aimed at controlling cancer rather than curing it. Therefore, it was proposed for aggressive cancers, such as metastatic castration-resistant prostate cancer (mCRPC) [44], that are irresponsive to conventional treatment or cancers that show early drug resistance such as advanced BRAF mutant melanoma [45]. Zhang and colleagues developed a mathematical model that takes the cellular competition for limited resources in the tumor and the proliferation differences within tumor subpopulations as its inputs. This model then predicts the optimal concentration and frequency of cytotoxic therapy that will permit the survival of a minimal number of chemosensitive cells, which will then keep the chemoresistant cells in check, as its output. To date, adaptive therapy has been applied to a clinical trial for the treatment of metastatic castrate-resistant prostate cancer. In this trial, all the patients were exposed to only 47% of the standard treatment dosage. Ten of the 11 patients in the adaptive therapy treatment arm have significantly improved remission time from 16.5 months to 27 months compared to the patients in the standard-of-care arm [44].

The efficacy of a drug also depends on its ability to go through various physical barriers in the stroma to reach the cancer cells. Considering the heterogeneity of tumors, a given drug might have a different uptake rate from tumor to tumor. To address this issue, Karolak and colleagues developed a mathematical model that takes the drug transport properties and tumor stroma topological information obtained from tissue section imaging as inputs [46]. This model predicts more accurate pharmacokinetics of a drug within a specific tumor microenvironment.

## **2.4 *Limitations of Computational and Mathematical Modeling***

Typically, computational and mathematical models rely on various laws of physics and biological observations, as the input, to predict a specific biological process, as the output. Hence, the accuracy of the prediction is highly dependent on the availability and accuracy of the required inputs. However, the required inputs are not always available, and to fill this gap, the model will need to rely on assumptions or neglect the role of some biological factors. For example, in the acid-induced toxicity model by Gatenby et al. [12], the authors assume that each cell has an optimal pH for its survival and any deviation from this pH level will lower cell viability. In the EGFR TKIs study by Poels et al. [40], the authors do not have the clinical toxicity data of combined osimertinib–dacomitinib treatment; hence, this was not accounted for in their model. Also, in the radiotherapy optimization model by Leder et al. [31], the authors excluded the effects of several key biological factors, including the immune system response, nutrient gradient, and tumor–stromal interactions. These assumptions might compromise the accuracy of the model at a certain level. Nevertheless, a mathematical model enables the fine-tuning of input variables to get a range of possible outcomes at a high resolution, a feat that otherwise will require a high level of resources experimentally or even not possible. Furthermore, the predictions made by the model are still based on real experimental data and might be extremely insightful to guide the respective studies.

## **3 *Microfluidics and Hydrogels in Cancer Studies***

Historically, wound healing assay is an in vitro method used to study cancer cell migration. This technique involves physically scraping cells off the culture plate and monitoring the time required for this gap to be covered by migrating cells. This technique is simple and widely used, but it does not recapitulate the in vivo 3D properties and chemical gradient. To solve some of the limitations posed by wound healing assay, scientists have used the Boyden chamber assay, which allows cells to migrate through a membrane with micron-sized pores in the direction of a chemical gradient. However, the phenotypes of the cells can only be studied before and after they go through the chamber, and imaging the within-constrictions morphology or biochemical changes that are temporal is very challenging with this assay. Microfluidic devices solve both the limitations of the Boyden chamber and wound healing assay; they allow real-time microscopy, and they can be easily fabricated to accommodate the complexity of a tumor environment.

In microfluidics, minute volumes of solvents and samples (e.g., cells) move through small channels embedded on a chip. One of the most common fabrication techniques for these microfluidic devices is soft lithography. Poly(dimethylsiloxane) (PDMS), being a transparent, non-toxic, and conformable silicon-based material, is a widely used material for microfluidic fabrication. In general, the process of



making a microfluidic device with PDMS-based soft lithography consists of the following steps: (i) computer-aided design of the microchannels, (ii) fabrication of photomask with the design, (iii) fabrication of a master mold by photolithography, (iv) fabrication of the PDMS microchannels by pouring PDMS on master with complementary reliefs, and (v) enclosure of the microchannels by bonding the PDMS onto a plasma-treated glass slides or coverslips [48].

The majority of cancer death is associated with metastasis [49]. This is a multistep process starting from the invasion of the basement membrane by the cancer cells, then their intravasation into the lymphatic system or bloodstream, then their migration in the circulation, and, finally, their extravasation into the secondary site where they form a new tumor niche [50]. During this migration, cancer cells need to migrate through various constrictions imposed by the dense tissue environment and the endothelial layer of the blood vessels. Using a microfluidic device with an array of constrictions, Irimia and Toner showed that cancer cells migrate constantly within the confinement channels and at a higher speed than unconfined cells. This confinement-induced migration can be hindered by the microtubule stabilizer chemotherapeutic agent paclitaxel, suggesting a role for the microtubule. Zanotelli and colleagues used microfluidic fabrication with Y-shaped micro-tracks of different confinements to show that migrating through confinement is an energy-intensive process for cells, and cells tend to migrate in the direction of less confinement, i.e., lesser energy demands [51]. In a breast cancer study, cancer cells were subjected to a chemical gradient-driven migration through a microfluidic device of varying confinements that models the tight spaces between ECM fibers *in vivo*. The cells migrating through tight lateral confinement of around 3  $\mu\text{m}$  showed modifications in cytoskeletal arrangement, in which microtubule polymerization was redirected toward the leading edge of the cell migration [52]. Hydraulic pressure also influences the direction of the migration of cells. Using a microfluidic device with trifurcating microchannels of different hydraulic pressures, Zhao and colleagues observed that in a calcium ion-mediated signaling pathway, TRPM7, a mechanosensor, senses a difference in hydraulic pressure and triggers the cells to move in the direction of low pressure [53]. In another study, Zervantonakis and colleagues designed a microfluidic device to study cancer cell intravasation through the endothelium of blood vessels [54]. The device consists of three channels: endothelial and cancer cells were seeded through the first and third channels, respectively, while the middle channel was filled with ECM hydrogels. Confluent endothelial monolayer formed in the first channel to mimic the endothelium. Then, the chemical gradient drove the migration of cancer cells through the ECM and the endothelial layer. Live imaging of the cancer cells showed that perturbations in the endothelial cell layer by TNF- $\alpha$  stimulation led to enhanced intravasation of cancer cells, suggesting the role of endothelium as a barrier to cancer cell invasion. The application of microfluidics technology is not limited to the study of cancer cell migration, however; for example, Karabacak and colleagues designed a microfluidic device that enables marker-free isolation of rare circulating tumor cells from patient's blood samples [55].



In addition to microfluidics, hydrogels are also widely used to study cell migration and response to physical cues. Hydrogels are fabricated by the physical or chemical cross-linking between their monomers, thereby transforming from liquid to a gel-like structure [56]. For example, collagen hydrogels self-assemble by physical cross-linking between the subunits or solubilized fibrils over time. Meanwhile, chemical cross-linking of acrylates is often induced by various stimuli, like photoinitiation or redox initiation, to initiate the chain-growth polymerization for rapid hydrogel formation. Hydrogels for cell culture can be classified as ECM-derived (e.g., collagen, fibrin, hyaluronic acid, Matrigel) and inert non-ECM-derived hydrogels (e.g., polyacrylamide, polyethylene glycol, alginate). Tunability of hydrogel properties such as pore size, stiffness, and degradability makes them important to study the influence of mechanical cues on cells [57].

Polyacrylamide (PA) hydrogel has been widely used in studying the role of substrate stiffness and extracellular matrix proteins in cancer progression. The stiffness of PA hydrogel can be finely tuned by varying the concentrations of acrylamide and its cross-linking reagents, to cover a wide range of stiffnesses to represent various tissues, such as the soft lymph node at  $\sim 0.1$  kPa, the pancreas at  $\sim 1$  kPa, and the lung at  $\sim 8$  kPa [58–60]. Typically PA hydrogel is used for 2D studies, where the cells are seeded onto the substrate. Due to the inert properties of PA gels, the gels need to be coated with ligands to allow cell adhesion, such as the extracellular matrix proteins collagen I, fibronectin, and laminin. Through the use of PA gels, stiff substrates have been shown to promote the proliferation of lung and breast cancer cells [61]. By using PA gels with fluorescently tagged fibronectin coating, a study also showed that stiff substrates promote the formation of invadopodia in breast cancer cells [62].

Hydrogels can also be used for 3D studies, where the cancer cells are embedded into the hydrogels before cross-linking. For example, collagen I hydrogels have been used to study the invasion of breast cancer and pancreatic cancer organoids. Interestingly, when mammary acini are cultured in collagen I gels, they can form physical connections with each other by modifying the collagen fibers and forming bridges of aligned collagen fibers between the acini, which then promotes the invasion phenotypes of the mammary cells [63]. In another study, polyethylene glycol gels were used to show that the interaction between laminin and integrin  $\alpha 3/\alpha 6$  is important for maintaining pancreatic cancer organoid growth [64]. Furthermore, by using an alginate hydrogel system, substrate stiffness was also shown to induce epigenetic changes that in turn drive tumorigenicity of the mammary cells [65]. Considering the breadth of topics covered in this section, it is clear that the use of physical sciences technologies, like microfluidic and hydrogel fabrication, has contributed significantly to the study of cancer biology.

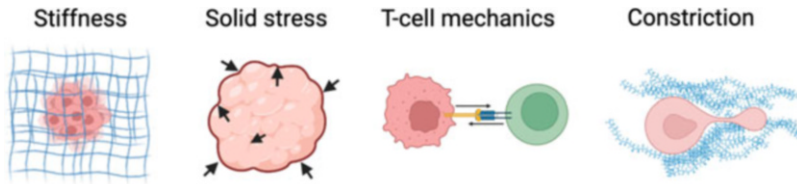


**Fig. 5** Some of the physical cues that affect cancer progression. (Image created in [Biorender.com](https://www.biorender.com))

## 4 Physical Cues in Cancer Biology

In this section, we will discuss several cancer studies that investigate various physical cues in tumor progression, ranging from tumor microenvironment stiffness, solid stress of the tumor, mechanical forces in T-cell interactions, and the impact of constrictions on cancer cell nucleus and genome (Fig. 5).

### 4.1 *Effect of Tumor Microenvironment Stiffness on Cancer Progression*

The organization and assembly of the ECM constituents determine the matrix's architecture and properties (e.g., stiffness or viscoelasticity), which, in turn, dictate the physical properties of the tissue [66]. Of more than 300 proteins found in the extracellular matrix, only the elastic fibers, glycosaminoglycans, and fibrillar collagen have a significant impact on the mechanical properties of the tissue [67, 68]. The elastic fibers are made up of elastin, fibulin, and fibrillin, and their major role is to allow the tissue to reverse its homeostatic state after being loaded with a mechanical force. Elastic fibers have been implicated in wrinkling of the skin and stiffening of the arteries with aging [69]. Collagen contributes to the stiffness and strength of the matrix and its remodeling by reorientation or cross-linking, and turnover helps to maintain the cell–matrix homeostasis.

The physical crosstalk between cells and their environment garner significant attention after the seminal work of Engler et al., which showed that the differentiation of naïve mesenchymal stem cells (MSCs) can be regulated by the elasticity of the substrate on which they are cultured [70]. They showed that MSCs cultured on compliant substrates (0.1–1 kPa) differentiated into neurogenic cells, while those cultured on stiff substrates (25–40 kPa) differentiated into osteogenic cells. The ability of cells to sense stiffness relies on the force-sensitive focal adhesion maturation [71]. When a cell lands on a substrate, the transmembrane protein, integrin, will bind to the ECM and initiate the formation of a focal adhesion complex inside the cell, which is connected to the actomyosin fibers (Fig. 6). On a stiff substrate, the integrin–ECM connection will be able to withstand the forces exerted by the actomyosin contraction, leading to the maturation of the focal adhesion, the

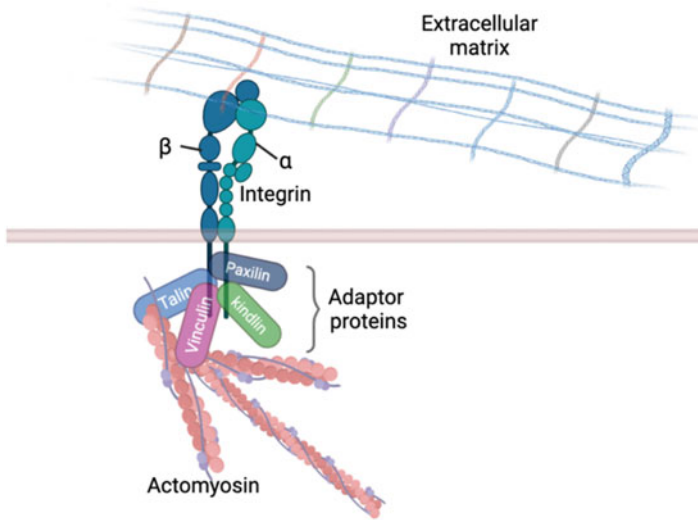


**Fig. 6** Physical connection between the cytoplasm and extracellular matrix. (Image created in [Bioreder.com](https://www.bioreder.com))

stability of actomyosin stress fibers, the increase in cellular contractility, and the spread cellular morphology on a 2D surface. In contrast, on a soft substrate, the focal adhesion cannot withstand actomyosin contraction, leading to lower cellular contractility and a more rounded cellular morphology.

The cells can translate physical cues, like stiffness, to functional chemical signaling through mechanotransduction. Dupont et al. revealed the role of the YAP/TAZ pathway in mechanotransduction. In this work, they cultured cells on fibronectin-coated polyacrylamide gel of varying stiffness. They found out that in cells cultured on a stiff substrate (i.e., cells with high actomyosin tension), YAP/TAZ resides in the nucleus where they upregulate the expression of genes such as CTGF and ANKRD1. While in cells grown on a compliant substrate, YAP/TAZ is mainly cytoplasmic and there is a reduction in the level of YAP/TAZ-regulated genes [72]. Swift et al. reported the translocation of RAR $\gamma$  transcription factor into the nucleus when cells are cultured on a stiff substrate, leading to the regulation of lamin-A/C expression [59].

In most solid tumors, disease progression is accompanied by desmoplasia-chronic fibroblast activation and remodeling of the ECM, which results in stiffened tissue stroma [73]. Stiffness is an intrinsic property that is regarded as the extent to which a substance can resist deformation. Cells probe ECM stiffness and viscoelasticity by the interaction of their transmembrane receptors, like integrins, with specific motifs within the ECM constituents. Subsequently, cells tune their contractility and behavior according to their environment's stiffness [74]. Aside from providing physical support to the cells, the ECM participates in tissue and tumor development by controlling the abundance of cytokines and specialized

receptors like discoidin domain receptors, pH of the tissue or tumor environment, and hydration [75].

Tissue stiffness correlates with the disease progression of breast cancer, and people with higher mammary matrix density, as a result of increased collagen cross-linking in the ECM, are more likely to develop breast tumors [76]. In breast cancer, stiff matrix activates malignant phenotype due to the activation of the Rho and actomyosin contractility [77]. However, ovarian cancer cells have been shown to be more invasive and resistant to drug treatment in a compliant matrix. Specifically, ovarian cancer cells undergo epithelial–mesenchymal transition and display enhanced migratory capacity on soft matrices [78]. According to Stephen Paget’s “Seed and Soil” hypothesis, stiff cancer cells (e.g., breast cancer) preferentially metastasize to stiff tissues (e.g., bone), and soft cancer cells tend to migrate to a compliant tissue [79]. In addition to invasion and disease progression [80], stiffness can also regulate TGF- $\beta$ 1-induced apoptosis [81], enhance immune infiltration [82], regulate DNA damage repair efficiency, and control sensitivity to genotoxic agents [83].

## ***4.2 Solid Stress and Tumor Progression***

Solid stress is one of the physical cues in a tumor. Solid stress is the compressive and mechanical forces exerted by the solid components of a tissue, such as cells and ECM. The total solid stress of the tumor is composed of two solid stresses: the growth-induced and the externally induced solid stress [84]. The growth-induced solid stress accumulates within the tumor when the cancer cells proliferate rapidly during tumor growth, causing deformation of the surrounding tumor microenvironment and stores strain energy. While the externally induced solid stress is applied by the surrounding tissues of the tumor. Growth-induced solid stress along with fluid pressure and externally applied stress was used to develop a mathematical model to predict the effect of solid stress on tumor progression [85]. This mathematical model, validated by in vivo experiments on murine tumors, shows that upon excision, a proliferating tumor releases its residual stress, and when it reaches a relaxed state, the tumor swells in the central region and retracts at the tumor boundary. This suggests that the intratumoral region of the tumor was under a compressive state, which compensates for the tensional stress in the peripheral region. Not surprisingly, solid stress differs among cancers, both between primary and metastatic cancer and between different cancer types. For example, pancreatic ductal adenocarcinoma primary tumors have a higher solid stress when compared to liver metastases, while primary colorectal cancers have low solid stress compared to corresponding liver metastases [86]. Solid stress can also compress the intratumoral blood and lymphatic vessels, a process that leads to hypoxia, immunosuppression, metastasis, and poor delivery of therapeutics [87]. Hence, combining cancer therapies with drugs that relax blood vessels may hold enormous potential in cancer treatment [88]. Indeed, multiple ongoing clinical trials are testing

the use of losartan in conjunction with chemotherapeutic agents for the treatment of pancreatic cancer [89, 90].

The externally applied solid stress can also modulate tumor morphology and progression. To study the effect of externally applied solid stress on cancer growth, Cheng et al. cultured carcinoma cell lines in 0.5% and 1.0% agarose gel. They found that cells in 0.5% were able to grow to about 50  $\mu\text{m}$  spheroid before apoptosis and necrosis were observed. However, for cells in 1.0% gel, cell death appeared earlier, and the spheroid could not grow bigger than approximately 30  $\mu\text{m}$ . Also, uniformly applied mechanical stress suppresses the overall growth of spherical cancer cell aggregates. In contrast, the application of nonuniform stress—allowing the spheroid to be exposed to low stress in some regions and high stress in other regions—revealed that cancer cells proliferate in regions with low stress while they undergo cell death in high-stress regions [91]. By using ultra-magnetic liposomes, Fernández-Sánchez and colleagues applied external solid stress to the colon cells of the Notch<sup>+</sup>Apc<sup>+1638N</sup> mouse and showed that mechanical pressure rapidly activates Ret, which then inhibits the interaction of E-cadherin with  $\beta$ -catenin, followed by  $\beta$ -catenin translocation into the nucleus. Furthermore, after a month of applying this solid stress, the expression of  $\beta$ -catenin-target genes was upregulated together with the formation of tumorous crypt foci [92]. These findings suggest a potential mechanism of tumorigenesis driven by a mechanical signaling pathway, where solid stress from the growing tumor may induce tumorigenic phenotypes of the surrounding healthy epithelial cells.

### 4.3 *T-Cells and Mechanical Forces*

Immunotherapy involves the use of monoclonal antibodies to block immune checkpoint inhibitors (and their ligands, e.g., CTLA-4, PD-1/PDL-1) that inhibit T-cell activity in an immune response, thereby allowing the host immune system to combat cancer cells [93]. Since the approval of ipilimumab, an anti-CTLA-4 inhibitor, by the Food and Drug Administration in 2011 for the treatment of stage III/IV melanoma, the oncology field has recorded a number of immunotherapies with enormous potential in cancer treatment.

During immunosurveillance, immune cells move through the blood and the lymphatic system looking for foreign agent-derived peptides on cell surface major histocompatibility complex (MHC). This process exposes the immune cells to various mechanical stresses that may cause changes in conformations of bonds between T-cell antigen receptor (TCR) and peptide-bound MHC (pMHC) on antigen-presenting cells and, by extension, affects antigen recognition and cytotoxicity activity [94]. Mechanistically, tensile force induces conformation change in the pMHC. By using a technique called biomembrane force probe [95], Liu and colleagues showed that the dissociation lifetime of the TCR-agonist pMHC bond increases with the application of tensile force; this tensional strengthening bond is called a catch bond [96]. The authors also showed that the application of 10 pN

tensile force triggers the highest  $\text{Ca}^{2+}$  flux, an indicator of T-cell activation. These findings suggest a key role of mechanical stress in the stabilization of the catch bond and T-cell activation. In contrast, the bond between TCR and antagonist pMHC dissociates faster with tensional force. The differential responses to tensile force amplify TCR specificity and discrimination. Wu and colleagues have shown that a specific mutation in the MHC can prevent force-induced conformational changes, thereby impairing the formation of catch bonds between TCR and agonist pMHC [97].

The role of substrate stiffness on cell migration potential has been demonstrated in a myriad of studies [98]. For example, Saitakis and colleagues studied the impact of substrate stiffness on the migration of human  $\text{CD4}^+$  T lymphoblast by culturing the cells on polyacrylamide gels with stiffnesses ranging from 0.5 kPa to 100 kPa [99]. The polyacrylamide gels were coated with ICAM-1 only or in addition to CD3 and CD28 antibodies, and then migration of T-cells was monitored through live imaging. The authors showed that both T-cell ICAM-1-dependent migration and TCR-induced stop signaling are influenced by substrate stiffness. Furthermore, another study showed that naïve T-cells are stiffer than effector T-cells [100]. This higher cellular stiffness leads to the formation of smaller immune synapses between naïve T-cells and antigen-presenting cells, suggesting the role of cellular stiffness on T-cell activation. Overall, it is clear that a better understanding of the role of physical cues on the immune response will help the development of a more effective immunotherapy against cancers.

## ***4.4 Physical Cues on Cancer Cell Nucleus and Genome***

### **4.4.1 Nucleus and the Nuclear Envelope**

The nuclear envelope is a lipid bilayer that protects the genome by controlling the exchange of materials between the nucleus and the cytoplasm via selective nuclear pore complexes [101]. The outer nuclear membrane of the nuclear envelope connects with the endoplasmic reticulum and is surrounded by ribosomes [102]. The inner envelope consists of hundreds of proteins including the SUN (Sad1-UNC-84 homology) and LEM (LAP2-emerin-MAN1) families, which have been described to play crucial roles in nuclear structure and positioning [103]. In addition to the nuclear envelope's role in regulating nucleocytoplasmic biochemical materials exchange, there is a dynamic transmission of force between the nucleus and the cytoskeletal network through the linker of nucleoskeleton and cytoskeleton (LINC) complex that spans through the nuclear envelope [104]. The LINC complex consists of SUN and KASH domains, which are located in the inner and the outer membranes of the nuclear envelope, respectively. The SUN proteins bind directly to the nuclear lamina within the nucleus, while the KASH proteins, like nesprins in mammalian cells, bind both directly and indirectly to the cytoskeletal network [105]. Ultimately,

these connections create a physical continuity between the cytoplasmic cytoskeletal network and the nucleus.

#### 4.4.2 Nuclear Lamina

The nuclear lamina is primarily made of a mesh network of lamins, type V intermediate filament proteins. Lamins have a short N-terminal domain, a central rod domain, and a long C-terminal tail characterized by an Ig-like domain [106]. A-type lamins and B-type lamins are the two groups of lamins. A-type lamins have an alternative splicing lamin C, both of which are from the *LMNA* gene [107]. B-type lamins are encoded by *LMNB1* (for lamin B1) and *LMNB2* (for lamin B2 and B3). By using proteomics analyses, Swift and colleagues showed that lamin-A protein level scales with tissue stiffness: The lamin-A protein level is 30-fold higher in stiff tissue when compared to softer tissue [59]. Moreover, by culturing mesenchymal stem cells in stiff and soft matrices, they found that lamin-A levels regulate nuclear translocation of the retinoic acid receptors, leading to the differentiation regulation of these stem cells. In another study, the interaction between lamin A/C and emerin has been shown to regulate the nuclear translocation of MKL1 as a cofactor of SRF pathway [108], while the interaction between nesprin1 and emerin has been shown to regulate the translocation of YAP and TAZ transcription factors of the Hippo pathway [109]. These findings suggest the role of nuclear proteins in mechanotransduction, i.e., nuclear mechanotransduction. Furthermore, the lamin-A protein level also dictates the stiffness of the nucleus itself [110, 111]. When a cancer cell migrates through micron-sized constrictions, like the tight spaces between ECM fibers, the nucleus, as the biggest organelle in the cell, needs to physically squeeze through these constrictions. The stiffer the nucleus, the harder it will be for the cell to pull the nucleus through such constrictions. Indeed, the lamin-A level, which dictates nuclear stiffness, has been reported to be the rate-determining factor in the migration of adenocarcinoma cell lines and mesenchymal stem cells through micron-sized constrictions [112].

#### 4.4.3 Effect of Constriction on DNA Damage

Alteration in the DNA when not properly repaired may lead to the acquisition of multiple mutations in both oncogenic and tumor suppression genes. These mutations give rise to various hallmarks of cancer, such as uncontrolled proliferation, evasion of cell death, and enhanced angiogenesis [1]. Normal cells have functional repair machinery known as the DNA damage response to maintain their genome integrity [113]. The DNA damage repair processes of cells within a tumor are perturbed and genome instability leads to clonal selection and enables the growth of dominant subclones that are more invasive and resistant to therapies. Ionizing radiation, alkylating agents, UV, replication errors, and spontaneous base deamination have

been well studied as causes of DNA damage [114]. In addition to these, physical cues like constriction and compression can also lead to an increase in DNA damage.

To mimic the *in vivo* constricted migration, cancer cells were subjected to constricted migration through Transwell micron-sized pores or microfluidic devices with sizes ranging from 1  $\mu\text{m}$  to 20  $\mu\text{m}$  [112, 115]. Nuclear deformation during constricted migration has been shown to cause nuclear envelope rupture and an increase in DNA damage [116, 117]. The mechanism behind the migration-induced increase in DNA damage is still unclear. However, the recruitment of cytoplasmic DNA binding protein cGAS has been observed at the nuclear rupture site, suggesting the exposure of chromatin to cytoplasmic factors that may induce DNA damage [116–118]. Furthermore, the migration of a nucleus through a micron-sized constriction has been shown to induce stretching of the chromatin, suggesting the application of mechanical stress on the chromatin itself, which may also induce DNA damage [119]. Alternatively, depletion of the DNA damage repair proteins during constriction migration has been shown in two different modes: the mislocalization of the DNA damage repair proteins into the cytoplasm during nuclear rupture and the segregation of the repair proteins away from the chromatin as the nucleus migrates through the constriction [120]. The depletion of DNA damage repair proteins from the damaged region may inhibit the repair processes. Furthermore, this migration-induced increase in DNA damage also represses the cell cycle and causes genomic instability [121, 122], suggesting its contribution to cancer cell heterogeneity and evolution. Hence, a better understanding of the underlying mechanisms of this phenomenon may shed light on potential therapeutic targets that inhibit cancer evolution and progression.

## 5 Summary and Future Direction

In this chapter, we described a number of studies that utilized physical sciences in cancer research. These studies cover a wide range of topics and highlight the significant contribution of physical sciences to studying cancer biology and to the development of more efficient therapies. Some of the studies involve the use of physical science approaches to studying the disease, such as the application of computational and mathematical modeling to better understand complex cancer biology and to improve cancer therapies. The use of microfluidics technology, a physical science instrument, in cancer research has resulted in numerous insights into cancer cell migration. Furthermore, many of the studies investigate the various physical factors that contribute to cancer progression, including the role of solid stress in suppressing drug penetration, the role of cellular contractility on cancer cell migration, the role of ECM compliance on cancer cell phenotypes, and even the role of mechanical stress in T-cell activation. A commonality among the studies and findings we discussed is that they provide a strong rationale for the continued involvement of physical science in cancer research and the further development of this field of research as part of the effort to finally beat cancer.



It is challenging to predict the future direction of this highly diverse transdisciplinary field. However, the following directions might help us to acquire a better understanding of cancer biology. First is the development of mathematical modeling that enables the integration of genomic data and phenotypic functional data to study cancer biology. Such a model will allow us to integrate the molecular aspects of cancer into our effort to predict the phenotype of interest. Furthermore, the ever-growing knowledge in cancer biology will also provide more and better data for the input of more accurate models. The application of microfluidics in cancer study is also rapidly and continuously growing, with the hope to develop a better and more accurate model that mimics the *in vivo* environment of a tumor. Physical sciences and engineering technologies are also an ever-growing field and resulted in novel tools that can be applied to cancer studies; one example is the 3D bioprinting technologies that may enable the fabrication of a more complex *in vitro* cancer model by using a biomimetic construct with spatially controlled seeding of various cell types, like cancer cells, immune cells, endothelial cells, and fibroblasts. Finally, although a myriad of studies has shown the importance of physical cues in cancer progression and treatment, we are still far from fully understanding the impact of physical cues in cancer biology; hence, further cancer mechanobiology studies should be pursued.

## References

1. Hanahan D, Weinberg RA (2011) Hallmarks of cancer: the next generation. *Cell* 144:646–674. <https://doi.org/10.1016/j.cell.2011.02.013>
2. Nia HT, Munn LL, Jain RK (2020) Physical traits of cancer. *Science* 370. <https://doi.org/10.1126/science.aaz0868>
3. Hui L, Chen Y (2015) Tumor microenvironment: sanctuary of the devil. *Cancer Lett* 368:7–13. <https://doi.org/10.1016/j.canlet.2015.07.039>
4. Romero-Garcia S, Moreno-Altamirano MM, Prado-Garcia H, Sanchez-Garcia FJ (2016) Lactate contribution to the tumor microenvironment: mechanisms, effects on immune cells and therapeutic relevance. *Front Immunol* 7:52. <https://doi.org/10.3389/fimmu.2016.00052>
5. DelNero P, Hopkins BD, Cantley LC, Fischbach C (2018) Cancer metabolism gets physical. *Sci Transl Med* 10. <https://doi.org/10.1126/scitranslmed.aag1011>
6. Weerasinghe HN, Burrage PM, Burrage K, Nicolau DV Jr (2019) Mathematical models of cancer cell plasticity. *J Oncol* 2019:2403483. <https://doi.org/10.1155/2019/2403483>
7. Metzcar J, Wang Y, Heiland R, Macklin P (2019) A review of cell-based computational modeling in cancer biology. *JCO Clin Cancer Inform* 3:1–13. <https://doi.org/10.1200/CCI.18.00069>
8. Graner F, Glazier JA (1992) Simulation of biological cell sorting using a two-dimensional extended Potts model. *Phys Rev Lett* 69:2013–2016. <https://doi.org/10.1103/PhysRevLett.69.2013>
9. Fletcher AG, Osterfield M, Baker RE, Shvartsman SY (2014) Vertex models of epithelial morphogenesis. *Biophys J* 106:2291–2304. <https://doi.org/10.1016/j.bpj.2013.11.4498>
10. Bauer AL, Jackson TL, Jiang Y (2007) A cell-based model exhibiting branching and anastomosis during tumor-induced angiogenesis. *Biophys J* 92:3105–3121. <https://doi.org/10.1529/biophysj.106.101501>

11. Chaplain MA, Graziano L, Preziosi L (2006) Mathematical modelling of the loss of tissue compression responsiveness and its role in solid tumour development. *Math Med Biol* 23:197–229. <https://doi.org/10.1093/imammb/dql009>
12. Gatenby RA, Gawlinski ET, Gmitro AF, Kaylor B, Gillies RJ (2006) Acid-mediated tumor invasion: a multidisciplinary study. *Cancer Res* 66:5216–5223. <https://doi.org/10.1158/0008-5472.CAN-05-4193>
13. Martin NK, Gaffney EA, Gatenby RA, Maini PK (2010) Tumour-stromal interactions in acid-mediated invasion: a mathematical model. *J Theor Biol* 267:461–470. <https://doi.org/10.1016/j.jtbi.2010.08.028>
14. Li L, He Y, Zhao M, Jiang J (2013) Collective cell migration: implications for wound healing and cancer invasion. *Burns Trauma* 1:21–26. <https://doi.org/10.4103/2321-3868.113331>
15. Ridley AJ et al (2003) Cell migration: integrating signals from front to back. *Science* 302:1704–1709. <https://doi.org/10.1126/science.1092053>
16. Bravo-Cordero JJ, Hodgson L, Condeelis J (2012) Directed cell invasion and migration during metastasis. *Curr Opin Cell Biol* 24:277–283. <https://doi.org/10.1016/j.ceb.2011.12.004>
17. Ray A, Slama ZM, Morford RK, Madden SA, Provenzano PP (2017) Enhanced directional migration of cancer stem cells in 3D aligned collagen matrices. *Biophys J* 112:1023–1036. <https://doi.org/10.1016/j.bpj.2017.01.007>
18. Yamada KM, Sixt M (2019) Mechanisms of 3D cell migration. *Nat Rev Mol Cell Biol* 20:738–752. <https://doi.org/10.1038/s41580-019-0172-9>
19. Chan CE, Odde DJ (2008) Traction dynamics of filopodia on compliant substrates. *Science* 322:1687–1691. <https://doi.org/10.1126/science.1163595>
20. Bangasser BL et al (2017) Shifting the optimal stiffness for cell migration. *Nat Commun* 8:15313. <https://doi.org/10.1038/ncomms15313>
21. Iliina O et al (2020) Cell-cell adhesion and 3D matrix confinement determine jamming transitions in breast cancer invasion. *Nat Cell Biol* 22:1103–1115. <https://doi.org/10.1038/s41556-020-0552-6>
22. Bazellieres E et al (2015) Control of cell-cell forces and collective cell dynamics by the intercellular adhesome. *Nat Cell Biol* 17:409–420. <https://doi.org/10.1038/ncb3135>
23. Kim JH et al (2020) Unjamming and collective migration in MCF10A breast cancer cell lines. *Biochem Biophys Res Commun* 521:706–715. <https://doi.org/10.1016/j.bbrc.2019.10.188>
24. Kang W et al (2021) A novel jamming phase diagram links tumor invasion to non-equilibrium phase separation. *iScience* 24:103252. <https://doi.org/10.1016/j.isci.2021.103252>
25. Nowell PC (1976) The clonal evolution of tumor cell populations. *Science* 194:23–28. <https://doi.org/10.1126/science.959840>
26. Greaves M, Maley CC (2012) Clonal evolution in cancer. *Nature* 481:306–313. <https://doi.org/10.1038/nature10762>
27. Marusyk A, Janiszewska M, Polyak K (2020) Intratumor heterogeneity: the Rosetta stone of therapy resistance. *Cancer Cell* 37:471–484. <https://doi.org/10.1016/j.ccell.2020.03.007>
28. Stupp R et al (2005) Radiotherapy plus concomitant and adjuvant temozolomide for glioblastoma. *N Engl J Med* 352:987–996. <https://doi.org/10.1056/NEJMoa043330>
29. Laperriere N, Zuraw L, Cairncross G, Cancer Care Ontario Practice Guidelines Initiative Neuro-Oncology Disease Site, G (2002) Radiotherapy for newly diagnosed malignant glioma in adults: a systematic review. *Radiother Oncol* 64:259–273. [https://doi.org/10.1016/s0167-8140\(02\)00078-6](https://doi.org/10.1016/s0167-8140(02)00078-6)
30. Gupta T, Dinshaw K (2005) Modified optimal fractionation for poor prognosis malignant gliomas: an elusive search. *Acta Oncol* 44:105–113. <https://doi.org/10.1080/02841860510007611>
31. Leder K et al (2014) Mathematical modeling of PDGF-driven glioblastoma reveals optimized radiation dosing schedules. *Cell* 156:603–616. <https://doi.org/10.1016/j.cell.2013.12.029>
32. Zhao J et al (2019) Immune and genomic correlates of response to anti-PD-1 immunotherapy in glioblastoma. *Nat Med* 25:462–469. <https://doi.org/10.1038/s41591-019-0349-y>

33. Huang CY et al (2018) Unfavorable mortality-to-incidence ratio of lung cancer is associated with health care disparity. *Int J Environ Res Public Health* 15. <https://doi.org/10.3390/ijerph15122889>
34. Bains MS (1991) Surgical treatment of lung cancer. *Chest* 100:826–837. <https://doi.org/10.1378/chest.100.3.826>
35. Zhang Z, Stiegler AL, Boggon TJ, Kobayashi S, Halmos B (2010) EGFR-mutated lung cancer: a paradigm of molecular oncology. *Oncotarget* 1:497–514. <https://doi.org/10.18632/oncotarget.186>
36. Maemondo M et al (2010) Gefitinib or chemotherapy for non-small-cell lung cancer with mutated EGFR. *N Engl J Med* 362:2380–2388. <https://doi.org/10.1056/NEJMoa0909530>
37. Yu HA et al (2013) Analysis of tumor specimens at the time of acquired resistance to EGFR-TKI therapy in 155 patients with EGFR-mutant lung cancers. *Clin Cancer Res* 19:2240–2247. <https://doi.org/10.1158/1078-0432.CCR-12-2246>
38. Remon J et al (2017) The APPLE trial: feasibility and activity of AZD9291 (Osimertinib) treatment on positive PLasma T790M in EGFR-mutant NSCLC patients. EORTC 1613. *Clin Lung Cancer* 18:583–588. <https://doi.org/10.1016/j.clcc.2017.02.005>
39. Piotrowska Z et al (2018) Landscape of acquired resistance to Osimertinib in EGFR-mutant NSCLC and clinical validation of combined EGFR and RET inhibition with Osimertinib and BLU-667 for acquired RET fusion. *Cancer Discov* 8:1529–1539. <https://doi.org/10.1158/2159-8290.CD-18-1022>
40. Poels KE et al (2021) Identification of optimal dosing schedules of dacomitinib and osimertinib for a phase I/II trial in advanced EGFR-mutant non-small cell lung cancer. *Nat Commun* 12:3697. <https://doi.org/10.1038/s41467-021-23912-4>
41. Su Y et al (2019) Phenotypic heterogeneity and evolution of melanoma cells associated with targeted therapy resistance. *PLoS Comput Biol* 15:e1007034. <https://doi.org/10.1371/journal.pcbi.1007034>
42. Rockne RC et al (2020) State-transition analysis of time-sequential gene expression identifies critical points that predict development of acute myeloid leukemia. *Cancer Res* 80:3157–3169. <https://doi.org/10.1158/0008-5472.CAN-20-0354>
43. West J et al (2020) Towards multidrug adaptive therapy. *Cancer Res* 80:1578–1589. <https://doi.org/10.1158/0008-5472.CAN-19-2669>
44. Zhang J, Cunningham JJ, Brown JS, Gatenby RA (2017) Integrating evolutionary dynamics into treatment of metastatic castrate-resistant prostate cancer. *Nat Commun* 8:1816. <https://doi.org/10.1038/s41467-017-01968-5>
45. Kim E, Brown JS, Eroglu Z, Anderson ARA (2021) Adaptive therapy for metastatic melanoma: predictions from patient calibrated mathematical models. *Cancers (Basel)* 13. <https://doi.org/10.3390/cancers13040823>
46. Karolak A et al (2018) Targeting ligand specificity linked to tumor tissue topological heterogeneity via single-cell micro-pharmacological modeling. *Sci Rep* 8:3638. <https://doi.org/10.1038/s41598-018-21883-z>
47. Hansen E, Read AF (2020) Modifying adaptive therapy to enhance competitive suppression. *Cancers (Basel)* 12. <https://doi.org/10.3390/cancers12123556>
48. Whitesides GM, Ostuni E, Takayama S, Jiang X, Ingber DE (2001) Soft lithography in biology and biochemistry. *Annu Rev Biomed Eng* 3:335–373. <https://doi.org/10.1146/annurev.bioeng.3.1.335>
49. Steeg PS (2016) Targeting metastasis. *Nat Rev Cancer* 16:201–218. <https://doi.org/10.1038/nrc.2016.25>
50. Wirtz D, Konstantopoulos K, Searson PC (2011) The physics of cancer: the role of physical interactions and mechanical forces in metastasis. *Nat Rev Cancer* 11:512–522. <https://doi.org/10.1038/nrc3080>
51. Zanotelli MR et al (2019) Energetic costs regulated by cell mechanics and confinement are predictive of migration path during decision-making. *Nat Commun* 10:4185. <https://doi.org/10.1038/s41467-019-12155-z>
52. Balzer EM et al (2012) Physical confinement alters tumor cell adhesion and migration phenotypes. *FASEB J* 26:4045–4056. <https://doi.org/10.1096/fj.12-211441>

53. Zhao R et al (2019) Cell sensing and decision-making in confinement: the role of TRPM7 in a tug of war between hydraulic pressure and cross-sectional area. *Sci Adv* 5:eaaw7243. <https://doi.org/10.1126/sciadv.aaw7243>
54. Zervantonakis IK et al (2012) Three-dimensional microfluidic model for tumor cell intravasation and endothelial barrier function. *Proc Natl Acad Sci U S A* 109:13515–13520. <https://doi.org/10.1073/pnas.1210182109>
55. Karabacak NM et al (2014) Microfluidic, marker-free isolation of circulating tumor cells from blood samples. *Nat Protoc* 9:694–710. <https://doi.org/10.1038/nprot.2014.044>
56. Caliari SR, Burdick JA (2016) A practical guide to hydrogels for cell culture. *Nat Methods* 13:405–414. <https://doi.org/10.1038/nmeth.3839>
57. Ingber DE (2006) Cellular mechanotransduction: putting all the pieces together again. *FASEB J* 20:811–827. <https://doi.org/10.1096/fj.05-5424rev>
58. Levental I, Georges PC, Janmey PA (2007) Soft biological materials and their impact on cell function. *Soft Matter* 3:299–306. <https://doi.org/10.1039/B610522J>
59. Swift J et al (2013) Nuclear lamin-A scales with tissue stiffness and enhances matrix-directed differentiation. *Science* 341:1240104. <https://doi.org/10.1126/science.1240104>
60. Laklai H et al (2016) Genotype tunes pancreatic ductal adenocarcinoma tissue tension to induce matricellular fibrosis and tumor progression. *Nat Med* 22:497–505. <https://doi.org/10.1038/nm.4082>
61. Tilghman RW et al (2012) Matrix rigidity regulates cancer cell growth by modulating cellular metabolism and protein synthesis. *PLoS One* 7:e37231. <https://doi.org/10.1371/journal.pone.0037231>
62. Alexander NR et al (2008) Extracellular matrix rigidity promotes invadopodia activity. *Curr Biol* 18:1295–1299. <https://doi.org/10.1016/j.cub.2008.07.090>
63. Shi Q et al (2014) Rapid disorganization of mechanically interacting systems of mammary acini. *Proc Natl Acad Sci U S A* 111:658–663. <https://doi.org/10.1073/pnas.1311312110>
64. Below CR et al (2022) A microenvironment-inspired synthetic three-dimensional model for pancreatic ductal adenocarcinoma organoids. *Nat Mater* 21:110–119. <https://doi.org/10.1038/s41563-021-01085-1>
65. Stowers RS et al (2019) Matrix stiffness induces a tumorigenic phenotype in mammary epithelium through changes in chromatin accessibility. *Nat Biomed Eng* 3:1009–1019. <https://doi.org/10.1038/s41551-019-0420-5>
66. Mouw JK, Ou G, Weaver VM (2014) Extracellular matrix assembly: a multiscale deconstruction. *Nat Rev Mol Cell Biol* 15:771–785. <https://doi.org/10.1038/nrm3902>
67. Hynes RO, Naba A (2012) Overview of the matrisome—an inventory of extracellular matrix constituents and functions. *Cold Spring Harb Perspect Biol* 4:a004903. <https://doi.org/10.1101/cshperspect.a004903>
68. Humphrey JD, Dufresne ER, Schwartz MA (2014) Mechanotransduction and extracellular matrix homeostasis. *Nat Rev Mol Cell Biol* 15:802–812. <https://doi.org/10.1038/nrm3896>
69. Kielty CM (2006) Elastic fibres in health and disease. *Expert Rev Mol Med* 8:1–23. <https://doi.org/10.1017/S146239940600007X>
70. Engler AJ, Sen S, Sweeney HL, Discher DE (2006) Matrix elasticity directs stem cell lineage specification. *Cell* 126:677–689. <https://doi.org/10.1016/j.cell.2006.06.044>
71. Moore SW, Roca-Cusachs P, Sheetz MP (2010) Stretchy proteins on stretchy substrates: the important elements of integrin-mediated rigidity sensing. *Dev Cell* 19:194–206. <https://doi.org/10.1016/j.devcel.2010.07.018>
72. Dupont S et al (2011) Role of YAP/TAZ in mechanotransduction. *Nature* 474:179–183. <https://doi.org/10.1038/nature10137>
73. Pickup MW, Mouw JK, Weaver VM (2014) The extracellular matrix modulates the hallmarks of cancer. *EMBO Rep* 15:1243–1253. <https://doi.org/10.15252/embr.201439246>
74. Kai F, Drain AP, Weaver VM (2019) The extracellular matrix modulates the metastatic journey. *Dev Cell* 49:332–346. <https://doi.org/10.1016/j.devcel.2019.03.026>
75. Mecham RP (2012) Overview of extracellular matrix. *Curr Protoc Cell Biol* Chapter 10:Unit 10.11. <https://doi.org/10.1002/0471143030.cb1001s57>

76. Wang HB, Dembo M, Wang YL (2000) Substrate flexibility regulates growth and apoptosis of normal but not transformed cells. *Am J Physiol Cell Physiol* 279:C1345–C1350. <https://doi.org/10.1152/ajpcell.2000.279.5.C1345>
77. Paszek MJ et al (2005) Tensional homeostasis and the malignant phenotype. *Cancer Cell* 8:241–254. <https://doi.org/10.1016/j.ccr.2005.08.010>
78. McGrail DJ, Kieu QM, Dawson MR (2014) The malignancy of metastatic ovarian cancer cells is increased on soft matrices through a mechanosensitive Rho-ROCK pathway. *J Cell Sci* 127:2621–2626. <https://doi.org/10.1242/jcs.144378>
79. Paget S (1989) The distribution of secondary growths in cancer of the breast. 1889. *Cancer Metastasis Rev* 8:98–101
80. Liu C et al (2021) Heterogeneous microenvironmental stiffness regulates pro-metastatic functions of breast cancer cells. *Acta Biomater* 131:326–340. <https://doi.org/10.1016/j.actbio.2021.07.009>
81. Leight JL, Wozniak MA, Chen S, Lynch ML, Chen CS (2012) Matrix rigidity regulates a switch between TGF-beta1-induced apoptosis and epithelial-mesenchymal transition. *Mol Biol Cell* 23:781–791. <https://doi.org/10.1091/mbc.E11-06-0537>
82. Acerbi I et al (2015) Human breast cancer invasion and aggression correlates with ECM stiffening and immune cell infiltration. *Integr Biol (Camb)* 7:1120–1134. <https://doi.org/10.1039/c5ib00040h>
83. Deng M et al (2020) Extracellular matrix stiffness determines DNA repair efficiency and cellular sensitivity to genotoxic agents. *Sci Adv* 6. <https://doi.org/10.1126/sciadv.abb2630>
84. Jain RK, Martin JD, Stylianopoulos T (2014) The role of mechanical forces in tumor growth and therapy. *Annu Rev Biomed Eng* 16:321–346. <https://doi.org/10.1146/annurev-bioeng-071813-105259>
85. Stylianopoulos T et al (2013) Coevolution of solid stress and interstitial fluid pressure in tumors during progression: implications for vascular collapse. *Cancer Res* 73:3833–3841. <https://doi.org/10.1158/0008-5472.CAN-12-4521>
86. Nia HT et al (2016) Solid stress and elastic energy as measures of tumour mechanopathology. *Nat Biomed Eng* 1. <https://doi.org/10.1038/s41551-016-0004>
87. Stylianopoulos T et al (2012) Causes, consequences, and remedies for growth-induced solid stress in murine and human tumors. *Proc Natl Acad Sci U S A* 109:15101–15108. <https://doi.org/10.1073/pnas.1213353109>
88. Zhao Y et al (2019) Losartan treatment enhances chemotherapy efficacy and reduces ascites in ovarian cancer models by normalizing the tumor stroma. *Proc Natl Acad Sci U S A* 116:2210–2219. <https://doi.org/10.1073/pnas.1818357116>
89. Massachusetts-General-Hospital (2019) Proton w/FOLFIRINOX-Losartan for pancreatic cancer. <https://clinicaltrials.gov/ct2/show/NCT01821729>
90. Massachusetts-General-Hospital (2021) Losartan and nivolumab in combination with FOLFIRINOX and SBRT in localized pancreatic cancer. <https://clinicaltrials.gov/ct2/show/record/NCT03563248>
91. Cheng G, Tse J, Jain RK, Munn LL (2009) Micro-environmental mechanical stress controls tumor spheroid size and morphology by suppressing proliferation and inducing apoptosis in cancer cells. *PLoS One* 4:e4632. <https://doi.org/10.1371/journal.pone.0004632>
92. Fernandez-Sanchez ME et al (2015) Mechanical induction of the tumorigenic beta-catenin pathway by tumour growth pressure. *Nature* 523:92–95. <https://doi.org/10.1038/nature14329>
93. Postow MA, Callahan MK, Wolchok JD (2015) Immune checkpoint blockade in cancer therapy. *J Clin Oncol* 33:1974–1982. <https://doi.org/10.1200/JCO.2014.59.4358>
94. Zhu C, Chen W, Lou J, Rittase W, Li K (2019) Mechanosensing through immunoreceptors. *Nat Immunol* 20:1269–1278. <https://doi.org/10.1038/s41590-019-0491-1>
95. Chen W, Zarnitsyna VI, Sarangapani KK, Huang J, Zhu C (2008) Measuring receptor-ligand binding kinetics on cell surfaces: from adhesion frequency to thermal fluctuation methods. *Cell Mol Bioeng* 1:276–288. <https://doi.org/10.1007/s12195-008-0024-8>

96. Liu B, Chen W, Evavold BD, Zhu C (2014) Accumulation of dynamic catch bonds between TCR and agonist peptide-MHC triggers T cell signaling. *Cell* 157:357–368. <https://doi.org/10.1016/j.cell.2014.02.053>
97. Wu P et al (2019) Mechano-regulation of peptide-MHC class I conformations determines TCR antigen recognition. *Mol Cell* 73:1015–1027 e1017. <https://doi.org/10.1016/j.molcel.2018.12.018>
98. van Helvert S, Storm C, Friedl P (2018) Mechanoreciprocity in cell migration. *Nat Cell Biol* 20:8–20. <https://doi.org/10.1038/s41556-017-0012-0>
99. Saitakis M et al (2017) Different TCR-induced T lymphocyte responses are potentiated by stiffness with variable sensitivity. *elife* 6. <https://doi.org/10.7554/eLife.23190>
100. Thauland TJ, Hu KH, Bruce MA, Butte MJ (2017) Cytoskeletal adaptivity regulates T cell receptor signaling. *Sci Signal* 10. <https://doi.org/10.1126/scisignal.aah3737>
101. Ungrich R, Kutay U (2017) Mechanisms and functions of nuclear envelope remodelling. *Nat Rev Mol Cell Biol* 18:229–245. <https://doi.org/10.1038/nrm.2016.153>
102. Gruenbaum Y, Margalit A, Goldman RD, Shumaker DK, Wilson KL (2005) The nuclear lamina comes of age. *Nat Rev Mol Cell Biol* 6:21–31. <https://doi.org/10.1038/nrm1550>
103. Mekhail K, Moazed D (2010) The nuclear envelope in genome organization, expression and stability. *Nat Rev Mol Cell Biol* 11:317–328. <https://doi.org/10.1038/nrm2894>
104. Lombardi ML et al (2011) The interaction between nesprins and sun proteins at the nuclear envelope is critical for force transmission between the nucleus and cytoskeleton. *J Biol Chem* 286:26743–26753. <https://doi.org/10.1074/jbc.M111.233700>
105. Wilson KL, Berk JM (2010) The nuclear envelope at a glance. *J Cell Sci* 123:1973–1978. <https://doi.org/10.1242/jcs.019042>
106. Dhe-Paganon S, Werner ED, Chi YI, Shoelson SE (2002) Structure of the globular tail of nuclear lamin. *J Biol Chem* 277:17381–17384. <https://doi.org/10.1074/jbc.C200038200>
107. Machiels BM et al (1996) An alternative splicing product of the lamin A/C gene lacks exon 10. *J Biol Chem* 271:9249–9253. <https://doi.org/10.1074/jbc.271.16.9249>
108. Ho CY, Jaalouk DE, Vartiainen MK, Lammerding J (2013) Lamin A/C and emerin regulate MKL1-SRF activity by modulating actin dynamics. *Nature* 497:507–511. <https://doi.org/10.1038/nature12105>
109. Guilluy C et al (2014) Isolated nuclei adapt to force and reveal a mechanotransduction pathway in the nucleus. *Nat Cell Biol* 16:376–381. <https://doi.org/10.1038/ncb2927>
110. Lammerding J et al (2004) Lamin A/C deficiency causes defective nuclear mechanics and mechanotransduction. *J Clin Invest* 113:370–378. <https://doi.org/10.1172/JCI19670>
111. Pajeroski JD, Dahl KN, Zhong FL, Sammak PJ, Discher DE (2007) Physical plasticity of the nucleus in stem cell differentiation. *Proc Natl Acad Sci U S A* 104:15619–15624. <https://doi.org/10.1073/pnas.0702576104>
112. Harada T et al (2014) Nuclear lamin stiffness is a barrier to 3D migration, but softness can limit survival. *J Cell Biol* 204:669–682. <https://doi.org/10.1083/jcb.201308029>
113. Ciccio A, Elledge SJ (2010) The DNA damage response: making it safe to play with knives. *Mol Cell* 40:179–204. <https://doi.org/10.1016/j.molcel.2010.09.019>
114. Chatterjee N, Walker GC (2017) Mechanisms of DNA damage, repair, and mutagenesis. *Environ Mol Mutagen* 58:235–263. <https://doi.org/10.1002/em.22087>
115. Davidson PM, Sliz J, Isermann P, Denais C, Lammerding J (2015) Design of a microfluidic device to quantify dynamic intra-nuclear deformation during cell migration through confining environments. *Integr Biol (Camb)* 7:1534–1546. <https://doi.org/10.1039/c5ib00200a>
116. Denais CM et al (2016) Nuclear envelope rupture and repair during cancer cell migration. *Science* 352:353–358. <https://doi.org/10.1126/science.aad7297>
117. Raab M et al (2016) ESCRT III repairs nuclear envelope ruptures during cell migration to limit DNA damage and cell death. *Science* 352:359–362. <https://doi.org/10.1126/science.aad7611>

118. Harding SM et al (2017) Mitotic progression following DNA damage enables pattern recognition within micronuclei. *Nature* 548:466–470. <https://doi.org/10.1038/nature23470>
119. Irianto J, Xia Y, Pfeifer CR, Greenberg RA, Discher DE (2017) As a nucleus enters a small pore, chromatin stretches and maintains integrity, even with DNA breaks. *Biophys J* 112:446–449. <https://doi.org/10.1016/j.bpj.2016.09.047>
120. Irianto J et al (2016) Nuclear constriction segregates mobile nuclear proteins away from chromatin. *Mol Biol Cell* 27:4011–4020. <https://doi.org/10.1091/mbc.E16-06-0428>
121. Pfeifer CR et al (2018) Constricted migration increases DNA damage and independently represses cell cycle. *Mol Biol Cell* 29:1948–1962. <https://doi.org/10.1091/mbc.E18-02-0079>
122. Irianto J et al (2017) DNA damage follows repair factor depletion and portends genome variation in cancer cells after pore migration. *Curr Biol* 27:210–223. <https://doi.org/10.1016/j.cub.2016.11.049>



# Index

## A

Agent-based models (ABMs), 87  
Animals, 9, 58, 87, 203, 219, 247, 260, 285,  
286, 288, 289, 291, 293, 294

## B

Biomaterial, 2, 15–18, 20, 21, 25, 26, 122, 163,  
188  
Breast cancer, 4, 13, 14, 18, 21, 23, 25, 44, 64,  
85, 98, 100, 115, 119, 121, 127, 131,  
141, 143, 144, 147–150, 152, 163–165,  
167–169, 171, 173, 178, 180, 183, 184,  
202, 203, 205–211, 216, 218–221, 233,  
258, 259, 264–266, 269, 271–273, 283,  
286, 291, 305, 306, 311, 312, 315

## C

Cancer-associated fibroblasts (CAFs), 5, 83,  
118, 119, 121, 143, 144, 146, 147, 150,  
152, 160, 161, 163–166, 169, 180, 183,  
187, 188, 236, 288, 299  
Cancer-macrophage dynamics, 203, 210–216  
Cell-cell interactions, 25, 57, 62, 81–84, 87,  
88, 91, 116, 232, 239, 244  
Cell rheology, 18, 45, 89, 91  
Cellular Potts model (CPM), 92–93, 97, 103,  
304  
Circulating tumor cells (CTCs), v, 60, 78, 86,  
125, 151, 255–273, 287, 289–293  
Cluster, 2, 4, 10, 19, 20, 47, 50, 51, 57–60, 78,  
79, 82–87, 92, 93, 101, 102, 118, 145,  
234, 238, 240, 257, 259, 261, 263–265,  
270, 273, 284, 289, 291

Computational modeling, 97, 301–310

## D

Dissemination, 2–4, 59, 60, 78, 85, 124, 125,  
140, 206, 234–236, 238, 288, 306  
Dynamic heterogeneity, 36, 37, 43, 45–47, 52,  
53, 57, 59, 140, 307

## E

Emergence, 38, 51, 53, 58, 59, 151  
Endometrium, 232  
Epithelial-mesenchymal transition (EMT), 2,  
6, 7, 19–25, 55, 60, 63–65, 78, 79, 81,  
84, 85, 99–101, 119, 123–125, 141,  
160, 163, 165–168, 171, 172, 174–187,  
256, 257, 259, 261, 264–266, 288, 293,  
315  
Exosomes, 115, 122, 123, 128

## F

Fallopian tubes, 232–235, 240, 242–243  
Flocking, 36, 38, 50, 57–59, 82, 84, 87  
Fluid shear stress, 124, 125, 244,  
258–260, 289

## G

Gene signatures, 216–220  
Glass transition, 7, 34, 37–39, 41, 44, 45  
Glycolysis, 11–15, 25, 141, 143–145, 147,  
148, 152, 302–304



**H**

Hemodynamics, 289, 290, 293  
 Hydrogel, 13, 17, 18, 80, 161, 170–172, 185,  
 211–213, 215, 216, 243, 262, 288, 306,  
 310–313

**J**

Jamming, 7, 8, 36–60, 63–66, 84, 85, 88, 90,  
 91, 306

**L**

Leukocyte, 3, 261, 262, 269, 271–273

**M**

Machine learning, 10, 25, 98–99  
 Macrophages, 5, 17, 23, 117, 119, 163,  
 201–221, 236, 283, 287  
 Matrix remodeling, 3, 4, 20, 118, 160, 187,  
 201–221, 305, 313  
 Matrix stiffness, *v.*, 13, 19, 20, 163, 168, 171,  
 174, 175, 177, 178, 180, 182–185, 203,  
 209, 211, 213  
 Mechanics, 2, 16, 18–21, 34, 41, 43, 45, 63,  
 88–90, 94, 97, 124–125, 127, 130,  
 160–163, 169, 170, 177, 178, 187, 216,  
 232  
 Mesothelium, 233–236  
 Metabolic heterogeneity, 11–15  
 Metabolic reprogramming, 140, 141  
 Metastasis, *v.*, 9, 21, 24, 27, 34, 60, 63–66,  
 77–104, 114–116, 118–121, 123, 124,  
 131, 140, 147, 151, 160, 165, 167,  
 174, 176, 179–181, 187, 207–209, 217,  
 219, 220, 236, 241, 256, 259, 261,  
 263–265, 283–294, 300, 303, 305,  
 311, 315  
 Metastatic colonization, *v.*, 16, 85, 263, 286,  
 289  
 Mice, 2, 15, 16, 20, 21, 23, 64, 115, 117, 147,  
 162, 168, 174, 176, 178, 180, 185–187,  
 205, 208, 219, 232, 233, 237, 241, 259,  
 260, 263, 265, 266, 285, 286, 289–293,  
 307, 316  
 Microfluidics, 26, 184, 210–214, 221,  
 244–246, 259–262, 264, 269, 271,  
 285, 288–294, 301, 310–313, 319,  
 320  
 Mitochondrial membrane potential, 145  
 Model systems, 86, 90, 152, 202, 221,  
 284–286, 288–292, 294

Monocytes, 203, 204, 209, 210, 215, 218, 220,  
 259, 272

Myocardin-related transcription factor  
 (MRTF), 128, 174, 177,  
 179–182, 187

**N**

Negative selection, 267, 269–270

**O**

Order parameter, 2, 7–10, 25, 37–39, 48, 51  
 Ordinary differential equations (ODEs), 86,  
 97, 100, 101  
 Organoid, 2, 15, 21–23, 60, 84, 184, 242–243,  
 264, 288, 312  
 Organotypic culture, 239–241, 243

**P**

Phase-field model, 94–95, 103  
 Phase transition, 2, 7–10, 33–66, 91, 306  
 Platelet, 78, 164, 236, 241, 244, 259, 261, 262,  
 265, 266, 269, 283  
 Polyploid giant cells, *v.*, 129–131

**R**

Rats, 17, 147, 169, 171, 232, 260, 285  
 Recruitment, 81, 120, 121, 145, 164, 202–204,  
 206–211, 220, 234, 237, 319

**S**

Senescence, *v.*, 115, 126–129  
 Soft matter, 10, 37, 39–43, 54, 58  
 Solid stress, *v.*, 114, 125, 140, 141, 145–151,  
 160, 313, 315–316  
 Stromal cells, 4, 5, 17, 114–117, 119, 121,  
 124–129, 143–152, 160, 207, 288, 289,  
 305

**T**

Therapy response, 203, 216, 220, 232  
 Traction force microscopy (TFM), 18, 46, 114,  
 171, 215, 216, 262  
 Tumor evolution, 241, 257, 301, 302  
 Tumor microenvironment (TME), *v.*, 113–132,  
 139–153, 159–188, 201–221, 257,  
 301–305, 309, 313–315  
 Tumor stiffening, 144

**V**

Vertex model, 47, 48, 54, 88–91, 103, 104, 304

**W**

Warburg effect, 141, 303

**X**

Xenograft, 143, 180, 187, 232, 285, 287

**Z**

Zebrafish, 44, 52, 286, 287, 289–291